Iosif Vulfson

Dynamics of Cyclic Machines

Foundations of Engineering Mechanics

Series editors

V.I. Babitsky, Loughborough, Leicestershire, UK
Jens Wittenburg, Karlsruhe, Germany

Iosif Vulfson

Dynamics of Cyclic Machines

Author
Iosif Vulfson
St. Petersburg
Russia

Translator
Valery Khitrik
St. Petersburg
Russia

In loving memory of Maria Vulfson

Preface

The book focuses on the methods of dynamic analysis and synthesis of machines, comprising cyclic action mechanisms, such as linkages, cams, steppers, etc. This book presents the modern methods of oscillation analysis in machines, including cyclic action mechanisms (linkage, cam, stepper, etc.). Basically, the intention is to build up a bridge between the classic theory of oscillations and its practical application in dynamic problems for cyclic machines.

Intensification of production processes always requires the growth of operating speeds, which in turn dictates the need for more in-depth and comprehensive accounting of the dynamic factors.

Obviously, problems of machine dynamics are discussed in a large number of textbooks and monographs, since this section of engineering science concerns both the wide variety of tasks and the various levels of coverage of each problem. The latter is associated both with the variety of interests pursued by the solution of a concrete engineering problem and with a large number of conditions and factors that determine the final outcome. Therefore, ready-made recipes are not very suitable for the formation of approaches to solve problems of this class.

Experience shows that the solution of scientific and engineering problems of machine dynamics depends on overcoming certain illusions. One of them is related to an assumption regarding the classical theory of mechanisms and machines, which presumes the absolute rigidity of links. Meanwhile, practical experience of machine operations shows that under modern operating speeds this assumption is acceptable only as a first approximation, but in some cases even leads to incorrect orientation in the analysis of complex dynamic processes and the selection of areas of further machine improvement. For instance, the indisputable influence of the geometric characteristics of cyclic mechanisms (position function, transfer functions, angles of pressure, etc.) on dynamic processes is sometimes wrongly perceived as the opportunity to solve a dynamic problem by purely geometric means. In this respect, the wide range of modifications of the so-called optimal laws of motion, which are credited with the capacity to eliminate the oscillations of the output links, irrespective of a system's frequency characteristics, is highly indicative. Thus, it is impossible to design modern machines without due regard to the

oscillatory processes that in many ways define the productivity, quality of production, durability, and reliability of the equipment, as well as the working conditions of a human operator.

Another illusion relates to an exaggeration of the omnipotence of the researcher equipped with modern computer facilities. Quite often it seems that it is enough to specify an arbitrary complex system as a model and the computer will take care of the rest. At the same time the computer's capacity to "digest" the initial information and present some results is perceived as the generation of an "accurate" solution to the problem. Such a formal approach presents the engineer with quite a few far-reaching dangers. A discussion of various aspects of this still-current problem can be found in an interesting monograph [10], which is devoted to the special features of applied mathematics in solving scientific and technical problems. We will only emphasize that, in addition to potential errors, another hidden danger here is that an engineer, whose knowledge of dynamics goes just as far as the scope of a computer user, will quite often lose the ability to challenge, and his sense of responsibility will be blunted.

The aforementioned tendencies, although diametrically opposed, have common roots. In either case, there is a propensity to "protect" oneself against ostensibly extraneous information. As a result, the inviting prospect of complete formalization of dynamic calculations generally produces a formal result of questionable value.

The modern dynamic analysis of machinery requires the accumulation and development of knowledge, particular features of the studied object, and should be based on the reasonable combination of analytical and numerical methods. Of course the implementation of analytical methods is also impossible without extensive use of computer, which is reflected in this book.

The analytical emphasis in presenting the material is reflected in the author's aspiration to keep simple the presentation of problems and to present the results in a form that allows the conveyance of physical interpretation and engineering evaluation. However, when working on this book, the author did not set the completely unrealistic goal of covering all aspects of the dynamics of cyclic machines.

This book is not a textbook, so it requires from the reader a certain level of knowledge of mathematics, mechanics and general engineering, and technical subjects. At the same time, in presenting the material, the author tried, as much as possible, to take into account that in the process of training engineers for jobs in engineering industries, producing cyclic machines, insufficient attention is paid till now to problems of dynamics and especially to oscillations. Missing information can be found in the known textbooks and monographs.

This book is a supplemented translation of the author's monograph "Dynamica cyclovyh mashin," published in Russian (publishing house "Politechnica," 2013).

Apart from additions and reviewing some of the chapters, the bibliographic details were partially changed, especially the references related to English language publications.

The author would like to thank Dr. Valery Khitrik and Eng. Raza All Khokhar for translation and proofreading of the manuscript.

St. Petersburg   Iosif Vulfson

Contents

Introduction

Cyclic mechanisms as part of the machine vibrating system have features that distinguish them as an independent class of dynamic problems. One of the main qualitative features is that cyclic mechanisms are simultaneously the source of oscillations and the object of vibration protection. This requires special approaches to the calculation of vibration activity and dynamic errors and ways to reduce them. Another feature is the increased complexity of oscillation systems, because the presence of cyclic mechanisms usually results in the emergence of parametric and nonlinear effects, caused both by the nonlinear transformation of coordinates and by the structural factors. In this book, as a main method for the calculation and study of oscillating systems with variable parameters, we used the method of conditional oscillator proposed in the study [59]. As is evident from the experience accumulated over the years, this method is well suited for solving problems of dynamic analysis and synthesis in systems of the given class.

In this book, methods of solving problems of cyclic machine dynamics, taking into account the elasticity of links, contained in a number of the author's monographs, as well as in reference books and textbooks [58, 62–64, 75, 83], were further developed. For the relatively long period of time that has elapsed since the publication of these books, newer problems in this field were solved, which were published in many articles that require collection and systematization. This particular task was given precedence by the author, while compiling this book. But at the same time, we did not consider it possible to repeatedly refer the reader to the publications that have become a rarity, so the first chapters of this book are devoted to the concise consideration of the main problems of oscillations of cyclic mechanisms and machines.

As examples, the book contains the results of theoretical and experimental studies and engineering calculations, carried out in regard to the textile machinery, light industry, printing, and other industrial manufacturing units, in which the role of cyclic mechanisms is particularly major. A certain amount of attention, while compiling analysis results, is paid to dynamic forecasting and engineering recommendations.

The material in the book is presented in order of increasing complexity of dynamic problems.

The first chapter contains, in short form, general information about cyclic mechanisms, methods of synthesis of laws of program motion of executive bodies, and the simplest criteria for dynamic synthesis of these laws.

Chapters 2 and 3 of the book contain the classification of typical dynamic models and a summary of the methods of analytical mechanics, applicable to the problem of their mathematical description.

Chapters 4 and 5 contain descriptions of the basic methods of solution of problems of dynamics of cyclic mechanisms with constant and variable parameters; the ways to reduce vibration activity and enhance the accuracy of reproduction of the given laws of program motion are also presented.

Chapters 6 and 7 are devoted to the methods of evaluations of many nonlinear factors in the given systems. In particular, Chap. 6 represents the methods of accounting of nonlinear dissipative forces at the polyharmonic oscillations on the basis of the limited information obtained through experiments during monoharmonic excitation. It is to be noted that the material in this chapter is of general engineering interest and its applicability is not limited to cyclic machines. Chapter 7 provides an analysis of the influence of clearances on the dynamic characteristics of cyclic mechanisms for the elimination of vibroimpact regimes.

Chapter 8 is devoted to the matrix method of analysis of oscillations in cyclic mechanisms. Unlike traditional transition matrices, apart from elastic and inertial elements, the kinematic analog of the cyclic mechanism is included in the matrix.

Chapters 9–12 are devoted to problems of dynamics of regular oscillatory systems. Let us discuss this issue in more detail. The theory of regular oscillatory systems with periodic spatial structure is reflected in the works of many prominent scientists. First of all, the one-dimensional lattice consisting of particles was studied by Newton when determining the speed of sound. Further studies are associated with the works of Daniel and Johann Bernoulli, Cauchy, Kelvin, Born, Karman, Debye, Brillouin, and others [12, 36]. These works formed the basis of the so-called theory of chains, which helps in analytically describing the dynamics of systems with many degrees of freedom, based on the analysis of a single structural element of the system. The main directions of further development of the regular systems theory are reflected in the monographs [25, 33, 37]. One of the common properties of regular systems is the spatial localization of energy generated in linear systems during deviations from strict regularity. This coincides with a local increase in amplitudes of oscillations in certain parts of the system. The theory of regular systems, besides physics, is used in chemistry, biology, and a number of other fields of science. At this time, only few publications are dedicated to solutions of the technical problems. The most well-known technical application of the chains theory is the oscillation of power lines. Among the monographs devoted to the regular systems analysis in the machines that are schematized in the form of models with constant parameters, we would single out a substantial monograph [7]. Over the last few decades, the theory of regular systems was developed by the author in relation to the investigation of dynamics of cyclic machines [63, 64, 72, 75, 77, 79, 85, 91].

In cyclic machines and automatic lines, we have to deal with regular oscillatory systems in view of the widespread dynamically identical modules used to implement similar technological and transport operations. In such cases, due to the natural tendency of unification and interchangeability of the individual units of the machine, there is a certain repeatability of the drive blocks of the dynamic models. With regard to machines with cyclic mechanisms, the theory of regular oscillatory systems requires additional development. Unlike classical chains, each repeating element has more complex internal structure and does not represent the point mass, but the node forming the oscillation subsystems of the branched, ring, and mixed structures. Apart from that, the need for a separate study of this problem is associated with the specific features of the cyclic mechanical systems, among which we note the nonlinearity of the position function, nonstationary state of dynamic connections, and the possibility of violation of the kinematic contact in clearances, etc.

The Appendix provides a summary of the harmonic linearization method, which is used to solve a number of problems discussed in the book.

The content of the book is divided into chapters, sections, and subsections. The formulae, figures, and tables are marked by double numbers. The first number corresponds to the chapter, the second being the number of the formula, figure, or table within that chapter.

Chapter 1
Cyclic Mechanisms

1.1 General Information About Cyclic Mechanisms

1.1.1 Functional Features of Cyclic Mechanisms

Cyclic mechanisms are widely used to form nonlinear position functions for output links in machines and automatic lines (Fig. 1.1). The distinctive feature of cyclic mechanisms is the nonlinearity of the position functions, transforming the coordinate of "input" into the mechanism, in coordinate of "Output" from the mechanism. Fig. 1.1 shows the most common varieties of the simplest cyclic mechanisms: the lever (Fig. 1.1a, b, c), cam (Fig. 1.1d), mechanisms with non-circular wheels (Fig. 1.1e), steppers, among which are the maltese gears (Fig. 1.1f), ratchet mechanisms (Fig. 1.1g) and worms (Fig. 1.1h).

There can be various combinations of these mechanisms, for example cam-lever, lever-step, cam-step etc. Apart from that, in accordance with the solved kinematic problem, these simple mechanisms may be significantly complicated, using the well-known method of layering of Assur's groups [21, 29, 39]. Sometimes the step type cyclic mechanism can be created on the basis of the mechanism with two degrees of freedom, implementing summation of uniform rotation with reciprocating or oscillating motion. An example of such a mechanism, which integrates the properties of worm gear and cam or lever mechanisms, is shown in Fig. 1.1h. In this case, the angular displacement of the worm wheel, caused by uniform rotation of the worm, is summed with the additional movement from the axial reciprocating screw motion, which is controlled, for example, with cam mechanism. A similar problem is solved by a differential mechanism, in which one of the drive wheels rotates uniformly, while the second acquires the vibration motion from the cam or lever mechanism.

Thus, all cyclic mechanisms can be divided into two groups: *reversible* and *irreversible*; depending on whether or not the average value of the first transfer function of the driven member is zero. In the first case, we have a reciprocating or

Fig. 1.1 Varieties of cyclic mechanisms
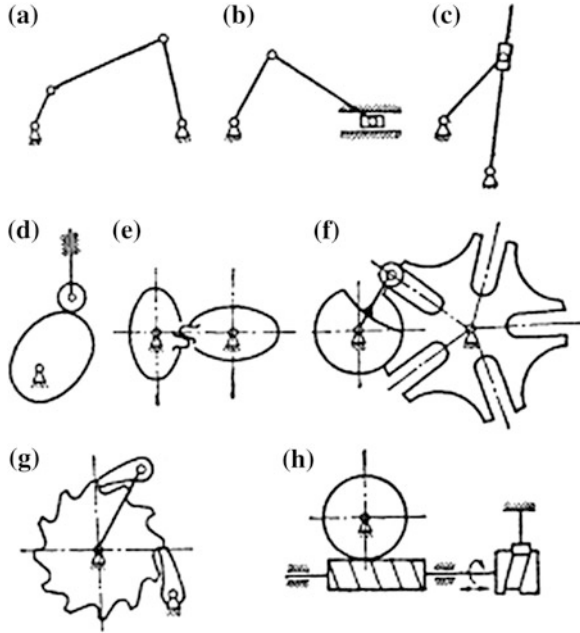
oscillating motion, of the links, about a fixed axis (Fig. 1.1a–d). In the second case the movement of the driven member has a non-zero average velocity (Fig. 1.1d–g), with a shift of the driven member, by one step, in each cycle.

Functions of link positions, implemented in cyclic mechanisms, can have or not have dwells (pauses). In accordance with this feature, all the mechanisms can be divided into two groups: *discrete* and *continuous* motion. In addition, you can select quasi-discrete motion, for the implementation of which multilink linkages with the approximate dwell of the driven member, are widely used in modern machines.

As per their functional purpose, the cyclic mechanisms may be *executive, transferring*, as well as can be used for *control, check, adjustment, feeding, transportation, sorting of products and automatic accounting of products etc*. Regardless of the performed operation, each of these mechanisms can play a very important role in the machine and can be subject to significant dynamic loads, so the division of the mechanisms, as per their functional assignment, is usually not essential from the standpoint of dynamic analysis of mechanisms. Sometimes the machine's functionality is labeled with special requirements regarding the permissible level of dynamic distortion of the laws of motion, dynamic loads etc., which should be taken into account, in the course of synthesis of the mechanism.

Kinematic and structural features of the different types of cyclic mechanisms were discussed in detail in textbooks about the theory of mechanisms and machines, [21, 29, 39] as well as in specialized monographs.

The following is the first stage of synthesis of the law of motion, based on a review of the so-called ideal kinetostatic model, in which clearances and manufacturing

errors are not taken into consideration, and all the links are taken as rigid bodies. Hereinafter these laws will be adjusted to reflect the elasticity of the links (see Chaps. 4 and 5). The possibility of change in laws of programmed motion takes root from the fact that kinematic requirements for the mechanism usually do not cause rigid laws of motion of its links and leave open the possibility of their selection, as per some criteria of dynamic nature. Such a situation arises, in particular, while solving the positioning problem, when kinematic requirements from the mechanism are reduced to the need to move the output link (working body) from a given initial to a given final position.

Regardless of executed operations these mechanisms, usually, play an important role in the machines, so their reliability and accuracy must correspond to fairly high levels of requirements.

Problems, arising out of the fulfillment of these requirements, are related to the fact that the dynamic conditions, with nonlinear position function, are more strained as compared with linear ones, because the output links of cyclic mechanisms move with variable velocities, which leads to significant inertial loads. Kinematic requirements, and hence the associated dynamic characteristics, cannot be implemented in various cyclic mechanisms equally. For example, in the cam mechanisms, we can directly implement the given law of motion, on the output link, by profiling the working surfaces of cams. In the lever mechanisms geometric characteristics are essentially laid in their scheme, therefore with the rational choice of a finite number of their parameters, you can just be closer to the specified standard.

If, during the comparison of dynamic parameters of cyclic mechanisms, we would rely only on the program laws of motion, without taking into account the possibilities of their practical implementation, the cam mechanisms would have obvious advantages, because they have great potential in case of synthesis to account for geometrically caused dynamic factors.

However, in many cases, an important role is played by the dynamic effects, caused by mechanism manufacturing and assembly errors. Here we have to take into account that the working surfaces of the elements of the lower kinematic pairs, used in the lever mechanisms, are very simple and in comparison to the complex cam profiles, can be made more accurately. On the other hand, it is extremely easy to carry-out complex laws of motion, using cam mechanisms, which can generally be implemented, only with a large number of links, when using lever mechanisms. Thus mass, dimensions and clearances increase, which has an overall adverse effect on the mechanism dynamics. So, without specifying the problem, we can only say one thing: the simpler the laws of motion, the more tangible are the benefits of lever mechanisms over the cam mechanisms.

Since using the cam mechanisms, the law of programmed motion can theoretically be reproduced exactly, we will focus on this class of mechanisms in further discussion. The laws of motion obtained, can be used as standards for approximate metric synthesis of lever mechanisms, as well as in solving the problem of positioning the working bodies using program controls [13, 18, 57].

Movement of the executive parts that ensure the fulfillment of the given technological or transport operations, is called the programmed motion. These motions

significantly influence the level of the excited oscillations; therefore the task of reducing machine vibration activity is closely related to the problem of forming the optimal laws of motion.

1.1.2 Position Function and Geometric Transfer Functions

We shall take the *ideal mechanism* as its kinetostatic model with an absolutely accurate reproduction of desired characteristics, i.e. such an abstract mechanism, in which the links are not deformed; there are no clearances and no manufacturing errors. If such mechanism has one degree of freedom, then the position of each link of the mechanism is uniquely determined as function of the angle of rotation of the input link φ_1. For certainty, we will assume that the link performs rotational or translational motion, described by one coordinate φ_n. Then

$$\varphi_n = \Pi_n(\varphi_1), \tag{1.1}$$

where Π_n is the position function of the link n.

Let's see the following functions obtained by differentiation (1.1)

$$\Pi'_n = \frac{d\Pi_n}{d\varphi_1}; \ \Pi''_n = \frac{d^2\Pi_n}{d\varphi_1^2}; \ \Pi'''_n = \frac{d^3\Pi_n}{d\varphi_1^3},$$

which are respectively called the *first, second and third geometric transfer functions,* or analogues of the speeds, accelerations and accelerations of the second order [21, 29, 39]. If φ_1 corresponds to the angular coordinate, then the dimensionality of the transfer functions coincides with the dimensionality of Π_n.

Plane-parallel motion of the link can be described with three functions of position, which fix the angular coordinate of the link and the position of one of its point. Connection of geometric characteristics Π'_n, Π''_n, Π'''_n with kinematic ones $\dot\varphi_n = d\varphi_n/dt$; $\ddot\varphi_n = d^2\varphi_n/dt^2$; $\dddot\varphi_n = d^3\varphi_n/dt^3$ is defined by the following relationships:

$$\left.\begin{array}{l} \dot\varphi_n = \Pi'_n(\varphi_1)\dot\varphi_1; \\ \ddot\varphi_n = \Pi''_n(\varphi_1)\dot\varphi_1^2 + \Pi'_n(\varphi_1)\ddot\varphi_1; \\ \dddot\varphi_n = \Pi'''_n(\varphi_1)\dot\varphi_1^3 + 3\Pi''_n(\varphi_1)\dot\varphi_1\ddot\varphi_1 + \Pi'_n(\varphi_1)\dddot\varphi_1. \end{array}\right\} \tag{1.2}$$

The structure of expression (1.2) shows that the use of position and transfer functions allows us to achieve clear differentiation between geometrical and kinematical characteristics, which define the motion of the mechanism under consideration. In the particular case of gear mechanisms with constant transmission ratio the position function is linear. As it implies as per dependency (1.2), in this case $\dot\varphi_n = \Pi'_n\dot\varphi_1$; $\ddot\varphi_n = \Pi'_n\ddot\varphi_1$; $\dddot\varphi_n = \Pi'_n\dddot\varphi_1$, whereas the proportionality factor in this

case is the first transfer function. Additionally if the input unit moves with constant speed $\dot{\varphi}_1$ = const, then output member will move uniformly. Consequently, the occurrence of inertial loads in such arrangements can only be due to a violation of conditions $\dot{\varphi}_1$ = const or Π'_n = const, due to manufacturing errors or other defects.

1.1.3 Simplest Criteria for Dynamic Synthesis

In case of nonlinear position function, which is typical for cyclic mechanisms (cam, lever, stepper, etc.), the dynamic functional conditions are more intense as compared to the mechanisms with linear function of position. Even in ideal cyclic mechanisms, the inertial loads are often very significant. In addition, there is an unfavorable force connection between the master (input) and slave (output) links.

If, for example, force F is applied to the output member n and which is balanced with the moment M, applied to the driving member, then in view of the virtual displacement principle

$$M = \Pi'_n(\varphi_1)F. \tag{1.3}$$

It is obvious that, even when $\Pi'_n \neq$ const the constant force F causes the emergence of variable torque on the input member that can excite the forced oscillations of the drive.

Another special case is also of interest. Let F be the force of inertia of the driven member n. Then, assuming for determination that the driven link performs translational motion, at $\dot{\varphi}_1$ = const we have

$$|F| = m\dot{\varphi}_1^2\left|\Pi''_n\right|. \tag{1.4}$$

Substituting this in (1.3), we obtain

$$|M| = m\dot{\varphi}_1^2\left|\Pi'_n\Pi''_n\right|. \tag{1.5}$$

It is easy to verify that $\Pi'_n\Pi''_n = (m\dot{\varphi}_1^3)^{-1}\frac{dT_n}{dt}$, where T_n is kinetic energy of the link n, dT_n/dt is kinetic power.

Expressions (1.3)–(1.5) show that the geometrical characteristics significantly affect the dynamics of the mechanism. Therefore, the extreme values of functions $|\Pi'|_{max}$, $|\Pi''|_{max}$, $|\Pi'\Pi''|_{max}$ can be used as simple dynamic criteria, by which a comparison is made between the different laws of motion, as well as the synthesis of new laws, having optimum properties in a certain sense.

To control the pulsation of inertial loads on the driven and driving, the following criteria can be used

$$K_1 = \Pi''_{max} + \xi_1 |\Pi''_{min}|; \quad K_2 = (\Pi'\Pi'')_{max} + \xi_2 |(\Pi'\Pi'')_{min}|. \quad (1.6)$$

Here ξ_1 and ξ_2 are some weights reflecting the level of importance of the components.

Issues related to the determination of the geometric characteristics of mechanisms, are covered in many monographs and textbooks, for example [21, 29, 39, 64]. Here we only emphasize that according to the method of formation of geometric characteristics of mechanisms, they can be divided into two groups: discrete synthesis and functional synthesis mechanisms.

The *first group* includes lever-type mechanisms, in which only a finite number of parameters can be determined with the help of synthesis. Geometrical characteristics of such mechanisms, in fact, are laid in their scheme, and therefore making a rational choice of parameters, can only bring close to the specified position function. The *second group* includes cam type mechanisms, in which profiling of working surfaces can help directly implement the given function. This in many cases significantly enhances the possibility of accounting dynamic factors in case of synthesis of such mechanisms.

The discussed criteria are based on geometric notions and of course, are limited and cannot exhaust the dynamic task (see Chaps. 4 and 5). However, their application is very useful, especially at the initial stages of solving such problems.

1.2 Program Motion of the Links of Cyclic Mechanisms

1.2.1 Methods for Obtaining Program Motion

In modern machines, there are two ways of forming the laws of motion of units. The *first method* is widely used in the cyclic process and energy machines, carrying out their functions under steady-state operation, when the engine speed ω, after a sort of a transient process reaches an approximately constant value. To implement the given laws of motion, we use the so-called *cyclic mechanisms* (lever, cam, maltese gears, etc.), which help us in the nonlinear transformation of the coordinates at the "input" $\varphi = \omega t$ to the corresponding coordinate at the "output".

In case of use of the *second method* the formation of the predetermined motions is provided with the help of the *program control*: servo motors (so-called "electronic cams"). In such cases, the mechanical system of the machine usually has simpler structure, because the mechanisms only perform linear coordinate transformation, as is the case, for example, in gears, with constant gear ratio.

Other undoubted advantages of this method include flexibility in configuration, reduction in mass and moments of inertia and therefore dynamic loads and reduction in structural dimensions etc. Typical examples of use of electronic cams include modern packing, printing and textile machines, automated assembly lines, woodworking machines etc.

At the same time, the use of this method is complicated, when the manufacturing process or the transport operation requires precise cyclic synchronization with other executive units. Similar tasks, in high-speed machines, are usually more reliably solved, by setting the input links of cyclic mechanisms on rigid camshaft.

Often the task of program control is solved by a human operator, for example, while controlling transport machines (cars, cranes, some kinds of industrial robots, etc.). Thereinafter we mostly restrict ourselves to the analysis of dynamic processes, implemented directly in the mechanical system.

1.2.2 Structure of Law of Motion. Dimensionless Characteristics

Regardless of the specific requirements, from the cyclic mechanism and its functionality in a particular machine, it must conform to a number of general dynamic conditions. Most often it is requirement of smooth motion, which excludes the possibility of breaking the continuity of the position functions Π and the first geometric transfer function Π'.

At the same time it is rather common to have structure of motion with three intermediate intervals, when the movement of the output link in one direction (forward or reverse) is considered as a set of three areas envisaged (Fig. 1.2): run-up, uniform motion 2 and run-out 3. In order to simplify the recording, the indices in geometrical characteristics that indicate the link's number, will be omitted in the future.

When synthesizing laws of motion, it is advisable to use the apparatus of dimensionless parameters. Let us enter the following functions for consideration:

$$\frac{\varphi}{\varphi_1} = \tau_1; \quad \frac{\Pi}{\Pi_1} = \theta_1(\tau_1) \ (\varphi \in [0, \ \varphi_1]);$$

$$\frac{\varphi_{III} - \varphi}{\varphi_{III} - \varphi_{II}} = \tau_3; \quad \frac{\Pi_{III} - \Pi}{\Pi_{III} - \Pi_{II}} = \theta_3(\tau_3) \quad (\varphi \in [\varphi_{II}, \varphi_{III}]). \tag{1.7}$$

Fig. 1.2 Graph of position function
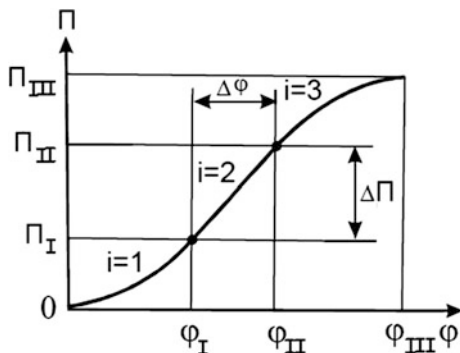
Table 1.1 Position functions and geometric transfer functions

Function	Run-up $\Pi'' \geq 0$	Uniform motion $\Pi'' = 0$	Run-out $\Pi'' \leq 0$
Π	$\Pi_I \theta_1(\tau_1)$	$\Pi_I + \dfrac{\Pi_{II} - \Pi_I}{\varphi_{II} - \varphi_I}(\varphi - \varphi_I)$	$\Pi_{III} - (\Pi_{III} - \Pi_{II})\theta_3(\tau_1)$
Π'	$\dfrac{\Pi_I}{\varphi_I}\theta'(\tau_1)$	$\dfrac{\Pi_{II} - \Pi_I}{\varphi_{II} - \varphi_I}$	$\dfrac{\Pi_{III} - \Pi_{II}}{\varphi_{III} - \varphi_{II}}\theta'_3(\tau_3)$
Π''	$\dfrac{\Pi_I}{\varphi_I^2}\theta''(\tau_1)$	0	$-\dfrac{\Pi_{III} - \Pi_{II}}{(\varphi_{III} - \varphi_{II})^2}\theta''_3(\tau_3)$

Functions $\tau_1 = 0$, $\theta_1 = 0$ at $\varphi = 0$; $\tau_1 = 1$, $\theta_1 = 1$; at $\varphi = \varphi_1$; $\tau_3 = 1$, $\theta_3 = 1$ at $\varphi = \varphi_{II}$; $\tau_3 = 0$, $\theta_3 = 0$, at $\varphi = \varphi_{III}$.

Thus, the dimensionless characteristics $\theta_1(\tau_1)$ and $\theta_3(\tau_3)$, fit into square, with sides equal to one. If we apply the same type of laws of motion at run-up and run-out, then the functions θ_1 and θ_3 are the same. Position functions and geometric transfer functions, expressed in dimensionless characteristics, are listed in Table 1.1.

Obviously the change of functions Π, $\Pi' = d\Pi/d\varphi$, $\Pi'' = d^2\Pi/d\varphi^2$ is controlled by functions θ_i, $\theta'_i = d\theta_i/d\tau_i$, $\theta''_i = d^2\theta_i/d\tau_i^2$; the remaining parameters are scale factors. If the introduction of geometric transfer functions separated the geometric and kinematic factors, then the introduction of the dimensionless characteristics, allowed to separate scale factors $\varphi_I, \varphi_{II}, \varphi_{III}, \Pi_I, \Pi_{II}, \Pi_{III}$, from transfer functions; with the help of which dimensionless characteristics of the motion law are "deformed" along the axis φ and Π. Hereinafter these scale factors will be called the *structural parameters* of the law of motion.

To exclude impact at the beginning and at the end we demand $\Pi'(0) = 0$ and $\Pi'(\varphi_{111}) = 0$, subsequently $\theta'_i(0) = 0$ and $\Pi'(\varphi_{111}) = 0$ ($i = 1, 3$). At $\tau_i = 1$ function $\theta'_i(\tau_i)$ reaches its maximum value θ'_{max}. It is easy to see that the constant θ'_{max} indicates, how much the maximum speed, in the considered area, is more than the average speed. Function $\theta''_i(\tau_i)$, depending on the chosen law of motion, can reach its maximum value at different values of τ_i. The ratio $\theta''_{max}/\theta'_{max}$ indicates, how many times the maximum acceleration, in the given area, is more than average value.

Table 1.2 shows the calculated dependencies and constants, for widely used in engineering practice family of dimensionless characteristics, known as the "modified trapezoid of general form". For this type of law of motion, the graph of the function $\theta''(\tau)$ is a trapezoid, whose sides are formed by segments of a sine wave (Fig. 1.3). The projections of the sides are defined by parameters s_1 and s_2, with which the law of program motion can be managed effectively. At $s_1 = 0$ and $s_2 = 0$, we have the so-called law of the rectangular acceleration; with $s_1 = s_2 = 0.5$ and with $s_1 = 0$, $s_2 = 1$—sine and cosine law of acceleration. Widely used is the law of equilateral trapezoid with $s_1 = s_2 = 0.25$ (for details of the impact of the parameters s_1, s_2 see Sect. 4.1.3).

Table 1.2 Dimensionless characteristics of functions of law of motion

Functions and constants	$0 \leq \tau \leq s_1$	$s_1 \leq \tau \leq 1 - s_2$	$1 - s_2 \leq \tau \leq 1$
θ	$\dfrac{2s_1}{\pi}\theta''_{max}\left(\tau - \dfrac{2s_1}{\pi}\sin\dfrac{\pi\tau}{2s_1}\right)$	$\theta''_{max}\left[\dfrac{\tau^2}{2} - s_1\tau\left(1 - \dfrac{2}{\pi}\right)\right.$ $\left. + s_1^2\left(\dfrac{1}{2} - \dfrac{4}{\pi^2}\right)\right]$	$\theta''_{max}\left\{\dfrac{4s_2^2}{\pi^2}\left[1 - \sin\dfrac{\pi(1-\tau)}{2s_2}\right]\right.$ $\left. + b_1(\tau_1 - 1 + s_2) + b_2\right\}$
θ'	$\dfrac{2s_1}{\pi}\theta''_{max}\left(1 - \cos\dfrac{\pi\tau}{2s_1}\right)$	$\theta''_{max}\left[\tau - s_1\left(1 - \dfrac{2}{\pi}\right)\right]$	$\theta''_{max}\left[b_1 + \dfrac{2s_2}{\pi}\cos\dfrac{\pi(1-\tau)}{2s_2}\right]$
θ''	$\theta''_{max}\sin\dfrac{\pi\tau}{2s_1}$	θ''_{max}	$\theta''_{max}\sin\dfrac{\pi(1-\tau)}{2s_2}$
$\theta'_{max}; \theta''_{max}$	$\theta'_{max} = \dfrac{\pi(2s_2 + b_1\pi)}{4s_2^2 + \pi^2(b_1s_2 + b_2)}; \quad \theta''_{max} = \dfrac{\pi^2}{4s_2^2 + \pi^2(b_1s_2 + b_2)};$		
$(\theta'\theta'')_{max}$	$(\theta'\theta'')_{max} = \left(\theta''_{max}\right)^2\sqrt{1 - b_3^2}\left[\dfrac{2s_2}{\pi}b_3 + b_1\right];$		
$b_1; b_2; b_3$	$b_1 = 1 - s_2 - s_1\left(1 - \dfrac{2}{\pi}\right); \quad b_2 = (1 - s_2)\left(\dfrac{1}{2} - \dfrac{s_2}{2} - s_1 + \dfrac{2s_1}{\pi}\right) + s_1^2\left(\dfrac{1}{2} - \dfrac{4}{\pi^2}\right);$ $b_3 = \dfrac{1}{4}\left(-\dfrac{\pi}{2s_2}b_1 + \sqrt{\dfrac{\pi^2}{4s_2^2}b_1^2 + 8}\right)$		
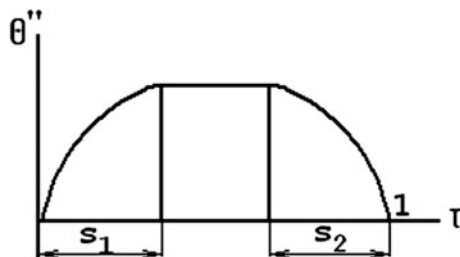
Fig. 1.3 Graph of dimensionless characteristic $\theta''(\tau)$

Out of all the possible laws, the smallest value $\theta'_{max} = 2$ is for the rectangular law of accelerations. However, under this law of acceleration, there are discontinuities (soft shocks), which leads to the excitation of intense vibrations. However, not every jump, inherent in the function θ'', necessarily leads to the soft shock. For example, if the cam follower is moving without dwell, it is possible to couple accelerations on the border of the forward and reverse strokes, without requiring the acceleration at the border to be equal to zero. The final decision about the admissibility and the merits of a particular law of motion, should be based on the account of characteristics of a specific vibration system (see Chap. 4).

1.2.3 Dimensionless Constants of Laws of Motion

Property 1 Constant θ'_{max} is inversely proportional to the value $1 - \tau_*$, where τ_* is abscissa of the Centre of gravity of the area limited with graph $\theta''(\tau)$ and axis of abscissas (see Fig. 1.3). For evidence of this provision we find τ_*:

$$\tau_* = \frac{\int_0^1 \tau\theta''(\tau)d\tau}{\int_0^1 \theta''(\tau)d\tau} = \frac{\theta'_{max} - 1}{\theta'_{max}}. \tag{1.8}$$

As per (1.8) we can see that

$$\theta'_{max} = 1/(1 - \tau_*). \tag{1.9}$$

It is clear that for all symmetric diagrams $\theta'(\tau)$ $\tau_* = 0.5$, and consequently $\theta'_{max} = 2$.

Property 2 Constant θ''_{max} is directly proportional to the constant θ'_{max} and inversely proportional to the filling coefficient σ. We consider the filling coefficient σ as the ratio of the area, limited by the graph θ''_{max} and axis of abscissas, to the area of circumscribed rectangle (see Fig. 1.3). So

$$\sigma = \int\limits_0^1 \theta''d\tau/\theta''_{max} = \theta'_{max}/\theta''_{max}.$$

It follows

$$\theta''_{max} = \theta'_{max}/\sigma = (1 - \tau_*)^{-1}\sigma^{-1}. \tag{1.10}$$

Since $\sigma_{max} = 1$ the minimum value $\theta''_{max} = 2$ is implemented with a rectangular law of acceleration.

Scope of the solution corresponds to the obvious restrictions $\sigma \leq 1$, $\theta'_{max} > 1$, $\theta''_{max} \geq 2$.

At this point we assume functions $\theta(\tau)$ as given. We will return to the issues related to rational choice of the dimensionless characteristics, at the end of this paragraph and in Sects. 1.2.4 and 4.1.3.

1.2.4 Typical Problems of Synthesis of Motion Law

The above mentioned six parameters cannot be set arbitrarily, because for prevention of shocks, they must be associated with two conditions of continuity of the

first geometric transfer function Π' on the interval borders, i.e. at $\varphi = \varphi_I$ and $\varphi = \varphi_{II}$:

$$\frac{\Pi_I}{\varphi_I}\theta'_{1max} = \frac{\Pi_{II} - \Pi_I}{\varphi_{II} - \varphi_I};$$
$$\frac{\Pi_{II} - \Pi_I}{\varphi_{II} - \varphi_I} = \frac{\Pi_{III} - \Pi_{II}}{\varphi_{III} - \varphi_{II}}\theta'_{3max}. \tag{1.11}$$

At $\varphi = 0$ and $\varphi = \varphi_{III}$ similar conditions are satisfied when $\theta'_i(0) = 0$. Thus *to uniquely solve the problem of motion law synthesis, except for dimensionless characteristics, it is necessary to* set four additional conditions, on the basis of the specific conditions.

Let's look at some common problems of synthesis of laws of program motion. First, we will introduce several dimensionless parameters, characterizing the relative value of the interval of uniform speed:

$$\zeta_n = (\Pi_{II} - \Pi_I)/\Pi_{III}; \qquad \zeta_\varphi = (\varphi_{II} - \varphi_I)/\varphi_{III}, \tag{1.12}$$

and the skewness factor of the law of motion

$$f = (\varphi_{III} - \varphi_{II})/\varphi_I. \tag{1.13}$$

At $f = 1$ the duration of run-up and run-out are equal to.

Problem 1 Given is: Π_{III}, φ_{III}, f, ζ_n.

On the basis of (1.11) in view of (1.12) and (1.13), after elementary calculations we obtain

$$\Pi_I = \Pi_{III}(1 - \zeta_n)/(1 + \nu_1 f); \quad \varphi_I = \varphi_{III}(1 - \zeta_\varphi)/(1 + f);$$
$$\Pi_{II} = \Pi_{III}(1 + \nu_1 f \zeta_n)/(1 + \nu_1 f); \quad \varphi_{II} = \varphi_{III}(1 + f \zeta_\varphi)/(1 + f), \tag{1.14}$$

where $\nu_1 = \theta'_{1max}/\theta'_{3max}$.

Now we need to define the unrecognized parameter ζ_φ. After substituting (1.14) in (1.12):

$$\frac{\zeta_n}{\zeta_\varphi} = \frac{(1 - \zeta_n)(1 + f)}{(1 + \nu_1 f)(1 - \zeta_\varphi)}\theta'_{1max}.$$

Solving this equation for ζ_φ we get

$$\zeta_\varphi = \frac{\zeta_n}{\zeta_n + U(1 - \zeta_n)\theta'_{1max}}, \tag{1.15}$$

where $U = (1 + f)/(1 + \nu_1 f)$.

If for run-up and the run-out the same type of law of motion is accepted, then $\theta'_{1max} = \theta'_{3max}$, $\nu_1 = 1$, and consequently $U = 1$. The expressions (1.14) and (1.15) uniquely determine the solution of the problem. If instead of parameter ζ_n given is the value of ζ_φ, the Eq. (1.15) must be solved relative to ζ_n.

Let's specify simple dynamic criteria, listed at the beginning of this paragraph, for the problem under consideration

$$\Pi'_{max} = \frac{\Pi_I}{\varphi_I} \theta'_{1max} = \frac{\Pi_{III} - \Pi_{II}}{\varphi_{III} - \varphi_{II}} \theta'_{3max}; \tag{1.16}$$

for run-up

$$\Pi''_{max} = \frac{\Pi_I}{\varphi_I^2} \theta''_{1max}; \qquad (\Pi'\Pi'')_{max} = \frac{\Pi_I^2}{\varphi_I^3} (\theta'_1 \theta''_1)_{max}; \tag{1.17}$$

for run-out

$$|\Pi''|_{max} = \frac{\Pi_{III} - \Pi_{II}}{(\varphi_{III} - \varphi_{II})^2} \theta''_{3max}; \qquad |\Pi'\Pi''|_{max} = \frac{(\Pi_{III} - \Pi_{II})^2}{(\varphi_{III} - \varphi_{II})^3} (\theta'_3 \theta''_3)_{max}. \tag{1.18}$$

According to formula (1.11), the structural parameters in general also depend on the dimensionless characteristics constants θ'_{1max}, θ'_{3max}, so the nature of their impact on the given criteria is not as obvious, as it formally looks from (1.16) to (1.18). In the simplest case, where there is no phase of uniform speed, ($\zeta_n = \zeta_\varphi = 0$) and $\theta'_{1max} = \theta'_{3max}$ ($\nu_1 = 1$), we obtain that the considered criteria are proportional to corresponding dimensionless constants.

With the increase in the interval of uniform speed, value Π'_{max} reduces, and $|\Pi''|_{max}$ usually grows. In extreme cases, when $\varphi_1 = 0$, $\varphi_{II} = \varphi_{III}$ ($\zeta_n = \zeta_\varphi = 1$), we obtain $\min \Pi'_{max} = \Pi_{III}/\varphi_{III}$; other criteria increase indefinitely. The opposite type of influence ζ_n (or ζ_φ) on Π'_{max} and $|\Pi''|_{max}$ proves that at certain interval of uniform velocity, there is a minimum of the criterion $|\Pi'\Pi''|_{max}$, which is proportional to the dynamic component of the drive torque.

Let us illustrate this with an example, in which the laws of motion at the run-up and run-out are accepted as similar and graphs θ'_1, θ'_3 are symmetric ($\tau_* = 0.5$); wherein $f = 1$, $\theta'_{max} = 2$, $\nu_1 = 1$.

On the basis (1.15) we have $\zeta_\varphi = \zeta_n/(2 - \zeta_n)$. Then at the run-up and run-out

$$|\Pi'\Pi''|_{max} = \frac{\Pi_{III}^2 (2 - \zeta_n)^3}{8\varphi_{III}^3 (1 - \zeta_n)} (\theta'\theta'')_{max}.$$

It is easily see that the minimum of this function, under variation of the parameter ζ_n, has the value $\zeta_n = 1/2$; wherein $\zeta_\varphi = 1/3$. Substituting these values

in (1.16)–(1.18) shows that due to the introduction of interval of uniform speed, the value $|\Pi'\Pi''|_{\max}$ decreased by 15.6 %, $\Pi'_{\max}$ decreased by 25 %; $|\Pi''|_{\max}$ increased by 12.5 %.

The nature of the influence of the skewness factor f will be analyzed, when considering the following problem.

Problem 2 Given is: Π_{III}, φ_{III}, ζ_n (or ζ_φ), $\lambda = \Pi''_{I\max}/|\Pi''_3|_{\max}$.

We will write the ratio of the extreme values of accelerations at the run-up and run-out (see Table 1.1):

$$\lambda = \frac{\Pi_I(\varphi_{III} - \varphi_{II})^2}{(\Pi_{III} - \Pi_{II})\varphi_I^2}\, v_2, \qquad (1.19)$$

where $v_2 = \theta''_{1\max}/\theta''_{3\max}$.

According to (1.13), (1.14) we have $(\varphi_{III} - \varphi_{II})^2/\varphi_I^2 = f^2$, $(\Pi_{III} - \Pi_{II})/\Pi_I = fv_1$. After substitution in (1.19)

$$\lambda = fv_2/v_1. \qquad (1.20)$$

So the skewness factor $f = \lambda v_1/v_2$ is uniquely determined by parameter λ. In doing so this problem is reduced to the conditions for the previous one. Equation (1.20) facilitates the analysis of the impact of the parameter f on $|\Pi''|_{\max}$. Taking into account (1.14), (1.17), (1.20), we have

$$\Pi''_{I\max} = \frac{\Pi_{III}(1 - \zeta_n)(1 + f)U\theta''_{1\max}}{(1 - \zeta_\varphi)^2}; \quad |\Pi''_3|_{\max} = \frac{v_1 \Pi''_{I\max}}{fv_2}. \qquad (1.21)$$

With the increase in parameter f the extreme value of the second transfer function in the run-up increases and in the run-out, it decreases. To select the optimum value of this parameter, we can use the condition of minimum criterion K_1 or K_2 [see (1.6)]. So, for example, at $v_1 = 1$, by substituting (1.21) into (1.6) and selecting for K_1 in the expression, the factors depending on f, we write

$$\Phi(f) = (1 + f)[1 + \xi_1 f/(v_2 f)].$$

Condition $d\varphi/df = 0$ gives the optimum value of the skewness factor

$$f_{\text{îïò}} = \sqrt{\xi_1/v_2},$$

at which pulsation of inertial loads will be minimum.

At $v_1 \neq 1$ conditions $\min K_1$, $\min K_2$ are quite cumbersome, so in the general case for optimization of the parameter f, it is more convenient to use numerical methods. However, we should note that the coefficient U in (1.21) weakly

depends on f. Thus, at increase of f from 0 to ∞ coefficient $U(f)$ varies monotonously from 1 to v_1^{-1}.

Problem 3 We accept given Π_{III}, φ_{III}, λ, Π'_{max}.

This problem occurs, when the working body must move in a certain interval with given uniform speed or at constant ratio of speeds of input and output links.

Examples of such situations include synthesis of the law of motion for sheet supply mechanisms in printing machines, mechanism for yarn destacking in textile machinery, mechanisms of tools provision in automated machine tool stations etc.

Figure 1.4a shows the typical drawing of the sheet supply mechanism in printing machine (pre-gripper).

Track 4, being driven member of the cam-lever mechanism (units 1–4), with its clappers 6 grasps the sheet 5, which is at rest, accelerates it to the peripheral speed of the impression cylinder 7 and transmits it to the cylinder clappers. In this case, the value $\Pi'_{\text{max}} = R_2/R_1$ is fixed; where R_1, R_2 are the radii of the cylinder and lever, and there is an interval of uniform velocity in the function of position (Fig. 1.4b).

Since in this problem, contrary to the previous case, the maximum value of the first geometric transfer function is given, we have to refuse from assignment of the relative interval of uniform speed determined by the parameters ζ_n or ζ_φ. From (1.7) to (1.8) follows the obvious relation

$$\zeta_n/\zeta_\varphi = \Pi'_{\text{max}}/\overline{\Pi}' > 1, \tag{1.22}$$
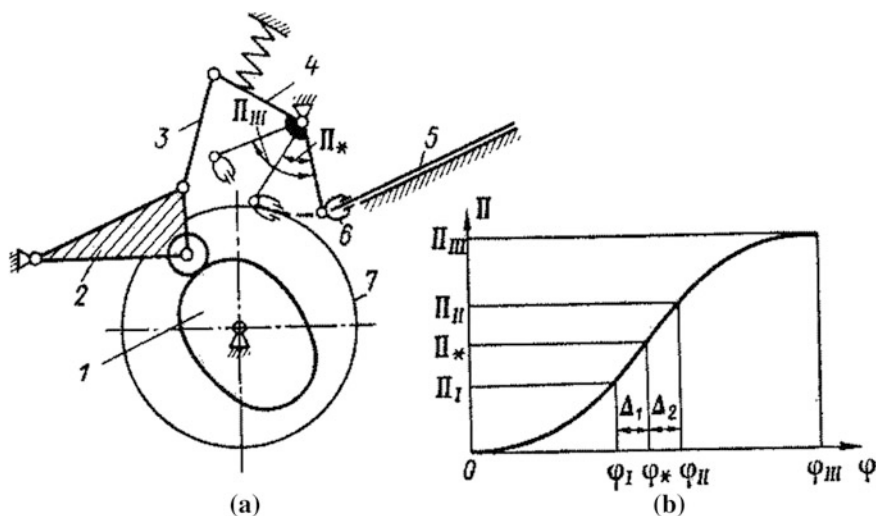
Fig. 1.4 Kinematic scheme and the position function for the stop-gripper mechanism

where $\overline{\Pi}\prime = \Pi_{III}/\varphi_{III}$ is the mean of the first geometric transfer function for the entire range of motion $\left(\overline{\Pi}' < \Pi'_{max}\right)$.

By solving the Eqs. (1.15) and (1.22) with respect to ζ_n, we find

$$\zeta_n = \frac{\theta'_{1max} U - \Pi'_{max}/\overline{\Pi}'}{\theta'_{1max} U - 1}. \tag{1.23}$$

Here function U is defined by formula (1.15) taking into consideration (1.20).

After determining parameter ζ_n as per (1.23), the initial conditions correspond to problem 2. Conditions for the existence of solutions are determined by the following obvious requirements: $0 \le \zeta_n \le 1$.

When $\zeta_n = 0$, the interval of uniform speed on the graph $\Pi(\varphi)$ (see Fig. 1.4b), constringes to a point, at $\zeta_n \to 1$ the intervals of running-up and running-out disappear that leads to shock at the beginning and end of the stroke. These conditions impose following restrictions on the input data

$$\Pi_{III} < \varphi_{III} \Pi'_{max} \le \Pi_{III} U \theta'_{1max}. \tag{1.24}$$

Rather often the initial conditions of the synthesis of law of motion are such that along with the given maximum value of the first geometric transfer function Π'_{max}, in certain way the length of the uniform speed interval is fixed. This additional requirement can be satisfied, if we exclude from the initial data the stroke of the working body Π_{III} or the corresponding phase angle φ_{III}.

On the basis of (1.14) and (1.23) in the first case we find

$$\Pi_{III} = \frac{1 + \zeta_\varphi(\theta'_{1max} U - 1)}{\theta'_{1max} U} \Pi'_{max} \varphi_{III}, \tag{1.25}$$

and in the second case

$$\varphi_{III} = \frac{\Pi_{III}}{\Pi'_{max}} \left[\theta'_{1max} U - \zeta_n(\theta'_{1max} U - 1)\right]. \tag{1.26}$$

Formulae (1.25) and (1.26) reduce the cases under consideration to the original conditions of the problem 3. At the same time the conditions of existence of solutions, defined by (1.24), remain valid.

On the basis of the considered common tasks of synthesis of laws of program motion, other tasks can also be solved, where a number of previously fixed parameters varies in a given interval [64].

In conclusion, we emphasize that for objective comparison of different types of laws of motion, defined with functions $\theta_i(\tau_i)$, we should express $\Pi'_{max}, |\Pi''_{max}|, |\Pi'\Pi''|_{max}$ in terms of independent initial conditions of the problem. As it was already noted, at the same time it is impossible to judge in general case, these

criteria as per the cognominal dimensionless constants θ'_{max}, θ''_{max}, $(\theta'\theta'')_{max}$, because the structural parameters of the law of motion, among other factors, according to (1.11) depend on the constant $\theta'_{i\,max}$. It follows from these equations in particular, that the laws of motion can be compared directly with the cognominal dimensionless constants, only with the same values of $\theta'_{i\,max}$.

Apart from above considered method, when synthesizing we operate with one or several families of laws of motion, comparing them as per the dynamic criteria, there is another approach, while using which for each case a new type of law of motion is created. Such an approach is justified for solving the specific problems of unique types of synthesis.

Chapter 2
Dynamic Models of Cyclic Mechanical Systems

2.1 Main Objectives of Machine Vibrations Analysis

The development of modern machinery raises many complicated technical problems for engineers. One of them is related to the tendency towards the intensification of technological and transport operations, which in turn stipulate increased operating velocities, dynamic loads and level of oscillations (vibrations).

The term "oscillations", as it is known, denotes the process of alternate increase and decay of physical values or its derivatives. In the case of mechanical oscillations such values are the coordinates, speeds, forces (or moments). The subject of the theory of oscillations is the study of the general laws of oscillatory processes and development of methods of their research on the basis of the laws of mechanics, modern mathematical apparatus and outcomes of the experiment.

Study of oscillations in machines, has the following objectives:

1. Elimination of emergency regimes, arising from resonance phenomena or fatigue failure of structural elements.
2. Provision of the normal working conditions for the machinery, devices, means of automation and other equipment. In technological machines cyclic mechanisms are commonly used for actuator's moving in accordance with given complex motion laws. In this case the problem of accurate reproducing of the kinematic characteristics, which substantially depends on oscillations, is very important.
3. The solution of the environmental problems, associated with machine functioning, to provide dependable staff protection against vibration and noise.
4. Use of oscillatory processes for the fulfillment of technological and transport operations. As valid examples, we can consider vibration tools, vibratory transportation, vibratory pile sinkage, vibratory separation of granular mixtures, etc.

2.2 Main Stages of Dynamic Analysis

We define the machine, mechanism or process as *physical object (PO)*; Fig. 2.1 shows the diagram of dynamic calculation. Even at the current level of development of machine mechanics and computers, the full description of dynamic behavior of an object is not possible and is not necessary. Therefore, *the first stage* of dynamic calculation is related to the reasonable simplification of the object, i.e. its replacement with some schematic or dynamic model, which depicts the most significant factors of the problem under consideration.

Thus, *the dynamic model (DM) is an idealized image of the considered system, used during its theoretical study and engineering calculations, that take into account the objectives and features of the problem* Since the number of tasks can be multiple, one single object depending on the purpose of calculation can correspond to several dynamic models (for details see Sect. 2.1).

The second stage is to set up the so-called mathematical model (MM), i.e. the mathematical description of the dynamic model. This term refers to the system of equations, derived by use the laws of mechanics and, if necessary, experimental data. Such a necessity arises, for example, for describing resistances of different physical nature. While designing the models, sometimes we can use some hypotheses and assumptions, compensating the lack of knowledge or simplifying future analysis.

The third step of dynamic calculation is *solving the equations.* At this stage both analytical methods that give a clear qualitative picture and reliable engineering
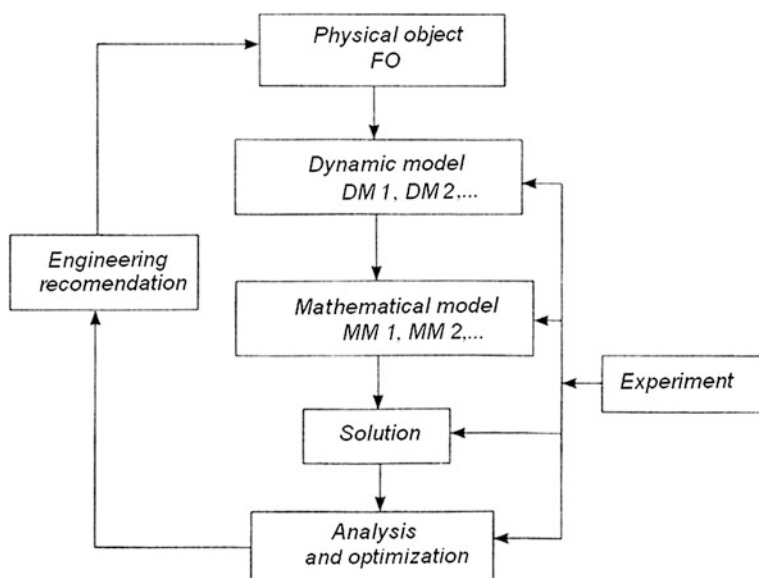
Fig. 2.1 Structure of dynamic analysis

evaluation and numerical methods, based on the great features of modern computing, are used. The numerical-analytical methods, based on a reasonable balance of both methods, have great prospects.

The fourth stage is the analysis of the obtained solutions, from the point of view of the given engineering problem. An *optimized problem* can often be formulated based on the analysis. In relation to the machines' oscillation systems, this problem is of interest, with the objective of reducing the vibration activity of mechanisms or more effective use of the vibrations, in the technological processes. On the basis of the fourth phase of calculation, *engineering recommendations*, for choosing machine parameters or correction of the initial parameter values, can be made.

The listed stages can be executed on a different level, both, in relation to the selected dynamic models and methods of their research, and/or to the accuracy of calculations, depending on the purpose and degree of responsibility. Of course the degree of reliability of the source information must also be taken into account.

Along with the theoretical methods of machine vibration analysis, sometimes it is necessary to *experiment*, to discover new phenomena, set some hypotheses and assumptions, and sometimes discover a new theory. Alongside natural experiments, performed directly on the investigated machine, physical modeling, making use of especially made units, is used for the design of some important mechanisms. Because of the wide variation of parameters and structure of the system, leading to large labor costs and expenses, the experiment should be based on the preliminary results of theoretical studies. At the same time, check of the adopted dynamic models plays a special role.

2.3 Classification of Mechanical Vibrations

According to the *kinematic features* mechanical vibrations can be: *periodic (steady) oscillations* in which the state of the system is repeated at regular intervals, called the period of the oscillations (Fig. 2.2a), *divergent oscillations,* in which the extreme deviations from the mean value is an increasing function (Fig. 2.2c) and *damped oscillations,* in which the extreme deviations from the mean value is a decreasing function (Fig. 2.2d). The system's position is characterized by generalized coordinates and their first derivatives (generalized velocities).

A very common special case of periodic oscillations are *harmonic oscillations,* in which the generalized coordinate or its derivative is proportional to the sine (cosine) with an argument, which is linearly time-dependent (Fig. 2.2b):

$$q = A \sin(\omega t + \alpha),$$

where A is the amplitude of the oscillations, i.e. the greatest deviation of the harmonic oscillation process from the average value; $\varphi = \omega t + \alpha$ is the oscillation phase; $\alpha = \varphi(0)$ is the initial phase; $\omega = d\varphi/dt$ is the angular frequency. The angular frequency is related to oscillation period τ at a ratio of $\omega = 2\pi/\tau$ and has
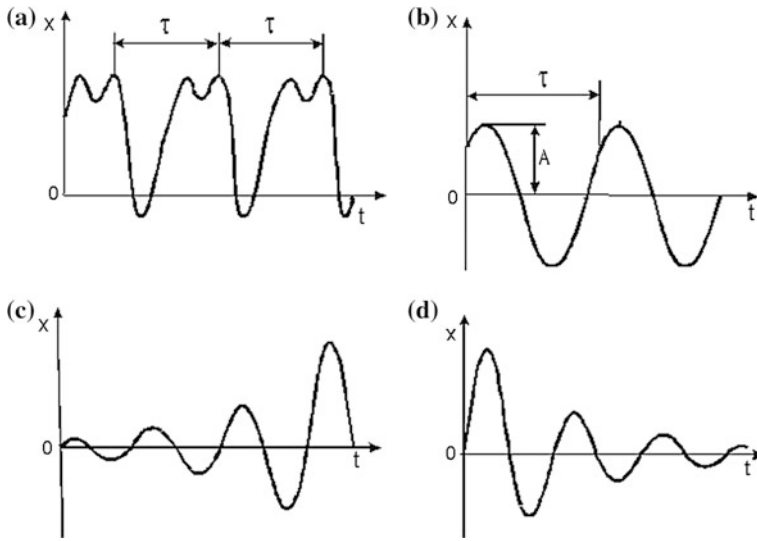
Fig. 2.2 Varieties of oscillations as per the kinematic features; types of vibration: **a** periodic (steady), **b** harmonic, **c** divergent, **d** damped

dimension s^{-1}. The frequency can also be measured in Hertz (Hz), i.e. number of oscillations per second $v = 1/\tau$. Obviously, $v = \omega/(2\pi)$.

As per the nature of disturbance, the oscillations can be attributed to the following types:

Free (natural) oscillations are oscillations that occur without an alternating external influence and external energy input. In case of free oscillations, the energy is supplied only in the initial moment, through the so-called initial conditions [initial deviations from equilibrium and initial speed (Fig. 2.3a)].

Forced oscillations, caused and supported by the force or kinematic excitation. In case of *forced excitation,* external time-dependent force or moment is applied to the system (Fig. 2.3b). In case of *kinematic excitation* any given point or section of system is forcibly moved as per the given law of motion (Fig. 2.3c).

Fig. 2.3 Simple examples of free and forced excitation of vibrations: **a** free, **b** forced, **c** forced when kinematic excitation
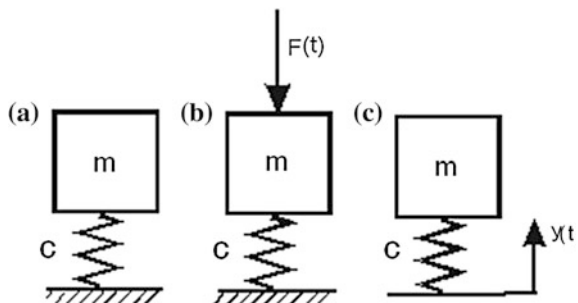
   Parametric oscillations, caused and supported by the change in time of one or more parameters of the system (reduced mass, reduced moment of inertia, stiffness coefficient, reduced length, etc.).

   Self-exciting oscillations are the process, regulated by the system's motion that occur in nonlinear systems with non-oscillatory source of energy or when the frequency of the source of energy differs a lot from the frequency of the self-excited oscillations. A famous technical example is the self-oscillations of the steam engine, in which constant steam pressure causes the reciprocating motion of the piston. Another example is self-exciting oscillations of a clock, because we can wind up the clock with frequency, incommensurable with the frequency of self-exciting oscillations.

   The *longitudinal oscillations* are differentiated as per the *type of deformations* (tension, compression); *torsional vibrations, bending vibrations.*

   By *type of dynamic model (DM)*: there are dynamic models with distributed and lumped parameters (see Sect. 2.1).

   By *type of mathematical model (MM)*: there are *linear oscillations* described by linear differential equations and *nonlinear oscillations,* described by nonlinear differential equations. In addition, the coefficients of these equations can be constant or variable.

2.4 Initial Data and the Principles of Dynamic Model Creation

As it was noted in Sect. 2.2, the study of dynamic processes, taking place in the machines, must begin with the drawing-up of the so-called dynamic model, adequate for these processes, i.e. suitable to describe those properties and characteristics that meet the objectives of the study.

   Dynamic model consists of several dynamic models of its functional parts, namely: a source of energy (the engine) and a mechanical system. In turn, the dynamic model of the mechanical system consists of dynamic models of its mechanisms.

   The simplest dynamic model is a mechanism with absolutely rigid links (kinetostatic model), which was discussed during the classical course of theory of mechanisms and machines. This model, however, does not allow the determination of the deformation errors of laws of motion and investigate the elastic oscillations of elements, which often results in violation of prescribed accuracy, increased wear and leads to breakdowns.

   When taking into account the deformability of the mechanism's links, the dynamic model of the mechanism is usually called the mechanism with elastic links. In this case it is believed that the links are elastic bodies, subordinate to Hooke's law. This means that after the removal of the load, causing the deformation, the original undistorted state is restored.

An important characteristic of the dynamic model is the number of degrees of freedom, i.e. the number of independent (generalized) coordinates that uniquely identify the system position. Since each link may be represented as totality of an infinite number of masses, connected by elementary "springs", any mechanism with elastic links has an infinite number of degrees of freedom. While schematizing the studied object, you can reflect this if you take advantage of dynamic models with distributed parameters that are described with systems of partial differential equations. Usually these types of models are used for a limited number of relatively simple (though very widespread) elements: rods, shafts, beams, plates, shells, etc. The analysis of the machine's drive, on the basis of only such models, is not considered possible, as well as necessary. So there is a widespread use, in engineering, of the dynamic models with lumped, i.e. discretely presented parameters, in which the number of degrees of freedom is finite.

The drawing-up of such models is based on the following principles:

1. The inertial properties of the system are reflected through the masses or moments of inertia, which are concentrated in separate locations or sections.
2. These points or sections are connected to each other by elastic, dissipative and geometric (or kinematic) constraints, deprived of inertial properties.

The term "dissipative" is used here to point to the accounting of the forces of resistance that cause dissipation of mechanical energy, i.e. its partial transition into other forms of energy. The application of these principles means that in kinematic chain and mechanisms the most massive elements and submissive links (links with the minimal rigidity) are taken into consideration.

Let us see the diagram of the drive (Fig. 2.4a), which consists of the motor 1, flexible coupling 2, gear train 3–4 leading into rotation the shaft 5 with drum 6. If all the links would be considered as absolutely rigid, then the number degrees of freedom for this drive will be equal to one. Such a model is called kinetostatic. In this case the number of degrees of freedom is equal to the so-called degrees of motion, used in the course of theory of mechanisms and machines. Considering the coupling stiffness, we can represent the design scheme as the dynamic model shown in Fig. 2.4b. The chain of inertial and kinematic elements, not interrupted by elastic and dissipative elements, can be replaced by one reduced moment of inertia J (Fig. 2.4c).

With increase in machine operating speeds the frequencies of machine excited oscillations are also increasing, leading to necessity of complicating the dynamic model. In these cases usually it is necessary to increase the number of accounted elastic elements of the machine, thus increasing the number of degrees of freedom of the studied vibration system.

Hence, for example if in the considered drive, we take into account the torsion compliance of the area of the shaft 5 between the wheel 4 and the drum 6, the dynamic model obtains an additional degree of freedom (Fig. 2.4d). Thus the total number of degrees of freedom $H = 3$.

Thus, for the study of the same object (machine, drive, mechanism), quite a different set of dynamic models can be used. This ambiguity of machine models, with elastic links, of course, complicates the dynamic analysis, because it requires
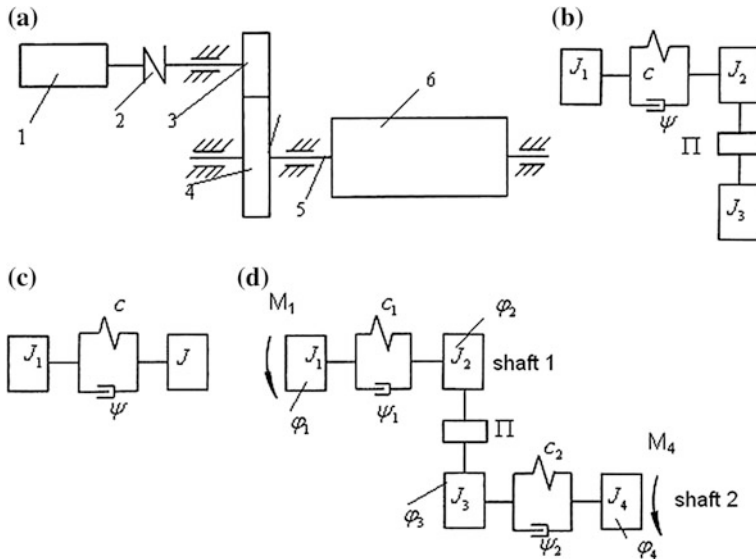
Fig. 2.4 To the method of drawing up a dynamic model; **a** diagram of the drive, **b** model with one elastic-dissipative element, **c** model with one elastic-dissipative element and reduced moment inertia, **d** model with two elastic-dissipative elements

the researcher to have clear ideas about the studied oscillatory processes. It often seems that the greater the number of degrees of freedom, which a dynamic model has, the smaller is the error expected at the end of problem solution. However, this statement is valid as long as it is supported by the appropriate level of reliability of the initial data. Meanwhile, the increasing complexity of the model results in additional difficulties, associated with the identification of its parameters (primarily stiffness coefficients and dissipation factors). The inevitable errors in their determination, lack of information and rough assumptions can negate the refinement that would be expected due to complexity of the model. Therefore, you should always choose the simplest dynamic models, capable of reflecting the studied phenomenon.

While conducting preliminary calculations at the stage of conceptual design, it is common to use a model of the machine with rigid links (kinetostatic model). On the basis of this model the engine is selected, the inertial loads, at first approximation, and reactions in the kinematic pairs, are estimated. When taking into account the dynamic characteristics of the motor on the basis of the kinetostatic model, the non-uniform rotation of the motor shaft can also be evaluated. Very often, in case of a small coefficient of irregularity, the input coordinate of the drive can be taken as $\varphi_0 = \omega t$, where ω is the angular velocity.

Hereafter, during the stage of technical design, elastic and dissipative elements are included in the model. In some cases the design features of the investigated drive allow the formation of one or more dynamic models. Examples of this approach have been illustrated above. However, in more complex cases, for the final selection of the successful model, some preliminary calculations are required
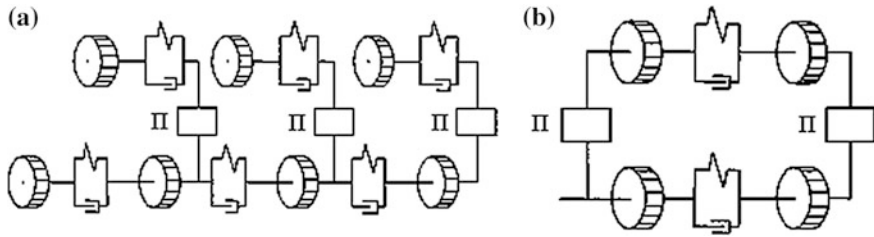
Fig. 2.5 Dynamic models with branched and ring structure; **a** branched structured model, **b** ring structured model

(for example, calculation of stiffness coefficients of some elements), and sometimes even a search experiment. It is often possible to identify such subsystems (mechanisms, drives, units, etc.), which in a first approximation, under certain simplifying assumptions can be considered separately, which allows the display of local dynamic processes in more depth.

Depending on the type of the connections of a model's elements, all models can be divided in several groups: chain models (see Fig. 2.4d), branched (Fig. 2.5a) and ring structured models (Fig. 2.5b). The selection of the dynamic model depends on the set of dynamic tasks and is usually multistage. The experience and skills of the researcher play an important role in this process.

2.5 Typical Dynamic Models of Cyclic Systems and Their Classification

Introductory remarks The result of any dynamic analysis is either the determination of forces at given motion (the first dynamic problem) or laws of motion of the links for given forces (the second dynamic problem). The first task is the main for systems with rigid links.

When taking into account the elastic properties of the links, we deal with the second task of dynamics, based on the solution of the system of differential equations. In this case, the specifics of cyclic mechanisms manifest not only in significantly large perturbations, but, as a rule, and in the more complex nature of the dynamic relations, due to the variability of the system parameters, kinematic nonlinearities contained in the position functions and other factors. Accordingly there are qualitatively more complex dynamic effects, which will be discussed later.

Dynamic calculations are carried-out both for solving the problem of analysis of mechanisms and for their rational synthesis. If for analysis, we answer the question, what is the dynamic effect of selected parameters of the mechanism, then, one of the major tasks of dynamic synthesis is the timely identification of rational (and sometimes, in a sense optimum) values of the parameters and their combinations.

Dynamic synthesis of mechanism is one of the most important and difficult problems, faced during the design of machine units. In this regard, the importance

of the first preliminary stage of synthesis should be emphasized, when the layout, kinematic and dynamic parameters of the designed mechanism, vary across a wide range. It is well known that this stage of the synthesis, which is still dominated by the intuitive approach, not sufficiently supported by engineering calculations, significantly affects not only the timeframe of design, but also greatly determines the technical perfection of the machine's prototype, as well as the volume of extra expenses, required during the mass production of the machine.

While solving the dynamic problems, the analysis and synthesis are usually closely connected. In particular, many of the problems of synthesis, which establish the rational values of the system's parameters, often base on preliminarily solved problem of analysis.

One of the most important and urgent tasks, for consideration, is the development of the optimization criteria. These criteria should be based on the most significant factors of the considered problem and at the same time have the foreseeable shape, to retain the role of active tool for the dynamic synthesis, when developing variants of a mechanism.

We have already analyzed some of the criteria identified during the study of the ideal mechanism. When taking into account the elasticity of links, the question of criteria, without losing its importance, is further complicated. In this case, in addition to geometric and kinematic characteristics, other factors, characterizing the frequency features of the system, level of proximity of working modes to the dynamically unstable modes, level of additional dynamic loads, caused by oscillations and many other factors, discussed in detail in following chapters, appear as dynamic criteria.

The choice of the mechanism structure and its design implementation, as one of the stages of analysis, is not an unambiguous task and, as it is known, largely depends on the experience and intuition of the designer. However, undoubtedly the role of objective dynamic parameters, in the choice of the type of mechanism, is increasing with the passage of time. In some cases it is possible to integrate this task directly into the algorithm of optimum synthesis. When choosing the schematic layout of the mechanism, the risk of unilateral estimation of the operational opportunities of various cyclic mechanisms, should be kept in mind. In this sense, as it was noted in Chap. 1, the example of "competition" between the lever and cam mechanisms is very indicative. As it is known, for a long time lever mechanisms were used only to achieve continuous movement of the driven member. However, over the decades, there is a tendency of replacement of cam mechanisms with lever ones, even in the cases where, in accordance with the predetermined cyclic machine diagram, significantly long dwells of the driven member are needed.

Cam mechanisms have great potential for the optimization of the laws of motion, but at high operating speeds the decisive role is often played by dynamic effects, caused by errors of manufacturing and assembly of the mechanism. Joints and slides, used in the kinematic pairs of lever mechanisms are quite simple to make and can be made more accurately as compared with complex profiles of the cams. In the lever mechanism there usually is no need for the forced closing, which positively affects the dynamics of the drive. These factors speak in favor of the lever mechanisms. Disadvantages of lever mechanisms are often manifested, when

operating under complex laws of motion, which require using multiple-link kinematic chains. This inevitably leads to the decrease in frequency characteristics of the mechanism, significant increase in dynamic loads, as well as to additional difficulties in constructing miniature components. It should also be noted that using lever mechanisms, with large number of kinematic pairs, leads to the increase in the dynamic errors and vibro-impact intensity, arising due to multiple inter-matings in the clearances (see Chap. 7). In addition the negative role of the dynamic errors, in the areas of dwell, related to the approximate nature of the metric synthesis of the laws of motion in the lever mechanism, is manifested. Often it is the dwells, where other mechanisms execute important technological operations, requiring heightened requirements for accuracy of kinematic characteristics. Meanwhile, such problems can be solved exceptionally easily by using cam mechanisms.

The contradictory character of foregoing considerations indicates that the mechanism structure by itself is not able to guarantee satisfactory dynamic conditions of the mechanism operations. So the question of applicability of a type of mechanism should not be decided in general, but only taking into account the specific terms, such as kinematic and dynamic factors, as well as the technological possibilities of their manufacture and assembly.

Classification of typical dynamic models of cyclic mechanisms Strictly speaking, all the mechanisms of the machine unit form a single coherent system, so starting the classification of dynamic models; we recall once again that each of them has a limited scope. However, in many cases, the consideration of the dynamics of machine unit assembly, as a process, as a single model is not possible, even with modern computing facilities. In fact, there is no special necessity for a global approach, because due to little connectivity of many vibration contours of machine unit, retaining sufficient level of accuracy of engineering calculations, they can be identified as separate models of mechanisms or groups of mechanisms.

For example, in determining non-uniformity of rotation of the driving links, we can use the dynamic model of the machine set (Fig. 2.6a), presented in the form of ensemble of the element D, representing the dynamic characteristic of the motor and the reduced moment of inertia of the machine (for details see Sects. 5.7 and 8.5). When considering this issue, we can either completely exclude, from consideration, the elastic and dissipative properties of the links or consider only the most malleable elements of the motor, such as belts, long transmission, etc. (Fig. 2.6b). The results of the analysis of this model make it possible to identify the coordinate $\varphi_0(t)$, defining at first approximation the motion of the driving link of the mechanism. Note that often
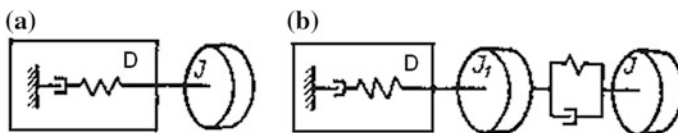
Fig. 2.6 Simple models, including the dynamic characteristics of motor; **a** model with regard to dynamic characteristics of motor and absolutely rigid drive, **b** model with regard to dynamic characteristics of motor and elastic-dissipative elements of the drive

with small coefficient of irregularity, we can take $\varphi_0 \approx \omega_0 t$, where ω_0 is the angular velocity. With this approach some typical dynamic models of cyclic mechanisms (shown in Table 2.1) can be selected, from the overall system of the machine unit.

In drawing up these models, in addition to the experience of dynamic calculations, it is also taken into consideration that, as a rule, maximum values of mass and moments of inertia are associated with the input and output links. To these two elements it is appropriate to reduce the inertial characteristics of the intermediate links, whose values, in case of rational design, are relatively small.

According to the structural features, as well as the degree of idealization of real dynamic processes, the considered models are divided into three classes and a number of modifications.

To class I, we refer dynamic models of mechanisms, formed by serial connection of elements. For facilitating of the necessary explanations we use the following symbolic notation, describing the structure of the dynamic model or its component: $H_1 - \Pi - H_2$, where H_1 and H_2—number of degrees of freedom of oscillatory contours, respectively the driving and driven parts of the mechanism.
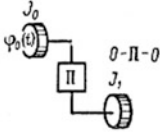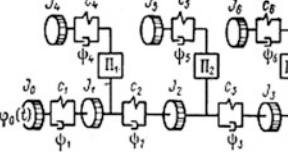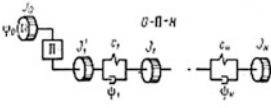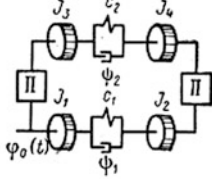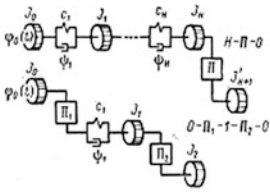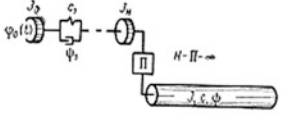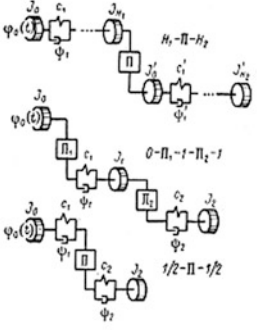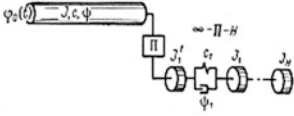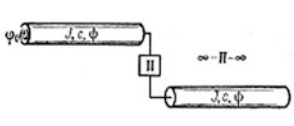
Among the models of *class I,* we can highlight four versions or modifications. To modification I we refer the simplest model with structure formula $0 - \Pi - 0$. In this model, all parts are accepted as rigid, so description of dynamic phenomena are not beyond kinetostatic ideas peculiar to the classical theory of mechanisms and machines. The kinetostatic model provides background information about the level of dynamic loading of the mechanism and is often successfully used for the synthesis of the mechanism at the preliminary stage.

However, for high-speed cyclic mechanisms, the results of the analysis of this model can only serve as "ideal" characteristics, giving an idea not so much about the actual dynamic loading, as about the level of disturbance causing these loads.

To the *modification 2* we refer the dynamic models $0 - \Pi - H$, for which the leading part is assumed as absolutely rigid, and the slave is presented as a vibrating system with H degrees of freedom. In case of *linearization of the dissipative forces*, this model is usually described with a system of linear differential equations with constant coefficients. The transition from modification 1 to modification 2, while making dynamic calculations, provides very rich material for the rational design of high-speed mechanisms, in which dynamic loads are dominant. The use of this material is particularly effective in the dynamic analysis and synthesis of the laws of motion of the members, driven with the cams. In many theoretical and experimental studies, it has been shown that the ideal kinematic functions, primarily acceleration, can be strongly distorted by vibrations, the intensity of which depends on the properties of the laws of motion (see Chap. 4). At the same time, the ideas about optimum laws of motion, changed significantly. Due to the rational synthesis of cam mechanisms, taking into account the elastic and damping properties of the driven mechanism, the performance of many machines of light, printing, textile and other industries has been significantly improved.

However, at the same time, a number of significant dynamic phenomena, being observed during the functioning of machines and limiting their performance, does not fit into the framework of modification model 2. Such phenomenon first of all

Table 2.1 Classification of the typical dynamic models of cyclic mechanisms

include various parametric phenomena, associated with the variability of the driving members, taking into account the elastic properties of the motor and variability of the reduced moments of inertia.

The simplest type of the model, capable of identifying these characteristics, is related to modification 3. In this and subsequent cases, the system of differential equations, strictly speaking, proves to be nonlinear and in some acceptable simplifications, can be reduced to a system of linear differential equations with variable coefficients. In addition to $H - \Pi - 0$, the models with several successive cyclic-type mechanisms $0 - \Pi_1 - 1 - \Pi_2 - 1$ type can also be assigned to this modification.

The most general type of models of class one, is related to modification 4. Several versions of such models are given in Table 2.1. In the first case we talk about mechanisms, whose calculative schematic includes oscillation contours of driving and driven links, connected to the mechanism through nonlinear position functions. In addition, this modification also includes the models of transfer mechanisms, consisting of several simple kinematic groups, linked with sufficiently malleable links $0 - \Pi_1 - 1 - \Pi_2 - 1$.

The model with one degree of freedom, taking into account the elastic and dissipative properties of the drive and inertial, elastic and dissipative properties of the driven member, is obtained from this scheme, in the absence of the first mechanism (Π_1), and relatively small moment of inertia of the intermediate subsystem. This extreme case is contingently marked as $1/2 - \Pi - 1/2$.

Dynamic models of modifications 4, allow us to take into account, more complex oscillatory phenomena, arising out of the mutual influence of contours, coupled with nonlinear position function.

Class II includes dynamic models of cyclic mechanisms, formed by serial-parallel connections of the members (modification 1) and models with closed loops (modification 2).

Camshaft with cyclic mechanisms can serve as an example of the first modification model.

Closed circuits of the cyclic mechanisms are widely used to drive massive operating tools, such as machines for textile and light industry (see Chaps. 8–12).

Class III includes dynamic models, in which the leading or driven parts of the mechanism, or both of them, are presented with subsystems with distributed parameters.

While making classification dynamic models of cyclic mechanisms, we deliberately excluded from consideration, the standard calculation schemes of beams and frames, used in the calculation of bending vibrations of links, keeping in mind that the bending vibrations, as a rule, are more local in nature. These models will be discussed in Chaps. 11 and 12.

Along with the structural classification of dynamic models of the cyclic mechanisms, at a certain level of dynamic analysis, a greater role is assigned to the classification, related to the nature of the corresponding differential equations and methods of their exact or approximate solutions. Here, first of all, we should note the linear and nonlinear models, models with stationary and non-stationary connections (see Chaps. 4–7).

It is to be noted that this model classification does not only present methodo-logical interest, but also contains valuable information about the principal capability of certain vibration processes (e.g., self-oscillation in nonlinear models, the para-metric resonances in systems with periodically varying parameters, etc.).

To select an effective method of analysis of systems, with non-stationary con-nections, very significant specifics of the model, is associated with the character of parameter changes. In this sense, it is possible to differentiate between models with slow and quick change of parameters (see Chap. 5).

Of course, when considering all aspects of the dynamic problem, any classifi-cation feature is in a sense conventional and, in any case, is limited. At the same time, taking into account the complexity of the problems and the need to obtain foreseeable engineering solutions, the use of the given classification facilitates the differentiated approach, to the choice of the method of dynamic analysis.

2.6 Elements of the Dynamic Model and Their Reduction

2.6.1 Inertial Characteristics

While determining the reduced mass and moments of inertia the kinetic energy of the system should be constant. If the reduction is not connected to the change of degrees of freedom, then the conditions for the balance of kinetic energy can be fulfilled accurately. Thus, for reduction of the inertia moment J_3 to the input link (see Fig. 2.1b, c) it is sufficient to maintain the balance of kinetic energy of the elements J_2 and J_3 before and after reduction

$$0.5J_2\dot{\varphi}_2^2 + 0.5J_3\dot{\varphi}_3^2 = 0.5J\dot{\varphi}_2^2,$$

where $\dot{\varphi}_2, \dot{\varphi}_3$ are angular velocities of the elements J_2 and J_3.

In general, instead of the square of gear ratio the reduction factor is the square of the first geometric transfer function $\Pi' = d\Pi/d\varphi$, where φ is input coordinate. Further we will look into the example, when reduction can be done only approx-imately. For the purpose let us consider torsional vibrations of the shaft (Fig. 2.7a).
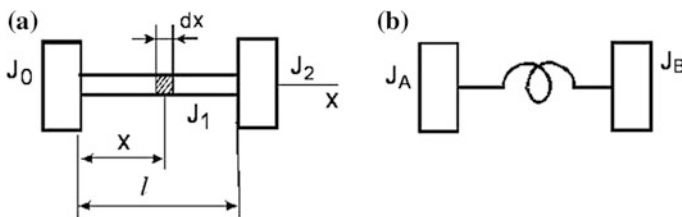
Fig. 2.7 By reducing the inertial characteristics; **a** initial model with distributed parameters, **b** model with lumped parameters

First, we assume that the disk J_0 is motionless. Reduce the distributed along the length of the shaft inertia moment J_1, to the cross section of the right disk; thus the transition to a simplified dynamic model, in which the disk with still unknown given inertia moment J_B is connected to restraint with weightless elastic element (Fig. 2.7b).

Select an elementary interval dx of the shaft with kinetic energy equal to

$$dT_1 = \frac{J_1}{2l} \dot{\varphi}^2(x,t)dx, \tag{2.1}$$

where $\dot{\varphi}(x,t)$ is the angular velocity in the section x.

Integrating (2.1) we get

$$T_1 = \frac{J_1}{2\ell} \int_0^l \dot{\varphi}^2(x,t)dx.$$

Therefore, the total kinetic energy is equal to

$$T = 0.5 \left[\frac{J_1}{l} \int_0^l \dot{\varphi}^2(x,t)dx + J_2\dot{\varphi}^2(l,t)\right]. \tag{2.2}$$

On the other hand, referring to the model shown in Fig. 2.7b, we get

$$T = 0.5J_{\hat{A}}\dot{\varphi}^2(l,t). \tag{2.3}$$

Hence, by equating (2.2) and (2.3)

$$J_{\hat{A}} = \frac{J_1}{l} \int_0^l \left[\frac{\dot{\varphi}(x,t)}{\dot{\varphi}(l,t)}\right]^2 dx + J_2. \tag{2.4}$$

Until now, calculations were rigorous. However, to obtain the final result we have to use some approximate assumptions. We assume for the relationship $f = \dot{\varphi}(x,t)/\dot{\varphi}(l,t)$, some believable law of distribution over x, which would not contradict with the true boundary conditions at $x = 0$ and $x = l$, for example $f = x/l$. Then on the basis of (2.4) $J_B = J_1/3 + J_2$. (Note that in the discussed, relatively simple example, it is possible to get an exact solution of the problem, considering the shaft as a system with distributed parameters.)

In this example the kinetic energy is related only to the oscillatory process. If the disc J_0 in program movement makes angular displacements as per a given law $\varphi(0,t) = \varphi_*(t)$, then

$$T = 0.5\left[J_0\dot{\varphi}_*^2 + \frac{J_1}{l}\int_0^l \dot{\varphi}^2(x,t)dx + J_2\dot{\varphi}^2(l,t)\right]. \tag{2.5}$$

On the other hand, for model with lumped parameters we get

$$T = 0.5\left[J_A\dot{\varphi}_*^2(t) + J_{\hat{A}}\dot{\varphi}^2(l,t)\right]. \tag{2.6}$$

Here $J_A, J_{\hat{A}}$ are reduced inertia moments on the left and right ends of the shaft.

The absolute angular velocity in an arbitrary section of the shaft $\dot{\varphi}(x,t)$ consists of two components: "programed" $\dot{\varphi}_*(t)$ and vibrating $\Delta\dot{\varphi}(x,t)$.

We require that the kinetic energy of the original system and the model should be equal in both extreme cases: at $\Delta\dot{\varphi} = 0$ (rigid system) and at $\dot{\varphi}_* = 0$ (the disk J_0 is motionless). Then, by equating (2.5) and (2.6) for these cases, and retaining the velocity distribution law, accepted in the previous example, we get $J_B = J_1/3 + J_2$.

$$J_A + J_{\hat{A}} = J_0 + J_1 + J_2; \quad J_B = J_1/3 + J_2.$$

Then $J_A = J_0 + 2J_1/3$.

It is rational to perform reduction to cross-sections, which host the bodies with relatively large inertia moments. For longitudinal vibrations all the above holds true for the procedure of reduction of masses.

2.6.2 Characteristics of Elastic Elements

An important characteristic of any element, in case of longitudinal elastic deformation x, is the stiffness $c = |dF/dx|$, where F is the restoring force, and in case of torsion deformations $c = |dM/d\varphi|$, where M is the resorting moment, φ is the angular deformation. In the first case stiffness factor has dimensionality of N/m, and in the second N m Inverse value $e = c^{-1}$ is called the coefficient of compliance.

The typical graphs of the restoring force $F(x)$ are represented in the Fig. 2.8a, to which graphs $c(x)$ shown in Fig. 2.8b, correspond. Obviously, for a linear characteristic, $c = F/x = $ const. The function $c(x)$ is determined by the material and the design of the elastic element.

For example, in the working range of stresses, metals typically obey the conditions of the Hooke's law (curve 1), whereas for rubber "hard" characteristic is inherent (curve 2), and for many polymers, it is the "soft" characteristic (curve 3). However in structures consisting only of metal components the occurrence of nonlinear restoring forces is also possible. In particular, it is observed in case of a
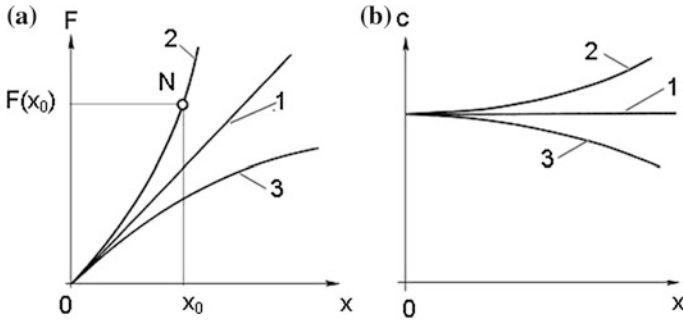
Fig. 2.8 To determination of the coefficients of stiffness; **a** graphs $F(x)$, **b** graphs $c(x)$

point or line contact of the two surfaces, which is typical for the elements of higher kinematic pairs.

In such cases, the contact stiffness increases with increase in stress. In addition to the mentioned causes, violation of linearity of the elastic characteristics of the restoring force can also occur due to the use of specially selected nonlinear elastic elements (conical springs, nonlinear couplings), connection or disconnection of some elements of the kinematic chain, the presence of clearances in the kinematic pairs, the installation of the stoppers, clamps and other factors.

Often, however, the nonlinear factors, in the overall stiffness balance, are unimportant. Furthermore, in case of study of small oscillations, occurring in the vicinity of a steady state of system x_0, nonlinear elastic characteristics can be linearized. Indeed, let $x = x_0 + \Delta x$ where Δx equals small oscillations about the position x_0 (see Fig. 2.8a). Then, expanding the function $F(x_0 + \Delta x)$ into Taylor series, we have

$$F(x_0 + \Delta x) = F(x_0) + \frac{dF}{dx}(x_0)\Delta x + 0.5\frac{d^2F}{dx^2}(x_0)\Delta x^2 + \cdots$$

Having restricted to first two terms of the series, we get $c = \frac{dF}{dx}(x_0)$. This means that the non-linear characteristic in the neighborhood of point N we replace approximately by tangent at this point. Of course, to make such a change justified, it is necessary that function $F(x)$ in the neighborhood of point N should be continuous and differentiable. While this condition is not met, the elastic characteristics are called *essentially nonlinear*.

It is worth noting here that the need to take into account the nonlinearities is usually associated with the consideration of such dynamic processes, which cause significant deformation of elastic elements, or in the cases where the subject of the study are specific effects, specific only to nonlinear systems (see Chaps. 6 and 7).

Reduction of the elastic characteristics is generally aimed at simplifying the model, which enables us to use the known solution of the problem. Let's, for example, reduce the parallel connected elastic elements (Fig. 2.9a) to one elastic element c_* (Fig. 2.9b). The unique property of parallel connection is the equality of
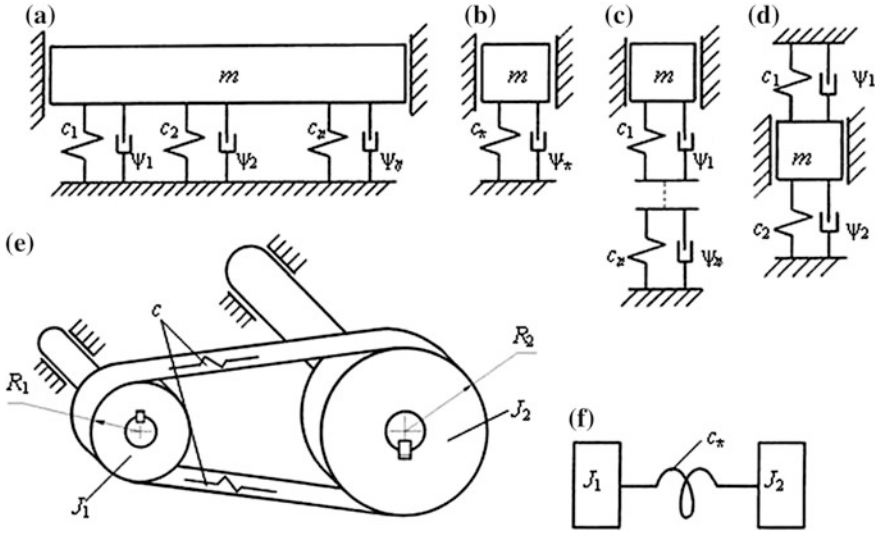
Fig. 2.9 To determination of the reduced stiffness coefficients; **a** model with parallel connection of elastic-dissipative elements (type 1), **b** model with reduced elastic-dissipative elements, **c** model with serial connection of elastic-dissipative elements, **d** model with parallel connection of elastic-dissipative elements (type 2), **e** the belt drive, **f** model of belt drive

absolute values of deformation: $|x_1| = |x_2| = \cdots = |x_n| = |x|$. In case of reduction, the system's potential energy should remain constant. For element i at deformation x_i restoring force equals $F_i = -c_i x_i$ then potential energy is

$$V_i = -\int_0^{x_i} F_i dx_i = \int_0^{x_i} c_i x_i dx_i = 0.5 c_i x_i^2.$$

Therefore $0.5 \sum_{i=1}^{n} c_i x_i^2 = 0.5 c_* x^2$, so

$$c_* = \sum_{i=1}^{n} c_i. \tag{2.7}$$

In case of serial connection (Fig. 2.9c), we have the equality the of absolute values of forces $|F_i| = |F|$. Similarly, we obtain

$$e_* = \sum_{i=1}^{n} e_i, \tag{2.8}$$

where $e_* = c_*^{-1}$; $e_i = c_i^{-1}$.

Note that the visible signs of the type of connection are sometimes misleading. For example, the connection shown in Fig. 2.9d may be taken by mistake as a serial connection; meanwhile with any moving mass m, the absolute elastic deformation

of both elements is identical, and therefore, the connection is parallel, thus $c_* = c_1 + c_2$.

In parallel connection the decisive role is played by the most rigid elements, and in serial connection it is the most compliant ones.

Sometimes the dimension of the stiffness may change while reducing. We perform, for example, the reduction of the elastic characteristics of the belt drive (Fig. 2.9e), which in case of transition to the design scheme is equivalent to elastic shaft rotating at an angular velocity same as of the driven pulley (Fig. 2.9f).

If the stiffness factor of one branch of the belt drive is c, then, considering both branches stretched, we can determine the potential energy as $v = cx^2$, where x is the deformation of one branch of the belt.

Next, we introduce an additional angle of rotation of the second shaft $\Delta\varphi$, corresponding to deformation x. Obviously, $\Delta\varphi = x/R_2$ where R_2 is the radius of the driven pulley, and as $V = cx^2 = 0.5c_*\Delta\varphi^2$ we finally have $c_* = 2cR_2^2$. Since there is a transition from linear deformation to angular, changed accordingly is the dimension of the stiffness factor from N/m to N m.

2.6.3 Parameters of Dissipation

Graphs of restoring forces in Fig. 2.8a are idealized, since in their formation, the deformable elements were accepted as perfectly elastic, i.e. deprived of dissipative properties. If we take into account the forces of inelastic resistance, which are opposite to the direction of the strain rate, the corresponding graph will have two branches, where the upper (curve 1) will correspond to load, and the bottom (curve 2)—to unloading (Fig. 2.10).

The area of the figure, demarked by branch 1 and the X-axis, corresponds to the work done during deformation and the area of the figure demarked on the top by branch 2, shows the work done by the elastic element during unloading. At the same time the selected area, whose outline is called the *hysteresis loop,* is

Fig. 2.10 The hysteresis loop of the mechanical system
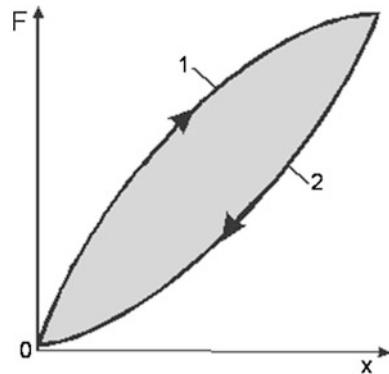
proportional to the work done per cycle to overcome the inelastic resistance. The ratio of the dissipated energy to the work, done during deformation, is called the coefficient of dissipation and is denoted by Ψ. The value and character of dependence of this parameter, on various factors, is first of all determined by the nature of the dissipative forces, which can be called into action due to different causes.

In mechanisms the forces of resistance are often the forces of friction, occurring in kinematic pairs and immobile joints of components. In the latter case we are talking about the so-called *structural damping,* arising in case of oscillations, on the area of joints, such as the junction, thread etc.

Sometimes the nature of the resistance forces is associated with type of damping device, specifically designed to increase the dissipative properties of the system. Such devices may be frictional, hydraulic or pneumatic.

In addition to these types of resistance forces, we should also note the internal friction forces in the material, which arise due to the deformation of elastic elements. In dynamics of mechanisms, these forces play a relatively minor role for metal parts, but for the parts made of plastics, rubber and other non-metallic materials, the forces of internal friction can be comparable with the other forces of resistance.

A large number of dissipative factors, the complexity and diversity of the processes, accompanying the oscillatory phenomena, lead to the fact that for solution of engineering problems we have to use the parameters obtained by experiment. In some cases, the experiment determines the coefficient of dissipation of individual structural elements or joints, and in the other cases, some reduced values, inherent to the whole mechanism, assembly, etc. Dissipation parameters are usually determined for mono-harmonic (i.e. single-frequency) oscillations in the mode of damped free vibrations or resonance mode, in case of forced oscillations. In the first case we have a decaying process (see Fig. 2.2d), for which the dissipation coefficient can be defined as

$$\Psi = 1 - (A_2/A_1)^2, \tag{2.9}$$

where A_1 and A_2 are two successive amplitude values, separated by a single period.

$\vartheta = \ln(A_1/A_2)$ is called the *logarithmic decrement*, wherein $\Psi = 1 - \exp(-2\vartheta)$. For smaller values of ϑ we have $\Psi = 2\vartheta$.

In the most general case, parameters Ψ and ϑ are not constant, but may depend on the oscillation amplitude and frequency. However, the analysis of many experimental materials shows that in the dynamics of mechanisms the dependence of dissipation parameters on the frequency practically does not appear or manifests very weakly. Strictly speaking, the parameters Ψ and ϑ do not depend on the amplitude only if the energy dissipated is proportional to the square of the amplitude, which occurs, for example, in case of linear resistance force or resistance force, proportional to the amplitude in the first degree. In more complex cases the coefficients Ψ or ϑ may be averaged within one or more oscillation periods. At the same time the function $\Psi(A)$ or $\vartheta(A)$ can be obtained from the experiment.

In the dynamic calculation, the dissipation coefficients allow us to establish certain energy equivalent, which takes into account the forces of resistance in the system of differential equations. Here we only point out that the most effective approach to accounting the dissipative forces, in engineering problems, is associated with the so-called equivalent linearization, in which the non-linear resistance force is replaced by the conditional linear force, maintaining the same amount of scattered energy per cycle. With this approach, the linearized resistance force can be expressed as $R = -b\dot{x}$ where b is the coefficient of proportionality (for details see Chap. 6).

Let us define the reduced value of the dissipation coefficient Ψ_* in parallel connection of the elastic elements having dissipative properties (see Fig. 2.9a). To move to the schematic, shown in Fig. 2.9b, it is enough to record the condition of dissipated energy balance

$$\Psi_* \sum_{i=1}^{n} V_i = \sum_{i=1}^{n} \Psi_i V_i, \tag{2.10}$$

where Ψ_i, V_i is the coefficient of dissipation and maximum potential energy of considered element i.

On the basis of (2.10) for parallel connection with $|x_1| = \cdots = |x_n| = |x|$ and taking into account $V_i = 0.5\, c_i x_i^2; \; V = c_* x^2$, we get

$$\Psi_* = \sum_{i=1}^{n} \Psi_i c_i / c_*.$$

Similarly, the relationship for Ψ_* can be obtained for a series connection of elastic elements with dissipative properties:

$$\Psi_* = \sum_{i=1}^{n} \Psi_i c_* / c_i.$$

In case of parallel connection the value Ψ_* is usually close to the values Ψ_i corresponding to the most rigid members, and in series to the most compliant.

Analysis of data, obtained for many mechanisms for textile, printing machines, and machine for other light industries, show that the reduced dissipation coefficient is usually in the range of values $0.3 < \Psi_* < 0.7$. These results as a guideline can be used in those cases, where there is no possibility to get specific information through preliminary calculations. More complex cases of dissipation accounting are in Chap. 6.

It should be noted that the mapping of dissipative properties of mechanical systems involves a number of issues, still unresolved, which has attracted the attention of many researchers.
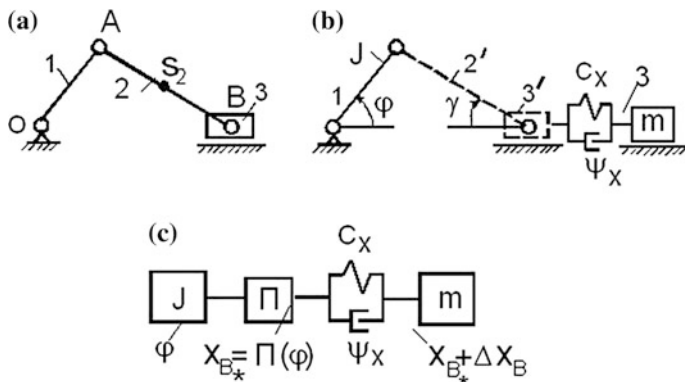
Fig. 2.11 To definition of reduced rigidity of the coupler; **a** slider-crank mechanism, **b** model with reduced characteristics, **c** generalized model of the mechanism

Example Let's make a simple model of slider-crank mechanism (Fig. 2.11a), in which the axial compliance of the connecting rod is taken into account. We make an approximate replacement of the rod mass m_2 with two masses m_{A2} and m_{B2} at the points A and B with subsequent inclusion of these masses in the inertial characteristics of the crank 1 and slider 3.

For the purpose, we can use, the well-known, from course on the theory of mechanisms and machines, the so-called static displacement of the masses, in which the total mass of the unit and the position of its center of mass remains unchanged, but the moment of inertia is slightly distorted ($m_{A2} = m_2 BS_2/AB$; $m_{B2} = m_2 AS_2/AB$; S_2 is the center of link 2 mass).

Now we present the model of the mechanism in the form of a crank with weightless coupler $2'$ and the slider $3'$ (kinematic analog of the "ideal" mechanism) with an attached block c_x, Ψ_x, m (Fig. 2.11b), taking into account reduced values of elastic, dissipative and inertial parameters of the system.

A more concise image of this dynamic model is presented in Fig. 2.11c. Here element Π corresponds to the transformation of the angle of the rotation of the input link φ into the motion of the link $3'$, i.e. $x_{B*} = \Pi(\varphi)$.

To determine reduced values c_x and Ψ_x we present the current coordinate of the slider as function of two variables $x_B = x_B(\varphi, L)$, where φ is the angle of the input link rotation; L is the length of the connecting rod, which consists of constant component L_* corresponding to the non-deformable connecting rod and deformation ΔL. Next, we expand x_B in Taylor series at interval ΔL, restricting ourselves to the consideration of the first two terms:

$$x_B = x_{B*} + \left(\frac{\partial x_B}{\partial L}\right)_* \Delta L.$$

Here asterisk corresponds to $\Delta L = 0$.

Obviously, the function x_B corresponds to the ideal position function, i.e. analogue of the "ideal" mechanism, formed with units 1, 2′, 3′, (see Fig. 2.11b), and the elastic element forms dynamic error $\Delta x_B = (\partial x_B/\partial L)_* \Delta L$ caused by deformation of the connecting rod ΔL.

We use the condition of potential energy balance again $0.5c\Delta L^2 = 0.5c_x\Delta x_B^2$. Hence

$$c_x = c(\Delta L/\Delta x_B)^2 \approx c(\partial L/\partial x_B)_*^2. \tag{2.11}$$

On the basis of cosine theorem we have $L^2 = r^2 + x_B^2 - 2rx_B\cos\varphi$. Differentiating this relation along x_B we get

$$2L \cdot (\partial L/\partial x_B)_* = 2x_B - 2r\cos\varphi;$$
$$(\partial L/\partial x_B)_* = \left[\frac{x_B - r\cos\varphi}{L}\right]_* = \cos\gamma_*; \; c_x = c\cos^2\gamma_*,$$

where γ_*, has sense of contact angle.

Since $\gamma_* = \gamma_*(\varphi)$ then stiffness c_x, strictly speaking, is variable, but for small values of γ_* we have $c_x = c$. The condition of balance of dissipated energy before and after reduction has the form $0.5\Psi c\Delta L^2 = 0.5\Psi_x c_x\Delta x_B^2$. Taking into account (2.11) we have $\Psi_x = \Psi$.

It is to be noted here that similarly we may select some "reference" links in any mechanism, which are connected via the kinematic pairs with frame and move translationally or perform angular movements about a fixed axis. Such units typically have the greatest masses and moments of inertia. Having this characteristic, the intermediate links, without appreciable loss in accuracy can be reduced to the reference links, as it is done in our example. With such a principle of modeling, we can achieve that the position of each inertial element is characterized by a single coordinate.

Chapter 3
Mathematical Model

3.1 Some Information About Analytical Mechanics, Applicable to the Analysis of Vibrations in Cyclic Mechanisms

Composition of the systems of differential equations (the so-called mathematical models) is one of the most important steps of any dynamic analysis. It should be borne in mind that if the equations are written incorrectly, then all the power of modern computers can't help. One of the methods of composing the systems of differential equations is based on using the general theorems of the dynamics that are based directly on Newton's laws. When we use these theorems with respect to non-free mechanical systems, which include mechanisms and machines, we have to dismember the systems, introducing the reactions of links as additional unknowns. In this case, the number of equations increases, accordingly.

Analytical mechanics, based on the fundamental works by G. Leibniz, L. Euler, J. Lagrange, provides general methods, using which we can compose differential equations of motion, without entering reactions of ideal connections. Methods of analytical mechanics have proven to be very fruitful in solving applied problems of machine dynamics. Along with these methods, for some systems, we use the so-called inverse method based on the D'Alembert's principle.

3.1.1 Constraints, Implemented in Mechanisms

Types of constraints Any mechanism can be considered as a mechanical system, subordinate to the so-called constraints i.e. limiting conditions of geometric or kinematic character. If the constraint equation can be written in general form as a function, which does not contain derivatives of the coordinates, then such constraint is called holonomic. In particular, an example of the holonomic constraint equations

can be the position function $\varphi_n = \Pi_n(\varphi_0)$, connecting coordinates of the input and output links, with finite dependence. Some kinematic dependencies can be reduced to holonomic connections. Suppose, for example, the gear ratio of the gears connecting two shaft is set $u_{21} = \omega_2 / \omega_1$. Then this connection equation can be integrated into a general form

$$\varphi_2 - \varphi_{2*} = \int\limits_{\varphi_{1*}}^{\varphi_1} u_{21}\, d\varphi_1 = u_{21}(\varphi_1 - \varphi_{1*}). \tag{3.1}$$

Here the asterisks denote the initial values of the coordinates φ_1 and φ_2.

However u_{21} in some mechanisms (for example, variable-speed drive) may be an explicit function of time. Since Eq. (3.1) cannot now be integrated in general form, it must be written as $u_{21}(t) = \dot\varphi_2/\dot\varphi_1$. In such cases, when the derivatives of the coordinates cannot be excluded from constraint equation, the corresponding connection is called *non-holonomic*.

The constraint is called *non-stationary* if the constraint equation explicitly includes time, otherwise it is called *stationary*. The position function, according to this definition, can be attributed to stationary connections. However if we can significantly consider that φ_1 has a component, which depends on time, in a given way, then such a connection proves to be nonstationary, for example $\varphi_2 = \Pi_2(\omega t + \Delta\varphi)$ where ωt characterizes the current ideal angle of the input link, and $\Delta\varphi$ describes oscillations of the input link.

In this and in many other cases, non-stationary connection in the problems of dynamics of mechanisms occurs as a result of idealization, caused by the desire to reduce the number of degrees of freedom of the oscillatory system. According to some methodological considerations in such cases, during the stage of composition of the system of differential equations, it is more convenient not to use this idealization and operate with fixed-link equations. It can be easily done at this stage if we do not reveal the functional relationship of the corresponding coordinate with time.

Constraints are called *ideal* if the sum of works of these constraints, for any possible displacements, is zero. In the real mechanisms, there always is a tangential component of the constraint reaction, which is equal to the force of friction; therefore any constraint is practically non-ideal. However, in practice it is possible to use the idea of the perfect constraints, if we introduce friction into the corresponding equations as the active forces. At the same time we should take into account, the additional relations, which are determined by the laws of friction, identified experimentally. With this approach, the use of the ideal constraints concept becomes quite multi-purpose. However, there is a wide class of so-called self-locking mechanisms, for which the possibility of movement, under the given external forces, is essentially dependent on the direction of transfer of the forces.

As per the nature of constraints, all systems are divided into *holonomic* and *non-holonomic*, as well as *scleronomous* systems (with fixed constraints) and *rheonomous* (with time-varying constraints).

Generalized and redundant coordinates As it was already mentioned, one of the most important features of any model is the *number degrees of freedom*, which, for holonomic systems, is determined by the number of independent coordinates, fully describing the position of each point of the system. These coordinates are called *generalized* and are designated by $q_1, \ldots, q_H$, where H is the number of degrees of freedom. Thus, the number of generalized coordinates is also the minimum number of coordinates, which embrace all the possible positions of the holonomic system.

The first and second derivatives of the generalized coordinates are respectively called the *generalized velocity* and *generalized acceleration.*

In addition to the generalized coordinates, it is advisable, for the analysis of dynamics of mechanisms, to use some auxiliary coordinates, associated with the generalized coordinates of the coupling equations. The coordinates of this kind are called *redundant* or superfluous. It is obvious that the number of superfluous coordinates must correspond to the number of additional constraint equations.

3.1.2 Presentation of Kinetic and Potential Energy in the Quadratic Forms

Based on the above remarks about accounting for non-stationary links, kinetic energy can be represented by the following positive-sign quadratic form of generalized velocities with inertial coefficients A_{ik} which are, in general, the functions of the generalized coordinates [34]:

$$T = 0.5 \sum_{i=1}^{H} \sum_{k=1}^{H} A_{ik} \dot{q}_i \dot{q}_k, \tag{3.2}$$

where $A_{ik} = A_{ki} = \sum_{s=1}^{N} m_s (\partial \vec{r}_s / \partial q_i)(\partial \vec{r}_s / \partial q_k)$; m_s is mass, $\vec{r}_s$ is radius vector (for practical definition, see below).

Often you may see that $A_{ik} = a_{ik} = \text{const}$. We would come to approximately the same result if we assume that all the generalized coordinates are small. In this case a_{ik} corresponds to the first term of series of expansions of function A_{ik} in Maclaurin series as per the powers of the generalized coordinates.

In expanded view, the quadratic form is somewhat reminds of the square of a polynomial. For example, for $H = 3$, $A_{ik} \approx a_{ik}$.

$$T = 0.5(a_{11}\dot{q}_1^2 + a_{22}\dot{q}_2^2 + a_{33}\dot{q}_3^2 + 2a_{12}\dot{q}_1\dot{q}_2 + 2a_{13}\dot{q}_1\dot{q}_3 + 2a_{23}\dot{q}_2\dot{q}_3). \tag{3.3}$$

Unlike gear units, with fixed transmission, for cyclic mechanisms we have $\partial T / \partial q_j \neq 0$ (see below).

In the mechanisms, the potential energy, involved in the formation of oscillatory processes, mainly forms due to the elastic deformations of the system's elements. In case of small oscillations in the vicinity of the stable equilibrium position, the potential energy can be presented as a positive-sign quadratic form of generalized coordinates:

$$V = 0.5 \sum_{i=1}^{H} \sum_{k=1}^{H} c_{ik} q_i q_k \qquad (c_{ik} = c_{ki}), \qquad (3.4)$$

where $c_{ik} = (\partial^2 V / \partial q_i \partial q_k)_0$ are quasi elastic coefficients (for practical definition, see below); $(\ )_0$ means that $q_1, \ldots, q_H = 0$. The structure of (3.4) in expanded form coincides with (3.3) if we replace a_{ik} with c_{ik} and $\dot{q}_i, \dot{q}_k$ with q_i, q_k.

3.1.3 Lagrange Equations of the Second Kind

Lagrange equations of the second kind have the form

$$\frac{d}{dt}\left(\frac{\partial T}{\partial \dot{q}_j}\right) - \frac{\partial T}{\partial q_j} = Q_j \qquad (j = \overline{1,H}).$$

The generalized force Q_j is defined as the dimensional coefficient in terms of the sum of elementary works on the virtual displacement δq_j:

$$\delta W = \sum_{j=1}^{H} Q_j \delta q_j.$$

Thus depending on whether q_j corresponds to the linear or angular coordinate Q_j has force or torque dimension.

The generalized force Q_j is composed of the potential Q_j^V and non-potential (nonconser vative) Q_j^* components. In this case, $Q_j^V = -\partial V / \partial q_j$ where V is the potential energy. Non-potential generalized forces in particular may be time dependent, generalized velocities and coordinates.

Then

$$\frac{d}{dt}\left(\frac{\partial T}{\partial \dot{q}_j}\right) - \frac{\partial T}{\partial q_j} + \frac{\partial V}{\partial q_j} = Q_j^*. \qquad (3.5)$$

Herein after asterisk in the generalized non-conservative force Q_j^* will be omitted.

In case of $A_{ik} = a_{ik} = $ const after substituting (3.2) and (3.4) in (3.5) we obtain the following system of differential equations:

$$\sum_{k=1}^{H} a_{jk}\ddot{q}_k + \sum_{k=1}^{H} c_{jk}q_k = Q_j \qquad (j = \overline{1,H}).. \tag{3.6}$$

In the inertial and quasi-elastic coefficients, in the system of Eq. (3.6), the first index j corresponds to the number of the equation, and the second k to the number of generalized acceleration or generalized coordinate. Unlike the gear mechanisms, with a constant gear ratio, in the presence of cyclic mechanisms within the oscillatory circuit $\partial T / \partial q_j \neq 0$, so the system of equations becomes more complicated (see below).

3.1.4 Special Form of the Second-Kind Lagrange Equations with Redundant Coordinates

When preparing the systems of differential equations, for the models with cyclic mechanisms, coefficients A_{ik} in the expression for kinetic energy cannot mostly be assumed as constant, since one or more of the generalized coordinates are not small quantities (see above).

Such a coordinate, for example, is the coordinate of the given program motion of the system's input link $\varphi_0(t)$. In the case of $A_{ik} \neq$ const, when substituting (3.2) in (3.5) we need to perform differentiation of complex expressions and produce cumbersome conversions, as in this case, the left side of each equation is complemented with summands.

$$\frac{1}{2}\sum_{k=1}^{H}\sum_{v=1}^{H}\left(\frac{\partial a_{jk}}{\partial q_v} + \frac{\partial a_{jv}}{\partial q_k} - \frac{\partial a_{kv}}{\partial q_j}\right)\dot{q}_k\dot{q}_v \qquad (j = \overline{1,H}) \tag{3.7}$$

The expression in parentheses in (3.7) is equal to twice the functional, called the first kind Christoffel symbol of the coefficient matrix of the quadratic form T (abbreviation $[k, v\,; j]$). This addition extremely complicates calculations and in fact often nullifies the above mentioned advantages, associated with the use of quadratic forms of the kinetic and potential energies. However, through the specific choice of the generalized coordinates, it is possible to make sure that in expression of the kinetic energy, summands with variable coefficients would have the form $T = 0.5a_{kk}\dot{q}_k^2$. Then $[k, v\,; j] = (\partial a_{jj} / \partial q_j)\,\dot{q}_j^2$.

Substantial simplification can be achieved by introducing redundant coordinates, eliminating the need for preliminary expression of all coordinates of the system in terms of independent generalized coordinates. Suppose that except for H generalized coordinates $q_1, \ldots, q_H$ we use n redundant coordinates $q_{H+1}, \ldots, q_{H+n}$.

Lagrange equations with redundant coordinates for holonomic and ideal constraints are [40]

$$\frac{d}{dt}\left(\frac{\partial T}{\partial \dot{q}_j}\right) - \frac{\partial T}{\partial q_j} + \frac{\partial V}{\partial q_j} = Q_j + \sum_{i=1}^{n} \frac{\partial \Phi_i}{\partial q_j} \Lambda_i \qquad (j = \overline{1, H+n}), \qquad (3.8)$$

where Λ_i are Lagrange multipliers; $\Phi_i(q_1, \ldots, q_{H+n})$ are constraint equations given in implicit form.

The physical meaning of the terms with the Lagrange multipliers is associated with the appearance of additional reactions for ideal constraints, which in contrast to (3.5) in this case are not completely excluded from the second-kind Lagrange equations, because the number of coordinates $H + n$ exceeds the number of degrees of freedom H.

We choose redundant coordinates in such a way that for all coordinates $\partial T / \partial q_j = 0$, wherein for all combinations i and k we have $A_{ik} = a_{ik} = \text{const.}$ Consequently, for linear elastic characteristics the expressions for kinetic and potential energies, with respect to all coordinates, including redundant, again convert to quadratic forms of (3.2) and (3.4). A corresponding system of differential equations can be written similar to (3.8)

$$\sum_{k=1}^{H+n} a_{jk} \ddot{q}_k + \sum_{k=1}^{H+n} c_{jk} q_k = Q_j + \sum_{i=1}^{n} \frac{\partial \Phi_i}{\partial q_j} \Lambda_i \qquad (j = \overline{1, H+n}). \qquad (3.9)$$

Lagrange multipliers can be expressed from any $H + n$ of the equations of system (3.9), but the simplest way of their definition is, when we adopt indexing coordinates from last n equations.

3.1.5   Generation of the Appell's Differential Equations for Holonomic Systems

Appell coined the conditional term of "energy of accelerations" U, which denotes the dependence, matching by the form to kinetic energy and differing only in that the velocities are replaced with accelerations. The Appell equations for systems, with holonomic constraints, have the form

$$\frac{\partial U}{\partial \ddot{q}_j} + \frac{\partial V}{\partial q_j} = Q_j^* \qquad (j = 1, \ldots, H). \qquad (3.10)$$

When determining energy of accelerations U it is sufficient to consider the terms that depend on the generalized accelerations $\ddot{q}_j$, since other members become null after differentiation.

3.1.6 Generation of Differential Equations by Using the Inverse Method

When composing the system of differential equations for bending oscillations of beams and shafts, with concentrated masses, preferential is the so-called inverse method, based on the principle of d'Alembert. We illustrate its application through the example of a beam with two masses (Fig. 3.1a). Confining ourselves to the consideration of the bending vibrations in the vertical plane only, we go first to the weightless elastic "skeleton" of the beam (Fig. 3.1b). To do this the connection should be applied with (in this case, the weightless elastic beam), except for external forces F_1 and F_2, also inertial forces $-m_1\ddot{y}_1$, $-m_2\ddot{y}_2$ according to the principle of d'Alembert, where $y_1(t), y_2(t)$ are the oscillations of corresponding masses. Thus we have reduced the problem to standard beam, exposed to the action of forces $P_1 = F_1 - m_1\ddot{y}_1$ and $P_2 = F_2 - m_2\ddot{y}_2$ i.e. to the problem considered in the course "strength of materials". Thus,

$$\left.\begin{array}{l} y_1 = e_{11}P_1 + e_{12}P_2; \\ y_2 = e_{21}P_1 + e_{22}P_2, \end{array}\right\} \tag{3.11}$$

where e_{jk} is the compliance coefficient, which is numerically equal to the deformation in section j under the action of a unit force applied in the section k $(e_{jk} = e_{kj})$.

The matrix of the compliance coefficients is equal to the inverse matrix of quasi-elastic coefficients, included in the quadratic form (3.4). Table 3.1 shows the formulae for calculation of the compliance coefficients (influence coefficients), depending on the type of shaft's support.
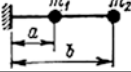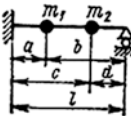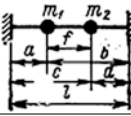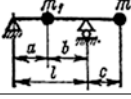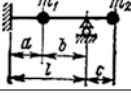
In this case, the following conventions are accepted: E is the modulus of elasticity of the shaft's material (for structural steel $E = 2.1 \times 10^{11}$ N/m^2); $I = d^4/64\pi$ is the axial moment of inertia of the shaft's cross-section, m^4; d is the diameter of the shaft, m.

Fig. 3.1 Model of an elastic beam with lumped masses
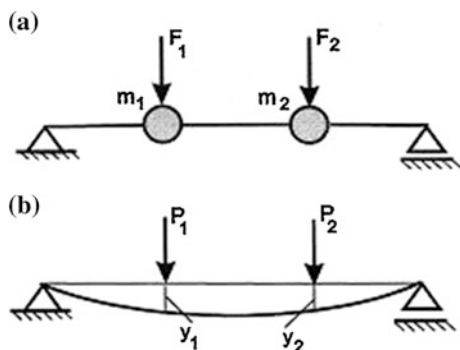
Table 3.1 The compliance coefficients for the typical beams

Scheme	e_{11}	e_{22}	e_{12}
	$\dfrac{a^3}{3EI}$	$\dfrac{b^3}{3EI}$	$\dfrac{a^2}{2EI}\left(b - \dfrac{a}{3}\right)$
	$\dfrac{a^2 b^2}{3EIl}$	$\dfrac{c^2 d^2}{3EIl}$	$\dfrac{ad}{6EIl}(l^2 - a^2 - d^2)$
	$\dfrac{a^3}{3EI}\left[1 - \dfrac{a(2l+b)^2}{4l^3}\right]$	$\dfrac{c^3}{3EI}\left[1 - \dfrac{c(2l+d)^2}{4l^3}\right]$	$\dfrac{a^2}{2EI}\left[c - \dfrac{a}{3} - \dfrac{3c^2}{2l^3}\left(l - \dfrac{a}{3}\right)\left(l - \dfrac{c}{3}\right)\right]$
	$\dfrac{a^3 b^3}{3EIl^3}$	$\dfrac{c^3 d^3}{3EIl^3}$	$\dfrac{ad}{6EIl^3}[bc(lf + 2ad) - l^2 f^2]$
	$\dfrac{a^2 b^2}{3EIl}$	$\dfrac{c^2}{3EI}(l + c)$	$-\dfrac{abc(l + a)}{6EIl}$
	$\dfrac{a^3}{3EI}\left[1 - \dfrac{a(2l+b)^2}{4l^3}\right]$	$\dfrac{c^3}{3EI}\left(1 + \dfrac{3l}{4c}\right)$	$-\dfrac{ca^2}{2EI}\left[\dfrac{3}{2}\left(1 - \dfrac{a}{3l}\right) - 1\right]$

After substituting P_1 and P_2 in (3.11) we have

$$\left.\begin{array}{l} e_{11}m_1\ddot{y}_1 + e_{12}m_2\ddot{y}_2 + y_1 = e_{11}F_1 + e_{12}F_2; \\ e_{21}m_1\ddot{y}_1 + e_{22}m_2\ddot{y}_2 + y_2 = e_{21}F_1 + e_{22}F_2, \end{array}\right\} \tag{3.12}$$

or in the general case,

$$\sum_{k=1}^{H} e_{jk}\, m_k\, \ddot{y}_k + y_j = \sum_{k=1}^{H} e_{jk}F_k \qquad (j = 1, \ldots, H), \tag{3.13}$$

where j is the number of the equation.

3.2 Specifics of Composition of Differential Equations for Drives with Cyclic Mechanisms

Use of the special form of the second-kind Lagrange equations Practical ways to use the methods of analytical mechanics (see Sect. 3.1) are illustrated with the help of the example of the dynamic model of a machine's drive, shown in Fig. 3.2,
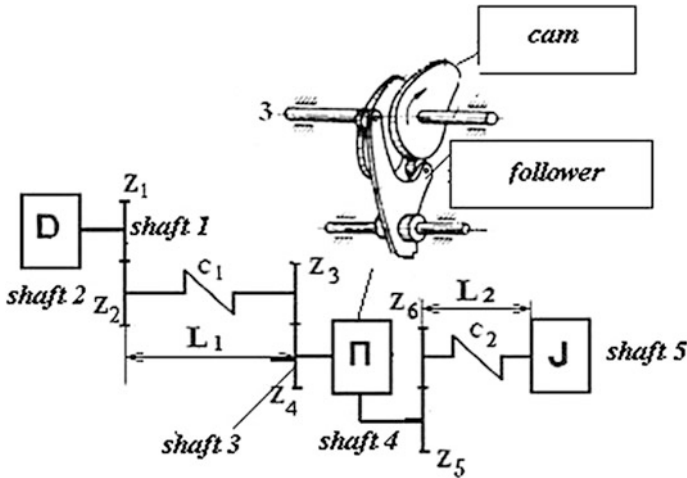
Fig. 3.2 Dynamic model of a drive with cam mechanism

in which shafts 3 and 4 are connected to each other by means of a cam mechanism, and the shafts 1–2, 2–3 and 4–5 by means of gears. We will accept the following notation: D is the motor, J_i are the gear's moments of inertia, u_{ij} are the gear ratios, c_{ij} are the stiffness coefficients of elastic shafts, J is the reduced moment of inertia of the actuator, Π is the position function of the cam mechanism.

For simplification of calculations we reduce the model to the form shown in Fig. 3.3. Thus inertial and elastic elements at the "input" are reduced to the shaft 3 and at the "output" to the shaft 4. Using the conditions of balance of the kinetic and potential energies in both models, we obtain $J_{11} = J_1 u_{31}^{-2} + J_2 u_{32}^{-2}$; $J_{12} = J_3 u_{32}^{-2} + J_4$; $J_{21} = J_5 + J_6 u_{54}^2$; $J_{22} = J u_{54}^2$; $c_1^* = c_1 u_{32}^{-2}$; $c_2^* = c_2 u_{54}^2$.

In addition to the generalized coordinates $q_1 = \varphi_{11}$; $q_2 = \varphi_{12} - \varphi_{11}$; $q_3 = \varphi_{22} - \varphi_{21}$ we take one redundant coordinate $q_4 = \varphi_{21}$. Thus we have one additional constraint equation ($n = 1$) $q_4 = \Pi(q_1 + q_2)$, that can be rewritten as

$$\Phi_1 = \Pi(q_1 + q_2) - q_4 = 0. \tag{3.14}$$
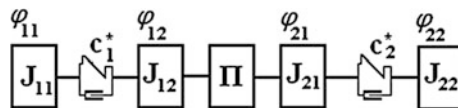
Fig. 3.3 Simplified form of the dynamic model

Let us set up the system of differential equations for the model considered in the form (3.8). While determining the coefficients of quadratic forms and the generalized forces, with redundant coordinates, should be treated in the same way, as the generalized ones. In our case we have

$$
\left.
\begin{aligned}
\mathrm{T} &= \frac{1}{2}(J_{11}\dot{\varphi}_{11}^2 + J_{12}\dot{\varphi}_{12}^2 + J_{21}\dot{\varphi}_{21}^2 + J_{22}\dot{\varphi}_{22}^2) \\
&= \frac{1}{2}[J_{11}\dot{q}_1^2 + J_{12}(\dot{q}_1 + \dot{q}_2)^2 + J_{21}\dot{q}_4^2 + J_{22}(\dot{q}_4 + \dot{q}_3)^2]; \\
V &= \frac{1}{2}[c_1^*(\varphi_{12} - \varphi_{11})^2 + c_2^*(\varphi_{22} - \varphi_{21})^2] = \frac{1}{2}(c_1^* q_2^2 + c_2^* q_3^2).
\end{aligned}
\right\}
\tag{3.15}
$$

Then $a_{11} = J_{11} + J_{12}$; $a_{22} = J_{12}$; $a_{33} = J_{22}$; $a_{44} = J_{21} + J_{22}$; $a_{12} = J_{12}$; $a_{34} = J_{22}$; $c_{22} = c_1^*$; $c_{33} = c_2^*$. The remaining coefficients are zero. Further, we find

$$
\frac{\partial \Phi_1}{\partial q_1} = \Pi'; \quad \frac{\partial \Phi_1}{\partial q_2} = \Pi'; \quad \frac{\partial \Phi_1}{\partial q_3} = 0; \quad \frac{\partial \Phi_1}{\partial q_4} = -1.
$$

After substituting in system (3.9), we finally have

$$
\left.
\begin{aligned}
(J_{11} + J_{12})\ddot{q}_1 + J_{12}\ddot{q}_2 &= Q_1^* + \Pi' \Lambda_1; \\
J_{12}\ddot{q}_1 + J_{12}\ddot{q}_2 + c_1^* q_2 &= Q_2^* + \Pi' \Lambda_1; \\
J_{22}\ddot{q}_3 + J_{22}\ddot{q}_4 + c_2^* q_3 &= Q_3^*; \\
J_{22}\ddot{q}_3 + (J_{21} + J_{22})\ddot{q}_4 &= Q_4^* - \Lambda_1.
\end{aligned}
\right\}
\tag{3.16}
$$

From the last equation of this system, we can directly express the Lagrange multiplier Λ_1 and substitute it in the previous equations.

$$
\ddot{q}_4 = [\Pi''(q_1 + q_2)](\dot{q}_1 + \dot{q}_2)^2 + [\Pi'(q_1 + q_2)](\ddot{q}_1 + \ddot{q}_2). \tag{3.17}
$$

However, it should be noted that in many cases of the system analysis, it is advisable to keep the Lagrange multipliers and derivatives of the redundant coordinates. Apart from the purely computational aspects of the problem, it often facilitates the evaluation of the degree of connectedness of the individual oscillation contours.

Application of Appell's equations To illustrate the application of Appell equations we use the dynamic model shown in Fig. 3.3. We will write expression for the energy of accelerations and will express it through the generalized coordinates and their derivatives from generalized coordinates, as before, will be $q_1 = \varphi_{11}$, $q_2 = \varphi_{12} - \varphi_{11}$, $q_3 = \varphi_{22} - \varphi_{21}$ (*variant 1*).

$$U = 0.5(J_{11}\ddot{\varphi}_{11}^2 + J_{12}\ddot{\varphi}_{12}^2 + J_{21}\ddot{\varphi}_{21}^2 + J_{22}\ddot{\varphi}_{22}^2)$$
$$= 0.5\{J_{11}\ddot{q}_1^2 + J_{12}(\ddot{q}_1 + \ddot{q}_2)^2 + J_{21}[(\dot{q}_1 + \dot{q}_2)^2\,\Pi'' \tag{3.18}$$
$$+ (\ddot{q}_1 + \ddot{q}_2)\,\Pi']^2 + J_{22}[(\dot{q}_1 + \dot{q}_2)^2\Pi'' + (\ddot{q}_1 + \ddot{q}_2)\Pi' + \ddot{q}_3]^2\}.$$

Here we have taken into account that

$$\ddot{\varphi}_{21} = \Pi''\dot{\varphi}_{12}^2 + \Pi'\ddot{\varphi}_{12} = (\dot{q}_1 + \dot{q}_2)^2\Pi'' + (\ddot{q}_1 + \ddot{q}_2)\,\Pi'.$$

Substitute function U and potential energy V in the Appell equation (3.10):

$$\left.\begin{array}{l}
J_{11}\ddot{q}_1 + J_{12}(\ddot{q}_1 + \ddot{q}_2) + J_{21}\Pi'[(\dot{q}_1 + \dot{q}_2)^2\Pi'' \\
\quad + (\ddot{q}_1 + \ddot{q}_2)\Pi'] + J_{22}\Pi'[(\dot{q}_1 + \dot{q}_2)^2\Pi'' + (\ddot{q}_1 + \ddot{q}_2)\Pi' + \ddot{q}_3] = Q_1; \\
J_{12}(\ddot{q}_1 + \ddot{q}_2) + J_{21}\Pi'[(\dot{q}_1 + \dot{q}_2)^2\Pi'' + (\ddot{q}_1 + \ddot{q}_2)\Pi'] \\
\quad + J_{22}\Pi'[(\dot{q}_1 + \dot{q}_2)^2\Pi'' + (\ddot{q}_1 + \ddot{q}_2)\Pi' + \ddot{q}_3] + c_1 q_2 = Q_2; \\
J_{22}[(\dot{q}_1 + \dot{q}_2)^2\Pi'' + (\ddot{q}_1 + \ddot{q}_2)\Pi' + \ddot{q}_3] + c_2 q_3 = Q_3.
\end{array}\right\} \tag{3.19}$$

Of course, in view of (3.17) the systems of Eqs. (3.16) and (3.19) coincide, and Eqs. (3.19) contain only generalized coordinates. Analyzing the resulting system of differential equations (3.19) or (3.8), we note that under *variant 1* of the generalized coordinates, the second derivatives are included in several members of some equations. This, in case of using some numerical methods of calculation, leads to certain inconveniences, because of the need to preserve in each equation only one member with the highest derivative. Therefore, in such cases it is preferable to use *variant 2* of assignment of generalized coordinates, where all generalized coordinates, except the first (cyclic) are the dynamical errors, i.e. these errors are deviations from ideal values, which are equal to the difference between the absolute element motion, taking into account its elasticity and absolute motion without elasticity. This method of assignment of generalized coordinates allows us to get rid of the "foreign" second derivative of the generalized coordinate in each of the differential equations of the system, which simplifies the procedure of numerical solution and analysis of the results. Thus $\varphi_{11} = \varphi_3 = q_1$ is the rotation angle of shaft 3 (input link of cam mechanism) in case of an absolutely rigid system, q_1 is the first generalized coordinate; $\dot{\varphi}_{11} = \dot{q}_1 = \omega$ $\ddot{\varphi}_{11} = \ddot{q}_1 = 0$; $\varphi_{12} = \varphi_{11} + q_2$; q_2 is the second generalized coordinate, equal to the dynamic error at the mechanism's "input", which in this case coincides with shaft 2 deformation, reduced to the third shaft. Thus, $\dot{\varphi}_{12} = \omega + \dot{q}_2$, $\ddot{\varphi}_{12} = \ddot{q}_2$; $\varphi_{21} = \Pi(\varphi_{12})$ which is the rotation angle of shaft 4 taking into account the deformation of shaft 2; $\dot{\varphi}_{21} = \Pi'(\varphi_{12})\dot{\varphi}_{12} = \Pi'(\varphi_{12})(\omega + \dot{q}_2)$, $\ddot{\varphi}_{21} = \Pi''(\varphi_{12})(\omega + \dot{q}_2)^2 + \Pi'(\varphi_{12})\ddot{q}_2$; $q_3 = \varphi_{22} - \Pi(\varphi_{11})$ is the dynamic error of the element J, reduced to shaft 4. Here φ_{22} is the reduced to shaft 4 absolute coordinate of the element J taking into account all of the deformations; $\Pi(\varphi_{11})$ is the ideal absolute

coordinate of the element J_{21} without elasticity. Thus, the kinematic characteristics of the output link are determined with the following relationships:

$$\varphi_{22} = \Pi(\varphi_{11}) + q_3, \quad \dot{\varphi}_{22} = \dot{q}_3 + \Pi'(\varphi_{11})\omega, \quad \ddot{\varphi}_{22} = \ddot{q}_3 + \Pi''(\varphi_{11})\omega^2.$$

We will again use the Appel's equations. For convenience we use the following notation: $\Pi_* = \Pi(\varphi_{11}), \quad \Pi = \Pi(\varphi_{12})$

Energy of accelerations:

$$
\begin{aligned}
U &= \frac{1}{2}\left(J_{11}\ddot{\varphi}_{11}^2 + J_{12}\ddot{\varphi}_{12}^2 + J_{21}\ddot{\varphi}_{21}^2 + J_{22}\ddot{\varphi}_{22}^2\right) \\
&= \frac{1}{2}\left(J_{12}\ddot{q}_2^2 + J_{21}[\Pi''(\omega + \dot{q}_2)^2 + \Pi'\ddot{q}_2]^2 + J_{22}(\ddot{q}_3 + \Pi''_*\omega^2)^2\right).
\end{aligned}
\tag{3.20}
$$

Potential energy:

$$V = \frac{1}{2}\left(c_1^*(\varphi_{12} - \varphi_{11})^2 + c_2^*(\varphi_{22} - \varphi_{11})^2\right) = \frac{1}{2}\left(c_1^* q_2^2 + c_2^*(q_3 - \Pi'_* q_2)^2\right).$$

Substituting these expressions into the Appel's equation, after some transformations we finally obtain:

$$
\begin{cases}
\left(J_{12} + J_{21}\Pi'^2\right)\ddot{q}_2 + \left(c_1^* + c_2^*\Pi'^2_*\right)q_2 - c_2^*\Pi'_* q_3 = Q_2 - J_{21}\Pi'\Pi''(\omega + \dot{q}_2)^2, \\
J_{22}\ddot{q}_3 + c_2^* q_3 - c_2^*\Pi'_* q_2 = Q_3 - J_{22}\Pi''_*\omega^2.
\end{cases}
\tag{3.21}
$$

Thus, using the Appel's equations we can, in the least cumbersome way, get a set of equations, describing oscillations and dynamic errors in the drive of the cyclic machine, with the additional requirement: *each equation should include just one corresponding to the equation number generalized acceleration*. As it was already noted, such form of equation corresponds to the most convenient method for computer modeling of the studied system, since using this form, without any additional procedures, a transition can be made to the system of differential equations, of first order.

Accounting of Coulomb friction The above mentioned mathematical model is valid for systems with ideal connections. Nevertheless for low frictional forces, we can, on the basis of this model, determine normal reactions with sufficient accuracy and then enter the corresponding frictional forces in the equations as active forces. However, in those cases, where the frictional forces are not small and strongly dependent on the dynamic process, such an approach may lead not only to quantitative errors, but also to the significant loss of quality. In particular, it is possible at the stage of the mathematical description of the system, to forcibly exclude from consideration such an important thing as self-locking.

Fig. 3.4 To the accounting of
non-ideal constraints
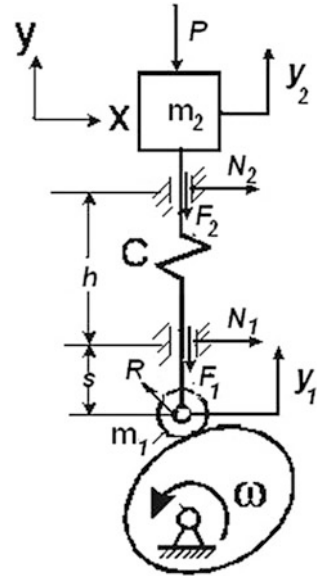
We will illustrate the method of taking the imperfect constraints into account, based on a single artificial method, in which we enter additional degrees of freedom and corresponding fictitious coordinates. Let us consider the problem of the dynamics of the elastic cam follower, the model of which is shown in Fig. 3.4.

In this case the following conventions are accepted: m_1, m_2 are the reduced masses of the driving and driven links; c is the stiffness of the elastic cam follower; P is the external force; R is the reaction of the cam on the cam follower (the reaction is assumed to be bilateral); α is the contact angle; N_i, F_i $(i = 1, 2)$ are the normal and tangential reactions in the sliding guides [the direction of these reactions in the scheme (Fig. 3.4) coincides with the positive direction of the reference; the true direction will become clear in the course of the calculation].

We will accept the following generalized coordinates: $q_1 = y_1$, $q_2 = y_2 - y_1$. To determine the reactions N_1 and N_2 we will introduce two additional fictitious coordinates: $x_1 = q_3 a_r^* = \sum_{i=1}^{H} \sum_{j=1}^{H} \alpha_{ir} \alpha_{jr} a_{ij}$; and $x_2 = q_4$ which are equal to the fictitious displacement, at the intersection of support points of the cam follower along the line of action of normal reactions. This technique allows us to operate with reactions N_i as with external forces, as it is done, for example, in solving the problems of statics, using the method of virtual displacements.

Further, to obtain such "extended" system, we write the second-kind Lagrange equations considering the friction forces F_i as conventionally known. Applying the abovementioned method of determining the inertial and quasi-elastic coefficients, we write: $T = 0.5 \left[m_1 \dot{q}_1^2 + m_2 (\dot{q}_1 + \dot{q}_2)^2 \right]$, $V = 0.5 \, c q_2^2$. In the expression for kinetic energy the terms depending on the fictitious generalized velocities $\dot{q}_3$ and $\dot{q}_4$ are

omitted since in the source system $q_3 = x_1 = $ const; $q_4 = x_2 = $ const. Thus $a_{11} = m_1 + m_2$; $a_{22} = m_2$; $a_{12} = m_2$; $c_{22} = c$; other coefficients become zero.

The works equation for the virtual displacements has the form:

$$\delta W = -P\delta(q_1 + q_2) + R\cos\alpha\,\delta q_1 + N_1\delta q_3 + N_2\delta q_4 + F_1\delta q_1 + F_2\delta(q_1 + q_2)$$
$$- R\sin\alpha\,\delta x_R\,,$$

where δx_R is the elementary displacement of the roller's center, corresponding to the virtual displacements of the supports δq_3, δq_4 (the direction of the friction forces F_1 and F_2 is taken into account in the mathematical description of these forces).

Taking into account that $\delta x_R = \delta q_4 + (\delta q_3 - \delta q_4)(l + s)/l = (1 + s/l)\delta q_3 - (s/l)\delta q_4$, we have

$$Q_1^* = -P_1 + F_1 + F_2 + R\cos\alpha; \quad Q_2^* = -P + F_2;$$
$$Q_3^* = N_1 - (1 + s/l)R\sin\alpha; \quad Q_4^* = N_2 + sR\sin\alpha/l.$$

Further we write the system of differential equations of the form (3.9)

$$\left.\begin{aligned}
(m_1 + m_2)\ddot{q}_1 + m_2\ddot{q}_2 &= -P + R\cos\alpha + F_1 + F_2;\\
m_2\ddot{q}_1 + m_2\ddot{q}_2 + cq_2 &= -P + F_2;\\
0 &= N_1 - (1 + s/l)R\sin\alpha;\\
0 &= N_2 + sR\sin\alpha/l.
\end{aligned}\right\} \tag{3.22}$$

On the basis of (3.22)

$$m_2\ddot{q}_2 + c_2q_2 = -m_2\ddot{q}_1(t) - P - fsl^{-1}R\,|\sin\alpha|\,\text{sign}(\dot{q}_1 + \dot{q}_2).$$

Assuming the given program movement is $q_1 = \Pi(\varphi)$, we get

$$R = \frac{(m_1 + m_2)\ddot{q}_1 + m_2\ddot{q}_2 + P}{\cos\alpha - f|\sin\alpha[sl^{-1}\text{sign}(\dot{q}_1 + \dot{q}_2) + (1 + sl^{-1})\text{sign}\dot{q}_1]|}. \tag{3.23}$$

Dependence (3.23) gives evidence of the possibility of self-braking, accompanied by jamming of the cam follower, when the denominator of this expression vanishes. To eliminate this phenomenon (with some reserve) the condition $|\text{ctan}\,\alpha_{\max}| > f(1 + s_*/\ell)$, should be satisfied, where s_* is the value at which $\alpha = \alpha_{\max}$.

Let us note that for the solution of real problems in dynamics of mechanisms, sometimes we need to take into account not only the elastic properties of the links, but other properties of the supports, joints, guides, etc. We particularly need to resort to such complication of model for statically undeterminable systems. Obviously in such cases the above-introduced additional coordinates q_3 and q_4 lose their fictitious character, being transformed into generalized coordinates, implementing

additional degrees of freedom. Frequently occurring errors in the signs of reactions and frictional forces, can be avoided with the help of the given method.

Mathematical model of the flexural-torsion oscillations of the drive with cyclic mechanisms Let us consider quite a general dynamic model (Fig. 3.5) that shows the camshaft, which moves N planar mechanisms, with nonlinear position functions, when each of them will be presented as multi-mass oscillatory contour. It is assumed that the camshaft can undergo both torsion and bending oscillations along the planes $x_0 y$ and $x_0 z$.

Let us accept the following notation: $i = \overline{1, N}$ is the number of the mechanism; m_i, J_i is the mass and moment of inertia in the section i of the camshaft; m_{ij}, J_i is the mass and moment of inertia relative to the center of masses for link j, belonging to mechanism i; φ_i, z_i, y_i are the current coordinates of the corresponding section of the camshaft; $\varphi_{ij}, z_{ij}, y_{ij}$ are the current coordinates characterizing the link's rotation angle and the center of mass position for link j; Π_{ij} is position function.

In many practical applications the most significant inertial elements of the model commit translational or rotational (or oscillatory) motion. In such cases element ij can be described by a single coordinate instead of three coordinates—linear or angular, and in the latter case J_{ij} corresponds to the moment of inertia relative to the axis of rotation.

Fig. 3.5 Dynamic model of the branched flexural-torsion system
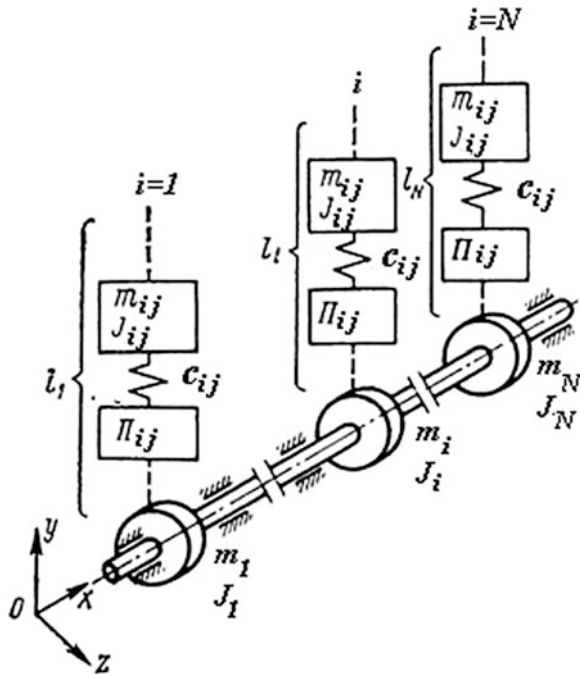
We will use a combination of two methods for producing the mathematical model. One of the methods is based on the use of the second-kind Lagrange equations, with redundant coordinates and the second is based on the inverse method (see Sects. 3.1.4 and 3.1.6).

Temporarily we will exclude from consideration, the bending vibrations of the camshaft. Then kinetic energy $T = T^*$ can be described as follows:

$$T^* = \frac{1}{2} \sum_{i=1}^{N} \left[J_i \dot{\varphi}_i^2 + \sum_{j=1}^{l_i} \left(J_{ij} \dot{\varphi}_{ij}^2 + m_{ij} \dot{z}_{ij}^2 + m_{ij} \dot{y}_{ij}^2 \right) \right], \qquad (3.24)$$

where $l_i = \max j$; here and below the asterisk indicates the exception of bending contour.

Let us choose n redundant coordinates so that the condition $\partial T^* / \partial q_s = 0$ was satisfied for all coordinates. Then no matter how small are $q_1, \ldots, q_{H_{1+n}}$, the kinetic energy T^* can be represented as quadratic form with $A_{kr} = a_{kr} = \text{const}$ (H_1 is the number of generalized coordinates without bending vibrations, i.e. assuming $m_i = 0$).

In our case the abovementioned condition is satisfied if the functions φ_{ij}, z_{ij}, y_{ij} are accepted as redundant coordinates. Differential equations for the considered subsystem can be written in the form

$$\sum_{s=1}^{H_1+n} a_{rs} \ddot{q}_s + \sum_{s=1}^{H_1+n} c_{rs} q_s = Q_r + \sum_{v=1}^{n} \frac{\partial \Phi_v}{\partial q_r} \Lambda_v \qquad (r = 1, \ldots, H_{1+n}). \qquad (3.25)$$

In Sect. 3.1.4 it was mentioned that group of summands, related to the Lagrange multipliers Λ_v, acts as the constraints' reaction, which in this case cannot be excluded from the equations due to the excess of the number of coordinates, as compared to the number of degrees of freedom.

Equations of the connection $\Phi_v = 0$ in this case can be written on the basis of the following considerations. Suppose for example $\varphi_{ij} = q_s$ when $\varphi_{ij} = f_{ij}^{(\varphi)}(q_1, \ldots, q_{H_{1+n}}, z_1, \ldots, z_N, y_1, \ldots, y_N)$. Then the corresponding constraint equation can be written as

$$\Phi_v = f_{ij}^{(\varphi)}(q_1, \ldots, q_{H_1+n}, z_1, \ldots, z_N, y_1, \ldots, y_N) - q_s = 0. \qquad (3.26)$$

Similarly the constraint's equations are written on the basis of the known relationships for $z_{ij} = f_{ij}^{(x)}$ and $y_{ij} = f_{ij}^{y}$. All coordinates, including redundant coordinates and coordinates describing bending vibration of the leading links, can be used as arguments of the functions $f_{ij}^{(z)}$ and $f_{ij}^{(y)}$ as well as for $f_{ij}^{(\varphi)}$. Let us note here that the functions $f_{ij}^{(z)}$ and $f_{ij}^{(y)}$, in essence, are the functions of position of relevant transformed mechanisms, which are used, for example, for studying problems

related to mechanism accuracy [16]; at the same time the driving link in these
mechanisms (mass m_i) performs translational motion along the axis z and y.

Now we turn to the subsystem, which performs bending vibrations and use the
abovementioned inverse method to describe it. It should be borne in mind that in
each cross-section i, applied, except for the external forces F_{ix}, F_{iy}, are the reactions
R_{iz}, R_{iy}, which are defined as follows:

$$R_{ix} = \sum_{v=1}^{n} \frac{\partial \Phi_v}{\partial z_i} \Lambda_v; \quad R_{iy} = \sum_{v=1}^{n} \frac{\partial \Phi_v}{\partial y_i} \Lambda_v. \tag{3.27}$$

The system of differential equations, describing bending vibrations, can be
written on the basis of (3.13) and (3.27) as follows:

$$\left. \begin{array}{l} \sum_{i=1}^{N} e_{si}^{z} m_i \ddot{z}_i + z_s = \sum_{i=1}^{N} e_{si}^{z} (F_{iz} + \sum_{v=1}^{N} \frac{\partial \Phi_v}{\partial z_i} \Lambda_v); \\ \sum_{i=1}^{N} e_{si}^{y} m_i \ddot{y}_i + y_s = \sum_{i=1}^{N} e_{si}^{y} (F_{iy} + \sum_{v=1}^{N} \frac{\partial \Phi_v}{\partial y_i} \Lambda_v) \end{array} \right\}. \tag{3.28}$$

$$(s = 1, \ldots, N)$$

The Eqs. (3.25) and (3.28) are connected to a single system by the constraints'
reactions. The total number of degrees of freedom of the oscillating system is equal
to $H = H_1 + 2N$.

Let us consider the dynamic model, in which, for simplification, we assume,
when conducting analysis of bending vibrations that masses m_1 and m_2 move only in
the vertical plane (Fig. 3.6). The model consists of two subsystems, corresponding to
the torsion-longitudinal (Fig. 3.6a) and bending oscillations (Fig. 3.6b, c). Let's
accept $q_1 = \varphi_1$; $q_2 = \varphi_2 - \varphi_1$; q_3 is the elastic deformation of the element with
stiffness coefficient c_2. To express the functions T^* and V^* as quadratic forms and to
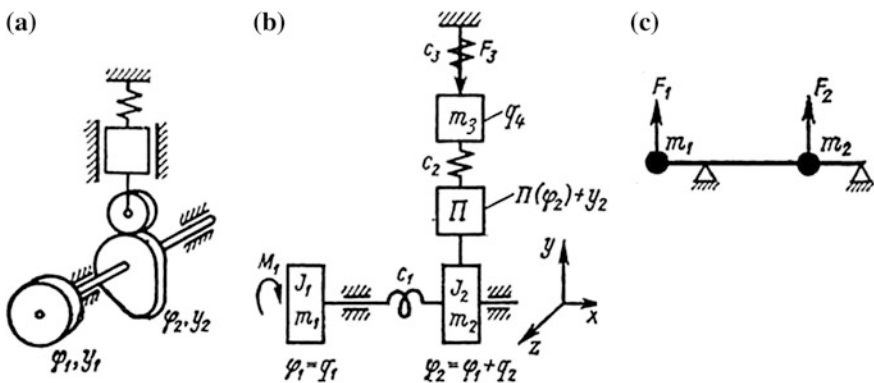
Fig. 3.6 Dynamic model of the cam mechanism drive

satisfy the conditions $\partial T^* / \partial q_s = 0$, in such cases, the coordinates of driven masses in absolute motion, should be accepted as redundant. In our case we denote q_4 as the absolute coordinate of the mass m_3.

Then:

$$T^* = \frac{1}{2}\left[J_1 \dot{q}_1^2 + J_2(\dot{q}_1 + \dot{q}_2)^2 + m_3 \dot{q}_4^2\right];$$
$$V^* = \frac{1}{2}(c_1 q_2^2 + c_2 q_3^2 + c_3 q_4^2).$$

Hence,

$$a_{11} = J_1 + J_2; \; a_{22} = J_2; \; a_{44} = m_3; \; a_{12} = J_2; c_{22} - c_1; \; c_{33} = c_2; \; c_{44} = c_3.$$

The rest of the inertial and quasi-elastic coefficients are zero. The equation of the constraint (3.26) has the form

$$\Phi_1 = \Pi(q_1 + q_2) + y_2 + q_3 - q_4 = 0. \tag{3.29}$$

Therefore

$$\frac{\partial \Phi_1}{\partial q_1} = \Pi'; \; \frac{\partial \Phi_1}{\partial q_2} = \Pi'; \; \frac{\partial \Phi_1}{\partial q_3} = 1; \; \frac{\partial \Phi_1}{\partial q_4} = -1; \; \frac{\partial \Phi_1}{\partial y_1} = 0; \; \frac{\partial \Phi_1}{\partial y_2} = 1.$$

To determine Q_r the equation of elementary works on the virtual displacements is to be recorded without taking into account the contour of bending vibrations

$$\delta W = M_1 \delta q_1 - F_3 \delta q_4.$$

Thus, $Q_1 = M_1; \; Q_4 = -F_3; \; Q_2 = Q_3 = 0.$
After substitution into (3.25) and (3.28) we obtain

$$\left.\begin{array}{l} (J_1 + J_2)\ddot{q}_1 + J_2\ddot{q}_2 = M_1 + \Pi'\Lambda_1; \\ J_2\ddot{q}_1 + J_2\ddot{q}_2 + c_1 q_2 = \Pi'\Lambda_1; \\ c_2 q_3 = \Lambda_1; \\ m_3\ddot{q}_4 + c_3 q_4 = -F_3 - \Lambda_1; \\ e_{11}m_1\ddot{q}_1 + e_{12}m_2\ddot{q}_2 + y_1 = e_{11}F_1 + e_{12}(F_2 + \Lambda_1); \\ e_{21}m_1\ddot{q}_1 + e_{22}m_2\ddot{q}_2 + y_2 = e_{21}F_1 + e_{22}(F_2 + \Lambda_1). \end{array}\right\} \tag{3.30}$$

(Index y under the coefficients of influence and external forces, is omitted everywhere).

Since we excluded from consideration the oscillations in the plane $x0z$ the total number of degrees of freedom is $H = H_1 + N = 3 + 2 = 5$. In order to exclude the

Lagrange multiplier Λ_1 from the system (3.30), we use the third equation, and for excluding redundant coordinate q_4 we use the equation of constraint (3.29).

Wherein

$$q_4 = \Pi(q_1 + q_2) + y_2 + q_3;$$

$$\ddot{q}_4 = (\dot{q}_1 + \dot{q}_2)^2 [\Pi''(q_1 + q_2)] + (\ddot{q}_1 + \ddot{q}_2)[\Pi'(q_1 + q_2)] + \ddot{q}_2 + \ddot{q}_3.$$

The considered method of mathematical description, of such dynamic models, is particularly effective in more complex multiply connected systems.

Generating the systems of differential equations for dynamic models of mechanisms, which consist of elements with distributed parameters In engineering practice, there often are cases when some of the working parts or other parts of the mechanism are massive and at the same time have considerable compliance. In these cases an attempt to represent the mechanism through a dynamic model, with a finite (but large) number of degrees of freedom, usually leads to the greater complexity of calculations, than the use of less-idealized calculation scheme, in which the corresponding element is represented as a subsystem with distributed parameters.

The composition of the mathematical model of such systems is illustrated with the help of the model shown in Fig. 3.7, in which the following notations are accepted: J_0, J_1, J_2 are the lumped moments of inertia; J is the moment of inertia of shaft 2 and rigidly associated parts; c_1, ψ_1 are the stiffness coefficients and dissipation coefficients of shaft 1; $\varphi_0(t)$, $\varphi_1(t)$, $\varphi_2(x, t)$ are the absolute coordinates respectively for J_0, J_1 and cross section x of shaft 2. In this case, $\varphi_2(0) = \Pi(\varphi_1)$, where Π is the mechanism's position function.

Let's accept $q_1 = \varphi_0$; $q_2 = \varphi_1 - \varphi_0$ as generalized coordinates. With cross section $x = 0$ we divide the model into subsystems with lumped and distributed parameters. It is obvious that two reaction moments M_- and M_+, which are equal in value and opposite in direction, i.e. $M_+ = -M_-$ must apply to the truncated parts in this section. However to avoid the possible errors in the choice of the sign of the reactive moment it is advisable to use the following rule: reactive torque at the "exit" of the element (in this case on the right) is considered positive if its direction coincides with the positive direction of the indication of the angle φ_2; for the reactive moment at the "input" of the element (in our case on the left) the sign rule is opposite. This rule, which we also use here, allows us to consider $M_- = M_+ = M$; and at the same time we can skip in calculations, the specification of the part of the system, to which the moment is attached. For external moments the rule of signs is set as for the reaction moment at the "exit".

For subsystem with lumped parameters the mathematical model can be composed as per one of the abovementioned methods, taking M_- as an external torque, applied to the driven link. We use, for example, the second-kind Lagrange's equation, which leads to the system of Eq. (3.8). We accept $q_3 = \varphi_2(0) = \Pi(\varphi_1)$

as redundant coordinate. Kinetic and potential energies of the considered subsystem can be expressed as follows:

$$T = \frac{1}{2}\left[J_0\dot{q}_1^2 + J_1(\dot{q}_1 + \dot{q}_2)^2 + J_2\dot{q}_3^2\right]; \quad V = \frac{1}{2}c_1q_2^2.$$

Hence $a_{11} = J_0 + J_1$; $a_{22} = J_1$; $a_{33} = J_2$; $a_{12} = J_1$; $c_{22} = c_1$; the rest of the inertial and quasi elastic coefficients are equal to zero. The constraint equation has the form $\Phi_1 = \Pi(q_1 + q_2) - q_3 = 0$. Thus $\partial\Phi_1/\partial q_1 = \Pi'$; $\partial\Phi_1/\partial q_3 = -1$.

After substitution into (3.8) we have

$$\left.\begin{array}{l} J_0\ddot{q}_1 + J_1\ddot{q}_2 = Q_1 + \Pi'\Lambda_1; \\ J_1\ddot{q}_1 + J_1\ddot{q}_2 + c_1q_2 = Q_2 + \Pi'\Lambda_1; \\ J_2\ddot{q}_3 = Q_3 - \Lambda_1. \end{array}\right\} \tag{3.31}$$

To determine the generalized forces Q_j, as it was shown above, we should use the equation of works on virtual displacements. It is easy to see that $Q_3 = M_- = M$.

Let us now turn to the subsystem with distributed parameters. Let us select on shaft 2 an elementary segment of length dx (Fig. 3.7) with moment of inertia equal to $\rho = \frac{\partial J}{\partial x}dx$.

In general case $\rho = \rho(x, t)$. If J denotes the variable reduced moment of inertia, which is also unequally distributed along the x axis, we might see that $\rho = \rho(x, t)$; when $J(t) = \text{const}$, we have $\rho = \rho(x)$. At uniform mass distribution $\rho = J/l = \text{const}$, where l is the length of shaft 2 (see Fig. 3.7).
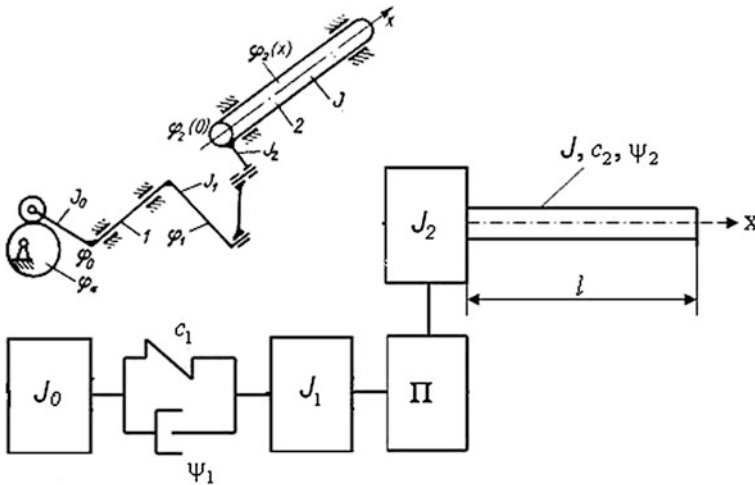
Fig. 3.7 Dynamic model with lumped and distributed parameters

For the selected segment we use the theorem of the angular momentum change, according to which the derivative of kinetic moment as per time is equal to attached external moments:

$$\frac{\partial}{\partial t}(\rho \frac{\partial \varphi_2}{\partial t})dx = -M + (M + dM) + \mu \, dx, \tag{3.32}$$

where $dM = \frac{\partial M}{\partial x} dx$ is an increment of the moment M on the segment dx; $\mu(x, t)$; is the distributed moment applied to shaft 2.

The elementary angular deformation $d\varphi_2$ can be expressed in the following way:

$$d\varphi_2 = \frac{M}{GI(x)} dx, \tag{3.33}$$

where G is shear modulus; $I(x)$ is the polar moment of inertia of the shaft, which in general case is variable.

Hence,

$$dM = G \frac{\partial}{\partial x}(I(x) \frac{\partial \varphi_2}{\partial x})dx.$$

After substituting this dependence in (3.32) we have

$$\frac{\partial}{\partial t}(\rho \frac{\partial \varphi_2}{\partial t}) - G \frac{\partial}{\partial x}(I \frac{\partial \varphi_2}{\partial x}) = \mu(x, t). \tag{3.34}$$

Using (3.32) we find

$$Q_3 = M_- = GI(0) \frac{\partial \varphi_2}{\partial x}(0). \tag{3.35}$$

Then we exclude Lagrange multiple Λ_1 from (3.31):

$$\left.\begin{aligned}
J_0\ddot{q}_1 + J_1\ddot{q}_2 + \Pi'\left[J_2\ddot{q}_3 - GI(0)\frac{\partial \varphi_2}{\partial x}(0)\right] &= Q_1; \\
J_1\ddot{q} + J_1\ddot{q}_2 + c_1 q_2 + \Pi'\left[J_2\ddot{q}_3 - GI(0)\frac{\partial \varphi_2}{\partial x}(0)\right] &= Q_2.
\end{aligned}\right\} \tag{3.36}$$

The system (3.31) must be solved together with the differential equation in partial derivatives (3.34), with next boundary conditions:

$$\begin{aligned}
\varphi_2(0, t) &= q_3 = \Pi(q_1 + q_2); \\
M(l) &= GI(l)\frac{\partial \varphi_2}{\partial x}(l) = 0.
\end{aligned} \tag{3.37}$$

Furthermore it must be taken into account in (3.31) that

$$\ddot{q}_3 = [\Pi''(q_1 + q_2)](\dot{q}_1 + \dot{q}_2)^2 + [\Pi'(q_1 + q_2)](\ddot{q}_1 + \ddot{q}_2).$$

If $\rho = \text{const}$ and $I = \text{const}$ (3.34) takes the form:

$$\rho\frac{\partial^2\varphi_2}{\partial t^2} - GI\frac{\partial^2\varphi_2}{\partial x^2} = \mu(x,\, t). \tag{3.38}$$

It is often more convenient to solve the equations and conduct the subsequent calculations using the coordinates, which correspond to small deviations caused by the elasticity of the links.

With reference to (3.32) the transition to the relative coordinates can be done as follows:

$$\varphi_2 = \varphi_2^*(t) + \gamma(x,\, t), \tag{3.39}$$

where φ_2^* is the ideal rotation angle of shaft 2 (Fig. 3.7), realized with absolutely rigid links of the mechanisms; γ is the angle error, i.e. deviation of the angle coordinate φ_2 from this value.

After substitution of (3.39) in Eq. (3.38) we have

$$\rho\frac{\partial^2\gamma}{\partial t^2} - GI\frac{\partial^2\gamma}{\partial x^2} = \mu(x,\, t) - \rho\,\ddot{\varphi}_2^*(t). \tag{3.40}$$

It should be taken into account that in (3.31) and boundary conditions (3.37) $\partial\varphi_2 / \partial x = \partial\gamma / \partial x;\ \ y(0,\, t) = \Pi(q_1 + q_2) - \Pi_1(q_1)$. If we consider $\varphi_0 = q_1$ as the given program motion, then the solution is determined from second equation of system (3.31) and equation for system with distributed parameters. The first Eq. (3.30) in such cases as it was shown above is selected for determination of the driving moment.

For large cyclic systems, including a lot of mechanisms and subsystems with distributed parameters, the methods of matrix analysis are developed. These methods allow us to combine the composition of mathematical model and its solution (see Chaps. 8–12).

Chapter 4
Dynamic Models with Constant Parameters

4.1 Models with One Degree of Freedom

4.1.1 General Solution

The dynamic models, under consideration in this chapter, include models $0-\Pi-H$ (see Table 2.1), to which a lot of modifications of the mechanisms can be associated. To facilitate and specify the consideration, without restricting generality, we define this model concretely for cam mechanisms with elastic cam follower (Fig. 4.1).

We write the differential equation for the given model having constant angular velocity of the input link ω (Fig 4.1a):

$$m\ddot{q} + b\dot{q} + (c + c_s)q = -F - m\ddot{x} - c_s x - F_s, \qquad (4.1)$$

where q is the deformation; m, c are the reduced mass and stiffness coefficients for the cam follower; b *is* the coefficient of the equivalent linear resistance (in details see Sect. 6.1); $x = \Pi(\varphi)$ is the law of the program motion, F is the external force; c_s, F_S is the coefficient of stiffness and the preliminary force of the closing spring; $\varphi = \omega t$ is the rotating angle of the input link.

If the output link of the mechanism is a balancing arm, with angular displacement around a fixed axis (Fig. 4.1b), then the mass is to be replaced with moment of inertia J, and the longitudinal stiffness is to be replaced with the torsional stiffness.

Dividing all the terms of the Eq. (4.1) by m, we write:

$$\ddot{q} + 2n\dot{q} + k^2 q = W(t), \qquad (4.2)$$

where $2n = b/m$; $k^2 = (c + c_s)/m$.

Fig. 4.1 Cam mechanisms
with elastic cam follower
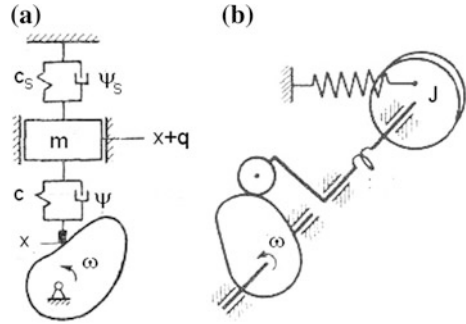
The right part of the Eq. (4.2), which will be called *the excitation function*, can
be written as:

$$W(t) = -\left(\Pi''\omega^2 + k_s^2\Pi + h\right). \tag{4.3}$$

Here $k_s^2 = c_s/m$; $h = (F + F_s)/m$; $\Pi'' = d^2\Pi/d\varphi^2$ is the second geometric
transfer function.

Having a linear position function Π, implemented, for example, in gearing-rack
train, as well as in cam mechanisms at the constant velocity intervals (see Sect. 1.2),
the first summand of the formula (4.3) is absent, because $\Pi' = const$ and $\Pi'' = 0$.

Suppose for some time interval of functions Π, W and their derivatives have
discontinuities. Then the solution for Eq. (4.2) looks like:

$$q = e^{-nt}(C_1 \cos k_1 t + C_2 \sin k_1 t) + Y(t). \tag{4.4}$$

Here $k_1 = \sqrt{k^2 - n^2}$; $Y(t)$ is the particular solution of the nonhomogeneous
equation; C_1, C_2 are the integration constants, which can be determined from
initial conditions when $t = 0 : q(0) = q_0; \dot{q}(0) = \dot{q}_0$.

Parameter k_1 is called *the frequency of free oscillations* or *natural frequency*.

Since $k_1 = k\sqrt{1 - \delta^2}$, and the coefficient $\delta = n/k$ in case of the absence of the
special damping devices it usually does not exceed the value of 0.1, we can accept
$k_1 \approx k$. Thus, the influence of the resistance forces on the natural frequency can be
neglected. Moreover, as $c_s \ll c$, $k \approx \sqrt{c/m}$.

After determining C_1 and C_2 we get

$$q = e^{-nt}(q_0 \cos kt + \frac{\dot{q}_0 + nq_0}{k}\sin kt) - e^{-nt}\left[Y(0)\cos kt + \frac{\dot{Y}(0) + nY(0)}{k}\sin kt\right]$$
$$+ Y(t). \tag{4.5}$$

The first group of terms describes the *free oscillations*, whose amplitude depends
on the initial conditions. The amplitudes of the free oscillations, in case of the linear

force of resistance, form an infinitely decreasing geometric progression, whose denominator e^{-nT} (where $T = 2\pi/k$ is the period of oscillations) is called the decrement of oscillations, and the value $\vartheta = nT$ is called the logarithmic decrement. This parameter is equal to the absolute value of the natural logarithm of the ratio of the two adjacent amplitudes, separated with the period.

The second group defines the so-called *accompanying oscillations,* the frequency of which is also equal to the natural frequency k, however, unlike free oscillations, their amplitude does not depend on the initial conditions and is determined with discontinuities of the particular solution and its derivatives at $t = 0$. Finally, the third summand corresponds to *the forced oscillations.* The kind of the particular solution is determined by the type of the excitation function (see below). The integral form of the particular solution is sometimes called the Duhamel's formula:

$$Y^0(t) = \frac{1}{k} \int\limits_0^t W(u) \exp[-n(t-u)] \sin k(t-u) du. \qquad (4.6)$$

When using (4.6) the second group of terms in (4.5) is explicitly absent, as in this case $Y^0(0) = 0$, $\dot{Y}^0(0)$. In this case accompanying oscillations are detected after the procedure of integration.

4.1.2 Solving for Steady Regimes

Harmonic excitation The right-hand side of the differential equation (4.2) reflects the dual nature of vibration excitation—*kinematic* and *forced*. In case of kinematic excitation, some point or section forcibly moves according to the given law of program motion; such point in this case is the inlet section of the cam follower, making contact with the cam profile. In case of forced excitation the oscillations are excited with time-varying driving force $F(t)$.

Let us first consider the case, where $F = \text{const}$ and the law of motion is described with harmonic function $\Pi = 0.5 x_{max}(1 - \cos \varphi)$. Then function of excitation (4.3) takes the form

$$W = W_0 + W_1 \cos \omega t, \qquad (4.7)$$

where $W_0 = -[0.5(\omega^2 + k_s^2)x_{max} + h]$; $W_1 = -0.5 x_{max}(\omega^2 - k_s^2)$.

In case of absence of discontinuities of functions Π and W, as was shown above, for steady regime $(t \to \infty)$ $q \to Y$. We find the particular solution Y of the

nonhomogeneous differential equation (4.2) as the sum of the constant component and harmonic function:

$$Y = A_0 + A_c \cos \omega t + A_s \sin \omega t = A_0 + A \cos(\omega t - \gamma), \tag{4.8}$$

where

$$\begin{aligned} A_0 &= W_0/k^2; \\ A &= \sqrt{A_c^2 + A_s^2} = 0.5 x_{\max} \kappa_k(z); \\ \gamma &= \arctan[2\delta z/(1 - z^2)](\gamma \in [0, \pi]). \end{aligned} \tag{4.9}$$

Here $z = \omega/k$ is the coefficient of frequency mismatch; $\delta = n/k$; $\kappa_k(z)$ is dynamicity factor in case of kinematic excitation, defined as:

$$\kappa_k = \frac{|z^2 - z_s^2|}{\sqrt{(1 - z^2)^2 + 4z^2\delta^2}}. \tag{4.10}$$

Here $z_s^2 = k_s^2/k^2$.

The dynamic magnification factor κ_k is the dimensionless *amplitude-frequency characteristic* (*AFC*). According to (4.9) it is the ratio of the amplitude of oscillation A to the amplitude of kinematic excitation $0.5x_{\max}$.

The typical graph of AFC is shown in the Fig. 4.2a. When $z \in [0, z_s]$ the function $\kappa_k(z)$ changes from value z_s^2 to zero, increasing after that to its maximum value $\kappa_{k\max}$. Using the conditions of extremum $d\kappa_k/dz = 0$, we find that the value $\kappa_{k\max}$ corresponds to

$$z_* = \sqrt{\frac{1 - z_s^2(1 - 2\delta^2)}{1 - z_s^2 - 2\delta^2}}. \tag{4.11}$$
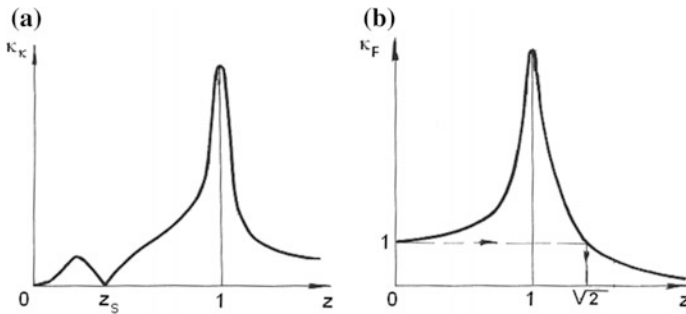
Fig. 4.2 Dynamicity factor in case of kinematic and forced excitations

Usually $z_s^2 \ll 1$ and $\delta \ll 1$, so $z_* \approx 1$ and $\kappa_{kmax} \approx 1/2\delta$. The value $z = 1$ $(\omega = k)$ corresponds to the resonance. In the beyond-resonance zone $(z > 1)$ the dynamicity factor decreases, asymptotically approaching the value $\kappa_k = 1$.

Significantly interesting is the regime $z = z_s$, in case of which $\omega = k_s$. In this mode $W_1 = 0$, therefore $q \to A_0 = \text{const}$. It is easy to see that in case of discontinuity of the kinematic connections, between the output and input links, the natural frequency of the system is equal to k_s. In case of $\omega = k_s$, the harmonic component of the restoring force in the terminating spring and the inertial force of the translational motion are equal in value and opposite in direction. This interesting effect and its use is discussed in Sect. 4.3.

In a similar way in case of the impact of the harmonic disturbing force $q_1^+ = q_i^- - \Delta x_i$; $\quad \dot{q}_1^+ = \dot{q}_i^- - \Delta \dot{x}_i$ $F = F_1 \cos(\omega t + \alpha)$ we get $q = B \cos(\omega t + \alpha - \gamma)$, with

$$B = B_{10}\kappa_F, \tag{4.12}$$

where $B_{10} = F_1/c$; $\quad \kappa_F = 1/\sqrt{(1 - z^2)^2 + 4z^2\delta^2}$. Here B_0 is the so-called *static amplitude*, equal to the deformation of the system under the influence of the peak value of the driving force, applied under static conditions; κ_F is the dynamicity factor in case of the forced excitation (Fig. 4.2b).

From dependence (4.9) it is clear that forced oscillations on the phase have offset relative to the excitation function at the value γ.

Dependencies $\gamma(\omega)$ or $\gamma(z)$ are called the phase-frequency characteristic (PFC). Figure 4.3 shows a group of curves $\gamma(z)$, corresponding to the dependence (4.9). In case of $z \ll 1$ we have $\gamma \approx 0$, in case of $z = 1$ (resonance) $\gamma = \pi/2$, *in case of* $z \to \infty$ the oscillations occur in the opposite phase $(\gamma \to \pi)$.

Determination of the solution for arbitrary periodic excitation functions using the method of harmonic analysis Here above we have analyzed the forced oscillations due to harmonic driving force, which is a special case of a periodic driving force. Getting into the consideration of this more general case, relative to a system with one degree of freedom, we recall that with the help of the normal (global) coordinates (see Sect. 4.2.2) the method described in this and the following

Fig. 4.3 Phase-frequency characteristic
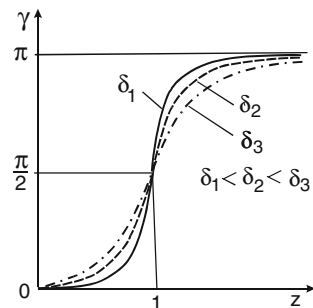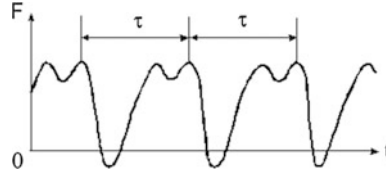
Fig. 4.4 Periodic changes of the driving force

paragraphs can be easily extended to a system with a finite number of degrees of freedom.

Now the differential equation looks like:

$$a\ddot{q} + b\dot{q} + cq = F(t), \tag{4.13}$$

where $F(t) = F(t + \tau)$ is the periodic driving force; τ is the period (Fig. 4.4).

Let us represent the function $F(t)$ as a Fourier series:

$$F(t) = F_0 + \sum_{j=1}^{\infty} (F_{jc} \cos j\omega t + F_{js} \sin j\omega t), \tag{4.14}$$

where $\omega = 2\pi/\tau$; F_0, F_{jc}, F_{js} are Fourier coefficients, defined as follows:

$$F_0 = \tau^{-1} \int_0^\tau F(t)dt; \ F_{jc} = 2\tau^{-1} \int_0^\tau F(t) \cos j\omega t dt; \ F_{js} = 2\tau^{-1} \int_0^\tau F(t) \sin j\omega t dt.$$

$$\tag{4.15}$$

For many typical cases F_0, F_{jc}, F_{js} are given in the references; additionally, there are standard software to find the Fourier coefficients, for certain number of values of the function $F(t)$.

When solving (4.13), we use the *principle of superposition* that is valid for linear systems. With respect to this problem, it means that the *oscillations arising from the sum of forces can be determined as the sum of the oscillations from each individual force.* Since the oscillations, in case of the harmonic driving force, were discussed above the problem can be considered solved basically.

Let us represent (4.14) as follows:

$$F(t) = F_0 + \sum_{j=1}^{\infty} F_j \sin(j\omega t + \alpha_j), \tag{4.16}$$

where $F_j = \sqrt{F_{jc}^2 + F_{js}^2}$; $\cos \alpha_j = F_{js}/F_j$; $\sin \alpha_j = F_{jc}/F_j$.

Each member of (4.16) is called the harmonic j. The deformation under constant component F_0 is equal to $A_0 = F_0/c$. Harmonic oscillations from the harmonic j of the driving forces are determined on the basis of (4.9) and (4.10)

$$q_j = A_j \sin(j\omega t + \alpha_j - \gamma_j),\tag{4.17}$$

where $A_j = A_{j0}\kappa_j$, $\kappa_j = 1/\sqrt{(1 - j^2 z^2)^2 + 4j^2 z^2 \delta^2}$; $z = \omega/k$; $A_{j0} = F_j/c$ is the static amplitude of the harmonic j; $k = \sqrt{c/a}$; $\gamma_j = \arctan[2\delta j z/(1 - j^2 z^2)]$ is phase frequency characteristic. (In case of the kinematic excitation, we need to use (4.9), (4.10) replacing z with jz).

So we finally have

$$q = F_0/c + \sum_{j=1}^{\infty} q_j.\tag{4.18}$$

When $jz = 1$ $(j\omega = k)$ the resonance of the harmonic j occurs; while $\kappa_{j*} = 1/(2\delta)$.

The solution (4.18) is mathematically accurate, but as the number of the summands in the Fourier series has to be limited to a finite number of harmonics j_{max}; therefore from the engineering perspective, it is an approximation. When choosing j_{max} we can take into account the following considerations. First of all, the most significant terms of the expansion F_j are to be considered. Secondly, to avoid severing the resonant mode, we should require $j_{max} > k/\omega + (1 \div 2)$.

Let us also note that the desire to maintain a large number of harmonics in Fourier series often creates an illusion of improvement in accuracy, as the accuracy of the determination of the higher harmonics is usually not much. Therefore this method of calculation of the forced oscillations is advisable for use in the problems of dynamics of the mechanisms without shocks, as well as in case of continuous and differentiable position functions, which have increased "smoothness". It is particular, for example, for the simple lever mechanisms and the cams, when during calculations you can limit yourself to a small number of harmonics.

The closed form of the solution In case of steady-state conditions $(t \to \infty)$, in accordance with (4.5), the free oscillations, due to the exponential factor, decay rapidly. At first glance, the same conclusion can be made about the accompanying oscillations. However, the latter is true only under the condition that the functions Π and W, and their derivatives do not have discontinuities. Otherwise accompanying oscillations are excited not only at $t = 0$, but also at times corresponding to these discontinuities.

Generalized coordinate q characterizing the oscillation process, in the example under consideration, directly describes the dynamic error of the output link, since the absolute coordinate of the output link is defined as $y = x + q$; accordingly, we have the dynamic errors in speed $\dot{q}$ and acceleration $\ddot{q}$.

The dynamic error q in this case, simultaneously characterizes the vibration activity of the mechanism, determined with reactive moment $M \approx cq\Pi'$, transmitted to the input link (here and below the prime means the derivative as per the angle of the input link φ).

Hereunder, we consider a number of typical cases of the determination of the dynamic errors.

Let us divide the time axis into segments, within which the functions $x = \Pi(\varphi)$ and $W(t)$ are continuous and differentiable. Then, for each section, the dependencies of type (4.4) are valid.

For example, for segment $i + 1$

$$q_i = e^{-n(t-t_i)}[C_{1i} \cos k(t - t_i) + C_{2i} \sin k(t - t_i)] + Y_{i+1}(t)(t > t_i). \qquad (4.19)$$

To determine the constants C_{1i} and C_{2i}, we use the conditions that the absolute coordinate $y = x + q$ and its derivative $\dot{y} = \dot{x} + \dot{q}$, preserve continuity on the borders of the intervals. Then

$$x_i^- + q_i^- = x_i^+ + q_i^+; \quad \dot{x}_i^- + \dot{q}_i^- = \dot{x}_i^+ + \dot{q}_i^+.$$

Here, the index "+" corresponds to the time moment $t_i + \varepsilon$ (ε is the infinitesimal), and the index "−" to $t_i - \varepsilon$. Thus, the conditions of the joining of solutions on the boundaries of the intervals can be written as follows:

$$q_i^+ = q_i^- - \Delta x_i; \, \dot{q}_1^+ = \dot{q}_i^- - \Delta \dot{x}_i, \qquad (4.20)$$

where $\Delta x_i = x_i^+ - x_i^-; \quad \Delta \dot{x}_i = \dot{x}_i^+ - \dot{x}_i^- = \omega(\Pi_i'^+ - \Pi_i'^-)$.

In order to identify the dynamic effects, associated with these discontinuities, we use the form of solutions in the shape of the series of derivatives of the perturbation function W, which is of particular interest in the problems of the synthesis of the laws of motion of the cam mechanisms. If we write the particular solution Y in integral form (4.6) and subject it to successive integration by parts, we get

$$Y^* \approx \sum_{m=1, \, 3, \, 5...}^{\infty} (-1)^{0.5(m-1)} w_{m(t)}, \qquad (4.21)$$

where

$$w_m = \frac{1}{k^{m+1}} \frac{d^{m-1}W}{dt^{m-1}}. \qquad (4.22)$$

Here Y^* is the new form of the particular solutions, from which the accompanying oscillations are completely eliminated (hereinafter the asterisk is omitted).

Using (4.20) and (4.21), we express the constants C_{1i} and C_{2i}:

$$C_{1i} = -\left[\Delta x_i + \sum_{m=1,3...}^{\infty} (-1)^{0.5(m-1)} \Delta w_{im}\right];$$

$$C_{2i} = -\left[\frac{\Delta \dot{x}_i}{k} + \sum_{m=2,4...}^{\infty} (-1)^{0.5m-1} \Delta w_{im}\right], \tag{4.23}$$

where $\Delta w_{im} = w_m(t_i + 0) - w_m(t_i - 0)$.

With (4.22) we get

$$q_i = D_i \exp[-n(t - t_i)] \sin[k(t - t_i) + \alpha_i], \tag{4.24}$$

where $D_i = \sqrt{C_{1i}^2 + C_{2i}^2}$; $\sin \alpha_i = C_{1i}/D_i$; $\cos \alpha_1 = C_{2i}/D_i$.

Hereinafter, for reasons of simplicity, we will call the amplitude D_i as *jump*.

In case of $\omega < k$ series as per m (4.21), (4.23) usually converge rapidly. In particular if the function $W(t)$ is represented as a polynomial, these series have a finite number of members. The sources of the accompanying oscillations, is clearly identified in these dependences, which enables us, during dynamic synthesis, to take measures for decreasing vibration activity.

Apart from the described analytical method of establishing a solution (4.24), we can also perform the integration of the original differential equation (4.2) using numerical methods (such as the Runge-Kutta method) with mandatory adherence to the conditions of (4.20).

Analyzing the formula (4.19), it is easy to see that on the one hand, the system is periodically excited by external disturbances and on the other hand, there is a constant outflow of energy due to the dissipative forces that reduce the level of oscillations. When $\omega = const$, as a result of the impact of these two factors (strictly speaking, when $t \to \infty$, and practically fast enough) there is some steady oscillatory mode, which we need to describe.

The most natural way to determine the dynamic errors in this case, at first glance, is the integration of the original differential equation until reaching the steady state. However, such approach, while using the numerical methods, usually leads to significant accumulated errors and increased working time for the calculation. Therefore we use the more accurate and economical method for composing the closed form of the solution.

Let us investigate the behavior of the oscillating system in an arbitrary period $\tau = 2\pi/\omega$. Taking as zero the beginning point for given period, we represent the solution of (4.22) as follows

$$q = q^0(C_1, C_2, t) + Y^0(t), \tag{4.25}$$

where $q^0 = e^{-nt}(C_1 \cos kt + C_2 \sin kt)$; $Y^0(t)$ is particular solution with zero initial conditions.

We should note that in this case we do not know the initial conditions, since the given period, under steady regime, is preceded by an infinite number of periods.

Integrating the original differential equation (4.2), with zero initial conditions, on the basis of (4.5) we obtain $Y(t) = Y^0(t)$ (here, as well as using the Duhamel's formula $Y^0(0) = 0$; $\dot{Y}^0(0) = 0$; with $q^0(0, 0, t) = 0$).

When in transition to the next cycle, due to the conditions of periodicity $y(0) = Y(\tau)$ and $\dot{y}(0) = \dot{y}(\tau)$, therefore on the basis of dependencies (4.23) and (4.25) we have

$$q^0(C_1, C_2, 0) = q^0(C_1, C_2, \tau) + Y^0(\tau) - \Delta x_0;$$
$$\dot{q}^0(C_1, C_2, 0) = \dot{q}^0(C_1, C_2, \tau) + \dot{Y}^0(\tau) - \Delta \dot{x}_0. \tag{4.26}$$

As the values of $Y^0(\tau)$ and $\dot{Y}^0(\tau)$ are already known, we only need to solve the resulting system of algebraic equations with respect to the two unknowns C_1, C_2.

To better illustrate this procedure, we first take $n = 0$. In this case the system (4.26) becomes

$$C_1 = C_1 \cos kt + C_2 \sin kt + Y^0(\tau) - \Delta x_0;$$
$$kC_2 = -C_1 \sin kt + C_2 k \cos kt + \dot{Y}^0(\tau) - \Delta \dot{x}_0. \tag{4.27}$$

After solving this system of equations, we get

$$C_1 = \frac{Y^0(\tau) - \Delta x_0}{2} + \frac{\dot{Y}^0(\tau) - \Delta \dot{x}_0}{2k} \cot \frac{k\tau}{2};$$
$$C_2 = \frac{\dot{Y}^0(\tau) - \Delta \dot{x}_0}{2k} + \frac{Y^0(\tau) - \Delta x_0}{2} \cot \frac{k\tau}{2}. \tag{4.28}$$

At $k\tau/2 = j\pi (j = 1, 2, \ldots)$ that corresponds to $j\omega = k$, we get $C_1 \to \infty$, $C_2 \to \infty$.

When $n \neq 0$ after similar, though more cumbersome, conversions and some simplifications, we get

$$C_1 = \frac{[Y^0(\tau) - \Delta x_0](1 - e^{-9N} \cos 2\pi N) + [\dot{Y}^0(\tau) - \Delta \dot{x}_0]k^{-1}e^{-9N} \sin 2\pi N}{1 - 2e^{-9N} \cos 2\pi N + e^{-29N}};$$
$$C_2 = \frac{[\dot{Y}^0(\tau) - \Delta \dot{x}_0]k^{-1}(1 - e^{-9N} \cos 2\pi N) - [Y^0(\tau) - \Delta x_0]e^{-9N} \sin 2\pi N)}{1 - 2e^{-9N} \cos 2\pi N + e^{-29N}}, \tag{4.29}$$

where $N = k/\omega$; ϑ is the logarithmic decrement.

Thus the initial conditions, corresponding to the steady oscillatory regime, are found:

$$q_0 = C_1; \dot{q}_0 = C_2 k - C_1 n = k(C_2 - C_1\delta) \approx kC_2 (\delta = n/k \ll 1). \tag{4.30}$$

Repeating the procedure of integration with these initial conditions, we find the final solution $q(t)$, determining the dynamic error.

Fig. 4.5 Factors of accumulation of disturbances
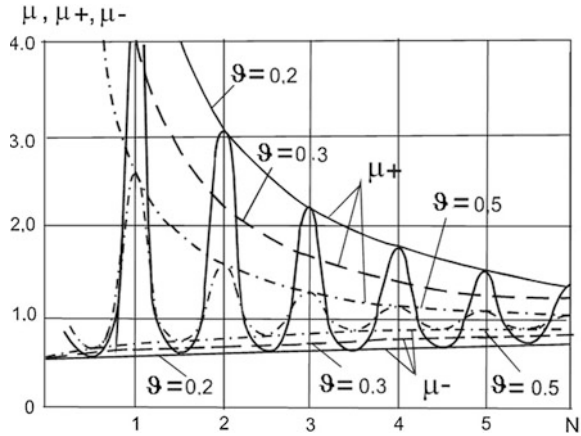
In accordance with (4.29), the amplitude of the accompanying oscillations, in the beginning of the cycle, is equal to:

$$D_0 = \sqrt{C_1^2 + C_2^2} = \mu\sqrt{[Y^0(\tau) - \Delta x_0]^2 + k^{-2}[\dot{Y}^0(\tau) - \Delta \dot{x}_0]}, \qquad (4.31)$$

where μ is the coefficient of accumulation of disturbances, determined as follows:

$$\mu = \frac{1}{\sqrt{1 - 2e^{-9N}\cos 2\pi N + e^{-29N}}}. \qquad (4.32)$$

The family of curves $\mu(N, \vartheta)$, where $N = k/\omega_0$, ϑ, is the logarithmic decrement, shown in Fig. 4.5. The coefficient μ can either be greater than one (the growth of the oscillations) or less than one (the attenuation of the oscillations).

The maximum value of μ^+ lies in the vicinity of integers N, and the minimum value of μ^-, when $2N$ is an odd number. From formula (4.32), it follows that:

$$\mu^+ = [1 - \exp(-9N)]^{-1}; \quad \mu^- = [1 + \exp(-9N)]^{-1}. \qquad (4.33)$$

The coincidence of phase of the earlier excited oscillations and the oscillations in the considered cycle correspond to the value μ^+; in case of $\mu = \mu^-$ these oscillations are in the opposite phase. The analysis of this important dynamic criterion is presented below.

Let us highlight the important feature of this method, associated with the possibility of the rational combination of numerical and analytical methods: numerical integration is used here only to determine the particular solution for the limited period of time; the conditions that correspond to the approach to the steady regime are found analytically. The last one significantly affects the accuracy of the solution. Of course, in case of relatively simple excitation functions, the closed form of the solutions can be obtained without using the numerical methods, directly using

solution (4.5) taking into consideration (4.29) and the analytical form of particular solution. The use of the combination of the numerical and analytical methods is especially useful in cases, where the geometric transfer functions or external forces have discontinuities, which is usually characteristic for the cam mechanisms.

4.1.3 Vibration Activity and Dynamic Errors

Preliminary notes *The vibration activity* of the mechanism is defined by the vibration load transmitted from the mechanism to the machine drive and through the supports to the body. A decrease in the vibration activity of the mechanical systems and dynamic errors is one of the central problems of dynamic synthesis, the solution of which significantly determines the productivity and technical perfection of the machine equipment. The study of this problem is developed in several directions. One of the first such directions is related to the rational synthesis of the laws of motion, which display optimum properties, on the basis of selected dynamic criterion (see Sect. 1.3).

Initially the dynamic criteria were totally based on the kinetostatic model that does not take into account the elasticity of the links and the related oscillatory processes. In this case the dynamic task was completely reduced essentially to a geometric one. With the growth of the operating speeds of machines, the limitations of this approach began to surface. Indeed, as follows from (4.1), (4.2), the characteristics of the laws of motion are included in the right-hand side of the equations and they largely define the excitation function $W(t)$ and consequently, the excited oscillations. A decrease in the excitation function can also be achieved through the installation of special unloading devices (see Sect. 4.3).

Another line of dynamic synthesis is associated with the reduction of the dynamic errors, through the focused change of the parameters of the oscillating system.

We should keep in mind that the solution for any of the particular problems of reduction in vibration activity often has a local character and sometimes is associated with an increase in vibrations in the other parts of the system. So, for example, the balancing of the mechanism with counterweights increases the variable portion of the inertial moment with all the associated negative consequences. Therefore it is very important for the engineer to adopt the integrated approach to the solving the problem, enabling in each case to find a compromise of a solution.

Sources of excitation of the accompanying oscillations First we define the accompanying oscillations associated with discontinuities of the functions $x = \Pi(\varphi)$, $\dot{x} = \Pi'(\varphi)\omega$, W at the moment in time $t = t_i$ on the border of the two intervals i and $i + 1$. As it was stated above, the oscillations on the interval $i + 1$ in

Table 4.1 Discontinuities of the geometric characteristics of the cyclic mechanism

Type of jump	D	$|\Delta\ddot{q}|_{max}$	α_1	α_2
$\Delta\Pi \neq 0$	$|\Delta\Pi|$	$k^2|\Delta\Pi|$	$3\pi/2$	$\pi/2$
$\Delta\Pi' \neq 0$	$\omega|\Delta\Pi'/k|$	$k\omega|\Delta\Pi'|$	π	0
$\Delta\Pi'' \neq 0$	$\omega^2|\Delta\Pi''|/k^2$	$\omega^2|\Delta\Pi''|$	$\pi/2$	$3\pi/2$
$\Delta\Pi''' \neq 0$	$\omega^3|\Delta\Pi'''|/k^3$	$\omega^3|\Delta\Pi'''|/k$	0	π

Note If the considered value of $\Delta\Pi$, $\Delta\Pi'$, $\Delta\Pi''$, or $\Delta\Pi'''$ is positive, then $\alpha = \alpha_1$; otherwise $\alpha = \alpha_2$.

this case are described with (4.19). The maximum value of additional accelerations caused by the jump D_i is equal to

$$|\Delta\ddot{q}_i|_{max} = k^2 D_i. \tag{4.34}$$

The influence of the discontinuities of the geometric characteristics on the values of D, α $|\Delta\ddot{q}|_{max}$ is determined using (4.21)–(4.24). For the cyclic mechanisms the most important jumps are specified in the Table 4.1 (here and hereafter the index i is omitted). Each row in the table corresponds to the discontinuities of only one response; while other functions are assumed to be continuous. Following are some explanations regarding the considered in Table 4.1 typical cases.

Discontinuity of the position function $\Delta\Pi$ This case in pure form may not be implemented, but it is close to the case of the stepped cam profile, occurring due to errors of fabrication. As the maximum additional acceleration is proportional to the square of the natural frequency, even a small jump of $\Delta\Pi$ can cause significant distortion of the given law of change in acceleration of $\ddot{x} = \Pi''(\varphi_1)\omega_0^2$. The observed effect, in this case, is similar to the effect of driving on a cobblestone street.

Discontinuity of the first geometric transfer function $\Delta\Pi'$ **("hard impact")** Dynamic effects of the hard impact increase with increase in the angular velocity of the input link ω_0 and the value of the natural frequency. Hard impacts occur not only with the abrupt change of the function Π', but with impacts, accompanying the adjustment of the clearances, connections of kinematic circuits with couplings, in case of locking of actions of some intermediate positions of the output link and in a number of other cases.

Discontinuity of the second geometric transfer function $\Delta\Pi''$ **("soft impact")** **(Fig. 4.6a)** In this case the maximum of the additional accelerations, caused by the jump in $\Delta\Pi''$, is approximately equal to the value of this jump, which leads to the significant distortion of the given program characteristics. For example Fig. 4.7 shows the accelerations of $\ddot{x}(t)$, changing in the program motion under the cosine law (curve 1) and $\ddot{y}(t) = \ddot{x}(t) + \ddot{q}(t)$ taking into consideration the excited vibrations (curve 2).
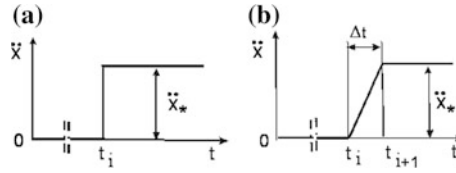
Fig. 4.6 Analysis of the effects of discontinuity of geometric characteristics
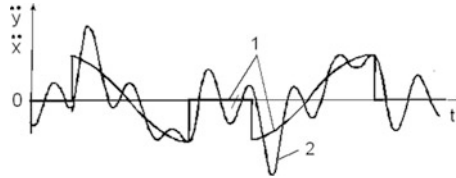
Fig. 4.7 Distortion of the ideal accelerations under the harmonic law of motion

Discontinuity of the third geometric transfer function $\Delta\Pi'''$ In this case there is a jump of the derivative $\dddot{x}(t) = \omega_0^3 \Pi'''$, called the second-order acceleration or jerk. Since the maximum additional acceleration unlike the case of the "hard" impact is inversely proportional to the natural frequency k; therefore the increase in rigidity leads to a positive effect.

The abrupt change in the function Π'' **(the equivalent jump)** We will discuss this problem using an example of the abrupt jump in acceleration of program motion $\ddot{x} = \Pi''\omega_0^2$ as per the linear fashion (Fig. 4.6b). We will show that for sufficiently small value of $\Delta t = t_{i+1} - t_i$ the system will respond to the changes in $\ddot{x}$ in much the same manner, as in case of the abrupt change of this function. First we will determine the accompanying oscillations q_*, caused at the interval $t > t_{i+1}$ by the two jumps $\Delta\Pi'''$ when $t = t_i$ and $t = t_{i+1}$, using (4.24):

$$q_* = \Delta q_i + \Delta q_{i+1} = D_i \exp[-n(t - t_i)] \sin[k(t - t_i) + \alpha_i]$$
$$+ D_{i+1} \exp[-n(t - t_{i+1})] \sin[k(t - t_{i+1}) + \alpha_{i+1}]. \tag{4.35}$$

In accordance with the formulae of Table 4.1

$$D_i = D_{i+1} = |\Delta\ddot{x}|/k^3 = \ddot{x}_* /(k^3 \Delta t); \quad \alpha_i = 0; \quad \alpha_{i+1} = \pi.$$

Hence, assuming $t_i = 0$ we have

$$q_* = \ddot{x}_*(k^3 \Delta t)^{-1} \exp[-n(t - \Delta t)][\exp(-n\Delta t) \sin kt - \sin k(t - \Delta t)].$$

Since $n\Delta t$ is small, for the purpose of simplification, we accept $\exp(-n\Delta t) \approx 1$.

Then

$$q_* = \ddot{x}_*(k^3 \Delta t)^{-1} \exp[-n(t - \Delta t)][\sin kt(1 - \cos k\Delta t) + \cos kt \sin k\Delta t.$$

Omitting the elementary transformations, we obtain

$$q_* = D_* \exp[-n(t - \Delta t)] \sin(kt + \alpha).$$

Here D_* is the equivalent jump defined as follows:

$$D_* = \ddot{x}_* \, \kappa^0(v)/k^2, \tag{4.36}$$

where $\kappa^0(v) = |\sin \pi v|/(\pi v)$; $v = \Delta t/T$; $T = 2\pi/k$. Hence when $t > t_{i+1}$,

$$|\ddot{q}_*|_{\max} \approx k^2 D_* = \ddot{x}_* \, \kappa^0(v). \tag{4.37}$$

When $v = 0$, we have $\kappa^0 = 1$, which corresponds to the soft stroke. When $v > 0$ accordingly $\kappa^0(v) < 1$. So this parameter is the measure of the softening of the dynamic effect, as compared to the soft stroke.

In the graph $\kappa^0(v)$ (Fig. 4.8) the curve $\delta = 0$ corresponds to the considered case that matches the above accepted assumption $\exp(-n\Delta t) \approx 1$. This means that within the period of time Δt we have neglected the damping of oscillation. When $\delta = 9/(2\pi) \neq 0$ (9 is the logarithmic decrement), the curves $\kappa^0(v)$ are located below with the exception of the small areas in the vicinity of integers v. This indicates that the resistance forces generally soften the dynamic effect of the abrupt change in the ideal acceleration $\ddot{x}$.

From the graphs $\kappa^0(v)$ it also follows that in case when $v \leq 0.25$, *the dynamic effect of the continuous change of the transfer function is practically equivalent to the effect of the jump*. It is illustrated in Fig. 4.9 with some graphs $\ddot{y}(t)$ in case of the

Fig. 4.8 Cushioning factor
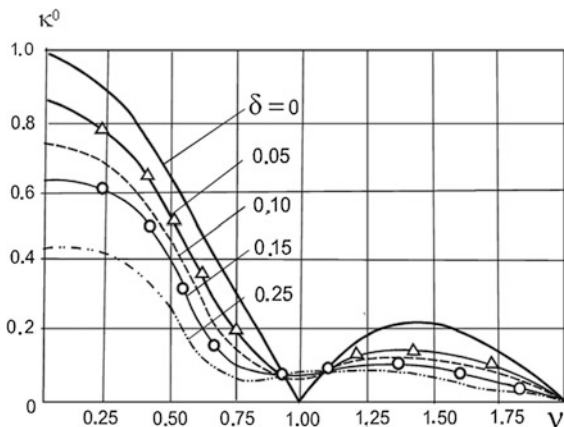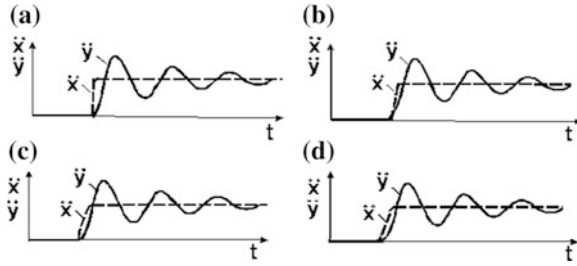
Fig. 4.9 Dynamic effect in case of abrupt changes in the program accelerations

soft impact i.e. at $\nu = 0$ (Fig. 4.9a) and in case of abrupt change of the $\ddot{x}(t)$ ($\nu = 0.25$) for the three cases: $\ddot{x}(t)$ varies linearly Fig. 4.9b; according to $\ddot{x}(t) = \ddot{x}_{\max} \sin 0.5\pi t/\Delta t$ (Fig. 4.9c) and in accordance with the law $\ddot{x} = \ddot{x}_{\max} 0.5(1 - \cos \pi t / \Delta t)$ (Fig. 4.8).

This effect once again manifests the impossibility of reducing the dynamic problem to the geometric one. In other words, it is impossible to suggest a law of motion, which would be the optimum in all cases, regardless of the frequency characteristics of the mechanism.

In case of large values of ν the coefficient $\kappa^0(\nu)$ decreases abruptly ($\kappa^0 \leq 1/(\pi\nu)$). The points $\nu = j\pi$ $(j = 1, 2, \ldots)$, in which $\kappa^0 \approx 0$ are of interest, in the graph $\kappa^0(\nu)$. These modes, corresponding to the so-called *quasi-static loading*, arise due to the mutual compensation of oscillations, caused by both the jumps of $\Delta\Pi'''$. The presence of the force of resistance, however, only leads to their partial compensation.

As per the current law of acceleration ("modified trapezoid"), there are no jumps of accelerations (see Sect. 1.2.2). Thus $\Delta\Pi'' = 0$, however, $\Delta\Pi''' \neq 0$. It can be shown that in this case

$$|\ddot{q}_*|_{\max} \approx \Delta w_* \kappa^0(\nu), \tag{4.38}$$

where $\Delta w_* = |w|_{\max}$ is the maximum value of the drop in acceleration in the program motion, $\nu = \Delta\varphi_i N/(2\pi), N = k/\omega; \Delta\varphi_i = s_i\varphi_i$ (see Sects. 1.2.2 and 1.2.3).

According to (4.38) the function $\kappa^0(\nu)$ determines the maximum value of the additional accelerations from one "equivalent jump." At $\nu = 0$ we have $\kappa^0 = 1$, which corresponds to the soft impact. In case of $\nu > 0$ accordingly $\kappa^0(\nu) < 1$, therefore this parameter is the index of the cushioning of the dynamic effect, as compared to the soft impact (see the example). For the law of motion called "modified trapezoid"

$$\kappa^0 = \frac{\sqrt{1 + 16\nu^2 - 8\nu \sin 2\pi\nu}}{|1 - 16\nu^2|}. \tag{4.39}$$

Fig. 4.10 Graph $\kappa^0(v)$ for law of acceleration "modified trapezoid"
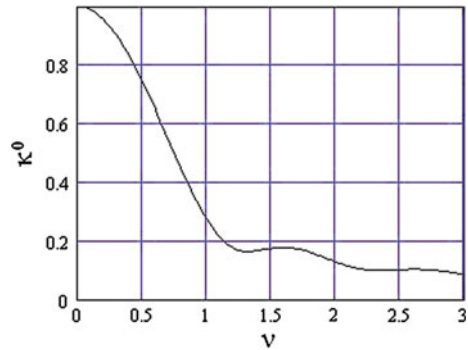
The analysis of the graph of the function $\kappa^0(\vartheta)$ (Fig. 4.10) shows that when $\vartheta < 0.25 \div 0.3$ the value of κ^0 is not very different from one, and when $\vartheta \geq 2$ it does not exceed 0.13. This condition can be used to rationally choose the parameters s_j and N.

Taking guide from the above considerations, the reduction of the maximum acceleration in the cam mechanism can be achieved to some extent through the adjustment of the law of motion. For one period 2π the second transfer function Π'' contains eight intervals, the relative value of which is determined by the parameter v_j.

When we define the condition $v_j \geq [v] = 2 \div 3$ (see Fig. 4.10), then in accordance with (4.38)

$$N \geq N_v = 2\pi \frac{[v]}{\Delta\varphi_i s_j}. \tag{4.40}$$

Here $\Delta\varphi_i$ are the angles of rotation of the input link, corresponding to the intervals of run-in and run-out at the direct and reverse strokes.

Thus, the conditions of (4.40), eliminate the possibility of significant vibration excitation in each cycle. This can be achieved by correcting the law of motion (parameter s_j) and the frequency criterion N. At the same time we should keep in mind that at each interval $s_1 + s_2 \leq 1$.

If the given conditions cannot be implemented on the basis of the law of motion, it is necessary to decrease ω (i.e. the machine's productivity) or increase its natural frequency.

For lever mechanisms the physical prerequisites for the excitation of the accompanying oscillation are the same as described above, but suppression of vibration is difficult, because of the limited capacity for the synthesis of the law of motion. At the same time, the laws of motion for the links of the lever mechanisms are described with "smoother" functions, so the accompanying oscillations often occur due to collisions in the clearances (see Chap. 7).

Restricting the accumulation of disturbances As the kinematic characteristics have the period $\tau = 2\pi/\omega_0$, where ω_0 is the angular velocity of the input link (cam),

the sum of the oscillations, excited by the identical jumps, must also be a periodic function. Therefore to evaluate the resulting mode, we can again use the closed form of solution, based on the conditions of the periodicity (see Sect. 4.1.2). Thus in accordance with (4.31) and (4.33) taking into account the jumps in the preceding cycles leads in the considered cycle to the jump D_1 transforming into μD_1, where μ is the coefficient of the accumulation of disturbances and the maximum additional acceleration, caused by this abrupt jump is determined as follows:

$$\sum_{i=1}^{\infty} |\Delta \ddot{q}_1|_{\max} = k^2 \mu D_1. \tag{4.41}$$

In case of dynamic synthesis, to restrict the level of the accompanying oscillations, it is advisable to accept $\mu < [\mu]$, where $[\mu]$ is the allowable value of the coefficient of accumulation of disturbances. Then on the basis of (4.32)

$$1 - 2 \exp(-\vartheta N) \cos 2\pi N + \exp(-2\vartheta N) < [\mu]^{-2}. \tag{4.42}$$

This inequality should be solved with respect to the frequency criterion N. For more evident results let us take $[\mu] = 1$. Then

$$0.5 \exp(-\vartheta N) < \cos 2\pi N. \tag{4.43}$$

In case of $\vartheta N \to 0$ the inequality (4.43) is satisfied when $N < E - 1/6$ or when $N > E + 1/6$, where E is an integer. In another limiting case, where, $N < E - 1/4$ or $N > E + 1/4$.

The resulting frequency tuning is practically effective only for smaller values of N (approximately $N < 4 \div 6$). Let us illustrate this with a simple example. Let $k = 170\,\text{s}^{-1}$; $\omega = 20\,\text{s}^{-1}$. Thus $N = k/\omega = 8.5$. This value corresponds to $\mu^- < 1$. However, when to reduce the speed of rotation just about to $1.1\,\text{s}^{-1}$ (which is quite possible in the real conditions), such as $N = 9$; for integer values of N we have $\mu = \mu^+ > 1$, therefore the level of vibrations is increased. Thus in this case the frequency criterion was not a reliable one. In such cases it is more appropriate to require $\mu^+ < [\mu]$, taking $[\mu] = 1 + [\Delta\mu]$, where $[\Delta\mu]$ is the small positive addition (for example, $[\Delta\mu] < 0.05 \div 0.1$). Then on the basis of (4.33) we get

$$N > \vartheta^{-1} \ln \frac{1 + [\Delta\mu]}{[\Delta\mu]}. \tag{4.44}$$

At $\vartheta N > 3$ we have $0.96 < \mu < 1.04$; it means that excited accompanying oscillations are practically damped for the duration of one revolution of the input link.

Let us note here that the limiting condition $\mu < [\mu]$ is highly desirable even in case of elimination of the obvious reasons of excitation of the accompanying oscillations, because the periodic disturbances, caused by random factors, are always there.

These disturbances are not included in the engineering calculations, which in case of having large values of μ can significantly increase the intensity of oscillations.

Engineering recommendations for dynamic synthesis of the cam mechanisms, taking into account the excited oscillations Based on the above mentioned analysis, the following conditions, which exclude the possibility of significant distortion of the kinematic characteristics of the given program motion, can be summarized as follows:

1. The discontinuities in position function $\Pi(\varphi)$ and in first and second transfer functions $\Pi'(\varphi) = d\Pi'/d\varphi$ and $\Pi''(\varphi) = d^2\Pi/d\varphi^2$ should be eliminated.
2. Since in case of small values of $\nu = \Delta t / T$ $(\nu < 0.25)$ the smooth change in acceleration is practically equivalent to soft impact, acceptable should be (with allowance) $\Delta t > (2 \div 3)T$, where $T = 2\pi / k$ is the period of free oscillations.
3. In order to restrict the dynamic effect of oscillations, excited during the previous cycles of motion, the maximum value of the coefficient of accumulation of disturbances μ^+ should be restricted. In particular, when $[\mu] < 1.1$, it is necessary to require that $N = k/\omega_0 > 2.4\vartheta^{-1}$. If, for example, $\vartheta = 0.2$, then the natural frequency k should be at least 12 times higher than the angular velocity of the cam ω.

During the process of rational dynamic synthesis of the laws of motion, taking into account the oscillations, there occurs a problem with opposite tendencies of effect of duration of transitional sector of the diagram of acceleration, determined by parameter s_j. On the one hand in case of an increase in s_j the value of $|\Pi''|_{max}$ increases due to the reduction in the fill factor (see Sect. 1.2.3), on the other hand, the average $\kappa^0(\vartheta)$ decreases. In such cases we can decisively select this parameter, providing the minimum value of $|\Pi''|_{max}(1 + \mu\kappa^0)$.

It should be noted, however, that the range of possible control by setting the parameter s_j is relatively small $(s_j \approx 0.15\ldots0.35)$. Relying on (4.34) we can formally conclude that in the acceleration function of the output link, we should eliminate the jump of derivatives of the highest possible order. We know various laws of motion, described by polynomials, which satisfy this requirement for derivatives of up to the fifth order and above. However, the practical use of these laws poses at least two risks. First of all, the elimination of the jump of derivatives does not exclude the possibility that the equivalent effect can remain in case of an abrupt change of the derivative; it can be reflected in corresponding value of the equivalent jump (see above). In addition, the higher the order of the derivative of the function $\Pi(\varphi)$, which is converted to zero at the beginning and end of the phase of motion, the more the levels of the graph of function $\Pi(\varphi)$ "spread" when approaching the extreme points (Fig. 4.11).

Let us assume that the accuracy of manufacturing determines some strips of width Δ, within the limits of which the value of the function Π is not guaranteed. Then in principle it is possible that the angle of rotation, corresponding to the working stroke, can be reduced from φ_x to φ_x^*. This can lead to the substantial increase in the value of Π''_{max}, as it is inversely proportional to the square of the
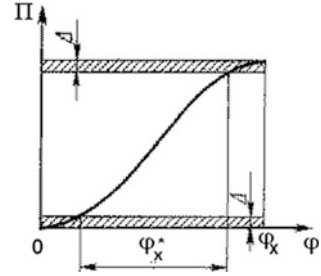
corresponding phase angle. Furthermore there can be impacts at the beginning and the end of the cycle. We can accordingly conclude: the smoother the curve $\Pi(\varphi)$ approaching towards the extreme values or, in other words, the higher the order of the derivative, converting at these points into zero, the stricter should be the technological requirements for reproduction of the given characteristics. Otherwise we create a false and harmful illusion of an optimum solution of the dynamic problem. This example is another clear demonstration of the importance of a comprehensive approach to solving the modern problems of machines' mechanics.

The mechanisms with unilateral constraints are widely used in modern machines, in which for the prevention of the loss of contact in the kinematic pairs the forced closure is used, which is implemented by means of springs. The spring closures are mostly seen in cam mechanisms, however, the terminal springs are often installed in links of lever, cam-lever and other mechanisms to partially or completely prevent the inter-mating of the working surfaces of the kinematic pairs, taking place during the changeovers in the clearances. This problem will be discussed in detail in Sect. 5.6.

4.2 Forced Vibrations of the Systems, with Finite Number of Degrees of Freedom

4.2.1 Harmonic Excitation

Discarding the dissipative forces, we get the system of differential equations, which looks like:

$$\mathbf{a}\ddot{\mathbf{q}} + \mathbf{c}\mathbf{q} = \mathbf{F}\cos \omega t, \tag{4.45}$$

where $\mathbf{a}, \mathbf{c}$ are the square matrices of the inertial and quasi elastic coefficients; $\mathbf{q}, \ddot{\mathbf{q}}, \mathbf{F}$ are vector-functions of the generalized coordinates, generalized accelerations and amplitudes of harmonic generalized forces. Accepting $\mathbf{q} = \mathbf{A}\cos \omega t$, where $\mathbf{A}$ is

the amplitude vector, after substitution in (4.45) we obtain the linear system of algebraic equations

$$(\mathbf{c} - \mathbf{a}\omega^2)\mathbf{A} = \mathbf{F}. \tag{4.46}$$

The roots of which are the sought-for amplitudes of the forced oscillations. Let us recall here that Eq. (4.46), when $\mathbf{F} = \mathbf{0}$, describes the free oscillations. Hence when $\mathbf{A} \neq \mathbf{0}$ and replacing ω with the "natural" frequency k, the condition $\det(\mathbf{c} - k^2\mathbf{a}) = \mathbf{0}$ or next matrix equation $(\mathbf{a}^{-1}\mathbf{c} - k^2\mathbf{E}) = \mathbf{0}$, where $\mathbf{E}$ is the identity matrix; $\mathbf{a}^{-1}$ is the inverse matrix of inertial coefficients, should be satisfied. As per the theory of matrix, it follows that the parameters $k_1^2, \ldots, k_H^2$ are the eigenvalues of the matrix $\mathbf{a}^{-1}\mathbf{c}$, and shape factors are the eigenvectors of this matrix. When $\omega = k_r$ without taking into account the dissipation, $A \to \infty$ (resonance).

In order to clarify the features of the forced vibrations of the systems with finite number of degrees of freedom, we will consider the machine's drive (Fig. 4.12). The drive consists of the motor D, connected using an elastic coupling with the main shaft, out of which S mechanisms branch-out. Each mechanism is displayed as a sub-system with one degree of freedom. The harmonic forcing moment $M = M_1 \cos \omega t$ is applied to the main shaft.

We will write the expressions for kinetic and potential energies, taking the deformations of the elastic elements as the generalized position coordinates q_i $(i = 1, \ldots, H)$.

Let us exclude, the cyclic coordinate $q_0 = \omega_0 t$, equal to the angle of rotation of motor, from consideration during the analysis of steady oscillations (see item 3.2).

$$T = 0.5[J_1\dot{q}_1^2 + \sum_{j=2}^{H} J_j(\dot{q}_1 + \dot{q}_j)^2];$$

$$V = 0.5\sum_{i=1}^{H} c_i q_i^2.$$

Then $a_{11} = \sum_{i=1}^{H} J_i$; $a_{1j} = J_j$; $a_{jj} = J_j$ when $j = 2, \ldots, H$; $c_{ii} = c_i$ (the remaining coefficients are zero). The system of differential equations has the form
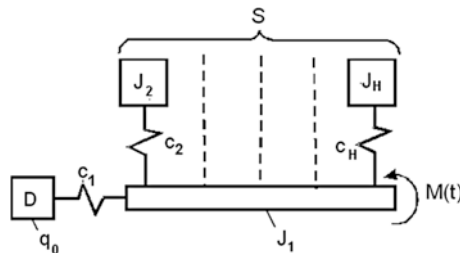
Fig. 4.12 Dynamic model with the finite number of degrees of freedom

$$
\left.
\begin{aligned}
&a_{11}\ddot{q}_1 + \sum_{j=2}^{H} a_{1j}\ddot{q}_j + c_{11}q_1 = M_1 \cos \omega t; \\
&a_{21}\ddot{q}_1 + a_{22}\ddot{q}_2 + c_{22}q_2 = 0; \\
&\cdots \\
&a_{H1}\ddot{q}_1 + a_{HH}\ddot{q} + c_{HH}q_H = 0.
\end{aligned}
\right\} \qquad (j = 2, \ldots, H). \qquad (4.47)
$$

After substitution of solution $q_i = A_i \cos \omega t$ in (4.47) we get

$$
\left.
\begin{aligned}
&(c_1 - \omega^2 a_{11})A_1 - \omega^2 \sum_{j=2}^{H} a_{1j}A_j = M_1; \\
&\cdots \\
&- \omega^2 a_{j1}A_1 + (c_j - a_{jj}\omega^2)A_j = 0
\end{aligned}
\right\} \qquad (j = 2, \ldots, H). \qquad (4.48)
$$

From the last $H - 1$ equations we express A_j in terms of A_1

$$
A_j = \frac{\omega^2 a_{j1}}{c_j - a_{jj}\omega^2} A_1 \qquad (4.49)
$$

and substituting (4.49) in the first equation of the system (4.48), we determine A_1

$$
A_1 = M_1 \left\{ c_1 - \omega^2 \left[\sum_{i=1}^{H} J_i + \sum_{j=2}^{H} \frac{J_j\omega^2}{c_j - J_j\omega^2} \right] \right\}^{-1}; \qquad (4.50)
$$

According to (4.50) $A_1 \to \infty$, when the denominator converts to zero; at the same time $\omega = k_r$ i.e. to the "natural" frequencies of the system that corresponds to the *resonant modes.* In case of $c_j - J_j\omega^2 = 0$, (i.e. when the frequency of the driving force is equal to the partial frequency $\omega = p_j = \sqrt{c_j/J_j}$) the denominator of the expression (4.50), enclosed in curly braces, increases indefinitely. This case, where $A_1 \to 0$, is called *anti-resonance.*

The typical AFC is shown in Fig. 4.13. Let us observe here that for the identical mechanisms $(c_j = c; J_j = J)$, the considered drive has two distinct natural
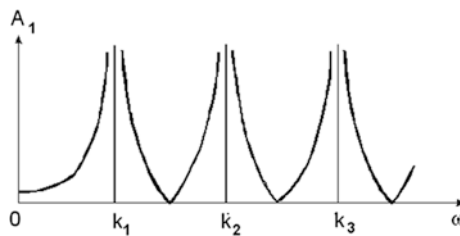
Fig. 4.13 Amplitude-frequency characteristic

frequencies and $H - 2$ identical natural frequencies $k_r = p = \sqrt{c/J}$, which in case of $H > 3$, turnout to be multiples.

However, the multiplicity of the frequencies, due to the structure of the quadratic forms, does not lead in this case to the anomalous solutions, associated with the emergence of the so-called "secular" members, whose amplitude increases infinitely. Although in this case the number of distinct roots, in the working frequency range reduces, the multiple frequencies often give the negative effect, as in this case there is an occurrence of beats and the overall vibration activity of the drive increases.

4.2.2 Normal Coordinates

Let us consider the oscillation system with two degrees of freedom, and shift from the original generalized coordinates q_1 and q_2 to the new coordinates θ_1 and θ_2. Then after substituting in the second-kind Lagrange equations with $H = 2$ and $A_{ik} = a_{ik} = $ const we have

$$
\left.
\begin{aligned}
T &= 0.5\left[a_{11}(\dot\theta_1 + \dot\theta_2)^2 + a_{22}(\beta_1\dot\theta_1 + \beta_2\dot\theta_2)^2 + 2a_{12}(\dot\theta_1 + \dot\theta_2)(\beta_1\dot\theta_1 + \beta_2\dot\theta_2)\right] \\
&= 0.5\left(a_1\dot\theta_1^2 + a_2\dot\theta_2^2 + 2a_*\dot\theta_1\dot\theta_2\right); \\
V &= 0.5\left[c_{11}(\theta_1 + \theta_2)^2 + c_{22}(\beta_1\theta_1 + \beta_2\theta_2)^2 + 2c_{12}(\theta_1 + \theta_2)(\beta_1\theta_1 + \beta_2\theta_2)\right] \\
&= 0.5\left(c_1\theta_1^2 + c_2\theta_2^2 + 2c_*\theta_1\theta_2\right).
\end{aligned}
\right\}
$$
(4.51)

It is assumed here that:

$$
\left.
\begin{aligned}
a_1 &= a_{11} + 2\beta_1 a_{12} + \beta_1^2 a_{22}; \\
a_2 &= a_{11} + 2\beta_2 a_{12} + \beta_2^2 a_{22}; \\
c_1 &= c_{11} + 2\beta_1 c_{12} + \beta_1^2 c_{22}; \\
c_2 &= c_{11} + 2\beta_2 c_{12} + \beta_2^2 c_{22}.
\end{aligned}
\right\}
$$
(4.52)

$$
\left.
\begin{aligned}
a_* &= a_{11} + (\beta_1 + \beta_2)a_{12} + \beta_1\beta_2 a_{22}; \\
c_* &= c_{11} + (\beta_1 + \beta_2)c_{12} + \beta_1\beta_2 c_{22}.
\end{aligned}
\right\}
$$
(4.53)

Let us assume the coefficients β_1 and β_2 as two unknown parameters in the system of equations obtained from (4.53) when $a_* = 0$ and $c_* = 0$. To solve this system of equations we use the substitution of $\beta_1 + \beta_2 = y_1$, $\beta_1\beta_2 = y_2$. Then,

$$y_1 = \frac{a_{22}c_{11} - a_{11}c_{22}}{a_{12}c_{22} - a_{22}c_{12}}; \quad y_2 = \frac{a_{11}c_{12} - a_{12}c_{11}}{a_{12}c_{22} - a_{22}c_{12}}.$$

On the basis of the Viet formulae, we write the following quadratic equation $\beta^2 - y_1\beta + y_2 = 0$, the roots of which are the sought-for values β_1 and β_2. We can show that these roots are the form factors.

Next substituting (4.51) in the Lagrange Eq. (3.5), we have

$$\left.\begin{array}{l} a_1\ddot{\theta}_1 + c_1\theta_1 = P_1; \\ a_2\ddot{\theta}_2 + c_2\theta_2 = P_2. \end{array}\right\} \tag{4.54}$$

The new dependencies for the generalized forces are easily determined from the balance of works on the virtual displacements: $\delta W = Q_1\delta q_1 + Q_2\delta q_2 = (Q_1 + \beta_1 Q_2)\delta\theta_1 + (Q_1 + \beta_2 Q_2)\delta\theta_2$.

Hence,

$$P_1 = Q_1 + \beta_1 Q_2; \quad P_2 = Q_1 + \beta_2 Q_2. \tag{4.55}$$

In the new coordinates θ_1 and θ_2, called *normal* or *principal*; each of these θ_1 and θ_2 can be determined from the corresponding differential equation of the second order, not from the system of equations, which, of course, is much easier:

$$a_i\ddot{\theta}_i + c_i\theta_i = P_i \quad (i = \overline{1, H}).$$

According to (4.54), the "natural" frequencies are equal to $k_i = \sqrt{c_i/a_i}$.

In case of transition to the normal coordinates for the systems with H degrees of freedom, it is convenient to use the matrix form of solution. In this case the inertial and quasi-elastic coefficients $\mathbf{a}_r$ and $\mathbf{c}_r$ are defined as follows:

$$\begin{array}{l} [\beta]^T[\mathbf{a}][\beta] = \mathrm{diag}\{a_1, \ldots, a_H\}; \\ [\beta]^T[\mathbf{c}][\beta] = \mathrm{diag}\{c_1, \ldots, c_H\}, \end{array} \tag{4.56}$$

and the new generalized forces as

$$P_r = \sum_{i=1}^{H} Q_i\beta_{ir}. \tag{4.57}$$

After solving the differential equations of type (4.54), the original generalized coordinates are defined as follows:

$$q_i = \sum_{r=1}^{H} \beta_{ir}\theta_r. \tag{4.58}$$

In conclusion we will emphasize that the normal coordinates with rare exceptions, have no physical meaning, i.e. do not correspond in the general to the actual movement of the elements of the system. Their use is just a convenient way to transform the original system of equations, facilitating the analysis and engineering calculations. In particular using the normal coordinates we can more accurately take into account the hysteretic dissipative forces (see Chap. 6).

4.3 Dynamic Unloading

General information about the unloading devices As it was noted above, one of the ways to reduce or redistribute the forces, acting on the links or reactions in the kinematic pairs, is associated with the installation of special unloading devices. It was shown above that the main source of vibrations are the variable driving forces that are caused not only by the performed technological process, but by the large inertial loads, arising out of the given program motion of the links. With the help of the unloading devices, we attempt to reduce, or at least to "smoothen" the perturbation function. The use of such devices, as the engineering practice shows, is often a very effective method for reducing the vibration activity and wear and tear of the parts of the kinematic pairs, which in turn increases the durability and longevity of the machine [39, 51, 58, 64, 81].

In the simplest case the role of the unloader can be performed by an ordinary spring. This is easily seen from the following example. Let the output link of the mechanism with mass m move according to the law of motion $y(t) = y_0 \cos \omega t$ (Fig. 4.14).

If we set the spring between the output link and the body, then $m\ddot{y} = R - c_0 y$, where c_0 is the spring's stiffness coefficient; R is the projection of reaction from the mechanism's side, acting as the driving force. After substituting $y(t)$, we have $R = (m\ddot{y} + c_0 y) = (c_0 - m\omega^2) y_0 \cos \omega t$. It is obvious that $R = 0$ when $\omega = \omega_* = \sqrt{c_0/m}$. We have already come across the similar effect in the example of the cam mechanism, with the spring closure (see Sect. 4.1.2), when it turned out that at a certain frequency of rotation $\omega = k_s$, the cam is subjected to the action of the

Fig. 4.14 Reactions in case of dynamic unloading
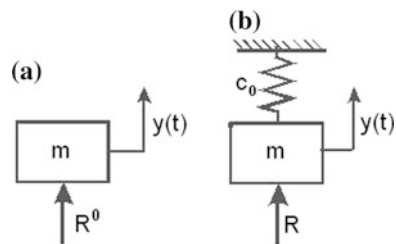
Fig. 4.15 Determination of
the ω_0
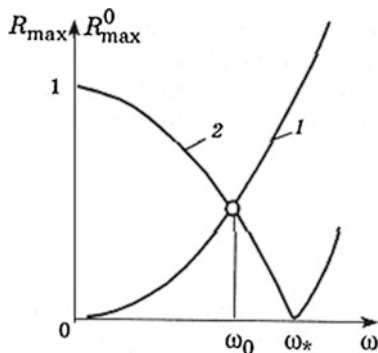
constant component of the closing force; whereas the variable harmonic component
is balanced by the force of inertia of the cam follower during its program move-
ment. The graphs of the maximum reactions R_{max}^0, R_{max} in the absence of the
unloading device (curve 1) and after its installation (curve 2) are shown in Fig. 4.15.
When $\omega = \omega_* = \sqrt{c_0/m}$, we have $R_{max}^0 = 0$. It is to be noted here that ω_* is not
equal to the "natural" frequency $k = \sqrt{(c_0 + c)/m}$, where c is the reduced coef-
ficient of stiffness of the mechanism. Usually $\omega_* \ll k$ and only when the output link
is disconnected from the drive $(c \rightarrow 0)$, we have $\omega_* \rightarrow k$.

The point of intersection of the two curves, determines the frequency interval
$\omega > \omega_0 = \omega_*/\sqrt{2}$, at which the installation of the unloader has a positive effect. At
start-up $R_{max}(\omega) = c_0 y_0 = m\omega_*^2 y_0$; therefore the installation of the unloading device
leads to an increase in the starting torque. This is a drawback, which can be
eliminated, by using an unloading mechanism with frequency tuning [18, 64].

Regardless of the design features, the unloading device is usually an accumulator
of potential or kinetic energy. In the first case we use the springs or pneumatic
devices (Fig. 4.16); whereas in the second case, we use the inertial links, driven by
special balancing mechanisms, which in most cases are lever and cam mechanisms
with significantly massive output links. For the first type of unloading devices, the
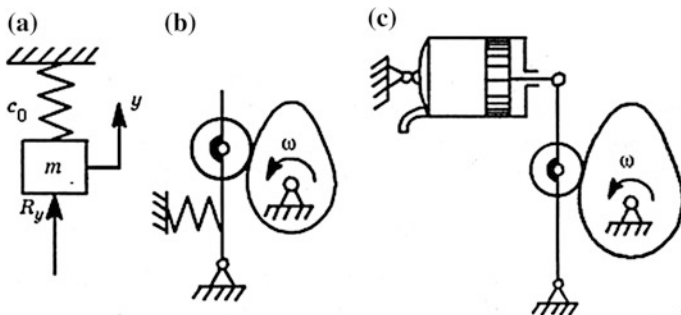
Fig. 4.16 Drawings of the dynamic unloading devices
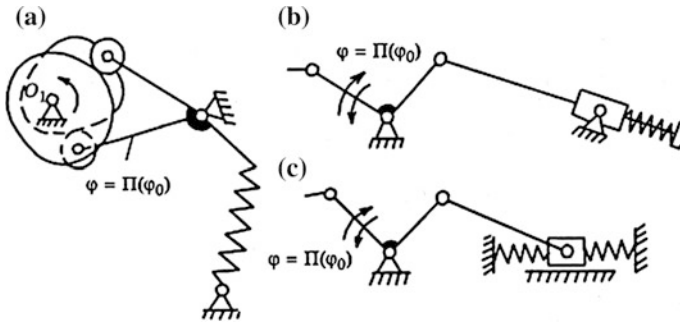
Fig. 4.17 Spring based dynamic unloading devices

counteracting force is the position function and does not depend on the velocity, whereas the counterbalanced dynamic loads are proportional to the square of the angular velocity of the input link. Therefore these devices should be tuned for a given velocity regime. In the devices of the second type, the unloading forces are also proportional to the square of the angular velocity; therefore with respect to dynamic components of the loads they are the followed load. In more advanced unloading devices there is always a program carrier, which usually comprises of a cyclic mechanism, such as a cam or lever mechanism.

To improve the efficiency of the unloader and to eliminate the possibility of additional excitation of vibrations in the system, its place of installation should be as close to the source of the oscillations as possible. As per the given point of view, it is advisable to attach it directly to the output link of the basic mechanism. In Fig. 4.17 we can see various types of the unloading devices, which consist of a simple lever mechanism and a spring (in Fig. 4.17b, c only the output link of the basic mechanism and the loader are represented).

To compensate the inertial loads of the output link, the unloader must store energy during run-out and return it during the run-in period. This is achieved by the change of sign of the unloading moment during the transition from a run-into a run-out.

Methods of calculation In general, the absolute value of the reaction from the working part on the machine's drive is equal to

$$|R| = |R_* + U|, \tag{4.59}$$

where R_* is the reaction in the absence of the unloading device; U is an additional component of the reaction after the installation of the unloading device.

If we use the spring based unloader (see Fig. 4.14b) then

$$U = u_0 + u_1 y, \tag{4.60}$$

where u_0 is the preliminary deformation of the spring; $u_1 = c_0$ is the stiffness coefficient of the spring. The function $R_*(y)$ in general case may not be equal for the

direct and the reverse stroke. Following the method of least squares, we determine
the parameters u_0 and u so as to provide the minimum of at the functional

$$\Psi = \oint (R_* + U)^2 dy \rightarrow \min. \tag{4.61}$$

Let $R_*(y)$ be two-valued function, namely $\vec{R}_*(y)$ for the direct stroke and $\overleftarrow{R}_*$ for the
reverse stroke. Then the condition of (4.61) is met by

$$\frac{\partial \Psi}{\partial u_i} = 2 \left[\int_0^{y_{max}} (\vec{R}_* + U) \frac{\partial U}{\partial u_i} |dy| + \int_0^{y_{max}} (\overleftarrow{R}_* + U) \frac{\partial U}{\partial u_i} |dy| \right] = 0 \quad (i = 0.1). \tag{4.62}$$

If $y = \Pi(\varphi)$, where φ is the rotation angle of the input link, then
$|dy| = |\Pi'(\varphi)| d\varphi$, where $\Pi'(\varphi)$ is the first geometric transfer function of the
mechanism. Taking into account that in accordance with (4.60) $\partial U / \partial u_0 = 1$ and
$\partial U / \partial u_1 = y$, on the basis of (4.62) we obtain the system of the two linear algebraic
equations with respect to u_0 and c_0

$$\left. \begin{array}{l} 2\Pi_{max} u_0 + \Pi_{max} c_0 = S_1; \\[2mm] \Pi_{max}^2 u_0 + \dfrac{2}{3} \Pi_{max}^3 c_0 = S_2, \end{array} \right\} \tag{4.63}$$

where $S_1 = -\int_0^{2\pi} R_*(\varphi) |\Pi'(\varphi)| d\varphi$; $S_2 = -\int_0^{2\pi} R_*(\varphi) \Pi(\varphi) |\Pi'(\varphi)| d\varphi$.

If the function $R_*(\varphi)$ is defined by a table, chart, or with the complex analytic
form, then S_1 and S_2 can be determined with any method of the numerical inte-
gration. On the basis of (4.63) we have

$$u_0 = (2S_1 \Pi_{max} - 3S_2)/\Pi_{max}^2; \quad c_0 = 3(2S_2 - \Pi_{max} S_1)/\Pi_{max}^3. \tag{4.64}$$

In Fig. 4.18 the typical graphs $R_*(y)$, $U(y)$ and the graph of the resulting reaction
after the installation of the unloader $R_1(y) = R_*(y) + U(y)$ are represented as an
illustration. From the graphs it follows that in this example the maximum reaction

Fig. 4.18 To analysis of the
efficiency of dynamic
unloading
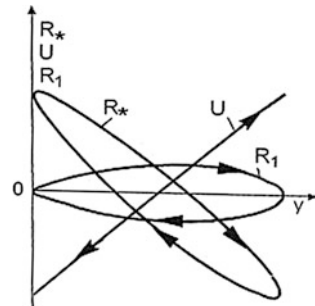
on the output link is reduced by about 4 times. In case of the harmonic movement of the working part (see above) the graph of the dynamic component of the reaction $R_*(y)$ degenerates into a straight line, and $U(y)$ into its mirror image. At the same time for the specified frequency ω_* the graph $R_1(y)$ coincides with the horizontal axis, i.e. we have absolute dynamic unloading.

In case of use of the unloading devices we should, however, take into account the possibility of the substantial reduction of the reactions in the kinematic pairs, that can lead to the arising of the vibration activity in the clearances of the kinematic pairs (see Chap. 7). Additionally, when using the spring type unloaders, it is necessary to check the level of the spring's oscillations (see Sect. 5.6).

4.4 Synthesis of the Cyclic Oscillatory Systems with Quasi-Constant Amplitude-Frequency Characteristic

This section is dedicated to the synthesis of one type of the cyclic mechanisms, for which we can make a significant qualitative transformation of the traditional frequency response with the appropriate selection of parameters. The detected anomaly of this characteristic can be used to create the mechanisms with the nearly constant amplitude of oscillations of the actuators regardless of the frequency of excitation. Apart from that, in case of resonance ratio of frequencies and effect of linear resistance, discovered is, at first glance, a paradoxical behavior of the oscillating system, when the dissipation of the resonant amplitude approaches zero [60, 70].

Such mechanisms may find application in technological and transport operations that require high-frequency displacements of actuators and in robotic systems, because of the small power requirements and the possibility of relatively simple regulation of the parameters of movement.

4.4.1 Dynamic Model and Its Modifications

Let us consider the dynamic model of the cyclic mechanism, mounted on the movable platform 0 with mass m_0, for showing which we have illustrated a lever mechanism in Fig. 4.19a.

The center mass of the crank 1 with the mass m_1 is displaced relative to the axis of rotation at a distance $O_1S = R$. Installed between the platform and the frame is an elastic element with stiffness coefficient c_0 and dissipation coefficient ψ_0. The output link is represented in the form of oscillatory system $m_2 - (c_1, \psi_1) - m_3 - (c_2, \psi_2)-$ frame, where m_i, c_i ψ_i are the reduced values of mass, stiffness and dissipation coefficients. Let the input link rotate with constant angular velocityω. Taking as generalized coordinates, the movement of the platform $(y_1 = q_1)$, displacement of

Fig. 4.19 Dynamic models
of the mechanisms with
anomalous characteristics
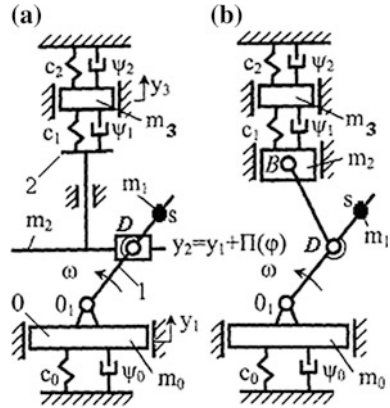
the mass m_3 $(y_3 = q_2)$ and temporarily omitting the dissipative terms, we write the system of differential equations as follows:

$$\left.\begin{array}{l} M\ddot{q}_1 + (c_0 + c_1)\,q_1 - c_1\,q_2 = -c_1\,r_0 \sin\omega t + m_1\omega^2 R \sin\omega t + m_2\omega^2 r_0 \sin\omega t + Q_1; \\ m_3\ddot{q}_2 - c_1 q_1 + (c_1 + c_2)\,q_2 = -c_1 r_0 \sin\omega t + Q_2, \end{array}\right\}$$

(4.65)

where $r_0 = O_1 D$; $M = m_0 + m_1 + m_2$; Q_1, Q_2; are non-conservative generalized forces (force of gravity can be excluded from the equations, as the measurement reference of the generalized coordinates is made from the position of static equilibrium).

4.4.2 Systems with One Degree of Freedom

Let $y_3 \equiv 0$; then the system has a single degree of freedom and is described with the differential equation

$$M\ddot{q} + \chi\dot{q} + (c_0 + c_1)q = -[c_1 r_0 - \omega^2(m_1 R + m_2 r_0)] \sin\omega t, \qquad (4.66)$$

where χ is the reduced coefficient of linear resistance; here and below only kinematic excitation is retained $(Q_i = 0)$.

If we accept $c_1 r_0 = \omega^2(m_1 R + m_2 r_0)$, then there occurs an instance of dynamic unloading, when at a certain frequency ω_* the kinematic excitation is completely compensated with the restoring force of the elastic element c_1 (see Sect. 4.3). However, in this case we are faced with another problem to provide for the oscillation of platform with an amplitude, which is independent (or the weakly

dependent) of the changes in ω. In accordance to (4.66) the amplitude of forced oscillations is determined as follows:

$$A = \frac{|c_1 r - \omega^2 (m_1 R + m_2 r_0)|}{(c_0 + c_1)\sqrt{(1 - z^2)^2 + 4\delta^2 z^4}}, \qquad (4.67)$$

where $z = \omega/p$ is the coefficient of the frequency detuning; $p \approx \sqrt{(c_0 + c_1)/M}$; $\delta = \psi_*$ is the dissipation coefficient; ψ_* is the reduced dissipation coefficient.

In case of dynamic synthesis of the system, we will define additional conditions:

$$c_1 r / (m_1 R + m_2 r_0) = p^2. \qquad (4.68)$$

Taking into account (4.68) on the basis of (4.67) we have

$$A = A_* = c_1 r_0 / (c_0 + c_1). \qquad (4.69)$$

For clearer physical understanding of the investigated problem, let us first consider a special case, in which the crank 1 is balanced ($R = 0$) and there are no dissipative forces ($\delta = 0$). Then formula (4.67) takes the form

$$A = r_0 \frac{|1 - \omega^2/k^2|}{(1 + \zeta)|1 - \omega^2/p^2|}, \qquad (4.70)$$

where $k = \sqrt{c_1/m_2}$; $\zeta = c_1/c_0$.

The expression $\frac{dA}{d\omega} = 0$ leads to the obvious condition $k = p$; therefore $c_1/c_0 = m_2/(m_1 + m_0)$ and according to (4.70)

$$A = r_0/(1 + \zeta) = \text{const.} \qquad (4.71)$$

This result indicates the non-trivial situation, when the "amplitude-frequency characteristic" (AFC) does not depend on the frequency of excitation. It is easily seen that the "natural" frequency of the system p is equal to the "natural" frequencies of the two subsystems, obtained in case of disconnection of the kinematic connection in the joints D (see Fig. 4.19). This means that in case of "hard" connection of the two subsystems, the "natural" frequency remains unchanged.

Further we shall return to the consideration of the general case corresponding to the initial model. Then

$$A = \frac{|c_1 r_0 - \omega^2 (m_2 r_0 + m_1 R)|}{(c_0 + c_1)\sqrt{(1 - z^2)^2 + 4\delta^2 z^4}} = \frac{r_0 k^2 |[1 - \omega^2(1 + \rho\mu_1)/k^2]|}{p^2 (1 + \zeta)\sqrt{(1 - z^2)^2 + 4\delta^2 z^4}}, \qquad (4.72)$$

where $\rho = R/r_0$, $\mu_1 = m_1/m_2$.

Fig. 4.20 Graph of the
dimensionless "natural"
frequency
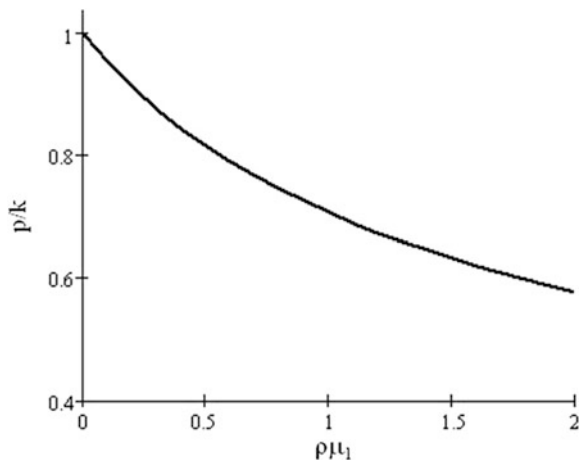
In case of satisfying the condition $k^2/(1 + \rho\mu_D) = p^2$ on the basis of (4.72) we
have

$$A = \frac{r\left|1 - z^2\right|}{(1 + \zeta)\sqrt{(1 - z^2)^2 + 4\delta^2 z^4}}. \tag{4.73}$$

Taking into account that on the other hand $p^2 = k^2(1 + \zeta)/\mu_\Sigma$, where
$\mu_\Sigma = 1 + \mu_0 + \mu_1$, $\mu_i = m_i/m_2$, we have the additional equation of the connection
between the dimensionless parameters:

$$\zeta = \mu_\Sigma/(1 + \rho\mu_1) - 1 > 0. \tag{4.74}$$

We note that in case of the given additional condition the dimensionless natural
frequency $\tilde{p} = p/k$ depends only on the product of $\rho\mu_1$ (Fig. 4.20).

In dimensionless form the final dependence, describing the amplitude-frequency
characteristic (AFC), has the form

$$a = a_*\kappa(z, \delta). \tag{4.75}$$

where $a = A/r_0$, $a_* = (1 + \zeta)^{-1} = (1 + \rho\mu_1)/M$ is the amplitude of the forced
vibrations of the platform and the "static" amplitude; $\kappa(z, \delta)$ is the factor of
dynamicity, defined as

$$\kappa = 1/\sqrt{1 + 4\delta^2 z^4/(1 - z^2)^2}. \tag{4.76}$$

(here and below the term "dimensionless" is omitted).

Then we will determine the oscillations of the output link:

$$y_2/r_0 = \sin \omega t - a \sin(\omega t - \gamma), \tag{4.77}$$

where $\gamma = \arctan[2\delta z/(1 - z^2)]$.

Using (4.76), we can show that

$$b = \max (y_2/r) = \sqrt{(1 - a \cos \gamma)^2 + a^2 \sin^2 \gamma}, \tag{4.78}$$

where b is the amplitude of the output link 2.

The family of quasi-constant amplitude frequency characteristics $a(z)$ of the platform 1 and $b(z)$ for the driven member 2, obtained on the basis of (4.74)–(4.77), is represented in the Fig. 4.21. The following input data are used for making graphs: $\mu_0 = 2$; $\mu_D = 0.5$; $\delta = 0.03$. Double indexation of the curves corresponds to $a - \rho$, $b - \rho$ (the numbers correspond to the numerical value of the parameter $\rho = R/r$).

Chart analysis reveals the following features of frequency response (AFC):

- With the exception of the narrow frequency range, in the vicinity of the resonance zone $z = 1$, the amplitude of forced oscillations of the platform (link 0) and the output link 2 practically remains constant.
- In case of resonance $(z = 1)$, the amplitude of the platform turns to zero (antiresonance) and for the output link 2, it takes the value $b = 1$ $(A_2 = \max(y_2) = r_0)$, which corresponds to resonance.

When $\rho = 0$, $\rho = 1$ we have $a < b$ and when $\rho = 3$ the amplitude of the platform exceeds the amplitude of the output link. Of utmost interest is the extreme case $a = b$. Accepting in case of the absence of dissipation in (4.78),

Fig. 4.21 Family of the amplitude-frequency characteristics
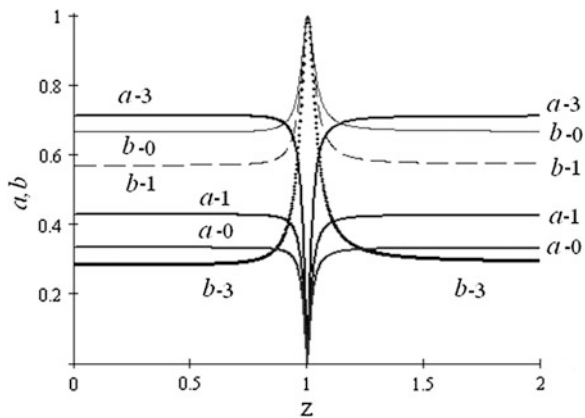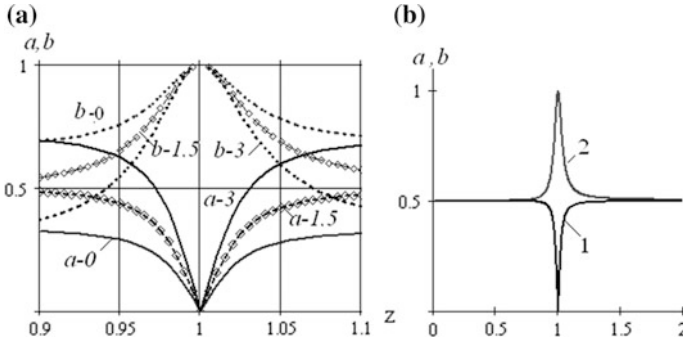
Fig. 4.22 Amplitude-frequency characteristics in resonance zone

$b = a$, $(\gamma = 0, \pi)$, we obtain $a = b = 0.5$. As in this case $a = a_*$, the extreme value of $\rho = \rho_*$ is determined as

$$\rho^* = 0.5(\mu_0 - 1)/\mu_1. \tag{4.79}$$

Thus, if $\rho < \rho^*$, we have $a < b$ and $a > b$ when $\rho > \rho^*$. In particular, for the above set parameters we obtain $\rho^* = 1.5$. For a more detailed study of the behavior of the system directly in the resonance zone in Fig. 4.22a the relevant frequency range is selected. Apart from the modes shown in Fig. 4.22b, the frequency response (AFC) for the regime $\rho^* = 1.5$ is presented (a—curve 1, b—curve 2).

The analysis of the graphs shows that when $\rho < \rho_*$ the platform and output link's phase of the oscillations, when entering the resonance zone, remains unchanged (curves $a - 0$, $b - 0$), and on the contrary, when $\rho > \rho^*$ it reverses (curves $a - 3$, $b - 3$). When $\rho = \rho^*$ and some distance from the resonance region, as might be expected, $a \approx b \approx a_*$. This regime is illustrated in Fig. 4.5b (a—curve 1; b—curve 2). Let us note here that the similar situation arises in case of dynamic dampening, when at a certain frequency the response of the unloader, on the subject of vibration protection, "balances" the external excitation.

In our case, however, there are significant differences. First of all, the dynamic damper along with the protected object, form an oscillating system, with many degrees of freedom, but at least two, while the considered system has one degree of freedom. From the given point of view, this effect is closer to the so-called dynamic unloading (see Sect. 4.3). Secondly, in case of the dynamic dampening, the accounting of the dissipation leads to some finite value of the amplitude of oscillations, which is different from zero and dependent on the level of dissipation. In the given system, when $z = 1$ the amplitudes are $a = 0$, $b = 1$, regardless of the level of dissipation.

The graphs $y_1(t)$, $y_2(t)$ obtained by computer simulation using $\rho = \rho^* = 1.5$ (for remaining data see above) are represented in the Fig. 4.23. In the non-resonance zone($z = 0.7$; Fig. 4.23a) the amplitudes of oscillations correspond to the above-obtained values (see Fig. 4.22b) and phases of oscillations of the links 0 and 3 are

Fig. 4.23 Oscillations in the non-resonance and resonance zones: *1* $y_1(t)$; *2* $y_2(t)$
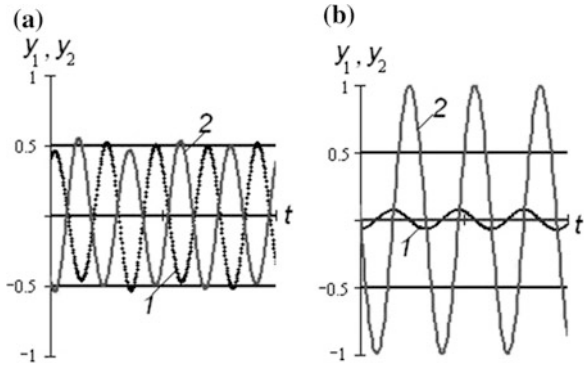
displaced on π. In the resonance zone ($z = 0.997$; Fig. 4.23b) the amplitude of the platform tends to zero, while the amplitude of the driven link tends to one. (Accepted value of z is slightly different from one, to illustrate the phase shift, close to the value $\pi/2$, at which curve 1 degenerates into a straight line.)

It should be noted that in case of intersection of the resonance zone the system usually does not have time to enter the steady state. However, the decrease in the amplitude of the platform's oscillations, in the resonant zone, appears quite clearly (Fig. 4.24).

The oscillations $y_1(t)$, $y_2(t)$ in case of change in coefficient of frequency detuning $z = \omega/p$ in the range $0 < z < 2$ for the two cases, are represented in the Fig. 4.25 fulfilment of the conditions of quasi-constant frequency response (AFC) (curves 1) and in case of the traditional kinematic excitation (y_1^*, y_2^*, curves 2). The graphs clearly show the significant differences in both the modes.

For the slider-crank mechanism (Fig. 4.19b) the position function with sufficient accuracy can be described by the bi-harmonic function

$$\Pi(\varphi) = r_0(\sin \varphi + 0.25\lambda \sin 2\varphi),$$

where r_0 is the radius of the crank; $\lambda = r_0/\ell$; ℓ is the length of the coupler.

Fig. 4.24 Transition across the resonance zone
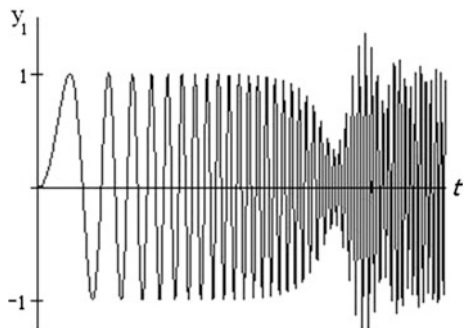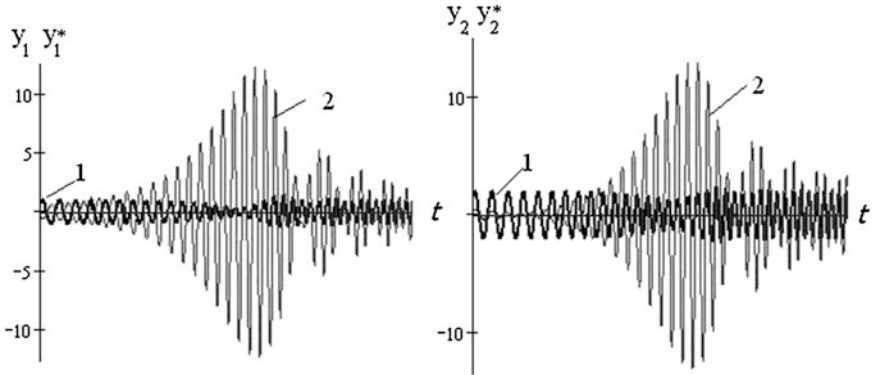
Fig. 4.25 Comparison of the oscillation regimes

We will require that for the main harmonic $j = 1$, the condition (4.69) should be satisfied. Then when $z = 1$ ($\omega = p$) we have $A_j = 0$, and when $z = 0.5$ ($\omega = 0.5p$) we get

$$A_1 \approx A_{1*}; \quad A_2 = 0.125\lambda A_{1*}/(\mu_1 \rho \delta). \tag{4.80}$$

It is assumed that the mass of the connecting rod is statically substituted with lumped masses in the joints D and B. It follows from (4.80) that in the balancing of the crank ($R = 0$) at the resonant frequency in the second harmonic ($\omega = 0.5p$).

4.4.3 Systems with Two Degrees of Freedom

Let us turn to the dynamic model with two degrees of freedom, which corresponds to the system of differential equations (4.65). Without narrowing the scope of generality in the formulation of the problem, we perform parametric synthesis of the oscillating system with anomalous properties in the case of monoharmonic excitation (see Fig. 4.19a).

In the absence of dissipation ($\delta = 0$) and $R = r$ the amplitude of forced vibrations of the platform is defined as follows:

$$A_1 = -r_0 \frac{c_1 c_2 - [c_1 m_3 + (c_1 + c_2)m_1^*]\omega^2 + m_1^* m_3 \omega^4}{m_3(m_0 + m_1^*)\omega^4 - [(m_0 + m_1^*)(c_1 + c_2) + m_3(c_0 + c_1)]\omega^2 + c_0 c_1 + c_0 c_2 + c_1 c_2}. \tag{4.81}$$

where $m_1^* = m_1 + m_2$.

We introduce the following notation: $c_0/c_1 = \zeta_0$; $c_2/c_1 = \zeta_2$; $m_0/m_1^* = \mu_0$; $m_3/m_1 = \mu_2$; $c_1/m_1 = \Omega^2$; $\omega/\Omega = z$. It can be shown that $dA_1/d\omega$ vanishes when

$$\mu_2^2(\zeta_0 - \mu_0)z^4 - 2\mu_2[\zeta_0(1 + \zeta_2) - \mu_0\zeta_2]z^2 + \zeta_0\mu_2 + (1 + \zeta_2)[\zeta_0(1 + \zeta_2) - \zeta_2\mu_0] = 0. \tag{4.82}$$

Condition (4.82) shows that the frequency factor z can be eliminated from the equation only when $\mu_2 = 0$, i.e. for a system with one degree of freedom. So in this case the point is not the constant amplitude, but the condition of extreme. At the same time, this condition characterizes the level of the derivative $dA_0/d\omega$; therefore its small values can be used to obtain the quasi constant amplitudes of the forced oscillations. For this purpose we take relatively small values of μ_2 and introduce one of the additional requirements of the form:

$$\zeta_0(1 + \zeta_2) - \mu_0\zeta_2 = 0; \tag{4.83}$$

$$\zeta_0\mu_2 + (1 + \zeta_2)[\zeta_0(1 + \zeta_2) - \mu_0\zeta_2] = 0. \tag{4.84}$$

In the first case, corresponding to the condition (4.83), the coefficient at z^2 vanishes, and under the condition (4.84) vanishes the free term. As shown in analysis, from the point of view of the specified problem, the preferable condition is (4.84). At the same time there are two extremes: when $z_{ext} = 0$ and $z_{ext} = \sqrt{2\zeta_0/[\mu_0 + \mu_2\zeta_0\zeta_2(1 + \zeta_2)]}$.

It can be shown that these extremes are "weak", which manifests itself in small changes of the derivative $dA_0/d\omega$ in the vicinity of these values. The latter, of course, indicates the quasi-constant character of the variations in amplitudes.

Observing the conditions of (4.83) and $\psi_i = 0$ $z_{ext} = \sqrt{4\zeta_2/\mu_2}$. Interestingly, in this case the amplitudes of the forced vibrations when $z = 0$ and when $z \to \infty$ coincide.

Further, for the correct accounting of the frequency-independent dissipation that is typical for the actual mechanisms, we make the transition to the normal coordinates η_i according to the expressions

$$q_1 = \eta_1 + \eta_2; \quad q_2 = \beta_1\eta_1 + \beta_2\eta_2. \tag{4.85}$$

Here β_1 and β_2 are the form factors, determined as the roots of the following quadratic equation $\beta^2 - S_1\beta + S_2 = 0$, where $S_1 = \zeta_0 + 1 - (1 + \mu_0)(1 + \zeta_2)\mu_2$ $S_2 = -(\mu_0 + 1)/\mu_2$.

After equivalent linearization of the dissipative forces it can be written as follows (see Sect. 6.1.2)

$$\begin{aligned} a_I\ddot{\eta}_1 + \chi_I\dot{\eta}_1 + c_I\eta_1 &= -r_0[c_1(1 - \beta_1) - m_1^*\omega^2]; \\ a_{II}\ddot{\eta}_2 + \chi_{II}\dot{\eta}_2 + c_{II}\eta_2 &= -r_0[c_1(1 - \beta_2) - m_1^*\omega^2], \end{aligned} \tag{4.86}$$

Fig. 4.26 Amplitude-frequency characteristic
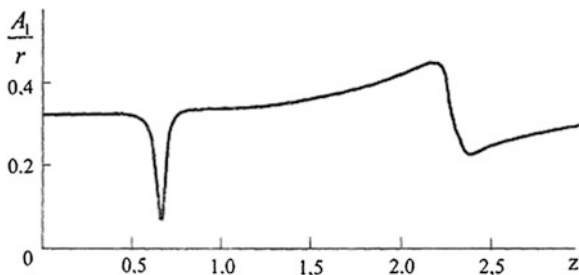
where $a_{\mathrm{I}} = m_0 + m_1^* + \beta_1^2 m_3$; $a_{\mathrm{II}} = m_0 + m_1^* + \beta_2^2 m_3$; $c_{\mathrm{I}} = c_0 + c_1 - 2\beta_1 c_1 + \beta_1^2$ $(c_1 + c_2)$; $c_{\mathrm{II}} = c_0 + c_1 - 2\beta_2 c_1 + \beta_2^2 (c_1 + c_2)$; $\chi_{\mathrm{I}}, \ \chi_{\mathrm{II}}$ are the reduced to the corresponding form coefficients of the equivalent linear resistance.

On the basis of (4.86), the amplitude of the forced oscillations is determined as follows:

$$\left.\begin{array}{l} A_1 = \sqrt{B_1^2 + B_2^2 + 2B_1 B_2 \cos\left(\gamma_1 - \gamma_2 - \alpha_1 + \alpha_2\right)}\,; \\[2mm] A_2 = \sqrt{\beta_1^2 B_1^2 + \beta_2^2 B_2^2 + 2\beta_1 \beta_2 B_1 B_2 \cos\left(\gamma_1 - \gamma_2 - \alpha_1 + \alpha_2\right)}\,. \end{array}\right\} \qquad (4.87)$$

Here

$$\left.\begin{array}{l} B_1 = \dfrac{\left|c_1(1 - \beta_1) - m_1\omega^2\right|}{c_{\mathrm{I}}\sqrt{\left(1 - z_1^2\right)^2 + 4\delta_1^2 z_1^2}}\,; \ B_2 = \dfrac{\left|c_1(1 - \beta_2) - m_1\omega^2\right|}{c_{\mathrm{II}}\sqrt{\left(1 - z_2^2\right)^2 + 4\delta_2^2 z_2^2}}\,; \\[4mm] \gamma_i = \arctan\dfrac{2\delta_i z_i}{1 - z_i^2}\,; \ \alpha_i = 0\,, \ \text{when} \ Q_i > 0\,; \ \alpha_i = \pi, \ \text{when} \ Q_i < 0\,, \end{array}\right\} \qquad (4.88)$$

where $z_i = \omega/p_i$; $\delta_i = \psi_i/(4\pi)$; Q_i is the right side of the corresponding Eq. (4.86); ψ_i is the reduced coefficient of dissipation.

Figure 4.26 shows the amplitude-frequency characteristic $A_1(z)/r$, where $z = \omega/\Omega$, $\Omega = \sqrt{c_1/m_1^*}$, that corresponds to the following source data: $\mu_0 = 2$; $\mu_2 = 0.4$; $\zeta_0 = 1$; $\zeta_2 = 1$; $\delta_i = 0.05$.

The analysis of the graph shows that, except for the resonance zones the amplitude of the forced oscillations remains relatively stable. In the zone of the first resonance the amplitude decreases abruptly and is close to zero, and in the area of the second resonance it has a slight splash in value, with subsequent stabilization.

When $\mu_2 = 0.2$ the deflection of the amplitudes in this area does not exceed 16 % of the mean value. It is to be noted that for smaller values $\mu_2 = 0.2$ the amplitude when $\omega \to \infty$ is close to the static amplitude, i.e. when $\omega = 0$. Thus with the accepted input data these amplitudes differ only by 6.6 %.

If required, as well as for the model with one degree of freedom, in the zone of the first resonance the condition $A_1 = 0$ can be achieved by selecting the parameter $\rho = R/r_0$ (earlier it was taken as $\rho = 1$). Analyzing (4.81), we can see that when $\rho \neq 1$ the numerator should be $m_1^* = m_2 + \rho m_1$, while the denominator remains unchanged. This indicates that the parameter ρ affects only the frequency detuning of the function of perturbations, without affecting the values of the "natural" frequencies.

Chapter 5
Dynamic Models with Variable Parameters

5.1 Linearization of the Geometric Characteristics of the Cyclic Mechanism in the Vicinity of the Program Motion

Let us consider the simplest dynamic model of the mechanism, with nonlinear position function, in which the drive is represented as an oscillatory contour with one degree of freedom, and the output links are accepted as absolutely rigid (Table 5.1, model 1). In this model the kinematic analog, which is represented with nonlinear position function $x = \Pi(\varphi)$, is "embedded" between the inertial elements J and m. This model allows us to determine, in the first approximation, the dynamic errors, occurring due to the torsional vibrations of the shaft, gears and other elements of the drive.

Let us accept the following notation: q is the angular deformation of the drive, reduced to the input link; $\varphi_* = \omega_0 t$ is the "ideal" rotation angle of the input link; $\varphi = \varphi_* + q$ is the angle of rotation of the input link taking into account the torsional vibrations; F is the external force applied to the output link, which will be taken as dependent on the time t and the angle φ; c_0, ψ are the coefficients of stiffness and dissipation of the drive part of the mechanism.
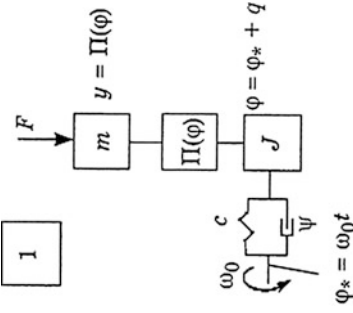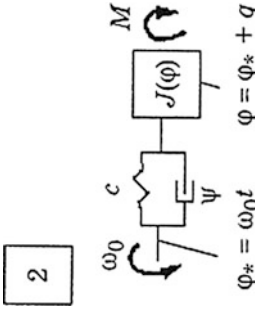
Using the outlined in Chap. 3 method of mathematical description of models, we can write the following differential equation

$$J\ddot{q} + b_0\dot{q} + c_0 q = -\Pi'(\varphi)(m\ddot{x} + F), \qquad (5.1)$$

where $\ddot{x} = \Pi''(\varphi)(\omega + \dot{q})^2 + \Pi'\ddot{q}$.

In Eq. (5.1), the reduced dissipative moment, which is proportional to the velocity $\dot{q}$ is also taken into account [the relation between the coefficient of proportionality b_0 and coefficient of dissipation ψ see Sect. 6.1, formula (6.3)]. The differential equation (5.1) is nonlinear, since the generalized coordinate and its derivatives are included as arguments of nonlinear functions.
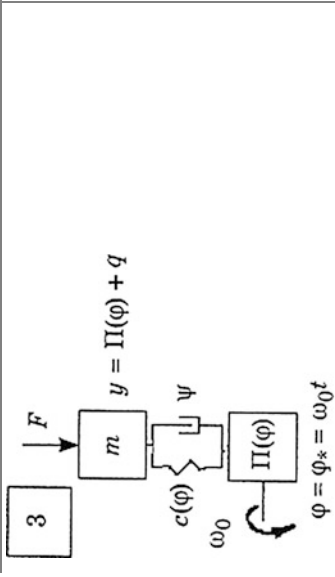
Table 5.1 Dynamic errors and the parameters of the mathematical model

Dynamic model	Dynamic error	Coefficients of equations
1	$\Delta y = \Pi(\varphi_* + q)$ $\Delta \dot{y} = \omega_0[(1 + \dot{q}/\omega_0)\Pi'(\varphi_*) - \Pi'(\varphi_*)]$ $\Delta \ddot{y} = \omega_0^2[(1 + \dot{q}/\omega_0)^2\Pi''(\varphi) + \Pi'(\varphi)\ddot{q}/\omega_0^2 - \Pi''(\varphi_*)]$	$k^2 = \dfrac{c(1 + \chi)}{J + m\Pi_*'^2}$ $n = \dfrac{\psi}{4\pi}k + \dfrac{m\Pi_*'\omega_0}{J + m\Pi_*'^2}$ $W = -\dfrac{\Pi_*'(m\omega_0^2\Pi_*'' + F_*)}{J + m\Pi_*'^2}$ $\chi = c^{-1}[m\omega_0^2(\Pi_*'' + \Pi_*'\Pi_*''')$ $+ \Pi_*''F_* + \Pi_*'(\partial F/\partial\varphi)_*]$
2	$\Delta\varphi = \varphi - \varphi_* = q$ $\Delta\dot\varphi = \dot\varphi - \omega_0 = \dot q$ $\Delta\ddot\varphi = \ddot\varphi = \ddot q$	$k^2 = \dfrac{c}{J_*}(1 + \chi)$ $n = \dfrac{\psi}{4\pi}k + \dfrac{J_*'\omega_0}{2J_*}$ $W = -\dfrac{0.5\,\omega_0^2 J_*' + M_*}{J_*}$ $\chi = c^{-1}(J_*''\omega_0^2/2 + M_*') \ll 1$

(continued)

Table 5.1 (continued)

Dynamic model	Dynamic error	Coefficients of equations
3 F m $y = \Pi(\varphi) + q$ $c(\varphi)$ ψ ω_0 $\Pi(\varphi)$ $\varphi = \varphi_* = \omega_0 t$	$\Delta y = y - \Pi(\varphi) = q$ $\Delta \dot{y} = \dot{y} - \Pi'(\varphi)\omega_0 = \dot{q}$ $\Delta \ddot{y} = \ddot{y} - \Pi''(\varphi)\omega_0^2 = \ddot{q}$	$k^2 = \dfrac{c(\varphi)}{m}$ $n = \dfrac{\psi}{4\pi} k$ $W = -\left(\Pi''\omega_0^2 + \dfrac{F'}{m}\right)$

Designations: m is the mass; J is the moment of inertia; c is the coefficient of stiffness; ψ is the coefficient of dissipation; the asterisk corresponds to argument $\varphi = \varphi_* = \omega_0 t$

Let us show that this equation, with the unimportant for dynamics simplifications can be reduced to the form of a linear differential equation with variable coefficients. Preliminarily we divide the phase angle of turn 2π, which corresponds to the total turnover of the input link, into time intervals, within which the functions $\Pi(\varphi)$, $F(\varphi, t)$ and some of the first derivatives of these functions on φ do not have discontinuities. Then expanding these nonlinear functions in Taylor's series as per the powers of the small values of q we have

$$
\begin{aligned}
\Pi'(\varphi) &\approx \Pi'(\varphi_*) + \Pi''(\varphi_*)q; \\
\Pi''(\varphi) &\approx \Pi''(\varphi_*) + \Pi'''(\varphi_*)q; \\
F(\varphi, t) &\approx F(\varphi_* t) + \frac{\partial F}{\partial \varphi}(\varphi_* t)q.
\end{aligned}
\tag{5.2}
$$

Let us call this procedure *the linearization in the vicinity of the program motion*. We should not mix this procedure with such linearization, when in the selected interval the nonlinear function is replaced with a linear one. In this case when we have relatively large argument $\varphi_* = \omega t$ all the functions have maintained their nonlinear properties and only the small angular deformations q are included into the corresponding expressions as linear. In particular, according to the first dependency (5.2) that can be interpreted as follows: in the small vicinity of the current value of φ_* the curve $\Pi'(\varphi)$ can be replaced by a tangent with variable slope $\Pi''(\varphi_*)$. This simplification allows us to use the *principle of superposition* (see Sect. 4.1.2) valid only for linear systems. After substituting (5.2) into (5.1), preserving in the resulting expressions the linear members relative to the coordinate q and its derivatives, we obtain

$$
a(t)\ddot{q} + b(t)\dot{q} + c(t)q = Q(t),
\tag{5.3}
$$

where

$$
\begin{aligned}
a(t) &= J + m\Pi_*'^2; \quad b(t) = b_0 + 2m\omega\Pi_*'\Pi_*''; \\
c(t) &= c_0\left\{1 + c_o^{-1}m\omega^2\left(\Pi_*''^2 + \Pi_*'\Pi_*'''\right) + c_0^{-1}[\Pi_*''F_* + \Pi_*'(\frac{\partial F}{\partial \varphi})_*]\right\}; \cdot \\
Q(t) &= -\Pi_*'\left(m\omega^2\Pi_*'' + F\right).
\end{aligned}
$$

Here the functions with argument φ_* are marked with an asterisk. In expression $c(t)$ the value of the function in the curly brackets is usually not much different one, so $c \approx c_0 = \text{const}$.

For elastic shaft line, with variable reduced moment of inertia $J(\varphi)$ (see Table 5.1, model 2), the differential equation is reduced to the form (5.1) when

$$
\begin{aligned}
a &= J_*; \quad b = b_0 + J_*'\omega; \quad c = c_0[1 + \omega^2 J''/(2c_0) + M_*'/c_0]; \\
Q(t) &= -0.5\omega^2 J_*' + M_*.
\end{aligned}
$$

Here $M_* = M(\varphi_*, t)$ is the external moment; $J_* = J(\varphi_*)\omega$; c_0 is the coefficient of stiffness of the drive; $(\ )' = d/d\varphi$.

Let us pay attention to the double origin of the coefficient b, in which the first summand corresponds to the dissipative factors and the second is equal to da/dt, i.e. related to the change in the inertial coefficient. Another important factor, determining the variability of the parameters of the dynamic model, is the change in time of the reduced stiffness. It is often related to the variability of the angles of pressure (see Sect. 2.6.3).

In Table 5.1 for a number of typical dynamic models with one degree of freedom and variable parameters, the coefficients of the linearized differential equations and absolute dynamic errors, i.e. deviation of the appropriating coordinate from the ideal values in the absence of vibrations, are also given. In a number of coefficients, the function $\chi \ll 1$, allowing to simplify the dependencies for calculation, is highlighted.

5.2 Method of the Conditional Oscillator

5.2.1 General Information About the Method of the Conditional Oscillator

To solve the differential equations, with variable coefficients, there are various approximate analytical methods [11, 20, 31, 40], the choice of which mostly depends on the specifics of the studied system and the goal of dynamic analysis. Provided hereunder is the information about the method of the conditional oscillator [59, 61–64, 75, 83], which can be attributed to the group of asymptotic methods of analysis of linear time-varying systems, containing the "large" parameter.

This method is based on one analogy between the parametric variations of the source system and forced oscillations of some auxiliary model, called the *conditional oscillator*. The method is well adapted to the specific tasks of the dynamics of mechanisms.

In particular, maintaining the unity of the approach, we can use this method to investigate the parametric effects, associated with the loss of the dynamic stability of the system and finding of the approximate solutions in both cases of "slow" and "fast" changes of the parameters.

Let us consider the following differential equation, which describes the systems with one degree of freedom

$$\ddot{q} + 2n(t)\dot{q} + k^2(t)q = w(t), \qquad (5.4)$$

where q is the generalized coordinate; $w(t)$ is the function of perturbations; $k^2(t)$, $n(t)$ are some functions of time, the first one of which is in the interval $[t_0, \ t_*]$ and should be continuous, and the second one is continuously differentiated.

Using the generalized Euler substitution, we introduce the new variable

$$y = q \exp\left[-\int_0^t n(t)dt\right], \tag{5.5}$$

and reduce (5.4) to the following form:

$$\ddot{y} + p^2(t)y = W(t), \tag{5.6}$$

where $p^2(t) = k^2(t) - n^2(t) - \dot{n}(t);\ W(t) = w(t)\exp\left[\int_0^t n(t)dt\right]$.

Here and below by analogy with the term, used for systems with constant parameters, the function $p(t)$ is named as the "*natural*" *frequency*. In accordance with the method of the conditional oscillator we find the solution for (5.6) as:

$$y = D(t)\cos\Phi(t). \tag{5.7}$$

Thus,

$$\ddot{y} = (\ddot{D} - D\dot{\Phi}^2)\cos\Phi(t) - (2\dot{D}\dot{\Phi} + D\ddot{\Phi})\sin\Phi(t). \tag{5.8}$$

Let us substitute (5.7) and (5.8) in (5.6) and equate the coefficients in case of $\cos\Phi$ and $\sin\Phi$ in both parts of the equality:

$$2\dot{D}\Omega + D\dot{\Omega} = 0; \tag{5.9}$$

$$p^2 - \Omega^2 + \ddot{D}/D = 0. \tag{5.10}$$

Here, $\Omega(t) = d\Phi/dt$.

The condition (5.9) is the first order differential equation with separable variables

$$\frac{dD}{D} = -0.5\,\frac{d\Omega}{\Omega}.$$

Hence,

$$D = D_0\sqrt{\Omega_0/\Omega(t)}, \tag{5.11}$$

where $D_0 = D(0);\ \Omega_0 = \Omega(0)$.

Substituting (5.11) into (5.7) and coming back with the help of (5.5) to the original variable q, we obtain

$$q = D_0 \exp[- \int_0^t n(t)dt]\sqrt{\Omega_0/\Omega(t)} \cos[\int_0^t \Omega(t)dt + \alpha], \qquad (5.12)$$

where D_0 and α are determined on the basis of initial conditions.

The relationship between function $\Omega(t)$ and "natural" frequency $p(t)$ is given by Eq. (5.10). Having taken $z = \ln(\Omega/\Omega_*)$, where Ω_* is an arbitrary parameter with the dimension of the frequency, acting as a normalizing multiplier and taking into account (5.11), we give this equation the following form

$$\ddot{z} - 0.5\,\dot{z}^2 + 2\,\Omega_*^2 e^{2z} = 2p^2(t). \qquad (5.13)$$

The differential equation (5.13) corresponds to some fictitious oscillatory system with the "hard" nonlinear characteristic, called the *conditional oscillator*. The role of the driving force is played by the function, which is proportional to the square of the "natural" frequency.

It is enough to have a particular solution for this equation, to transform (5.12) into the calculation dependence, describing the oscillatory process.

As a "convenient" positive property of conditional oscillator, we would note that *its parameters, displayed in the left-hand side of the equation, are of a general nature and do not depend on the parameters of the system.*

Relation (5.7) can be reduced to the following form

$$q = D_0 \exp[- \int_0^t n(t)dt - 0.5\,(z - z_0)] \cos\left[\Omega_* \int_0^t e^z dt + \gamma\right], \qquad (5.14)$$

where $z_0 = z(0)$.

The dependencies (5.12) and (5.14) correspond to the accurate solution. Their approximate character only associates with the functions Ω or z (see below).

The analysis of the coefficient $n = b^*/(2a^*)$ shows, that it can be represented as a sum $n = n_0 + n_1$, where $n_0 \approx \psi p/(4\pi)$ characterizes the dissipative component, and $n_1 = 0.5\,\dot{a}^*/a^*$ characterizes the gyroscopic component, when

$$\int_0^t n_1 d\xi = \ln\sqrt{a^*(t)/a^*(0)}.$$

Hence for the solution of (5.13) we should accept

$$\exp\left[-\int_0^t n(\xi)d\xi\right] = \sqrt{a^*(0)/a^*(t)}\,\exp\left[-\int_0^t n_0(\xi)d\xi\right]. \qquad (5.15)$$

In accordance with (5.15), in case of the periodic variation of the inertial coefficient, the first multiplier in the period turns to one. As expected the attenuation of the oscillations in the period is due only to the dissipative component, since the work of the gyroscopic forces over the period is equal to zero. In case of the instantaneous change of the inertial coefficient $a^*(t)$, this factor also changes abruptly. The function $q(t)$, however, remains continuous, and the speed $\dot{q}$ changes as well as at the impact pulse $\dot{q}_{j+} = a^*_{j-} \dot{q}_{j-} / a^*_{j+}$, where plus corresponds to the moment $t_j + 0$, and minus to $t_j - 0$. Thus the phase jump of the solution is equal to

$$\Delta\gamma_j = \arccos\left[\sqrt{a^*_{j+}/a^*_{j-}} \; \cos(\Phi_j + \gamma_{j-})\right] - (\Phi_j + \gamma_{j-}),$$

where $\Phi_j = \int\limits_0^{t_j} \Omega(\xi)d\xi$.

Having the particular solutions of the homogeneous linear differential equation, to obtain the particular solution of nonhomogeneous differential equations, we can use the method of variation of the arbitrary constants.

Taking into account (5.15), we finally obtain

$$
\begin{aligned}
q = &A_0 \exp\left[-\int\limits_0^t n_0 dt\right] \sqrt{\frac{a(0)\Omega(0)}{a(t)\Omega(t)}} \cos\left[\int\limits_0^t \Omega dt + \gamma\right] \\
&+ \frac{1}{\sqrt{\Omega(t)}} \int\limits_0^t \frac{W(u)}{\sqrt{\Omega(u)}} \exp\left[-\int\limits_u^t n(\xi)d\xi\right] \sin\left[\int\limits_u^t \Omega(\xi)d\xi\right] du
\end{aligned}
\tag{5.16}
$$

Depending on the kind of changes in the function $p^2(t)$, we can determine the approximate and in some cases, the exact solution of Eq. (5.13). A detailed analysis of the equation of the conditional oscillator is given in the monographs [59, 62–64]. Here, we will only consider several important special cases.

Slow changes in the parameters In this case the change of the model's parameters in the average period of free oscillations can be considered small as compared to their average values for this period (this case should not be confused with the case of small changes of parameters relative to their average values over a long period of time, for example, the kinematic cycle of the mechanism). The inequality $2.5\ddot{p}/p^3 - 3.75(\dot{p}/p^2)^2 \leq 1$ can serve as the quantitative criterion for this case.

At the same time $p \approx \Omega$ and the solution of (5.14) and (5.16) coincides with the WKB approximation of the first order [20].

Stepped change of the "natural" frequency Let the function $p^2(t)$ change abruptly from value p_0^2 up to p_1^2. Introducing the dimensionless time $\tau = 2p_0 t$, we write the differential equation of the conditional oscillator:

$$\ddot{z}'' - 0.5\,z'^2 + 0.5\,e^{2z} = 0.5\,v^2(\tau), \tag{5.17}$$

where $v = \dfrac{p}{p_0}; \quad z' = \dfrac{d\,z}{d\tau}; \quad z'' = \dfrac{d^2 z}{d\tau^2}.$

In case of $v = const$, taking $z'^2 = x$, we represent the Eq. (5.17) as follows:

$$\frac{dx}{dz} - x = \left(v^2 - e^{2z}\right), \tag{5.18}$$

The solution of which is

$$x = Ce^z - \left(v^2 - e^{2z}\right).$$

After determining the arbitrary constant C and transition to the original variable z, we obtain

$$z' = \pm\sqrt{(z_0'^2 + v^2 + e^{2z_0})e^{z-z_0} - (v^2 + e^{2z})}. \tag{5.19}$$

Let us test this dependence for the phase plane $z'(z)$. We take $\Omega_* = p_1$. Then $v_0 = p_0/p_1$, $v = v_1 = 1$. Further, assigning $\Omega_0 = p_0$ and $\dot{\Omega}_0 = 0$ we have $z_0 = \ln v_0$ and $z_0' = 0$, therefore in case of $z_0 = \pm \ln v_0$ in accordance with (5.19) z' vanishes. These values correspond to the extremes of z. In Fig. 5.1, we can see a number of closed curves, symmetric with respect to the axis of abscissa and intersecting this axis at two points, situated at an equal distance from the start of the coordinate. The phase trajectory $\tau_* = 0$ corresponds to the abrupt change of p; other curves correspond to the monotonous variation of p at the given interval of the dimensionless time $\tau_* = 2p_0 t_*$ [intervals $N_1 N_j$ $(j = 2, \ldots, 5)$]. The curves z_{ex}', limiting the extreme values of the phase trajectories along the Y-axis, are plotted in the phase plane. In case of increase in τ_* have $z_{min} \to 0$; this extreme case corresponds to the slow change of parameters.

The nature of these curves indicates that we are dealing with a specific kind of steady-state oscillation mode, in which for the area $z' < 0$ the damping of oscillations takes place, and for $z' > 0$ it's the buildup. In general the level of the energy of the oscillatory process, per cycle, remains constant. In other words the conditional oscillator behaves, in this case, as an autonomous conservative system. It can be shown that time period of a full cycle of a closed phase trajectory is equal to $T_z = \pi/p_1$. Thus the main "natural" frequency of the conditional oscillator is found to be $2p_1$, which in case of the periodic frequency oscillation of the original system corresponds to the zone of principal parametric resonance. Later we will discuss this interesting and quite "natural" result, in more details.

Harmonic pulsation of the function $p^2 = p_0^2[1 - 2\varepsilon \cos(\omega_P t + \gamma)]$. We find the approximate solution of the conditional oscillator equation (5.13) in the form

Fig. 5.1 Phase portrait of the conditional oscillator
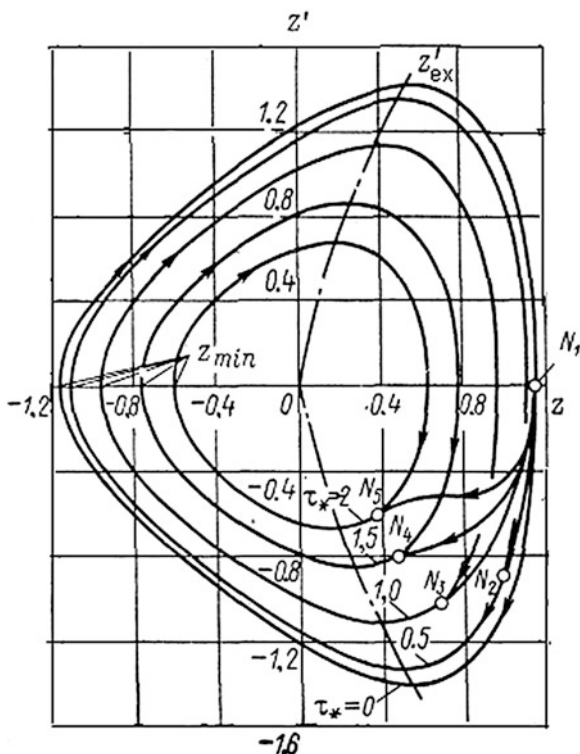
$z = a_0 + a\cos(\omega t)$. Using the method of harmonic linearization (see Appendix) we get

$$a = \frac{\varepsilon k_0^2(a)}{\left|k_0^2(a) - [\omega_P/(2p_0)]^2\right|} \frac{a I_0(2a)}{I_1(2a)}; \quad a_0 = 0.5\,\ln\frac{p_0^2 + 0.125\,\omega_P^2}{p_0^2 I_0(2a)}. \qquad (5.20)$$

Here the function $k_0(a)$ corresponds to the "natural" frequency of the conditional oscillator and is determined as follows

$$k_0^2(a) = \frac{I_1(2a)}{a[I_0(2a) - 0.5a\,I_1(2a)]},$$

where $I_k(2a) = i^{-k} J_k(2ai)$; $i = \sqrt{-1}$; J_k is the Bessel function of the first order in case of imaginary argument $2a\,i$.

In Fig. 5.2, We can see the amplitude-frequency characteristics of the conditional oscillator with fixed values of the depth of pulsation $\varepsilon = 0.2;\ 0.4;\ldots;\ 1$ (thin lines). With increase in ε the curves became estranged from the skeleton curve (thick line). As the analysis shows, when $z \leq 1$, which corresponds to an almost three-fold change in Ω, the deviation of the backbone curve (thick line) from the
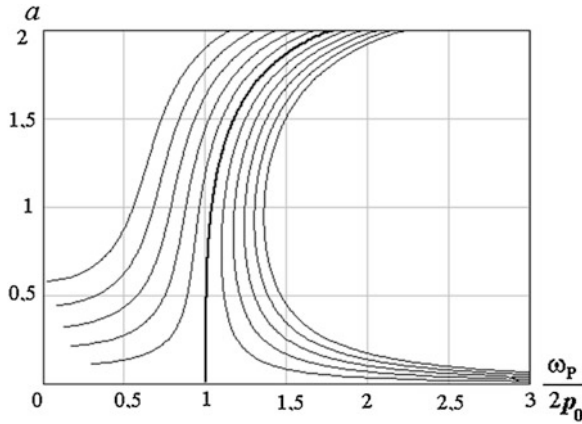
Fig. 5.2 Amplitude-frequency characteristic of the conditional oscillator

unit does not exceed 3.5 %. This allows, in the given case, to linearize the coefficients of Eq. (5.17), after which it takes the form

$$\ddot{z} + 4\bar{p}^2 z = 2(p^2 - \bar{p}^2), \qquad (5.21)$$

where $\bar{p}^2 = \Omega_*^2$ is the average value of the function $p^2(t)$.

We can see, in the Fig. 5.3, the phase trajectories for exact (solid line) and approximate solution (dotted line), which confirm the efficiency of linearization.

Let us illustrate the effect of parametric excitations in the zone of the main parametric resonance. Suppose, for example, there is a pulsation of the function
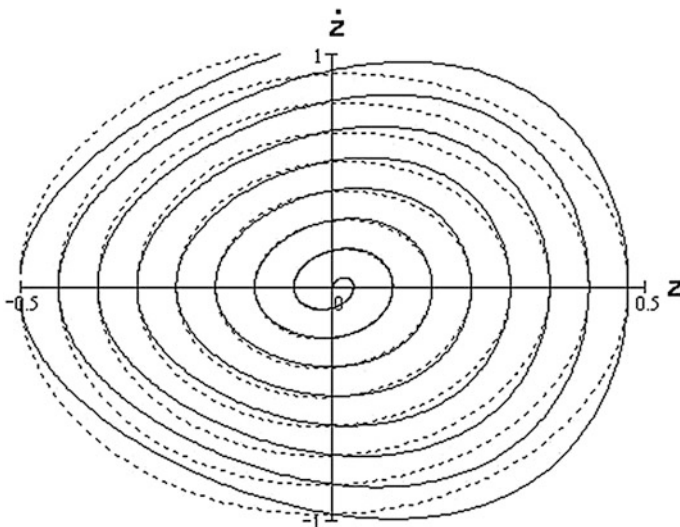
Fig. 5.3 Phase portraits for exact and approximate solutions

$p^2(t)$ around the mean value $\overline{p}^2$: $p^2 = \overline{p}^2(1 - \varepsilon \cos \omega_P t)$, where ε is the depth of pulsation. Then on the basis of (5.20) $\ddot{z} + 4\overline{p}^2 z = -2\varepsilon \cos \omega_P t$. Obviously the conditional oscillator resonates at $\omega_P = 2\overline{p}$ that corresponds to the main parametric resonance of the original system. The buildup of conditional oscillator is the necessary, though not sufficient, condition for the dynamic instability of the original system. On the other hand, we can confirm that the limitation of the variable amplitude in the first summand of the solution (5.16) is sufficient (but not necessary) to ensure dynamic stability (see below).

Family of the exact solutions If the function $p^2(t)$ is piecewise constant, then the equation of the condition oscillator (5.13) has an exact analytical solution. Therewith the accurate solutions can be constructed for many families of function $p^2(t)$, having certain properties. Further we consider the method of forming the exact solution. We use the earlier considered method of determining the parameters of free and forced vibrations under monotonous and rather abrupt change of function $p^2(t)$ [62]. Let's consider the monotonous change of $p^2(t) \in \left[p_0^2, p_*^2\right]$ at a certain period of time $t \in [0, t_*]$. The particular solution z_* is given in the form of some family of the functions with free parameters $\beta_1, \ldots, \beta_m$

$$z_* = \tilde{z}(t, \beta_1, \ldots, \beta_m). \tag{5.22}$$

After the substitution of (5.22) in (5.14) we get some function $\tilde{p}^2(t, \beta_1, \ldots, \beta_m)$, defined as follows

$$\tilde{p}^2(t, \beta_1, \ldots, \beta_m) = 0.5\ddot{\tilde{z}} - 0.25\dot{\tilde{z}}^2 + \Omega_*^2 e^{2\tilde{z}}. \tag{5.23}$$

Further we write the differential equation

$$\ddot{u} + \tilde{p}^2(t, \beta_1, \ldots, \beta_m)u = W(t). \tag{5.24}$$

It is obvious that Eq. (5.24) has an exact analytical solution, defined with dependencies (5.17), (5.18) and (5.20)–(5.22).

We can choose the free parameters β_i in such a way as to provide sufficient proximity between functions $\tilde{p}^2(t)$ and $p^2(t)$. In particular in case of minimization of the quadratic deviation we get

$$\int\limits_0^{t_*} p^2 \frac{\partial \tilde{p}^2}{\partial \beta_i}\, dt = \int\limits_0^{t_*} \tilde{p}^2 \frac{\partial \tilde{p}^2}{\partial \beta_i}\, dt. \qquad (i = 1, \ldots, m).$$

Often in case of monotonous variation of these functions, satisfactory accuracy is achieved, if we limit ourselves to their equality on the boundaries of the interval.

It is interesting that when $z = -2\ln(\beta_1 p_0 t + \beta_2)$, then the sum of the two first summands on the right side of the Eq. (5.26) is equal to zero. Then $\Omega = p_0 \exp \tilde{z} = \tilde{p}$, i.e. it is defined similarly in the first WKB-approximation, applied for slow-

changing parameters. The slow character of change in $p(t)$ is not stated explicitly, however, the exact solution, obtained using this method, imposes certain restrictions on the form of the function $p(t)$.

It can be shown that the homogeneous differential equation obtained from (5.24), with given method of forming $\tilde{p}^2(t)$, is the modified Bessel equation of the following form [31]

$$\ddot{u} + \left[\frac{1}{2}\frac{\ddot{\Phi}}{\Phi} - \frac{3}{4}\left(\frac{\ddot{\Phi}}{\dot{\Phi}}\right)^2 + (\frac{1}{4} - k^2)\left(\frac{\dot{\Phi}}{\Phi}\right)^2\right]u = 0,$$

when $k = 1/2$.

The solution of this equation is $u = Z_k(\Phi)\sqrt{\Phi/\dot{\Phi}}$, where $Z_k(\Phi) = C_1 J_k(\Phi) + C_2 Y_k(\Phi)$. J_r, Y_k are Bessel functions of the first and second order; C_1, C_2 are the arbitrary constants.

This result, with some modification of the arbitrary constants, completely coincides with the solution of the homogeneous equation, shown above.

5.2.2 Analytical Method of Solving for Steady-State Regimes

Let's introduce the dimensionless time $\Phi = \bar{p} \int_0^t e^z \, dt$, where $\bar{p}^2$ is the mean value of $p^2(t)$, and the new variable

$$v = q \, \exp[\int_0^t n_1(t)dt + 0.5 z]. \tag{5.25}$$

In the new coordinates, (5.25) takes the form of a differential equation with constant coefficients:

$$\frac{d^2 v}{d\Phi^2} + 2\delta \frac{dv}{d\Phi} + (1 + \delta^2)v = L(\Phi), \tag{5.26}$$

where $\delta = n_0\bar{p}$; $L = W\bar{p}^{-2}\exp[\int_0^t n_1(t)dt - 1.5z]$.

In the non-resonant modes, the function $n_1(t)$ and the forced oscillations of the conditional oscillator $z(t)$, are the periodic functions of the period $\tau = 2\pi/\omega$, where ω is the average value of $\dot{q}_0$. It is obvious that in this case the function $L(\Phi)$ is also periodic, with the dimensionless value of time for this function being equal to $\Phi(\tau) = \bar{p}\tau = 2\pi\bar{p}/\omega$. The dimensionless time Φ is a monotonously increasing function of time, as $d\Phi/dt = \Omega(t) = \bar{p}e^z > 0$.

As noted above, in practical calculations, usually the condition $|z| < 1$ is satisfied; therefore the forced oscillations of the conditional oscillator can be determined from the simple equation (5.24). Therewith in many cases, the additional simplification is related to the possibility of replacing e^z in the integrand for $\Phi(t)$ with several members of expansion of the Maclaurin series: $e^z \approx 1 + z + 0.5\,z^2$.

Let us represent the periodic function $L(\Phi)$ in the form of a Fourier series with respect to the argument Φ

$$L(\Phi) = L_0 + \sum_{j=1}^{\infty} (L_{cj} \cos j\tilde{\omega}\Phi + L_{sj} \sin j\tilde{\omega}\Phi), \qquad (5.27)$$

where

$$L_0 = \frac{1}{\Phi(\tau)} \int_0^{\Phi(\tau)} L(\Phi)\,d\Phi = \frac{\overline{p}}{\Phi(\tau)} \int_0^{\tau} L(t) e^{z(t)}\,dt;$$

$$L_{cj} = \frac{2}{\Phi(\tau)} \int_0^{\Phi(\tau)} L(\Phi) \cos(j\tilde{\omega}\Phi)\,d\Phi = \frac{2\overline{p}}{\Phi(\tau)} \int_0^{\tau} L(t) e^{z(t)} \cos[j\tilde{\omega}\Phi(t)]\,dt;$$

$$L_{sj} = \frac{2}{\Phi(\tau)} \int_0^{\Phi(\tau)} L(\Phi) \sin(j\tilde{\omega}\Phi)\,d\Phi = \frac{2\overline{p}}{\Phi(\tau)} \int_0^{\tau} L(t) e^{z(t)} \sin[j\tilde{\omega}\Phi(t)]\,dt;$$

$$\tilde{\omega} = 2\pi/\Phi(\tau) \approx 2\pi/(\overline{p}\tau).$$

Having solved the differential equation (5.26), taking into account (5.25) and (5.27), we obtain

$$q = \exp\left[-\int_0^t n_1(t)dt - 0.5\,z\right] \left[L_0 + \sum_{j=1}^{\infty} \frac{L_j \sin(j\tilde{\omega}\Phi(t) + \alpha_j - \Delta_j)}{\sqrt{(1 - j^2\tilde{\omega}^2)^2 + 4j^2\tilde{\omega}^2\delta^2}} \right], \qquad (5.28)$$

where $\delta = n_0/\overline{p}$ $(\delta^2 \ll 1)$; $L_j = \sqrt{L_{cj}^2 + L_{sj}^2}$; $\sin\alpha_j = L_{cj}/L_j$; $\cos\alpha_j = L_{sj}/L_j$; $\Delta_j = \arctan(2j\tilde{\omega}\delta/(1 - j^2\tilde{\omega}\alpha))$; $j\tilde{\omega} \neq 2$.

This method is especially useful for sufficiently smooth functions $p(t)$ and $W(t)$, which are usually used in the lever mechanisms, when during the expansion of the periodic functions into the Fourier series, we can restrict the process to a small number of members.

In case of abrupt changes of functions $W(t)$, as well as for the laws of motion with dwells, for the implementation of which we usually use the cam or step mechanisms, it is more preferable to use the closed form of solutions (see 4.1.2).

In clause 4.1.3 we showed the analytical method of solution formation, on the basis of expansion of the particular solution into series, with respect to its derivatives. The advantage of this method is in the clear identification of the sources of vibration activity. When analyzing we can also use the combined numerical and analytical method, which is described hereunder.

5.2.3 Numerical-Analytical Method of Solving for Steady-State Regimes

When calculating the steady-state regimes, the use of the purely numerical methods of calculation often lead to significant accumulated errors, due to the large number of steps of integration. In this case we can use the numerical and analytical way of solving the problem, which is devoid of the marked disadvantages and consists of several stages.

1. *Numerical integration of the differential equation of the conditional oscillator* (5.14) *with zero initial conditions over the period* $\tau = 2\pi/\omega_0$. The average for the cycle τ value of the "natural" frequency $p(t)$ i.e. $\Omega_* = \bar{p}$ is conveniently taken as the normalized value of Ω_*. At this stage we calculate $z(\tau),\ \dot{z}(\tau)$,
   $$\Phi(\tau) = \bar{p} \int_0^\tau e^z dt,\ \Omega(t) = \bar{p}\, e^{z(\tau)}.$$

2. *The determination of the particular solution Y with the help of the numerical integration of the original differential equation* (5.4) *with zero initial conditions:* Herein we find $Y(\tau)$ and $\dot{Y}(\tau)$. When performing numerical integration in the case of the discontinuity of moment t_j of the inertial factor a^* for joining of the solution, we should accept as follows $q(t_j - 0) = q(t_j + 0); a^*(t_j - 0)\dot{q}(t_j - 0) = a^*(t_j + 0)\dot{q}(t_j + 0)$.

3. *Analytical determination of the initial conditions corresponding to the steady state regime.* We first find $\xi = \sqrt{\xi_1^2 + \xi_2^2}$, where $\xi_1 = Y(\tau)$, $\xi_2 = \Omega^{-1}(\tau)\big[\dot{Y}(\tau) + 0.5\, \dot{z}(\tau)Y(\tau)\big]$.

   Furthermore we determine the factor of accumulation of perturbations μ, taking into account the oscillations, excited during the previous cycles (see Sect. 4.2)

$$\mu = \frac{1}{\sqrt{1 - 2e^{-\vartheta N} \cos 2\pi N + e^{-2\vartheta N}}}, \qquad (5.29)$$

where $N = \bar{p}/\omega$; ϑ is the logarithmic decrement (the graph of the factor μ is represented in Fig. 4.5).

The final expressions for the initial conditions in an arbitrary cycle of the steady motion regime are:

$$q_0 = \mu\xi \sin\gamma^0; \quad \dot{q}_0 = \mu\xi\bar{p}e^{z(\tau)} \cos\gamma^0, \tag{5.30}$$

where $\gamma^0 = \gamma + \arcsin\left[\mu e^{-9N} \sin 2\pi N\right]$; $\sin\gamma = \xi_1/\xi$; $\cos\gamma = \xi_2/\xi$.

4. *The numerical integration of the original differential equation with initial conditions of* (5.30).

Using the given method of numerical integration, only some intermediate functions are determined, calculated for a limited period of time; the conditions of periodicity of the solution are embedded in solution analytically, using the method of conditional oscillator. This method significantly affects the accuracy of the solution and also enables the achievement of effective engineering evaluations. In particular, formula (5.29) allows us to determine the highest and lowest effects due to oscillations, excited during the previous cycles. It is easy to see that for integer values of N $\mu = \mu_{max} = (1 - e^{-9N})^{-1}$; if $2N$ is an odd number, then $\mu = \mu_{min} = (1 + e^{-9N})^{-1}$ (see Fig. 4.5).

If the system's parameters are slowly changing, we can use some simplification of the described method. In this case, there is no need to integrate the conventional oscillator's differential equations, as $\Omega = \bar{p}e^z \approx p$; $\Phi = \int_0^\tau pdt$; $z = \ln p/\bar{p}$; $N = \bar{p}/\omega$.

5.2.4 Systems with Many Degrees of Freedom

As noted above, the parameter n in the problems of dynamics of mechanisms usually influences the "natural" frequency p very little and at the same time significantly influences the amplitudes of oscillations. A similar picture emerges from the analysis of the systems with variable parameters, displayed with the help of the models with many degrees of freedom. Then in the case of discretely assigned parameters, after linearization in the vicinity of the program motion, the frequency and the modal analysis are based on the system of the homogeneous differential equations

$$\mathbf{a}(t)\ddot{q} + \mathbf{c}(t)\mathbf{q} = 0, \tag{5.31}$$

where $\mathbf{a}(t)$, $\mathbf{c}(t)$ are the square matrices of inertial and quasi-elastic coefficients; $\mathbf{q}$ is the vector of the function of the generalized coordinates.

It can be shown that for up to the terms first order of smallness the kinetic and potential energies are defined accurately with dependencies $T = 0.5 \sum_{r=1}^{H} a_r^* \dot{\eta}_r^2$; $V = 0.5 \sum_{r=1}^{H} c_r^* \eta_r^2$, where η_r are the quasi-normal coordinates; H is the number of the degrees of freedom of the oscillatory system [40]. At the same time

the variable "natural" frequencies in the first approximation can be determined on the basis of the formal frequency equation, in which time acts as a parameter

$$\det\left(c_{ij}(t) - a_{ij}p(t)^2\right) = 0. \tag{5.32}$$

The relation between p_r and Ω_r, as earlier, is described by the equation of the conditional oscillator

$$\ddot{z}_r - 0.5\,\dot{z}_r^2 + 2\Omega_{*r}^2 e^{2z_r} = 2p_r^2(t),$$

where $z_r = \ln(\Omega_r/\Omega_{*r})$.

In the quasi-normal coordinates the system of the equations takes the following form

$$a_r^*(t)\ddot{\eta}_r + [b_r^*(t) + \dot{a}_r^*(t)]\dot{\eta}_r + c_r^*(t)\eta_r = M_r(t). \qquad (r = \overline{1,\,H}) \tag{5.33}$$

Here $M_r(t) = \sum_{i=1}^{H} \alpha_{ir} Q_{ir}^*$; Q_{ir}^* is the non-conservative generalized force from the external loads and kinematic excitation; $b_r^*(t)$ is the factor of the equivalent linear resistance reduced to the form r.

$a_r^* = \sum_{i=1}^{H} \sum_{j=1}^{H} \alpha_{ir}\alpha_{jr}a_{ij}$; $c_r^* = \sum_{i=1}^{H} \sum_{j=1}^{H} \alpha_{ir}\alpha_{jr}c_{ij}$, where α_{ij} are non-stationary shape factors.

In matrix form, we have

$$\alpha^T \mathbf{a}\,\alpha = \mathrm{diag}\{a_1^*, \ldots a_H^*\}; \quad \alpha^T \mathbf{c}\,\alpha = \mathrm{diag}\{c_1^*, \ldots c_H^*\}. \tag{5.34}$$

With the above mentioned method of determination of the quasi-normal coordinates of the form of oscillations, based on the physical assumptions, are accepted to be the slowly changing functions; as for the rest their determination doesn't differ from the similar procedure as for the case of constant parameters. Elimination of the "fast" components of the factors of the mode is not an obstacle for the analysis of the fast components $p_r^2(t)$ in the equation of the conditional oscillator. This is due to the relatively low sensitivity of the "natural" frequencies towards the changes of the modes of oscillations. This is the base feature, in particular, for the methods of Rayleigh, Galerkin and a number of other effective approximate methods of frequency analysis.

5.3 Dynamic Synthesis of Cyclic Mechanisms with Slow Changing Parameters

Manifestation of vibrations in systems with slowly varying parameters is sufficiently diverse and in each specific case it is reflected in the functions $q_i(t)$, corresponding to the relative dynamic errors (see Sect. 4.1.3). In turn the absolute

dynamic errors, i.e. the deviations of the kinematic characteristics of the links from the "ideal" values, corresponding to the program motion, depend on them.

The most significant effects in these models are usually associated with the oscillations of the input links of the mechanisms, since these lead to the violation of the linear relation between the angle of rotation of the input link and time (see also Chap. 7 and Sect. 8.5). We can see in Fig. 5.4a the illustration, where the experimental record, produced on the cam mechanism for the given symmetric sinusoidal law of accelerations of the cam follower and significant oscillations of the input link, is shown. As it can be seen from the oscillogram the velocity (curve 1) and acceleration (curve 2) of the cam follower have undergone significant distortion. In particular, there was redistribution between the intervals of run-in and run-out, which led to a sharp asymmetry of the law of motion and very large values of the accelerations in the run-out phase. Here we will focus on the main directions of the dynamic design of the mechanisms; this term means the rational management of the dynamic parameters of the system, at the design stage, on the basis of the specified dynamic criteria.

5.3.1 Stability Within an Arbitrary Time Interval

Section 5.2.1 showed the possibility of the buildup of the system in the areas of parametric resonance, when for accepted model, for arbitrarily small initial conditions, the amplitude of the free oscillations increases indefinitely (see details in Sect. 5.4). However apart from these cases in the systems with variable parameters, even when they change slowly, the *violations of the conditions of dynamic stability in the finite time interval.*

We can clearly see the corresponding dynamic effect in the experimental record (Fig. 5.4b).
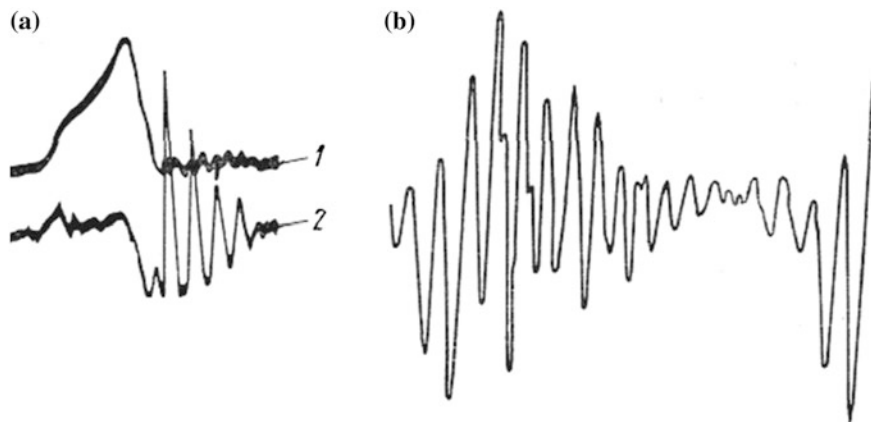
Fig. 5.4 Experimental records of the kinematic characteristics; **a** symmetry violation of the initial kinematic characteristics, **b** violations of the conditions of dynamic stability in the finite time interval

The zone of increase in oscillations alternates with the zone of attenuation, forming specific amplitude modulation of the oscillations, which is significantly manifested in the level of the system's vibration activity.

Dynamic model with one degree of freedom   For the analysis of the issue under consideration, we use the solution (5.16), in which we select the variable component of the amplitude of the accompanying vibrations.

$$Z = [a^*(t)p^*(t)]^{-0.5} \exp[-\int n_0(t)dt]. \tag{5.35}$$

To eliminate the possibility of increase in the accompanying oscillations, we will require $dZ/dt < 0$ for any moment in time. Then the condition of dynamic stability, on an arbitrary interval of the kinematic cycle, takes the form [64]

$$\tilde{\vartheta} = -\pi\vartheta^{-1}p^{-1}(\dot{a}^*/a^* + \dot{p}/p) < 1, \tag{5.36}$$

where ϑ is the logarithmic decrement.

Similar conditions for the vibration velocity and acceleration have the form

$$\tilde{\vartheta} = \pi p^{-1}\vartheta^{-1}(\dot{p}/p - \dot{a}^*/a^*) < 1; \quad \tilde{\vartheta} = \pi p^{-1}\vartheta^{-1}(3\dot{p}/p - \dot{a}^*/a^*) < 1. \tag{5.37}$$

It is interesting that these conditions can also be obtained in case of the arbitrary character of the changes $p(t)$ on the basis of the direct Lyapunov's method, which establishes sufficient conditions for the asymptotic stability [62]. In the considered case of slow change of parameters this condition on the level of the accepted approximate solution, turns out to be necessary as well.

If the variability of the parameters is determined by a single function $\Pi' \neq \text{const}$ then the inequalities (5.36) and (5.37) can comfortably be represented, with some allowance, as follows:

$$\tilde{\vartheta} = \pi\omega_0\vartheta^{-1}p_{\min}^{-1}|\Pi''_{\max}||v_1\beta_p + v_2\beta_a|_{\max} < 1, \tag{5.38}$$

where $\beta_p = p^{-1}dp/d\Pi'$; $\beta_a = (a^*)^{-1}da^*/d\Pi'$; for oscillation displacement $v_1 = v_2 = 1$; for oscillation velocity $v_1 = 1, v_2 = -1$; for oscillation acceleration $v_1 = 3, v_2 = -1$.

In particular for the dynamic model 1 (see Table 5.1) we obtain

$$\tilde{\vartheta} = -\frac{\pi(2s+1)\Pi'_*\Pi''_*\omega_0}{\vartheta k_0\rho^2\sqrt{1+(\Pi'_*/\rho)^2}} < 1, \tag{5.39}$$

where $s = 0$ corresponds to the condition (5.36), and $s = 1; 2$ to the conditions (5.41); $\rho = \sqrt{J/m}$; $k_0 = \sqrt{c/J}$.

As it follows from (5.39) the increase of the amplitudes should be expected in run-out areas of the driven link, when the kinetic power, proportional to the product of $\Pi'_*\Pi''_*$, is negative. In this case the determining factor is the condition recorded for the accelerations of oscillations ($s = 2$). The function $\tilde{\vartheta}$ can be used as a comprehensive criterion that characterizes the level of the dynamic load of the tested mode. This criterion increases with the increase in the $\Pi'_*\Pi''_*$ and angular velocity ω_0, and decreases with the increase in $k_0 = \sqrt{c/J}$, ρ and the logarithmic decrement ϑ.

As the amplitude growth is seen to increase for the time interval, equal to the period $T \approx 2\pi/p(t)$, therefore the given conditions can be relaxed if it is approximate to express the derivatives, in terms of finite increments in a period. In this case, condition (5.36) takes the following form

$$\tilde{\vartheta} = 0.5\, \vartheta^{-1} \ln[a^*_- p_- / (a^*_+ p_+)] < 1, \tag{5.40}$$

where plus corresponds to the time moment $t + 0.5\,T$, and minus to $t - 0.5\,T$. It follows from (5.40) that the risk of the violation of dynamic stability occurs when $a^*_+ p_+ < a^*_- p_-$ and when $a^* = $ const the increase in the amplitudes is possible when $p_+ < p_-$ and when $c^* = $ const if $p_+ > p_-$. Thus in general, it is impossible to make conclusions on the basis of the changes in the "natural" frequency only.

Dynamic model with many degrees of freedom As it is shown in Sect. 5.2.4, after the transition to the quasi-normal coordinates, the problem is reduced to the analysis of H differential equations of the second order with variable coefficients (5.37). After performing similar calculations, we obtain the conditions of dynamic stability in the form

$$\vartheta_r > \pi p_r^{-1}(\xi \dot{p}_r / p_r - \dot{a}^*_r / a^*_r) \quad (r = \overline{1, H}), \tag{5.41}$$

where $\xi = -1$ corresponds to the coordinate η_r; $\xi = 1$ corresponds to the velocity $\dot{\eta}_r$; $\xi = 3$ corresponds to the accelerations $\ddot{\eta}_r$. As under these conditions the system loses its most dangerous unsteady properties, they can be treated as quasi-stationary conditions. In some cases, corresponding to certain modes of oscillations, such conditions are realized because of the structure of the drive or the introduction of specific correcting chains.

5.3.2 Ways to Vibration Activity Reduce and Some Dynamic Criteria

Elimination of the jumps and abrupt changes of function $W(t)$ Just as in the mechanisms, depicted by dynamic models with constant parameters, the level of accompanying oscillations largely depends on the degree of smoothness of the function W (see formulae of Table 4.1). To eliminate the discontinuities of this function and its derivative, the conditions of the smoothness must be required from Π'_*, Π''_*, Π'''_*, F. Furthermore we should eliminate the equivalent jumps, when calculating with formulae, shown in Sect. 4.1.3, taking the average values of the "natural" frequency p for the considered time interval Δt. This requirement is met, in the first approximation, by the following correlation

$$N_{r\,\min} > [N_r]_\kappa,$$

where $N_{r\,\min} = p_{r\,\min}/\omega_0$; $[N_r]_\kappa = 6\pi/\Delta\varphi_*$; $\Delta\varphi_*$ is the ideal angle of the rotation of the input link, corresponding to the interval of abrupt change of the function W_r. Special attention should be paid, while taking into account the torsion compliance of the drive, to the value of the interval $\Delta\varphi_*$, embosomed between the extreme points of $(\Pi'_*\Pi''_*)_{\max}$ and $(\Pi'_*\Pi''_*)_{\min}$. As the perturbation function W_r, in the problems of dynamics of mechanisms, greatly depends on the laws of motion, the dynamic factors must necessarily be taken into account when conducting the synthesis of the mechanisms. In case of the slowly varying parameters the dynamic errors mainly depend on the pulse of the function W_r/p_r^2, describing the coordinate of the instantaneous position of the dynamic equilibrium of the system. This function can also be used as the minimized dynamic criterion [62].

Limitation of the coefficient of the accumulation of perturbations $\tilde{\mu}_r$ Using the formula (4.44) we obtain the following condition

$$N_{r\min} > [N_r]_\mu,$$

where $[N_r]_\mu = \vartheta_r^{-1}\ln(\mu_r^*/(\mu_r^* - 1))$; μ_r^* is allowable value for the coefficient of accumulation of perturbations ($\mu_r^* \approx 1.05 - 1.1$).

Reduction in the vibration activity of the drives of cyclic mechanisms using unloading devices: Apart from the indicated methods, to reduce the dynamic errors, we can use the special unloading devices, whose approximate calculations can be performed using averaging values of the parameters (see Sect. 4.3). In this case, however, one should not overlook the dynamic characteristics of the unloader itself, as otherwise, contrary to its intended purpose it may become the source of additional perturbations.

5.4 Conditions of Dynamic Stability in the Areas
   of Parametric Resonances

5.4.1 General Information About the Parametric Resonance

We have already mentioned the parametric resonance, associated with the certain pulse of the system parameters, such as reduced moment of inertia, or the reduced stiffness. The engineer, much more often, has to deal with the force-resonance, caused by the action on the system of the periodic driving force, than with the parametric resonance, arising in case of sufficiently precise frequency tuning. Because of this, the parametric resonance is sometimes regarded as an unlikely and insignificant side effect. Meanwhile in some cases it is not only a source of disruption of normal functioning of machinery, but also can lead to accidents, threatening the safety of operating personnel.

As the parametric resonance is the manifestation of the instability of motion (or particularly—the equilibrium state), we will give a brief explanation associated with the term "*stability of the movement*". *If the motion with the changed initial conditions is taken as perturbed motion, then the stability can be regarded as follows: when initial perturbations are arbitrarily small, then the perturbed motion differs arbitrarily small from the unperturbed motion.*

Moreover, when at $t \to \infty$, the motion tends to the undistorted motion, it is said to be *asymptotically stable*. Let $\varphi_j(t)$ be the investigated decision, ξ_j be the perturbation. Then according to A.M. Lyapunov the solution of $\varphi_j(t)$ will be stable if for any arbitrarily small number $\varepsilon > 0$ we can find a positive number $\eta(\varepsilon)$ such that for $\left|\xi_j(t_0)\right| \le \eta$ for any $t > t_0$ inequality $\left|\xi_j(t)\right| < \varepsilon$ will be satisfied. When in case of $t \to \infty$ the movement tends to the unperturbed, i.e. condition $\lim_{t\to\infty}\left|\xi_j(t)\right| = 0$ is satisfied, then the solution will be *asymptotically stable*. Initial perturbation, necessary apart from the other factors to arouse parametric resonance, are always present in the real system.

For example, the swaying of a swing would have been impossible in case of strictly zero initial conditions. We should note here that the studied dynamic model is not entirely adequate for its physical original; differences between them are substantially equivalent to the disturbances of the analyzed system. Providing the conditions of dynamic stability, as a rule, is one of the most important objectives of the design of machines. These conditions gain particular significance, when using cyclic mechanisms, which predetermine the variability of the parameters of the oscillatory system. It should be taken into consideration that the unstable motion is essentially uncontrollable, and therefore, any random disturbance for a sufficiently large period of time can lead to emergency consequences.

The problem of motion stability has been studied in an extensive number of papers. With regard to the problems of parametric excitation of mechanisms these issues are discussed in the following works: [15, 16, 58, 62–64, 83] etc.
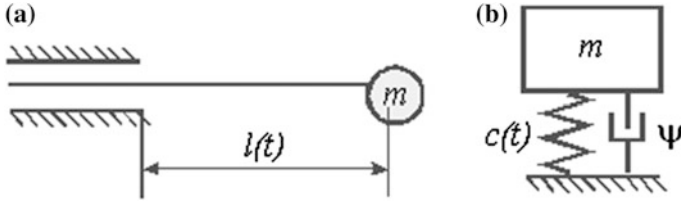
Fig. 5.5 Examples of systems with variable stiffness; **a** initial scheme, **b** dynamic model

We will illustrate the excitation of parametric resonance with the example of the changes in the coefficient of reduced stiffness, which we have already encountered during the analysis of the slider-crank mechanism (see Sect. 2.6.1). Similarly the reduced bending stiffness of the needles of textile and sewing machines or the spindle of the machine tool can change (Fig. 5.5a). In such cases the task is reduced to the analysis of the dynamic model, shown in Fig. 5.5b. Quite often, the change in the coefficient of reduced stiffness can be approximated using the harmonic function of the form $c(t) = c_0 - \Delta c \sin \omega_P t$, where c_0, Δc are the mean values and amplitude of the variable part of the coefficient of stiffness. Hence we can write the differential equation (5.3) as follows

$$m\ddot{y} + b\dot{y} + c_0(1 - \varepsilon \sin \omega_P t)y = 0. \tag{5.42}$$

The ratio $\varepsilon = \Delta c/c_0$ is called the *depth of pulsation*; ω_P *is the frequency of the parametric excitation,* $\tau = 2\pi/\omega_P$ *is the period of parametric excitation.*

According to (5.42) occurring is the pulse of the square of the "natural" frequency with respect to the mean value $k_0^2 = c_0/m$ (minor influence of dissipation is not taken into account)

$$k^2(t) = k_0^2(1 - \varepsilon \sin \omega_P t), \tag{5.43}$$

As it was shown in Sect. 5.2.1, the conditional oscillator is subjected to the excitation $-2\varepsilon k_0^2 \sin \omega_P t$ and consequently, it resonates at $\omega_P = 2k_0$, which corresponds to the *main parametric resonance.* A more detailed analysis shows that in addition to this resonant frequency the areas of dynamic instability are located in the vicinity of the values

$$\omega_{P*} = 2k_0/s, \tag{5.44}$$

where $s = 1, 2, 3, \ldots, \infty$.

These areas are marked, on the coordinate plane ε, ω_P/k_0, with hatching (Fig. 5.6). The methods of determination of the boundaries of these areas is shown in many monographs, textbooks and reference books. From an engineering point of view, the minima of the instability regions are of greater interest (see below).
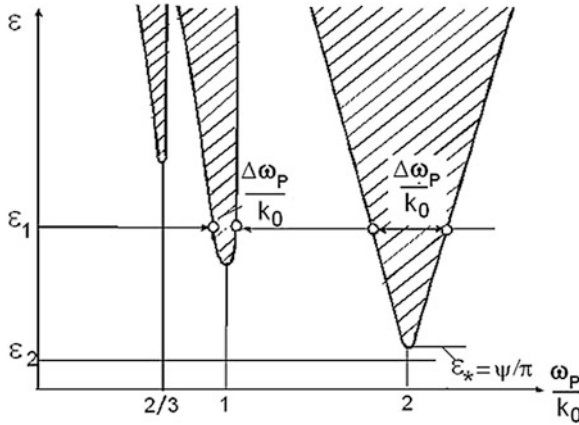
Fig. 5.6 Areas of dynamic instability

Suppose, for example $\varepsilon = \varepsilon_1$, which corresponds to a line in the diagram, parallel to the X-axis. The points of intersection of this line with the boundaries of the areas of dynamic instability restrict the range of critical frequencies $\Delta\omega_P$ which host parametric resonance.

5.4.2 Methods of Elimination of the Parametric Resonance

Let us use the diagram, shown in Fig. 5.6, to outline the two principal possibilities of elimination of parametric excitation. The first method is related to frequency detuning from the critical areas, in which the values ω_P are sufficiently removed from ω_{P*}. The second method is illustrated in Fig. 5.6, with a straight line $\varepsilon = \varepsilon_2$. Obviously if $\varepsilon_2 < \varepsilon_*$, where ε_* is the critical depth of pulsation, then the line ε_2 does not intersect any of the regions of instability, and therefore, regardless of the frequency of the parametric excitation, the system is dynamically stable over the whole frequency range. The second method is more reliable, because when using actual input data, the boundaries of the areas are located in the small vicinity of the critical zones. To determine the critical pulse depth we will use the energy method. Let us represent Eq. (5.42) as follows:

$$m\ddot{y} + c_0 y = -b\dot{y} + \varepsilon c_0 y \, \sin\omega_P t. \tag{5.45}$$

Multiplying both sides of this equation by $dy = \dot{y}dt$, we get $dE = Q\dot{y}dt$; where E is the total energy; Q is the right side of the Eq. (5.3). Hence

$$\Delta E_- = -b \int_0^T \dot{y}^2 dt; \quad \Delta E_+ = \varepsilon c_0 \int_0^T y\dot{y} \sin \omega_\mathrm{P} t \, dt,$$

where $\Delta E_-, \Delta E_+$ are withdrawn and supplied energies for a single period of oscillation $T \approx 2\pi/k_0$ $(k_0 = \sqrt{c_0/m})$. We approximately take within the single period of oscillation $y \approx A \sin(k_0 t + \alpha)$, where A is the average value of the amplitude for the given period. Then

$$\Delta E_- = 0.5 \, \psi c_0 A^2;$$
$$\Delta E_+ = \varepsilon c_0 k_0 A^2 \int_0^T \sin \omega_\mathrm{P} t \, \sin(k_0 t + \alpha) \cos(k_0 t + \alpha) dt.$$

Let $\omega_\mathrm{P} = \omega_{\mathrm{P}*} = 2k_0$, which corresponds to the main parametric resonance. In this case after integration we obtain $\Delta E_+ = 0.5 \, \varepsilon c_0 A^2 \pi \cos 2\alpha$. The phase shift $\alpha = 0$ corresponds to maximum input energy. Thus,

$$\Delta E = \Delta E_+ - \Delta E_- = 0.5 \, \pi c_0 \varepsilon A^2 - 0.5 \, \psi c_0 A^2. \tag{5.46}$$

$\Delta E < 0$ corresponds to the attenuation of oscillations. Then on the basis of (5.46),

$$\varepsilon < \varepsilon_* = \psi/\pi. \tag{5.47}$$

Thus, a certain level of dissipative forces serves as an energy barrier that prevents parametric excitation. The correlation $\varepsilon_*/\varepsilon$ determines the stability allowance of the system.

If instead of linear force of resistance, the system is subjected to the force of dry friction H, then $\Delta E_- = 4|H|A$, and condition $\Delta E_+ - \Delta E_- < 0$ when $\Omega = 2k_0$ takes the form

$$A < A_* = 8H/(\pi c_0 \varepsilon). \tag{5.48}$$

This means that under constant force of resistance, there exists a critical value of the amplitude A_*, below which the conditions of dynamic stability are provided for. In case of $A > A_*$, in the area of main parametric resonance, the amplitudes of oscillations will increase. In case of the violation of the conditions of dynamic stability, the amplitudes increase very rapidly. Therefore even a short interval of time in the critical zone may cause an accident. Hence to ensure trouble-free and reliable operation of high-speed mechanisms, the implementation of the condition $\varepsilon < \varepsilon_*$ is more justified than the frequency detuning of the operating modes from the closer critical zones (for details see Sects. 6.3.5 and 6.3.6).

5.4.3 Estimation of Resonant Amplitudes Under the Joint Action of the Disturbing Force and Parametric Excitation

In the differential equation (5.4) we will accept $k^2 = k_0^2(1 - \varepsilon \sin \omega_2 t)$ and $W = h \sin(\omega_1 t - \gamma_1)$ when $\omega_2 = 2k_0 = 2\omega_1$ that corresponds to the "forced" resonance and simultaneously to the main parametric resonance. Let us write the expression that determines the energy increment for the period $T_1 = 2\pi/\omega_1$:

$$\Delta E = \int_{E_1}^{E_2} dE = \int_0^{T_1} [h\dot{q}\sin(\omega_1 t - \gamma_1) - 2n\dot{q}^2 + \varepsilon k_0^2 q\dot{q}\sin\omega_2 t]dt.$$

In the steady regime $\Delta E = 0$. Hence, taking as an approximate solution $q = A\sin(\omega_1 t - \gamma_2)$, after integration we obtain

$$A = \pi k_0^{-2} h \sin(\gamma_2 - \gamma_1)/(\vartheta - \vartheta_* \cos 2\gamma_2), \qquad (5.49)$$

where $\vartheta_* = 0.5\,\pi\varepsilon$.

In case of resonance $\gamma_2 - \gamma_1 = \pi/2$. Thus the amplitude of resonance A on the basis of (5.49) corresponds to the conditional system without parametric excitation, but with the changed level of dissipation corresponding to $\vartheta_1 = \vartheta - \vartheta_* \cos 2\gamma_2$. Depending on the phase shift γ_2 this parameter takes value in the range $\vartheta_1 \in [\vartheta - \vartheta_*,\ \vartheta + \vartheta_*]$, so amplitude A may be either higher or lower than the value obtained, when $\varepsilon = 0$. Of course, with $\vartheta < \vartheta_*$ the question of the maximum amplitude is meaningless, as in this case the system is dynamically unstable. Thus, the above identified conditions for the asymptotic stability of equilibrium remain valid in case of forced oscillations, however, in this case they do not show attenuation of oscillations, but indicate the asymptotic approximation of the perturbed motion to the tested mode.

When analyzing parametric resonance in multi-masses systems, we can take advantage of the transition to quasi-normal coordinates for the averaged values of the coefficients of the forms.

Of course the different modes of oscillations of the rheonomous systems are interconnected, which leads to errors in calculation. Therewith "averaging" the shapes of oscillations, we thereby exclude the inertial components, which arise in case of change of the earlier. Usually, however, the connectivity of the systems in this class of problems is rather weak. At the same time, the forced separation of modes, into the main areas of the parametric excitation, usually, enhances the allowance of stability.

These considerations allow us to assume that the zones of parametric resonance, in the first approximation, correspond to the vicinity of the frequencies, for which the relation $i\omega = \bar{p}_r/j$ is valid; where $j = 1/2, 1, 3/2, 2, \ldots$ are the averaged, for the period, values of the roots of the formal frequency equation (5.32). In the

quasi-normal coordinates the differential equations have the form of (5.33), so the technique to study these modes and methods of suppressing parametric resonances are no different from those used above in the study of systems with one degree of freedom. However, the use of this approach involves qualitative loss of sorts.

The fact is that apart from the parametric resonances, the system can be excited by the so-called *combination resonances*, when $i\omega$ is equal to the linear combination of several averaged "natural" frequencies. In the simplest of cases $i\omega = \bar{p}_{r2} \pm \bar{p}_{r1}$, where the minus sign corresponds to the "difference", and plus to the "total" combination resonance; $\bar{p}_{r1}, \bar{p}_{r2}$ are the two values of $\bar{p}_r$. The analysis of the conditions, ensuring the suppression of the combination resonances in cyclic mechanical systems is given in [18]. Here we will merely note that when the stability conditions are performed with a certain allowance in the areas of the main parametric resonances the combination resonances are also supposed to be suppressed.

5.5 Parametric Impulse

In oscillatory systems with cyclic mechanisms, the short splash of the "natural" frequency sometimes takes place, with subsequent recovery of the initial value. Let us call such behavior of change of the system's parameters as *the parametric impulse.* The occurrence of such modes may be associated as much with the change in the elastic as inertial characteristics. Parametric impulses are observed in the cyclic mechanisms, described with models 1, 2, 3 (see Table 5.1) in case of pulsed nature of the variation of the first transfer function Π'. The latter in particular is typical for mechanisms, in which the kinematic cycle consists of large areas of uniform motion of the output link and the small transition intervals of reverse, as, for example, it is true for traverse mechanisms of the textile machines, automatic machine tools, flat-bed printing machines etc.

5.5.1 Single Parametric Impulse

Let us consider the following initial conditions. Let (Fig. 5.7a)

$$p = \begin{cases} p_0 & t < 0, \qquad \text{interval I} \\ p_1, & t < t < t_1, \quad \text{interval II} \\ p_0 & t > t_1, \qquad \text{interval III.} \end{cases}$$

As shown by analysis, for small values of the length of time t_1 the above representation of $p(t)$ as a piecewise constant function can be used not only in the mechanisms of variable structure, but as a fairly good approximation of the
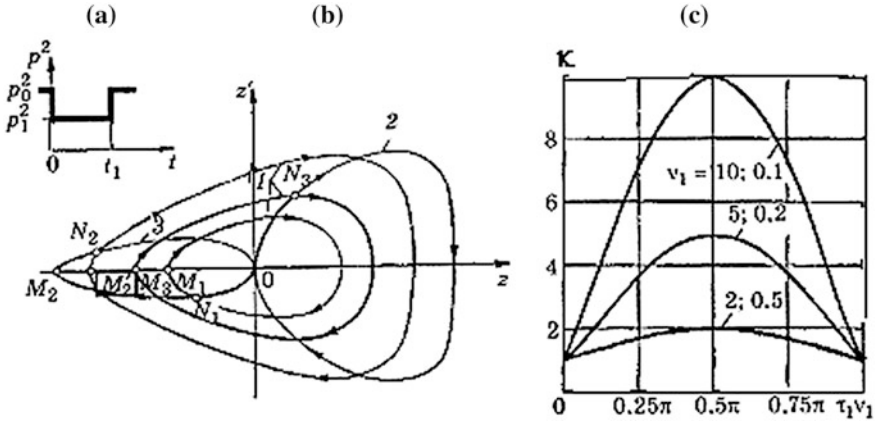
Fig. 5.7 To the analysis of parametric impulse; **a** graph $p_2(t)$, **b** phase trajectories, **c** graphs of the factor of increase in amplitude

corresponding functions, obtained for mechanisms with smooth variation of the "natural" frequency.

To describe the amplitudes of oscillations we use the exact solution of the conditional oscillator for piecewise constant characteristics of $p(t)$ set out in Sect. 5.2. First we investigate the behavior of the system in the phase plane of the conditional oscillator $z'(z)$. Let us accept $\Omega_* = p_0$; $\tau = p_0 t$.

The values of $z_{\min}$, which determine the maximum amplitude of the function $y_*(t)$ are of most interest on the phase trajectories (Fig. 5.7b; points M_i, $i = 1, 2, 3$).

$$A_{\max} = A_0 \exp[-0.5 (z_{\min} - z_0)], \tag{5.50}$$

where $A_0 = A(0)$.

While solving the problem of the parametric impulses, $v = p/p_0$ as the dimensionless frequency, is more preferable. Then in the first and third intervals $v = 1$, whereas $v = v_1$ in the second interval.

Case 1 At the first interval $z = z_0 = \ln(p/p_0) = 0$, which corresponds to the origin of coordinate (point 0). In the second interval, the phase trajectory, on the basis of (5.21), is described as:

$$z = \ln \frac{2v^2 v_0}{v^2 + v_0^2 + (v^2 - v_0^2) \cos 2v(\tau - \tau_0)},$$

$$z' = \pm 2 \sqrt{(0.25 z_0'^2 + v^2 + e^{2z_0}) e^{z - z_0} - (v^2 + e^{2z})}. \tag{5.51}$$

Here τ_0, v_0 correspond to the values at the end of previous interval. In this case, we should accept $v_0 = 1$; $v = v_1$, $\tau_0 = 0$; $z_0 = z_0' = 0$.

Assuming the current values of τ, with (5.51) we can draw up the phase trajectory (Fig. 5.7b, curve 3). Switching point N_i, corresponding to the border of the areas *II*

and *III*, is determined at $\tau = \tau_1 = p_0 t_1$. There can be two outcomes: If $\tau_1 = p_0 t_1 < \pi/2\nu_1$, then switching will take place in point N_1, hence function z does not reach the minimum on the second interval. When $\tau_1 > \pi/2\nu_1$, the switching point will be N_2, so the minimum value $z_{min} = 2 \ln \nu_1$ is located on the second interval.

On the interval *III* the phase trajectory (curve 1) is defined with the same dependencies (5.51), if we accept $\nu_0 = \nu_1$; $\tau_0 = \tau_1$; $z_0 = z(\tau_1) = z_1$; $z'_0 = z'(\tau_1) = z'_1$. The value z_{min} is determined as less than the root of the next quadratic equation, obtained from (5.51) when $z' = 0$:

$$e^{2z_{min}} - e^{z_{min}} \left[1 + \nu_1^2 + \left(1 - \nu_1^2 \right) e^{-z_1} \right] + 1 = 0. \tag{5.52}$$

The points M_1, M'_2 on the phase plane of the conditional oscillator correspond to the value z_{min}.

Case 2 $\nu_1 = p_1/p_0 > 1$. This case can also be analyzed with the help of dependence (5.51). In this case the phase trajectory passes along curve 2 from point 0 to point N_3, whereupon it passes along curves of the family 1 (see Fig. 5.7a). This case differs from the above mentioned one, because the minimum value of the function z is equal to zero in the interval *II*. It means that within this interval $A \leq A_0$. However increase of the amplitude in the interval *III* can be very considerable and depends on value of z_{min} (point M_3).

Using (5.52) we will determine the factor of increase in amplitude $\kappa = A^*_{max}/A_0$, where A^*_{max} is the maximum possible value of the amplitude outside the parametric impulse zone. It can be shown, that

$$\kappa = \left[\frac{\sqrt{H + \sqrt{\left(H^2 - 16\nu_1^4 \right)}}}{2\nu_1} \right]^m,$$

where $H = \left(1 + \nu_1^2 \right)^2 - \left(1 - \nu_1^2 \right)^2 \cos 2\nu_1 \tau_1$; $m = \text{sign}(\nu_1 - 1)$.

The analysis of the function $\kappa(\nu_1 \tau_1)$ (Fig. 5.7c), shows that the amplitude of free vibrations, during the passage through the zone of single parametric impulse, is limited by the following inequality $\kappa \leq \nu_1^m$. Thus, even under the most unfavorable phase shifts within the same period T_ω we get

$$q_{max} \leq A_0 \kappa \exp \left[- \int\limits_0^{T_\omega} n dt \right]. \tag{5.53}$$

Thus, the above mentioned technique allows to get the very concise engineering estimation, which is used to determine the highest level of possible dynamic aftereffect. This method can be applied to the more complex forms of parametric impulse. So, if the parametric impulse has the form as shown in Fig. 5.8a, then the

phase trajectory consists of three sections and has two switching points N_1 and N_2 (Fig. 5.8c, curve 1). The values of z_1 and z_1' are determined with (5.51).

To find the parameters, corresponding to the second point of shift, we can use the same dependencies if we accept z_0 and z_0' as the initial values in the given interval (i.e. in our case $z_0 = z_1$ and $z_0' = z_1'$) and the value of v_0 as the value of v on the previous interval (i.e. in our case $v_0 = v_1$). The issue of the minimum value of z is solved in a similar fashion as for the cases considered above, and does not require additional calculations.

The parametric impulse consisting of four sections is shown in Fig. 5.8b, which correspond to the following segments of the phase trajectory (Fig. 5.8c, curve 2): $0 - N_1'$ $(v = v_1)$; $N_2' - N_3'$ $(v = v_2)$; $N_3' - M' - \ldots$ $(v = 1)$.

Let us note that the above mentioned phase trajectories are used only to illustrate the calculations and their compilation isn't required while solving a particular problem, since all the characteristic points of the phase plane are determined as per the derived final analytical functions.
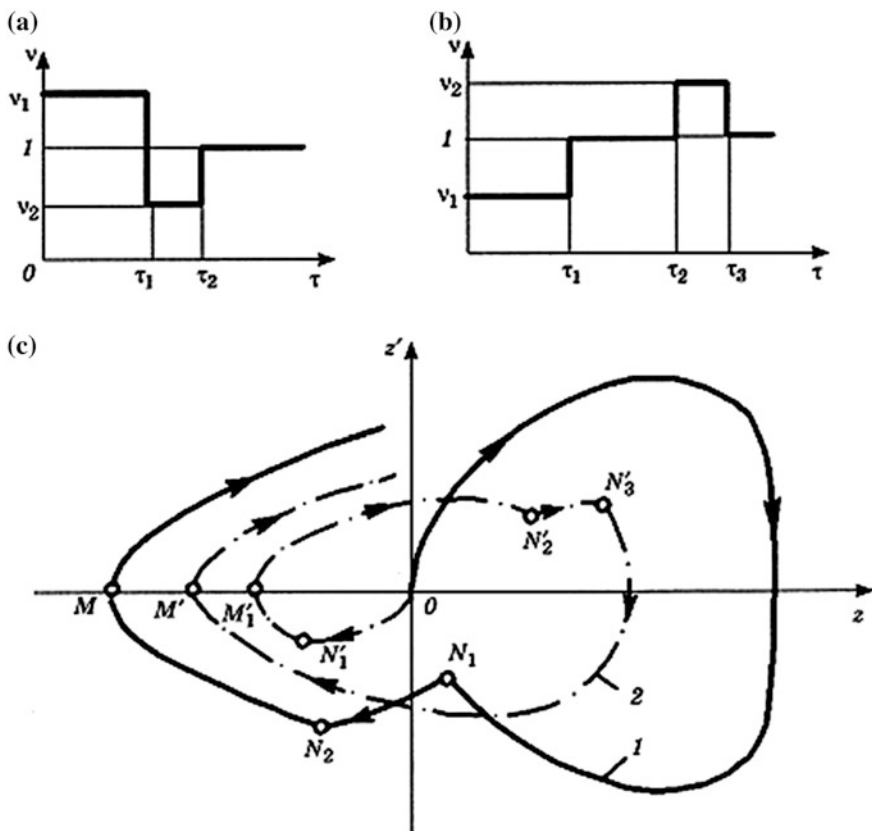
Fig. 5.8 To the analysis of the parametric impulses with many switching points; **a** parametric impulse consisting of three sections, **b** parametric impulse consisting of four sections, **c** phase trajectories

5.5.2 Dynamic Effect Due to Action of Periodic Parametric Impulses

In case of periodic repeatability of the parametric impulses, the maximum value of the amplitude of free oscillations, after one period of the kinematic cycle, can reach

$$A_1 = A_0 \exp\left[-\int_0^\tau n(t)dt\right] \prod_{i=1}^s \kappa_i, \qquad (5.54)$$

where s is the number of parametric impulses in one period.

Equations (5.53) and (5.54) show that the dynamic effect of parametric impulses can be equivalent to the decrease in dissipation level of the system. When $A_1/A_0 > 1$ there is a possibility of occurrence of parametric resonance. The sufficient condition of the dynamic stability has the form

$$\exp\left[-\int_0^\tau n(t)\right] \prod_{i=1}^s \kappa_i < 1. \qquad (5.55)$$

5.6 Cyclic Mechanisms with Force Closure

5.6.1 The Influence of the Drive's Vibrations on Conditions of Force Closure

In modern machines, mechanisms with unilateral constraints, using the force closure consisting of springs, to prevent the loss of contact in the kinematic pairs, are widely used. It is the cam mechanisms, in which we most commonly encounter spring closure, however, quite often the closing springs are installed on links of lever, cam-lever and other mechanisms for the partial or complete elimination of inter-mating of the working surfaces, arising from the relining in the clearances, of the kinematic pairs. The reliable operation of the closing system can be impaired due to various reasons, among which the oscillations of the springs and the oscillations of the mechanism's links, excited among others, by the closing force, are the most important ones. If dynamic loads are predominant, then the condition $F = \xi|P^i|_{max}$, where P^i is the inertial force; F is the closing force, $\xi > 1$ is the safety factor, should be observed. During the oscillations the closing force and the force of inertia, defined on the basis of kinetostatic model, can vary substantially. The latter fact may lead to the breach of the forced closure, irremovable by increasing the closing force. This effect is due to the non-stationary character of the kinematic connections, because of which in case of the nonlinear position function, even the constant component of the closing force transforms into variable torque

(a)   **(b)**
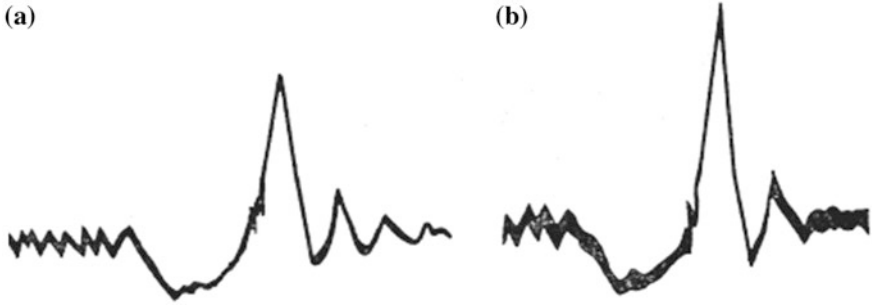
Fig. 5.9 To the analysis of the dynamic effect resulting from the increase in the closing force; **a** initial value of the closing force, **b** an enlarged value of the closing force

$M_0 = \Pi' F_0$, acting on the drive. In this case the forced oscillations of input link are additionally excited, causing the increment of inertial loads on the output unit.

We can see in Fig. 5.9, the two oscillograms, obtained when recording accelerations of the cam follower on the experimental stand of the cam mechanism with the spring closure [62]. Input data for the recording of these oscillograms is identical, except the forces of the preliminary deformation, which in the second case (Fig. 5.9b) as compared to the first (Fig. 5.9a) was increased by 1.5 times. As a result, the maximum acceleration of the cam follower increased by about 40 %.

Let $F = F_0 + c_0 \Pi$, where c_0, F_0 are the coefficient of stiffness and force from preliminary deformation of the closing spring, Π is the position function of the output link.

There is a functional connection $\left| P^i \right|_{max} = \Psi(F_0)$ between $\left| P^i \right|_{max}$ and F_0. Let us give some increment to the force F_0, equal to ΔF_0. Then, restricting to linear approximation, we have

$$\left| P^i \right|_{max} + \Delta P^i \approx \Psi(F_0) + \frac{\partial \Psi}{\partial F_0}(F_0) \Delta F. \tag{5.56}$$

Let us introduce the notion of the ideal increment of the factor of allowance $\Delta \xi_0 = \Delta F / \left| P^i \right|_{max}$ in case of absolutely rigid drive, i.e. when $\Delta P^i = 0$. Using (5.56) we can show that when taking into account the drive's elasticity $\Delta \xi = \zeta \Delta \xi_0$, where

$$\zeta = (1 - h)/(1 + h \, \delta \xi_0). \tag{5.57}$$

Here $h = \dfrac{\partial \Psi}{\partial F_0}(F_0)$; $\delta \xi_0 = \Delta \xi_0 / \xi$.

The graph $\zeta(h)$ clearly shows three distinct modes of operation of the closing system (Fig. 5.10). For small values of h the coefficient ζ is close to unity. This means that increment in the factor of allowance $\Delta \xi$ is only slightly below its ideal value $\Delta \xi_0$. When $h \approx 1$ we have $\zeta \approx 0$. This corresponds to the case where an increase of the closing force does not lead to any noticeable change of the initial

value of factor of allowance ξ. At last, when $h > 1$ we have $\zeta < 0$. In this mode it can be expected that increase in the closing force leads to increase in the intensity of the discontinuities of the kinematic connections and the further deterioration of the mechanism's operation. This means that the attempt to eliminate the discontinuities of the kinematic contact by increasing the closing force, will fail, and the locking system completely loses sensitivity to the installation and operating regulations, that is, in fact, it turns out to be uncontrollable.

As it can be seen from the represented graphs, on the real range of variation $\Delta \xi_0 = \Delta \xi_0 / \xi < 1$, this parameter has relatively weak influence on the value of ζ. We now turn to some of the "preventive" measures, which eliminate the possibility of the operation of the mechanism in the dead zone of the closing system. We restrict the change of the parameter ζ to some admissible value $\zeta < [\zeta]$. When choosing the value of $[\zeta]$ it should be taken into account that the closing force, which prevents the disclosing of the system in run-down, is a very significant additional load on the links and kinematic pairs of the mechanism during the run-in, which can lead to increased wear and tear, as well as decreased the mechanism's efficiency, durability and reliability. Therefore it seems reasonable to accept $[\zeta] \approx 0.8$. This limit, taking into account (5.57) can be written as follows

$$h < [h] = (1 - [\zeta])/(1 + \delta \xi_0). \qquad (5.58)$$

To eliminate the effect of uncontrollability of the locking force, remaining within the limits of the dynamic model 1-Π-1 (see item 2.3), we can ensure that in the first approximation

$$h \approx (3 \div 4) \left| \frac{P_*^i \sigma_*^2 \Pi''_{\max}}{(\sigma_*^2 - 1) c_1} \right|. \qquad (5.59)$$

Here c_1 is the reduced torsion stiffness of the drive; $\sigma_* = p_2/p_1$, where p_1, p_2 are the partial frequencies of the driving and driven subsystems of the mechanism; P_*^i is the ideal force of inertia (or moment of inertia forces) in the area of possible discontinuity of the kinematic chain.

From (5.59) it follows that marked phenomenon cannot be eliminated by changing the parameters of the closing spring and is defined by the dynamic characteristics of the drive and in the first place its reduced stiffness, which must satisfy the following condition:

$$c_1 > c_1^* \approx \frac{20 \sigma_*^2 (1 + \delta \xi_0)}{\left| \sigma_*^2 - 1 \right|} |\Pi''|_{\max} P_*^i \xi.$$

When $c_1 \to \infty$, according to (5.59) we have $h \to 0$; thus the actual increment of the factor of safety coincides with ideal value, i.e. $\zeta \to 0$ (see Fig. 5.10).
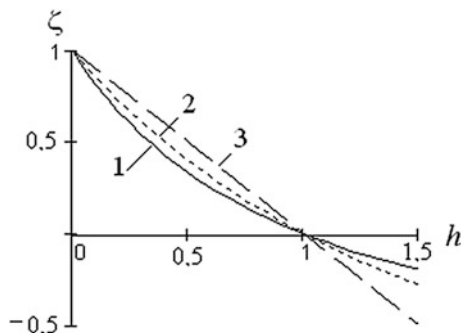
Fig. 5.10 Graph $\zeta(h)$: $1 - \delta\xi_0 = 1$; 2–3–$\delta\xi_0 = 0$

5.6.2 Longitudinal Oscillations of the Closing Springs

Thus, the increase of the closing force to overcome the inertial loads of the output link under certain conditions may not be effective, since at the same time the force of inertia caused by this force increases. This leads to the lack of controllability of the closing system and to the increase in the vibration activity of the system. Furthermore we consider this problem in conjunction with the analysis of the oscillations in the closing spring itself that makes possible a more complete assessment of the considered phenomenon and the relative engineering recommendations. Let us turn to the dynamic model (Fig. 5.11), which shows the cyclic mechanism in the form of a consecutive chain of inertial elements (J_0, J_1, m) and elastic and dissipative (c_1, ψ_1) elements.

The input part of mechanism J is separated from the output part m with element Π that simulates the transformation of the input coordinate $\varphi_0 + q$ to the output coordinate $s = \Pi(\varphi_0)$. The angular velocity of the element J_0 is assumed to be constant ω_0. The closing spring attached to the output link at the point N_1 is, strictly speaking, the spatial curve beam, however at relatively small lifting angles of the helix the spring, as it is known, can be replaced with a straight beam [56]. When determining the frequency response of the system the dissipation can be neglected. Let us write the homogeneous differential equation of the schematized spring
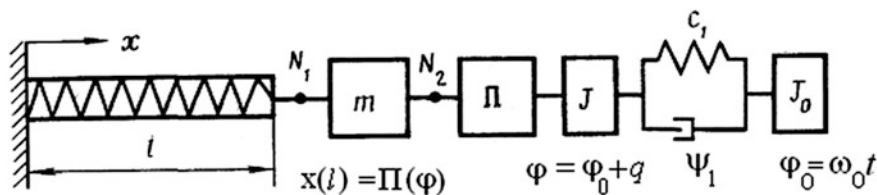
Fig. 5.11 Model of the cyclic mechanism with spring closing

$$\frac{\partial^2 u}{\partial x^2} - g_0^{-2}\frac{\partial^2 u}{\partial t^2} = 0, \tag{5.60}$$

where $u(x,t)$ is the displacement of the section x; $g_0^2 = ES/\mu_0$; ES; μ_0 are the stiffness of the section of the equivalent "rod" and mass per unit length; E is the modulus of elasticity; S is the cross-sectional area of the rod.

Assuming that the length of the equivalent rod is equal to the average height of the spring l, for cylinder helix spring made of steel wire of round section we have $ES = 8 \times 10^{10}d^4\ell/8D^3 n$; $g_0 = 2.264 \times 10^3 d\ell/(\pi D^3 n)$, where d is the diameter of the wire; D is the average diameter of the spring; n is the number of active coils. As the parameters of the real mechanisms are slowly varying functions of time, one of the boundary conditions of (5.60) also has a non-stationary character. According to the method of conditional oscillator the particular solution of (5.60) can be written as $u = X(x,\tau)\Psi(t)$ where τ is slow time. Then Eq. (5.60) corresponds to the following ordinary differential equation describing the time-varying oscillation form

$$X'' + \lambda^2(\tau)X = 0, \tag{5.61}$$

where $(\ )' = \partial/\partial x$; $\lambda^2(\tau) = \mu_0 p^2(\tau)/(ES)$; $p(\tau)$ is the varying "natural" frequency.

Approximate solution of (5.61) can be written as

$$X = \alpha\cos\lambda x + \sin\lambda x. \tag{5.62}$$

As $X(0,\tau) \equiv 0$ we have $\alpha = 0$. Furthermore, normalizing the form in such a way that $X(\ell,\tau) \equiv 1$ we represent (5.62) as

$$X = \sin\theta/\sin\theta_*, \tag{5.63}$$

where $\theta = \lambda x$, $\theta_* = \lambda\ell$.

The second unused boundary condition is defined on the basis of the equality of the amplitude values of the forces in the cross section N_1, taking into account $u = -s = -\Pi(\varphi)$:

$$\ell X'(\theta_*)/X(\theta_*) = -R/c_0, \tag{5.64}$$

where $c_0 = ES/\ell$ is the stiffness coefficient of the spring; R is the dynamic stiffness of the mechanism. On the basis of (5.63) and (5.64) after determining the dynamic stiffness of the mechanism the formal frequency equation can be written as follows:

$$\frac{\tan\theta_*}{\theta_*}\left[\frac{\theta_*^2 g_0^2(J + m\Pi'^2_*)}{c_1\ell^2} - 1\right] = \frac{c_0\Pi'^2_*}{c_1}. \tag{5.65}$$

Equation (5.65) has an infinite number of roots $\theta_{*r}(\tau)$ $r = (\overline{1, \infty})$. The variable "natural" frequency is determined as $p_r(\tau) = g_0 \theta_{*r}(\tau)/\ell$. In view of the specific conditions of the considered problem, it is usually not necessary to solve the transcendental equation (5.65). The point is that in the right-hand of the equation there is a member $\varepsilon = c_0 \Pi_*'^2 / c_1$, that characterizes the relation of stiffness of the spring to the stiffness of the link (reduced values). Obviously, when using the actual values of parameters, generally $\varepsilon \ll 1$. If we accept as the first approximation $\varepsilon = 0$, then (5.72) splits into two equations, the roots of which can be found from simple relations:

$$\theta_{*r} = \sqrt{c_1/(J + m\Pi_*'^2)}, \quad \theta_{*\,r+1} = r\pi, \quad (r = \overline{1, \infty}). \tag{5.66}$$

Thus in this model practically only one frequency (usually the first one) varies in time, and the rest do not depend on time or on the parameters of the mechanism. We will use this circumstance in determining the forced oscillations of the system.

So, the performed frequency analysis provides the basis for a separate examination of the forced oscillations of the spring, i.e. for decomposition of the original system. The law of motion for the spring's end is $u = -\Pi(\varphi_0 + q) \approx -\Pi(\varphi_0) - \Pi'(\varphi_0)q$.

However, in case of small oscillations $\Pi'q \ll \Pi_{\max}$, so we can assume that the section $x = \ell$ moves as per the ideal law of motion, which is represented by Fourier series:

$$u(\ell, t) = b_0 + \sum_{j=1}^{\infty} b_j \sin(j\omega t + \gamma_j). \tag{5.67}$$

In solving this problem, we cannot directly use the Fourier method, since the boundary conditions are not uniform. This difficulty is eliminated by the substitution $u = u_1 + w$, where $w = \kappa_1(t) + [\kappa_2(t) - \kappa_1(t)]x/\ell$; $\kappa_1 = u(0, t)$; $\kappa_2(t) = u(\ell, t)$ (in our case $\kappa_2 = 0$). For the new variable u_1 we have zero boundary conditions $u_1(0, t) = 0$; $u_1(\ell, t) = 0$, but the equation becomes nonhomogeneous:

$$\frac{\partial^2 u_1}{\partial x^2} - g_0^{-2} \frac{\partial^2 u_1}{\partial t^2} = \frac{x}{g_0^2 \ell} \frac{d^2 \kappa_2}{dt^2}. \tag{5.68}$$

We find solution as follows:

$$u_1 = \sum_{j=1}^{\infty} v_j(x) \sin(j\omega t + \gamma_j). \tag{5.69}$$

After substituting (5.69) into (5.68), taking into account the boundary conditions and the transition to the original variables, we finally obtain:

$$u = \sum_{j=1}^{\infty} b_j \sin(j\omega t + \gamma_j) \sin(j\omega x/g_0)/ \sin(j\omega\ell/g_0) + b_0 x/\ell. \qquad (5.70)$$

The closing force in this case is determined as к $F = (ES)_0 \dfrac{\partial u}{\partial x}(\ell)$. Thus

$$F = \chi_1\omega \sum_{j=1}^{\infty} jb_j\cot(j\omega\ell/g_0) \sin(j\omega t + \gamma_j) + \chi_2 b_0, \qquad (5.71)$$

where, for the spring made of steel wire $\chi_1 = 1,387 \times 10^7 d^3/D$ kg/s; $\chi_2 = 10^{10}d^4/(D^3 n)$ kg/s^2; n is the number of volutes.

The conditions of forced closing will be met if for the whole kinematic cycle $F < 0$ for compression springs and $F > 0$ for tension springs, which is equivalent to the requirement

$$\chi_1\omega \sum_{j=1}^{\infty} jb_j|\cot(j\omega\ell/g_0)| < \chi_2|b_0|. \qquad (5.72)$$

When $j\omega\ell/g_0 = \pi s$ ($s = \overline{1, \infty}$) and assuming the absence of dissipation, there is an infinite increase on the left side of this inequality that corresponds to the resonant frequency $j\omega = k = s\dfrac{\pi g_0}{\ell} = 2.264 \times 10^3 \dfrac{d}{D^2 n}$. However, the normal operation of the closing device is violated even on the verge of the resonance zone. Thus, when we have monoharmonic nature of the law of motion ($j = 1$), taking $|b_0| = \xi b_1$, where $\xi > 1$ is the original coefficient of allowance, we obtain the condition

$$\xi > \chi_1\omega|\cot(\omega\ell/g_0)|/\chi_2. \qquad (5.73)$$

If $\omega \to 0$, after evaluation of interminate form, the formula (5.73) gives the result $\xi > 1$. Further, with the growth of ω, the right-hand side decreases reaching zero at $\omega\ell/g_0 = \pi/2$. This increase of the safety factor is due to the effect of dynamic unloading (see Sect. 4.3). With further increase in ω, as we approach the resonance mode $\omega = \pi g_0/\ell$, the right-hand side of the inequality increases, which ultimately leads to the violation of the condition (5.73). This indicates that then spring no longer performs the forced closing.

If we assume that in the cyclic mechanism the dynamic load, associated with non-uniform mass m movement, dominates, then to exclude the unlocking in section N_2 (see Fig. 5.11) the condition (5.73) must be stricter

$$F_0 > \chi_1\omega_0 \sum_{j=4}^{\infty} j|\cot(j\omega_0\ell/g_0)| - mw, \qquad (5.74)$$

where w is the acceleration of the mass m, which depends on both the acceleration of the program motion and oscillations q of the input link $F_0 = \chi_0|b_0|$.

To determine $q(t)$ we can use the truncated model, based on the revealed-above possibility of system decomposition. This model, which shows the oscillatory system of the drive with variable moment of inertia $J + m\Pi_*'^2$, is described by the following linear differential equation with variable coefficients:

$$(J + m\Pi_*'^2)\ddot{q} + (\beta + 2\,m\omega_0\Pi_*'\Pi_*'')\dot{q} + c_0 q = \Pi_*'[F(t) - m\omega_0^2\Pi''], \qquad (5.75)$$

where β is the equivalent coefficient of linear resistance; asterisk corresponds to the argument $\varphi_0 = \omega_0 t$; $F(t)$ is given by formula (5.71).

Further on we assume that the parameters of the system correspond to the conditions of dynamic stability, both in the areas of parametric resonance and in the finite segment of the kinematic cycle (see Sects. 5.3.1 and 5.4.2). A sufficient condition for dynamic stability is reduced to the form $\beta > p_1(J + m\Pi_*'^2) \cdot dp_1/dt$.

The approximate analytical solution of Eq. (5.75), obtained using the method of conditional oscillator, is given in Sect. 5.2. When we have the known solution $q(t)$ the acceleration is described by the relation:

$$w = \Pi''\omega_0^2(1 + \dot{q}/\omega_0)^2 + \Pi'\ddot{q}, \qquad (5.76)$$

After which inequality (5.74) can be checked for any moment of current time. Violation of this inequality is primarily expected to be in the vicinity of the rotation angles φ_0, corresponding to the minimum of the second geometric transfer function Π''. According to (5.71) and (5.74) in case of increase in F_0 the driving force also increases and hence the extreme values of acceleration $w(t)$ of the cam follower also increases.

Along with the above test, during the synthesis of the closing system, it is desirable to have the estimated conditions, which could serve as the guideline for the design and as material for further clarification. For the purpose, using the principle of superposition, we select from solution $q(t)$ the component, which is proportional to the average value of the closing force

$$q = q_0 + F_0 \sum_{j=1}^{\infty} D_j \cos(j\omega_0 t + \alpha). \qquad (5.77)$$

As shown by the analysis, the "strongest" harmonics at some distance from the resonance zones $D_j \approx \kappa_j j b_j/c_1$, where $\kappa_j \approx [1 - (j\omega_0/\bar{p}_1)^2]^{-1}$; $\bar{p}_1$ is the average frequency p_1.

Further, taking into account that in real mechanisms $\dot{q}/\omega_0 < 0.1$ we perform the linearization of the function (5.76)

$$w \approx \Pi_*''\omega_0^2(1 + 2\dot{q}/\omega_0) + \Pi_*'\ddot{q}. \qquad (5.78)$$

Hence, according to (5.74), (5.77) and (5.78) we get with certain factor of margin

$$F_0 = \frac{\chi_1 \omega_0 \sum_{j=1}^{\infty} j b_j |\cot(j\omega_0 \ell / g_0)| - K \Pi''_{\min} \omega_0^2 m}{1 - 2|\Pi''_{\min}| \omega_0^2 m \sum_{j=1}^{\infty} j^2 D_j (1 + 0.5 jN)}, \qquad (5.79)$$

where $K = |w^0_{\min} / (\Pi''_{\min} \omega_0^2)|$; $w^0 = w(q_0)$; $N = |\Pi'_{**} / \Pi''_{\min}|$; Π'_{**} is the value of the function Π', corresponding to the position at which $\Pi'' = \Pi''_{\min}$. If we keep in the function Π' and Π'' one dominant harmonic ν, $\Delta \dot{q} \approx -F_0 \nu b_\nu \kappa_\nu \omega_0 c_1^{-1} \sin(\nu \omega_0 t + \alpha_\nu)$, $\Delta \ddot{q} \simeq F_0 \nu^2 b_\nu \kappa_\nu \omega_0^2 c_1^{-1} \cos(\nu \omega_0 t + \alpha_\nu)$, where $\Delta q = q - q_0$.

In this case, we get

$$F_0 > \frac{\chi_1 \omega_0 \sum_{j=1}^{\infty} j b_j |\cot(j\omega_0 \ell / g_0)| - K \Pi''_{\min} \omega_0^2 m}{1 - \kappa_\nu \nu^2 b_\nu^2 \omega_0^2 m c_1^{-1}}. \qquad (5.80)$$

In case of substantial reduction of the denominator in (5.79) and (5.80) the mean value of the force F_0, required for reliable closing, significantly increases and if the denominator is equal to zero, the effect of absence of the controllability of the closing system appears, the physical meaning of which was explained above.

To exclude the possibility of this effect, it is necessary to ensure through the choice of the coefficient of torsion stiffness c_1 the satisfaction of the condition, under which the denominators in these formulae remained close to unity (one). For example, in the particular case, corresponding to the formula (5.80), it should be required that $c_1 \gg \kappa_\nu \nu^2 b_\nu^2 \omega_0^2 m$. We can consider the reciprocal value of the denominator as the criterion, characterizing the increase in the inertial forces due to the increase in the mean value of the closing force.

5.6.3 Transverse Vibrations of Closing Springs

System of differential equations. When calculating the transverse oscillations of the spring it is also replaced by the equivalent rod. However, in this case, we have to take into account not only the bending in the plane of the volute of the spring, but also the torsional and longitudinal deformation of the volute element. Taking into account the shifts, the rotational inertia of the cross sections and longitudinal loads, the system of differential equations, which describes the transverse vibrations of the springs, has the form [56]

$$\begin{aligned} \frac{\partial^2 y}{\partial x^2} - \frac{m}{S_2} \frac{\partial^2 y}{\partial t^2} - (1 - \frac{F}{S_2}) \frac{\partial \theta}{\partial x} = 0; \\ \frac{\partial^2 y}{\partial x^2} - \frac{\rho}{S_1} \frac{\partial^2 \theta}{\partial x^2} + \frac{S_2}{S_1} (1 - \frac{F}{S_2})(\frac{\partial y}{\partial x} - \theta) = 0, \end{aligned} \qquad (5.81)$$

where y is the transverse displacement; θ is the average angle of rotation of the cross section; m; ρ are mass and moment of inertia of the equivalent rod of unit

length; F is the longitudinal load ($F > 0$ is stretching; $F < 0$ is compression); S_1, S_2 are the bending and shear stiffness of the section of the equivalent rod. For springs made of round wire

$$m = \rho_0 \frac{\pi^2 D d^2 n}{4l}; \quad \rho = \rho_0 \frac{\pi^2 D^3 d^2 n}{32l}; \quad S_1 = \frac{2\ell EI}{\pi D n (2 + \mu_P)}; \quad S_2 = \frac{8\ell EI}{\pi D^3 n},$$

where D is the diameter of the wire; ℓ is the height of the spring under average load; d is the diameter of the wire; ρ_0 is the density of the material; E *is the* elastic modulus; $I = \pi d^4/64$ is the moment of inertia of the section; μ_P is Poisson's ratio (for steel $\mu_P = 0.3$); n is the number of the working volutes.

When using the springs for forced closing of the kinematic pairs, its ends are often attached to the movable links. In this case, the boundary conditions are given as functions of time.

Let $y(0, t) = \kappa_1(t)$, $y(\ell, t) = \kappa_2(t)$ ($\kappa_1 \ll \ell$, $\kappa_2 \ll \ell$). We could also require $\theta(0, t) = \kappa_3(t)$, $\theta(\ell, t) = \kappa_4(t)$. However, when designing the mechanisms, special measures are taken to ensure that the bearing surfaces would not "break out" the spring, so the presence of such boundary conditions indicates the taking of an unsatisfactory constructive decision. In other words when using the movable ends of the closing spring, the possibility of the self-aligning of the plane of the ends should be provided for, which corresponds to the absence of bending moments in these sections, i.e. to pivoted support. Let us introduce the substitution

$$y = (x, t) = y_1(x, t) + w(x, t), \tag{5.82}$$

where $w(x, t) = \kappa_1(t) + [\kappa_2(t) - \kappa_1(t)]x/\ell$.

Then $w(0, t) = \kappa_1(t)$, $w(\ell, t) = \kappa_2(t)$, $y_1(0, t) = y_1(\ell, t) = 0$ and the system of differential equations is reduced to the form

$$\frac{\partial^2 y_1}{\partial x^2} - \frac{m}{S_2} \frac{\partial^2 y_1}{\partial t^2} - (1 - f)\frac{\partial \theta}{\partial x} = \frac{m}{S_2}\left[\frac{d^2\kappa_1}{dt^2} + (\frac{d^2\kappa_2}{dt^2} - \frac{d^2\kappa_1}{dt^2})\frac{x}{\ell}\right];$$

$$\frac{\partial^2 \theta}{\partial x^2} - \frac{\rho}{S_1}\frac{\partial^2 \theta}{\partial t^2} = -\frac{S_2}{S_1}(1-f)\left[\frac{\partial y_1}{\partial x} - \theta + \frac{\kappa_2 - \kappa_1}{\ell}\right], \tag{5.83}$$

where $f = F/S_2$.

Determination of the "natural" frequencies and mode shapes of vibrations Let us substitute in the system of homogeneous differential equations obtained from (5.83) when $\kappa_1 = \kappa_2 = 0$, $y_1 = Y_1(x)\sin(kt)$, $\theta = v(x)\sin(kt)$. After reduction to $\sin kt$ we get the following system of differential equations:

$$Y_1'' + \frac{mk^2}{S_2}Y_1 - (1-f)v' = 0; \quad \frac{S_2}{S_1}(1-f)Y_1' + v'' + \left[\frac{\rho k^2}{S_1} - \frac{S_2}{S_1}(1-f)\right]v = 0, \tag{5.84}$$

where $( )' = \partial/\partial x$.

Assuming $Y_1 = Ae^{\lambda x}$ and $v = Be^{\lambda x}$, we transform (5.84) into a homogeneous system of algebraic equations relatively to A and B. Furthermore, turning to zero the determinant of this system, we obtain the characteristic equation

$$\lambda^4 + 2b_1^2\lambda^2 - b_2^4 = 0, \tag{5.85}$$

where $b_1^2 = 0.5 \left[k^2 \left(\dfrac{m}{S_2} + \dfrac{\rho}{S_1} \right) - \dfrac{S_2}{S_1} f(1-f) \right]$; $b_2^4 = \dfrac{mk^2}{S_1}(1-f - \dfrac{\rho k^2}{S_2})$.

It follows: $\lambda_{1,2} = \pm i\alpha_1$ $(i = \sqrt{-1})$; $\lambda_{3,4} = \pm\alpha_2$, and besides $\alpha_1 = \sqrt{b_1^2 + \sqrt{b_1^4 + b_2^4}}$; $\alpha_2 = \sqrt{-b_1^2 + \sqrt{b_1^4 + b_2^4}}$. Then

$$
\begin{aligned}
Y_1 &= C_1 \cos(\alpha_1 x) + C_2 \sin(\alpha_1 x) + C_3 \mathrm{ch}(\alpha_2 x) + C_4 \mathrm{sh}(\alpha_2 x); \\
v' &= \beta_1[C_1 \cos(\alpha_1 x) + C_2 \sin(\alpha_1 x)] + \beta_2[C_3 \mathrm{ch}(\alpha_2 x) + C_4 (\mathrm{sh}\alpha_2 x)],
\end{aligned}
\tag{5.86}
$$

where $\beta_1 = (mk^2 S_2^{-1} - \alpha_1^2)/(1-f)$; $\beta_2 = (mk^2 S_2^{-1} + \alpha_2^2)/(1-f)$.

The constants C_1, C_2, C_3, C_4 are found from the boundary conditions, which in case of pivoted support of the spring's ends have the following form: $Y_1(0) = Y_1(\ell) = 0$; $v'(0) = v'(\ell) = 0$ (absence of the bending moments). Omitting the calculations, on the basis of (5.86) we get the following frequency equation:

$$\zeta_1 \tilde{k}^4 - z^2 \left[z^2(1-f) + \zeta_2 \right] \tilde{k}^2 + z^4 \left[1 + \zeta_3 z^2 f(1-f) \right] = 0, \tag{5.87}$$

where $\tilde{k} = k/k_0$; $k_0 = j^2 \pi^2 \ell^{-2} \sqrt{S_1/m}$; $z = \ell/D$ (index of the spring).

For springs made of round steel wire $\zeta_1 = 1.32$; $\zeta_2 = 2.31$; $\zeta_3 = 0.932$.

As it follows from the analysis, the tensile strength ($F > 0$, $f > 0$) increases the lower "natural" frequency, whereas the compressive strength ($F < 0$, $f < 0$) decreases it.

When $\tilde{k} \leq 0$, the straight shape of the spring's equilibrium, becomes unstable. Obviously, the corresponding critical value of the spring's compression force $F_* = f_* S_2$ corresponds to the vanishing of the free term of the Eq. (5.87); thus f_* is determined as the negative root of the quadratic equation

$$\zeta_3 z^2 f_*^2 - \zeta_3 z^2 f_* - 1 = 0. \tag{5.88}$$

To determine the forms of oscillations, at the accepted boundary conditions, we should substitute corresponding values k when $C_1 = C_3 = 0$; $C_2 = 1$; $C_4 = -\sin\alpha_1\ell/\mathrm{sh}\alpha_2\ell$ in expression (5.86).

With the given side sections of the springs we have the following boundary conditions: $Y_1(0) = Y_1(\ell) = 0$ (the absence of deflection); $v(0) = v(\ell) = 0$ (the absence of the angular deformation in the side section of the spring). In this case, the frequency equation appears to be transcendental:

$$\begin{vmatrix} \cos\alpha_1\ell + \mathrm{ch}\alpha_2\ell & \sin\alpha_1\ell + \dfrac{\alpha_2\beta_1}{\alpha_1\beta_2}\mathrm{sh}\alpha_2\ell \\[2mm] \dfrac{\beta_1}{\alpha_1}\sin\alpha_1\ell - \dfrac{\beta_2}{\alpha_2}\mathrm{sh}\alpha_2\ell & \dfrac{\beta_1}{\alpha_1}(\mathrm{ch}\alpha_2\ell - \cos\alpha_1\ell) \end{vmatrix} = 0. \tag{5.89}$$

The critical value of the parameter $f_* < 0$, corresponding to the loss of stability of the rectilinear form of the spring's equilibrium, is determined from (5.85) to (5.89) with the substitution of $k = 0$.

Forced oscillations in case of kinematic excitation Let's suppose that the spring's ends oscillate perpendicular to its axis for a relatively small value $\kappa_1 = a_1\sin\omega t$, $\kappa_2 = a_2\sin\omega t$ $(a_1 \ll \ell,\ a_2 \ll \ell)$. We use again the representation of solutions in form (5.89) and write the functions $y_1(t)$ and $\theta(t)$ as $y_1(x,t) = Y_\omega(x)\sin\omega t$, $\theta(x,t) = v_\omega(x)\sin\omega t$. Substituting these functions in (5.83) we get

$$\begin{aligned} Y_\omega'' + \frac{m\omega^2}{S_2}Y_\omega - (1-f)v_\omega' &= \frac{m\omega^2}{S_2}\left[a_1 + (a_2 - a_1)\frac{x}{\ell}\right]; \\ \frac{S_2}{S_1}(1-f)Y_\omega' + v_\omega'' + \left[\frac{\rho\omega^2}{S_1} - \frac{S_2}{S_1}(1-f)\right]v_\omega &= \frac{(a_1 - a_2)(1-f)S_2}{S_1\ell}, \end{aligned} \tag{5.90}$$

where $(\ )' = \partial/\partial x$.

The solution of the system (5.90) has the form:

$$\begin{aligned} Y_\omega &= h_1\cos\alpha_1 x + h_2\sin\alpha_1 x + h_3\mathrm{ch}\alpha_2 x + h_4\mathrm{sh}\alpha_2 x + h_5 x + h_6; \\ v_\omega &= \beta_1\alpha_1^{-1}(h_1\sin\alpha_1 x - h_2\cos\alpha_1 x) + \beta_2\alpha_2^{-1}(h_3\mathrm{sh}\alpha_2 x + h_4\mathrm{ch}\alpha_2 x), \end{aligned} \tag{5.91}$$

where $h_i(i = \overline{1,\ 6})$ are the some constants.

Functions β_1, β_2, α_1, α_2 are determined as per the above mentioned formulae by replacing the natural frequency k with the frequency of kinematic excitation ω.

The last two terms in dependencies for Y_ω correspond to the particular solution, the substitution of which in (5.83) gives $h_5 = (a_2 - a_1)/\ell$, $h_6 = a_1$. Other constants are found from the boundary conditions for simply supported ends of the spring $Y_\omega(0) = Y_\omega(\ell) = 0$; $v_\omega'(0) = v_\omega'(\ell) = 0$.

From the first equation of (5.90) it follows that the last two boundary conditions are equivalent to $Y_\omega''(0) = m\omega^2 a_1/S_2$ and $Y_\omega''(\ell) = m\omega^2 a_2/S_2$. On the basis of (5.91) we get

$$h_1 = -\frac{a_1\alpha_2^2}{\alpha_1^2 + \alpha_2^2}; \qquad h_2 = \frac{\alpha_2^2(a_1\cos\alpha_1\ell - a_2)}{(\alpha_1^2 + \alpha_2^2)\sin\alpha_1\ell};$$

$$h_3 = -\frac{a_1\alpha_1^2}{\alpha_1^2 + \alpha_2^2}; \qquad h_4 = \frac{\alpha_1^2(a_1\cosh\alpha_2\ell - a_2)}{(\alpha_1^2 + \alpha_2^2)\sinh\alpha_2\ell}.$$

In case of resonance $\omega = k$, we have $\sin \alpha_1 \ell = 0$; then under the condition that $a_1 \neq a_2$, $h_2 \to \infty$ $Y_\omega \to \infty$. If $a_1 = a_2$, then with resonance only symmetric mode shapes are excited, i.e. $\alpha_1 \ell = (2j - 1)\pi$. If the kinematic excitation of the sides of the spring has the similar amplitudes, but the phase shift is equal to π $(a_1 = -a_2)$, then the resonance equals $\alpha_1 \ell = 2j\pi$; at the same time only antisymmetric shapes are excited. We find the total displacement of the arbitrary section of the spring as $y_\omega = [Y_\omega(x) + a_1 + (a_2 - a_1)x/\ell] \sin \omega t$.

When using the Fourier series the given dependencies are easily generalized to the case when the functions $\kappa_1(t)$ and $\kappa_2(t)$ are arbitrary periodic functions.

Parametric and combination resonances of the springs As it follows from (5.87), the longitudinal disturbance, which is associated with the variability of the spring's parameters, leads to the pulsation of "natural" frequencies that may be the cause of the parametric excitation.

As it was already mentioned, the basic parametric resonances occur in the vicinity of the frequencies $\omega_* = 2\bar{p}_{1,2}$ and combination resonances when $\omega_* = \bar{p}_2 \pm \bar{p}_1$. When calculating $\bar{p}_{1,2}$ the dimensionless frequency coefficient $\bar{p}_{1,2} \approx \bar{k}_{1,2}$ is determined by substituting into (5.87) the average values of the parameters.

The specifics of parametric excitation of the springs is associated with small values of the logarithmic decrement ϑ (usually $\vartheta < 0.1$), so the provision of conditions of dynamic stability is mainly due to the detuning from the critical zones. Furthermore, it should be understood that the longitudinal driving force is always applied to the spring eccentrically, not strictly parallel to the axis of the spring, which leads to the inevitable excitation of transverse vibrations. The latter may interact with parametric oscillations.

5.7 Some Problems of Dynamics of Cyclic Mechanisms, Schematized as Chain Systems with Variable Parameters

5.7.1 Dynamic Errors of the Operating Members with Increased Dimensions

In many technological machines the working parts are mounted on the shafts or rods, committing the given non-uniform program movement. This movement is complimented by undesirable vibrations, caused by the kinematic disturbance, and as the analysis shows, especially significant dynamic errors occur due to vibratory accelerations (see Chap. 4).

Dynamic model The dynamic model presented in Fig. 5.12 consists of two elements with elastic and dissipative properties, separated by the element that simulates the position function of the output link of the cyclic mechanism $\varphi_1 = \Pi(\varphi)$ and the executive body, schematized as the disc and shaft with moments of inertia
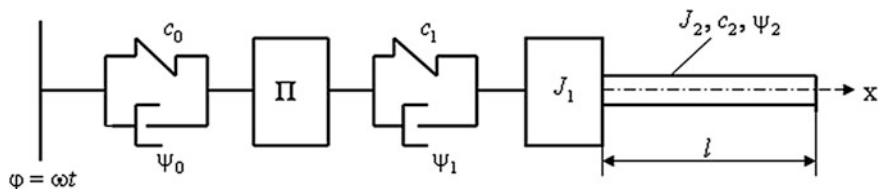
Fig. 5.12 Dynamic model

J_1 and J_2. Let us introduce the following notations: ω, $\varphi = \omega t$ are the angular velocity and coordinate of the input link; $\varphi_2(x,t)$ is the coordinate of the output link; c_0, c_1 are the stiffness coefficients; ψ_0, ψ_1 are the dissipation coefficients; G is the shear modulus; I is the polar moment of inertia. Using the energy balance condition, we reduce the elastic and dissipative characteristics c_0, ψ_0 to the axis of the executive body. At the same time we assume $d\Pi/d\varphi = r_0 \sin \varphi$, which corresponds to the widespread event of program motion of the output link. Then the reduced coefficients of stiffness and dissipation are defined as follows

$$c = c_1(1 + \chi \sin^2 \varphi)^{-1}; \quad \psi = (\psi_0 c_1/c_0 + \psi_1)(1 + \chi \sin^2 \varphi)^{-1}, \qquad (5.92)$$

where $\chi = r_0^2 c_1/c_0$.

The differential equation of the oscillations of the executive body in the coordinate system $\varphi_1 = \Pi(\varphi)$ has the form

$$GI\frac{\partial^2 u}{\partial x^2} - \rho\frac{\partial^2 u}{\partial t^2} - b\frac{\partial u}{\partial t} = \rho\omega^2\frac{d^2\Pi}{d\varphi^2} - M(x,t), \qquad (5.93)$$

where $u = \varphi_2(x,t) - \Pi(\varphi)$ is the dynamic error in the section x; $\rho = J_2/l$ is the moment of inertia of the running length; b is the equivalent coefficient of the linear force of resistance (see below); $M(x,t)$ is the intensity of the distributed external moment.

According to (5.92) the reduced elastic and dissipative characteristics of the transmission mechanism are the functions of "slow" time $\tau = \varphi/\omega$. In this case the boundary conditions are defined as follows:

$$GI\frac{\partial u}{\partial x}(0) = c(\tau)u(0) + b(\tau)\frac{\partial u}{\partial t}(0) + J_1\frac{\partial^2 u}{\partial t^2}(0); \quad \frac{\partial u}{\partial x}(0) = 0. \qquad (5.94)$$

The frequency and modal analysis Taking into account the negligible influence of the resistance forces on the "natural" frequencies and mode shapes, at this stage, we accept $b \equiv 0$. According to the method of conditional oscillator the solution of the homogeneous differential equation, obtained from (5.92) with vanishing right-hand side, we find in the form:

$$u = X(x, \tau) \cos \Phi(t), \qquad (5.95)$$

where τ is "slow time".

In one of the sections (for example, at $x = \ell$) functions $X(\ell, \tau)$ and Φ, according to the method of the conditional oscillator, can be associated with additional condition (see Sect. 5.2)

$$2\frac{dB}{d\tau}p + B\frac{dp}{d\tau} = 0. \qquad (5.96)$$

Here $p(\tau) = d\Phi/dt$ is "natural" frequency; $B = X(\ell, \tau)$.

On the basis of (5.93)–(5.96) the formal frequency equation can be written as

$$\theta(\tau)[\theta(\tau) + \mu \tan \theta(\tau)] = \sigma_0^2 (1 + \chi \sin^2 \omega\tau)^{-1}, \qquad (5.97)$$

where $\mu = \rho l/J_1$; $\sigma_0 = k_1/k_2$; $k_1 = \sqrt{c_1/J_1}$; $k_2 = \sqrt{GI/(J_2 l)}$; $\theta_r(\tau) = p_r(\tau)/k_2$.

Equation (5.97) has an unlimited set of roots $(\theta_r(\tau))$, $(r = \overline{1, \infty})$, to which correspond the "natural" frequencies $p_r(\tau) = k_2 \theta_r(\tau)$. If we take $B = 1$ when $\tau = 0$ then non-stationary mode shape is determined with the following relationship:

$$X_r(x, \tau) = \sqrt{\frac{\theta_r(0)}{\theta_r(\tau)}} \cos[\Phi_r(\tau)(1 - x/l)], \qquad (5.98)$$

where r is the number of the frequency.

The evolution of mode shapes for $\chi = 1$, $\varphi = \pi/2$ at variation of parameters μ and σ_0 is shown in Fig. 5.13. Thus the solid line corresponds to $\mu = 0.5$, $\sigma_0 = 1$, the hatching line corresponds to $\mu = 3$, $\sigma_0 = 1$, the hatch-dotted line corresponds to $\mu = 1$, $\sigma_0 = 0.5$, the dotted line corresponds to $\mu = 1$, $\sigma_0 = 2$.

Fig. 5.13 Evolution of oscillatory mode shapes
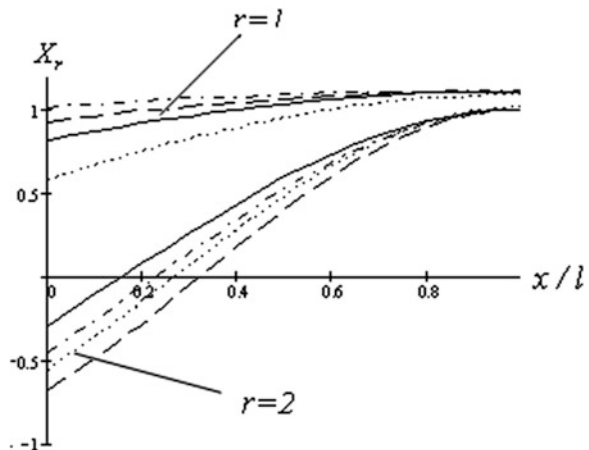
Analysis of the dynamic errors Using the apparatus of quasi-normal coordinates, we will represent the solution of the nonhomogeneous differential equation (5.93) as

$$u = \sum_{r=1}^{\infty} X_r(x, \tau)\, U_r(t), \tag{5.99}$$

where function U_r is determined from the following differential equation:

$$\ddot{U}_r + 2n_r(\tau)\dot{U}_r + p_r^2(\tau)U_r = W_r(t). \tag{5.100}$$

The dissipative term, omitted in frequency analysis, is included in the left-hand side of this equation, for the determination of which we can use the following dependence, obtained with the exclusion of dissipative connections between the different mode shapes (see Chap. 6).

$$\psi_r^*(\tau) = \frac{c(\tau)l\psi(\tau) + GID_r(\tau)\psi_r}{c(\tau)l + GID_r(\tau)}, \tag{5.101}$$

where $D_r = l^{-1} \int_0^l X_r'^2(x, \tau)dx = 0.5\,\theta_r(\tau)[\theta_r(\tau) - 0.5\,\sin 2\theta_r(\tau)];$ $\psi,\ \psi_r$ are   the dissipation coefficients for both considered subsystems respectively; ψ_r^* is the reduced to the mode shape r dissipation coefficient. At the same time $n_r(\tau) \approx \psi_r^*(\tau)\,p_r(\tau)/(4\pi)$.

The right-hand side of the differential equation (5.100) can be found as

$$W_r = -w_*(t) \int_0^l X_r dx / \int_0^l X_r^2 dx = -w_*(t)H_r(\tau),$$

where $H_r(\tau) = \dfrac{2\sin\theta_r(\tau)}{\theta_r(\tau) + 0.5\,\sin 2\theta_r(\tau)}$.

On the basis of the method of the conditional oscillator the particular solution of Eq. (5.100) for slowly varying coefficients can be written as follows:

$$U_r = \frac{1}{\sqrt{p_r(t)}} \int_0^t \frac{W_r(z)}{\sqrt{p_r(z)}} \exp[- \int_z^t n_r(\xi)d\xi] \sin[\int_z^t p_r(\xi)d\xi]dz. \tag{5.102}$$

For engineering estimations, the function $\ddot{u}_{\max}(x/\ell)$, characterizing the distribution of additional accelerations along the x axis, is of great interest. It should be noted that using the actual values of the parameters, the vibration accelerations, caused by

abrupt changes of acceleration of the program movement $d^2\varphi_1/dt^2$, are the source of increased vibration activity, which limits the performance of the machines.

As shown by the analysis of these dependencies, in case of change of program acceleration from 0 to w_{max} for the time Δt

$$\ddot{u}_{max} = w_{max} \sum_{r=1}^{\infty} \kappa_r(\nu_r)H_rX_r, \qquad (5.103)$$

where $\nu_r = \Delta t/T_r$; $T_r = 2\pi/\bar{p}_r$; $\bar{p}_r$ is the average value of $p_r(\tau)$ in the interval $[0, \Delta t]$, w_{max} is the maximum value of $|w(t)|$. For a number of the typical shapes of $w_*(t)$ the functions $\kappa_r(\nu_r)$ are given in Sect. 4.1. Since in case of adopted normalized forms $X_r(\ell) = 1$, it follows from (5.103), that sum of $K = \sum_{r=1}^{\infty} \kappa_r|H_r|$ can be used as criterion for estimation of the dynamic error in vibration accelerations. The components of this sum characterize the distribution of the accelerations over the various vibration modes. The most significant contribution is made by the member K_1.

It can be shown that $\nu_r = \Delta\varphi_1 k_2\bar{\theta}_r/(2\pi\omega\sigma_0)$, where $\Delta\varphi$ is the rotation angle of the main shaft, corresponding to the change of $w(t)$ between extremes, $\bar{\theta}$ is the average value of θ. For small values of ν_r the criterion K_1 is not very different from unity. Consequently, $\ddot{u}_{max} \approx w_{*max}$ that corresponds to the so-called soft impact. With the growth of the parameter θ, which is proportional to the "natural" frequency, this criterion abruptly decreases. Interestingly, for some small values of ν_1 the criterion has the maximum, which exceeds one in value. This, however, does not mean that the maximum of additional acceleration $\ddot{u}_{max}$, arising from a single discontinuity $w_*(t)$ may become larger than w_{*max}. The matter is that criterion K_1 characterizes only the first mode shape, which when summed as per formula (5.103), is compensated by other components.

When criterion K is formed, usually the next as per importance is member K_3. The relatively small influence of the members, corresponding to even modes, follows from nearness to the anti-symmetric modes of oscillations, for which the elementary work from the given symmetric load is relatively small.

To analyze the character of distribution of vibration acceleration along the X-axis, we introduce the function $Z_1 = K_1(\nu)X_1(x/l)/X_1(0)$, which corresponds to the lowest mode of oscillations. In the Fig. 5.14 we can see the graphs of this function when $\chi = 1$, $\mu = 1$ for two values $\nu_1 = 0.1$ and $\nu_1 = 1$. In this case, the solid lines correspond to $\sigma_0 = 4$, hatched lines correspond to $\sigma_0 = 3$, hatch-dotted ones correspond to $\sigma_0 = 2$. As it follows from the graphs, with decrease in σ_0 the accelerations is more evenly distributed along the length of the executive body.

To control the level of vibration activity we will define the load, transmitted to the drive $c(\tau)u(0,t) = c(\tau)\sum_{r=1}^{\infty} X_r(0,\tau)U_r(t)$. The criterion of evaluation of each of the components of the sum, included in this dependence, is $N_r = |X_r(0,\tau)U_r|_{max}$.

The analysis of this criterion indicates that the satisfaction of the condition $\nu_1 \geq 2 \div 3$ is also useful for the reduction of the system's vibration activity (see 4.1.3). Consideration of the other program accelerations leads to similar conclusions.

Fig. 5.14 Distribution of the oscillation accelerations
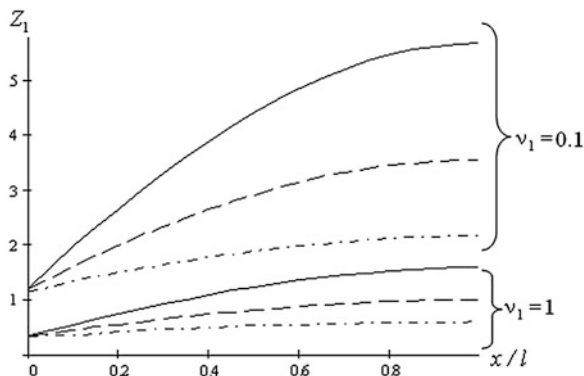
Conditions of dynamic stability on a finite interval of the kinematic cycle As shown above, the main source of vibration activity are the accompanying free vibrations, arising out of the quasi-impulsive kinematic excitation. In a system with constant oscillation parameters, arising from each pulse, are damped. In case of variable parameters, we can alternate the intervals of increase and decrease of the amplitudes, which is due to the violation of the conditions of dynamic stability for a finite time interval. At the same time there is a kind of an amplitude modulation, during which the level of oscillations may increase significantly (see Sect. 5.3.1).

In the given problem the conditions of stability for lowest frequency $(r = 1)$ are reduced to the form $\vartheta_1 > \vartheta_* = \pi\omega k_2^{-1}|\Psi_1(\varphi)|$ (vibrations and vibration-velocity), $\vartheta_1 > \vartheta_* = 3\pi\omega k_2^{-1}|\Psi_1(\varphi)|$ (vibration accelerations). Here ϑ_1, ϑ_* are logarithmic decrements and its critical value and function $\Psi_1(\varphi)$ is determined with the following dependence: $\Psi_1(\varphi) = \theta_1^{-2}d\theta_1/d\varphi$. As shown by the analysis, the conditions, establishing the stability in vibration accelerations, turns out to be defining ones.

5.7.2 Vibrations in the Differential Mechanism with Built-In Cyclic Mechanism

A combination of the differential mechanisms, with mechanisms that implement some kind of nonlinear functions, connecting the kinematic and dynamic characteristics of certain links, are often used in the drives of the technological and industrial machines. Among them the mechanical impulse transmissions, with surplus number of the degrees of freedom of the differential mechanism, are widely used for automatic transformation of torque, the formation of impulse actions and

solutions of some other dynamic problems [50]. In such drives, usually freewheel mechanisms combined with lever mechanisms are used. In this class of the mechanisms, the connections are not positional, so they cannot be used in cases, where it is necessary to ensure strict cyclic working of various mechanisms, which is typical for many machines used in the textile industry, printing, food industry and many other industries.

The additional positional relationship with respect to the differential mechanism can be either external or internal. An example of a mechanism with an external positional connection is discussed in the monograph [1]. In this case one of the two input links of the differential mechanism, is kinematically linked to the balancing arm of the cam follower, which results in the output link's rotation with variable angular velocity, which is the linear combination of the input link's angular velocities that is basically distinct from the systems with internal nonlinear position connections. In particular, such mechanisms are used to rotate the lens turret of the movie-camera. What follows are the typical problems of kinematics and dynamics of the differential mechanisms with cyclic mechanisms with nonlinear position relationships, considered in the general formulation, with specific focus on accounting of the elastic and dissipative properties and methods of reduction of the dynamic loads.

Kinematic characteristics The kinematic characteristics largely determine the dynamic properties of mechanisms of the given class. In Fig. 5.15, we can see the schematic diagram of the differential-cyclic mechanism, consisting of a differential mechanism D, a cyclic mechanism with a nonlinear position function $\Pi(\varphi_n)$ and two transmission gears with constant ratio $u_{nk} = \omega_n/\omega_k$ and $u_{HN} = \omega_H/\omega_N$ where ω_i are the angular velocities of the corresponding links, the index H corresponds to the carrier of the differential mechanism, and the index N to the output link of the mechanism.
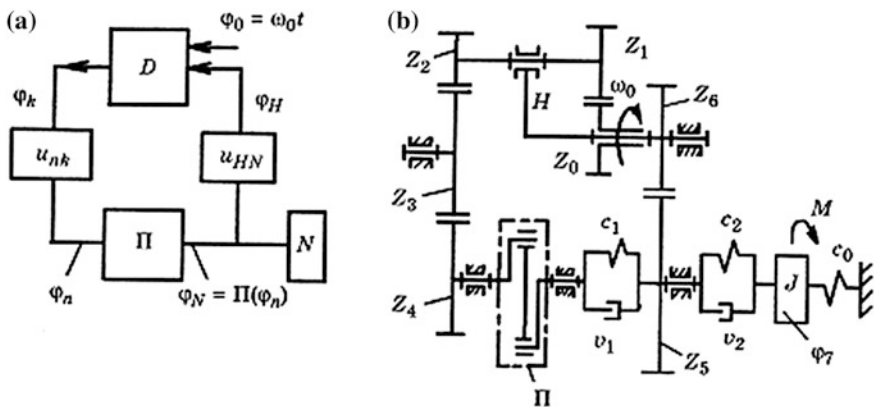
Fig. 5.15 Schematic and dynamic model of the differential mechanism with cyclic subsystem; **a** block diagram, **b** dynamic model

The functional connection between the angular velocities has the following form:

$$\omega_n = [u_D \Pi'(\varphi_n) + u_z]\omega_0, \tag{5.104}$$

where $u_D = u_{HN}(u_{0k}^{(H)})$, $u_z = u_{nk}^{-1}u_{0k}^{(H)}$, $\Pi'(\varphi_n) = d\varphi_N/d\varphi_n$.

On the basis of (5.104) we get $u_z \int\limits_0^{\varphi_n} B(\varphi_n)d\varphi_n = \int\limits_0^{\varphi_0} d\varphi_0 = \varphi_0$, where $B(\varphi_n) = h\Pi'(\varphi_n) + 1$, $h = u_D/u_z$. Hence, the equation of the position feedback has the form

$$h\Pi(\varphi_n) + \varphi_n = u_z^{-1}\varphi_0. \tag{5.105}$$

Henceforth, without the loss of generality, out of methodological reasons, we assume $\varphi_n \geq 0$, $\Pi(\varphi_n) \geq 0$, that corresponds to $\omega_n > 0$ and $B(\varphi_n) > 0$. The movement phase, in which $h\Pi' > 0$, will be called direct passage, and if $h\Pi' < 0$— the reverse passage. Let us introduce the kinematic characteristics of the mechanism when $\Pi(\varphi_n) \equiv 0$, $\Pi'(\varphi_n) \equiv 0$, $\omega_{n0} = u_z^{-1}\omega_0$, $\varphi_{n0} = u_z^{-1}\varphi_0$. Obviously, these characteristics correspond to the mechanism with the connected carrier.

When $\omega_0 = \text{const}$, we have $\omega_{n0} = \text{const}$, $\varphi_{n0} = \omega_{n0}t$. Then

$$\begin{aligned}
&\omega_n/\omega_{n0} = 1/B(\varphi_n); \quad \varepsilon_n/\omega_{n0}^2 = -h\Pi''(\varphi_n)/B^3(\varphi_n); \\
&\omega_N/\omega_{n0} = \Pi'(\varphi_n)/B(\varphi_n); \quad \varepsilon_N/\omega_{n0}^2 = \Pi''(\varphi_n)/B^3(\varphi_n),
\end{aligned} \tag{5.106}$$

where $\Pi''(\varphi_n) = d^2\Pi/d\varphi_n^2$; ε_n, ε_N are the angular accelerations.

In spite of the nonlinearity of the function $\Pi(\varphi_n)$, taking into account the positional feedback, between the accelerations of the input and output links of the cyclic mechanism, it can be shown that these accelerations are connected with the simple linear relationship $\varepsilon_n = -h\varepsilon_N$. According to (5.105) the angles of rotation of the input link φ_n characterizing the direct and reverse passages are determined with expressions $\varphi_n + h\Pi_{max} = \varphi_{n0}$, $\varphi_n - h\Pi_{max} = \varphi_{n0}$. Since the angles φ_{n0} are proportional to the relevant time intervals, these dependencies indicate that there is a "stretching" in time during the direct passage, and conversely, "compression" during the reverse passage. Subjected to the observation of the mandatory condition $B(\varphi_n) > 0$ the element n rotates with variable angular velocity, while link N and the associated carrier oscillate.

We will illustrate the kinematic and dynamic properties of the considered class of mechanisms using the model, presented in the Fig. 5.15b with following initial data: $z_0 = 40$, $z_1 = 20$, $z_2 = z_3 = 30$, $z_4 = 60$, $z_5 = 54$, $z_6 = 18$, $\Pi = \alpha(1 - \cos\varphi_n)$, where z_i is the number of the teeth; $\alpha = 0.5\,\Pi_{max}$. when $h = 1.5$.

The analysis of the dimensionless kinematic characteristics (Fig. 5.16) shows that the original symmetrical harmonic law of motion during the forward and reverse passages can be changed as desired. In particular without deterioration of the initial pressure angles, corresponding to the symmetry of the direct and reverse
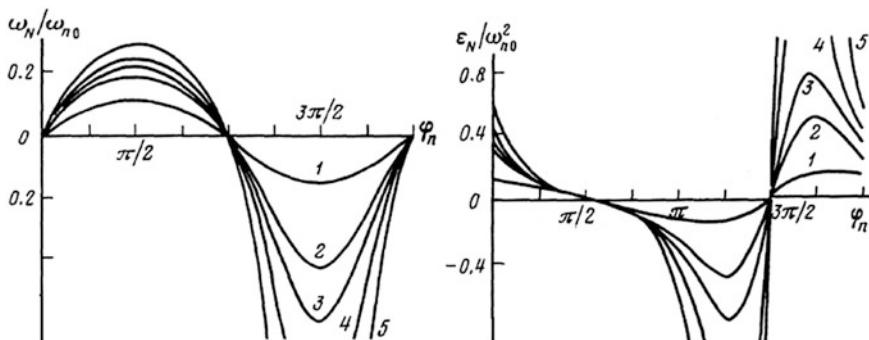
Fig. 5.16 Kinematic characteristics: $1 - \alpha = \pi/24, 2 - \pi/12, 3 - \pi/10, 4 - \pi/8, 5 - \pi/6$

passages, we can substantially increase the productivity ratio of the mechanism. $\varphi_{N0}/\varphi_{n0}$.

Another advantage of such mechanism is the ability to change the kinematic characteristics with the same cyclic mechanism, only by varying the ratios of gears. For example, if the gear ratio u_{HN} is realized with the variable-speed drive, then the readjustment does not require the mechanism to be dismantled. The use of variable-speed drive in the inverse kinematic chain, in this case, does not lead to the cumulative error, associated with slippage, and can only make minor phase shifts of the kinematic characteristics within the loop, which usually do not violate the given cyclic diagram of the machine.

The extreme values of the angular velocity and accelerations of the links n and N are of interest. According to (5.106) extremes of angular velocities occur when $\Pi''(\varphi_n) = 0$ and for acceleration at φ_n^*, which are the roots of the equation.

$$\Pi'''(\varphi_n^*)[h\Pi'(\varphi_n^*) + 1] = 3\,h\Pi''^2(\varphi_n^*). \tag{5.107}$$

For considered law of motion we have

$$\varphi_n^* = \pi\nu - (-1)^\nu \arcsin[(1 - \sqrt{1 + 24\,h^2\alpha^2})/(4\,h\alpha)], \quad \nu = 1,\ 2.$$

With $B \to 0$, which corresponds to $\Pi'_{\min}h \to -1$, the extreme acceleration values increase infinitely. At the same time there is an impact that is eliminated by observing the condition $B > 0$. In case of the harmonic law of motion the greatest values of the accelerations during the direct passage are achieved when $\varphi_n = 0,\ \pi$ and during the reverse passage, the extremities shift to the zone of increasing values of $|\Pi'|$.

If the law of motion consists of a three-interval structure, then the area of constant velocity is retained even in the given class of mechanisms, when the value of $|\omega_N|_{\max}$ is proportional to $|\Pi'|_{\max}/(1 \pm |\Pi'|_{\max})$, where the plus sign corresponds to the direct passage and the minus sign corresponds to the reverse passage.

Dynamic model For the dynamic model (Fig. 5.15b) we will take the following parameters as the generalized coordinates: the angle of rotation of the input link $\varphi_0 = q_0$; absolute dynamic errors, equal to the deviations of coordinates of the appropriate links while taking into account the elastic deformations $q_1 = \varphi_4 - \varphi_4^0$, $q_2 = \varphi_7 - \varphi_7^0$, where φ_i^0 corresponds to the program motion for rigid mechanism. Using the constraint equation (5.105) and the linearization procedure in the vicinity of the program motion (see Sect. 5.1), it can be shown that the elastic deformations, corresponding to the coefficients of stiffness c_1 and c_2 are respectively equal to $\Delta\varphi_5 = -Bh^{-1}q_1$ and $\Delta\varphi_7 = -Bh^{-1}q_1 + q_2$.

For the purpose of dynamic unloading, the relatively elastic element c_0 is included in the model (see Fig. 5.15), the deformation of which when $c_0 \leq c_1$, $c_0 \leq c_2$ is weakly dependent on q_1 and q_2 and is defined with the program motion φ_5^0.

Let us introduce the following notation: $J_\mathrm{I} = J_k u_{kn}^2 + J_n$, $J_\mathrm{II} = J_N + J_H u_{HN}^2 + m_p r_H^2 u_{HN}^2$, $J_p = J_1 + J_2$, where m_p, J_p are the mass and moment of inertia of the satellites; r_H is the radius of the carrier; J is the moment of inertia of the output link (see Fig. 5.15). At the same time the kinetic and potential energies are described as follows:

$$T = 0.5 \{ J_0 \dot{q}_0^2 + J_\mathrm{I}(\dot{\varphi}_n^0 + \dot{q}_1)^2 + J_\mathrm{II}(\dot{\varphi}_N^0 - \dot{q}_1 h^{-1})^2$$

$$+ J_p[\dot{\varphi}_p^0 - u_{HN}(1 - u_{10}^{(H)})\dot{q}_1 h^{-1}]^2 + J(\dot{\varphi}_N^0 - \dot{q}_2)^2 \},$$

$$V = 0.5 [c_1 h^{-2} B^2 q_1^2 + c_2(h^{-1}q_1 + q_2)^2 + c_0(\dot{\varphi}_N^0)^2],$$

where $\dot{\varphi}_p^0 = \omega_0 u_{10}^{(H)} + \dot{\varphi}_N^0 u_{HN}(1 - u_{10}^{(H)})$.

After substitution into the second-kind Lagrange equation the system of differential equations takes the following form:

$$\sum_{i=1}^{2} a_{ji}\ddot{q}_i + \sum_{i=1}^{2} b_{ji}(\varphi_n^0)\dot{q}_i + \sum_{i=1}^{2} c_{ji}(\varphi_n^0)q_i = Q_j^0 + Q_j^K, \ j = 1,\ 2,$$

where $a_{11} = J_\mathrm{I} + J_\mathrm{II} + J_p u_{HN}^2 (1 - u_{10}^{(H)})^2 h^{-2}$; $a_{12} = a_{21} = 0$; $a_{22} = J$; $c_{11} = (c_1 B^2 + c_2)h^{-2}$; $c_{12} = c_{21} = c_2 h^{-1}$; $c_{22} = c_2$; b_{ji} are the coefficients of the equivalent linear resistance; $Q_1^0 = M_1(t)$; $Q_2^0 = M_2(t) - c_0[\Pi(\varphi_n^0 + \Delta]$; $Q_1^K = -[J_\mathrm{I} + J_\mathrm{II}h^{-2} + J_p u_{HN}^2 (1 - u_{10}^{(H)})^2 h^{-2}]\ddot{\varphi}_n^0$; $Q_2^K = -J\ddot{\varphi}_N^0$; $M_j(t)$ are the external moments; Δ is the preliminary deformation of the elastic unloader. The variable "natural" frequency p_r can be determined without taking into account the dissipation on the basis of formal frequency equation

$$\det[c_{ij} - a_{ij}p^2(\varphi_n^0)] = 0. \tag{5.108}$$

Assuming that the logarithmic decrements ϑ_1 and ϑ_2, reduced to the oscillations modes are known, we find the coefficients b_{ij} *as* the matrix entries (see Chap. 6).

$$b = [\theta^{-1}]^{\mathrm{T}} \mathrm{diag}\{b_1^*, b_2^*\}\theta^{-1}, \tag{5.109}$$

where θ is the matrix of the non-stationary mode shapes factors.

Specifying (5.109) for the considered model, we have

$$b_{11} = (b_1^* + b_2^*\theta_{21}^2)/(1 - \theta_{12}\theta_{21}), b_{12} = b_{21} = -(b_1^*\theta_{12} + b_2^*\theta_{21})/(1 - \theta_{12}\theta_{21})^2,$$
$$b_{22} = (b_2^* + b_1^*\theta_{12}^2)/(1 - \theta_{12}\theta_{21})^2,$$

where $\theta_{ir} = -(c_{ii} - a_{ii}p_r^2)/(c_{ir} - a_{ir}p_r^2)$ at $i \neq r$; $r = 1, 2$; p_r is the root of the Eq. (5.108).

In the considered problem, the coefficients of the equations are functions of the angle φ_n^0, associated with the temporary nonlinear equation (5.105), which should be solved for each step of integration.

This can be avoided if we switch to the "dimensionless" time φ_n^0. Then $\dot{q}_i = q_i'\omega_{n0}/B(\varphi_n^0)$, $\ddot{q}_i = q_i''B^{-2}(\varphi_n^0)\omega_{n0}^2 - h\Pi''(\varphi_n^0)B^{-3}(\varphi_n^0)\omega_{n0}^2 q_i'$, where $()' = d/d\varphi_n^0$, $\omega_{n0} = u_z^{-1}\omega_0$.

Let us consider a few special cases. If $c_{22}/a_{22} \gg c_{11}/a_{11}$, the decisive role in the formation of oscillatory processes, is played by the oscillating contour, associated with the coefficient of stiffness c_1, which is described with the differential equation

$$a_1^*\ddot{q}_1 + b_1^*\dot{q}_1 + c_1^*(\varphi_n^0)q_1 = Q_1, \tag{5.110}$$

where $a_1^* = a_{11} + Jh^{-2}$, $c_1^* = h^{-2}B^2(\varphi_n^0)c_1$, $Q_1 = M(t) - [J_I + (J_{II} + J)h^{-2} + J_p u_{HN}^2(1 - u_{10}^{(H)})^2]\ddot{\varphi}_n^0 - c_0[\Pi(\varphi_n^0) + \Delta]$.

The variable "natural" frequency p is proportional to the function $B(\varphi_n^0)$: $p = B(\varphi_n^0)h^{-1}p_0$, where $p_0 = \sqrt{c_1/a_1^*}$. We can see the family of frequency characteristics p/p_0 in Fig. 5.17. An interesting feature of this mechanism is the increase in the "natural" frequency during the direct passage ($\Pi' > 0$) and decrease during the reverse passage ($\Pi' < 0$).

Due to the variability of the "natural" frequency, in certain areas of the kinematic cycle, local violation of dynamic stability are possible, manifested in the form of amplitude modulation of the free oscillations (see Sect. 5.3.1). To investigate this question, we will write the homogeneous differential equation, corresponding to (5.110), using the stated transition to dimensionless time φ_{n0}.

$$q'' + 2(\beta_0 + \beta_1)q' + \tilde{p}_0^2 h^{-2}B^4(\varphi_n^0)q = 0, \tag{5.111}$$

where $\tilde{p}_0 = p_0/\omega_{h0}$, $\beta_0 = \tilde{p}\vartheta/(2\pi)$, $\beta_1 = -0.5 h\Pi''(\varphi_n^0)/B(\varphi_n^0)$, ϑ is the reduced value of the logarithmic decrement.
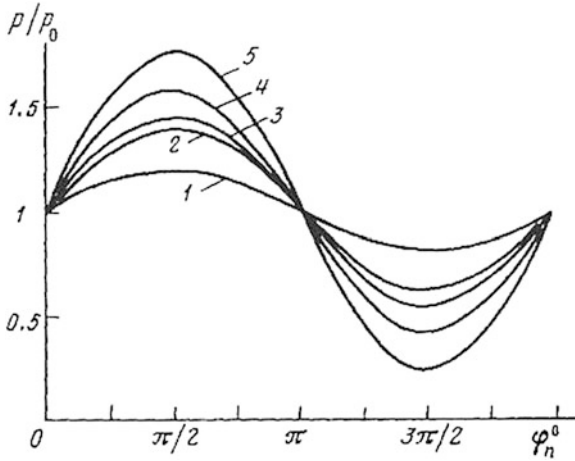
Fig. 5.17 Frequency characteristics: $1 - \alpha = \pi/24, 2 - \pi/12, 3 - \pi/10, 4 - \pi/8, 5 - \pi/6$

On the basis of the method of the conditional oscillator (see Sect. 5.2) to eliminate the possibility of growth of the amplitude of free oscillations, we will require

$$\frac{d}{d\varphi_n^0} \left\{ B^{-1}(\varphi_n^0) \exp\left[-\int_0^{\varphi_n^0} (\beta_0 + \beta_1(\xi)d\xi \right] \right\} < 0. \qquad (5.112)$$

Omitting the calculations we will write the condition (5.112) as follows:

$$\tilde{p}_0 \nu > -\pi h \Pi''(\varphi_n^0)/[h\Pi'(\varphi_n^0) + 1].$$

For the example under consideration, the right side of this inequality takes its maximum value when $\varphi_n^0 = \pi + \arcsin(\alpha h)$. The analysis shows that the most intense vibrations are excited during the reverse passage in case of abrupt change of the kinematic characteristics (see Fig. 5.16). In this zone, the given effect is also enhanced due to the parametric impulse, associated with the rapid changes of frequency characteristics.

A similar effect occurs for $c_{11}/a_{11} \gg c_{22}/a_{22}$, when the role of the mechanism is practically limited to kinematic excitation. Thus, for all of the considered models of the differential-cyclic mechanisms, particular attention is required for the interval $\delta\varphi_n^0 = \varphi_{n2}^* - \varphi_{n1}^*$, where φ_{n1}^*, φ_{n2}^* are the roots of the Eq. (5.107), corresponding to the extreme values of the angular acceleration $(\ddot{\varphi}_n^0)_{\max}$ and $(\ddot{\varphi}_n^0)_{\min}$.

The time segment δt determined with the constraint equation (5.105), corresponds to this interval

$$h[\Pi(\varphi^*_{n2}) - \Pi(\varphi^*_{n1})] + \delta\varphi^0_n = \omega_{n0}\delta t.$$

Hence we know that in the considered zone, when $\Pi' \approx \Pi'_{\min} < 0$ we have

$$\delta t = (1 - h|\Pi'_{\min}|)\delta\varphi^0_n/\omega_{n0}. \tag{5.113}$$

The dependence (5.113) shows the "phase compression", which can lead to the significant reduction of the segment δt, as compared to the conventional case, when the relationship between the angles of rotation of the cyclic mechanism's input link and the time in the first approximation is displayed with a linear function. As shown above, to eliminate the possibility of the soft impact, it is necessary to require $\delta t > (2 \div 3)2\pi/p_{\min}$, where $p_{\min}$ is the minimum value of the "natural" frequency.

Dynamic unloading For dynamic unloading of the differential-cyclic mechanism, we can use an elastic element, installed between the output link and the housing (see Fig. 5.15). The coefficient of torsional stiffness of this element c_0 and the value of preliminary deformation Δ are determined by the procedure of optimization of moment on one of the links (see Sect. 4.3). Thus, in particular, the driving torque on the input link, arising due to the kinetostatic load is equal to:

$$M_0 = B^{-1}(\varphi^0_n)\{[A_{11} - A_{22}\Pi'(\varphi^0_n) - A_{02}B(\varphi^0_n)h^{-1}]\varphi^0_n \\ + M_N\Pi'(\varphi^0_n) + c_0\Pi'(\varphi^0_n)[\Pi(\varphi^0_n) + \Delta]\}, \tag{5.114}$$

where $A_{11} = J_{\mathrm{I}}$, $A_{22} = J_{\mathrm{II}} + J + J_p u^2_{HN}(1 - u^{(H)}_{10})^2 h^{-2}$, $A_{02} = J_p u_{HN}(1 - u^{(H)}_{10})$.

We can see the results of optimization, when $\alpha = \pi/12$, $A_{22}/A_{11} = 0.4$, $A_{02}/A_{11} = 0.1$, $M_N = 0$, for the considered example in Fig. 5.18 as the graphs of the dimensionless moment $\mu = M_0/(A_{11}\omega^2_0)$.

Fig. 5.18 Graphs of the dimensionless driving moment
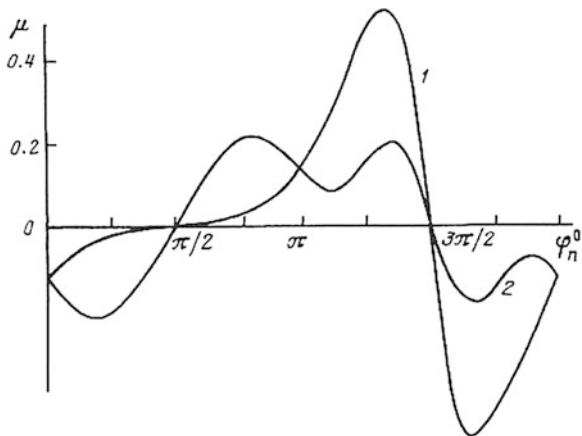
Curve 1 corresponds to $c_0 = 0$, curve 2 to c_0 and Δ, obtained from (5.114), while minimizing the difference between the extreme values of μ, for forward and reverse passages. The installation of the unloader leads to the reduction of the extreme values of torque on the input link by more than 2.5 times. Thus, despite of the great difference in kinetostatic load on the forward and reverse passages, the load on the drive of the differential-cyclic mechanism can be substantially aligned with the help of the unloader. At the same time the driving forces and vibration activity of the drive also decrease.

At the end, we will note that using the differential-cyclic mechanisms, we can with a single constructive solution, carry-out the complex laws of motion for the executive bodies and change these laws with easy readjustments.

5.7.3 Bending Vibrations of the Actuator, Schematized as a Cantilever Beam with Variable Length

Let us consider the dynamic model of the cantilever beam of variable length, as shown in Fig. 5.19. A similar pattern occurs in the calculation of bending vibrations of pullout spindles, needles of the row of knitting machines and in some other cases.

Let us accept $\ell(t) = \ell_0 + x(t)$, where $x(t) = vt$, v is the velocity. We will transform the original dynamic model of the beam, with distributed parameters, to the beam with lumped mass at its end. We will assume that the frequencies of the original and reduced beams, for the considered oscillations' modes, are equal. On the basis of the frequency equation $\cos \sigma \ell \cdot \cosh \sigma \ell = -1$, we get $p_r = \sigma_r^2 \sqrt{EI/\rho}$, where E, I are elastic modulus and equatorial moment of inertia; ρ is the mass of the unit length. When $r = 1$, $r = 2$ the roots of the frequency equation are $\sigma_1 \ell = 1.875$; $\sigma_2 \ell = 4.694$. Omitting the elementary calculations, we get for the first oscillations' mode $m(t) = 0.243 \rho \ell(t)$; $c(t) = 3EI/\ell(t)^3$. Hence

$$p(t)^2 = p_0^2/(1 + \alpha t)^4, \tag{5.115}$$

where $p_0^2 = c(\ell_0)/m(\ell_0)$, $\alpha = v/\ell_0$.

After the transition to the new variable $\tau = p_0 t$, assuming $v = p/p_0$, we get $v = \tilde{v}$, where according to (5.115) $\tilde{v}$ corresponds to the family of the exact solutions of the conditional oscillator $z = -2 \ln(\beta_1 p_0 t + \beta_2)$ at $\beta_1 = \alpha/p_0 = v/(\ell_0 p_0)$; $\beta_2 = 1$ (see Sect. 5.2.1).
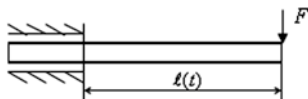
Fig. 5.19 Dynamic model

Fig. 5.20 Graphs $z(\tau)$: 1, 2
… $v_* = 0.1$; 0.2 when
$\tau_* = 50$; 3.4 − $v_* = 0.1$; 0.2
when $\tau_* = 50$
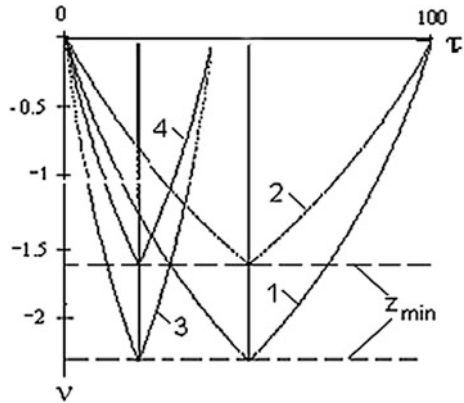
We can see in the Figs. 5.20 and 5.21, the coordinates of the conditional oscillator and the corresponding graphs of changes in the dimensionless "natural" frequency, in the range of dimensionless time $2\tau_*$, when $\tau = \tau_*$, the sign of velocity v changes. The analysis of these graphs is primarily of interest as an opportunity to predict the maximum variation of the amplitudes of free oscillations, without solving the original differential equation.

Indeed according to (5.50) we have

$$\max y_* \leq A \exp[-0.5 \, (z_{min} - z_0)]. \tag{5.116}$$

These graphs illustrate an interesting property: the rate of increase in amplitudes κ without dissipation is determined only by drops of frequencies (parameter v_*) and is independent of τ_* (Fig. 5.22, line 1). When taking into account the structural damping, we have $q = y_* \exp[-\delta \int_0^t p(\xi)d\xi]$, where $\delta = \vartheta/(2\pi)$, ϑ is the logarithmic decrement. The lower curves 2 and 3 correspond to the interval τ_* and the top curves 2 and 3 correspond to the interval $2\tau_*$, i.e. to the full cycle of motion.

Fig. 5.21 Graphs $v(\tau)$: 1, 2, 3
… $v_* = 0.1$; 0.2; 0.5 when
$\tau_* = 50$; 4.5 − $v_* = 0.5$ when
$\tau_* = 30$; 20
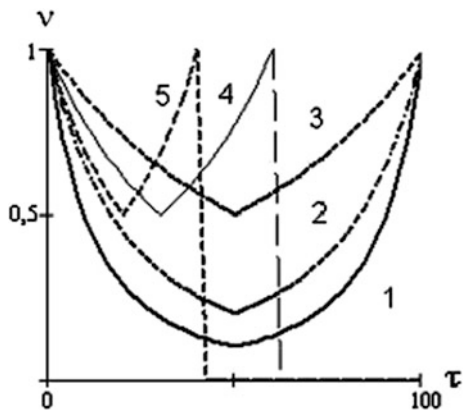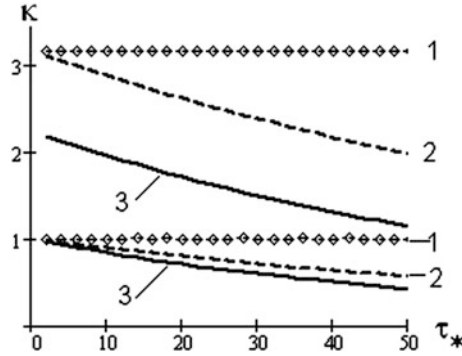
Fig. 5.22 Graphs $\kappa(\tau_*)$: $1 - \nu_* = 0.1$; $\delta = 0$: $2 - \nu_* = 0.1$; $\delta = 0.03$; $3 - \nu_* = 0.2$; $\delta = 0.03$

The integral in the exponent depicts the change of the phase of oscillations, which after the transition to the variable τ is equal to $\tau/(1 + \beta_1 \tau)$.

In Fig. 5.23, we can see the typical graphs of free oscillations in the absence of dissipation $(q = y_*)$ and taking it into account. The graphs clearly illustrate the increase in the amplitudes of oscillation in case of transition to the zone of low frequencies. This effect, which occurs in case of violation of dynamic stability conditions in the finite time interval, manifests to a lesser degree in case of presence of dissipation. Due to this, we can set a problem regarding the critical dissipation level, at which the damping character of free oscillations is provided.

Based on the study of this problem, in relation to our case, we have the following condition:

$\delta > \delta_* = 0.5 \, \beta_1/(1 + \beta_1 \tau)$. It can be shown that the amplitude of free oscillations is in the range, bounded by two extreme cases, corresponding to an abrupt and slow change in "natural" frequency. Thus, $A(0)/\sqrt{\nu_*} < \max y_* < A(0)/\nu_*$. In case
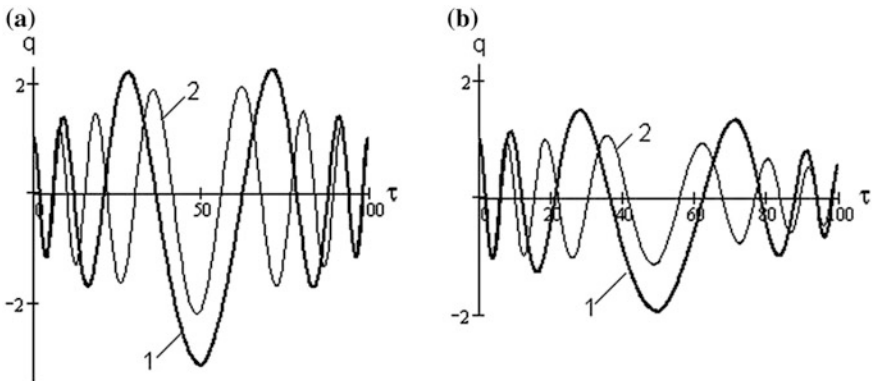
Fig. 5.23 Free oscillations in case of $\delta = 0$ (**a**) and $\delta = 0.03$ (**b**): $1 - \nu_* = 0.1$; $2 - \nu_* = 0.2$
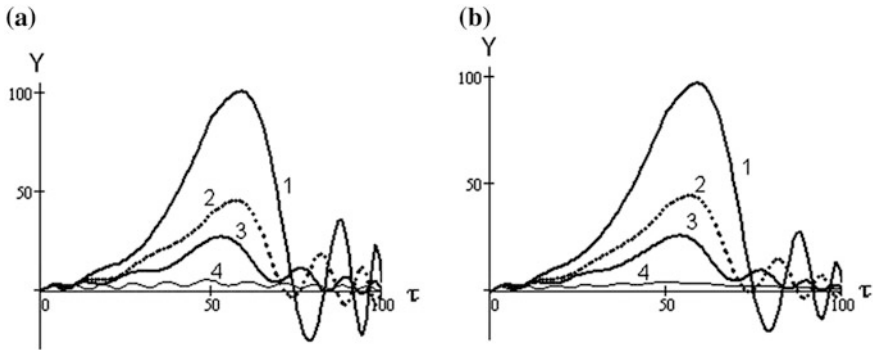
Fig. 5.24 Forced oscillations of case $\delta = 0$ (**a**) and $\delta = 0.03$ (**b**) : $1 - v_* = 0.1$; $2 - v_* = 0.15$; $3 - v_* = 0.2$; $4 - v_* = 0.5$, $1 - n_* = 0.1$; $2 - n_* = 0.15$; $3 - n_* = 0.2$; $4 - n_* = 0.5$.

of $v_* \tau_* > 2\pi$, the change in parameters can be considered as slow. To determine the forced oscillations, we use (5.16), which, taking into account the dissipation, takes the form

$$Y = \exp[-0.5\, z(\tau)] \int_0^\tau \{ W(s) \exp[-0.5\, z(s) - \delta \int_s^\tau v(\xi)d\xi] \sin \int_s^\tau v(\xi)d\xi \} ds.$$

Below we can see the typical graphs of forced oscillations, when $W = 1$, $\tau_* = 50$, $\delta = 0$ (Fig. 5.24a) $\delta = 0.03$ (Fig. 5.24b).

The analysis of the graphs shows that in case of significant and abrupt change in the "natural" frequencies, the system responds to the constant force almost as if to the application of instantaneous load. In such cases, within the same cycle the influence of the dissipative forces is weak.

5.7.4 Vibrations of the Drives of Cyclic Machine, Taking into Account the Dynamic Characteristics of the Motor

Here above during the dynamic analysis of the mechanisms, we assumed that the angular velocity of the motor is permanent or is a known function of time. However, this approach requires verification and sometimes some adjustment of the results. As noted in Sect. 2.5, the dynamic model of the executive machine, strictly speaking, should be supplemented by taking into account the dynamic characteristics of the power source (motor), which allows us to determine the non-uniform rotation of the driving links and the associated vibration activity of the drive.

For some automated drives and robotic devices, we should also take into account the control system of motion [13, 18, 26, 57]. Here we will restrict ourselves to the problems, which have a direct relation to the dynamics of the cyclical technological

machines, in which control, due to strict limitations, is determined by the cyclogram of the program motion of the working parts. In Sect. 8.5, we will discuss the matrix method of analytical solution for the given class of problems.

The electric motors belong to the group of electro-mechanical systems, in which the dynamic processes are characterized by the correlation of forms of motion: electrical and mechanical. The description of electromagnetic oscillatory processes in the motors is associated with the solution of quite complex systems of nonlinear differential equations. However, with regard to the established regimes, in the engineering practice, the approximate linearized equation, called the *dynamic characteristics* of the motor, is widespread; for DC motors and asynchronous motors these characteristics can be represented as follows:

$$\omega_m = \omega_m^0 \left[1 - \nu_m (M + T_m \dot{M}) \right], \tag{5.117}$$

where ω_m, ω_m^0 are the angular velocities of the electric motor and rate of the ideal idle run; ν_m is the slope factor of the static characteristic; M is the motor's moment; T_m is the motor's electromagnetic time constant, depending on the parameters of its electrical circuit.

For asynchronous electric motors and T_m are determined by the following approximate dependencies: $\grave{O}_m = 1/(2\pi f_{\text{Ñ}} s_{\hat{\text{E}}})$; $\nu_m = s_{\hat{\text{E}}}/(2\grave{I}_{\text{n}} \xi)$, where $s_{\text{K}} = (1 - \omega_m^n/\omega_m^0)(\xi + \sqrt{\xi^2 + 1})$ is the critical sliding; M_n, ω_m^n are the nominal torque and angular speed of the motor; $f_{\text{Ñ}}$ is the line frequency, Hz; ξ is the ratio of the maximum torque to the nominal.

The input data for the determination of $\grave{O}_m$ and ν_m is taken from the motor's catalogue. For $\grave{O}_m = 0$ in Eq. (5.117) the characteristic of the electric motor is called *static*.

Case J = const: If the reduced to the motor's shaft moment of inertia J is constant, then

$$J\dot{\omega}_m = \grave{I} - \grave{I}_{\tilde{\text{N}}}, \tag{5.118}$$

where $M_{\tilde{\text{N}}}$ is the reduced to the motor's shaft moment of resistance. Hence $M = J\, d\omega_m/dt + M_{\text{C}}$ and $dM/dt = J(d^2\omega_m/dt^2) + dM_{\text{C}}/dt$. After substituting M and dM/dt in (5.118) we get

$$\nu_m T_{\ddot{A}} J\ddot{\omega}_m + \nu_m J\dot{\omega}_m + \omega_m/\omega_m^0 = 1 - \nu_m(\grave{I}_{\tilde{\text{N}}} + \grave{O}_m \grave{I}_{\tilde{\text{N}}}). \tag{5.119}$$

Further we will represent the moment of resistance $M_{\tilde{\text{N}}}$ as the sum of the average value $\grave{I}_{\text{C}}^{-}$ and the variable component $\Delta \grave{I}_{\tilde{\text{N}}}(t)$. Accordingly the function $\omega_m(t)$ can also be represented as $\omega_m(t) = \bar{\omega}_m + \Delta\omega_m(t)$. The constant component $\bar{\omega}_m$ is determined by the static characteristic of the motor:

Fig. 5.25 Graphs $\bar{M}_m$, $\bar{M}_C$
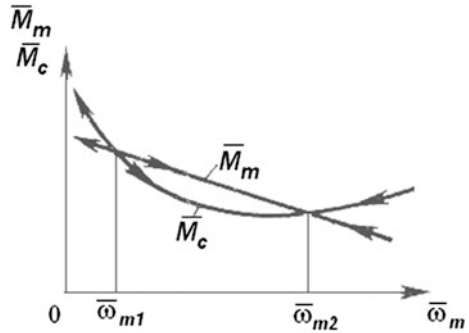
$$\bar{\omega}_m = \omega_m^0(1 - \nu_m \bar{I}_{\bar{N}}). \tag{5.120}$$

In the engineering practice, situations occur, when the determination of $\bar{\omega}_m$ requires some clarification. Suppose, for example, graphs, $\bar{M}_m$ and $\bar{M}_C$ have the form shown in Fig. 5.25.

The points of intersection of the curves correspond to the two stationary regimes. However, in case of the angular velocity $\bar{\omega}_{m1}$, the regime is unstable, as any deviation from it leads to the emergence of destabilizing moment. Value ω_{m2} corresponds to stable stationary state.

When taking into account (5.120), we will rewrite Eq. (5.119) as follows:

$$\Delta\ddot{\omega}_m + 2n\Delta\dot{\omega}_m + k^2\omega_m = W(t), \tag{5.121}$$

where $n = 0.5\,\dot{O}_m^{-1}$; $k^2 = (\nu_m T_m J \omega_m^0)^{-1}$; $W(t) = -(\Delta M_{\bar{N}} \dot{O}_m^{-1} + \Delta \dot{I}_{\bar{N}})/J$; $\Delta M_C = M_C - \bar{M}_C$.

Thus, the finding of the variable component of angular velocity of the motor $\Delta\omega_m$, which determines the non-uniformity of the machine's input link's rotation, again is reduced to the solution of the linear nonhomogeneous differential equation of the second order, investigated in details in this chapter. Let us note here, however, that unlike the previously discussed cases, where the dissipative force was basically caused by structural damping, parameter n here could be comparable to k. So when calculating the natural frequency k_1 (see Sect. 4.2), we should use the formula:

$$k_1 = \sqrt{k^2 - n^2} = \sqrt{(J\nu_m T_m \omega_m^0)^{-1} - 0.25\,T_m^{-2}}.$$

When $T_m = T_m^* = 0.25\,\nu_m \omega_m^0 J$, the "natural" frequency vanishes. Thus when $T_m \le T_m^*$ the solution of the homogeneous differential equation, corresponding to (5.121), becomes non-periodic. Increasing T_m up to $T_m^{**} = 0.5\,\nu_m \omega_m^0 J$ the value of k_1 increases to its maximum value $k_{1\max} = (\nu_m \omega_m^0 J)^{-1}$; in case of $T_m > T_m^{**}$ the

"natural" frequency with the increase in the electromagnetic constant of time T_m accordingly decreases.

This character of influence of parameter T_m is related to the fact that the dynamic characteristics of the motor correspond to the model, in which the rotor is connected to the stator by means of an "elastic element" with the stiffness coefficient $c_m = (v_m \omega_m^0 T_m)^{-1}$ and the sequentially included damper, enhancing the resistance moment, proportional to the first stage of velocity with the coefficient of proportionality $b_m = (v_m \omega_m^0)^{-1}$. Therefore, for small values of T_m, the damper plays the decisive role, which leads to the possibility of non-periodic solutions; for larger values of T_m the "stiffness" decreases, and accordingly the "natural" frequency decreases.

As the analysis shows, the characteristic of an asynchronous motor and DC motor are equivalent to the compliance of the elastic element, which is usually much greater than the elastic elements of the drive. This enables us in case of study of the machine's dynamics, research the non-uniformity of rotation of the motor's shaft, by means of the relatively simple models, assuming in the first approximation, that the rest of the kinematic chain is either rigid or taking into account only the most flexible elements of the drive.

One of the traditional ways of reducing irregular rotation of the input link of the machines' drives is to increase the moment of inertia J by installing the flywheel. However, as the analysis shows, increasing J reduces $\Delta\omega_m$ only in above-resonance regimes, when the frequency of the driving torque $\Omega > k_1$. If in this case, we accept $\Omega \geq \sqrt{2}k_1$ for detuning from resonance, then in case of installation of the flywheel, the condition $J > 2(\omega_m^2 \omega_m^0 v_m T_m)^{-1}$ to be satisfied. Next, based on the solutions of the Eq. (5.121) maybe we can determine the irregularity factor $\delta_{ir} \approx 2|\Delta\omega_m|_{max}/\bar{\omega}_m r$, where $\bar{\omega}_m$ is the average angular velocity of the motor.

It should, however, be kept in mind that the substantial increase in the moment of inertia J is not desirable for transient modes, as this increases the dynamic loads during the machine's run-up.

Case $J \neq$ const: Cyclic recurrence of change of parameters of the system is determined by the average angular velocity of the main shaft $\bar{\omega}$. In this case, instead of the dependence (5.118) we should write

$$J(\varphi)\dot{\omega}_m + 0.5\,\omega_m^2 \frac{dJ}{d\varphi}(\varphi) = M(\omega_m) - M_c(\Omega, \varphi). \qquad (5.122)$$

Here φ is the rotation angle of the main shaft; $\Omega = d\varphi/dt$.

Then, again, representing the angular velocity of the motor as the sum of the fixed and variable components, after linearization in the vicinity of program motion, we obtain

$$\Delta\ddot{\omega}_m + 2n(\varphi_*)\Delta\dot{\omega}_m + k^2(\varphi_*)\Delta\omega_m = W(\varphi_*), \tag{5.123}$$

where $2n = T_m^{-1} + 2J'\bar{\Omega}/J$; $k^2 = J^{-1}[(\nu_m T_m \bar{\omega}_m)^{-1} + \bar{\Omega}J'T_m^{-1}]$; $W = -J(\Delta M T_m^{-1} + \Delta M'\bar{\Omega} + 0.5\bar{\Omega}^2 uJ'T_m^{-1})$; $u = \bar{\Omega}/\bar{\omega}_m$ is the drive ratio; $\Delta M = M - \bar{M}$; $(\,)' = d/d\varphi$; dash corresponds to the average value for the period $\tau = 2\pi/\bar{\Omega}$.

Thus, as regards to $\Delta\omega_m$, we again have a linear differential equation of the second order with variable coefficients. The "natural" frequency as per (5.6) is equal to $p = \sqrt{k^2 - n^2} - \dot{n}$. The specifics of this model include the relatively large value of the dissipative term, which practically eliminates the possibility of parametric resonance at this frequency. In addition it can lead to the large difference between k and p and even to transition to the non-periodic regime. Let us note here that often sufficient accuracy is provided by the solution when using average value of $J \approx \bar{J} = $ const (see above). The analytical solution of the oscillatory regimes, taking into account the characteristics of the electric motor and the variable reduced moment of inertia, is discussed in detail in [18, 26].

Dynamic errors and the effects, associated with taking into account the characteristics of the engine, in the cyclic oscillatory systems In a number of machines program motion is performed by a massive executive body or unit, which essentially determines the dynamic load of the electric motor. This situation occurs in the drive of the flat-bed printing machine table, the drive of carriages and other massive executive parts of the textile machinery, in machines and automatic lines in a wide variety of industries. In such cases the dynamic processes, occurring in the

Fig. 5.26 Distortion of the program motion characteristics: *1*—velocity; *2*—accelerations; *3*—areas of the kinematic contact discontinuity; *4*—markers of the beginning and the end of the program motion
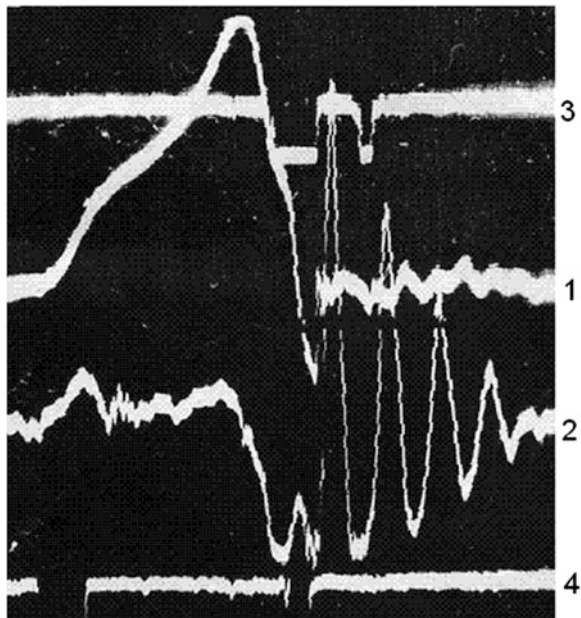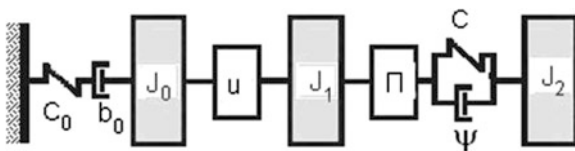
Fig. 5.27 Dynamic model of the cyclic machine with motor

engine, are manifested not only in case of change of the force system character-
istics, but also in case of dynamic errors of the given program motion. As an
example, Fig. 5.26 shows the oscillogram of the kinematic characteristics of the
output link of the cam mechanism in case of symmetric law of the program motion.
On the run-in due to large inertial loads the angular velocity of the motor has
declined substantially, leading to the significant acceleration during the run-down
and, as a result, to vibration impact regime, in the interval of theoretical dwell (see
Chap. 7).

Let us consider the dynamic model (Fig. 5.27), which takes into account char-
acteristics of the engine, drive and oscillatory system of the output link.

To identify the distortions of the given program motion, we first consider a
special case with an absolutely rigid mechanism ($c \rightarrow \infty$). We can see in Fig. 5.28
the graphics of the function $w = -\ddot{q}(\varphi_*)$ that are obtained by computer simulation
and are proportional to the moment of inertial forces of the output link. At the same
time the curve 1 corresponds to the original harmonic law of change of acceleration,
and curves 2, 3 correspond to static and dynamic characteristics of the electric
motor respectively.

It follows from the analysis of the graphs that the most significant distortions
occur under the static characteristics. This is due to the appearance of the second
harmonic in the moment of inertial forces, reduced to the motor's shaft, which is
proportional to $\Pi'\Pi''$ (see Sect. 1.3). When taking into account the dynamic
characteristics, this effect is smoothed due to the influence of the electromagnetic
time constant, however, as compared to the initial accelerations, the extreme
accelerations increase.

Fig. 5.28 Distortions of the
program motion's
accelerations, associated with
the influence of the motor
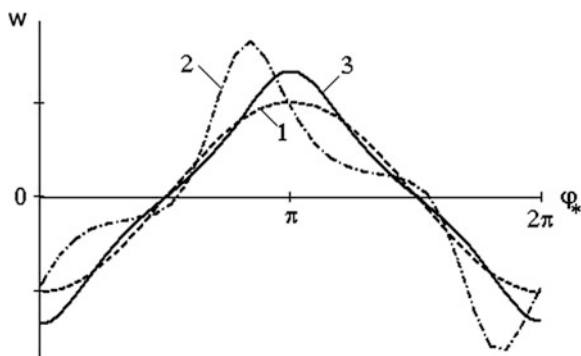
Fig. 5.29 The consolidated graph of the characteristics of cyclic electromechanical system
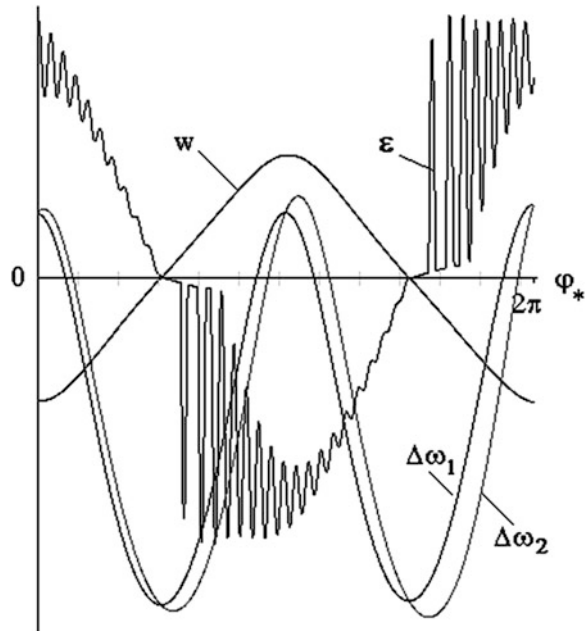
Furthermore, we will estimate, as to how much do the high-frequency-oscillations, excited in the output link, distort, taking into account the characteristic of the engine. In the Fig. 5.29 some results of the analysis of the original model are presented (see Fig. 5.27). At the same time in the zone of transition through the clearance (see Chap. 7), impulse excitation occurs, causing high-frequency oscillations of the output link (curve ε). The curves $\Delta\omega_1$ and $\Delta\omega_2$, corresponding to the dynamic error of the electric motor's angular velocity, differ in such a way that in the second case the phase shifts of the rotation angle of the main shaft are taken into account additionally. Curve w corresponds to the original harmonic law of program motion, distorted due to the irregular rotation of the motor's rotor. As it can be seen in Fig. 5.26, in some cases it can lead to inappropriate operating modes.

Analysis of graphs leads to the following conclusions:

1. Because of the significant difference between the partial frequencies of the motor and the mechanical system, the high frequency oscillations of the output link, generally, do not influence the angular velocity of the motor.
2. Low-frequency oscillations of the output link, caused by program motion (curve w), can lead to significant non-uniformity of rotation of the main shaft (curves $\Delta\omega_1, \Delta\omega_2$). Thus, not only do the extreme values of the kinematic characteristics of the program motion change, but also the time intervals, corresponding to the transition lengths of changes in program accelerations. This, in turn, manifests itself at the level of excited oscillations of the output link (see Sect. 4.1.3).

3. The phase shifts in angle φ can significantly distort the duration given by the program motion, run-in and run-down intervals, which leads to impaired accuracy of the reproduction of kinematic characteristics of the output link. This is particularly important in the cyclic force-closing mechanisms, when discontinuities of kinematic contact and vibration-impact regimes can occur (see Fig. 5.6 and Chap. 7).

Chapter 6
Nonlinear Dissipative Forces

6.1 Accounting of Nonlinear Dissipative Forces in Case of Mono-harmonic Oscillations

6.1.1 Preliminary Remarks

In case of oscillations in the elastic systems, the power dissipates in the machinery joints, in the material of the elastic elements, as well as in the environment, i.e. the mechanical energy transforms into other forms of energy. The role played by the dissipative forces in the formation of oscillatory processes of frequencies close to its natural ones, is extremely extensive. In particular, the level of dissipation affects the amplitude of the resonant oscillations and conditions for the occurrence of parametric, sub-harmonic and self-excited oscillations.

Theoretical and experimental investigations of the dissipative forces were the subject matter of many scientific publications. The detailed review of which, is neither the purpose of this book nor does it fit in its scope. Various aspects of this multifaceted problem were reflected in many monographs, reference books, research reports and other publications, for example, [9, 15, 16, 24, 26, 27, 30, 42, 43, 45, 46, 49, 55, 58, 60, 88, 89]. Based on the above, it seems appropriate to focus only on the publications that are relevant to the dynamics of machines and mechanisms.

For systems, with one degree of freedom, the force of resistance that occurs, in case of oscillations, can be described as follows:

$$R = -|R(q, \dot{q})|\text{sign}\dot{q}, \tag{6.1}$$

where q is the generalized coordinate, which characterizes the oscillatory process.

In some cases, the module of the force of resistance does not depend on the generalized coordinate q. In particular, in case of the so-called viscous resistance, which occurs in case of small oscillations in a viscous medium (liquid or gas)

$R = -b\dot{q}$. At high vibration rates, there is quadratic dependence of the force of resistance on velocity or higher order of this dependence.

In other cases, typical for the dynamics of machines, the module of force of friction normally depends on the generalized coordinates and is practically independent of vibration velocity. At the same time $R = -|R(q)|\mathrm{sign}\dot{q}$; in this case the force of resistance is called *positional*. If $|R| = P = \mathrm{const}$, then the force is called dry friction (or Coulomb) force. Another distinguishing type is the positional-viscous friction, in case of which $R = -f(q)\dot{q}$.

It should be noted that the separation of the elastodissipative force into its elastodissipative components is, strictly speaking, conditional and is often impossible; therefore during engineering calculations the point can be made of using the effective approximate methods, which allow us to estimate the influence of dissipation on the oscillatory processes. At the same time we usually only have limited background information in the form of some integral characteristics, such as the coefficient of dissipation ψ or the logarithmic decrement ϑ, which are obtained experimentally using mono-harmonic h (single-frequency) modes.

6.1.2 Equivalent Linearization of Dissipative Forces in the Oscillatory System with One Degree of Freedom

Let us consider the differential equation corresponding to the oscillations of the system with one degree of freedom

$$m\ddot{q} + cq = F(t) - |R(q, \dot{q})|\mathrm{sign}\dot{q}, \tag{6.2}$$

where m, c are the reduced mass and reduced stiffness coefficient; $F(t)$ is the driving force.

Hereunder we will consider the positional dissipative forces, typical for machines and mechanisms. Strictly speaking, the differential Eq. (6.2) is nonlinear due to the nonlinearity of the dissipative forces. However, as a rule, the dissipative forces very slightly influence the frequency of free oscillations and in the given case it determines the intensity of the mechanical attenuations and the amplitude level in case of resonance. On the basis of such limited manifestations of nonlinear dissipative forces, we will call the considered oscillatory system as *quasi-linear*. For the nonlinear force $-R(q, \dot{q})$ we can find energetically equivalent linear force $R_L = -b\dot{q}$. If $F(t) = F_0 \sin \omega t$, then under the stationary forced oscillations $q = A\sin(\omega t - \gamma)$. In this case, the dissipated in one period energy is equal to

$$\Delta E_- = A \int_0^{2\pi} |R(A\sin\varphi, \omega A\cos\varphi)\cos\varphi| d\varphi = \psi c A^2 / 2.$$

On the other hand $\Delta E_- = \pi b A^2 \omega$. Hence,

$$b = \Delta E_- / (\pi A^2 \omega) = \psi c / (2\pi \omega). \tag{6.3}$$

This result coincides with the corresponding coefficient, obtained by the method of harmonic linearization (see Appendix), which seems quite natural if we take into account that background information about the coefficient of dissipation ψ was obtained with single-frequency harmonic oscillations. In a certain sense, according to this point of view, the coefficient of dissipation ψ can be regarded as the result of "harmonic linearization", performed experimentally. Usually when using formula (6.3) the frequency of the driving force ω can be replaced by natural frequency k, as dissipative forces play a significant role in the vicinity of this frequency.

It follows from (6.3) that the dissipative properties, for mono-harmonic mode, are determined by the area of the hysteresis loop and do not depend on the shape of the loop. Furthermore, it is obvious that the dissipation coefficient ψ does not depend on the amplitude, only if the value ΔE_- is proportional to the square of the amplitude. This, for example, takes place in case of linear force of resistance or force of resistance, proportional to the amplitude in the first degree.

Analysis of the experimental materials indicates that the dissipation coefficient ψ, and hence, the logarithmic decrement ϑ usually very weakly depend on frequency of oscillations. Then according to (6.3) coefficient b turns out to be inversely proportional to the frequency of oscillations. Let us note here that in case of this kind of dissipation, which is often called *frequency independent,* one of the most typical mistakes, made by varying the parameters of the oscillatory system, is to keep obtained value b as constant. The fact that indicates the probable consequences of such mistake, shows that in case of $b = $ const, the reduction in the coefficient of stiffness c, in case of positional friction can apparently cause the transition to the non-periodic regime, since the natural frequency is equal to $k_1 = \sqrt{c/m - b^2/(2m)^2}$. However, in fact in this case when $\psi = $ const, we have $k_1 = \sqrt{c(1 - \delta^2)/m}$, where $\delta \approx \psi/(4\pi)$, and hence, the possibility of occurrence of the non-periodic regimes due to a decrease in the coefficient of stiffness, c is excluded.

Equation (6.3) shows that "inelastic" resistance $R = -b\dot{q}$, in case of single-frequency oscillations, is proportional to the restoring force, but is shifted in phase $\pi/2$ relative to the latter. This is the basis of the proposal by Sorokin [55] to use a complex form of writing the dissipative force as follows:

$$R = -2\,\delta\,cq \cdot i, \tag{6.4}$$

where $i = \sqrt{-1}$ is the imaginary unit, corresponding to the rotation of the vector of the restoring force on $\pi/2$ (this very angle corresponds to the phase shift between q and $\dot{q}$ in case of the harmonic oscillations). Hence, taking into account (6.4), while

representing elastodissipative forces in complex form, the differential Eq. (6.2) can be written as

$$m\ddot{q} + \tilde{c}q = F_0 e^{i\omega t}, \tag{6.5}$$

where the right hand side of the equation corresponds to the harmonic driving force with frequency ω; $\tilde{c} = c(1 + i \cdot 2\delta)$ is the complex coefficient of stiffness.

In case of parallel or serial connection of the elastodissipative elements, under the fair rules of reduction of the complex coefficients of stiffness, according to which, in the first case the stiffness coefficients of individual elements are added, and in the second case, the reduced coefficient of compliances (inverse of the stiffness coefficients) is equal to the sum of the relevant values of elements (see Sect. 2.6.3).

We will find the particular solution of Eq. (6.5), corresponding to the forced oscillations, in the form

$$\tilde{q} = \tilde{A}e^{i\omega t}. \tag{6.6}$$

Here $\tilde{A} = |A|e^{i\alpha}$ is the complex amplitude of the forced oscillations; α is the phase of the oscillations. Substituting (6.6) in (6.5) we get

$$\tilde{A} = \frac{F_0}{c} \frac{1}{(1 - \omega^2/k^2 + 2\delta i)}. \tag{6.7}$$

The module $|A|$ coincides with the well-known formula (4.12), which determines the resonant amplitude. However, using modern standard computing, it is not necessary to determine $|A|$ with the help of the analytical procedures.

6.1.3 Equivalent Linearization of Dissipative Forces in Oscillatory Systems with Many Degrees of Freedom

The described method of accounting of the nonlinear forces can be extended to systems with both lumped and distributed parameter [43, 64, 75, 88]. As before, we will assume the dynamic model to be quasi-linear in that, nonlinear dissipative forces have negligible influence on the natural frequencies and mode shapes.

We represent the system of differential equations of the model with H degrees of freedom in the form

$$\mathbf{a}\ddot{\mathbf{q}} + \mathbf{c}\mathbf{q} = \mathbf{Q}, \tag{6.8}$$

where $\mathbf{a}$, $\mathbf{c}$ are the square matrices of inertial and quasi-elastic coefficients; $\mathbf{q}$ is the vector-matrix (column) of the generalized coordinates; $\mathbf{Q}$ is the vector matrix of non-conservative forces.

From the vector of generalized forces, we select dissipative component $\mathbf{R}(q, \dot{q})$, which will be presented as

$$\mathbf{R} = -\mathbf{b}\dot{\mathbf{q}}, \tag{6.9}$$

where $\mathbf{b}$ is the square matrix of equivalent dissipative coefficients; $\dot{\mathbf{q}}$ is the vector of generalized velocities.

The task is to find the reliable (in terms of engineering calculation of vibrations in machines) value of the coefficients of linear damping b_{jv}, the determination of which would base on the available information about the dissipation coefficients (or logarithmic decrements) of the individual elastodissipative elements of the system.

For purely viscous friction, where the force of resistance is proportional to the first order of velocity, for describing the dissipative properties, we usually use the dissipation function of Rayleigh Φ_R, which characterizes the intensity of the change in the total energy of the system E:

$$\Phi_R = -\frac{1}{2}\frac{dE}{dt} = \frac{1}{2}\sum_{j=1}^{H}\sum_{v=1}^{H} b_{jv}\dot{q}_j\dot{q}_v. \tag{6.10}$$

However, for frequency-independent dissipation the coefficients b_{jv} are unknown and they can be used only with approximate approach. In this case it is sensible to consider several steps of idealization of dissipative forces. Let us introduce the normal (main) coordinates θ_r

$$q_j = \sum_{r=1}^{H} \beta_{jr}\theta_r. \tag{6.11}$$

Here β_{jr} are the shape factors, determined without taking into account the dissipative forces.

Then the original system of differential Eq. (6.8) can be written as follows:

$$\mathbf{a}^*\ddot{\boldsymbol{\theta}} + \mathbf{c}^*\boldsymbol{\theta} = \mathbf{Q}^*, \tag{6.12}$$

where $\mathbf{a}^* = \boldsymbol{\beta}^{\mathbf{T}}\mathbf{a}\boldsymbol{\beta}$, $\mathbf{c}^* = \boldsymbol{\beta}^{\mathbf{T}}\mathbf{c}\boldsymbol{\beta}$ are the diagonal matrices of inertial and quasi-elastic coefficients after the transition to the normal coordinates; $\boldsymbol{\theta}, \mathbf{Q}^*$ are the vector-matrices of the normal coordinates and generalized non-conservative forces; $\boldsymbol{\beta}$ is the matrix of the shape modes coefficients.

Let us note here that when using the given procedure of drawing up Eq. (6.12) the assumption of the absence of dissipative connections, between different modes, was used in principle form. Then we introduce the equivalent dissipative force $R_r = -b_r^*\dot{\theta}_r$ in every equation of the system (6.12):

$$a_r^* \ddot{\theta}_r + b_r^* \dot{\theta}_r + c_r^* \theta = F_r^*(t) \qquad (r = 1, \ldots, H). \tag{6.13}$$

Here $F_r^* = \sum_{j=1}^{H} Q_j \beta_{jr}$ ($\mathbf{F}^* = \boldsymbol{\beta} \mathbf{Q}$).

Dissipation coefficient ψ_r^* corresponding to r mode is determined as:

$$\psi_r^* = \sum_{j=1}^{H} \psi_j c_j \beta_{jr}^2 / \sum_{j=1}^{H} c_j \beta_{jr}^2. \tag{6.14}$$

Hence with (6.3)

$$b_r^* = \psi_r^* c_r / (2\pi k_r), \tag{6.15}$$

where $k_r = \sqrt{c_r / a_r}$.

The described above method of using numerical methods, for solving the system of differential equations, may cause some inconvenience, since as an interim procedure, it requires the transition to normal coordinates. However, retaining the idea of this method, the said procedure can be eliminated. Let the equivalent dissipative forces be described in the original system as follows:

$$\mathbf{R} = -\mathbf{b}\dot{\mathbf{q}} = -\mathbf{b}\boldsymbol{\beta}\,\dot{\boldsymbol{\theta}}, \tag{6.16}$$

where $\mathbf{b}$ is the square matrix of unknown dissipative coefficients.

On the other hand

$$\mathbf{R}^* = \boldsymbol{\beta}^{\mathbf{T}} \mathbf{R} = -\mathbf{b}^* \dot{\boldsymbol{\theta}}, \tag{6.17}$$

where $\mathbf{R}^*$ is the vector-matrix of the dissipative forces, after the transition to the normal coordinates; $\boldsymbol{\beta}^{\mathbf{T}}$ is the transposed matrix of the mode coefficients $\mathbf{b}^* = \mathrm{diag}[b_1^*, \ldots, b_H^*]$.

With (6.16) and (6.17) we get

$$\mathbf{b} = (\boldsymbol{\beta}^{\mathbf{T}})^{-1} \mathbf{b}^* (\boldsymbol{\beta})^{-1}. \tag{6.18}$$

The square matrix $\mathbf{b}$, in the general case, is not diagonal. So, when using (6.18), the original differential Eq. (6.8), after selecting the dissipative components from the non-conservative generalized forces, takes the form

$$\mathbf{a}\,\ddot{\mathbf{q}} + \mathbf{b}\,\dot{\mathbf{q}} + \mathbf{c}\mathbf{q} = \mathbf{F}(t). \tag{6.19}$$

The procedure of determination of matrix $\mathbf{b}$ is greatly simplified if, in addition to the accepted assumptions, we suppose that only one mode of oscillations is in the regime of mono-harmonic oscillations. This situation, in particular, occurs when

excited resonance mode dominates over others. One can show that in this case $b_{jj} \approx \psi_j c_j/(2\pi k_j)$; $b_{jv} = 0$; $(j \neq v)$. This result is almost identical to the result obtained on the basis of conditions of balance of energy.

6.2 Reduced Characteristics of Elasto-Dissipative Elements of Machine Drives

While conducting engineering calculations, we often come across specific issues related to the correct use of the limited information about the dissipative forces and the rational use of this information, in order to reduce machine's vibration activity. As it was shown in Sect. 2.6.3 for parallel and serial connections of the elasto-dissipative elements, the reduced values of the dissipation coefficient ψ_* on the basis of the condition of balance of energy, can be written as follows:

$$\left.\begin{array}{l} \psi_* = \sum_{i=1}^{n} c_i \psi_i / \sum_{i=1}^{n} c_i \quad (parallel\, connection), \\[3mm] \psi_* = \sum_{i=1}^{n} \overset{\circ}{a}_i \psi_i / \sum_{i=1}^{n} e_i \quad (series\, connection), \end{array}\right\} \tag{6.20}$$

where c_i is the stiffness coefficient; e_i is the compliance coefficient; n is the number of the elastodissipative elements.

Equation (6.20) show that the role of one or the other elastodissipative element, in the formation of dissipative properties of the system, depends not only on the dissipation coefficient ψ_i, but also on the energy intensity of the given element.

Therefore, sometimes we discover opposite tendencies of influence, when the activation of the elastodissipative element is accompanied by decrease in the reduced stiffness. In particular, such effect, in case of use of damping coatings, is observed in the damping of the tightened tapered and threaded connections [88]. Thus, the task of reducing the vibration activity of the system and optimization of its parameters requires an integrated approach to the problem.

It should be emphasized that there exists a substantial difference between the serial and parallel connection of the elastodissipative elements. This difference is shown in the fact that in the latter case, strictly speaking, the order of the system of differential equations, with each element, increments by one. It is often treated as an additional 1/2 degree of freedom of the oscillatory system. In case of engineering calculations of the machines' vibrations, such situation generally occurs, when the point of application of the dominant generalized dissipative forces does not coincide with the location of the concentrated mass and moments of inertia [24, 43, 88].

In Fig. 6.1 we can see the model of a two-stage connection of the elastodissipative elements, commonly used in engineering applications. From a rheological point of view, this model displays a serial connection of two elements of the

Fig. 6.1 Model of a two-stage connection
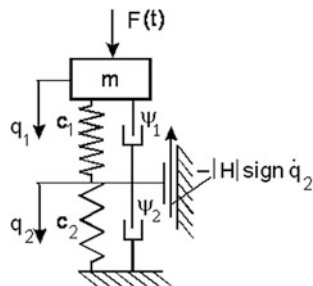
Kelvin-Voigt, separated by the Saint-Venant element, and is described by the following system of differential equations:

$$\left. \begin{array}{l} m\ddot{q}_1 + b_1\dot{q}_1 - b_1\dot{q}_2 + c_1 q_1 - c_1 q_2 = Q(t), \\ - b_1\dot{q}_1 + (b_2 + b_1)\dot{q}_2 - c_1 q_1 + (c_1 + c_2)q_2 = -|H|\mathrm{sign}\dot{q}_2. \end{array} \right\} \tag{6.21}$$

Here, in addition to the previously introduced notations, the following is accepted: m is the mass; q_1, q_2 are the generalized coordinates; Q is the generalized force; $H = |H|\mathrm{sign}\dot{q}_2$ is the force of Coulomb friction; b_i is the coefficient of equivalent force of linear resistance.

Let us consider some of the features of this model, in the absence of Coulomb friction ($H = 0$). In this case, the problem is usually reduced to the analysis of the system with one degree of freedom with natural frequency

$$p = k_1\sqrt{\zeta(1 - \delta_*^2)/(1 + \zeta)} = k_2\sqrt{(1 - \delta_*^2)/(1 + \zeta)}, \tag{6.22}$$

where $\zeta = c_2/c_1$, $\quad k_1 = \sqrt{c_1/m}$, $\quad k_2 = \sqrt{c_2/m}$, $\quad \delta_* = \psi/(4\pi)$.

Formula (6.22) are valid for the so-called frequency-independent resistance, when $\psi_i = const$, $\quad b_i = \psi_i c_i/(2\pi\omega)$, where ω is the frequency of oscillations. Let us note here that the change of the parameter ζ has a double origin, which is particularly important in the extreme cases. So when $c_1 = const$, we have $p \to 0$ for $\zeta \to 0$ and $p \to k_1\sqrt{1 - \delta_1^2}$ for $\zeta \to \infty$. In case of the fixed value of $c_2 = const$, we have $p = k_2\sqrt{1 - \delta_2^2}$ for $\zeta \to 0$ and $p \to 0$ for $\zeta \to \infty$.

The analysis of (6.22) shows that when $\delta_* < 1$ the non-periodic solution is absent for any ζ. Let us note that we can come to a completely different conclusion if we assume resistance to be purely viscous.

Then

$$p = \sqrt{c_*/m - b_*^2/(2m)^2}, \tag{6.23}$$

where $b_* = (b_1\zeta^2 + b_2)/(1 + \zeta)^2$, $\quad c_* = c_1\zeta/(1 + \zeta)$.

According to (6.23), in this case if we assume a fixed value b_i, by reducing the value of c_*, the regime can turn out to be non-periodic. Thus, for example, when $\zeta \to \infty$ we have $p = \sqrt{c_1/m - b_1^2/(2m)^2}$, consequently when $c_1 \leq 0.25 b_1^2/m$ the oscillatory mode is absent.

The question that arises here is, that how much did the transition from a system with one and half degrees of freedom to the system with one degree of freedom, distort the frequency and dissipation characteristics?

The system (6.21) when $P = 0$, corresponds to the following characteristic equation:

$$m(b_1 + b_2)\lambda^3 + [m(c_1 + c_2) + b_1 b_2]\lambda^2 + (b_1 c_1 + b_2 c_2)\lambda + c_1 c_2 = 0 \qquad (6.24)$$

Two complex-conjugate roots of Eq. (6.24) and one real root $\lambda_{1,2} = -n \pm ip$, $\lambda_3 = -\alpha$. correspond to the oscillatory regime. Then when $Q = 0$

$$q_1 = e^{-nt}(C_1 \cos pt + C_2 \sin pt) + C_3 e^{-\alpha t}, \qquad (6.25)$$

where C_i are the arbitrary constants.

Strictly speaking, the system of Eq. (6.21) when $H = 0$ appears to be linear, only at purely viscous friction, when $b_i = const$. In engineering practice, we often have to deal with cases, where at least one of the dissipative elements corresponds to linearly equivalent resistance with frequency-independent hysteresis resistance. Let us consider two of the most common cases.

Case 1 $\psi_1 = const$, $\psi_2 = const$ (frequency-independent resistance in the both contours). In this case in dimensionless form, Eq. (6.24) takes the following form

$$2\delta_2(1 + \zeta)^{-1}(\zeta + \beta_1)\tilde\lambda_1^3 + (1 + 4\delta_2^2\beta_1)\tilde\lambda_1^2 + 2\delta_2(1 + \beta_1)\tilde\lambda + 1 = 0, \qquad (6.26)$$

where $\bar\lambda = \lambda/k_*$ is the normalized value of the characteristic index, $k_* = \sqrt{c_*/m}$ is the natural frequency. In case of $\beta_1 = \delta_1 + \delta_2 = 1$, the dissipative properties of the system, according to (6.26) are independent of ζ. Similar conclusion can be drawn on the basis of the analysis of reduced value of $\delta_* = \delta_2(\zeta + \beta_1)/(\zeta + 1)$.

As could be expected, when $\delta_1 = \delta_2 = 0$, we have $\tilde\lambda_1 = \pm i$ therefore $p = k_*$, and when

$$\zeta \to 0(c_1 \to \infty) \quad \tilde\lambda = -\delta_2 + i\sqrt{1 - \delta_2^2} \text{ so } p = k_*\sqrt{1 - \delta_2^2}, \quad n = \delta_2 k_*.$$

A correlation of the numerical results, obtained using the above mentioned methods, shows that the difference makes up a fraction of one percent. At the same time, we should note that in this case, the roots of the Eq. (6.26), even from the principal point of view, should not be seen as a refinement, because the original model is not linear, and the system of Eq. (6.21) implements an attempt to represent

nonlinear forces of resistance using equivalent linearization. At first glance the principal adjustments are related only to the last term of formula (6.25) and the additional condition $q_2(0)$. However, the analysis shows that the real root of the Eq. (6.26) has the order δ_*^{-1}, which for small values of δ_1 and δ_2 leads to rapid decrease in $\exp(-\alpha t)$.

So, for case 1, the engineering calculations can be performed using (6.20), (6.22), i.e. on the basis of the reduced values of the model with one degree of freedom.

In this case, the possibility of selecting optimum parameters, which correspond to the minimum value of resonant amplitude, is of special interest. Thus for the fixed values of c_1 and ψ_2, corresponding to the minimum of resonant amplitude, is condition $\zeta = (1 - 2\delta_1)^{-1}$, which can be realized when $\beta_1 < 0.5$.

Case 2 $\psi = \text{const}$, $b_2 = \text{const}$. In this case, a frequency-independent resistance is there in the first contour and viscous resistance is in the second one. Such a situation, may particularly, occur, when analyzing the machine taking into account the dynamic characteristics of the motor (see Sect. 5.7.4), as well as in some systems of vibration-insulation with quasi-zero stiffness [27]. As the analysis showed, in the particular case with $\psi_1 = 0$ and in case of low values of $\zeta = c_2/c_1$, there is a significant influence of the additional degree of freedom on change in parameters of frequency and dissipation. In order to avoid uncertainty in case of $c_2 \to 0$, we take c_1 as a fixed parameter, and the transition to the dimensionless form of the characteristic index will be defined as $\lambda = \bar{\lambda}_1 k_1$ (Let us recall that for case 1 we accepted $\lambda = \bar{\lambda}_1 k_*$, then when $\zeta \to 0$ we have $k_* \to \infty$).

The characteristic Eq. (6.24) has the following dimensionless form

$$(\xi_1 + \xi_2)\bar{\lambda}_2^3 + (1 + \zeta\xi_1\xi_2)\bar{\lambda}_2^2 + (\xi_1\zeta + \xi_2)\bar{\lambda}_2 + \zeta = 0, \qquad (6.27)$$

where $\xi_1 = 2\delta_1 k_1/\omega$, $\quad \xi_2 = b_2/\sqrt{c/m}$.

During the analysis of the free oscillations, to determine ξ_1, we should accept $\omega = p$, however, since the natural frequency P is not yet known to us, we can use the method of sequential approximations. Significant difference between p and k_* occurs only for large values of viscous resistance. Usually $\xi_2 \gg \xi_1$, therefore the characteristic features of the system should be studied first when $\xi_1 = 0$.

As will be shown hereunder, the traditional approach to the problems of accounting of dissipative characteristics, based on the dependencies (6.20), for small values of ζ and relatively large viscous resistance, in the second contour, can lead to not only quantitative but qualitative mistakes.

If the decrease in ζ is due to the condition $c_1 \to \infty$, then the accepted model degenerates into a rheological model of Kelvin-Voigt, for which the formulae, for the single degree of freedom systems, are valid. However, when $\zeta \to 0$ due to $c_2 \to 0$, the system corresponds to the Maxwell model, which comprises of a serial connection of Hooke and Newton models [44]. For the latter case, when $\zeta = 0\xi_1 = 0$, $\xi_2 > 0.5$,

according to the Eq. (6.27), we have, in addition to a zero root $\bar{\lambda}_2 = 0$, two mutually conjugate complex roots, which corresponds to the natural frequency

$$p_0 = k_1 \sqrt{1 - 0.25\xi_2^{-2}}. \tag{6.28}$$

Contrary to traditional concepts, the increase in dissipation, in the second contour, according to (6.28), increases the natural frequency. This is due to the fact that for large values of ξ_2 the dissipative element prevents oscillations, described with coordinate q_2, and in the limit when $\xi_2 \to \infty$, we have $p_0 \to k_1$.

The dimensionless damping coefficient $n/k_1 = 0.5\xi_2^{-1}$ decreases with increase in the viscous resistance in the second contour. To linearize the dynamic characteristics of the induction electric motor and the DC motor, we should adopt $c_1 = \left(v_m\omega_m^0 T_m\right)^{-1}$, $b_2 = \left(v_m\omega_m^0\right)^{-1}$ where ω_m^0 is the angular velocity of the ideal idle pass, v_m is the slope coefficient of the static characteristic, T_m is the electromagnetic time constant. In this case, after substitution into (6.28) we obtain

$$p_0 = \sqrt{\left(v_m\omega_m^0 T_m J\right)^{-1} - 0.25 T_m^{-2}}, \tag{6.29}$$

where J is the reduced inertial moment of the machine.

In case of $T \leq T_* = 0.25 v\omega_* J$, the solution turns-out to be aperiodic. By increasing T to the value of $T_{**} = 0.5 v\omega_* J$, the natural frequency increases to its maximum value $p_{0\,\text{max}} = (v\omega_* J)^{-1}$, and in case of $T > T_{**}$, it accordingly decreases. Such influence of electromagnetic time constant is due to its dual role as inertial, as well as dissipative, coefficient.

As the analysis showed, the influence of the dissipative properties of the first contour ($\delta_1 \neq 0$) on the natural frequency is negligible, however, for larger values, it can cause significant adjustments to the parameter $\bar{n} = n/k_1$.

In case of $\psi = 0$ and inertial perturbations, the amplitude of the forced oscillations is proportional to the square of the frequency. In this case the choice of the optimum value, minimizing the amplitude of resonance, is possible in principle; however, these values are usually so large that their practical implementation turns out to be problematic.

In the presence of Coulomb friction, the system shown in Fig. 6.1, appears to be significantly nonlinear. Such models are used in particular in positioning systems, including a device for adjustment of clearances, in systems with dry friction dampers, in rope systems for cargo movements, in spring pivot suspension arms and in other devices [5, 8, 9, 27, 43, 57, 83, 89]. This problem will be discussed in detail in Sect. 6.5. Here we will focus only on the selection of optimum parameters of the model, which enable us to minimize the amplitude of resonance, when harmonic driving force $F = F_0 \sin \omega t$. The condition of equilibrium between the input and withdrawn energies, for one period of oscillations, can be reduced to the form

$$U = h^2 - h\kappa(1 + 0.125\psi) + 0.25\kappa[\pi(1 + \zeta) - 0.5\kappa\psi\zeta] = 0, \qquad (6.30)$$

where $h = |H|/F_0$, $\kappa = Ac_1/F_0$ is the coefficient of dynamicity in case of resonance; ψ is the reduced dissipation coefficient (see below).

When composing the Eq. (6.30) we used the approximating dependencies of the harmonic linearization factors, given in [27]. According to (6.30), when $\psi = 0$, the condition $h > 0.25\pi(1 + \zeta)$, corresponds to the restricted amplitude of resonance. Let us find the value of κ_{min} from the condition

$$d\kappa/dh = -(\partial U/\partial h)/(\partial U/\partial \kappa) = 0 \qquad (6.31)$$

With (6.11), (6.12) we get

$$h = h_* = \frac{0.5\pi(1 + \zeta)}{1 + 0.5\psi(\zeta + 0.25)}; \quad \kappa_{min} = \frac{\pi(1 + \zeta)}{1 + 0.5\psi(\zeta + 0.25)}. \qquad (6.32)$$

Included in (6.30) and (6.32), reduced dissipation coefficient was earlier determined with the help of formula (6.20), when concluding which, we did not take into account the stages of dwells of the intermediate link; therefore in the given case $\psi \neq \psi_*$. If during deduction we use the coefficients of harmonic linearization, then according to (6.32), we obtain $\psi \approx (\zeta + 0.5)(\psi_1 + \psi_2\zeta^{-1})/(1 + \zeta)$.

The conducted analysis showed that in case of the combined nature of the two-stage elastodissipative elements it is possible to realize relatively small resonance amplitudes at acceptable values of the parameters of the system.

6.3 Accounting of Nonlinear Dissipative Forces in Case of Multi-frequency Oscillations

6.3.1 Preliminary Remarks

In the course of dynamic calculations of mechanisms and machines we often come across vibrations of distinct multi-frequency nature. In particular, such a situation is observed in the cyclic mechanisms with forced oscillations and simultaneous excitation of intense free accompanying vibrations; in case of resonance at a certain harmonic of the driving force and sufficiently intensive excitation of vibrations of other frequencies, in case of joint parametric and forced excitation, etc.

In such cases, the role of dissipative forces is seen only, when the frequency of the tested mode is close to the frequency of free oscillations, while the level of vibrations on the "alien" frequencies practically does not depend on dissipation. In Sect. 6.1, in case of equivalent linearization of dissipative forces, we used the assumption of single-frequency (monoharmonic) character of the oscillatory mode.

Previously, it did not lead to contradictions, because it was this mode, in which the experimental values of the coefficient of dissipation ψ or the logarithmic decrement ϑ, were obtained. Naturally, this correspondence, in case of oscillations with several frequencies, is violated, and under certain conditions, this occurs significantly. It follows that the initial information about the dissipative properties of the system, requires corrections.

As per the character of the influence of the dissipative forces, the vibration modes can be divided into two groups. The first group includes the modes, the level of amplitude of which depends on the level of dissipation, such as free oscillations and forced resonance oscillations. The second group comprises of modes, the existence of which is possible only after overcoming some energy barrier, determined by dissipation, such as parametric and sub-harmonic resonances, as well as self-oscillations.

The analytical study of the problem of accounting of nonlinear dissipative forces, in case of multi-harmonic perturbation, is based on the idea of separation of motions [9]. Thus, there are several possible approaches. In one approach, the system's movement is considered as a combination of two movements, namely, substantially dependent on dissipation (e.g., resonant) and substantially independent of dissipation (e.g., non-resonant). This approach, which is based on the methods of harmonic and statistical linearization, was used in study [26], applicable to the dry friction systems and in [43, 60, 64, 72, 74, 80] for positional hysteresis resistance forces. In case of applying the other approach, developed by Blehman, determined are the so-called vibration forces, reflecting the impact of high-frequency components of excitation on slow motion [9]. This paper focuses on some specific effects, related to the issue under consideration, and on the development of computer simulation methods, applicable to the problems of dynamics of machines. At the same time the "alien" oscillations can be both of high-frequency, as well as of low-frequency.

6.3.2 Free Vibrations

Let us consider a simple model, consisting of an elastic element with stiffness coefficient c and s slider of mass m. The slider moves along the guide at the absolute speed $v(t) = \dot{x}_0(t) + \dot{q}(t)$, where $\dot{x}_0(t), \dot{q}(t)$ are the speed of the translational motion and relative velocity that occurs in case of free vibrations. Under the effect of the force of Coulomb friction $R = H = -|H|\mathrm{sign}(\dot{x}_0 + \dot{q})$, the differential equation of motion is

$$m\,\ddot{q} + cq = -|H|\mathrm{sign}(\dot{x}_0 + \dot{q}) - m\,\ddot{x}_0. \tag{6.33}$$

When $\dot{x}_0 = v_0 = \text{const}$, the oscillations in general can be described as $q = A_0 + A(t)\sin(kt + \alpha)$, where $A(t)$ is the slowly changing amplitude, $k = \sqrt{c/m}$ is the natural frequency, α is the initial phase.

The withdrawn energy ΔE_- in the period $T = 2\pi/k$ is equal to

$$\Delta E_- = \oint |R|\text{sign}(\dot{x}_0 + \dot{q})dq = |R| \int\limits_0^T \dot{q}\,\text{sign}(\dot{x}_0 + \dot{q})dt. \qquad (6.34)$$

When $v_0 = 0$, we have $\Delta E_- = 4|R|A$. At the same time, the amplitude of the excited under initial conditions free oscillations, decreases linearly, the equivalent force of linear resistance is equal to $R = -b\dot{q}$, where $b = 4|R|/(\pi Ak)$, and the dissipation coefficient is equal to $\psi = 8|R|/(cA)$. We can see in Fig. 6.2a, the graphs $q(t)$, produced using computer simulation when $v_0 = 0$ (curve 1). This result is rather often extended by mistake for case $v_0 \neq 0$ (curve 2). Let, for example $v_0 > 0$, at that $v_0 = \text{const}$. Then in accordance with (6.21), in the time segment, where $\dot{q} < v_0$, the work spent to overcome the force of friction is equal to zero. The inner region of the phase portrait, unfilled with phase trajectories (Fig. 6.2b) corresponds to this effect. So, beginning at some certain moment in time, attenuation of the oscillations is stopped. Therefore if we exclude the effect of dissipation of a different nature, the system has damping properties, only when $\dot{q} > v_0$.

Let us see another illustrative example, explaining the role of Coulomb friction, as a damping factor, in the oscillations of the cyclic mechanisms' executive links. Let $x_0(t) = \Pi(\omega t)$, where $\Pi(\omega t) = 1 - \cos\omega t$ is the position function of the output link, ω is the angular velocity of the input link. With the selected harmonic acceleration law (without dwells) the source of excitation of the free accompanying oscillations, in the given example, are the jumps of the force of friction, at the time of change of sign of absolute velocity of the output link. If taking into account the dissipations, we neglect the translational movement, then the velocity v and acceleration w of the output link have the form of the curves, shown in Fig. 6.3a. Similar curves, obtained while determining the loss of energy taking into account the translational motion on the basis of (6.34), are displayed in Fig. 6.3b.

Thus, there is a significant reduction in dissipation in case of additional movement of the system, as compared to mono-harmonic. The accounting of this effect,

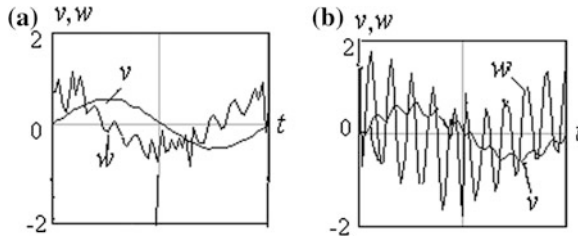**Fig. 6.2** Free oscillations in case of Coulomb friction
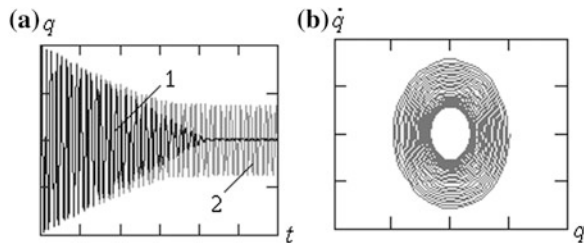
Fig. 6.3 The influence of translational motion on the excitation of accompanying oscillations

in engineering calculations, is also very important while studying the vibro-impact regimes, arising from the change of surface contact in the clearances.

6.3.3 Analytical Description of Coefficients of Dissipation in Case of Multi-frequency Regimes

The resonant oscillations of a system with one degree of freedom and nonlinear position dissipative force under biharmonic excitation with the frequencies ω_1 and ω_2 (see below) have been investigated in [60]. Let us suppose that there is resonance at frequency $\omega_1 = k$. In this case the specific unilateral correlation occurs, when the process with frequency ω_2, changing the equivalent dissipative force, may have a significant influence on resonant amplitude A_1, while the effect on the amplitude of forced vibrations A_2 with frequency ω_2 is negligible. At the same time the updated value of the dissipation coefficient ψ and the logarithmic decrement ϑ is determined as

$$\psi = \psi_0 \Phi_s, \quad \vartheta = \vartheta_0 \Phi_s. \tag{6.35}$$

Here ψ_0, ϑ_0 are dissipation parameters, determined at mono-harmonic oscillations; $\Phi_s = \Phi_s(z)$ is the coefficient, depending on the ratio of vibration velocities $z = A_1\omega_1/(A_2\omega_2)$ and the form of the hysteresis loop.

It can be shown that [43, 60]

$$\Phi_s = \frac{\int_0^{2\pi} \lambda_s(A_1 \sin \varphi) \cos \varphi \, sign(\dot{q}_2 + A_1 k \cos\varphi) d\varphi}{\int_0^{2\pi} \lambda_s(A_1 \sin \varphi)|\cos \varphi| d\varphi} \quad (\omega_2 \ll k),$$

$$\Phi_s = \frac{\int_o^{2\pi} \lambda_s \xi \cos\varphi d\varphi}{\int_0^{2\pi} \lambda |\cos \varphi| d\varphi} \quad (\omega_2 \gg k), \tag{6.36}$$

where

$$\xi(\varphi, z) = \begin{cases} 2\pi^{-1}\arcsin(z\cos\varphi) & (|\cos\varphi| \leq z^{-1}), \\ \mathrm{sign}(\cos\varphi) & (|\cos\varphi| \geq z^{-1}). \end{cases}$$

The parameter λ_s for the rectangular hysteresis loop is equal to one, for an elliptical loop it is equal to $|\cos\varphi|$ and for the triangular (spring characteristic) it is $|\sin\varphi|$. The functions Φ_s determined by (6.36), for the above mentioned forms of hysteresis loops, are presented in [43, 58, 60]. Similarly the force of Coulomb friction $H = H_0\Phi_1(z)$, is adjusted, where index 1 corresponds to the rectangular hysteresis loop.

The calculation results show that, just as in case of mono-harmonic oscillations, the damping properties of the system are weakly dependent on the shape of the contour of the hysteresis loop, but are, basically, determined by the area of the loop, proportional to the dissipation coefficient ψ_0. Based on the analysis of (6.36) the theoretical dependencies, approximating average characteristic, with some allowance, for typical loop is obtained

$$\Phi = z(0.4 + 0.5z)/(1 + 0.5z^2). \tag{6.37}$$

Function Φ varies from zero to one (Fig. 6.4). For small values of z ($z < 0.4$), function $\Phi(z)$ according to (6.37) is close to linear, i.e. proportional to amplitude A_1. Then if in case of mono-harmonic mode, the dissipation coefficient ψ_0 is inversely proportional to the amplitude, then $\psi = \psi_0\Phi = $ const. This situation in particular, takes place in case of Coulomb friction, when, according to (6.37), we have $\psi_0 \approx 2|H|k/(cA_1\Omega)$, $b_0 \approx |H|/(\pi A_1\Omega)$. Since $\psi = $ const corresponds to the linear force of resistance, so in such cases the so-called vibration linearization of Coulomb friction forces takes place, to which specific effects are related, which have many technical applications. Let us also note that this dynamic effect is usually associated only with high-frequency components of excitation, while the ratio of the

Fig. 6.4 Graph $\Phi(z)$
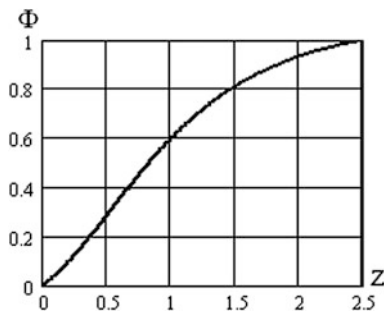
speeds z of the tested and "alien" regimes plays the decisive role, regardless of the frequency structure of the latter. In particular, as indicated above, this effect is observed, even at the constant speed of additional movement (see Fig. 6.2). When $z > 2$, we can accept $\Phi = 1$ as in this range the correction of the dissipative characteristics are not supported by the original reliable information.

If we use the methods of accounting of nonlinear dissipative forces in case of poly-harmonic perturbations, based on the method of linearization as per the distribution function [36, 47], we can apply formula (6.37), with $z = A_j \omega_j / (\sqrt{2} \sigma_v^*)$. Here $\sigma_v^{*2} = \sum_{i=1}^{N}{}' A_i^2 \omega_1^2$ is the dispersion the velocity of the oscillatory process, from which the oscillations with frequency ω_j are excluded (the prime means skipping the summation of the members of the index $i = j$); A_j, A_i are the amplitudes of the oscillations of the corresponding harmonics. Let us note here that the amplitude A_j greatly depends on the level of dissipation, while the amplitudes A_i are practically independent.

Physical preconditions of the analyzed dynamic effect are connected with the arising of the so-called partial hysteresis loops, arranged inside the main loop, corresponding to the oscillations with the main frequency [30, 43]. Provided that these loops are closed, their total area is proportional to the work of the resistance forces, carried out by the "alien" movement. At the same time the effective area of the hysteresis loop, for the tested mode, is reduced, which is manifested in the reduction of the above dissipative characteristics. Let us emphasize that for the emergence of particular local loops and implementation of the tested effect the velocity has to change its sign at intermediate sections of the main loop contour.

The mathematical description of the hysteresis loop, in case of oscillations with several frequencies, is a rather complicated and time-consuming task, even under static formulation of the problem, is poorly adapted for the solution of practical engineering problems of dynamics of machines.

As it was noted above, we are not interested in the contour of the hysteresis loop, but in the equivalent energy, which determines its effective area.

As already mentioned, the source of information about the dissipative properties of the system is usually the logarithmic decrement ϑ_0 or the dissipation coefficient ψ_0, obtained in case of harmonic oscillations. In view of the above, the refined positional dissipative force f, per unit mass, can be expressed as

$$f_1(q, \dot{q}) = -|f_0| u(|\dot{q}| - |v|) \mathrm{sign}\dot{q}, \tag{6.38}$$

where v is the velocity, connected with the additional motion ("alien" harmonics, translational motion etc.); u is the unit function ($u = 1$ at $|\dot{q}| > |v|$ and $u = 0$ when $|\dot{q}| < |v|$), $f_0 = R(q)/m$.

To solve the problem analytically the function $u(|\dot{q}| - |v|)$ is averaged and is transformed into the function $\Phi(z)$ (see above). Thus, both of the approaches are substantially identical and differ only in the averaging procedure. If the initial

Fig. 6.5 Typical hysteretic loops
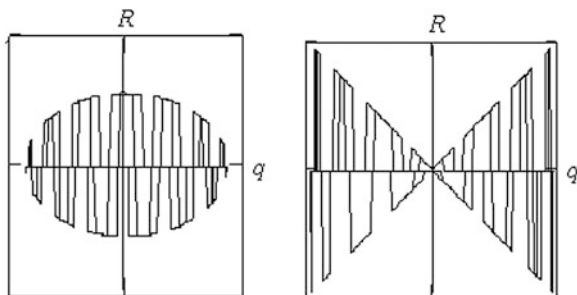
Fig. 6.6 Free oscillations in case of additional excitations
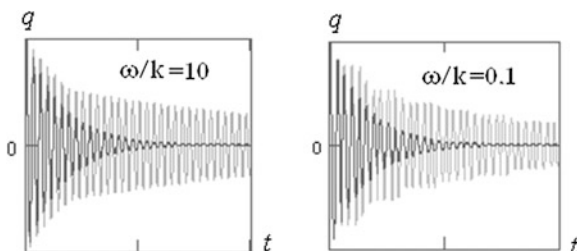
information, about the dissipative forces, is given by the logarithmic decrement in case of single-frequency oscillations λ_0, then

$$f_1(q, \dot{q}) = -\vartheta_0 \pi^{-1} k \dot{q} u(|\dot{q}| - |v|). \qquad (6.39)$$

We can see in Fig. 6.5, the hysteresis loops, corrected as per (6.39), for the cases of the original elliptical loop and of spring characteristics, when the module of the force of resistance is proportional to q. The reduction of the original areas of both the loops is clearly visible in the diagram.

Figure 6.6 shows the attenuated oscillations in case of the elliptical hysteresis loop and $v = v_* \sin \omega t$, obtained by computer simulation taking into account (6.39), whereas in the first case $\omega/k = 10$ and in the second case $\omega/k = 0.1$. Here, as above, the darker shade of the curves corresponds to the absence of additional oscillations ($v \equiv 0$).

As it follows from the graphs, the effect of the reduction in dissipation is observed both in case of high, as well as low-frequency additional excitation. Thus, there is an influence not only of the fast movements on the slow ones, but also of the slow movements on the fast ones [79].

6.3.4 Resonant Oscillations

Let us look into the forced oscillations, in a system with one degree of freedom, described by the following differential equation

$$m\ddot{q} + cq = -|R(q)|\,\mathrm{sign}\dot{q} + F_1 \sin \omega_1 t + F_2 \sin \omega_2 t. \tag{6.40}$$

Let frequency ω_1 be equal to the natural frequency $k = \sqrt{c/m}$, whereas frequency ω_2 is significantly different from it. Hereafter, frequency ω_1 and forced oscillations with this frequency $q_1 = A_1 \sin(\omega_1 t - \gamma_1)$ will be called the basic, and $q_2 = A_2 \sin(\omega_2 t - \gamma_2)$ as optional. If the dissipative force would had been linear, as, for example, it happens in case of viscous friction, the problem would had been solved very simply using the principle of superposition. However, in this case because of the nonlinear nature of the dissipative forces, this principle cannot be used.

After separation of the motion into main and additional, we obtain the following two modified differential equations:

$$\left.\begin{aligned}
\ddot{q}_1 + f(q_1, \dot{q}_1) + k^2 q_1 &= w_1 \sin \omega_1 t; \\
\ddot{q}_2 + k^2 q_2 &= -\omega_2^2 a_0 \sin \omega_2 t,
\end{aligned}\right\} \tag{6.41}$$

where $w_1 = F_1/m, f = -f_1$ [see (6.39)], a_0 is the amplitude of kinematic excitation.

Since the frequency ω_2 significantly differs from the resonant, the amplitude of forced oscillations A_2, at this frequency, is practically independent of dissipation. Thus, $A_2 \approx \omega_2^2 a_0 / |k^2 - \omega_2^2|$, and the resonant amplitude A_1, found using analytical method, is determined as

$$A_1 = \pi A_* / (\vartheta_0 \Phi(z)), \tag{6.42}$$

where $A_* = F_1/c$, $z = A_1 \omega_1 / (A_2 \omega_2)$.

As the right-hand side of this expression also depends on the unknown value of A_1, the expression (6.42) is the equation, which can be reduced to the following form:

$$\chi = \Phi^{-1}(\chi z_0). \tag{6.43}$$

Here $\chi = A_1/A_{10}$ is the rate of increase in amplitude of resonance $z_0 = z(A_{10})$, where $A_{10} = \pi A_*/\lambda_0$ is the known value of the amplitude of resonance without taking into account the correcting effect of the additional "alien" oscillations.

The graph of the function $\chi(z_0)$, calculated with the help of the approximate expression (6.37), is represented in the Fig. 6.7.

Fig. 6.7 Graph $\chi(z_0)$
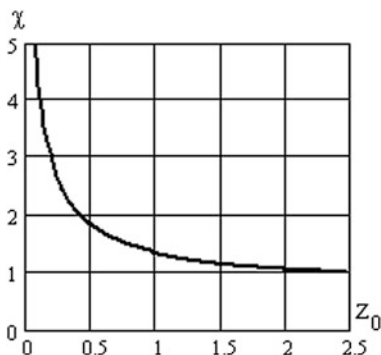
Without restricting the scope of generality of the problem, we will consider the following reference example. Let $m = 1$ kg, $c = 1$ N/m, $\omega_1 = 1\,\text{s}^{-1}$, $\omega_2 = 5.3\,\text{s}^{-1}$, $F_1 = 1$ N, $F_2 = -m\omega_2^2 a_0$, $\vartheta_0 = 0.5$, $|f| = \zeta|q|$ when $\zeta = 0.15$ (spring characteristic). We can see in Fig. 6.8, the curves obtained by computer simulation. Here $q(t)$ corresponds to the original differential Eq. (6.40), (Fig. 6.8a; curve 1), and $q_1(t)$ to the modified Eq. (6.41) (Fig. 6.8b; curve 2). Apart from that, both diagrams have curves 3, showing the forced oscillations with resonant frequency in case of the formal use of the principle of superposition. In this case as before, the dark curves in the diagrams correspond to the given event.

The analysis of the above graphs shows that, first of all, the ignorance of the nonlinear nature of the dissipative forces can lead to the substantial error in estimating the amplitude of resonance. Thus, in this example, $A_1^0 = \left|q_1^0\right|_{\max} = 6.21$, while $|q|_{\max} \approx 14.3$. Secondly, we have the satisfactory match of the most recent result with the solution of the modified differential equation $A_1 = |q_1|_{\max} = 13.9$. Some discrepancies in results are mainly related to the fact that the function $q(t)$ reflects the bi-harmonic nature of excitations and in the function $q_1(t)$ we only have oscillations with resonant frequency.

The good agreement of these results, which are tested by varying parameters in a wide range both in $\omega_2 > \omega_1$, and $\omega_2 < \omega_1$, is also supported by the results of the analytical solution based on Eq. (6.40), whereas the difference is usually no more than (10–15 %).
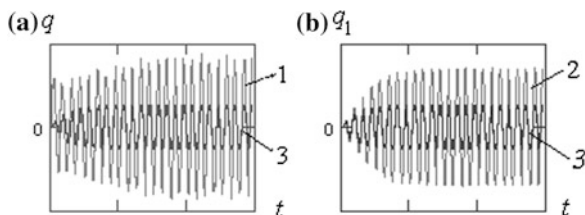
Fig. 6.8 Forced oscillations in case of additional excitation

6.3.5 Refined Conditions of Dynamic Stability in Case of the Main Parametric Resonance

Let the original differential equation, describing the oscillations in case of the simultaneous action of the parametric and forced excitations, has the form

$$\ddot{q} + k^2 q = -[|f(q)|\text{sign}\dot{q} - \varepsilon k^2 q \sin\Omega t] + w\sin\omega t, \qquad (6.44)$$

where ε, Ω are the depth of pulsation and the frequency of parametric excitation.

Let us assume that $\omega \gg k$, $\Omega = 2k$; the last condition corresponds to the zone of the main parametric resonance. Using the method outlined above, we represent the corresponding modified differential equation, in the form

$$\ddot{q}_1 + f(q_1, \dot{q}_1, v) + k^2(1 - \varepsilon\sin\Omega t)q_1 = 0. \qquad (6.45)$$

Thus, in this equation, the member corresponding to the driving force, with relevant correction of the dissipative component, is omitted. Let us recall that in case of analytical solution of the problem $f = \pi^{-1}k\vartheta_0(A)\Phi(z)$. In this case $z = Ak/(A_1\omega)$, where A, A_1, are the amplitudes of the oscillations with frequencies k (parametric resonance) and ω (forced oscillations).

The terms of dynamic stability in the zone of the main parametric resonance, are reduced to the form:

$$\sigma_0 > \sigma_* = \Phi^{-1}(z), \qquad (6.46)$$

where $\sigma_0 = 2\vartheta_0/(\pi\varepsilon)$.

Let us look into two cases.

Case 1 ($w = 0$): In this case the forced oscillations are absent, therefore $z \to \infty$ and $\Phi \to 1$, consequently, the dynamic stability condition has the form $\sigma_0 > 1$.

Case 2 ($w \neq 0$): Since $\Phi(z) < 1$ the area of dynamic instability is expanding. Therefore, the conditions that ensure dynamic stability, in the absence of high-frequency excitation, can now turn out to be violated. To a better illustration of the behavior of the system, under the combined forced and parametric excitations, we will use the plane of the parameters $z - \sigma_0$ or $A - \sigma_0$ (Fig. 6.9).

In the area 1 ($\sigma_0 < 1$), the system is always dynamically unstable, irrespective of the effect of additional excitation, which in this case is seen only due to the increase in the intensity of the growth in amplitude. This is clearly seen in the superimposed graph $q_1(t)$ and $q_1^0(t)$ (superscript 0 corresponds to case 1, which is represented by the darker curve in the diagram). In the area 2 the system is stable in case of $w = 0$ and $\sigma_0 > 1$ (case 1) and unstable when $w \neq 0$ and $\sigma_0 < \sigma_*$. Finally, in the area 3 ($\sigma_0 > \sigma_*$), the terms of dynamic stability are satisfied irrespective of the additional excitation.
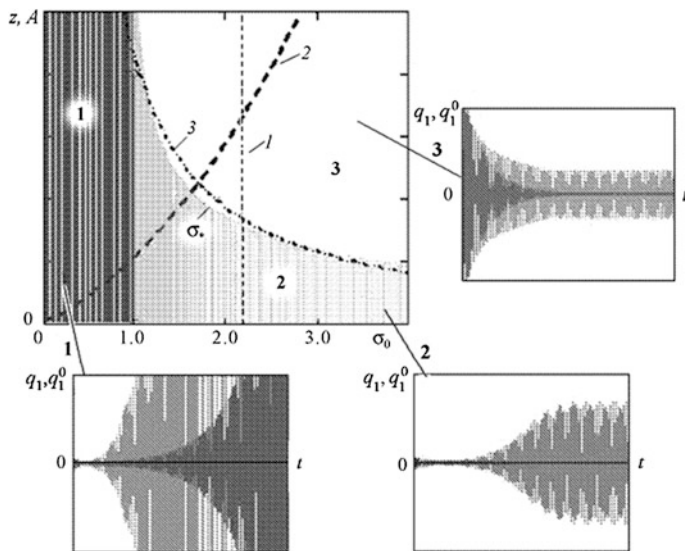
Fig. 6.9 Influence of the additional excitation on the parametric oscillations

Three typical cases of change in the logarithmic decrement, depending on the amplitude, are shown in the plane of the parameters with hatching lines. If $\vartheta_0 =$ const (straight line 1), then the amplitude increases in area 2, and decreases in area 3. Consequently, the amplitude of the steady state corresponds to the boundary of the asymptotic stability σ_*. The graphs $q_1(t)$ and $q_1^0(t)$—it is visible that when $w \neq 0$ the oscillations reach the steady state, and when $w = 0$ the oscillations rapidly attenuate. Similar nature of the behavior of the system occurs in case of increase in function $\vartheta_0(A)$ (curve 2).

In case of descending nature of the change in $\vartheta_0(A)$, two cases are possible. If curve 3 intersects the curve σ_* twice, then the upper point of intersection corresponds to the unstable mode, and the bottom one corresponds to the stable mode. In the absence of the lower points of intersection, as, for example, it occurs in case of Coulomb friction, the oscillations when $\sigma_0 > \sigma_*$ completely attenuate $(A \to 0)$.

6.3.6 The Influence of the High-Frequency Impacts on the Resonant Vibrations, in Case of Joint Action of Force and Parametric Excitations

As shown in Sect. 5.4.3, when $\omega = k_0$ (resonance) and parametric perturbation at a frequency $2k_0$ (the main parametric resonance), the amplitude of the forced

oscillations A, among other factors, depends on the phase shift between the driving force and the harmonic pulsation of the parameter. Thus,

$$2\pi A_* / (\psi_0 + \pi\varepsilon) \leq A \leq 2\pi A_* / (\psi_0 - \pi\varepsilon), \tag{6.47}$$

where A_* is the static amplitude.

According to (6.47), the amplitudes A can be both below and above the value determined in the absence of the parametric perturbations, i.e. when $\varepsilon = 0$. Thus, in case of the most unfavorable phase ratio, the maximum resonant amplitude, corresponds, in the first approximation, to some arbitrary system, without parametric excitation, but with reduced dissipation, corresponding to $\psi_0 - \pi\varepsilon$.

When taking into account the high-frequency impact according to (6.35), the effective dissipation coefficient decreases. Herewith, the maximum values of the coefficient of increase in resonant amplitude χ (see above), is determined with the following equation:

$$\chi_{\max} = \psi_0 / [\psi_0 \Phi(z) - \pi\varepsilon]. \tag{6.48}$$

In the left-hand side of the Eq. (6.48) $\chi_{\max}$, is also included in hidden form, because the ratio of vibration velocities z depends on the sought after resonant amplitude. The solution of this equation is reduced to

$$\chi_{\max} = 0.5 \left[1 + fL + \sqrt{(1 + fL)^2 + 4f(1 - L)} \right] / (1 - L), \tag{6.49}$$

where $L = \pi\varepsilon / \psi_o$, $f = \Phi^{-1}(z_0) - 1$.

In this case, parameter z_0 is determined in the absence of the parametric and high-frequency excitations, i.e. when $\chi = 1$. At the same time parameter L reflects the influence of the parametric excitation and parameter f reflects high-frequency influence. In case of $L \to 1$ the conditions of dynamic stability are violated, so $\chi_{\max} \to \infty$, regardless of the value of f.

6.3.7 Refined Conditions for the Emergence of the Sub-Harmonic Resonances

Let us consider the differential equation, describing the nonlinear forced oscillations in the system with one degree of freedom, in case of biharmonic excitations and positional friction.

$$\ddot{q} + |R(q)|\mathrm{sign}\dot{q} + P(q) = w_0 + w_1 \sin(\Omega_1 t + \varphi) + a\Omega_2^2 \sin \Omega_2 t. \tag{6.50}$$

It is assumed here that $\Omega_2 > \Omega_1$, at the same time when the component with frequency Ω_2 corresponds to kinematic excitation. (All forces are assigned to the

unit of the mass). To study the subharmonic oscillations, taking into account the additional excitation, not limiting the scope of generality in approach to the problem, we assume $|R(q)| = \zeta|P(q)|$, that corresponds to the so-called spring characteristics of the forces of resistance, encountered in many engineering applications. Apart from that we will concretize function $P(q)$, which is proportional to the non-linear restoring force $P(q) = k_0^2(1 + \alpha q^2)q$, where k_0 is the natural frequency when $\alpha q^2 \ll 1$. The accepted function $P(q)$ corresponds to Duffing's equation, the analysis of which is discussed in a broad range of literature [6, 36]. The adopted elastic characteristics play the role of the mathematical model, illustrating the opportunities of this approach towards solving the given problem.

After the transition to the dimensionless time $\tau = k_0 t$, we represent the Eq. (6.50) in the form

$$q'' + \zeta(1 + \alpha q^2)|q|\mathrm{sign}q' + (1 + \alpha q^2)q = f_0 + f_1 \sin(\omega_1 \tau + \varphi) + a\omega_2^2 \sin \omega_2 \tau, \tag{6.51}$$

where $f_0 = w_0/k_0^2$, $f_1 = w_1/k_1^2$, $\omega_1 = \Omega_1/k_0$, $\omega_2 = \Omega_2/k_0$, $(\cdot)' = d/d\tau$.

On the basis of (6.51), we will investigate the conditions of excitation of subharmonic resonance of the order 1/3. As already mentioned, sub-harmonic oscillations can be represented, with sufficient accuracy, as the free oscillations, without friction. Then, using the energy balance conditions, when $f_0 = 0$, $a = 0$, we get [6, 27]

$$q \approx A\sin\omega_0\tau + A_3 \sin 3\omega_0\tau,$$

where $\omega_0 = 1 + 0.75\alpha A^2$, $\omega_1 = 3\omega_0$, $A_3 = \alpha A^3/(32 + 21\alpha A^2)$.

Thus, in our case, the energy of the unit mass withdrawn for one period $2\pi/\omega_0$, is equal to $\Delta E_- = 2\zeta^0(A^2 + 0.5\alpha A^4)k_0^2$, and the input energy, which is equal to the work of the driving force, is equal to $\Delta E_+ = 3\pi f_1 A^3 \alpha k_0^2 \sin \varphi/(32 + 21A^2)$.

The conditions of existence of sub-harmonic resonance are defined as $\Delta E_- < (\Delta E_+)_{\max}(\varphi = \pi/2)$. Thus,

$$\zeta^0 < \zeta_*^0 = 1.5\pi\alpha f_1 A(1 + 0.5\alpha A^2)^{-1}(32 + 21\alpha A^2)^{-1}. \tag{6.52}$$

To confirm the effectiveness of the approaches used in the analytical solution of the problem, we represent some results of computer simulation for some typical regimes. As it was shown by the numerical experiment, when $f_1 = 5$, $\alpha = 0.5$, $\omega_1 = 6$ and in the absence of the high-frequency excitation ($a = 0$), the sub-harmonic resonance is excited when $\zeta^0 \leq 0.069$ that is slightly lower than the resultant of formula (6.52). This is due to the fact that in the vicinity of ζ_*^0 the excitation of sub-harmonic resonance usually depends a lot on the initial conditions, whereupon the opportunity to enter the tested mode can remain unrealized. The amplitude of the sub-harmonic

resonance corresponds to the point on the skeleton curve $\omega_0^2 = 1 + 0.75\alpha A^2$. When $\omega_0 = 1/3$ and $\alpha = 0.5$, we have $A = 2.82$, which at a high level of accuracy, coincides with the result of the numerical experiment.

It should be emphasized here that in contrast to the resonant modes, whose amplitude is determined by the level of dissipation, in this case the dissipation only sets some energy barrier, in case of overcoming which the sub-harmonic resonance may occur. The dissipation sets similar "barrier" in parametric resonance and "rigid" self-excitation of oscillations.

Proposed in [43, 60] approach to the accounting of dissipation, in case of poly-harmonic excitation, is based on the fact that in the tested mode, the effective force of dissipation is only formed in a closed hysteresis loop. Let us recall that, if due to additional perturbations, in this mode there is no change of the sign of velocity, then their effect on dissipation is absent. On the other hand, as already noted, in case of the change of sign of velocity, within the cycle, the total area, bounded by the closed contours, is less than the original area of the loop, which reduces the effective force of dissipation in the given mode (see Fig. 6.5). Thus, in the time intervals, corresponding to the counter speed as compared to the speed of the main mode, there is practically no dissipation. In accordance with the above mentioned we will shift from Eq. (6.51) to the modified equation, in which there are no additional perturbation of frequency ω_2, but the correction of the dissipative component is introduced

$$q'' + \zeta^0(1 + \alpha q^2)|q|\eta(|q'| - |v\cos\omega_2\tau|) + (1 + \alpha q^2)q = f_0 + f_1\sin(\omega_1\tau + \varphi), \tag{6.53}$$

where v is the amplitude of the dimensionless velocity for harmonics of ω_2 (at a reasonable distance from the resonant zone; the influence of dissipation on v can be neglected); η is the unit function.

We can see, in Fig. 6.10, graphs $q(\tau)$ and $q'(q)$, obtained by the Runge-Kutta method for a number of modes for the given above input parameters. At the same time parameter $\zeta_*^0 = 0.22$, for all of the reduced modes, corresponds to the upper boundary of the existence of sub-harmonic oscillations.

In the first case (Fig. 6.10a) the solution was determined on the basis of (6.51), and in the second on the basis of the modified Eq. (6.53) when $v = 8.75$ (Fig. 6.10b), and in both cases $\omega_2 = 10$. The comparison of the graphs $q(\tau)$ shows that this method practically eliminates the small influence of high-frequency component on the level of amplitude, leaving almost unchanged the condition of the existence of the sub-harmonic oscillations. The phase trajectory in the first case demonstrates the repeated change of the sign of velocity, which leads to the decrease in effective dissipation and increase in ζ_*.

In the second case the phase trajectory is "cleaned" of the high-frequency component at the same amplitude level of oscillations. Graph $q(\tau)$ and the phase trajectory $q'(q)$ were almost completely identical in case of $\zeta_*^0 = 0.069$, in the absence of additional excitation, i.e. $f_2 = 0$ (see above). The third case (Fig. 6.10c) differs in a

Fig. 6.10 Sub-harmonic
resonance
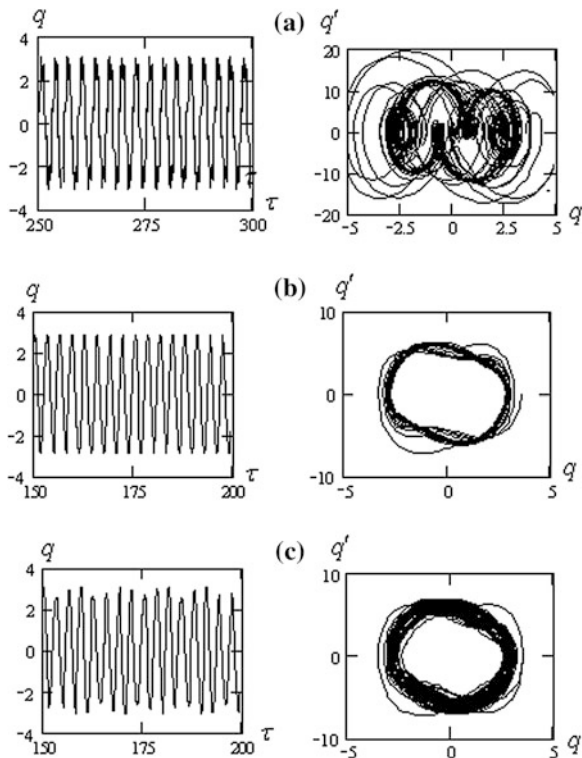
way that the additional perturbations have low frequency ($\omega_2 = 0.3$, $v = 8.75$).
In this case there is a small amplitude modulation, at the same average value of
amplitude $A = 2.82$. This regime is of interest, because it requires only sufficient
distance from the tested resonant mode, and allows to analyze also the cases when
$\Omega_2 < k_0$ ($\omega_2 < 1$); it is not based on the assumption of a high-frequency nature of the
additional effects. On the basis of the modified differential Eq. (6.53), using the
method of harmonic linearization, the work of dissipative forces was determined,
taking into account the additional oscillations. In this case the dependence obtained
is similar to (6.35): $\zeta(z) = \zeta^0\Phi(z)$, where

$$\Phi(z) = \begin{cases} \left[z\sqrt{1-z^2} - (1-2z^2)\arcsin z\right]/(\pi z^2) & (z \le 1); \\ 1 - 1/(2z^2) & (z > 1). \end{cases} \qquad (6.54)$$

When solving the applied problems of the dynamics of machines, along with
harmonic driving forces, there usually is a constant force, which on the right hand
side of the differential Eqs. (6.51) and (6.53) corresponds to the member $f_0 \ne 0$. In
this case, the free oscillations of the considered nonlinear system, without taking
into account the dissipative forces, after harmonic linearization, is described using
the following equation:

$$q'' + \omega_0^2(A, A_0)q = f_0. \tag{6.55}$$

Here the solution of Eq. (6.55) is accepted in the form $q \approx A_0 + A\sin(\omega_0\tau + \gamma)$ when

$$\left.\begin{array}{l} A_0\left[\alpha\left(A_0^2 + 1.5A^2 + 1\right] = f_0; \\ \alpha\left(3A_0^2 + 0.75A^2\right) + 1 = \omega_0^2. \end{array}\right\} \tag{6.56}$$

The analysis of the solution of the system of nonlinear Eq. (6.56) shows that when $f_0 \neq 0$ the skeleton curve, in the vicinity of the relatively small values of A, has the inflection point, which corresponds to the unstable modes boundary. At the same time it appears that in case of excitation of the sub-harmonic resonances, the characteristics of $A(\omega_0)$, weakly depend on the value of f_0. At the same time the existence area boundaries of these modes, depends on f_0 quite significantly. Let us turn our attention on this issue. It can be shown that when $A_0 \neq 0$ the value ΔE_-, proportional to the withdrawn per one cycle energy (see above), is determined as

$$\Delta E_- = \zeta\Psi(A_0, A)\Phi(z), \tag{6.57}$$

where

$$\Psi(A_0, A) = 2\left(A_0^2 + A^2\right) + 0.5\alpha\left[(A_0 - A)^4 + (A_0 + A)^4\right]. \tag{6.58}$$

Further using the condition of the balance of input and withdrawn energies, taking into account (6.54), (6.56)–(6.58), we get

$$\zeta < \zeta_* = \frac{3\pi f_1 \alpha A^3}{(32 + 21\alpha A^2)\Phi(z)\Psi(A, f_0)}. \tag{6.59}$$

It can be shown that in case of increase in the constant component f_0, we can observe the intensive growth of the effective level of dissipation. Often, along with the hysteresis characteristic of the form considered, the force of Coulomb friction $H = -|H|\text{sign}\dot{q}$, influences the system. In this case, formula (6.57) is corrected as follows:

$$\Delta E_- = [\zeta\Psi(A_0, A) + 4hA]\Phi(z), \tag{6.60}$$

where $h = |H|/m, m$ is the reduced mass (or the moment of inertia).

Taking into account (6.60) the condition (6.59) takes the form

$$\zeta < \zeta_* = \left[\frac{3\pi f_1 \alpha A^3}{(32 + 21A^2)\Phi(z)} - 4hA\right]\Psi^{-1}(A, f_0). \tag{6.61}$$

According to (6.61) for the excitation of sub-harmonic resonances, it is necessary (but not sufficient) to have the first term in square brackets, greater than the second one. In the absence of additional perturbations ($\Phi = 1$) this requirement can be expressed as

$$A > \sqrt{128h/(3\pi f_1 \alpha - 84h)}. \tag{6.62}$$

When $\Phi(z) < 1$ in the condition (6.62), h should be replaced by $h\Phi(z)$, which leads to the transcendental equation for A, as Φ is a non-linear function of $z = A\Omega_0/v_2$.

6.3.8 The Influence of High-Frequency Disturbances on the Emergence of Stick-Slip Frictional Self-excited Oscillations

When operating machinery the frictional oscillations occur most often under slow movement of the sliding boxes on guides or under shaft's rotation at small angular velocities. In particular, movement with periodic stops can occur instead of the required uniform motion when moving heavy units in machine tools. This exclude the possibility of precise tool feed. A similar phenomenon is observed in the drawing rollers of the spinning machines, in which the frictional self-excited oscillation causes yarn unevenness and increases its breakage. The problem of frictional self-excited oscillations is the subject of many studies, a review of which is not given here. We confine ourselves to the brief information on the conditions of excitation of frictional self-excited oscillations and taking into account the influence of high-frequency disturbances on these conditions.

We consider the model shown in Fig. 6.11.

Let us imagine that from link 1, moving with constant velocity $v_0 > 0$, motion through elastic dissipative element 2 is transmitted to unit 3, having mass m, to which the force of friction H is applied. As the generalized coordinate, we accept the deformation of the elastic element q. Then the velocity of the link 3 is equal to $v = v_0 + \dot{q}$. Obviously, under $H = H_0 = \text{const}$, we have $q = -H_0/c = \text{const}$, and therefore $v = v_0$. However, the frictional force depends on many factors, including
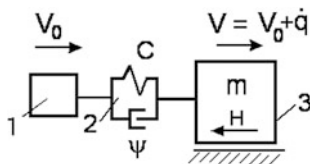

Fig. 6.11 Dynamic model

sliding velocity and, therefore, in general, $H(v) \neq$ const at that $\dot{q} \neq 0$. We assume simplified characteristics of the frictional forces, according to which the absence of sliding $(v = 0)$, frictional force is equal to the force of static friction $H = H_0$ and under motion $(v > 0)$ $H = H_1 < H_0$.

Let us write the differential equation for the phase of mass m movement $(0 < t < t_1)$

$$m\ddot{q} + b\dot{q} + cq = -H_1, \tag{6.63}$$

where $b = \psi\sqrt{cm/(2\pi)}$ is the factor of equivalent linear resistance; ψ is the dissipation factor.

Transform (6.63) to the form

$$\ddot{q} + k^2 q = -H_1/m - 2n\dot{q}.$$

Here $k^2 = c/m$; $2n = b/m$.

Let's input "dimensionless time" $\varphi = kt$. Then

$$q'' + q = \Delta(q'), \tag{6.64}$$

where $\Delta = -F_1/c - 2\delta q'$; $\delta = n/k = \vartheta_0/(2\pi)$; the derivative with respect to φ is denoted with prime mark.

The phase-plane portrait shown in Fig. 6.12, for several typical cases, corresponds to (6.64). Let's consider first of all the case, when there is no linear resistance $(\delta = 0)$. At the same time in the area of motion, the phase trajectory is presented as a circle centered at the point $\Delta_* = -H_1/c$ (Fig. 6.12, curve 1). Let's establish initial conditions. The movement begins only when the restoring force balances the force of static friction. When $t = 0$ we have $q_0 = -H_0/c$. The second initial condition is determined on the basis of the obvious equality $v = v_0 + \dot{q}_0 = 0$; hence $\dot{q}_0 = -v_0$. The point N_0 with coordinates $x_0 = q_0$ and $y_0 = q'_0 = -v_0/k$ corresponds to the initial conditions in the phase plane.

Fig. 6.12 Phase-plane portrait
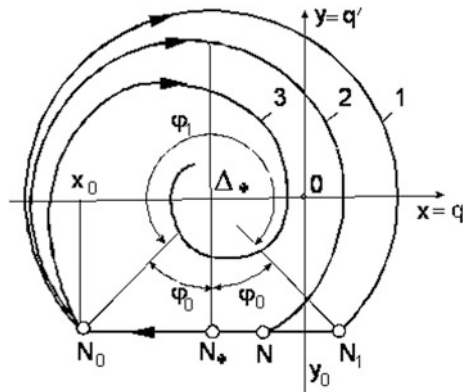
Movement of mass will continue as long as the phase trajectory will not come to the point N_1. The value $v = v_0 + \dot{q} = 0$ corresponds to this point, so the frictional force becomes equal to the force of static friction H_0. In the zone of dwell $y = -v_0/k = $ const, the plot phase trajectory is a straight line $N_1 N_0$. Further, the above-described oscillatory process is repeated. Thus, uniform motion of input link 1 transformed into relaxation oscillations with dwells (stick-slip motion). The area of movement corresponds to the angle $\varphi_1 = 2(\pi - \varphi_0)$ and time interval $t_1 = \varphi_1/k$. The angle φ_0 is defined as

$$\varphi_0 = \arctan|(x_0 - \Delta_*)/y_0| = \arctan[k\Delta H/(cv_0)]. \tag{6.65}$$

Here $\Delta H = H_0 - H_1$ is the difference between static and sliding friction.

We will find the period of self-excited oscillations $\tau = t_2$, from the obvious equality of the distances passed with the link 1 and mass m for one cycle

$$\Delta s = v_0 \tau = v_0 t_1 + q(t_1) - q_0,$$

where $q(t_1) - q_0 = N_0 N_1 = 2\Delta H/c$.

Considering, $t_1 = \varphi_1/k = 2(\pi - \varphi_0)/k$, we get

$$\tau = 2(\pi - \varphi_0)/k + 2\Delta H/(cv_0) \tag{6.66}$$

The dimensionless value of the period of self-excited oscillations is equal to

$$\varphi_2 = k\tau = 2\pi + 2(\tan \varphi_0 - \varphi_0). \tag{6.67}$$

It follows from (6.65)–(6.67), that when $\Delta H \to 0$, we have $\varphi_0 \to 0$, $\tau \to 2\pi/k$, $\varphi_2 \to 2\pi$.

The amplitude of oscillations A_0 is determined as

$$A_0 = \sqrt{x_0^2 + y_0^2} = \sqrt{(\Delta H/c)^2 + (v_0/k)^2}. \tag{6.68}$$

Next, we take into account the effect of the linear resistance, the influence of which will manifest itself in the fact that the amplitude will decrease by the law $A = A_0 e^{-nt}$. At the same time the phase trajectory (curve 2) is located within a circle 1 of radius A_0, and the dwell begins at the point N.

The graph $\dot{q}(t)$ shown in Fig. 6.13a corresponds to this case. However it may be, that $v_{min} = v_0 + \dot{q}_{min} > 0$ and therefore $\dot{q}_{min} > -v_0$. Then the area of dwell is absent and oscillations will attenuate by exponential law (Fig. 6.13b). At that the phase trajectory takes the form of curve 3 (see Fig. 6.12).

The critical value of v_0^*, which separates these two cases, corresponds to the point of touching of the phase trajectory with the straight line $N_0 N_1$. The analysis

Fig. 6.13 To the determination of the dwell area
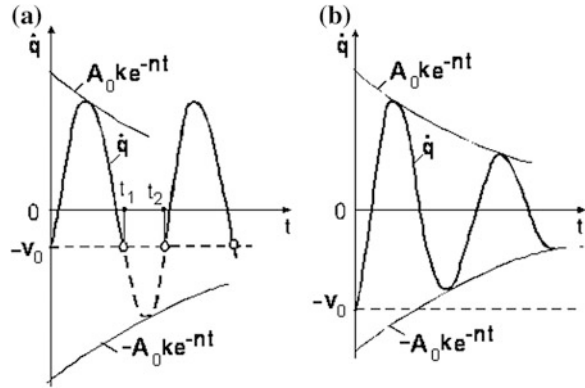
shows that the influence of linear dissipation on the position of the point contact is negligible and it is located in the vicinity of N_*. At that

$$A_0 k \exp(-n t_1^*) = v_0^*, \qquad (6.69)$$

where, $t_1 = t_1^* = (2\pi - \varphi_0^*)/k$. (The parameters values corresponding to this critical case are marked with the asterisk).

On the basis of (6.69) and phase-plane portrait analysis, we get $\cos \varphi_0^* = v_0^*/(kA_0) = \exp[-\vartheta_0(1 - \varphi_0^*/2\pi)]$ (Here ϑ_0 is the logarithmic decrement.) It follows that

$$\vartheta_0(1 - \varphi_0^*/2\pi) = -\ln(\cos \varphi_0^*). \qquad (6.70)$$

On the basis of (6.70) when $0.2 \le \vartheta_0 \le 0.8$, we get $\varphi_0^* \approx [\pi/6 \div \pi/3]$.
Next, using (6.68), (6.69), we finally get

$$v_0^* = \frac{k \,\Delta H}{c \sqrt{\exp(2\vartheta_1) - 1}} = \frac{k \,\Delta H}{c} \sqrt{\frac{1 - \psi_1}{\psi_1}}, \qquad (6.71)$$

where, $\vartheta_1 = \vartheta_0(1 - \varphi_0^*/(2\pi)) \approx [5/6 \div 11/12]\vartheta_0$; $\psi_1 = 1 - \exp(-2\vartheta_1)$ are the corrected values of logarithmic decrement ϑ_0 and dissipation factor ψ_0. Taking into account the degree of validity of the initial information and smallness of the corrected modification, we can accept $\vartheta_1 \approx \vartheta_0$; $\psi_1 \approx \psi_0$.

It should be emphasized that it is the dissipative properties of the drive, which determine the final value of the v_0^*, since when $\psi_0 \to 0$, we have $v_0^* \to \infty$. This means that, excluding the linear resistance, we can see that the self-excited oscillations of the considered type can occur at any velocity v_0. Typically, the critical velocity v_0^* is sufficiently small. Suppose, for example, $k = 100\,\text{s}^{-1}$, $\Delta f = 0.05$; $\vartheta_0 = 0.2$. At that $\varphi_0^* = 0.584\,\text{rad}$; $v_0^* = 0.741 \cdot 10^{-2}\,\text{m/s}$.

As it was already mentioned, while designing machine tools, devices and other equipment, occurring in case of frictional self-oscillations, transformations of

uniform movement into stick-slip movement (i.e. motion with dwells and jumps) is highly undesirable. The point is the value of jump Δs ultimately determines the so-called positioning accuracy, i.e. realized accuracy of the executive body in achieving the specified position.

We consider two critical cases for estimation of Δs. In case of velocity v_0, nearest to the critical value of v_0^*, we have $\varphi_1 \approx 2\pi - \varphi_0^*$, where $\varphi_0^* = \varphi_0(v_0^*)$. Then

$$\Delta s_* = v_0^*(2\pi - \varphi_0^*)/k + q(t_1) - q_0.$$

In this case $\Delta q = q(t_1) - q_0 \approx N_* N_0 = v_0^* k^{-1} \tan \varphi_0^* = \Delta H/c$. It follows that

$$\Delta s_* = (v_0^*/k)[2\pi - \arctan(k\Delta H)/(cv_0^*)] + \Delta H/c.$$

The period $\tau_* = \Delta s_*/v_0^*$ corresponds to this jump. When velocity v_0 transits through critical value of v_0^* period decreases with a jump to the value $\tau = 2\pi/k$, i.e. by the value of $\Delta \tau_* = (\tan \varphi_0^* - \varphi_0^*)/k$. Under accepted initial data, we have $\varphi_0^* = 0.584 \, \text{rad}$; $\Delta s_* = 0.471 \, \text{mm}$; $\tau_* = 6.36 \cdot 10^{-2} \text{s}$; $\Delta \tau_* = 7.68 \cdot 10^{-4} \text{s}$.

The other critical case is realized when $v_0/k < \Delta H/c$. Such a situation occurs in case of small driving velocity. In this case $\varphi_0 \to \pi/2$. Then in accordance with (6.66)

$$\left.\begin{array}{l} \tau = \pi/k + 2\Delta H/(cv_0) \approx 2\Delta H/(cv_0); \\ \Delta s = \pi v_0/k + 2\Delta F/c \approx 2\Delta H/c. \end{array}\right\} \tag{6.72}$$

In this critical case, we see the clear manifestation of another curious feature of frictional self-oscillations. As it follows from (6.72), the period of self-excited oscillation, now, is practically determined by the time interval of mass dwell, when the deformation of the elastic element takes place. Further mass almost instantly "jumps" to the value of Δs.

At that the oscillations turn out to be essentially discontinuous. The malleable drive in this case acts as the energy storage device and appears to be a kind of mediator between the external source and the oscillatory system. As value of v_0 approach the critical value of v_0^* the frictional form of self-oscillations becomes less pronounced.

Further we will assume that the speed, of sliding along the guides, has a high-frequency component $v + a\omega \sin \omega t$, where a is the amplitude of oscillations ($\omega \gg k$). This situation in particular occurs under the high frequency vibration of the entire system, which leads to the additional kinematic excitation of the moving mass. Maximum of velocity oscillations, with a frequency k is determined by the dependence $v_k \approx k\sqrt{(\Delta H/c)^2 + (v/k)^2}$.

When $\omega \gg k$ we have $z \approx v_k/(a\omega)$, and at high frequencies ω, even very small amplitudes of the high-frequency excitations a can lead to a significant decrease in the value of parameter z and functions $\Phi(z)$ (see Fig. 6.4). In the considered model the difference between frictional forces $\Delta H_z = \Delta H \Phi(z)$ and dissipation

factor $\psi_z = \psi_0 \Phi(z)$ is corrected simultaneously; here index z corresponds to taking into account the high-frequency oscillations (see Sect. 6.3.3).

On the basis of (6.71)

$$v_{**} = \frac{k\Delta H}{c} \sqrt{\Phi(1 - \psi_0\Phi)/\psi_0}, \tag{6.73}$$

where, v_{**} is the critical velocity, taking into account the high-frequency component of oscillations.

Equation (6.73) shows the opposite trend with decreasing Φ. This is related to the fact that, the efficiency value of the differential frictional forces ΔH_z and the dissipation factor of the drive ψ_z, decrease simultaneously. The first of these factors leads to a decrease in v_*, and the second—to increase. In Fig. 6.14a is shown the graphs $f(z, \psi_0) = v_{**}/w$ and the locus of points max $f(z)$.

On the basis of (6.71) and (6.73) $v_{**} = v_* K(\Phi)$, where the correction function $K(\Phi)$ has the form

$$K(\Phi) = \sqrt{\Phi(1 - \psi_0\Phi)/(1 - \psi_0)}. \tag{6.74}$$

According to (6.74) max $K(\Phi)$ corresponds to the condition $\Phi = \Phi_* = 1/(2\psi_0)$. As $\Phi < 1$ when $\psi_0 < 0.5$ $\Phi \in [0, \Phi_*]$ function $K(\Phi)$ on the whole interval [0,1] is increasing. When $\psi_0 > 0.5$, $\Phi \in [0, \Phi_*]$ the function $K(\Phi)$ increases, and when $\Phi \in [\Phi_*, 1]$ it decreases. Figure 6.14b shows a family of curves $K(z, \psi_0)$.

The analysis shows that to reduce the critical speed of excitation of self-oscillations, more than two times, when $\varphi_0 > 0.25$, it is necessary that $\Phi \leq 0.2$, at that $z \leq 0,4$. Similar dynamic effects can also occur in case of the high-frequency excitation [impact] in the direction perpendicular to the plane of motion [9]. One way to eliminate the identified "jumps" is to use the materials with low difference between coefficients of friction in rest and motion, such as filled fluoroplasts (PTFE, Teflon, flourlon) paired with tempered steel. Of course, a more radical way is to start using [motors] drives with ball bearings, in which the sliding friction is
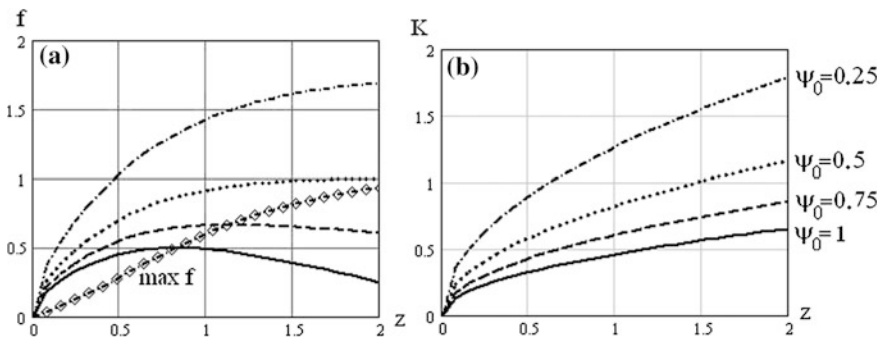

Fig. 6.14 Graphs $f(z, \psi_0)$, $K(z, \psi_0)$

completely eliminated. However, in this case usually the reduced stiffness of the drive is decreased and the lower natural frequency increases, which is related to the elimination of the effect of self-braking, which in the given case acts positively, reducing the "length" of kinematic chain of the drive, which is prone to excited oscillations.

In conclusion, we will note that the occurrence of differential friction forces ΔH, according to modern ideas, is treated as feedback broadband random disturbances, arising during sliding of rough deformable bodies. The friction itself, strictly speaking, is formed in an oscillating system directly by the locally occurring dynamic processes. Therefore the use, in the engineering calculations, of quasi-static friction characteristics is approximate.

6.4 Nonlinear Resonance Oscillations on the Frequency of the Amplitude Modulation Caused by the High-Frequency Excitation

Let us take a look at the dynamic model of the drive of the cyclic mechanism (see Table 5.1, fragment 1), described with differential equations [72]

$$J\ddot{q} + |R(q)|\mathrm{sign}\dot{q} + P(q) = \Pi'(\varphi)[F_1 \sin \Omega t - m(\Pi''(\varphi)(\omega + \dot{q})^2 + \Pi'(\varphi)\ddot{q})],$$

(6.75)

where J is the moment of inertia of the input link; m is the mass of the output link; ω is the assigned ideal frequency of rotation of the input link; Ω, F_1 are the frequency and amplitude of the driving force, applied to the output link $(\Omega \gg \omega)$; $\Pi'(\varphi), \Pi''(\varphi)$ are the first and second geometric transfer functions of the cyclic mechanism; $\varphi = \omega t$; q is the generalized coordinate, which describes the drive's torsional oscillations; $-|R(q)|\mathrm{sign}\dot{q}$ is the positive dissipative force; $-P(q)$ the force of restoration (odd function q).

Let $\Pi' = r\sin\varphi, \Pi'' = r\cos\varphi$, and the nonlinear force of restoration corresponds to the coupling with cubic characteristics. Then on the basis of (6.75) after the linearization of the position function $\Pi(\varphi)$ and its derivatives in the vicinity of program motion, we have

$$(1 + \mu \sin^2 \omega t)\ddot{q} + 2\delta\omega\dot{q} + p_0^2(1 + \alpha q^2)q = w_1 \sin \omega t \cos \Omega t - 0.5\mu\omega^2 \sin 2\omega t,$$

(6.76)

where $\mu = mr^2/J, w_1 = F_1/J; p_0$ is the natural frequency when $\mu = 0$ and $\alpha = 0$; $\delta = \vartheta/(2\pi)$ is the effective value of the reduced coefficient of dissipation, when the logarithmic decrement is ϑ and the frequency ω (see hereunder).

In Eq. (6.76) omitted is the component, proportional to $\dot{q}$, which corresponds to the gyroscopic force; the work of this force for the period $2\pi/\omega$ converts to zero.

Differential Eq. (6.76) serves as the mathematical model for many oscillatory systems and as per the coverage of the problem far exceeds the limits for the models of cyclic mechanisms. Among these problems we can point out parametric resonance in linear system, combined effect of parametric and forced excitation, influence of poly-harmonic excitation on dissipative properties, definition of conditions of excitation of parametric and subharmonic resonances etc. Usually is considered the case $w_1 = 0$, when there is no high-frequency amplitude modulation of the driving force. Case $w_1 \neq 0$, in case of viscous friction, was studied in paper [28].

Taking into account the presented in this paper problem and to "clean" the researched effect of the influence of other factors, we will eliminate the possibility of excitation of main parametric resonance, as well as sub-harmonic resonances. For the purpose we will adopt $\vartheta \gg 0.5\,\pi\mu$ and $\Omega \gg \omega$. Without restricting the generality, hereunder we will adopt $p_0 = 1$, which simultaneously corresponds to the procedure of transition to dimensionless time $\tau = p_0 t$. At the same time we will retain the accepted arbitrary values of frequencies, to which now correspond the dimensionless values ω/p_0 and Ω/p_0.

We dwell on the physical nature of the studied effect and establish, why the resonant oscillations, at frequency ω, are possible only in the nonlinear system. When $\mu \ll 1$ we have $w_1 \sin\omega\tau\cos\Omega\tau(1 + \mu\sin^2\omega\tau)^{-1} \approx 0$, $5w_1[\sin(\omega + \Omega) - \sin(\Omega - \omega)]$. Thus, the system is subject to two driving forces with near similar frequencies. In the absence of nonlinearity ($\alpha = 0$) the principle of superposition is valid, therefore these forces lead to the beating mode, however, the prerequisites for the occurrence of resonance, at frequency ω, do not exist.

The amplitude of oscillations is proportional to $|\sin\omega\tau| \approx \frac{2}{\pi}(1 - \frac{2}{3}\cos 2\omega\tau)$, which in the nonlinear system ($\alpha \neq 0$) leads to the pulsation of "natural" frequency and is the prerequisite for the violation of the conditions of dynamic stability and excitation of main parametric resonance. Illustrated in Fig. 6.15 are some of the steady oscillatory modes, determined with the help of computer simulation at $\alpha = -0, 2$ (soft characteristic) $\omega = 0.85 - 0.88$, $\Omega = 20$ (modes 1–5), $\Omega = 12$ (mode 6) and the variation of the coefficient of dissipation δ. As shown by analysis, when $\mu < 0, 1$ this parameter in case of adopted initial data, practically, does not influence the final result, therefore in future we will adopt $\mu = 0$.

In case of large amounts of dissipation (mode 1) we notice beating relative to zero level. Similar view when $\omega = 1$ is in graph $q(\tau)$ when the linear elastic characteristic is ($\alpha = 0$). With the decrease in the level of dissipation, the beating mode shifts to low-frequency resonant mode with frequency ω, at the same time when the level of amplitude of this component changes very slightly. As in case of sub-harmonic resonances, dissipation in this case acts as the former of an energy barrier, which hinders the occurrence of these modes.

As it was shown earlier, in case of occurrence of bi-harmonic mode, the effective values of dissipative parameters can decrease significantly, which leads to the change in the conditions for the occurrence of resonant oscillations at the amplitude modulation frequencies of high-frequency oscillations. In case of a significant change in high frequency (mode 6) of configuration of bending, similar to mode 2,

Fig. 6.15 Evolution of
oscillatory modes in case of
change in the level of
dissipation
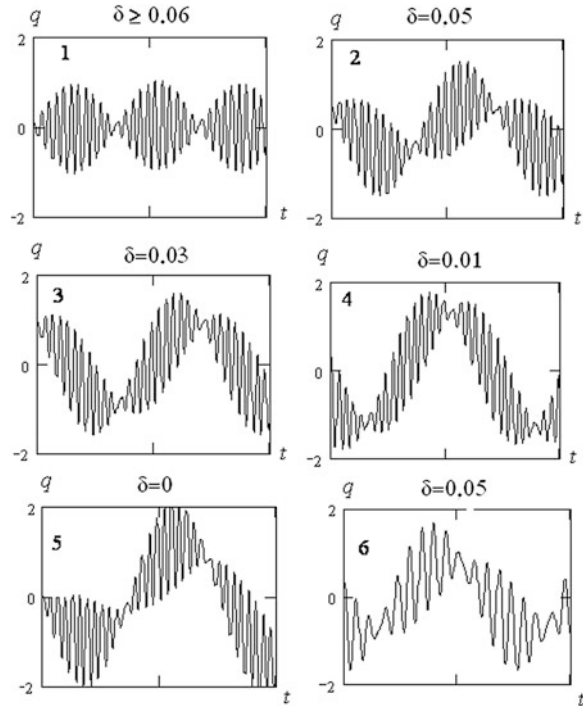
which eliminates the possibility of supposing about the sub-harmonic nature of the
considered modes.

Qualitatively similar results are shown in paper [72] for the cases, when non-
linear nature of the restoring force requires the presence of a clearance in the
subsystem of the motor.

6.5 Vibrations in the Systems with Intermediate Friction Connections

During the analysis of dynamic models with Coulomb friction, we can select an
original group of systems with intermediate friction connections [43, 89]. The
distinguishing feature of these systems is that the most significant frictional forces
are applied to the links with relatively low mass (during schematization, often these
masses can be considered equal to zero), which are separated with elastic elements
from the nearby elements, having large masses.

Systems with intermediate friction connections occur in the machine tool drives
(for example, tracer-controlled and boring); in the drives, which use pre-tightened
closed kinematic chains; in systems with braking devices; in some designs of the

shock absorbers and dry friction dampers; in some models of the marine power equipments etc.

In this case, the intermediate frictional connection can perform not only the usual dissipative role, but also as a kind of "vibro cut-off device" that in case of appropriate choice of its parameters, prevents the penetration of vibrations deep into the kinematic chain and has a significant effect on the frequency spectrum of the system. Apart from that, in a certain range of the system parameters, the increase in friction in the intermediate friction pairs, contrary to traditional notions, may lead not to decrease but increase in the resonant amplitude of forced oscillations.

6.5.1 Dynamic Model with Finite Number of Degrees of Freedom

The represented in the Fig. 6.16a dynamic model, with discrete parameters, is described by the following system of nonlinear differential equations:

$$
\left.\begin{array}{l}
\ddot{q}_0 + \frac{2\delta_0 k^2}{\omega(1+\xi_1)}\dot{q}_0 + k^2(q_0 - q_1) = w_0 \sin(\omega t + \gamma); \\
\text{---------------------} \\
2\omega^{-1}\dot{q}_i(\xi_i\delta_i + \xi_{i-1}\delta_{i-1}) + [Y_i + H_i c_i^{-1}\mathrm{sign}\dot{q}_i]\eta(|Y_i| - H_i c_i^{-1}) = 0.
\end{array}\right\} \quad (6.77)
$$

Here the following notations are adopted: q_i are the generalized coordinates ($i = 0$ meets mass m, $i = \overline{1, n}$ meets friction elements); H_i are the forces of Coulomb friction; $\xi_i = c_i/c_0$, where c_i, c_0 are the stiffness coefficients; $k^2 = c_0/m$; $w_0 = F_0/m$, $\delta_i = \psi_i/(4\pi)$, where F_0- is the amplitude of the driving force $F(t) = F_0 \sin(\omega t + \gamma)$; ψ_i is the reduced dissipation coefficient corresponding to the
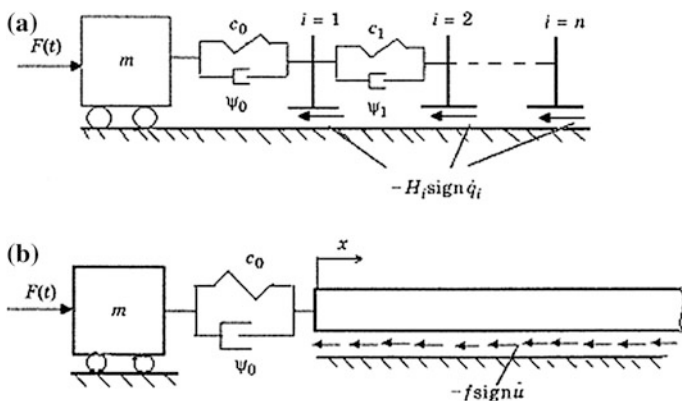

Fig. 6.16 Dynamic models

positional resistance, arising in case of structural dissipation of the elastodissipative element i.

For a number of special cases Vulfson obtained the analytical solutions by using the modification of the harmonic linearization method [43]. In this case the motion of the mass m was presented as $q_0 = a_0 \sin \omega t$, however, while describing the motion of the intermediate elements the dwell zones, determined by force correlations, were taken into account. The characteristic features of such systems can be illustrated by a simple dynamic model, with one intermediate friction element ($n = 1$), whose motion is described with the help of the differential equation of the second order

$$m\ddot{q}_0 + c_0(q_0 - q_1) = F_0 \sin(\omega t + \alpha) \tag{6.78}$$

and with one equation of the connection between the generalized coordinates q_0 and q_1

$$c_1 q_1 - c_0(q_0 - q_1) = H \operatorname{sign}\dot{q}_1 \tag{6.79}$$

Here $q_0 = q$ characterizes the absolute motion of the body mass m, q is the displacement of the moving friction element; F_0 is the amplitude of the driving force; H is the absolute value of the maximum value of friction.

Depending on the oscillating system parameters, the perturbation and the magnitude of friction, the system can either be linear (when the total impact on the intermediate link with the elastic elements is not sufficient to overcome the friction in the contact pair) or nonlinear. In the latter case, the motion occurs with the breakdowns of the intermediate element from the supporting pad. In the oscillatory motion of the nonlinear system, in practice, a specific switching sequence, which allows the highlighting of four phases of motion during one period of the disturbing force, exists.

Let us adopt the following notation: a_0, a_1 are the amplitudes of the mass and frictional element; R, R_1 are the restoring forces; $\tilde{H} = H/F_0$. On the hysteresis characteristics $R(q), R_1(q_1)$, shown in Fig. 6.17, the elastodissipative force is represented as a piecewise-linear function, describing the hysteresis loop of the polygonal form, these four stages correspond to intervals 1–2, 2–3, 3–4, 4–1. Under the adopted switching regime the Eq. (6.78) with (6.79) can be converted to the traditional form of nonlinear differential equation

$$\ddot{q} + R(q, \dot{q}) = w_0 \sin(\omega t + \alpha). \tag{6.80}$$

To study the dynamics of the given system, we use the modification of the harmonic linearization method (see appendix). According to this modification the movement of the mass is harmonized and the movement of the intermediate inertia-free element is determined by force correlations identified under this assumption. The resulting solution allows us to describe not only the areas of intermediate element motion, but also its dwells.

Fig. 6.17 Hysteretic characteristic
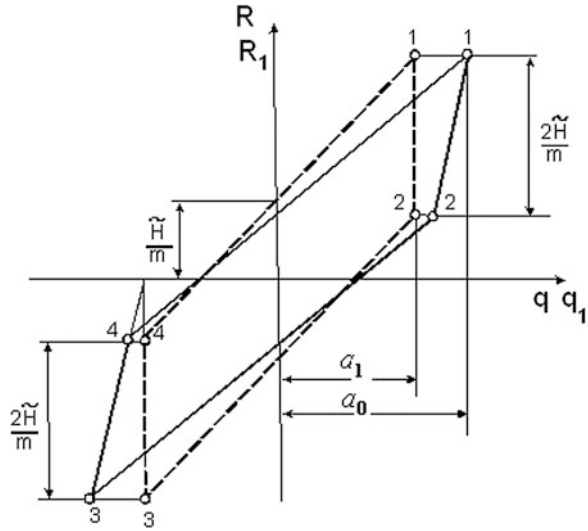
The amplitude-frequency characteristics $\kappa(z)$, in dimensionless form, are described by the equation [43]

$$z^4 - 2z^2\beta(\kappa) + [\beta^2(\kappa) + \frac{16\zeta^2\tilde{H}^2(\kappa - \tilde{H})^2}{\pi\kappa^4(1+\zeta)^2} - \kappa^{-2}] = 0. \qquad (6.81)$$

Here $\kappa = a_0/a_{s\delta}$ is the coefficient of dynamicity; $a_{s\delta} = w_0/k^2$; $\beta(\kappa) = p^2/k^2$; p^2 is the coefficient of the harmonic linearization; $\zeta = c_1/c_0$; $z = \omega/k$.

The analysis of the amplitude-frequency characteristics allowed us to establish the existence of two regions of values of parameters, corresponding to the restricted and unrestricted amplitudes of resonance. The amplitude of the resonance is limited under condition

$$\tilde{H} \geq 0,25\pi(1+\varsigma). \qquad (6.82)$$

If this condition is satisfied, the resonant value of the coefficient of dynamicity is given by

$$\kappa_{max} = \frac{4\tilde{H}}{4\tilde{H} - \pi(1+\varsigma)}. \qquad (6.83)$$

We can see in the Fig. 6.18, the graphs of the coefficients of dynamicity for $\zeta = 0.25$ with $\tilde{H} = 1, \tilde{H} = 2, \tilde{H} = 4$. The analysis of these graphs, clearly shows that the value κ_{max} depending on $\tilde{H}$ can have some minimum value (shown in the Figure with dotted curve, depicts the locus of the maximums of the coefficients of dynamicity). The value κ_{max} reaches its minimum, when $\tilde{H}_{opt} = 0.5\pi(1+\zeta)$.

Fig. 6.18 Amplitude-
frequency characteristics
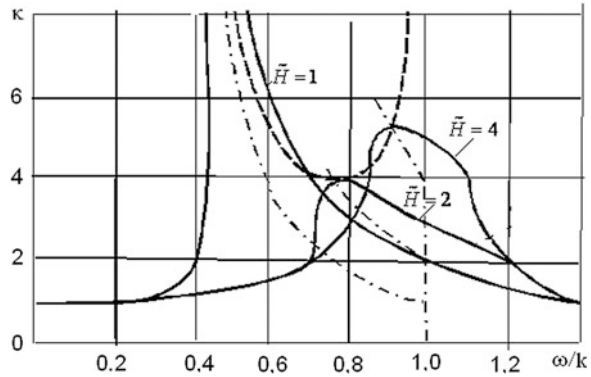
$$\min \max \kappa = \pi(1 + \varsigma). \tag{6.84}$$

In a number of practical cases, the information about the parameters, of the just steadied process, is insufficient. For example, for engineers it is often of interest to find the real time of the system's run-in to reach the steady state, the behavior of the system under intermittent action of the driving force, the analysis of possible amplitudes of oscillations, when the system goes through the resonance, damping conditions, etc.

For steady-state oscillations of the model we implement, as a rule, one of three modes of movement. The first regime occurs in the case, when the velocity of the intermediate element, during the entire period of the oscillations, is less than the velocity of the supporting pad. The second mode is characterized by two switching points, specified by one kinematic and one force conditions. In the third mode, four switching points are determined by two kinematic and two force conditions.

6.5.2 Study of the Forced Vibrations of the Drive Using the Model with Distributed Elastic-Friction Elements

Hereunder, we will consider the discrete-continuum model, on the basis of which we not only formulate the exact qualitative ideas about the occurrence of dynamic modes, but also the effective criteria and engineering estimations, which significantly ease the procedure of dynamic synthesis of such systems (see Fig. 6.20b) [89].

If our study is restricted to the static formulation of the problem, then the distributed elastic-friction element, which is the part of the dynamic model, shown in Fig. 6.12b, can be regarded as a subsystem with the so-called structural friction (structural hysteresis). This term means the friction between the contacting surfaces, in the nominally fixed joints, in case of small relative displacements (slippage). In such systems, there is a significant correlation between the distribution of friction and deformations.

In the considered model, the distributed elastic-friction element serves as the fragment of a continuum model of a large number of discrete friction elements, separated with elastodissipative connections, forming an oscillatory system. Thus, what we are talking here is about the dynamic formulation of the problem. In this case the high frequency components of perturbations, leading to the vibration linearization of friction, can play some corrective role. In connection to this problem, we should also note the study of Palmov [44], dedicated to the problem of the vibration propagation in the nonlinear dissipative medium, with respect to the elastic-plastic semi-infinite rod.

The studied machine drive hereunder, is schematized as a model, consisting of a massive working body, connected through elastodissipative element with the semi-infinite rod, to which the distributed force of dry friction is applied, from the stationary base (see Fig. 6.12b). (Here and below, the term "rod" is used purely conventionally, in particular, in case of angular displacements of the working body of the model, under corresponding parameters, corresponds to torsion oscillations of the drive.)

Let us adopt the following arbitrary notations: m is the mass of the working body; c_0 is the stiffness coefficient; ψ_0 is the coefficient of dissipation; f, ζ, μ are the absolute value of friction, compliance coefficient and mass per unit length of the rod; q is the mass m coordinate; $u(x,t)$ is the deformation of the rod.

If the driving force $F(t) = F_0 \sin \omega t$ is applied to the working body, its oscillations are described by the system of differential equations

$$\left. \begin{array}{c} m\ddot{q} + b(\dot{q} - \dot{u}(0)) + c(q - u(0)) = F_0 \sin(\omega t + \gamma); \\[2mm] \zeta^{-1}\dfrac{\partial^2 u}{\partial x^2} - \mu\dfrac{\partial^2 u}{\partial t^2} + f\,\mathrm{sign}\,\dfrac{\partial u}{\partial t} = 0. \end{array} \right\}$$
(6.85)

The second equation of (6.85) is rather complex, which is due not only to its nonlinear nature, but to the boundary conditions, depending on the unknown effective length of the rod l, which is determined in the course of finding the solution.

Keeping in mind the level of the considered model's idealization and the engineering trend of the analysis, we will use some simplifications. We will search for an approximate solution, describing the forced oscillations in the form $q = A\sin(\omega t)$, $u(0) \approx a\sin(\omega t)$ (strictly speaking, the phases of both the harmonic movements may vary).

First of all, we exclude from consideration the influence of inertial characteristics of the rod, which corresponds to the formulation of the problem, outlined above. This assumption, in the first approximation, corresponds to $\mu\omega^2 \ll f$ (see the clarification below). Then the second equation of system (6.85) takes the form $u'' = \pm f\zeta$ where $(\ )' = \partial u/\partial x$. Hence

$$u = \pm 0.5\zeta f x^2 + C_1 x + C_2,$$
(6.86)

where C_1, C_2 are the arbitrary constants, determined from the boundary conditions $u(0) = u_0$; $u(l) = 0$.

The last boundary condition, corresponding to the absence of movement in the cross section $x = l$, in this case is incomplete, since in the "end" of the vibration chain, the restoring force should be fully balanced with the forces of friction, which corresponds to the additional condition $u'(l) = 0$. After substitution in (6.86) we obtain

$$u(x) = u_0 - \zeta fx[\sqrt{2|u_0|/(\zeta f)} - 0,5x]; \tag{6.87}$$

$$l = \sqrt{2|u_0|/(\zeta f)}. \tag{6.88}$$

Let us define the potential energy, developing in case of deformation of the rod $V_1 = 0.5\zeta \int_0^l F^2(x)dx$, where $F(x)$ is the restoring force. Herewith, taking into account, that $F(x) = \zeta^{-1}(\partial u/\partial x)$, on the basis of (6.87), (6.88) we get

$$V_1 = |u_0|\sqrt{|u_0|}/(3h), \tag{6.89}$$

where $h = \sqrt{2\zeta/f}$.

At the same time the potential energy of the whole system is determined as:

$$V = V_1 + 0.5(q - u_0)^2 c_0. \tag{6.90}$$

Furthermore, we will find the relation between u_0 and q, for which we equate the reactions when $x = 0$. At the same time we will restrict ourselves to considering the elastic components of the reaction, which corresponds, in the first approximation, to averaging in the period of oscillations (about the accounting of the dissipative component, see below). On the basis of (6.86), (6.89) and (6.90) we obtain the following quadratic equation

$$h\chi^2 + 2\chi e_0 - hq = 0,$$

where $\chi = \sqrt{|u_0|}$, $e_0 = c_0^{-1}$.

Hence

$$u_0(q) = h^{-2}[-e_0 + \sqrt{e_0^2 + h^2|q|}]^2 \text{sign}q. \tag{6.91}$$

With (6.86), (6.91) the considered system can be described with the next non-linear differential equation

$$\ddot{q} + \Psi(q, \dot{q}) = W\sin(\omega t + \gamma), \tag{6.92}$$

where $W = F_0/m$.

The function Ψ consists of the potential and dissipative components. The potential component is defined as

$$\frac{dV}{dq} = \frac{\partial V}{\partial q} + \frac{\partial V}{\partial u_0}\frac{du_0}{dq}. \tag{6.93}$$

On the basis of (6.89), (6.90), (6.92), (6.93) we get

$$\frac{\partial V}{\partial q} = S(q)u_0(q)h^{-1} + e_0^{-1}(q - u_0)(1 - 2\sqrt{|u_0|}S(q)), \tag{6.94}$$

where $S(q) = h/\sqrt{e_0^2 + h^2|q|}$.

If we use the harmonic linearization method, this component is $p^2(A)q$, where $p(A)$ is the frequency of free oscillations. However, the direct use of the harmonic linearization method, with respect to (6.94), requires numerical integration. In such cases, the method of linearization as per the distribution function, proposed by Kolovsky and Pervozvansky [27], is more efficient. Thus,

$$p^2(A) = \frac{2}{mA\sqrt{3}}\frac{\partial V}{\partial q}(A\sqrt{3}/2). \tag{6.95}$$

The graphs $p(A, h)$, obtained from (6.95) are shown in Fig. 6.19 (solid lines). Here and below, to illustrate the result, the following input data is used: $c_0 = 1$, $m = 1$, $W = 1$. Let us note that in case of the data, the results correspond to the transition to the dimensionless form and become general if we take the

Fig. 6.19 Graphs $p(A)$ and $\delta(A)$
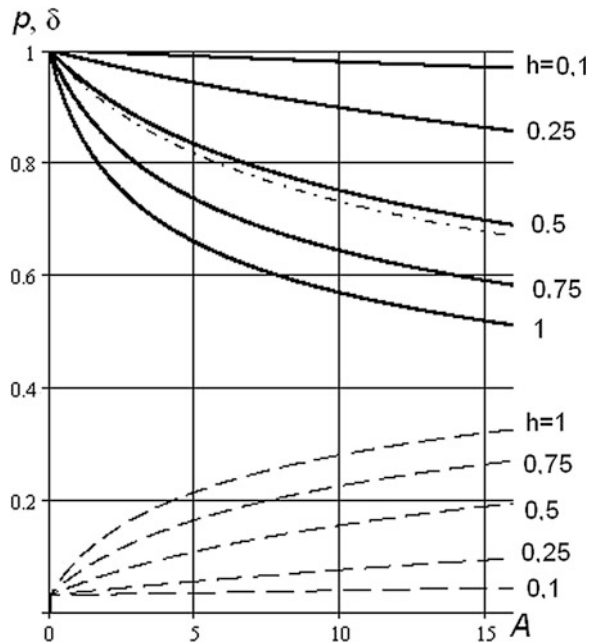
frequency parameter ω equal to the ratio of the frequency of the driving force, to the frequency $p_0 = \sqrt{c_0/m}$.

For the particular case $h = 0.5$, the curve $p(A)$, obtained with the calculation of the simplified formula $p = 1/\sqrt{[e_0 + e_1(A)]m}$ where $e_1 = \zeta \ell(A)$, is drawn with hatch-dotted line in the graph. As follows from the graph, the results are almost identical.

The analysis of graphs suggests the possibility of the substantial reduction in "natural" frequency, due to increase in amplitude of oscillations and parameter h. Let us recall that this parameter increases with increase of the rod's compliance factor and with the reduction in the specific force of friction per unit of the length.

Henceforth, we pass to the accounting of dissipative factors. In this case, we will use the terms of the balance of energy, to which the dissipative component of the function $\Psi(q, \dot{q})$, corresponds in case of use of the method of harmonic linearization. Let the amplitude of oscillations in the cross section of the rod x be $a(x)$. Scattered in one oscillation period energy is $\Delta E = \Delta E_0 + \Delta E_1$, where $\Delta E_0 = \psi_0 c_0[A - a(0)]^2/2$ corresponds to the elastic element c_0, and ΔE_1 to the rod. Thus,

$$\Delta E_1 = 4f \int_0^\ell a(x)dx.$$

The function $a(x)$ is determined by the relation (6.87) in case of exchange of u with a and u_0 with $a_0 = a(0)$. After integration and simplification, taking into account (6.80), we obtain

$$\delta(A) = \frac{1,33 Y^3(A) h^{-1} 0,5\pi c_0 [\sqrt{3}A/2 - Y^2(A)]^2 \delta_0}{\left\{ 2Y^3(A)/(3h) + 0,5c_0[\sqrt{3}A/2 - Y^2(A)]^2 \right\} \pi}. \tag{6.96}$$

Here $\delta(A) = (4\pi)^{-1} \Delta E/V$ is the reduced dissipation coefficient of the system; $\delta_0 = \psi_0/(4\pi)$; $Y(A) = h^{-1}(-e_0 + \sqrt{e_0^2 + 0,5h^2 A\sqrt{3}})$.

The family of the curves $\delta(A, h)$ is shown in Fig. 6.19 with hatching lines.

The evolution of the hysteresis loops, at fixed amplitude of oscillations, depending on the parameter h is shown in Fig. 6.20. Here $R(q)$ is the reduced elastodissipative force (solid line) and elastic component of this force (hatched line), per unit mass.

At first glance, it seems paradoxical that with the increase in parameter h the area of the hysteresis loop is also increasing: in case of fixed stiffness of the rod, this means reduction of specific friction. However, the marked contradiction is only apparent, since in this case the effective length of the rod is growing and with it the total work, to overcome the forces of friction.
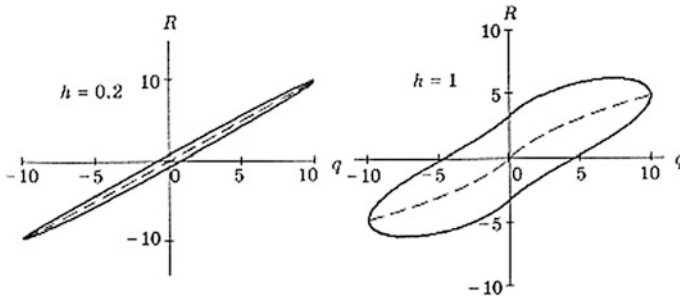
Fig. 6.20 Evolution of the hysteresis loop

Based on the above mentioned, we can write the linearized differential Eq. (6.83) as follows:

$$\ddot{q} + 2\delta(A)p(A)\dot{q} + p^2(A)q = W\sin(\omega t + \gamma). \qquad (6.97)$$

Let us estimate the influence of the unaccounted for above inertial properties of the rod on the frequency response of the system. The kinetic energy of the element of the rod dx is $dT_1 = 0.5\mu\,\dot{u}^2(x,t)dx$. Taking $u = a(x)\sin pt$, after integration over the length ℓ and simple calculations, the expression for the maximum kinetic energy of the system T takes the form

$$T = 0.5\,mA^2p^2[1 + \varepsilon(A)], \qquad (6.98)$$

where $\varepsilon(A) = 1.5A^{-2}Y^5(A)\xi$; $\xi = \mu h/(\varsigma m)$.

Further with (6.91), (6.92), (6.98) as per the Rayleigh formula, we obtain the following formula for the frequency of free oscillations p_μ:

$$p_\mu(A) = p(A)/\sqrt{1 + \varepsilon(A)}. \qquad (6.99)$$

Analysis of formula (6.99) shows that at the dimensionless amplitude $A < 5 \div 8$ and $\xi < 1$ relative magnitude of the refinement $[p(A) - p_\mu(A)]/p(A)$ does not exceed 5 %.

According to (6.90) the amplitude of the forced oscillations is determined as

$$A = \frac{W}{\sqrt{[p^2(A) - \omega^2]^2 + 4\delta^2(A)p^4(A)}}. \qquad (6.100)$$

We will present (6.100) as the biquadratic equation with respect to ω

$$\omega^4 - 2p^2(A)\omega^2 + p^4(A)[1 + 4\delta^2(A)] - W^2/A^2 = 0.$$

Hence

$$\omega(A) = \sqrt{p^2(A) \pm \sqrt{W/A^2 - 4\,\delta^2(A)p^4(A)}}. \tag{6.101}$$

Dependence (6.101), taking into account (6.95) and (6.96), determines, in the closed form, the amplitude-frequency characteristic.

Figure 6.21 shows the family of curves $A(\omega, h)$. It follows from the graph that depending on the parameter h, the envelope curve of the amplitude-frequency characteristic peaks, has a minimum. Let us recall that parameter h increases with increase in the rod specific compliance and decrease in the specific friction f. The equation of the envelope curve on the basis of (6.101), in the parametric form, can be written as follows:

$$2\omega_*(A)A\,\delta(A) - W = 0; \ \omega_*(A) = p(A), \tag{6.102}$$

where $\omega_*(A)$ is the resonance frequency.

The obtained characteristics, as per the qualitative level, are in line with the results of the analysis of the models with the discrete predetermined friction elements [43, 83, 89]. In particular, replacing the endless elastic rod with the elastic element with stiffness coefficient c and the weightless element with the concentrated friction force, we have $\min \max(\kappa) = \pi(1 + c_1/c_0)$ at $H = H_{opt} = 0.5$ $\pi(1 + c_1 + c_0)F_0$, where $\kappa = Ac_0/F_0$ is the dynamicity coefficient. As the calculations show, the values of $\min \max \kappa$ for the models with discrete and distributed parameters are relatively close. At the same time, the corresponding values of the forces of friction are strongly dependent on the method of their application.

Fig. 6.21 Amplitude-frequency characteristics
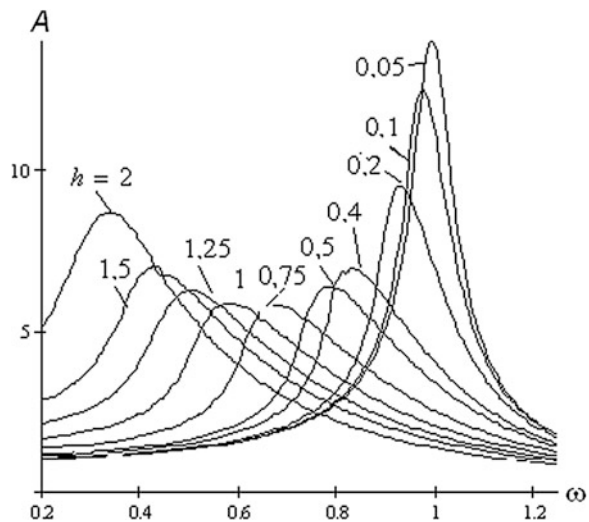
The latter is associated with the significant evolution of the hysteresis loop, with one friction pad and the extreme form of this loop in the system with distributed friction characteristics. In the first case the loop has the shape of a parallelogram and has distinct "locking" properties. With the increase in the number of friction pads the loop takes the polygonal shape that approximates to the above case. Herewith, the effective length of the oscillatory chain changes smoothly, without distinct abrupt transitions, associated with changes in the dynamic structure of the oscillatory system.

As an illustration, as well as to verify the analytical results of the above study, the computer simulation of the dynamic model was carried out, in which the rod was replaced by the n elastic members, separated by intermediate "pads", which were subjected to the concentrated forces of the Coulomb friction.

In the Fig. 6.22 we can see two graphs $q_i(t)$ for the discrete model with three areas. In this case $i = 0$ corresponds to the motion of mass m, the other values of i correspond to the number of the pad, depending on its distance from the mass m.

During the simulation, frequency ω varied so as to provide the approach to the resonant mode. Both of the considered regimes have the various friction forces $H = F_0$ (the first mode), $H = 10F_0$ (second mode). At the same time $c_i/c_0 = 1$, the other parameters correspond to the values, previously adopted in the analytical study.

The analysis of the first mode indicates that all areas, upon approach of the steady state, move, herewith $q_{0max} = A = 5.25$; $q_{1max} = 2.49$; $q_{2max} = 0.746$; $q_{3max} = 0$ and the resonant frequency $\omega = 0.72$. (Let us recall that under the assumed unit values of the parameters all the reduced parameters have the dimensionless form.)

This given mode is very similar to the mode corresponding to the minimum of the envelope curve of the amplitude-frequency characteristics (see Fig. 6.21), to which $\omega = 0.68$, $A = 5.84$ respond.

The second mode corresponds to the tenfold increase in the force of friction, with the permanent elastic characteristics of the system. At the same time the resonant
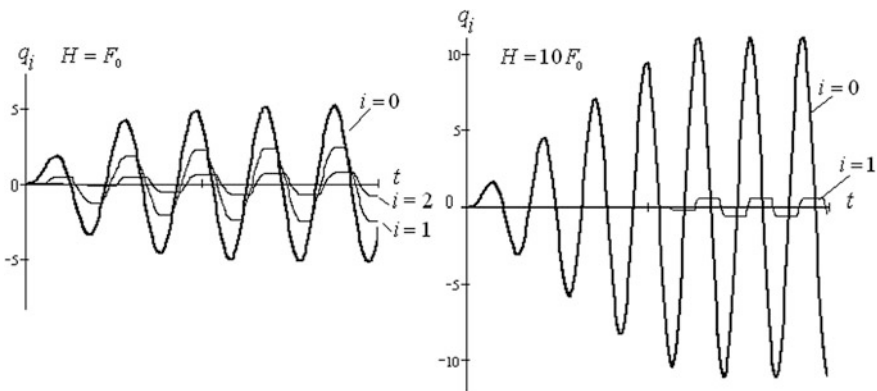

Fig. 6.22 To the analysis of the results of the computer simulation

oscillation amplitude of the mass increased almost two-fold ($A = 11.06$). With the exception of minor oscillations of the first pad ($q_{1max} = 0.526$) other pads are motionless. The resonant frequency, as expected, is close to $p_0 \omega \approx 0.97$ and the resonance amplitude is close to the value $1/(2\delta_0)$ corresponding to the non-deformable rod.

Figure 6.23 shows the graphs $A^0(\omega_*)$ (hatched line), as well as the family of the envelope curves $A^0(\omega_*, \xi)$, obtained by numerical integration of the system. Here $\omega_*(A^0) = p(A^0)$ is the resonant frequency. It is interesting that the amplitude-frequency characteristics, in case of the large number n, are determined with parameter h, which depends on the relationship ξ/f, in which both stiffness and friction properties of the system are simultaneously reflected. Therefore this parameter can serve as the complex criterion for dynamic synthesis of such systems. In the graphs, we can clearly see the presence of a minimum of resonance amplitudes.

A significant difference between the results of the analytical and numerical analysis for small ω_* is natural, since in this case in the "discrete" system the condition of frictional closedness (see above) is violated. This, in particular, is clear in selected areas adjoining the analytic curve, where the transition from movement over two pads to movement over 3 pads takes place.

In the latter case, part of load is balanced with the reaction in the build-in support, whereas in case of analytical approach the number of the frictional elements always corresponds to the total balance of elastic and frictional components.

Under additional perturbations with frequencies, significantly differing from ω, the resonant oscillations can be changed significantly, due to the linearization of dissipative forces. In Fig. 6.24 we can see the family of the amplitude-frequency characteristics, for the four groups of values of h (curves : $1 - h = 0.05$; $2 - h = 0.2$; $3 - h = 0.5$; $4 - h = 1$).

Fig. 6.23 Geometric locus of resonant amplitudes
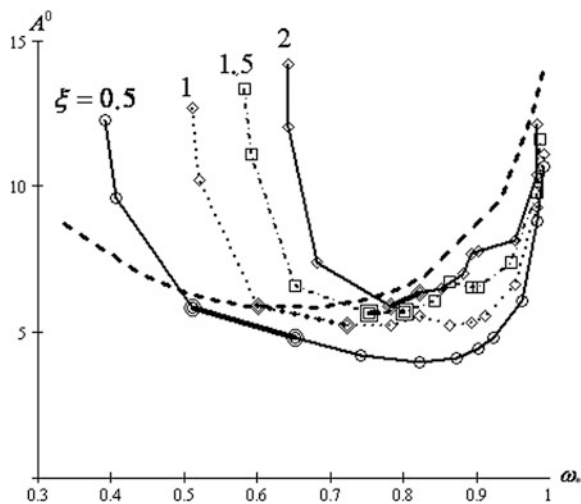
Fig. 6.24 Family AFC, in case of variation of parameter h
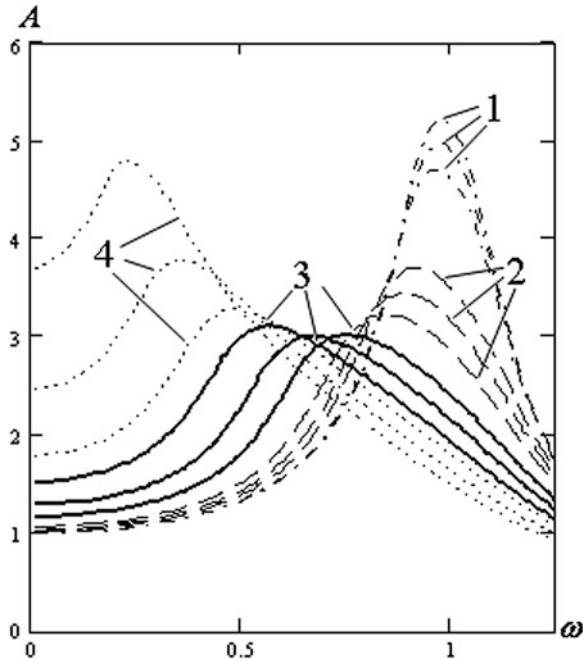
To each of the groups three curves, with different parameter z_i (0.5, 0.8, 1.5), which is the ratio of vibration speed $\dot{q}_i$ to the given speed of the vibrating base, correspond. Herewith, with decrease in z_i the reduced distributed friction force f decreases; therefore parameter h increases, which ultimately leads to the displacement of resonance curves, towards the small values of ω, and to decrease of the minimum of the resonance amplitudes. We will note, in conclusion that the obtained results in addition to the applications, indicated in the start of the chapter, may be useful, when forecasting the level of dissipations in the structural damping, particularly in case of the tightened tapered joints, threaded connections and a number of other similar cases.

Chapter 7
Clearances

7.1 Dynamic Effects and Mathematical Description

The clearance is generally a concomitant factor in any kinematic pair, performing a movable connection of the mechanism's links. In the absence of clearances, even with the ideal manufacturing of the kinematic pair components, the danger of the significant growth of the reactions arises. In particular, this occurs in case of thermal expansion of the parts, that in turn causes an increase in friction and eventually may lead, even, to the complete jamming of the mechanism.

Strictly speaking, the kinematic pair should be considered as a unilateral constraint, to which the moving connections of the links with one-way contact are usually related. Indeed, although the kinematic pair as a whole implements two-way connection, it performs this role only partially: in case of reversals in the clearance, local discontinuities of the kinematic chain arise, which are typical for systems with unilateral constraints. Such connections can be characterized as pseudo-bilateral constraints. In this chapter, we will focus on common approaches to this problem and some of the characteristic dynamic manifestations of the clearances, in the cyclic mechanisms [17, 23, 41, 54, 64, 74, 75, 84–87].

According to the influence on the oscillatory system, we can conditionally select two characteristic cases of the manifestation of clearances. Each case is characterized by the corresponding area of changing parameters and external perturbations.

In the first case the clearance manifests itself as a nonlinear element, which substantially affects the frequency spectrum of free oscillations. *In the second case* the effect of the clearance is mainly manifested as the pulse perturbation in the limited time interval in case of absence of any significant distortion of the frequency spectrum of the initial linear system. This, however, leaves the possibility of multiple collisions leading to vibration impacts, under which the dynamic effect of the clearances is close to the first case. The analysis, carried out using the results obtained in [41], indicates that in practice the interphase transition during the relatively small time interval is accompanied by the so-called quasi-plastic impact.

Herewith, a high-frequency chatter arises, which rather quickly attenuates. The resulting dynamic effect is analogous to a perfectly inelastic impact.

The problem of rational dynamic synthesis of oscillatory systems, taking clearances into account, is particularly important in designing high-speed cyclic mechanisms, with nonlinear position functions since in this class of mechanisms the clearances may lead to large distortions of the given program motion of actuators, as well as to increased noise and vibration activity of the drive. It is often the size of the clearances, which ultimately limits the performance and operating characteristics of many modern technological machines. This makes it significantly important to tighten the precision requirements for their manufacturing and assembly. The restoring force, corresponding to the scheme (Fig. 7.1a) and graph $F(q)$ (Fig. 7.1b), is described as follows:

$$F = c(q - \Delta \mathrm{sign} q)[u(|q| - \Delta)], \tag{7.1}$$

where q is the generalized coordinate; $\Delta = 0.5\, s$; s is the clearance's value; u is the unit function ($u = 0$ at $|q| < \Delta$; $u = 1$ at $|q| \geq \Delta$).

The abrupt change in the unit function corresponds to the moment of restructuring the oscillatory system. Some difficulties are sometimes related to implementation of these switching moments. For example, when using the numerical methods the special "sliding" modes, with a large number of switchings for a limited time interval, may appear [1]. In analytical studies the abrupt character of the dependencies can complicate the analysis and optimization synthesis due to violating the conditions of differentiability in the vicinity of these areas. To eliminate this disadvantage, while preserving the nonlinear properties of the function (7.1), we use an approximation of $|F(q)|\mathrm{sign} q$ with continuous functions $|F(q)|u(q_1)$, where

$$u(q_1) = 0.5 + \pi^{-1} \arctan(Lq_1/\Delta). \tag{7.2}$$

Here $q_1(q) = |q| - \Delta; L \gg 1$ (the number L should be usually several orders greater than q_1/Δ).

In case of alteration of sign x of the function $u(q_1)$, according to (7.2), fairly quickly changes from 0 up to 1, keeping a continuous character. A similar procedure is sometimes referred to as a smooth approximation.

Experiments have shown that a smooth approximation of the clearence is often even more accurate than the initial step function. This apparently has connection
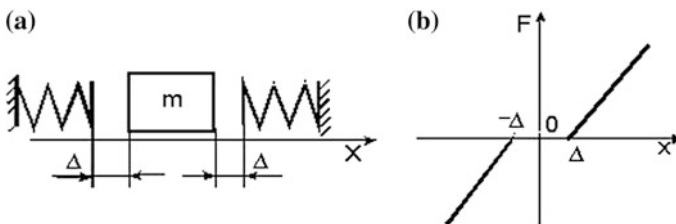

Fig. 7.1 Dynamic model of the elastic element with clearance

with the reduction of contact rigidity of elements of kinematic pair in the vicinity of the switching zones, the presence of a layer of lubricant and other smoothing factors.

7.2 Excitation of Vibrations Due to Impacts in the Kinematic Pairs

We will illustrate the peculiarities of the occurrence of clearances in case of oscillations, using the example of a cyclic mechanism, the dynamic model of which is presented in Fig. 7.2.

In addition to the conventional elements in the model, the element s, corresponding to the clearance, is shown in Fig. 7.2. This model, taking into account (7.1), (7.2), corresponds to the following differential equation:

$$\ddot{q} + k_0^2(2\delta\,k_0^{-1}\dot{q} + q)\Psi(q) = w(t). \tag{7.3}$$

It is assumed here that the absolute coordinate of the output link is represented as $y(\varphi_1) = \Pi(\varphi_1) + q \pm s$, where $\Pi(\varphi_1)$ is the mechanism's position function; $\varphi_1 = \omega t$, ω is the angular velocity of the input link; q is the generalized coordinate; $k_0 = \sqrt{c/m}$ is the "natural" frequency, in the absence of the clearances; $\Psi(q) = F(q)/m$.

Let $w(t) = w_0 \cos \omega t$, where $w_0 = \Pi''_{\max}\omega^2$, which corresponds to the harmonic law of motion of the output link, without oscillations. In particular, such a position function, with sufficient accuracy, corresponds to the motion of a crank-slider mechanism $\Pi \approx r_0(1 - \cos\varphi_1)$. In order to present the result of the analysis, in a more general view, we turn to a new variable, which we will take as "dimensionless time" $\varphi_1 = \omega t$. Then, Eq. (7.3) takes the form

$$\bar{q}'' + N^2(2\delta N^{-1}\bar{q}' + \bar{q})\Psi(\bar{q}) = \cos\varphi_1, \tag{7.4}$$

where $N = k_0/\omega, \delta \approx \psi/(4\pi)$; the line corresponds to the derivative with respect to φ_1; $\bar{q} = q/r_0$ is the dimensionless coordinate.

In Fig. 7.3 we see the graph $\bar{q}(\varphi_1)$, which is derived by solving Eq. (7.4), using the numerical method, with $N = 30$, $\delta = 0.03$, $\bar{s} = s/r_0 = 10^{-3}$. Transiting in the

$$\varphi_1 = \omega t \qquad\qquad y = \Pi \pm s + q$$
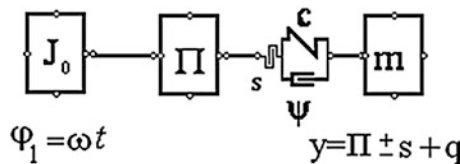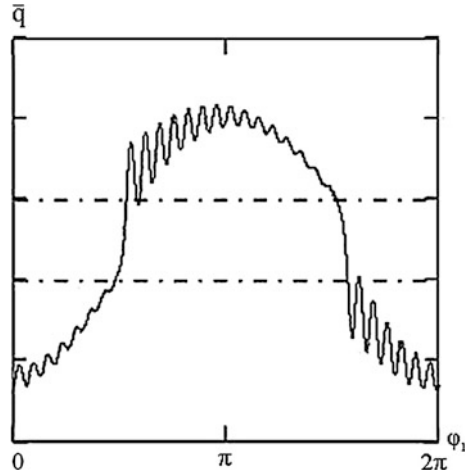
Fig. 7.2 Dynamic model of the cyclic mechanism with the clearance

Fig. 7.3 Graphs $\bar{q}(\varphi_1)$

clearance occurs when $-5 \times 10^{-4} < \bar{q} < 5 \times 10^{-4}$ (the boundaries of this interval are shown in the graph with dash-dot lines). The graph clearly shows a pulsed excitation of oscillations, after each pass through the clearance. As the regime under consideration, after the clearance adjustment, have no repeated collisions, the clearance practically has no influence on the natural frequencies. It is even more clearly seen in the graph of function $\bar{q}''(\varphi_1)$, with the inertial forces, arising in case of oscillations, are proportional to this function (Fig. 7.4).

A completely different picture is observed in case of vibroimpact modes. For example, Fig. 7.5 shows a graph of function $\bar{q}(\varphi_1)$, while preserving the accepted above input data, but with full dynamic unloading and single excitation pulse.

In this mode the oscillation's frequency k is substantially lower than value k_0. To estimate the frequency k, in such cases, we can use the method of harmonic linearization (see Appendix), according to which $k^2(A) \approx k_0^2[(1 - 4\Delta/(\pi A)]$, where A is the oscillation's amplitude.

Fig. 7.4 Graphs $\bar{q}''(\varphi_1)$
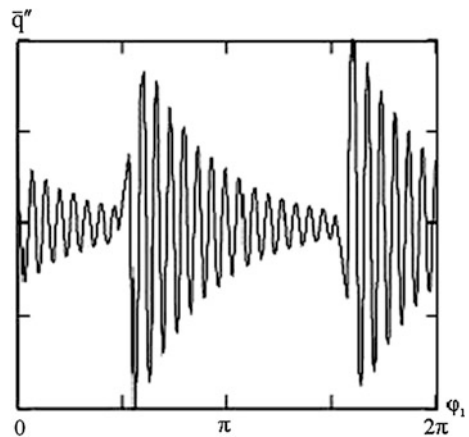
Fig. 7.5 Dynamic effect from repeated impacts
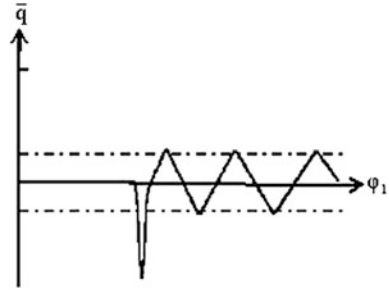
It should, however, be noted that this formula can give a large error. This is due to the significant difference of the vibro-impact regimes from the harmonic oscillations. In such cases the more effective method of the estimation of natural frequencies, is harmonic linearization, with respect to the force, since the restoring force is rather accurately described by the function $F = F_0 + F_1 \sin \omega t$. If we use the coefficients of harmonic linearization, with respect to force [5], the series connection of an element c_0, with the clearance $s = 2\Delta$, is equivalent to the elastic element, the compliance of which is $e_* = c_*^{-1} = e_0 + e_\Delta$, where

$$
\left.
\begin{aligned}
&e_0 = c_0^{-1}; \\
&e_\Delta = \frac{4\Delta}{\pi F_1} \sqrt{1 - \left(\frac{F_0}{F_1}\right)^2} \text{ at } F_1 \geq F_0; \\
&e_\Delta = 0 \text{ at } F_1 \leq F_0.
\end{aligned}
\right\}
\tag{7.5}
$$

The possible arising of such vibro-impact modes should be excluded or limited at the stage of machine creation. In the mode under consideration, in connection with the presence of clearances, also of interest is the negative effect of full dynamic unloading (see below).

Hereafter, we will present some analytical estimations and dynamic criteria [73]. We will analyze the dynamic effect of reversals in the clearance, using the example of the cam mechanism (Fig. 7.6a), which implements the position function of the cam follower $\Pi(\varphi)$ (Fig. 7.6b). Let us draw two curves on the graph of the position function $\Pi(\varphi)$, shifted on the reduced size of the clearance s (Fig. 7.6b, curves 1, 2). Suppose when $\varphi = \varphi_*$, at point B detachment from curve 1 takes place, and at point B' on curve 2 the restoration of the kinematic contact occurs. We will assume that the rotation angle $\Delta\varphi = \omega\Delta t$, corresponding to the zone of the "free flight", is small. In this case we can reasonably assume that the motion in this section occurs with the constant speed, which is equal to the separation velocity at point B.

According to the differential equation (7.3), we will distinguish two phases of motion. In the *first phase,* the clearance is selected, consequently, exactly as the constant $y = \Pi(\varphi) + q$. In the *second phase,* when passing through the small clearance, the output link moves due to inertia almost with a constant speed. We
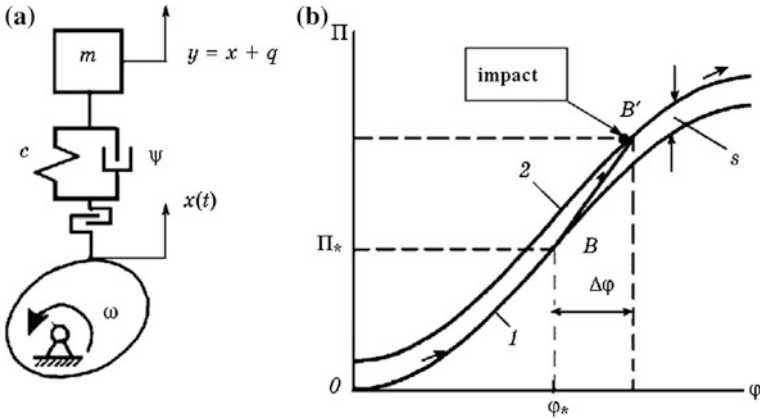
Fig. 7.6 To the determination of the dynamic effect on the transition across a clearance

will define the level of additional oscillations, excited in case of recovery of the kinematic contact. Then

$$\Pi(\varphi_1^* + \Delta\varphi_1) + s = \Pi(\varphi_1^*) + \Pi'(\varphi_1^*)\Delta\varphi_1, \qquad (7.6)$$

where φ_1^* is the rotation angle of the input link, at the instant of change in the reaction's sign in the kinematic pair; s is the value of the clearance.

Then, introducing the function $\Pi(\varphi_1^* + \Delta\varphi_1)$, in the vicinity of φ_1^* as in the truncated Taylor series, on the basis of (7.6) we get

$$\frac{1}{6}\Pi'''_*\Delta\varphi_1^3 + \frac{1}{2}\Pi''_*\Delta\varphi_1^2 + s = 0. \qquad (7.7)$$

Here Π''_*, Π'''_* correspond to argument φ_1^*.

In modern high-speed cyclic mechanisms, the dynamic load, caused by kinematic excitation, is usually much greater than the force of resistance, so the transition across the clearance practically occurs when $\Pi''_* = 0$. Then, according to (7.7)

$$\Delta\varphi_1 = \sqrt[3]{6s/|\Pi'''_*|}. \qquad (7.8)$$

Here we have taken into account that $\Pi'''_* < 0$.

When restoring kinematic contact, the jump of the first transfer function $\Delta\Pi'$, takes place, which according to (7.8) is defined as follows:

$$\Delta\Pi' = \sqrt[3]{4,5s^2|\Pi'''|}. \qquad (7.9)$$

As shown in Sect. 4.1, in this case we have a hard impact. Similarly, the perturbations associated with jumps $\Delta\Pi''$ and $\Delta\Pi'''$ can be taken into account. We will introduce the parameter $\xi = |\Delta y''|_{\max}/|\Pi''|_{\max}$, equal to the ratio of the

additional extreme acceleration (after adjustment of the clearance), to the extreme of the ideal acceleration. In case of a single impact we get

$$\xi = \Pi_*''' \sqrt{(4,5)^{2/3} \beta_1^4 N^2 + N^{-2}}, \qquad (7.10)$$

where $\beta_1 = \sqrt{[3]s / |\Pi_*'''|}$, $N = k_0 / \omega$.

The family of curves $\xi(N, \beta_1)$, with $\beta_1 = 10^{-3}$ (curve 1), $\beta_1 = 5 \times 10^{-4}$ (curve 2), $\beta_1 = 10^{-4}$ (curve 3) is represented in the Fig. 7.7. Parameter β_1 is an important dynamic criterion. On the basis of (7.10) the parameters of the system, satisfying the requirement $\xi \leq \xi_*$, where ξ_*, is the allowable value of the additional acceleration level, caused by the clearance, can be determined. (Usually- $\xi_* < 0.1 \div 0.2$).

To exclude the possibility of occurrence of vibro-impact modes during clearance adjustment, it is very important to eliminate the repeated collisions. Repeated collisions may occur with a certain phase shift with respect to the angle φ_1^*, corresponding to the discontinuity of the kinematic connection, in case of "input" into the clearance: $\Delta\varphi = \Delta\varphi_1 + \Delta\varphi_2$ (see Fig. 7.3). The value of $\Delta\varphi_1$ is determined using formula (7.8) and $\Delta\varphi_2 \approx \Delta t_2 / \omega = \alpha N^{-1}$, where the time interval Δt_2 corresponds to the first minimum of the function $\bar{q}$ after the clearance adjustment; $\alpha \approx 4.45 \div 6.28$ [41, 66].

On the basis of (7.8)–(7.10) we can show that in the first approximation, the following condition must be satisfied:

$$\beta_2 = \beta_1 N^{-1} < 0.3 \exp(\delta\alpha) \left[1 + \sqrt{1 + 29.4 \exp(-\delta\alpha)} \right]. \qquad (7.11)$$

Fig. 7.7 Determination of the additional accelerations, excited by a single reversal in the clearance
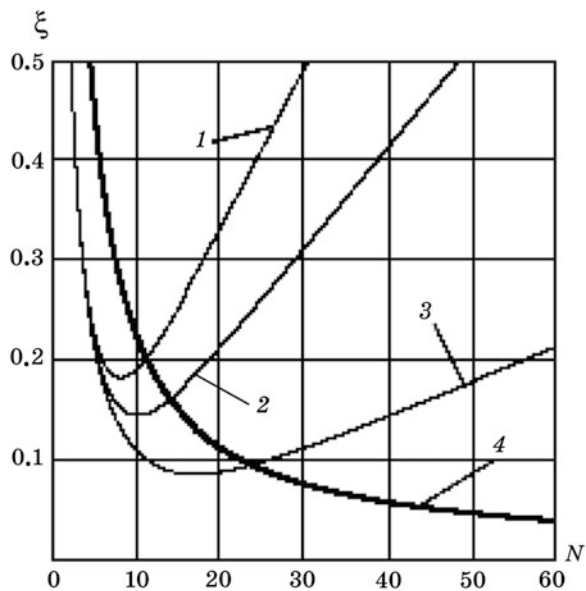
The formula (7.11) takes into account the damping of oscillations in a small period of time Δt_2. However, the analysis shows that $\exp(\delta\alpha) \approx 1$. Then, $\beta_2 < \beta_2^*$, where $\beta_2^* \approx 1.9$. In Fig. 7.7 the points, located below the curve 4, correspond to this condition.

7.3 Excitation of Vibrations During Shockless Reversals in Clearance—Joint. Pseudo-Impact

Dynamic Model The development of criteria, on the basis of which the dynamic effects, accompanying the impact-free shift into clearances, are predicted, are discussed in many researches, a partial review of which is given in [16, 17, 23, 54, 90]. At the initial stage, the main objective of this research was to use the results of the kinetostatic model analysis to ensure the continuity of the kinematic contact in the joint. Further, the elastic properties of the contact were taken into account. In particular, in [17] it was proposed that the criterion, called the index of the impact prediction IPN (Impact Prediction Number), in which the contact stiffness of the joint and the parameters of an elliptical trajectory were taken into account. However, this criterion doesn't reflect many essential dynamic factors, such as interaction of the two oscillating contours, predetermining pulsation of the "natural" frequencies and the possibility of "negative dissipation", in case of which a local buildup of the system occurs, etc. It is assumed that the most significant original prerequisite, of favorable conditions for reversals in clearance, is the absence of the kinematic contact violations. In [74, 79, 85, 86] a new model of the clearance is proposed, in which the comprehensive accounting of the "pendulum" motion, in the joint and elastodissipative properties of the system, are performed. This model is used below for designing criteria evaluations of the studied dynamic effect in case of the quasi-elliptic reaction's locus in the joint.

The simplest model of the joint (model DM1) is represented in Fig. 7.8a. Let a body with mass m, associated with point O, performs, together with the joint's finger (point O'), a plane program motion.

Thus, $OO' = 0.5\,s$, where s is the value of the clearance. So, in each joint of the kinematic chains, there appears an additional weightless link adding one degree of freedom. This link represents the unilateral constraint, in the normal direction, so in this case the analogy with the thread is more appropriate.

Let us assume that the normal and tangential stiffness coefficients of the pivot pin are equal to c. The reduced stiffness of these components may vary slightly by taking into account the contact stiffness in the joint, however, as the analysis shows the bending stiffness of the finger joint usually dominates. In the coordinate system, associated with the translational program motion, model DM1 takes the form of a pendulum of length $0.5\,s$, the support of which is elastically connected to the body (Fig. 7.8b). If $c \to \infty$, the "natural" frequency of the pendulum is equal to
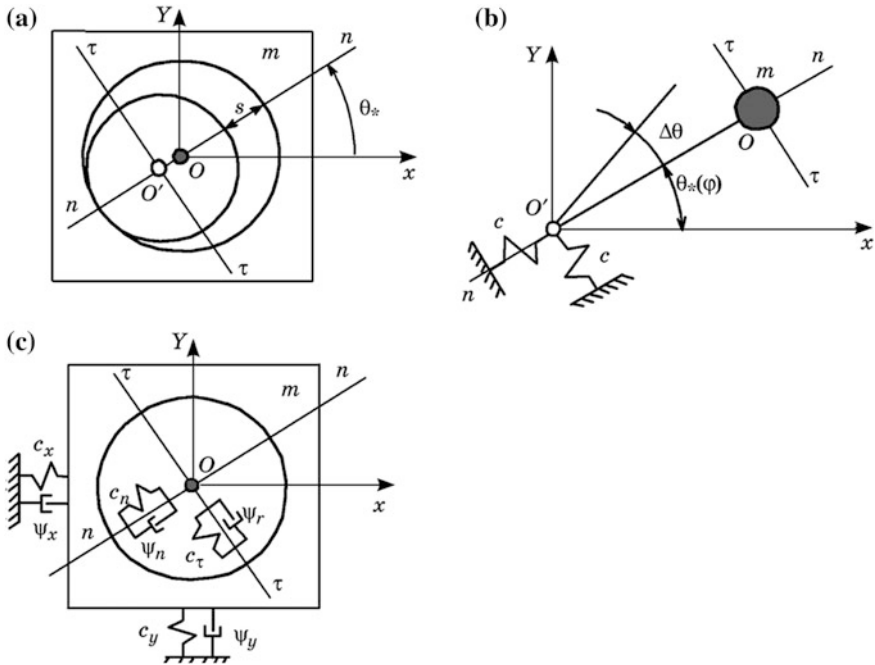
Fig. 7.8 Modification of the dynamic models, in case of absence of the kinematic contact discontinuities

$$k_0 = \sqrt{2|F_*(\varphi)/(ms)|}. \qquad (7.12)$$

Here $F_*(\varphi)$ is the reaction between the finger and the body, $\varphi = \omega t$ is the rotation angle of the mechanism's input link. (Usually in the first approximation we can assume $\varphi \approx \omega t$, where $\omega = d\varphi/dt = \text{const}$).

The position of the pendulum, in the plane, is characterized by the angle $\theta = \theta_*(\varphi) + \Delta\theta$, where $\theta_*(\varphi)$ is the "slow" component, defined as $\theta_* = \arctan(F_y^*/F_x^*)$ and $\Delta\theta$ is the "fast" component, arising in case of implementation of the additional degree of freedom, due to the pendulum's oscillations. (Here F_x^*, F_y^* are the corresponding projections of the reaction F^*). Often the angle θ, is determined at the kinetostatic level that corresponds to the assumption $\theta = \theta_*$ and $\Delta\theta = 0$. However, in this case we ignore the possibility of oscillations around the centered mass m positions, thereby we eliminate the additional degree of freedom, associated with the "pendulum's" movement in the joint at the clearance. When $c \neq \infty$, the reduced tangential component of the coefficient of stiffness c_τ, corresponds to the serial connection of the element c and $c_{\tau 0} = 2|F|/s$. In the corresponding dynamic model DM 2 (Fig. 7.8c) the normal and tangential components of stiffness can be expressed as follows

$$c_n = c; \quad c_\tau = c|F_*(\varphi)|/[0.5cs + |F_*(\varphi)|]. \tag{7.13}$$

The dissipative components (ψ are the dissipation coefficients) and the elasto-dissipative elements c_x, ψ_x and c_y, ψ_y, corresponding to the connection with the body frame, are taken into account in the model DM 2. The necessity to take these components into account appears, for example, in case of increased compliance of the links and guides in various modifications of the lever mechanisms. When $c_x \to \infty$, $c_y \to \infty$, the potential energy is equal to

$$V_1 = 0.5(c_n\Delta_n^2 + c_\tau\Delta_\tau^2), \tag{7.14}$$

where Δ_n, Δ_τ are the deformations along the axis $n - n$ and $\tau - \tau$.

Taking into account that $\Delta_n = \Delta x_1 \cos \theta_* - \Delta y_1 \sin \theta_*$, $\Delta\tau = \Delta x_1 \sin \theta_* + \Delta y_1 \cos \theta_*$, we have $V_1 = 0.5(c_{xx}\Delta x_1^2 + c_{yy}\Delta y_1^2 + +2c_{xy}\Delta x\Delta y)$, where $\Delta x_1, \Delta y_1$ are the projections of the deformations Δ_n, Δ_τ; $c_{yy} = c_n \sin^2 \theta_* + c_\tau \cos^2 \theta_*$; $c_{xy} = 0.5 \sin 2\theta_*(c_\tau - c_n)\Delta x\Delta y$.

In the absence of the clearance $(s = 0)$, according to (7.13), $c_\tau = c$. Then, $c_{xx} = c_{yy} = c$, $c_{xy} = 0$. In this case the reduced stiffness coefficients don't depend on φ. When $F_* \to 0$, we have $c_\tau \to 0$. When $c_x \neq 0$, $c_y \neq 0$

$$V = 0.5\left[\left(\frac{\partial V_1}{\partial \Delta x_1}\right)^2 (c_x^{-1} + c_{xx}^{-1}) + \left(\frac{\partial V_1}{\partial \Delta y_1}\right)^2 (c_y^{-1} + c_{yy}^{-1})\right]. \tag{7.15}$$

We will adopt the positional components of the dynamic errors $\Delta x = q_1$ and $\Delta y = q_2$ as generalized coordinates. By this term we will mean the variations, determined with generalized positional coordinates, included in the potential energy expression. Thus, the absolute motion x, y consists of translational motion $x^0 = x_*^0 + 0.5s \cos \theta_*$, $y^0 = y_*^0 + 0.5s \sin \theta_*$ (cyclic generalized coordinates) and relative motion $(\Delta x, \Delta y)$.

Furthermore, according to (7.13)–(7.15), we will present the expression for potential energy in the form of the following quadratic equation:

$$V = 0.5(c_{11}q_1^2 + c_{22}q_2^2 + 2c_{12}q_1q_2). \tag{7.16}$$

Here

$$c_{11} = \frac{c_x^2}{D^2}\left\{\frac{c_y^2 c_y}{c_y^*} + \frac{\left[c_{xx}(c_y + c_{yy}) - c_{xy}^2\right]^2}{c_x^*}\right\}; \quad c_{22} = \frac{c_y^2}{D^2}\left\{\frac{c_x^2 c_{xy}^2}{c_x^*} + \frac{\left[c_{yy}(c_x + c_{xx}) - c_{xy}^2\right]^2}{c_y^*}\right\};$$

$$c_{12} = \frac{c_x c_y c_{xy}}{D^2}\left\{\frac{c_x\left[c_{xx}(c_y + c_{yy}) - c_{xy}^2\right]}{c_x^*} + \frac{c_y\left[c_{yy}(c_x + c_{xx}) - c_{xy}^2\right]}{c_y^*}\right\},$$

$$\tag{7.17}$$

where $c_x^* = (c_x^{-1} + c_{xx}^{-1})^{-1}$; $c_y^* = (c_y^{-1} + c_{yy}^{-1})^{-1}$; $D = (c_x + c_{xx})(c_y + c_{yy}) - c_{xy}^2$.

The system of differential equations for model DM 2 has the form:

$$\left.\begin{array}{l} \ddot{q}_1 + (2n_{11}\dot{q}_1 + 2n_{12}\dot{q}_2 + k_{11}^2 q_1 + k_{12}^2 q_2)\Psi_1(q_1, q_2) = w_1(t); \\ \ddot{q}_2 + (2n_{21}\dot{q}_1 + 2n_{22}\dot{q}_2 + k_{21}^2 q_1 + k_{22}^2 q_2)\Psi_2(q_1, q_2) = w_2(t), \end{array}\right\} \tag{7.18}$$

where $k_{ij}^2 = c_{ij}/m$; $w_1(t) = Q_1(t)/m$; $w_2(t) = Q_2(t)/m$; n_{ij} are the dissipation coefficients (see below); $Q_1(t), Q_2(t)$ are the generalized forces; Ψ_i are the unit functions, vanishing when $\Delta_n \leq 0$, i.e. in case of the violation of the kinematic contact in the joint.

Let us note here that, strictly speaking, the system of Eq. (7.18) is nonlinear, even in the absence of the kinematic contact discontinuities, because the stiffness coefficients, according to (7.13), depend on the reaction in the kinematic pair. However, with the selection of the slow component of this reaction F_* and the subsequent linearization in its vicinity, we transform the nonlinear differential equations to the form of linear equations, with variable coefficients. Thus, $n_{ij} = n_{ij}(\varphi)$ and $k_{ij} = k_{ij}(\varphi)$, where $\varphi = \omega t$.

We transform the system of differential equations (7.18) to the dimensionless form. For this purpose we introduce "dimensionless" time $\varphi = \omega t$ and dimensionless coordinates $\bar{q}_i = q_i/r$, where r is the normalization parameter; it is convenient to take the radius of the crank of the input link of the lever mechanism, as this parameter. Let us define the following notation:

$\eta_0^2 = c/(m\omega^2)$; $P_{11} = c_{11}/(m\omega^2)$; $P_{22} = c_{22}/(m\omega^2)$; $P_{12} = c_{12}/(m\omega^2)$; $\beta_{11} = \vartheta_1\pi^{-1}\sqrt{P_{11}}$; $\beta_{22} = \vartheta_2\pi^{-1}\sqrt{P_{22}}$; $\Delta = 0.5s/r$. Then

$$\left.\begin{array}{l} \bar{q}_1'' + (\beta_{11}(\varphi)\bar{q}_1' + P_{11}(\varphi)\bar{q}_1 + P_{12}(\varphi)\bar{q}_2)\Psi_1(\bar{q}_1, \bar{q}_2) = f_1(\varphi); \\ \bar{q}_2'' + (\beta_{22}(\varphi)\bar{q}_2' + P_{21}(\varphi)\bar{q}_1 + P_{22}(\varphi)\bar{q}_2)\Psi_2(\bar{q}_1, \bar{q}_2) = f_2(\varphi), \end{array}\right\} \tag{7.19}$$

where $(\ )' = d/d\varphi$, $f_i(\varphi) = w_i/(m\omega^2 r)$. (A more strict accounting of the dissipative components, see Chap. 6).

When $c_x \gg c$, $c_y \gg c$

$$\left.\begin{array}{l} P_{11}(\varphi) = P_{11}^0(\varphi) = \eta_0^2\left[\cos^2\theta_*(\varphi) + \chi_1\sin^2\theta_*(\varphi)\right]; \\ P_{22}(\varphi) = P_{22}^0(\varphi) = \eta_0^2\left[\sin^2\theta_*(\varphi) + \chi_1\cos^2\theta_*(\varphi)\right]; \\ P_{12}(\varphi) = P_{12}^0 = -0.5(1 - \chi_1)\sin 2\theta_*(\varphi), \end{array}\right\} \tag{7.20}$$

where $\chi_1 = |F_*|/(\eta_0^2\Delta + |F_*|)$.

Pulsation of the "Natural" Frequencies, Due to Reversals in the Clearance

When determining the dimensionless "natural" frequencies $\eta_i(\varphi) = p_i(\varphi)/\omega$ (p_i is the "natural" frequency), we exclude the small effect of dissipative forces from our consideration. In this case the formal frequency equation has the following form

$$\det \begin{pmatrix} P_{11}(\varphi) - \eta^2 & P_{12}(\varphi) \\ P_{21}(\varphi) & P_{22}(\varphi) - \eta^2 \end{pmatrix} = 0. \tag{7.21}$$

Hence

$$\eta_{1,2} = \sqrt{0.5(P_{11} + P_{22}) \mp \sqrt{0.25(P_{11} - P_{22})^2 + P_{12}^2}}.$$

(Here and hereunder, argument φ, in the corresponding functions, is omitted.)

To specify the results of the analysis, we will take the quasi-elliptic configuration of the hodograph of reaction in the joint. Such a situation, in particular, occurs in case of kinematic excitation in the slider-crank mechanism, as well as in other lever mechanisms with the trajectory of progressive motion of the output link, which is close to the elliptical one. Let the elliptical trajectory of the mass m be described with dependencies $x_0^* = r \cos \varphi$, $y_0^* = \alpha r \sin \varphi$. In this case the right-hand sides of the Eq. (7.19) take the form

$$f_1(\varphi) = \cos \varphi + 0.5\bar{s}[\theta'^2_*(\varphi) \cos \theta_*(\varphi) + \theta''_* \sin \theta_*(\varphi)];$$
$$f_2(\varphi) = \alpha \sin \varphi + 0.5\bar{s}[\theta'^2_*(\varphi) \sin \theta_*(\varphi) - \theta''_*(\varphi) \cos \theta_*(\varphi)].$$

The graphs of the dimensionless "natural" frequencies $\eta_1(\varphi, \alpha)$ and $\eta_2(\varphi, \alpha)$ when $\eta_0 = 30$, $\bar{s} = s/r = 10^{-3}$, $c_x/c \gg 1, c_y/c = 5$, $\alpha = 0.05$ (curve 1), $\alpha = 0.2$ (curve 2), $\alpha = 0.5$ (curve 3) are presented in Fig. 7.9.

In the graphs, we can see the decrease in the pulsation of the "natural" frequencies, with the increase in parameter α, which characterizes the ratio of the amplitudes of reaction along the axis x and y (see above). The role of decrease in the lowest frequency η_1, is especially important. The physical origin of this effect is due to the "pendulum's" frequency, so, to estimate the lower frequency with some margin, we can use the following relationship:
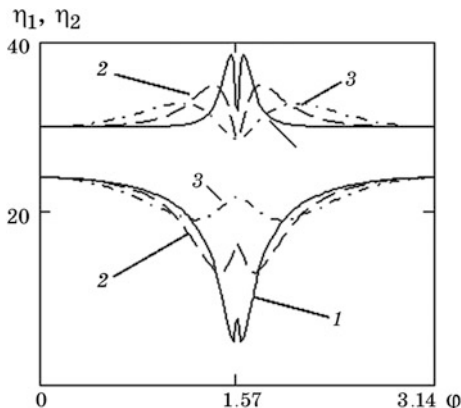
$$\min \eta_1 \approx \sqrt{c_\tau/m}/\omega.$$

The decisive role, in the formation of the studied dynamic effect, is played by the function $\theta_*(\varphi)$ (see Fig. 7.8b) and its derivatives, represented by the following dependencies:

$$\theta_*(\varphi) = \arctan(F_*^y/F_*^x); \; \theta_*'(\varphi) = [F_*^x(F_*^y)' - F_*^y(F_*^x)']/F_*^2;$$
$$\theta''(\varphi)_* = [F_*^x(F_*^y)'' - F_*^y(F_*^x)'']/F_*^2 - 2[F_*^x(F_*^y)' + F_*^y(F_*^x)'][F_*^x(F_*^y)' - F_*^y(F_*^x)']/F_*^4, \tag{7.22}$$

where $F_* = \sqrt{(F_*^x)^2 + (F_*^y)^2}$.

Fig. 7.9 Graphs of the dimensionless frequencies $\eta_1(\varphi, \alpha), \eta_2(\varphi, \alpha)$

For the adopted elliptic locus of the reaction's characteristics, on the basis of (7.22), we get. $\theta'_*(\varphi) = \alpha/B(\varphi); \theta''_*(\varphi) = \alpha(1 - \alpha^2) \sin 2\varphi/B^2(\varphi)$, where $B(\varphi) = \alpha^2 \sin^2 \varphi + \cos^2 \varphi$.

The analysis shows that for small values of α the variation of θ_*, in the interval of reversals in the clearance ($\varphi \approx \pi/2, 3\pi/2$), is close to a jump. Figure 7.10 shows the graphs $\theta'_*(\varphi, \alpha)$ and $\theta''_*(\varphi, \alpha)$. The function θ'_* reaches its maximum $\theta'_{*\max} = \alpha^{-1}$ at $\varphi = \pi/2$ and $\varphi = 3\pi/2$. It can be shown that the extreme values of the function θ''_* occur at values $\varphi = \varphi_*$ that are determined as per the following equation

$$(1 - \alpha^2) \cos^2 2\varphi_* - (1 + \alpha^2) \cos 2\varphi_* + (1 - \alpha^2) = 0. \qquad (7.23)$$

Taking into account that the extremes of θ''_*, are located in the small vicinity of values 0.5π and 1.5π on the basis of (7.23), we have $\varphi_* = j\pi/2 \pm \Delta\varphi_1 (j = 1, 3)$ when $\Delta\varphi_1 \approx 0.64\alpha$.

An additional source of excitation is the rotating, weightless, link of length $0.5\,s$. For small α, in the clearance area, the lowest "natural" frequency abruptly decreases. At the same time the real time of the link's rotation at an angle π may be commensurate with $(0.25 \div 0.3)$ of the free oscillations' period (at the lowest frequency), which is substantially equivalent to the impact (see Sect. 4.1). The significant role, in the formation of the dynamic effect, is also played by the non-stationary nature of the mode factors and the values of the dimensionless "natural" frequencies $\eta_1(\varphi), \eta_2(\varphi)$, due to local violations of the dynamic stability in the finite interval of the kinematic cycle (see Sect. 5.3). To eliminate this undesirable effect, leading to an increase in the maximum vibration acceleration, the following conditions must be satisfied: $\vartheta_r > \vartheta_r^*(\varphi) = 3\pi(d\eta_r/d\varphi)/\eta_r^2 (r = 1, 2)$. Here $\vartheta_r, \vartheta_r^*(\varphi)$ are reduced to form r logarithmic decrements and its critical values.

Furthermore, when α is small the effect of "parametric impulse" manifests, in case of which, the abrupt change of the "kinetostatic" equilibrium position, can occur (see Sect. 5.5) [16, 61, 62, 85]. The analysis shows that the above mentioned
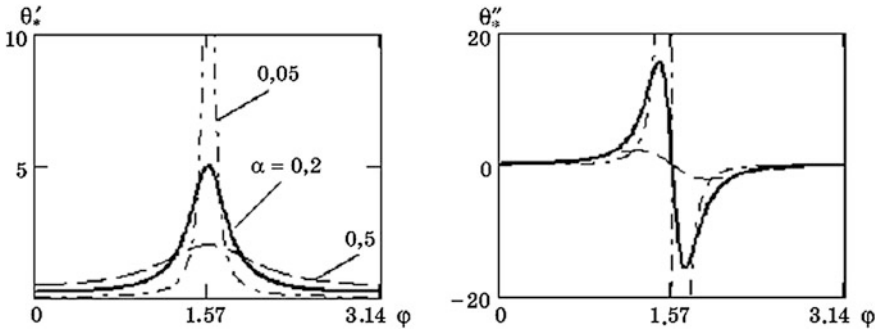
Fig. 7.10 Graphs $\theta'_*(\varphi, \alpha), \theta''_*(\varphi, \alpha)$

causes can lead to the seeming paradox, when the accelerations, in case of pseudo impact (i.e. in the absence of the kinematic contact discontinuities in the joint), may be higher than in case of discontinuity in the kinematic contact. Therefore, when solving the problem of reducing the vibration activity of the lever mechanisms, one should not limit to the elimination of collisions.

7.4 Mathematical Models for the Study of Vibrations, Excited by Pseudo-Impacts in the Clearances

7.4.1 Crank-and-Rocker Mechanism

Set of Differential Equations Here we will consider a dynamic model of the crank-and-rocker mechanism, taking into account the clearances and elastiodissipative characteristics in the joints A and B. In the kinematic plan, as well as in many studies, the clearance is simulated as the weightless link, the length of which is equal to half of the clearance: $A'A'' = \delta_A = 0.5\Delta; B'B'' = \delta_B = 0.5\Delta_2$, where Δ_i is the value of the clearance (Fig. 7.11). Angles φ_i characterize the current position of the moving links and angles θ_i characterize the position of the weightless links of $A'A''$ and $B'B''$, determined as per the direction of the reaction, between contiguous links.

Current dynamic model corresponds to the oscillatory system with four degrees of freedom, in which the generalized coordinates are taken as the dynamic errors, caused by the deformations of the joints A and B, namely the deflection of the coordinates of the mass center of the connecting rod $\Delta x_{s2} = q_1, \Delta y_{s2} = q_2$, the angular positions of the connecting rod $\Delta\varphi_2 = q_3$ and the balancing arm $\Delta\varphi_3 = q_4$.

The analysis, of the actual structures of the lever mechanisms, shows that the coefficients of stiffness of the joints in the normal direction, are, substantially, defined by the bending stiffness of the joint's fingers, wherein the contact stiffness usually plays a minor role. According to (7.13), the characteristics of the restoring moment,

Fig. 7.11 A kinetostatic model with pseudo impact
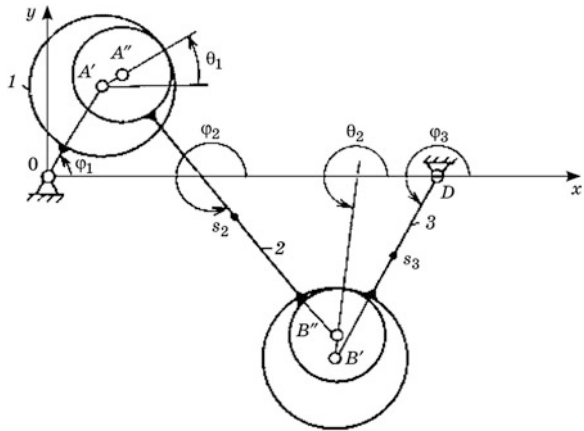
arising when angles θ_i deviate from the values θ_{i*}, obtained by the kinetostatic analysis, significantly affect the stiffness in the tangential direction.

In case of minor oscillations

$\Delta\theta_i = \theta_i - \theta_{i*} \approx \sum\limits_{j=1}^{L} (\partial\theta_i/\partial q_j)_{q_j=0} q_j$ ($i = 1, 2$). Thus, the system of differential equations takes the form:

$$
\left.
\begin{aligned}
&\tilde{m}_2\tilde{q}_1'' + \sum_{i=1}^{4}\beta_{1i}\tilde{q}_i' + \sum_{i=1}^{4}\zeta_{1i}\tilde{q}_i = \tilde{Q}, \\
&\tilde{m}_2\tilde{q}_2'' + \sum_{i=1}^{4}\beta_{21}\tilde{q}_i' + \sum_{i=1}^{4}\zeta_{21}\tilde{q}_i = \tilde{Q}_2, \\
&\tilde{m}_2\rho_2^2 l_1^{-2}\tilde{q}_3'' + \sum_{i=1}^{4}\beta_{3i}\tilde{q}_i' + \sum_{i=1}^{4}\zeta_{3i}\tilde{q}_i = \tilde{Q}_3, \\
&\rho_3^2 l_1^{-2}\tilde{q}_4'' + \sum_{i=1}^{4}\beta_{4i}\tilde{q}_i' + \sum_{i=1}^{4}\zeta_{4i}\tilde{q}_i = \tilde{Q}_4,
\end{aligned}
\right\}
\tag{7.24}
$$

where

$\rho_2^2 = J_{2s}/m_2;\quad \rho_3^2 = J_{3D}/m_3;\quad ()' = d/d\varphi_1;\quad \tilde{q}_{1,2} = q_{1,2}/l_1;\quad \tilde{q}_{3,4} = q_{3,4};$

$\tilde{m}_2 = m_2/m_3;\quad \tilde{Q}_1 = -\tilde{m}_2\tilde{x}_{s2*}'';\quad \tilde{Q}_2 = -\tilde{m}_2\left(\tilde{y}_{s2*}'' + g\omega_1^{-2}l_1^{-1}\right);\quad \tilde{Q}_3 = -\tilde{m}_2\rho_2^2 l_1^{-2}\varphi_{2*}'';$

$\tilde{Q}_4 = -\rho_3^2 l_1^{-2}\varphi_{3*}'' + M_3/\left(m_3\omega_1^2 l_1^2\right) - g\tilde{l}_{31}l_1^{-1}\omega_1^{-2}\cos\varphi_{3*};\quad \tilde{l}_{31} = DS_3/l_1;\quad \tilde{x}_{s2*} = x_{s2*}/l_1;$

$\tilde{y}_{s2*} = y_{s2*}/l_1; g = 9.81$ m · s^{-2}; M_3 is the external moment applied to the link 3; ζ_{ji}, β_{ji} are normalized quasi-elastic and dissipative coefficients; $\dot{\varphi}_1 = \omega_1 = \text{const}$; m_2 is the connecting rod mass; J_{2s}, J_{3D} are the inertial moments of links 2 and 3,

with regard to the corresponding points, $\ell_{21} = A''S_2$; $\ell_{22} = B''S_2$. (An asterisk denotes the ideal coordinate values, realized in the infinitely rigid joints.)

To obtain comparable results, when varying the parameters of the system, the stiffness $c_0 = J_{3D}p_0^2/l_3^2$, where p_0 is the maximum value of the "natural" frequency, which is realized at $|\sin(\varphi_{3*} - \varphi_{2*})| = 1$, weightless coupler and crank, and in the absence of clearances, was accepted as the base value for the normalization of the quasi-elastic coefficients.

For this case c_0 means the reduced stiffness coefficient of joints A and B. Let us introduce the following conditional notation:

$$h = c_A^n/\zeta_B^n; \quad \zeta_A^n = c_A^n/c_0 = 1 + h; \quad \zeta_B^n = c_B^n/c_0 = (1+h)/h;$$
$$\zeta_A^\tau = c_A^\tau/c_0; \quad \zeta_B^\tau = c_B^\tau/c_0.$$

With (7.13) we have

$$\zeta_{A,B}^\tau = \tilde{R}_{A,B}\zeta_{A,B}^n / \left(\tilde{R}_{A,B} + \zeta_{A,B}^n \eta_0^2 \tilde{\delta}_{A,B}\rho_3^2 l_3^{-2}\right),$$

where $\tilde{R}_{A,B} = |R_{A,B}|/(\omega_1^2 m_3 l_1)$; $\quad \tilde{\delta}_{A,B} = \delta_{A,B}/l_1$; $\quad \eta_0 = p_0/\omega_1$.

The coefficients $\zeta_{ji} = \zeta_{ij}$ are represented below.

$$\zeta_{11} = \left(\zeta_A^n \cos^2\theta_{1*} + \zeta_A^\tau \sin^2\theta_{1*} + \zeta_B^n \cos^2\theta_{2*} + \zeta_B^\tau \sin^2\theta_{2*}\right)\rho_3^2\eta_0^2 l_3^{-2};$$

$$\zeta_{12} = \zeta_{21} = 0.5\left[\left(\zeta_A^n - \zeta_A^\tau\right)\sin 2\theta_{1*} + \left(\zeta_B^n - \zeta_B^\tau\right)\sin 2\theta_{2*}\right]\rho_3^2\eta_0^2 l_3^{-2};$$

$$\zeta_{13} = \left[-\zeta_A^n \tilde{l}_{21}\cos\theta_{1*}\sin(\theta_{1*} - \varphi_{2*}) + \zeta_A^\tau \tilde{l}_{21}\sin\theta_{1*}\cos(\theta_{1*} - \varphi_{2*})\right.$$
$$\left. + \zeta_B^n \tilde{l}_{22}\cos\theta_{2*}\sin(\theta_{2*} - \varphi_{2*}) - \zeta_B^\tau \tilde{l}_{22}\sin\theta_{2*}\cos(\theta_{2*} - \varphi_{2*})\right]\rho_3^2\eta_0^2 l_3^{-2};$$

$$\zeta_{14} = \left[-\zeta_B^n \tilde{l}_3 \cos\theta_{2*}\sin(\theta_{2*} - \varphi_{3*}) + \zeta_B^\tau \tilde{l}_3 \sin\theta_{2*}\cos(\theta_{2*} - \varphi_{3*})\right]\rho_3^2\eta_0^2 l_3^{-2};$$

$$\zeta_{22} = \left(\zeta_A^n \sin^2\theta_{1*} + \zeta_A^\tau \cos^2\theta_{1*} + \zeta_B^n \sin^2\theta_{2*} + \zeta_B^\tau \cos^2\theta_{2*}\right)\rho_3^2\eta_0^2 l_3^{-2},$$

$$\zeta_{23} = \left[-\zeta_A^n \tilde{l}_{21}\sin\theta_{1*}\sin(\theta_{1*} - \varphi_{2*}) - \zeta_A^\tau \tilde{l}_{21}\cos(\theta_{1*} - \varphi_{2*}) + \zeta_B^n \tilde{l}_{22}\sin\theta_{2*}\sin(\theta_{2*} - \varphi_{2*})\right.$$
$$\left. + \zeta_B^\tau \tilde{l}_{22}\cos\theta_{2*}\cos(\theta_{2*} - \varphi_{2*})\right]\rho_3^2\eta_0^2 l_3^{-2},$$

$$\zeta_{24} = \left[-\zeta_B^n \tilde{l}_3 \sin\theta_{2*}\sin(\theta_{2*} - \varphi_{3*}) - \zeta_B^\tau \tilde{l}_3 \cos\theta_{2*}\cos(\theta_{2*} - \varphi_{3*})\right]\rho_3^2\eta_0^2 l_3^{-2},$$

$$\zeta_{33} = \left[\zeta_A^n \tilde{l}_{21}^2 \sin^2(\theta_{1*} - \varphi_{2*}) + \zeta_A^\tau \tilde{l}_{21}^2 \cos^2(\theta_{1*} - \varphi_{2*}) + \zeta_B^n \tilde{l}_{22}^2 \sin^2(\theta_{2*} - \varphi_{3*})\right.$$
$$\left. + \zeta_B^\tau \tilde{l}_{22}^2 \cos^2(\theta_{2*} - \varphi_{2*})\right]\rho_3^2\eta_0^2 l_3^{-2},$$

$$\zeta_{34} = \left[-\zeta_B^n \tilde{l}_{22}\tilde{l}_3 \sin(\theta_{2*} - \varphi_{2*})\sin(\theta_{2*} - \varphi_{3*})\right.$$
$$\left. - \zeta_B^\tau \tilde{l}_{22}\tilde{l}_3 \cos(\theta_{2*} - \varphi_{2*})\cos(\theta_{2*} - \varphi_{3*})\right]\rho_3^2\eta_0^2 l_3^{-2},$$

$$\zeta_{44} = \left[\zeta_B^n \tilde{l}_3^2 \sin^2(\theta_{2*} - \varphi_{3*}) + \zeta_B^\tau \tilde{l}_3^2 \cos^2(\theta_{2*} - \varphi_{3*})\right]\rho_3^2\eta_0^2 l_3^{-2}, \quad \tilde{l}_i = l_i/l_1$$

If we restrict ourselves to taking into account only the clearance and elasto-dissipative properties of joint B, then the number of the degrees of freedom of dynamic model is reduced to two, and the system of differential equations takes the form

$$\tilde{m}_2\left(\tilde{l}_{21}^2 + p_2^2 l_1^{-2}\right)q_3'' + \beta_{33}^0 q_3' + \beta_{34}^0 q_4' + \zeta_{33}^0 q_3 + \zeta_{34}^0 q_4 = \tilde{m}_2 \rho_2^2 l_1^{-2}\varphi_{2*}''$$

$$+ \tilde{m}_2\tilde{l}_{21}\left[\left(\tilde{x}_{s2*}'' + \tilde{y}_{s2*}'\varphi_{2*}'\right)\sin\varphi_{2*} + \left(\tilde{x}_{s2*}'\varphi_{2*}' - y_{s2*} - g\omega_1^{-2}l_1^{-1}\tilde{l}_{21}^{-1}\right)\cos\varphi_{2*}\right],$$

$$\rho_3^2 l_1^{-2}q_4'' + \beta_{43}^0 q_3' + \beta_{44}^0 q_4' + \zeta_{43}^0 q_3 + \zeta_{44}^0 q_4 = \tilde{Q}_4,$$

$$\tag{7.25}$$

where

$$\zeta_{33}^0 = \left[\zeta_B^n \sin^2(\theta_{2*} - \varphi_{2*}) + \zeta_B^\tau \cos^2(\theta_{2*} - \varphi_{2*})\right]\rho_3^2\eta_0^2\tilde{l}_2^2 l_3^{-2},$$

$$\zeta_{34}^0 = -\left[\zeta_B^n \sin(\theta_{2*} - \varphi_{2*})\sin(\theta_{2*} - \varphi_{3*}) + \zeta_B^\tau \cos(\theta_{2*} - \varphi_{2*})\cos(\theta_{2*} - \varphi_{3*})\right]\rho_3^2\eta_0^2\tilde{l}_2\tilde{l}_3 l_3^{-2},$$

$$\zeta_{44}^0 = \left[\zeta_B^n \sin^2(\theta_{2*} - \varphi_{3*}) + \zeta_B^\tau \cos^2(\theta_{2*} - \varphi_{3*})\right]\rho_3^2\eta_0^2\tilde{l}_3^2 l_3^{-2}.$$

Analysis of the "Natural" Frequencies Dimensionless "natural" frequencies η_r are determined on the basis of (7.24) or (7.25). In determining η_r, for systems of the given class, the dissipative factors can be excluded from consideration, as their influence on the "natural" frequency is negligible.

The graphs describing the clearance's effect on the change of the lower "natural" frequencies, for the crank-and-rocker mechanism, are shown in Fig. 7.12. It follows from the graphs that, even in the absence of the kinematic chain discontinuities, with the increase in parameter $\eta_0 = p_0/\omega_1$, the slow change in the frequencies is disturbed, by parametric impulses, with great depth of pulsation. This can lead to the significant increase in dynamic errors and the vibration activity of the mechanism. At the same time, at relatively low values of η_0, (e.g. when $\eta_0 = 10$), the influence of the clearance on the frequency spectrum is weak. Analysis of the modal characteristics of the mechanism shows that the first mode substantially corresponds to the oscillations of the output link (coordinate q_4), the inertial characteristics of which, generally, are the most significant. The identified areas, of parametric pulses, strictly correspond to the unfavorable angles of the mechanism's pressure, determined as per the position of the weightless links, simulating the clearance.
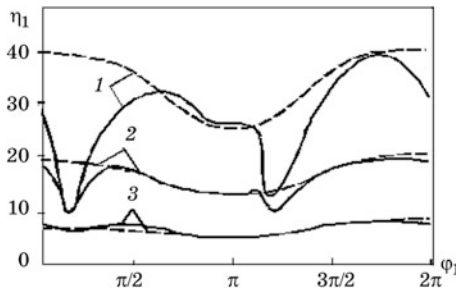

Fig. 7.12 Influence of the clearances on the lower "natural" frequencies: $\tilde{\delta}_A = \tilde{\delta}_B = 0$ (*hatched line*), $\tilde{\delta}_A = \tilde{\delta}_B = 5.75 \times 10^{-3}$ (*solid line*); $1 - \eta_0 = 50.2 - \eta_0 = 25.3 - \eta_0 = 10$

When the tangential stiffness of the joint, converts to null, zero frequencies appear in the oscillatory system. For example, for the system of Eq. (7.25), the free term of the formal frequency equation is reduced to the form $\zeta_{33}^0\zeta_{44}^0 - \left(\zeta_{34}^0\right)^2 = \zeta_B^n\zeta_B^\tau \sin^2(\varphi_{3*} - \varphi_{2*})$. Therefore, at $\zeta_B^\tau = 0$, we have $\eta_1 = 0$ and the system becomes semi-definite.

Small values of $\zeta_{A,B}^\tau \ll 1$, lead to a similar result which in accordance with relation (7.13), corresponds to the small values of normal reactions in the kinematic pairs. From this point of view, the desire to significantly reduce the load in the kinematic pair, at the kinetostatic level, may lead to undesirable consequences.

Excitation of the Oscillations and Transformation of the Pseudo- Impact into Impact To illustrate the studied dynamic effect, in Fig. 7.13, we demonstrate the graphs of functions φ_{2*}'', φ_{3*}'', that are proportional to the ideal angular accelerations of the coupler 2 and rocker 3 and graphs $\varphi_2'' = \varphi_{2*}'' + q_3''$, $\varphi_3'' = \varphi_{3*}'' + q_4''$, obtained by computer simulation, taking into account the clearance and elasto-dissipative properties of joint B. It follows from the graphs that at relatively high value of $\eta_0 = p_0/\omega_1 = 50$ (Fig. 7.13a) in the zones of parametric pulses, occurs, intense excitement of the accompanying free oscillations, which leads to significant increase in the maximum acceleration and vibration activity of the mechanism. When $\eta_0 = 10$ (Fig. 7.13b) this effect significantly mitigates, however, excessive reduction of this parameter can lead to the increase in the amplitude of
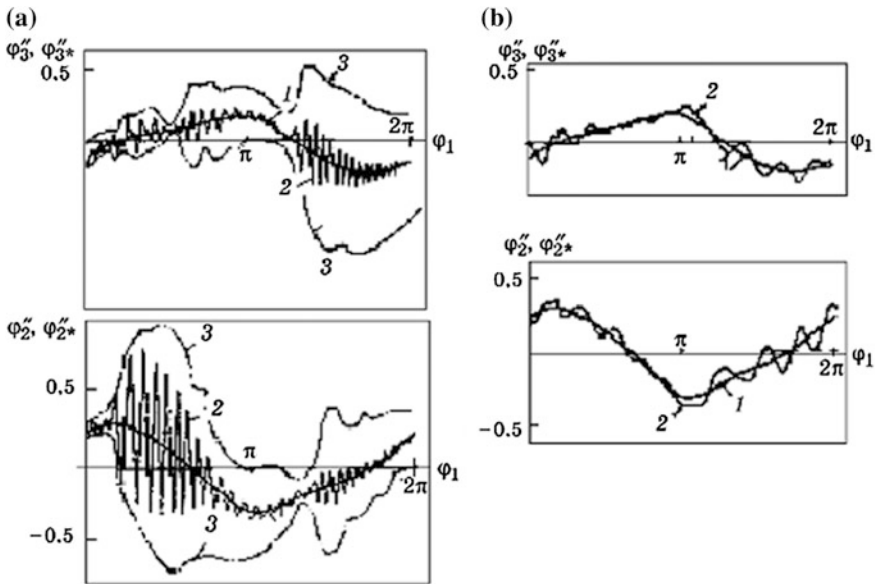
Fig. 7.13 Graphs of the functions φ_{2*}'', φ_2'', φ_{3*}'', φ_3'': $1 - \varphi_{2*}''$, φ_{3*}'', $2 - \varphi_2''$, φ_3'' (at $\vartheta_1 = \vartheta_2 = 0.2$); 3—the envelope of the curves φ_2'' и φ_3'' (at $\vartheta_1 = \vartheta_2 = 0.06$)

oscillations, corresponding to the "strong" harmonics of the kinematic and power disturbances.

The transition from pseudo-inpact to impact is illustrated in Fig. 7.14, using computer simulation of two regimes when $\eta_0 = 20$, $\eta_0 = 30$, and $\vartheta_1 = 0.2$. Circle 1 with radius, equal to half of the clearance, corresponds to the trajectory of the contact point, in the joint of the "rigid" mechanism, curve 2 corresponds to the static deformation, and the curves 3 corresponds to the total effect, in case of taking into account of oscillations.

In the first case the curves surround the circle, indicating the absence of the kinematic opening (pseudo-impact). In the second case the curves intersect the circle, which corresponds to the impact character of the interaction between the elements of the joint. In case of a further increase in η_0 the multiple intersection of the circle occurs, that indicates the arising of the vibroimpact regimes.

Some conclusions We accept the ratio of the maximum vibration acceleration value to the maximum acceleration value in the program motion ξ_i, as one of the criteria of vibration activity. In Fig. 7.15, we can see graphs $\xi_x(\alpha)$, $\xi_y(\alpha)$, where α is the ratio of the amplitudes of harmonic program motion, along the X-axis and Y-axis.

The solid lines of the graphs correspond to the results obtained under the assumption of absence of discontinuities in the joint's contact (pseudo- impact), and the dash-dot lines correspond to the mixed effect from the pseudo-impact, transforming into impact.

An important role, in the transformation of pseudo-impact regime into impact regime, is played by the local violations of conditions of dynamic stability, over the finite interval of the kinematic cycle (see Sect. 5.3.1). The area of increase in amplitudes is alternated with the zone of attenuation. The methods, of excluding this undesirable effect, are described above.

The analysis of "natural" frequencies, in case of fixed inertial parameters, allows us to make the following conclusions:
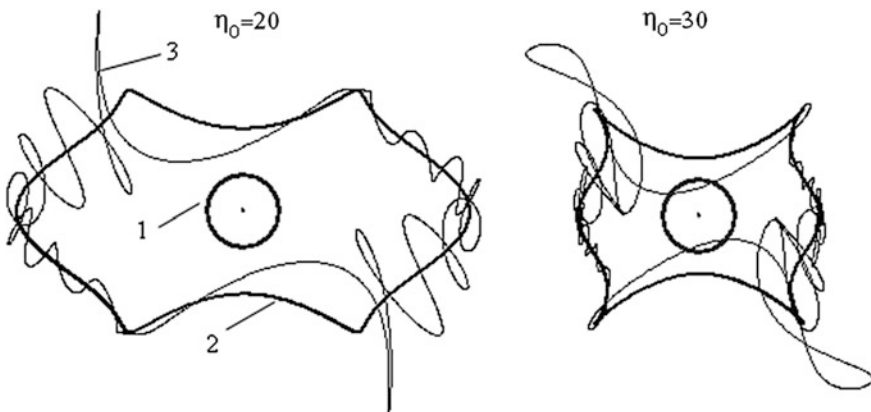
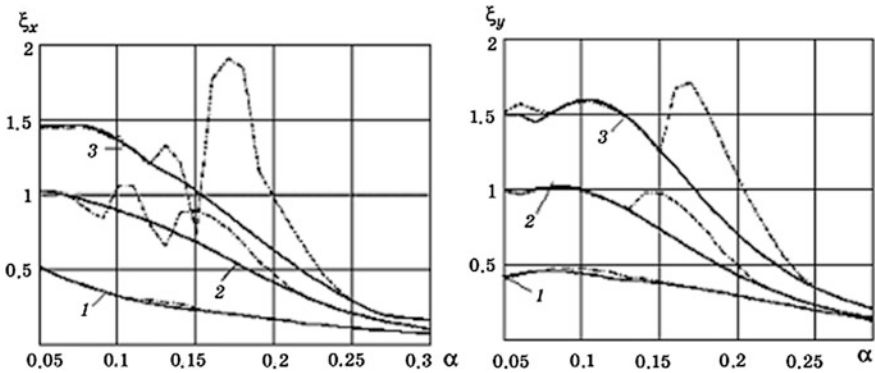**Fig. 7.14** Transformation of the pseudo- impact into impact

Fig. 7.15 Graphs $\xi_x(\alpha)$, $\xi_y(\alpha)$: $\mathit{1} - \eta_0 = 20; \mathit{2} - \eta_0 = 30; \mathit{3} - \eta_0 = 40$

- maximum values of the lowest frequency are defined mainly by elastic properties of the joints;
- minimum values of the lowest frequency, in case of real values of clearances, weakly depend on the elastic properties of the joint and are determined, with sufficient accuracy, on the basis of the "rigid" mechanism: $p_{1\min} \approx \sqrt{2R^*_{\min}/(sm)}$, where m is the reduced mass.
- At large values of $p_{\min}/\omega > 25 \div 50$, the significant influence of the clearance on the pulsation of the lowest "natural" frequency is real, while when $p_{\min}/\omega \leq 10 \div 15$, the influence of the clearance on the frequency spectrum is minor.

7.4.2 Slider-Crank Mechanism

In Fig. 7.16 the kinetostatic model of the slider-crank mechanism, with clearance in joint B, is represented. As the methods of dynamic analysis were described above, we restrict ourselves here to the representation of the system of differential equations.

As the generalized coordinates, we accept the dynamic errors of the position of the slider $q_1 = \Delta x_B = x_B - x_{B*}$ and the connecting rod $q_2 = \Delta \varphi_2 = \varphi_2 - \varphi_{2*}$. When composing the system of differential equations, we pass to the dimensionless form of linear values, relating them to the length of the crank, for example, $\tilde{q}_1 = q_1/l_1$, where $l_1 = OA$. The system of differential equations corresponding to pseudo-impact takes the form
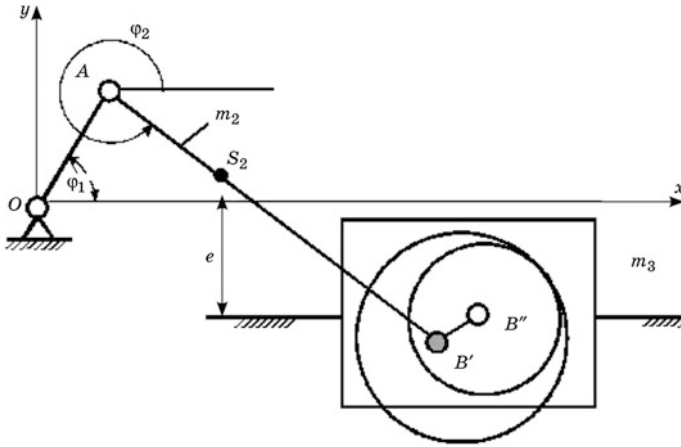
Fig. 7.16 Kinetostatic model in case of pseudo impact in joint B

$$\left.\begin{array}{l} \tilde{q}_1'' + \beta_{11}(\varphi_1)\tilde{q}_1 + \beta_{12}(\varphi_1)q_2' + \zeta_{11}(\varphi_1)\tilde{q}_1 + \zeta_{12}(\varphi_1)q_2 = Q_1, \\ \tilde{m}_2(l_{21}^2 + \rho_2^2/l_1^2)q_2'' + \beta_{21}(\varphi_1)\tilde{q}_1' + \beta_{22}(\varphi_1)q_2' + \zeta_{21}(\varphi_1)\tilde{q}_1 + \zeta_{22}(\varphi_1)q_2 = Q_2, \end{array}\right\}$$

(7.26)

where $()' = d/d\varphi_1$, $\tilde{m}_2 = m_2/m_3$ is the normalized value of the coupler's mass; $\rho_2^2 = J_{s2}/m_2$, J_{s2} is the moment of inertia of the coupler, at point S_2;

$$Q_1 = -\tilde{x}_B'' + P/(m_3\omega_1^2 l_1),$$
$$Q_2 = -\tilde{m}_2\rho_2^2 l_1^{-2}\varphi_{2*}'' + \tilde{m}_2\tilde{l}_{21}\left[(\tilde{x}_{s*}'' + \tilde{y}_{s*}'\varphi_{2*}')\sin\varphi_{2*} + (\tilde{x}_{s*}'\varphi_{2*}' - g\omega_1^2\tilde{l}_{21}^{-1}l_1^{-1} - \tilde{y}_{s*}'')\cos\varphi_{2*}\right].$$

Here P is the external force; $\tilde{l}_{21} = AS_2/l_1$. (When rationing quasi-elastic coefficients as the reference values, the coefficient of stiffness $c_0 = m_3k^2$ was accepted).

Then

$$\left.\begin{array}{l} \zeta_{11} = \eta_0^2(\zeta^n\cos^2\theta_* + \zeta^\tau\sin^2\theta_*); \\ \zeta_{22} = \eta_0^2\tilde{l}_2^2[\zeta^n\sin^2(\theta_* - \varphi_{2*}) + \zeta^\tau\cos^2(\theta_* - \varphi_{2*})]; \\ \zeta_{12} = \zeta_{21} = -\eta_0^2\tilde{l}_2[\zeta^n\sin(\theta_* - \varphi_{2*})\cos\theta_* - \zeta^\tau\cos(\theta_* - \varphi_{2*})\sin\theta_{2*}], \end{array}\right\}$$

(7.27)

where $\eta_0 = k/\omega_1$; $\zeta^n = c^n/c_0$; $\zeta^\tau = c^\tau/c_0$; $\tilde{l}_2 = AB/l_1$.

7.4.3 Spatial Crank-and-Rocker Mechanism

First of all, let's turn to the model of the rigid crank-and-rocker mechanism, in which the clearances in the spherical joints A and B are simulated as weightless links $A'A'' = r_A$, $B'B'' = r_B$, whose length is equal to half of the clearance (Fig. 7.17). Let's exclude from consideration the rotation of links, around their own axis, because herewith, the spatial position, of all the links of the mechanism, remains unchanged. Thus, in each spherical joint, during the relative movement of links, we should take into account, two degrees of freedom. A similar result is achieved, when imposing special restrictors. Taking into account the above mentioned, retaining the kinematic contact in all joints, the discussed mechanism has five degrees of freedom. To describe the spatial position of the links $A'A''$, $A''B''$, $B''B'$, we use the so-called high-speed axis, which are the special case of aircraft axis.

If each of these links is considered as vector $\bar{r}$, directed along the axis of the link, the angular position of the vector, relative to the fixed coordinate system $O'x^0y^0z^0$, is characterized by two parameters: the angle of inclination β and the angle of attack α. Transition from constantly-oriented coordinate system, to the translational movement together with the beginning of the vector in the coordinate system O_1xyz, associated with the link, is carried out by two turns, namely the turn around y-axis (the angle β) and about the axis z (angle α). Then the axis O_1x is coincident with the axis of the link, i.e. vector $\bar{r}$. At the same time the coordinates, in the moving and fixed coordinate systems are connected by the following relations:

$$\left[\begin{array}{c} x^0 \\ y^0 \\ z^0 \end{array}\right] = \left[\begin{array}{ccc} \cos\alpha\cos\beta & -\cos\beta\sin\alpha & \sin\beta \\ \sin\alpha & \cos\alpha & 0 \\ -\cos\alpha\sin\beta & \sin\beta\sin\alpha & \cos\beta \end{array}\right] \left[\begin{array}{c} x \\ y \\ z \end{array}\right] \Bigg\}$$

and the projections of the angular velocities of the moving coordinates of axis are defined as $\omega_* = \dot{\beta}\sin\alpha$; $\omega_y = \dot{\beta}\cos\alpha$; $\omega_z = \dot{\alpha}$.

To the system under consideration, one cyclic coordinate (the angle φ_1) and four positional coordinates, describing the oscillatory system, correspond. When taking into account the compliance of joints, the oscillatory system additionally gains two

Fig. 7.17 Kinetostatic model of the spatial four-link chain
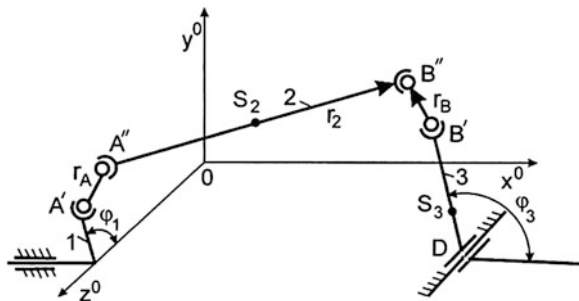
more degrees of freedom and can be described by six neralized coordinates: $q_1 = \varphi_3 - \varphi_{3*}$; $q_2 = \alpha_2 - \alpha_{2*}$; $q_3 = \beta_2 - \beta_{2*}$; $q_4 = \Delta x_A$; $q_5 = \Delta y_A$; $q_6 = \Delta z_A$.

Here, we introduce the following notations: φ_3 is the angle of the rocker's rotation; α_2, β_2 are the angles determining the position of the axis of the coupler (see above); Δx_A, Δy_A, Δz_A are the projections of vector $\bar{r}_A$, on the corresponding axis of the fixed coordinate system (asterisks denotes the coordinates of a perfectly rigid mechanism, with no clearances).

In case of small variations in assumption of the steady unseparated motion of the links, the system of differential equations, with clearances, on the basis of the proposed pseudo impact model, takes the form

$$\sum_{j=1}^{6} a_{js}\tilde{q}_s'' + \sum_{j=1}^{6} \left(b_{js} + a_{js}'\right)\tilde{q}_s' + \sum_{j=1}^{6} \zeta_{js}\tilde{q} = Q_j(\varphi_1) \quad (j = \overline{1,6}). \tag{7.28}$$

At the same time the following notation is introduced: $\varphi = \omega t$ is the "dimensionless time";

$()' = d/d\varphi_1$; $\tilde{q}_s = q_s$ at $s = 1, 2, 3$ и $\tilde{q}_s = q_s/l_1$ at $s = 4, 5, 6$; $a_{js}(\varphi_1)$, $b_{js}(\varphi_1)$, $c_{js}(\varphi_1)$ and $Q_j(\varphi_1)$ are the dimensionless inertial, dissipative, quasi-elastic coefficients and non-conservative generalized forces, defined by the dependencies given in [85].

7.5 Some Criteria of Efficiency of Dynamic Unloading, Taking into Account the Clearances

As noted in Sect. 4.3, one way to reduce the dynamic loads of the cyclic driving mechanisms, executing periodic movement of the links of the working machines, is dynamic unloading using the elastic elements, installed between the output member and the machine's frame. Here we represent some general criteria, taking into account the variability of the parameters and the clearance-effects. Optimization of the elastic characteristics of the unloader, for absolutely rigid mechanism, is achieved by minimizing the functional (see Sect. 4.3).

$$K_0 = \min \int_0^{2\pi} (Q + U)^2 |d\Pi/d\varphi| d\varphi, \tag{7.29}$$

where φ is the rotation angle of the main shaft; Q is the generalized force (before the installation of the unloader); $U(u_1, \ldots, u_n)$ is the control action, implemented by the unloader; u_j are the parameters of the unloader; $\Pi(\varphi)$ is the mechanism's position function.

The simplest dynamic constructive solution, of the dynamic unloader, is the elastic element c_0, installed between the output link of the mechanism and the body.

Let y_0 be the preliminary deformation value of the unloader's elastic element, $F(\varphi)$ be the technological force. Then when $\Pi = r_0(1 - \cos\varphi)$, the function $w(\varphi)$, which is proportional to the generalized force, can be represented in the dimensionless form as

$$w(\varphi) = p_0^2 \cos\varphi(\varepsilon + 1 + 0.25\cos\varphi) + f(\varphi), \qquad (7.30)$$

where $p_0^2 = c_0/(m\omega^2 r_0)$, $\varepsilon = y_0/r_0$, $f(\varphi) = F(\varphi)/(m\omega^2 r_0)$,

The optimizing dynamic synthesis of the unloader is a multi-criteria task. On the stage of the analytical prediction, we exclude the effect of collisions, in the clearances ($\Delta = 0$). According to (7.29) and (7.30)

$$|\bar{q}|_{\max} \leq \left[(\varepsilon + 1)p_0^2 + |1 - p_0^2|\bigg/\sqrt{(1 - p^{-2})^2 + \vartheta^2/\pi p^2}\right]p^{-2}.$$

At the kinetostatic analysis level, as noted above, about the smallness of some components, the dimensionless moment attached to the main shaft, without accounting of the technological force, is defined as follows:

$$M(\varphi) = -\left[(1 - p_0^2)\cos\varphi - (1 + \varepsilon)p_0^2\right]\sin\varphi. \qquad (7.31)$$

Further as the functional to be minimized we accept

$$\Psi_0 = \int_0^{2\pi} M^2 d\varphi. \qquad (7.32)$$

The condition $\partial\Psi_0/\partial p_0 = 0$ taking into account (7.31), (7.32), is met by the following dependence:

$$\varepsilon = \varepsilon_1 = 0.5\sqrt{(1 - p_0^2)/p_0^2} - 1. \qquad (7.33)$$

Thus, the optimum value of preliminary deformation of the elastic element of the unloader $y_0^* = \varepsilon_1 r_0$, depends on its stiffness coefficient. When $p_0^2 = 1$, we have $\varepsilon_1 = -1$ that, in the absence of other restrictions (see below), corresponds to the optimum. Indeed, in this case, according to (7.31) $M(\varphi) \equiv 0$.

As already mentioned, the total unloading, when $M(\varphi) \equiv 0$, can lead to vibro-impact regimes, arising in case of multiple resurfacings in the clearances. It was found that to eliminate such regimes, the value of $p = k/\omega$, should not exceed $25 \div 35$.

For comparison of the oscillatory modes, taking into account the clearances, and for the selection of the optimum parameters of the unloader, some integral criteria are required. In addition to the above criteria, we propose the criteria that take into account the influence of the unloader on the level of the excited oscillations.

1. *The criterion that characterizes the root mean square value of the dynamic component of the reaction:*

$$\Psi_1 = \frac{2}{\pi} \sqrt{\int_{\pi/2}^{\pi} R^2(\varphi)d\varphi}$$

where $R(\varphi) = \bar{q}''(\varphi) - w(\varphi)$. (Here and below the averaging is accomplished in the area of the run-down of the forward stroke.)

2. *The criterion that characterizes the root mean square value of the torque transmitted to the main shaft of the machine:*

$$\Psi_2 = \frac{2}{\pi} \sqrt{\int_{\pi/2}^{\pi} R^2(\varphi) \sin^2 \varphi \, d\varphi}$$

3. *The criterion that characterizes the root mean square value of the additional acceleration caused by oscillations:*

$$\Psi_3 = \frac{2}{\pi} \sqrt{\int_{\pi/2}^{\pi} (\bar{q}''(\varphi))^2 d\varphi}$$

4. *The criterion characterizing the relative total duration of the discontinuities of the kinematic contact, because of clearances (see Sect.* 7.1*):*

$$\Psi_4 = \frac{2}{\pi} \int_{\pi/2}^{\pi} u(|q(\varphi)| - \Delta)d\varphi.$$

For the three characteristic regimes, the results are shown in the Table 7.1. Moreover, for all regimes, illustrated below, the following dimensionless initial data were adopted: $\Delta = 10^{-3}$, $p = 30$, $\vartheta = 0.2$.

Regime 1 corresponds to the absence of the unloader. Thus, there are discontinuities in kinematic contact in the clearance ($\Psi_4 \neq 0$) and significant dynamic errors of the law of program motion.

Table 7.1 Criterion of dynamic unloading

No.	p_0^2	ε	Ψ_1	Ψ_2	Ψ_3	Ψ_4
1	0	0	0.491	0.249	0.129	0.088
2	1	−1	0.231	0.139	0.13	0.626
3	0.86	−0.7	0.3	0.201	0.035	0

Regime 2 corresponds to the installation of the unloader, with an optimum setting, without taking into account the clearances. In this case, there are also collisions in the clearances.

Regime 3 corresponds to the installation of the unloader, with the optimum frequency tuning and taking into account the clearances. In this case, in case of acceptable values of Ψ_1, Ψ_2, Ψ_3 very significant, from the point of view of noise characteristics and wear and tear, is the absence of the resurfacings in the clearances ($\Psi_4 = 0$) that leads to the decrease in the additional stresses caused by vibrations.

Figure 7.18 shows the graphs of oscillations of the output link of the cyclic mechanism, obtained by computer simulation of the three considered modes of oscillation. The boundaries of the clearance are depicted as dash-dot line. The graphs clearly reflect substantial excitation in the clearance, without the unloader (mode 1), and also in case of fully unloaded dynamic mode (2), and in this case the repeated collisions occur in the clearance, which are completely eliminated in mode 3.

5. *The criterion of dynamic stability for the finite time interval*

   As shown in Sect. 5.3, in the oscillatory systems with cyclic mechanisms, there is a slowly varying range of "natural" frequencies, which can lead to the violation of the "traditional" attenuating nature of free oscillations. At the same time, over a certain part of the kinematic cycle, the amplitude of free oscillations increases.

6. *Energy criterion.*

   We make a comparison of the maximum energy $\mathring{A}_*$ when $\Delta \neq 0$ and E_0 under $\Delta = 0$. As $\mathring{A}_* = 0.5c_0^{-1}(F_0 + F_1)^2$ we find that $\mathring{A}_*/\mathring{A}_0 = 1 + K_\Delta$ where

$$K_\Delta = \frac{4c_0\Delta}{\pi F_1}\sqrt{1 - \left(\frac{F_0}{F_1}\right)^2} \qquad (F_1 \geq F_0).$$

Parameter K_Δ can serve as an effective energy criterion, for estimation of dynamic effect of the clearance. This criterion increases with increase in Δ and stiffness coefficient c_0 and decreases with increase in F_1 and F_0. When $F_1 \leq F_0$, we have $K_\Delta = 0$, which fully corresponds to the adjusted clearance, during all the
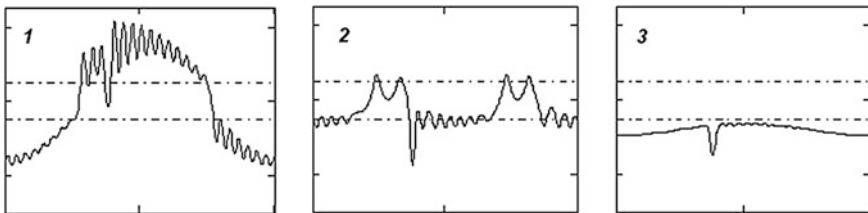
Fig. 7.18 Results of computer simulation

cycle. Analysis of the engineering calculations and the results of the experimental studies, show that to limit the level of vibrations, caused by the clearances, condition $K_\Delta \leq 0.2 \div 0.4$ should be fulfilled.

The problem under consideration is multi-criteria. Sometimes in such cases, using the coefficients of weights, we can formulate the generalized criteria of optimality. At the same time, however, it is difficult to avoid subjectivity in determining the degree of importance of each of the criteria.

Chapter 8
Vibration Analysis of Cyclic Machines Using Modified Transition Matrices

8.1 Modified Transition Matrices

For solving the problems considered in this chapter, we use the transition matrices that allow us to perform the dynamic calculation of complex mechanical systems, in the form of a sequence of algebraic operations, corresponding to the transition from one part of the system to another.

The transition matrices have become more widespread in the analysis of harmonic oscillations of the linear oscillatory systems, with constant parameters. With the help of the transition-matrix apparatus, we can determine the "natural" frequencies and oscillation modes, as well as the amplitude of the forced oscillations, bypassing the formal composing of the systems of differential equations and calculating the coefficients of these equations. Moreover the undoubted advantage of the transition matrices is their adaptability to the specific computer calculations.

In a number of papers by the author of this book [62, 64, 75, 77, 78], the transition matrices, on the basis of the method of conditional oscillator, has been developed with reference to the problems of dynamics of machines and mechanisms that form the oscillatory systems, with variable parameters. Such transition matrices are called the *modified* ones. Hereunder, this term will be used only in those cases, where it is necessary to emphasize this feature. The possibility of such "non-traditional" transition matrices is due to the fact that in case of the additional conditions (5.9), implemented in the method of conditional oscillator, the generalized coordinates and generalized accelerations are described by the same harmonic functions.

The apparatus of the modified transition matrices is particularly suitable for the drives of machines, forming the oscillatory systems, with slowly varying parameters. Such systems are typical for the technological machines of light, textile, printing, food processing and other industries that experience the high dynamic loads and elevated levels of vibrations, caused by the cyclic mechanisms.

In this chapter we restrict ourselves to considering the torsion and longitudinal vibrations of the drive elements. In these cases we are dealing with the so-called simply-connected systems. *The connectivity of the system shows the number of possible displacements of any cross section or, what is the same thing, the number of reactions, which in this cross section substitute the action of one part of system to another.*

Transition Matrices of Dynamic Model's Elements and the Rule of Signs If we exclude from consideration the influence of the dissipative forces, the harmonic vibrations of various sections of the system occur in a single phase or in the opposite phases. Then the oscillation in any section can be characterized by its amplitude a, which is assumed to be positive if its phase coincides with the phase of the oscillatory element, taken as the original, and negative if the oscillations are in antiphase i.e., differ in π.

Similar conclusion is valid also with respect to the amplitudes of forces Q. However, to avoid errors in the determination of reactions in the cross-sections, we should agree about the signs of forces (or moments), acting on the "left" and "right" sides of the system. We accept the following rule of signs: the reactive force or torque on the "input" of the element j will be considered positive if its direction coincides with the positive direction of the reference frame (Fig. 8.1a, section $j - 1$). For the "output" (section j) the rule of sign is opposite.

From the theory of linear systems, it is known that the number a_{j-1} and Q_{j-1} ("input") and the number a_j and Q_j ("exit") in case of harmonic oscillations, with the frequency ω, are connected among themselves, with the following linear relations:

$$\left.\begin{array}{l} a_j = A_j a_{j-1} + B_j Q_{j-1}; \\ Q_j = C_j a_{j-1} + D_j Q_{j-1}. \end{array}\right\} \tag{8.1}$$
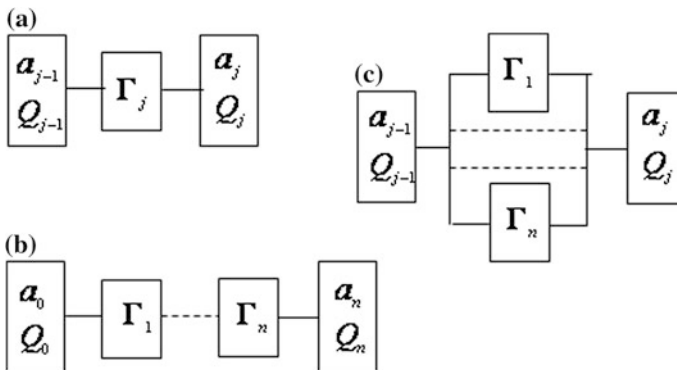
Fig. 8.1 Kinds of connections of transition matrices

Here A_j, B_j, C_j, D_j are coefficients, depending generally on the system's parameters, (mass, moments of inertia, stiffness coefficients) and the frequency ω of the harmonic oscillations.

Herewith, the matrix form of (8.1) is valid:

$$\begin{pmatrix} a_j \\ Q_j \end{pmatrix} = \begin{pmatrix} A_j & B_j \\ C_j & D_j \end{pmatrix} \begin{pmatrix} a_{j-1} \\ Q_{j-1} \end{pmatrix} \tag{8.2}$$

The square matrix $\boldsymbol{\Gamma}_j$, formed by the elements, A_j, B_j, C_j, D_j, is called *the transition matrix.* The ratio Q_j/a_j is called *the dynamic stiffness* and the reciprocal value a_j/Q_j is called the *dynamic compliance.*

Let's note here that in spite of the convention on the selection of signs, the sign of the dynamic stiffness is independent of the direction of reference system, but only on the phase shift between the oscillations and the forces. In the other words, the dynamic stiffness is positive, if the phase of the force coincides with the phase of phase displacement at the frequency considered, and in the case of the anti-phase, it is negative.

It should be emphasized that when using transition matrices in the problems of dynamics of machines, we accept the absolute dynamic errors, as generalized coordinates; the dynamic errors are the deviations of the absolute coordinates, at the given point or section, from the ideal value at program motion (that is, in case of absolutely rigid links).

Let us see the matrices of transition of some simple elements.

Elastic Element with Stiffness Coefficient c_j In this case, the amplitude of displacements, at its ends, differs as much as the value of the amplitude of deformation and the amplitude of forces, according to Newton third law, are equal to each other:

$$\left.\begin{array}{l} a_j = a_{j-1} + Q_{j-1}/c_j; \\ Q_j = Q_{j-1}. \end{array}\right\} \tag{8.3}$$

Thus according to (8.2) and (8.3) the elements of the transition matrix are determined as $A_j = 1$, $B_j = c_j^{-1}$, $C_j = 0$, $D_j = 1$.

Inertial element J_j or m_j Similarly, we obtain $A_j = 1$, $B_j = 0$, $C_j = -J_j\omega^2$, $D_j = 1$.

Transition matrices with complex elements: Dissipation element We represent the harmonic oscillations $q = a\sin(\omega t + \alpha)$ in the complex form

$$q = ae^{i(\omega t + \alpha)} \tag{8.4}$$

Let $\tilde{a} = a e^{i\alpha}$ be the complex amplitude, whose module is equal to the amplitude of the oscillations, and argument α is equal to the phase of the oscillations. Similarly, harmonic force in complex form corresponds to $\tilde{Q} = Q e^{i\alpha}$.

In Sect. 6.1.2, we presented the dependence of the coefficient of complex stiffness $\tilde{c} = c(1 + 2\delta\, i)$, corresponding to the elastodissipative element, taking into account the positional friction force, with the dissipation coefficient $\delta = \vartheta/(2\pi) \approx \psi/(4\pi)$. Thus, in this case, to account for the dissipative force, in the recurrent dependencies (8.1) and their representation in matrix form (8.2), it is enough to replace the stiffness coefficient c with its complex form $\tilde{c}$. Thus,

$$\left.\begin{array}{l} \tilde{a}_j = \tilde{A}_j \tilde{a}_{j-1} + \tilde{B}_j \tilde{Q}_{j-1}; \\ \tilde{Q}_j = \tilde{C}_j \tilde{a}_{j-1} + \tilde{D}_j \tilde{Q}_{j-1}, \end{array}\right\} \tag{8.5}$$

where $\tilde{A}_j, \tilde{B}_j, \tilde{C}_j, \tilde{D}_j$, are generally complex elements of the transition matrix (taking into account the elastodissipative element $\tilde{A}_j = A_j = 1$, $\tilde{B}_j = \tilde{c}^{-1}$, $\tilde{C}_j = 0$, $\tilde{D}_j = D_j = 1$).

If the resistance corresponds to the so-called viscous friction, then $R = -b\dot{q}$. On the basis of (8.4) $\dot{q} = i\tilde{a}\omega e^{i\omega t}$. Then in dependencies (8.5) taking into account the rule of signs, we should accept $\tilde{A}_j = 1$, $\tilde{B}_j = (b\omega i)^{-1}$, $\tilde{C}_j = 0$, $\tilde{D}_j = 1$. With these corrections, the discussed in this chapter matrix method of analysis of oscillations, acquires a general character.

Element for the transformation of coordinates in the ideal mechanism We use the linearization of position function, in the vicinity of the program motion (see Sect. 5.1), for the kinematic analogue of a mechanism, corresponding to its conversion during "transition" through the mechanism. Then $a_j = a_{j-1}\Pi'$, $Q_j = Q_{j-1}(\Pi')^{-1}$. Hence, as per (8.5) $A_j = \Pi'_j$; $B_j = 0$; $C_j = 0$; $D_j = (\Pi'_j)^{-1}$, where $\Pi'(\varphi)$ is the absolute value of the first geometric transfer function in the program motion.

Let us pay attention to the fact that the function Π', should be taken in absolute value, as the sign change in the amplitude transformations, using transition matrices, testifies that oscillations are in the opposite phases, while in the kinematic calculations, this change corresponds to the direction of the motion, with respect to the chosen reference system. (For simplicity, the sign of the absolute value is omitted everywhere.) In the particular case of gears, function Π' is transformed into a constant gear ratio. Let us pay attention to the following property of the transition matrices

$$\det \mathbf{\Gamma}_j = A_j D_j - C_j B_j \equiv 1. \tag{8.6}$$

Here $\det \mathbf{\Gamma}_j$ is the determinant of the matrix $\mathbf{\Gamma}_j$.

Serial connection of the model's blocks Let the dynamic model be formed using serial connection of the blocks (Fig. 8.1b). For such models we sometimes use the term *chain system*. With successive substitution of (8.2) we obtain

$$\begin{pmatrix} a_n \\ Q_n \end{pmatrix} = \begin{pmatrix} A_n & B_n \\ C_n & D_n \end{pmatrix} \times \cdots \times \begin{pmatrix} A_1 & B_1 \\ C_1 & D_1 \end{pmatrix} \begin{pmatrix} a_0 \\ Q_0 \end{pmatrix}. \tag{8.7}$$

So the transition matrix of the oscillatory chain, consisting of serially connected blocks, is the product in the reverse order of the transition matrices of these blocks:

$$\Gamma = \prod_{j=n}^{1} \Gamma_j. \tag{8.8}$$

Let us emphasize that the reverse order of the multipliers, in comparison with the sequence of the blocks themselves, in the oscillatory chain, appears to be imperative, since the matrix product does not have commutative properties. Table 8.1, along with the above simplest elements of the transition matrices, also contains the elements of these matrices for typical serially connected blocks.

The last line of the table corresponds to the transition matrix for the element with distributed parameters in case of torsion oscillations in the area of the shaft. Here we use the following notations: $\sigma = (GI\rho)^{-0.5}$; $\theta = p(t)\ell/g$; $g = \sqrt{GI/\rho}$, where G is the shear modulus; I is the polar moment of inertia; ρ is the linear inertia; ℓ is the length of the element.

In Table 8.1, along with the described above simplest elements of transition matrix, we can also see the elements of these matrices for typical events of serial connection of blocks.

Table 8.1 Transition matrix elements for typical serial connections

Connection	A	B	C	D
c	1	c^{-1}	0	1
J	1	0	$-Jp^2$	1
Π	Π'	0	0	$1/\Pi'$
$c - J - \Pi$	Π'	$\Pi'c^{-1}$	$-Jp^2/\Pi'$	$(1 - Jp^2c^{-1})/\Pi'$
$c - \Pi - J$	Π'	$\Pi'c^{-1}$	$-Jp^2\Pi'$	$-Jp^2\Pi'c^{-1} + 1/\Pi'$
$J - c - \Pi$	$\Pi'(1 - Jp^2c^{-1})$	$\Pi'c^{-1}$	$-Jp^2/\Pi'$	$1/\Pi'$
$J - \Pi - c$	$\Pi' - Jp^2/(c\Pi')$	$(c\Pi')^{-1}$	$-Jp^2/\Pi'$	$1/\Pi'$
$\Pi - J - c$	$\Pi'(1 - Jp^2c^{-1})$	$(c\Pi')^{-1}$	$-Jp^2\Pi'$	$1/\Pi'$
$\Pi - c - J$	Π'	$(c\Pi')^{-1}$	$-Jp^2\Pi'$	$(1 - Jp^2c^{-1})/\Pi'$
Element with distributed parameters	$\cos\theta$	$\sigma p^{-1}\sin\theta$	$-\sigma^{-1}p\sin\theta$	$\cos\theta$

Parallel connection of the blocks of the model (Fig. 8.1c) In this case for each of the elements (or entire blocks with serial connection of elements), the following matrix equation is valid:

$$\begin{pmatrix} a_{jv} \\ Q_{jv} \end{pmatrix} = \begin{pmatrix} A_{jv} & B_{jv} \\ C_{jv} & D_{jv} \end{pmatrix} \begin{pmatrix} a_{j-1,v} \\ Q_{j-1,v} \end{pmatrix} (v = \overline{1,n}) \tag{8.9}$$

Here v is the current block number, n is number of blocks.

Since in case of parallel connection the coordinates in the input and output are equal for all blocks, and therefore don't depend on v, we have $a_{jv} = a_j$, $a_{j-1,v} = a_{j-1}$. Thus,

$$\left. \begin{array}{l} a_j = A_{jv}a_{j-1} + B_{jv}Q_{j-1,v}; \\ Q_{jv} = C_{jv}a_{j-1} + D_{jv}Q_{j-1,v}. \end{array} \right\} \tag{8.10}$$

The total load Q_{j-1} and Q_j in accordance with (8.9) and (8.10) can be represented as

$$\left. \begin{array}{l} Q_{j-1} = \sum\limits_{v=1}^{n} Q_{j-1,v} = -a_{j-1}\gamma_1 + a_j\gamma_2; \\ Q_j = \sum\limits_{v=1}^{n} Q_{jv} = -a_{j-1}\gamma_2 + a_j\gamma_3, \end{array} \right\} \tag{8.11}$$

where $\gamma_1 = \sum_{v=1}^{n} A_{jv}/B_{jv}$; $\gamma_2 = \sum_{v=1}^{n} B_{jv}^{-1}$; $\gamma_3 = \sum_{v=1}^{n} D_{jv}/B_{jv}$.

The transition matrix $\mathbf{\Gamma}_j$, for the entire set of blocks connected in parallel, must satisfy the matrix equation (8.2). Thus, on the basis of (8.10) and (8.11), the elements of matrix $\mathbf{\Gamma}_j$ are defined by the relationship:

$$A_j = \gamma_1/\gamma_2; \quad B_j = 1/\gamma_2; \quad C_j = (\gamma_1\gamma_3 - \gamma_2^2)/\gamma_2; \quad D_j = \gamma_3/\gamma_2.$$

It is easy to see that these values A_j, B_j, C_j, D_j satisfy the identical equation (8.6). In the special case of parallel connection of elastic elements, with the stiffness coefficients c_{jv}, we have $A_{jv} = 1$, $B_{jv} = c_{jv}^{-1}$, $C_{jv} = 0$, $D_{jv} = 1$. Herewith $\gamma_1 = \gamma_2 = \gamma_3 = c_j$, where $c_j = \sum_{v=1}^{n} c_{jv}$. Consequently $A_j = 1$, $B_j = c_j^{-1}$, $C_j = 0$, $D_j = 1$.

Thus, as expected, the stiffness of the elements with parallel connection is equal to the sum of the stiffness coefficients of these elements.

8.2   Determination of "Natural" Frequencies and Non-stationary Mode Shapes

To indicate the frequencies of the free oscillations, here forth, we will use the term "natural", although, strictly speaking, this term corresponds to the system with constant parameters.

The method for determining the spectrum of "natural" frequencies will be explained using the example of the torsion oscillations of the drive, consisting of the main shaft and n cyclic mechanisms (Fig. 8.2).

Suppose the input section of the shaft ($j = 0$), rotates with the constant angular velocity ω_0, which in the first approximation is close to real situation. This assumption is adequate to the assumption that the moment of inertia in the "input" of the shaft is sufficiently large, which allows us to consider the input section, during the frequency analysis as clamped. Because of the small effect of the linear (or linearized) dissipative forces on the "natural" frequencies, we exclude them at this stage from consideration.

We divide the oscillating system in n blocks, each of which consists of the portion of the main shaft with stiffness coefficient c_{0j}, lumped moment of inertia J_{0j} and the mechanism, which forms the chain elements $\Pi_j - c_j - m_j$ (or $\Pi_j - c_j - J_j$).

The transformation of the values of amplitudes of vibrations and loads, when crossing block j, corresponds to the following matrix relationship:

$$\begin{pmatrix} a_{0j} \\ Q_{0j} \end{pmatrix} = \begin{pmatrix} 1 & 0 \\ -p^2 J_{0j} & 1 \end{pmatrix} \begin{pmatrix} 1 & c_{0j}^{-1} \\ 0 & 1 \end{pmatrix} \begin{pmatrix} a_{0,j-1} \\ Q_{0,j-1} \end{pmatrix} + \begin{pmatrix} 0 \\ Q_j \end{pmatrix}. \tag{8.12}$$

The first summand in expression (8.12), corresponds to serial connection of the main shaft elements $c_{0j} - J_{0j}$ and the second corresponds to the additional reaction Q_j from the mechanism j. To determinate this reaction we write

Fig. 8.2 Dynamic model of the branched structure
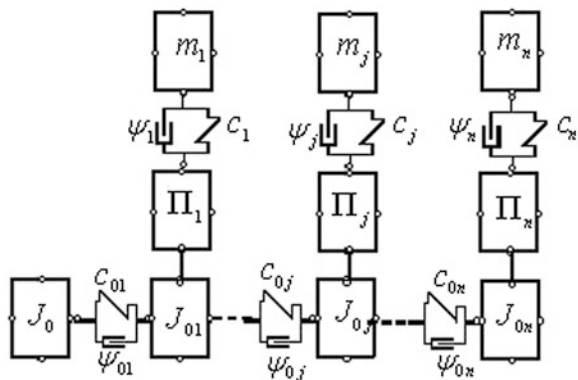
$$\begin{pmatrix} a_j^+ \\ Q_j^+ \end{pmatrix} = \begin{pmatrix} A_j & B_j \\ C_j & D_j \end{pmatrix} \begin{pmatrix} a_j^- \\ Q_j^- \end{pmatrix}. \tag{8.13}$$

Here the index "plus" corresponds to the amplitude values at the mechanism's "output", and "minus" at the "input"; A_j, B_j, C_j, D_j correspond to the connection $\Pi - c - m$ (see Table 8.1 when changing m with J).

In our case $Q_j^+ = 0$, $a_j^- = a_{0j}$, $Q_j^- = Q_j$. Then on the basis of (8.13) we have

$$\left. \begin{array}{l} a_j^+ = A_j a_{0j} + B_j Q_j; \\ 0 \;\; = C_j a_{0j} + D_j Q_j. \end{array} \right\} \tag{8.14}$$

Hence

$$Q_j = -\frac{C_j}{D_j} a_{0j} = R_j a_{0j}, \tag{8.15}$$

where $R_j = -C_j/D_j$ is the dynamic stiffness of the mechanism j (see Sect. 8.1).

For the model under consideration $R_j = -mp^2 \Pi'^2/(1 - mp^2/c)$.

Sometimes the output link is connected with the body, with an elastic member. This situation in particular occurs in case of spring closing of the cam follower, as well as in case of using the spring based dynamic unloaders (see Sect. 4.3). In such cases, in the first Eq. (8.14), we should take $a_j^+ = 0$; the left side of the second equation is equal to the unknown reaction of the body Q_j^+. This way we similarly obtain $R_j = -A_j/B_j$.

On the basis of (8.12) and (8.15), we have

$$\begin{pmatrix} a_{0j} \\ Q_{0j} \end{pmatrix} = \mathbf{\Gamma}_{0j} \begin{pmatrix} a_{0,j-1} \\ Q_{0,j-1} \end{pmatrix}, \tag{8.16}$$

where $\mathbf{\Gamma}_{0j}$ is the transition matrix of block j, whose elements are determined as follows:

$$A_{0j} = 1; \quad B_{0j} = c_{0j}^{-1}; \quad C_{0j} = R_j - J_{oj}p^2; \quad D_{0j} = 1 + (R_j - J_{0j}p^2)/c_{0j}. \tag{8.17}$$

Let us note here that $R_j - J_{0j}p^2 = R_j^*$ corresponds to the dynamic stiffness of the mechanism j, if we add to its elements the inertial moment of the input link J_{0j}.

Here, we will present one interpretation of the result. On the basis of formulae, presented in Table 8.1, values $A = 1$, $B = c^{-1}$, $C = -Jp^2$, $D = 1 - Jp^2/c$ correspond to the connection $c - J$ (for the use of these formulae, for corresponding connections, in this case it is necessary to accept $\Pi' = 1$). If we compare these formulae with $A_{0j}, B_{0j}, C_{0j}, D_{0j}$, it is easy to make sure that they coincide in case of $J = J_{0j}^* = J_{0j} - R_j/p^2$. Thus, J_{0j}^* makes sense as the reduced to the main shaft

moment of inertia. So, to take into account the kinematic branch, it is quite enough to correct, in this way, the moment of inertia of the input link.

Using for the model under consideration, the above formula, determining the dynamic stiffness R_j we have

$$J_{0j}^* = J_{0j} + \frac{m_j \Pi_j'^2}{1 - p^2/k_j^2}, \tag{8.18}$$

where $k_j = \sqrt{c_j/m_j}$.

In particular, when $\Pi_j' = 0$ and $m_j \to 0$, as expected, $J_{0j}^* = J_{0j}$, and in case of an absolutely "rigid" mechanism $(c_j \to \infty)$ $J_{0j}^* = J_{0j} + m_j \Pi_j'^2$, which corresponds to the known expression, met during the course of theory of mechanisms and machines, reduced to the input link of the mechanism on the basis of the kinetic energy balance. Thus, we transformed the initial branched system into serially connected blocks, for which the following matrix equation is valid:

$$\begin{pmatrix} a_{0n} \\ Q_{0n} \end{pmatrix} = \begin{pmatrix} A & B \\ C & D \end{pmatrix} \begin{pmatrix} a_{00} \\ Q_{00} \end{pmatrix}, \tag{8.19}$$

where A, B, C, D are the elements of the matrix.

$$\mathbf{\Gamma} = \prod_{j=n}^{1} \mathbf{\Gamma}_{0j}. \tag{8.20}$$

When defining the boundary conditions, the following cases are possible:

Case 1 "Input" is clamped, "output" is clamped $(a_{00} = 0, \ a_{0n} = 0)$. When $a_{0n} = Aa_{00} + BQ_{00} = BQ_{00}$, we have $B(p) = 0$. This result serves as the frequency equation.

Case 2 "Input" is clamped, "output" is free $(a_{00} = 0, \ Q_{0n} = 0)$. According to (8.19) $Q_{0n} = Ca_{00} + DQ_{00} = DQ_{00} = 0$, at $Q_{00} \neq 0$. Hence, $D(p) = 0$.

Case 3 "Input" is free, "output" is free $(Q_{00} = 0, \ Q_{0n} = 0)$. Similarly, we get $C(p) = 0$.

Case 4 "Input" is free, "output" is clamped $(Q_{00} = 0, \ a_{0n} = 0)$. At the same time $A(p) = 0$.

Thus, according to (8.20), to calculate the "natural" frequency, it is necessary to multiply, in the reverse order, the square matrices of separate blocks and equate to zero the corresponding element of the obtained matrix $\mathbf{\Gamma}_0$. However, there is an easier way to define the elements of the matrix. On the basis of (8.19), we write

$$\left.\begin{array}{l} a_{0n} = A(p)a_{00} + B(p)Q_{00}; \\ Q_{0n} = C(p)a_{00} + D(p)Q_{00}. \end{array}\right\} \tag{8.21}$$

For case 1, assuming, in the first equation, that $Q_{00} = 1$, we get $a_{0n} = B(p)$. To determine $D(p)$ (case 2), it is enough, in the second equation of the system (8.21), to assume the boundary conditions $Q_{00} = 1$. Since $a_{00} = 0$, then we have $Q_{0n} = D(p)$. In case 3, we should use the second equation when $a_{00} = 1$, herewith, $Q_{0n} = C(p)$. Finally, in case 4, from the first equation, when $a_{00} = 1$, it follows that $a_{0n} = A(p)$. In case of using the described method, we practically operate only with column matrices (vector-matrices) of the boundary conditions.

At first glance, it seems that the above way of simplifying calculations, in case of the present level of computer technology, is not particularly interesting. However, it's not about saving the estimated time. As the practice of the engineering calculations shows, in case of transition matrix multiplication, for long oscillation chains, the elements of these matrices quickly reach enormous values, which affects the accuracy, when searching for the roots. This disadvantage is eliminated, by using the above method for transformation of vectors.

To determine the frequency spectrum, it is sufficient to find the point of intersection of the graph of the corresponding function $B(p)$ (case 1) and $D(p)$ (case 2), with the horizontal axis, or use the known computer methods of finding the roots.

Let us emphasize here that for the drives with the cyclic mechanisms, in contrast to the mechanisms with constant ratios, "natural" frequencies are not constant, but vary, depending on the angle of rotation of the main shaft $\varphi_0 = \omega_0 t$. This is due to the variability of the first transfer functions $\Pi'_j(\varphi_0)$ in the corresponding transition matrices. Then, in case of slow change of parameters, free oscillations, without taking into account the resistance, are described as follows (see Sect. 5.2):

$$q_i = \sum_{r=1}^{H} a_{ir}^0 \sqrt{\frac{p_r(0)}{p_r(t)}} \cos\left[\int_0^t p_r(u)du + \alpha_r\right], \tag{8.22}$$

where H is the number of the degrees of freedom; r is the frequency number; i is the number of the element or section; a_{ir}^0 and α_r are determined from the initial conditions.

The totality $a_{ir}(t) = a_{ir}^0 \sqrt{p_r(0)/p_r(t)}$, in case of fixed "natural" frequency p_r, forms the oscillation mode, which in our case is time varying, as it also depends on $\varphi_0 = \omega_0 t$. To determine the time-dependent coefficients of the form, any section of the system should be subjected to unit amplitude or force. If, for example, in case 1, we require $a_{0n}(p_r) = 1$, then from the first equation of (8.20), it follows that $Q_{00}(p_r) = 1/B(p_r)$ (Method of defining $B(p)$ was described above).

For frequency p_r, the positive value $a_{ir}(t)$, indicates towards the coincidence of phases, and negative—towards the anti-phase of the oscillations of element i, compared to the oscillations of the element with the single form factor.

Earlier, during the analysis of the model shown in the Fig. 8.2, we have given analytical expressions, for the elements of transition matrices. This was done to illustrate the physical content of each of the components, which allows us to explain some of the observed effects. Of course, with computer calculations, the submission of elements of the matrices, in the analytical form, is not required; it is sufficient to specify the type of connection (stiffness, mass and moment of inertia, kinematic similar of the mechanism) and the corresponding transition matrix, after which all the necessary changes are made in the process of calculations.

8.3 Forced Vibrations

Let us again turn to the drive model, shown in Fig. 8.2. Let the periodic disturbing forces, represented in the form of Fourier series, be applied to the output links of the mechanism.

$$F_j(t) = F_{j0} + \sum_{v=1}^{\infty} \left(F_{jv}^c \cos v\Omega t + F_{jv}^s \sin v\Omega t \right). \tag{8.23}$$

Here, as above, j is the number of the mechanism.

The origin of the disturbing forces may be both, forced and kinematic. In the first case, they are usually associated with performed technological operation, and in the second case, with the forces of inertia of the mechanism's links, in translational motion. In particular, for this model, these inertial forces are determined as $-m_j \omega_0^2 \, \Pi_j''(\omega_0 t)$. Usually the value Ω coincides with the the angular velocity of the main shaft $(\Omega \approx \omega_0)$.

As before, at this stage we will exclude from consideration the resonant modes, which allow us to ignore the effect of dissipative forces. In addition, we restrict ourselves to the event of slow change Π_j'; however, the disturbing forces can change quickly and have large harmonic of these forces, when $v\Omega \gg \omega_0$.

It is easy to see that in these cases, in case of transition, through the kinematic analogue of the mechanism, only amplitude transformation of force, according to relation $F_{jv}^{c,s}\Pi_j'$, occurs and its frequency remains practically unchanged. In these cases the above relation contains the products of $\sin \omega_0 t \cos v\omega_0 t$ or $\sin \omega_0 t \sin v\omega_0 t$, which when $v \gg 1$ essentially describes the harmonic oscillations, with frequency $v\omega_0$, in case of amplitude modulation, of frequency ω_0, which resembles the beat mode (see Sects. 5.2 and 6.4).

Let us also note the following feature of systems with variable parameters: the constant force component of the force F_{j0}, in the mechanism, transforms into an alternating torque $F_{j0}\Pi_j'$, applied to the main shaft, and harmonic ω_0 $(v = 1)$ transforms to harmonic $2\omega_0$ of the driving moment. For example, in the slider-crank mechanism, the first harmonic of the first transfer function is equal to $l_1 \sin \omega_0 t$,

where l_1 is the length of the crank and the inertial force in translation motion is equal to $-m\omega^2 l_1 \cos \omega t$. Herewith, the moment from this force, on the main shaft, is equal to $-0.5 m\omega^2 l_1^2 \sin 2\omega_0 t$. Quite often, the "natural" frequencies, in the considered range of practical interest, are close to constants. Herewith, variability of the first transfer function of the mechanism is shown only on the amplitudes and frequencies of the disturbing forces, reduced to the main shaft, as it was shown above.

The forced oscillations with the frequency $\Omega_\nu = \nu\omega_0$ are described as

$$\left.\begin{array}{l} q_{0j} = a_{0j}^c \cos \omega t + a_{0j}^s \sin \omega t; \\ q_j = a_j^c \cos \omega t + a_j^s \sin \omega t. \end{array}\right\} \tag{8.24}$$

Here, as before, the index $0j$ corresponds to the main shaft, and index j to the corresponding mechanism. (In formulae (8.24) and below, for simplicity of description, we accept $\Omega_\nu = \omega$.)

When calculating both, the forced and the free oscillations, transformation of harmonic functions takes place; therefore the shape of all the presented-above transition matrices is preserved, when changing frequency p with frequency ω.

First, we will define the amplitude of reactive torque Q_j^C, acting on the main shaft, from the force $F_j^c \cos \omega t$, applied to the output mechanism j. We will use the system of Eq. (8.14), which now takes the form

$$\left.\begin{array}{l} a_j^c = A_j(\omega)a_{0j}^c + B_j(\omega)Q_j^C; \\ -F_j^c = C_j(\omega)a_{oj}^c + D_j(\omega)Q_j^c. \end{array}\right\} \tag{8.25}$$

With (8.6) and (8.15) on the basis of (8.25), we get

$$Q_j^c = R_j a_{oj}^c - F_j^c / D_j. \tag{8.26}$$

The sign, when F_j^c, corresponds to the application of force at the "exit" (see above).

Herewith, transit through block j now corresponds to the following recursive dependencies:

$$\left.\begin{array}{l} a_{0j}^c = A_{oj}(\omega)a_{0,j-1}^c + B_{0j}(\omega)Q_{0,j-1}^c; \\ Q_{0j}^c = C_{0j}(\omega)a_{o,j-1}^c + D_{oj}(\omega)Q_{0,j-1}^c - F_j^c / D_j(\omega). \end{array}\right\}. \tag{8.27}$$

As F_j^c enters this equation linearly, the principle of superposition is valid. According to this principle, we represent the amplitudes at the "exit" as

$$\left.\begin{array}{l} a_{on}^c = S_{11}(\omega)a_{00}^c + S_{12}(\omega)Q_{00}^c + S_{13}(\omega, F_1^c, \ldots, F_n^c); \\ Q_{0n}^c = S_{21}(\omega)a_{00}^c + S_{22}(\omega)Q_{00}^c + S_{23}(\omega, F_1^c, \ldots, F_n^c). \end{array}\right\}. \tag{8.28}$$

For the considered model $a_{00}^c = 0$ (clamping), $Q_{0n}^c = 0$ (the free end). The unknown coefficients $S_{12}, S_{13}, S_{22}, S_{23}$ are determined on the basis of (8.28), by means of several simple calculations.

Calculation number **1**: $Q_{00}^c \equiv 1$, $F_1^c = \cdots = F_n^c \equiv 0$. Then $(a_{0n}^c)_1 = S_{12}$; $(Q_{on}^c)_1 = S_{22}$ (Here and below the index near the brackets, indicates the number of calculation.).

Calculation number **2**: $Q_{00}^c \equiv 0$. Now $(a_{0n}^c)_2 = S_{13}$ and $(Q_{0n}^c)_2 = S_{23}$ (Hence, using the condition $Q_{on}^c = 0$, we obtain the unknown boundary condition Q_{00}^c).

$$Q_{00}^c = -S_{23}(\omega)/S_{22}(\omega). \tag{8.29}$$

The frequency response in the arbitrary cross-section $a_{0j}^c(\omega)$ is determined as per dependencies (8.27) (or with the multiplication of the corresponding matrices), taking into account the boundary condition, at the "input", obtained as per the formula (8.29). Let us emphasis that when $S_{22}(\omega) = 0$, we get $\omega = p_r$, which corresponds to resonance. If, in our case, $\omega = \omega_j = \sqrt{c_j/m_j}$, then according to (8.18) $J_{0j}^* \to \infty$. Herewith, the oscillation node (anti-resonance) is located in the inlet section of mechanism j, and the mechanism itself plays the role of a dynamic absorber.

If for two or more mechanisms, the anti-resonant frequencies coincide, then in the vicinity of these values, some natural frequencies are placed. When the main shaft is absolutely rigid, this frequency is the multiple of the natural frequency.

In case of replacement of F_j^c with F_j^s, the value $a_{0j}^s(\omega)$ is determined similarly, then the amplitude in section j is obtained as $a_{0j}(\omega) = \sqrt{\left[a_{0j}^c(\omega)\right]^2 + \left[a_{0j}^s(\omega)\right]^2}$.

8.4 Frequency and Modal Analysis of Systems with Complex Structure

Let us look into a fairly general pattern of the cyclic machine (Fig. 8.3a), when the motion of drive is transmitted to the shaft 2 of the machine, from which a large number of mechanisms are branching off: gears, linkages, cams, etc., observed in Sect. 8.3. Furthermore, along with branches of type 3, there are mechanisms of type 5, which make up, together with actuators 4 and the main shaft 2, statically inde-terminate oscillatory contour of the ring structure [16, 18, 62–64].

As a "global" model we will take the system (Fig. 8.3b), which consists of a number of torsion subsystems, with distributed parameters $m = \overline{0, m_*}$, corre-sponding to the main shaft 2 ($m = 0$), to the actuators 4, as well as a number of sub-systems with discrete parameters, which correspond to the driving mechanism 1, simple mechanisms of type 3, and mechanisms of type 5, working in a parallel fashion and included in contours of the ring structure. In such systems, with

(a)   **(b)**
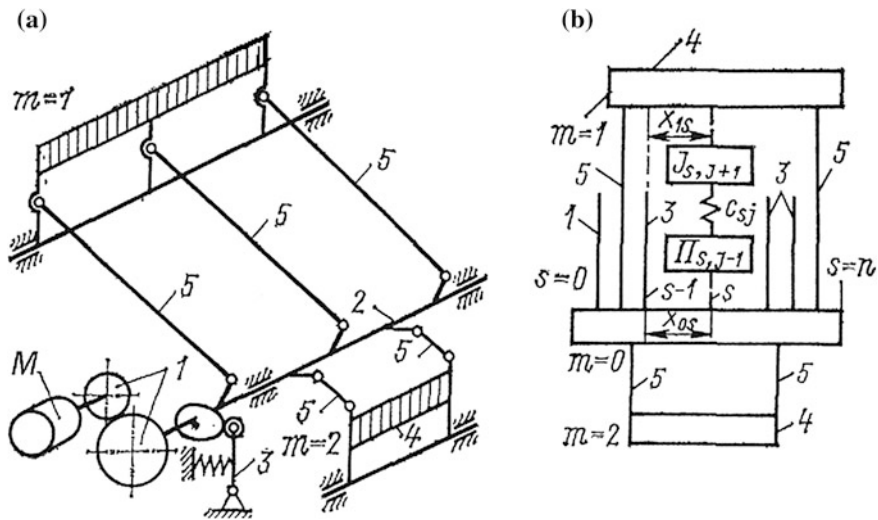
Fig. 8.3 Dynamic model of the ring structure

increased complexity of the structure, the transfer matrix has a large dimensionality, so we use the combined method described below.

For the coefficients $K_{ms} = a_{ms}$, $N_{ms} = Q_{ms}/(G_{ms}I_{ms})$ following recurrent relations are valid:

$$
\begin{aligned}
K_{ms} &= K_{m,\,s-1}\cos\theta_{ms} + N_{m,\,s-1}\sin\theta_{ms}; \\
N_{ms} &= \tilde{\sigma}_{ms}(-K_{m,\,s-1}\sin\theta_{ms} + N_{m,\,s-1}\cos\theta_{ms} + R_{ms}),
\end{aligned} \tag{8.30}
$$

where $\tilde{\sigma}_{ms} = \sigma_{m,\,s+1}/\tilde{\sigma}_{ms}$ $(\tilde{\sigma}_{mn} = 1)$; $\tilde{\sigma}_{ms} = (G_{ms}I_{ms}\rho_{ms})^{-0.5}$; $\theta_{ms} = \vartheta_{ms}(\Delta\ell_{ms})$. The remaining symbols see Sect. 8.1.

Functions R_{ms}, proportional to the amplitudes of the reactive moments, applied to the subsystems m in the sections s, are determined depending on the type of fixing of the second end of the branch 5 as per the formulae given in Table 8.2. Herewith, each of these cases corresponds to ν_{ms}. In matrix form the recurrent dependencies (8.30) correspond to

$$
\begin{pmatrix} a_{0s} \\ Q_{0s} \end{pmatrix} = \begin{pmatrix} 1 & 0 \\ -p^2 J_{0s} & 1 \end{pmatrix} \begin{pmatrix} 1 & c_{0s}^{-1} \\ 0 & 1 \end{pmatrix} \begin{pmatrix} a_{0,s-1} \\ Q_{0,s-1} \end{pmatrix} + \begin{pmatrix} 0 \\ R_{ms}G_{ms}I_{ms} \end{pmatrix}. \tag{8.31}
$$

If the chain s has intermediate branches, they can be taken into account with the help of the structural transformations, described in Sect. 8.2, with the introduction of the corresponding fictive moment of inertia, in the place of the connection of this branch to the chain s.

Let's start taking into consideration the boundary conditions, and assume that the drive based mechanism is attached to the main shaft in section n. The absence of

Table 8.2 Functions R_{ms}

v_{ms}	R_{0s} $(m = 0)$	R_{ms} $(m = \overline{1,\ m_*})$	Type of connection
0	0	0	No connection chain s with the subsystem m
1	$\dfrac{\sigma_{0s}C_sK_{0s}}{pD_s}$	$\dfrac{\sigma_{ms}C_sK_{ms}}{pD_s}$	The end of the chain s is free
2	$\dfrac{\sigma_{0s}A_sK_{0s}}{pB_s}$	$\dfrac{\sigma_{0s}A_sK_{0s}}{pB_s}$	The end of the chain s is fixed
3	$\dfrac{\sigma_{0s}(A_sK_{0s} - K_{us})}{pB_s}$	$\dfrac{\sigma_{us}(D_sK_{us} - K_{0s})}{pB_s}$	The connection of the subsystem $m = 0$ with the subsystem $m = u$ by means of the mechanism s

Note A_s, B_s, C_s, D_s are elements of the transition matrix of the mechanism s

loads, on all parts of the subsystems, with distributed parameters, corresponds to the following conditions: $N_{m0} = 0$ and $K_{mn} = 0$ with $m = \overline{0,\ m_*}$. However, in order to satisfy these requirements, based on the recurrent relations (8.30), we have to set the stroboscopic form, in the initial section, i.e. to set the values of K_{m0}. In comparison with the similar situation in the drives of the branched structure, an additional difficulty occurs, which is related to the fact that only one value of K_{m0}, for example, $K_{00} = 1$ can be taken independently; the remaining values of K_{m0} $(m = \overline{1,\ m_*})$, and the frequency p should be determined from the foregoing boundary conditions.

The analytical expressions, for the function K_{m0}, in such systems, are very cumbersome, poorly convenient for calculations and also change their appearance, depending on the structure of the system. We will use the more convenient method of "numerical experiment", which we have used in Sect. 8.3. It is obvious that in this linear problem functions N_{mn} are the linear combination of K_{m0}, so when $N_{m0} = 0$, we have the following system of equations:

$$\sum_{i}^{m_*} S_{mi}(p)K_{i0} = N_{mn}, \quad (m = 0,\ m_*), \tag{8.32}$$

where $S_{mi}(p)$ are the unknown coefficients.

Let's indulge with the following matrix of fictitious boundary conditions: $K_{m0}^{(k)} = \chi_{mk}$, where $k = \overline{0,\ m_*}$ is the number of the count, when $\|\chi_{mk}\| = \mathrm{diag}\{1,\ 1,\ \ldots 1\}$.

It is easy to see that for these fictitious boundary conditions, each equation of the system (8.30) gives $S_{mk} = N_{mn}^{(k)}$. Thus, to determine all the unknown coefficients S_{mk}, we should $m_* + 1$ times do the calculations as per the recurrent dependencies (8.30) and for each count in the matrix χ has a corresponding column of boundary conditions.

Further, we will select one of the equations of system (8.32), for example, the equation $m = 0$, and in the rest of the system $m_* = 2$ equations, we substitute the true boundary conditions $K_{00} = 1$ and $N_{mn} = 0$. Having solved this system of equations, we find the true values of $K_{10},\ K_{20}, \ldots K_{m_*0}$ $(m_*$ values).

Let's illustrate the definition of the unknown boundary conditions, using an example. Suppose that the number of subsystems, associated with the camshaft, is equal to two (m_*). Then for the given p, we should perform three calculations with fictitious boundary conditions, namely when $K_{00}^{(0)} = 1$; $K_{10}^{(0)} = K_{20}^{(0)} = 0$ ($k = 0$); at $K_{10}^{(1)} = K_{20}^{(1)} = 0$; $K_{10}^{(1)} = 1$ ($k = 1$) and at $K_{00}^{(2)} = K_{10}^{(2)} = 0$, $K_{20}^{(2)} = 1$ ($k = 2$).

Each calculation gives three values $N_{mn}^{(k)} = S_{mk}$. Unknown true boundary conditions K_{10} and K_{20} are determined from the system of two equations

$$S_{11}K_{00} + S_{12}K_{20} = -S_{10};$$
$$S_{21}K_{10} + S_{22}K_{20} = -S_{20}.$$

In case of one subsystem of the ring structure ($m_* = 1$) $K_{10} = -S_{10}/S_{11}$, where $S_{10} = N_{1n}^{(0)}$, when $k = 0$ ($K_{00}^{(0)} = 1$, $K_{10}^{(0)} = 0$) and $S_{11} = N_{1n}^{(1)}$, when $k = 1$ ($K_{00}^{(1)} = 0$, $K_{10}^{(1)} = 1$).

To find the unknown frequency p, we now have several options (see Sect. 8.2). For example, the selected above equation $m = 0$, when $N_{0n} = 0$, can serve as the formal frequency equation, namely,

$$U(p) = \sum_{m=0}^{m_*} S_{0m}(p)K_{m0}(p) = 0, \tag{8.33}$$

where S_{0m} and K_{m0} for given value of p were determined earlier using the numeral experiment. Transcendental equation (8.33) is solved numerically, for example, with the sequential "pass" of the given frequency range, identifying the values $p = p_r$ corresponding to the change of the sign of the function $U(p)$, when $|U(p)| < \varepsilon$, where ε is the given small quantity. The oscillation mode is characterized by the values of $K_{ms}(p_r)$, where p_r are the "natural" frequencies. For an arbitrary element sj (branch s, index number j) mode factors to be determined as per the formulae:

$$a_{sj}^{(r)} = [A_{sj}^* K_{0s} - B_{sj}^* R_{0s}p/\sigma_{0s}]_{p=p_r} \quad (v_{0s} \neq 0);$$
$$a_{sj}^{(r)} = [(A_{sj}^* - B_{sj}^* C_s/D_s)K_{ms}]_{p=p_r} \quad (v_{ms} = 1; v_{0s} = 0);$$
$$a_{sj}^{(r)} = [(A_{sj}^* - B_{sj}^* A_s/B_s)K_{ms}]_{p=p_r} \quad (v_{ms} = 2; v_{0s} = 0),$$

where A_{sj}^*, B_{sj}^* are the elements of the first row of the matrix $\Gamma_{sj}^* = \prod_{u=j}^{1} \Gamma_{su}$; v_{ms} (see Table 8.1).

In the matrix form, this procedure corresponds to the definition of eigenvalues and eigenvectors of the matrix $\mathbf{S}(p) = 0$.

Quite often, in drives, it turns-out that $\theta_{ms} \ll 1$; it indicates that the subsystems can be represented as a set of discrete elastic and inertial elements. Herewith,

$\cos \theta_{ms} \approx 1$; $\sin \theta_{ms} \approx \theta_{ms} = p\sqrt{\Delta J_{ms}/\Delta c_{ms}}$, $\sigma_{ms} = (\Delta J_{ms}\Delta c_{ms})^{-0.5}$, $g_{ms} = \Delta\ell_{ms}\sqrt{\Delta c_{ms}/\Delta J_{ms}}$ where ΔJ_{ms}, Δc_{ms} are the moment of inertia and torsion stiffness coefficient of the section s of the subsystem m, respectively.

When using the above mentioned methods of frequency and modal analysis, the transition to the digital parameters does not give any tangible simplification of calculation. However, on the basis of the conditional oscillator method, the description of their "natural" modes and corresponding frequencies can be reduced to solving the complete eigenvalue problem (elements of the matrix in this case are varying in time). With this approach to the problem, for the fixed sequence t, we can use standard software.

8.5 Joint Accounting of Dynamic Characteristics of the Motor and the Machine Drive

Let us consider the dynamic model, formed using serial connection of the subsystems of the motor and machine drive (Fig. 8.4).

As noted in Sect. 5.7.4, the features of an induction motor and DC motor, at steady state, correspond to the model, in which the stator (rigid support) is connected to the rotor, which has the moment of inertia equal to J_{m}, through the serial connection of the damper $(b_{\mathrm{m}} = (v_{\mathrm{m}}\omega_{\mathrm{m}}^0)^{-1})$ and the elastic element $(\tilde{n}_{\mathrm{m}} = (v_{\mathrm{m}}\omega_{\mathrm{m}}^0 T_{\mathrm{m}})^{-1})$. Here ω_{m}^0, v_{m}, T_{m} are respectively ideal angular velocity, slope coefficient of static characteristics and the electromagnetic constant of the motor [26, 57, 62, 75].

Let us define the transition matrix of the motor subsystem, which is highlighted in Fig. 8.4 with hatch-dotted lines.

$$\mathbf{\Gamma}_{\mathrm{m}} = \mathbf{\Gamma}_{J0} \cdot \mathbf{\Gamma}_{c} \cdot \mathbf{\Gamma}_{b}. \tag{8.34}$$

Here $\mathbf{\Gamma}_{J0} = \begin{pmatrix} 1 & 0 \\ -J_0\omega^2 & 1 \end{pmatrix}$; $\mathbf{\Gamma}_{c} = \begin{pmatrix} 1 & c_{\mathrm{m}}^{-1} \\ 0 & 1 \end{pmatrix}$; $\mathbf{\Gamma}_{b} = \begin{pmatrix} 1 & (b_{\mathrm{m}}\omega\ i)^{-1} \\ 0 & 1 \end{pmatrix}$, where ω is the frequency of the harmonic disturbing force (moment).

Let us represent the "elastodissipative" component of this characteristic as follows:

$$\mathbf{\Gamma}_{cb} = \mathbf{\Gamma}_{c} \cdot \mathbf{\Gamma}_{b} = \begin{pmatrix} 1 & 1/c_{\mathrm{m}} - i/(b_{\mathrm{m}}\ \omega) \\ 0 & 1 \end{pmatrix}. \tag{8.35}$$

From (8.35), it follows that matrix $\mathbf{\Gamma}_{cb}$ has the permutation properties, i.e. it does not depend on the type of sequence of elements c_{m} and b_{m}. The mechanical system, in the considered model, is represented with elastodissipative element $\tilde{n}_1$, ψ_1, which
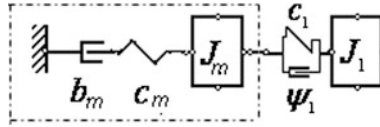
Fig. 8.4 The dynamic model of the mechanical drive with a motor

corresponds to the complex coefficient of stiffness $\tilde{c}_1$ and reduced moment of inertia J_1. The transition matrix of this subsystem is: $\Gamma_i = \Gamma_{J1} \cdot \Gamma_{c1}$, where

$$\Gamma_{J1} = \begin{pmatrix} 1 & 0 \\ J_1\omega^2 & 1 \end{pmatrix}; \quad \Gamma_{c1} = \begin{pmatrix} 1 & \tilde{c}_1^{-1} \\ 0 & 1 \end{pmatrix}; \tilde{c}_1 = c_1(1 + 2\delta_1 i).$$

Let the harmonic driving moment $M = M_1 \sin \omega t$ be applied to the output element of the system. Then

$$\begin{pmatrix} \tilde{a}_1 \\ M_1 \end{pmatrix} \begin{pmatrix} \tilde{A} & \tilde{B} \\ \tilde{C} & \tilde{D} \end{pmatrix} \begin{pmatrix} 0 \\ \tilde{M}_m \end{pmatrix}.$$

Here $\tilde{A}, \tilde{B}, \tilde{C}, \tilde{D}$ are the elements of transition matrix $\Gamma = \Gamma_i \Gamma_m$; $\tilde{a}_1$ is the complex amplitude at the "output" (element J_1); $\tilde{M}_m$ is the complex amplitude of the driving moment.

Hence, $\tilde{M}_m = M_1/\tilde{D}$; $\tilde{a}_1 = M_1\tilde{B}/\tilde{D}$. The peak values of torque and the drive vibrations are defined as absolute values and the oscillations phase as the arguments of the corresponding complex numbers. This procedure, as well as all intermediate calculations, is easy to implement with modern computer programs.

Example Let us study the drive dynamics, schematized as dynamic model represented in Fig. 8.4 with the following parameters: $\omega_m^0 = 157 \text{ s}^{-1}$; $v_m = 3 \times 10^{-3}(\text{N} \cdot \text{m})^{-1}$; $T_m = 0.043 \text{ s}$; $J_0 = 0.224 \text{ kg} \cdot \text{m}^2$; $J_1 = J_0h$; $p_1 = 150 \text{ s}^{-1}$; $c_1 = p_1^2 J_1$; $\delta_1 = \psi_1/(4\pi) = 0.02$; $M_1 = 1 \text{ N} \cdot \text{m}$. Here p_1 is the partial frequency of the mechanical subsystem, δ_1 is the dissipation coefficient, $h = J_1/J_0$.

The partial frequency of the electric motor is determined as $p_0 = \sqrt{k^2 - n^2}$, where $k^2 = (v_m T_m J_0 \omega_m^0)^{-1}$, $n^2 = 0.25T_m^{-2}$. According to the initial data we have: $p_0 = 9.2 \text{ s}^{-1}$. In Fig. 8.5 the amplitude-frequency and phase-frequency characteristics $a(\omega, h)$, $\gamma(\omega, h)$, where $a = |\tilde{a}|$, $\gamma = -\arg \tilde{a}$ are represented. The parameter h has values: $h = 0.25$ (solid line), $h = 0.5$ (dotted line), $h = 1$ (hatched line), $h = 3$ (hatch-dotted line).

In Fig. 8.6 the family of curves that characterize the irregularity factor of the motor's rotation $\chi_\omega = \Delta\omega_m/\bar{\omega}_m$, are shown, where $\bar{\omega}_m$ is the average value of ω_m; $\chi_\omega = |\tilde{\chi}_\omega|$; $\tilde{\chi}_\omega \approx v_m\tilde{M}_m(1 + iT_m)$. In these graphs, as above, the role of parameter h, in the formation of dynamic distortions of the ideal kinematic characteristics, is clearly shown.
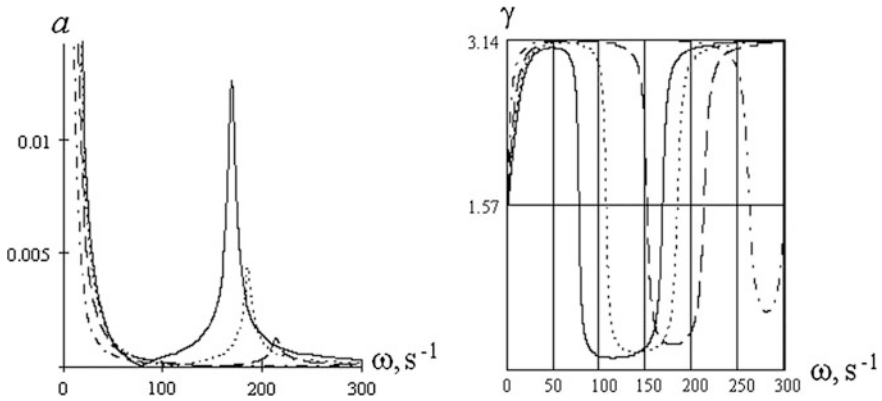
Fig. 8.5 Amplitude-frequency and phase-frequency characteristics

Fig. 8.6 Graphs of the non-uniformity coefficients
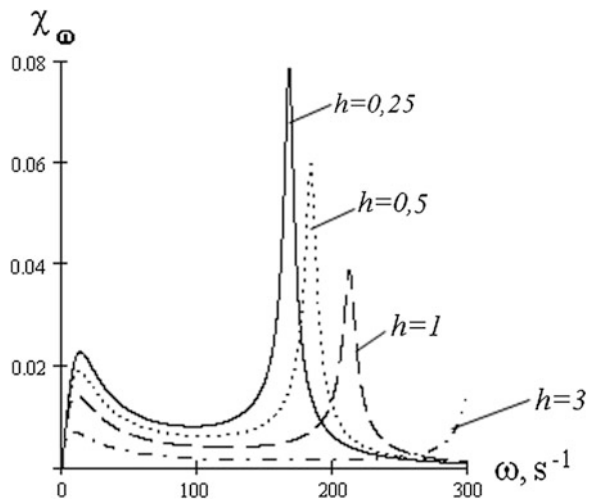
Usually, the reduced moment of inertia, of the machine's drive, is less than the rotor's moment of inertia ($h<1$). In such cases the increase in the coefficient of non-uniformity can be expected in the vicinity of the partial frequencies of the motor and drive system.

Chapter 9
Regular Torsional Cyclic Systems with Branched Structure

9.1 Overview of Regular Systems

The term "regularity" means the coincidence, of the dynamic structure and the parameters of the individual subsystems (modules). The theory of regular oscillatory systems is reflected in the works of many prominent scientists. First, one-dimensional lattice, consisting of the point particles, was studied by Newton, while determining the speed of sound. Further studies are associated with the works of Daniel and Johann Bernoulli, Cauchy, Kelvin, Born, Karman, Debye, Brillouin, and others [12, 25, 36, 37], that formed the basis of the so-called theory of chains (or lattices). With help of this theory we can perform analytical description of the dynamics of systems with many degrees of freedom, based on the analysis of one of the structural elements of the system. The objects, for use with the theory of chains apparatus, were the crystalline lattices and a number of other problems of theoretical physics.

Among the technical problems of analysis of such class, we can mention the theory of electrical lines, as well as some problems arising in the calculation of strain and vibration in frames, girders, etc. [6–8, 19].

Regular oscillatory systems are often included in cyclic machines and automatic transfer lines, with dynamically identical sections, used in case of extended lengths of the zone of technological process, as well as for the implementation of uniform technological and transportation operations. In such cases, in view of the "natural" desire for unification and interchangeability of individual components or entire units of the machine, arises the certain repeatability of blocks of the dynamic model of the drive. This situation is particularly common in textile machinery, light industry, food, printing and several other industries.

With regard to the machines with cyclic mechanisms, the theory of regular oscillatory systems requires additional development, which is performed in the works [16, 63, 64, 73–78, 91].

First of all, the dynamic models of drives have more complex internal structures. Moreover, unlike classical chains, each repeating element is not a point mass, but represents a branched, ring and branched-ring oscillatory system. Secondly, the need for a separate study of this problem is associated with the specific features of cyclic mechanical systems, among which we note the nonlinearity of the position function, non-stationary nature of the dynamic connections, the possibility of violation of the kinematic contact in the clearances, etc.

From the standpoint of machine dynamics, the regularity is associated with some specific effects and as a rule, is undesirable. In case of absolutely rigid main shaft and identical mechanisms, there are multiple "natural" frequencies, which, in case of accounting of elasticity of a shaft, are transformed into a frequency range of increased density. This leads to an increase in vibration activity and in the calculation plan, to certain difficulties, which include increased sensitivity of results, to small changes in parameters. On the other hand, for regular systems, some special methods of analysis can be used: they can promote analytical methods further. Thus, not only the computational difficulties are eliminated, but created also are the effective ways of rational dynamic machine design. Some general properties of regular systems are illustrated, using the example of one of the "classical" one-dimensional chains, consisting of point masses connected by an elastic-dissipative element (Fig. 9.1). We temporarily exclude from consideration the dissipative components, usually having little influence on the specter of "natural" frequencies.

We will write the system of differential equations as generalized equation for arbitrary mass $s\,(s = \overline{(1, n)}$.

$$m\ddot{q}_s + c_1(2q_s - q_{s-1} - q_{s+1}) + cq_s = 0. \tag{9.1}$$

Next, assuming $q_s = a_s \sin pt$; $a_s = ae^{is\theta}$, after substituting in (9.1) and elementary transformations, we get

$$p = p_* \sqrt{1 + 4\zeta \sin^2 \theta}, \tag{9.2}$$

where, $p_* = \sqrt{c/m}$; $\zeta = c_1/c$.

The relationship between the "natural" frequencies and function θ is defined by the boundary conditions (see below). However, regardless of the boundary conditions and the number of elements in chain n, from (9.2) it follows that

Fig. 9.1 Chain of pointed masses
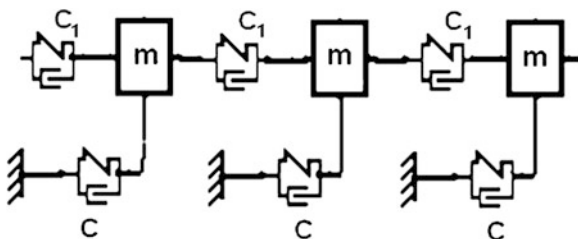
$p_* \le p < \sqrt{1 + 4\zeta}$. In particular, for the elementary chain, when $c = 0$, we have $p \le 2\sqrt{c_1/m}$, and when $c_1 = 0$, as it should be expected, $p = p_*$. On the basis of these simple dependencies, it can be argued that for small ζ and large n, the spectrum of "natural" frequencies would be very dense. For the continuous idealization of the model under consideration, the upper limit of frequency tends to infinity, while the bottom one remains unchanged. The physical object, corresponding to this model, is the string on the elastic foundation [25]. In this case, frequency p_* corresponds to the motion of the string as a solid unit.

Let us consider the generalized dynamic model, consisting of n blocks (modules) that form the K-connected oscillatory system, with periodic spatial structure (Fig. 9.2). The term "connected" we will understand the number of reactions in case of discontinuity of connections. Each module also generally may be a k-connected system. Elements M1 and M2 correspond to the machine's drive. Obviously, the transition matrices of the regular part of the system coincide.

The eigenvalues of the transition matrix are the roots of the characteristic equation

$$\lambda^{2K} + h_1\lambda^{2K-1} + h_2\lambda^{2K-2} + \cdots + h_2\lambda^2 + h_1\lambda + 1 = 0,$$

whose coefficients are determined in accordance with the method of D.K. Faddeev as [22]:

$$\left.\begin{array}{l} h_1 = -\mathrm{Sp}\,\mathbf{G}_1; \quad \mathbf{B}_1 = \mathbf{G}_1 - h_1\mathbf{E}^0; \quad \mathbf{G}_2 = \mathbf{G}_1\mathbf{B}_1; \\ h_2 = -\frac{1}{2}\mathrm{Sp}\,\mathbf{G}_2; \quad \mathbf{B}_2 = \mathbf{G}_2 - h_2\mathbf{E}^0; \quad \mathbf{G}_3 = \mathbf{G}_1\mathbf{B}_2; \\ \cdots \\ h_{2K-1} = -\frac{1}{2K-1}\mathrm{Sp}\,\mathbf{G}_{2K-1}; \quad \mathbf{B}_{2K-1} = \mathbf{G}_{2K-1} - h_{2K-1}\mathbf{E}^0; \quad \mathbf{G}_{2K} = \mathbf{G}_1\mathbf{B}_{2K-1}, \end{array}\right\}$$

$$(9.3)$$

where, $\mathbf{G}_1 = \boldsymbol{\Gamma}$; $\mathrm{Sp}\,\mathbf{G}_i$ is the spur of a matrix; $\mathbf{G}_i$; $\mathbf{E}^0$ is the identity matrix.

In this and the subsequent chapters, the practical application of the matrix method, of calculating the oscillations, is illustrated using the example of cyclic mechanical systems, with complex structures, taking into account the variability of parameters.
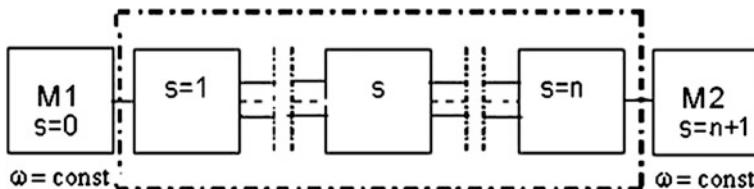
Fig. 9.2 Generalized dynamic model of regular structure

9.2 Model with Lumped Parameters

Frequency analysis Let us take into consideration the dynamic model of the drive, consisting of a main shaft and n identical executive members (see Fig. 8.2). As shown in Sect. 8.2, the transformation of amplitudes and forces, when passing through block j, is described by Eq. (8.13), which corresponds to the following recursive relationship:

$$\left.\begin{aligned} a_{0j} = A_{0j}a_{0,j-1} + B_{0j}Q_{0,j-1}; \\ Q_{0j} = C_{0j}a_{0,j-1} + D_{0j}Q_{0,j-1}. \end{aligned}\right\} \tag{9.4}$$

Let us recall here that each unit j consists of a section of the shaft, with the coefficient of torsion stiffness c_{0j} and some conventional disk with the moment of inertia J_{0j}^*, including, according to (8.18), the moment of inertia of the input link J_{0j} and an additional term related to the dynamic stiffness of mechanism j. In case of identical mechanisms, the elements of matrix Γ_{0j} are not dependent on j, so hereon, we accept $A_{0j} = A_0$, $B_{0j} = B_0$, $C_{0j} = C_0$, $D_{0j} = D_0$.

Dependencies (9.4) can be considered as the linear system of differential equations, whose solution will be sought in the form $a_{0j} = \eta a_{0,j-1}$; $Q_{oj} = \eta Q_{0,j-1}$

$$\left.\begin{aligned} (A_0 - \eta)a_{0,j-1} + B_0 Q_{0,j-1} = 0; \\ C_0 a_{0,j-1} + (D - \eta)Q_{0,j-1} = 0. \end{aligned}\right\} \tag{9.5}$$

Excluding the trivial zero solution, we convert the determinant of this system into zero. The roots of the obtained square characteristic equation are the eigenvalues of the transition matrix Γ_{0j}; they are equal to

$$\eta = \xi \pm i\sqrt{1 - \xi^2}, \tag{9.6}$$

where $\xi = 0.5(A_0 + D_0)$; $i = \sqrt{-1}$. (taken into account here that $\det \Gamma_{0j} \equiv 1$.)

The sum of the elements of the main diagonal of the matrix is called the spur of the matrix. Thus, $\xi = 0.5\mathrm{Sp}\Gamma_{0j}$, where $\mathrm{Sp}\Gamma_{0j}$ is the spur of the block transition matrix. Depending on the value of η, we can consider the cases $\xi < 1$, $\xi > 1$, $\xi < -1$. When $\xi < 1$, the coefficient of the imaginary part is $\mathrm{Im}\eta \neq 0$. Then the eigenvalues are the mutually conjugate complex numbers, with a modulus equal to one. Taking $\xi = \cos\gamma$, on the basis of (9.6), we have

$$\eta = \cos\gamma \pm i\sin\gamma = \mathrm{e}^{\pm i\gamma}. \tag{9.7}$$

Similarly, as in the case of solution of the linear differential equations, in this case the solution of (9.4) is determined by trigonometric functions. Thus,

$$a_{0j} = h_1 \cos j\gamma + h_2 \sin j\gamma,$$
$$\left. Q_{0j}B_0 = h_1[\cos(j+1)\gamma - \cos j\gamma] + h_2[\sin(j+1)\gamma - \sin j\gamma]. \right\} \qquad (9.8)$$

Values h_1 and h_2 are determined from the boundary conditions; $r = 1, \ldots, n$ is the number of the main shaft oscillation form.

In Sect. 8.2 four cases of boundary conditions were examined. We will start our analysis by considering the simplest case 1, when, $a_{00} = 0$, $a_{0,n+1} = 0$ (the "input" and "output" are clamped). Let us recall that the term "clamping" is not to be taken literally. As already noted, if the oscillatory system has, in the "input" or "output", the elements with relatively large masses or moments of inertia, the corresponding section in the relative movement (in this case, under oscillations) can be considered as clamped, in the first approximation. A similar situation occurs in case of forced movement of these sections, which is the equivalent of infinitely large stiffness. Taking $j = 0$ and $j = n + 1$, we have $h_1 = 0$ and $\sin(n + 1)\gamma = 0$ that leads to expression

$$\gamma_r = r\pi/(n+1), \qquad (9.9)$$

At that the frequency equation in general can be written as follows:

$$\xi_r = \cos \gamma_r(p) = 0.5[A_0(p) + D_0(p)]. \qquad (9.10)$$

If we replace free end with clamped end, in the drive's model, shown in Fig. 8.2, then taking into account $A_0 = 1$, $D_0 = 1 - J_0^*(p)p^2$, on the basis of (9.10), we get

$$1 - \cos \gamma_r = 0.5J_0^*(p)p^2/c_0. \qquad (9.11)$$

First of all, we will consider the case, when $J_0^* = J_0 = \text{const}$. In this case, the roots of Eq. (9.11), corresponding to the "natural" frequencies, are determined by the following relationship:

$$p_r = 2p_0 \sin \frac{r\pi}{2(n+1)}, \qquad (9.12)$$

where, $p_0 = \sqrt{c_0/J_0}$.

The oscillation form r is described by the relation (9.7), after substituting $h_1 = 0$, $\gamma = \gamma_r$, and the number of main shaft forms n coincide with the number of "natural" frequencies.

When taking into account the elasticity of mechanisms, function $J_0^*(p)$ is described by relation (8.18). Then (9.11) is reduced to a biquadratic equation, with regard to p, the solution of which, at fixed r, provides two real roots: p_{r1} and p_{r2} ($p_{r2} > p_{r1}$). Now the number of "natural" frequencies is equal to $2n$ and is twice the number of the main shaft forms. However, for the system, as a whole, the two

groups of forms differ in that when $p_r = p_{r1}$, the "input" and "output" of the mechanisms, oscillate in the same phase, while when $p_r = p_{r2}$, in anti-phase.

Case 2, ($a_{00} = 0$, $Q_{0n} = 0$), corresponds to the boundary conditions of the model, shown in Fig. 8.2. The boundary condition at the "input", according to (9.8), again determines the sinusoidal form of the main shaft oscillations. At that $h_1 = 0$ and $a_{0j} = h_2 \sin j\gamma$. On the basis of the first equation of system (9.3), $B_0 Q_j = a_{j+1} - A_0 a_j$. Then taking into account $A_0 = 1$, after substituting in (9.8), we get

$$B_0 Q_n = h_2[\sin(n+1)\gamma - \sin n\gamma] = 0.$$

As $h_2 \neq 0$, consequently

$$\sin(n+1)\gamma - \sin n\gamma = 2 \cos(n+0.5\gamma) \sin 0.5\gamma = 0,$$

which taking into account $\gamma \neq 0$, leads to the equation $\cos(n + 0.5\gamma) = 0$.
Therefore,

$$\gamma_r = \pi \frac{2r - 1}{2(n + 0.5)} \qquad r = 1, \ldots, n. \tag{9.13}$$

The frequency equation retains the form of (9.11), but in case of a different value of γ_r, obtained according to relation (9.13). When $J_0^* = J_0 = $ const, the oscillatory system has n degrees of freedom. The "natural" frequencies are obtained, just as in the previous case:

$$p_r = 2p_0 \sin[\pi \frac{2r - 1}{4(n + 0.5)}]. \tag{9.14}$$

In Fig. 9.3, for this case, the graphs of p_r/p_0 are represented, where $n = 6$ (curve 1), $n = 9$ (curve 2) and $n = 12$ (curve 3).

If each of the mechanisms is schematized in the form of the oscillatory system with one degree of freedom (see formula 8.18), for a given value of r, as before, we

Fig. 9.3 Graphs p_r/p_0
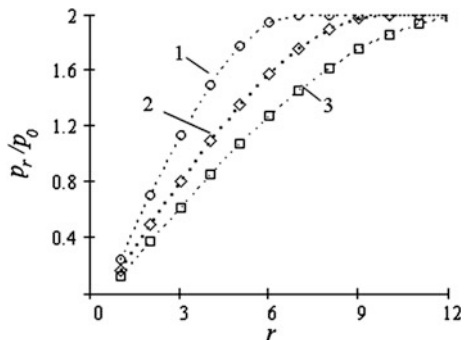
reduce (9.10) to the form of the biquadratic equation, whose solution gives the two values of frequency. Thus, the number of "natural" frequencies is equal to the number of degrees of freedom $2n$. Formulae (9.12), (9.14) set the boundaries of existence of the spectrum of "natural" frequencies. It is often referred to as "range of transmission" area. For example, from formula (9.12), it follows:

$$2p_0 \sin \frac{\pi}{2(n+1)} \leq p_r < 2p_0,$$

and from formula (9.14)

$$-2p_0 \sin \frac{\pi}{2(2n+1)} \leq p_r < 2p_0.$$

The above analysis clearly showed the "might" of the apparatus of study of the regular systems. Indeed, we analytically determined the range of the "natural" frequencies for the oscillatory system, with any finite number of degrees of freedom!

In the leading text we have reviewed the most common case, when $\xi < 1$. This is the case for almost all of the frequency range, except for the narrow bands, in the vicinity of $J_0^* \to \infty$. In these areas, there is a high density of "natural" frequencies, along with the case $\xi \leq 1$, there are cases as $\xi \leq 1$ and $\xi < -1$. When $\xi > 1$ (Im$\eta = 0$), taking $\xi = \mathrm{ch}\gamma$ and carrying out similar calculations, we obtain the expressions that differ from the above only in that the trigonometric functions are replaced by the same name hyperbolic ones. When $\xi < -1$ (Im$\eta = 0$), the condition $\xi = \mathrm{ch}\gamma$ is satisfied, only when $\gamma = \gamma^0 + i\pi$ ($i = \sqrt{-1}$). In this case, we have

$$\cos(\gamma^0 + i\pi) = \cosh\gamma^0 \cosh i\pi + \sinh\gamma^0 \sinh i\pi = -\cosh\gamma^0 \leq -1.$$

Thus, we should accept $\cosh\gamma^0 = -\xi$, and now γ^0 is a real number. On the basis of the Moivre theorem, we have $\cosh j\gamma = (-1)^j \cosh j\gamma^0$ and $\sinh j\gamma = (-1)^j \sinh j\gamma^0$. With these adjustments the dependencies, for case $\xi > 1$, are valid.

Thus, along with the conventional cases, when the forms of oscillations have the usual trigonometric appearance, at a certain frequency range ($|\xi| > 1$), they are described with hyperbolic functions. With reference to the drive model (see Fig. 8.2), this leads to the fact that there is a peculiar spatial attenuation, in which the amplitude of the blocks $|a_{0j}|$ decreases, as it approaches the clamping. A characteristic feature of the case $\xi < -1$, lies in the fact that the sign of a_{0j} changes, when passing through each block.

Forced oscillations We will define the amplitude of forced oscillations from the actions of the disturbing force $F(t) = F^c \cos \omega t + F^s \sin \omega t$, applied to the output link of each of the identical mechanisms. As the method of calculation for both

components of the disturbing force is identical, we restrict ourselves to the cosine component. Then, the recurrent dependencies have the form of (8.27) and represent the non-uniform system of differential equations. In this case, instead of dependence (9.8), we now get

$$a_{0j}^c(\omega) = h_1^c(\omega) \cos j\gamma + h_2^c(\omega) \sin j\gamma + Y_a^c \quad (j = \overline{1, n}). \tag{9.15}$$

Here Y_a^c is the particular solution, which can be determined from the system of Eq. (8.27). From the second equation of the system, it implies that a particular solution (by force) is $Y_Q^c = -F^c/D_j(\omega)$. After substituting $Q_{0,j-1}^c = Y_Q^c$ in the first equation of system (8.27), we have $Y_a^c = -B_0(\omega)F^c/D_j(\omega)$. For the model shown in Fig.8.2, $D_j = (1 - m\,\omega^2/c)/\Pi'$, $Y_Q^c = -F^c\Pi'/(1 - m\,\omega^2/c)$. Since identical mechanisms are subjected to identical forces, index j can be omitted. The particular solution Y_Q^c corresponds to the reduced, to the shaft, maximum moment of the force applied to the output link, and Y_a^c corresponds to the angular deformation of the shaft's section, under the action of this moment.

The boundary conditions are taken into account, in the same way as, when determining the "natural" frequency spectrum. In particular, in case 1, when both ends of the shaft correspond, in the translational movement to the clamping, on the basis of (9.14), we obtain

$$\begin{aligned} a_{00}^c &= h_1(\omega) + Y_a^c = 0 & (j = 0); \\ a_{0,n+1} &= h_1(\omega) \cos(n+1)\gamma + h_2(\omega) \sin(n+1)\gamma = 0 & (j = n+1). \end{aligned}$$

It follows, that $h_1(\omega) = -Y_a^c$; $h_2(\omega) = -h_1(\omega) \cot(n+1)\gamma$. In its final view, formula (9.15) takes the following form:

$$a_{0j}^c(\omega) = \frac{B_0 F^c}{D_j} [\cos j\gamma - \cot(n+1)\gamma \sin j\gamma - 1]. \tag{9.16}$$

Let us recall that $\cos\gamma = \xi = 0.5[A_0(\omega) + D_0(\omega)]$; it corresponds to formula (9.10), but in contrast to free oscillations, instead of frequency p_r, the frequency of the disturbing force ω, appears. If $\omega = p_r$, then according to (9.9) $\gamma = \pi r/(n+1)$, hence $|\cot(n+1)\gamma| \to \infty$ and resonance occurs.

Similarly, we find $a_{0j}^s(\omega)$, after which the amplitude-frequency response, in the arbitrary cross-section, is determined as

$$a_{0j}(\omega) = \sqrt{(a_{0j}^c(\omega))^2 + (a_{0j}^s(\omega))^2}. \tag{9.17}$$

When $a_{00} = 0$, $Q_{0n} = 0$, (case 2)

$$\left.\begin{array}{l} h_1^{c,s}(\omega) + Y_a^{c,s} = 0; \\ h_1^{c,s}(\omega)[\cos(n+1)\gamma - \cos n\gamma] + h_2^{c,s}(\omega)[\sin(n+1)\gamma - \sin n\gamma] = 0. \end{array}\right\}$$

The solution of this system of equations is

$$\left.\begin{array}{l} h_1^{c,s}(\omega) = F^{c,s}B_0(\omega)/D_j(\omega); \\ h_2^{c,s}(\omega) = F^{c,s}B_0(\omega)\tan(n+0.5)\gamma/D_j(\omega). \end{array}\right\} \tag{9.18}$$

After substituting (9.18) into (9.15), we obtain the relation that defines the frequency response in arbitrary section j of the main shaft

$$a_{0j}^{c,s}(\omega) = \frac{F^{c,s}B_0(\omega)}{D_j(\omega)}[\cos j\gamma - 1 + \tan(n+0.5)\gamma \sin j\gamma]. \tag{9.19}$$

When $\omega = p_r$, according to (9.15), we get $\gamma = \gamma_r$; at the same time $|\tan(n+0.5)\gamma_r| \to \infty$, $a_{0j}^{c,s}(\omega) \to \infty$, which corresponds to the resonance.

Formula (9.19) shows yet another possible resonant state of the system, which is associated with the possibility of nullifying $D_j(\omega)$. Indeed, for the model under consideration

$$D_j(\omega) = 1 - J_*(\omega)\,\omega^2/c_0 = 1 - [J_0 + m\Pi'^2/(1 - \omega^2/k_j^2)]\omega^2/c_0,$$

where, $k_j^2 = c_j/m_j$.

Just formally, turning this expression into zero, we can find the corresponding critical frequency ω. It should, however, be borne in mind that the considered trigonometric form of oscillations, corresponds to the condition $\xi = \cos\gamma = 1 - 0.5\,J_*\omega^2/c_0$, so $|1 - 0.5\,J_*\omega^2/c_0| \le 1$. Hence, $J_*(\omega) < 0$ or $J_*(\omega)\,\omega^2/c_0 > 2$. In case of violation of these conditions, as already noted, the form of oscillations is described using the hyperbolic functions. Typically, this occurs on the limited frequency band, in the vicinity of the values of k_j. When $\omega = k_j$, we have $D_j(\omega) \to \infty$. Then, on the basis of (9.18), $a_{0j}^{c,s}(k_j) = 0$; it means, that at the given frequency, anti-resonance occurs and the mechanisms play the role of dynamic absorbers. However, in case of larger numbers of mechanisms n, in the vicinity of frequency k_j, the thickening of "natural" frequencies is observed and hence, the resonance zones, so the reliable tuning for the mode of dynamic damping, cannot be realized.

For stricter analysis of the forced oscillations, taking into account the dissipative forces, see Chaps. 10, 11, 12.

9.3 Model with Distributed Parameters

Preliminary notes   The complexity of modern machinery and large dynamic coupling of its individual units, as already mentioned, leads to the necessity of studying the oscillatory systems with many degrees of freedom. During analysis, especially during the dynamic synthesis of such systems, there often arises some difficulties of computational nature, characterized by the figurative term "*curse of dimensionality*". In addition, the array of generalized coordinates and varied parameters becomes difficult to comprehend.

To overcome these difficulties in the study of complex objects of mechanics, automatic control, and economy, currently becoming more common are the ideas of system aggregation, based on the integral representation of its parameters. Applied to the problems of dynamics of machines, in the development of such approaches, the continuum models were proposed, in which the kinematic, elastic and inertial properties of the mechanisms are mapped with some "pseudo medium". This allows us to operate with the generalized representation of the variables and to significantly reduce the number of characteristics, describing the oscillatory system [47, 63, 64]. As a result, we can greatly simplify the dynamic analysis and synthesis of the systems and in many cases represent the solution in the analytical form.

Mathematical model   We will concretize the technique of using the continuum model with respect to the problems of dynamics of machines, using the example of a drive with *n* identical cyclic mechanisms, branching from the main shaft (see Fig. 8.2). As opposed to the drive with a regular structure, discussed in Sect. 9.2, we represent the main shaft as the torsion subsystem, with distributed parameters and the mechanisms attached to the shaft, as the pseudo medium (Fig. 9.4).

Each element of this pseudo medium, shown in the model with vertical lines, is formed by "spreading" the elastic, inertial and kinematic characteristics along the shaft's axis and has the property to transmit motion and force. At the same time, the interaction between the elements of the pseudo-medium takes place only through the main shaft. The set of parallel and stretched unrelated threads (but not the cloth!), mounted on a common base, can serve as some analogy of this model.

Fig. 9.4 Continuum dynamic model
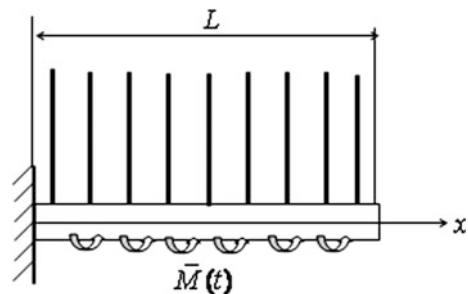
   This model corresponds to the relative coordinate system, therefore, section $x = 0$, rotating with the constant translational angular velocity ω_0, is shown as the clamping.

   With the regular system of identical mechanisms, the "density" of the medium is constant, that corresponds to the uniform distribution of elements, along the shaft. The characteristic of the medium is the distributed modified transition matrix of the mechanism $\bar{\Gamma} = \prod\limits_{j=n}^{1} \bar{\Gamma}_j$, which is formed as the product, in the reverse order, of the transition matrices of mechanisms (see Chap. 8), with the difference, however, that when determining $\bar{\Gamma}_j$, the inertia and elastic elements must be distributed along the axis of the shaft. In this case, instead of mass or moment of inertia, we use $\bar{m} = nm_j/L$, $\bar{J} = nJ_j/L$, and instead of the stiffness coefficient—$\bar{c} = nc_j/L$.

   As was shown in Sect. 8.2, consideration of the dynamic characteristics of mechanism j, according to (8.17), can be performed, by introducing reduced moment J^*_{0j}. Then, the linear moment of inertia of the shaft is defined as $\rho(p) = \rho_0 - nR_j(p)/(\rho^2 L)$, where ρ_0 is the distributed moment of inertia of the shaft itself; p is the "natural" frequency (in the calculation of the forced oscillations, frequency p should be substituted with disturbing force ω). If the first transfer function of the mechanisms is constant ($\Pi'_j = $ const), as this, for example, takes place in the gear mechanisms with the constant gear ratio, we have $\rho(p) = $ const. In this case we obtain the following differential equation in partial derivatives

$$\rho \frac{\partial^2 \varphi}{\partial t^2} + GI_0 \frac{\partial^2 \varphi}{\partial x^2} = \bar{M}(t), \qquad (9.20)$$

where $\varphi(x, t)$ is the angular coordinate of the main shaft, corresponding to the oscillations; G is the shear modulus; I_0 is the polar moment of inertia; $\bar{M}(t)$ is the reduced, to the main shaft, driving moment per unit length (see below).

Definition of "natural" frequencies and non-stationary shape modes   When solving this problem, in Eq. (9.20), we should accept $\bar{M}(t) = 0$. For cyclic mechanisms, the first transfer function Π', when $\omega \ll p$, changes slowly, depending on $\varphi_0 = \omega_0 t$, where ω_0 is the angular velocity of the main shaft. In this case, functions $J^*_{0j}(\varphi_0)$, $R^*_j(\varphi_0)$, $\rho(\varphi_0)$ are also slowly changing and the free oscillations, on the basis of the conditional oscillator method, are described by the dependence, similar to (5.102). We find the particular solution of Eq. (9.19) in the form

$$\varphi(x, \varphi_0) = X(x, \varphi_0)\sqrt{p(0)/p(\varphi_0)} \sin\left(\int\limits_0^{\varphi_0} p(u)du + \alpha\right).$$

   After substitution in the differential equation (9.19), we obtain the equation with respect to amplitude function $X(x, \varphi_0)$.

$$\frac{\partial^2 X}{\partial x^2} + P(\varphi_0)X = 0, \tag{9.21}$$

where, $P(\varphi_0) = \rho(\varphi_0)p^2/(GI_0)$.

In general, the function $\rho(\varphi_0)$ can take both positive and negative values. For the model shown in Fig. 8.2, $\rho = \rho_0 + \bar{m}\Pi'^2/(1 - p^2/k^2)$, where $k = \sqrt{c_j/m_j}$, is the partial frequency of the mechanism responsible for the clamping of its "input". Then, condition $\rho(\varphi_0) > 0$ is met by frequency ranges $p/k < 1$ and $p/k > \sqrt{1 + \bar{m}\Pi'^2/\rho_0 2}$, and the interval $1 < p/k < \sqrt{1 + \bar{m}\Pi'^2/\rho_0}$ is met by condition $\rho(\varphi_0) < 0$.

When $\rho(\varphi_0) > 0$, $P(\varphi_0) > 0$, function X has the trigonometric form

$$X(x, \varphi_0) = h_1(\varphi_0) \cos \sigma x + h_2(\varphi_0) \sin \sigma x,$$

where $\sigma(\varphi_0) = \sqrt{P(\varphi_0)}$.

In this example the boundary conditions have the form $X(0, \varphi_0) = 0$, $\partial X/\partial x(L, \varphi_0) = 0$. It follows that $\cos(\sigma(\varphi_0)L) = 0$. After substitution of function $P(\varphi_0)$ and elementary transformations, we get the frequency equation in the following form

$$p_r^2(\varphi_0) = \frac{c\pi^2(2r-1)^2}{4\{\bar{J} + nm_j\Pi'^2/[1 - p_r^2(\varphi_0)/k^2]\}}. \tag{9.22}$$

Here $c = GI_0/L$ is the coefficient of torsion stiffness of the shaft; r is the number of the mode of main shaft's oscillations.

We will reduce Eq. (9.22) to the form of the biquadratic equation, which has two real roots $p_{r1}(\varphi_0)$ and $p_{r2}(\varphi_0)$. The first root corresponds to the inphase oscillations of the input and output elements of the mechanism, whereas the second one corresponds to the anti-phase oscillations. When $c_j \to \infty$ on the basis of (9.22), we obtain

$$p_r(\varphi_0) = \frac{\pi(2r-1)}{2}\sqrt{\frac{c}{J_0 + nm_j\Pi'^2(\varphi_0)}}.$$

The oscillations mode is described as

$$X_r(x, \varphi_0) = \sin(\sigma_r(\varphi_0)x),$$

where, $\sigma_r(\varphi_0) = p_r(\varphi_0)\sqrt{\rho(\varphi_0)/(GI_0)}$.

When $\rho(\varphi_0) < 0$ $(P(\varphi_0) < 0)$, the amplitude function X is described with hyperbolic functions: $X(x, \varphi_0) = h_1(\varphi_0) \cosh \sigma^0 x + h_2(\varphi_0) \sinh \sigma^0 x$, where, $\sigma^0(\varphi_0) = \sqrt{|P(\varphi_0)|}$.

The boundary condition $X(0, \varphi_0) = 0$ is satisfied, when $h_1(\varphi_0) = 0$. The second boundary condition, $\partial X / \partial x (L, \varphi_0) = 0$, when $h_2(\varphi_0) \neq 0$, takes the form $\sigma^0 \mathrm{ch}\sigma^0 L = 0$. As $\mathrm{ch}\sigma^0 L \geq 1$, we obtain $\sigma^0(p) = 0$. For the given model, this condition leads to the expression

$$p_*(\varphi_0)/k = \sqrt{1 + \bar{m}\Pi'^2(\varphi_0)/\rho_0}. \tag{9.23}$$

However, the condition $\sigma^0(p) = 0$ is contrary to the original assumption $\rho < 0$, since, in this case $\rho = 0$. In this case, in Eq. (9.20), we should accept $P(\varphi_0) = 0$. Then the oscillations mode is described as follows: $X = 0.5x^2 - Lx$.

Forced oscillations   Let us assume that to the output link of each of the mechanisms, disturbing force $Q_j = F_j \cos \omega t$ is applied. As shown in Sect. 8.2, each of these forces transmits to the main shaft, moment $M_j = -F_j D_j^{-1} \cos \omega t$. At the same time, the distributed, along the x axis reactive driving moment, is equal to $\bar{M}(t) = -FnD^{-1}L^{-1} \cos \omega t$. (Since the mechanisms and the applied disturbing forces are identical, index j can be omitted.) Restricting ourselves to considering the non-resonant case, we find the solution of (9.19), in the following form

$$\varphi(x, t) = Y(x, \varphi_0) \cos \omega t. \tag{9.24}$$

Here, $Y(x, \varphi_0)$ is the amplitude function, which slowly changes depending on the so-called *slow time* $\varphi_0 = \omega_0 t$.

After substituting (9.24) in (9.20), we obtain the differential equation, with respect to amplitude function $Y(x, \varphi_0)$:

$$\partial^2 Y / \partial x^2 + P(\varphi_0)Y = \bar{M}_*(\varphi_0)/(GI_0), \tag{9.25}$$

where $\bar{M}_*(\varphi_0) = -FD^{-1}(\varphi_0)L^{-1}$; $P(\varphi_0) = \rho(\varphi_0)\omega^2/(GI_0)$. (Functions $P(\varphi_0)$ and $\rho(\varphi_0)$ differ from the ones used in Eq. (9.21), only with replacement of the free oscillation frequency p for the frequency of disturbing forces ω.) When $\rho(\varphi_0) > 0$ the solution of Eq. (9.25) has the form

$$Y = h_1 \cos \sigma x + h_2 \sin \sigma x + Y_*, \tag{9.26}$$

where $\sigma(\varphi_0) = \sqrt{P(\varphi_0)}$; $Y_* = \bar{M}_*/(\rho(\varphi_0)\omega^2)$ is the particular solution.

For the given model

$$Y_*(\varphi_0) = -\frac{F\Pi'(\varphi_0)}{\omega^2 \left[\rho_0(1 - \omega^2/k^2) + \bar{m}\Pi'^2(\varphi_0)\right]}. \tag{9.27}$$

In case of boundary conditions $Y(0, \varphi_0) = 0$ and $\partial Y / \partial x (L, \varphi_0) = 0$, we have $Y = -Y_*(\cos \sigma x + \tan\sigma L \sin \sigma x)$.

As expected, when $\omega = p_r(\varphi_0)$, resonance occurs ($|\tan\sigma L| \to \infty$). It should, however, be borne in mind that the "natural" frequency p_r is the slowly varying function, so the resonant frequency "floats". In this case instead of seeing an explicit resonance peak, we usually observe a beat mode.

When $\rho(\varphi_0) < 0$, we find the solution in the form of hyperbolic functions. Then

$$Y = Y_*[\cosh(\sigma^0 x) - \tanh(\sigma^0 L)\sinh(\sigma^0 x)], \quad \text{where } \sigma^0 = \sqrt{|P(\varphi_0)|}.$$

From formula (9.27), it follows that $|Y_*(\varphi_0)| \to \infty$, when

$$\frac{\omega}{k} = \sqrt{1 + \frac{\bar{m}\Pi'^2}{\rho_0}}. \tag{9.28}$$

When $\omega = p_*$, formulae (9.28) and (9.23) coincide.

Conciseness of the above mentioned calculations and the final form of the obtained analytical relationships, proves the great predictive capabilities of continuum models, which is particularly important at the stage of dynamic synthesis of complex oscillatory systems of this class.

Chapter 10
Regular Cyclic Systems with Ring and Branched-Ring Structure

10.1 Model of Ring Structure, with Lumped Parameters

Dynamic model In machines for the textile, printing, light, and a number of other industries, manufacturing operations are carried out by the executive members of the increased extension. In such cases, to provide the required stiffness of the system and to avoid the high level of vibration activity, the executive body is driven by multiple duplicated cyclic mechanisms. This oscillatory drive system forms the closed contours and acquires the so-called ring structure, which is associated with the number of specific features [16, 62–64, 73, 78]. A dynamic model of the drive (Fig. 10.1), consisting of the subsystems of the main shaft $(k = 1)$ and the executive body $(k = 2)$, linked to the main shaft with n cyclic mechanisms, is under consideration.

Every mechanism is represented as a serial connection of elements, which take into account inertial, elastodissipative and kinematic characteristics. Further, the following conditional notes are accepted: $J_{j,k}$ are the moments of inertia; $c_{j,k}$, c_j are the stiffness coefficients; $\psi_{j,k}$, ψ_j are the dissipation coefficients; $\Pi(\varphi_j)$ is the position function. It is assumed that the dynamic characteristics of the main shaft and the executive body are reduced to the input and output links of the cyclic mechanisms. Herewith, the angular velocity ω, at the "input", is assumed to be constant, which is usually valid, in the first approximation, for the real machines, with the rational choice of electric motor characteristics and the geared drive. The oscillatory system under consideration has $2n + 1$ degrees of freedom.

Frequency and modal analysis At this stage of analysis, we will exclude from consideration the external excitations and the negligible effect of the dissipative components, as well as taking into account the identity of modules $c_{1j} = c_1$; $c_{2j} = c_2$; $c_j = c$; $J_{1j} = J_1$; $J_{2j} = J_2$; $J_j = J$. As generalized coordinates, we accept the deviations from the coordinates of program motion, caused by the oscillations: q_{1j} and q_{2j}. The angle of rotation of the main shaft in section j is equal to $\varphi_j = \varphi + q_{1j}$,
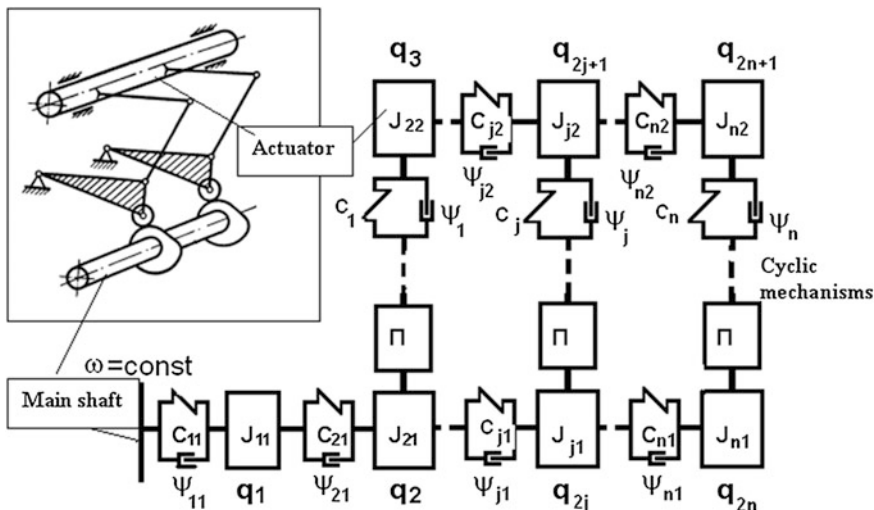
Fig. 10.1 Dynamic model

where $\varphi = \omega t$ is the ideal rotation angle. After linearization of the position function, in the vicinity of the program motion, we have $\Pi(\varphi + q_{1j}) \approx \Pi(\varphi) + \Pi'(\varphi)q_{1j}$, where, $\Pi'(\varphi) = d\Pi/d\varphi$ is the first geometric transfer function (analogue of speed).

The system under consideration is the complicated model of the linear chain of repeating units, to which the method of analysis, similar to the one used for the system of branched structure, can be applied. System parameters are *slowly* changing. When, $c_{11} \to \infty$, the system has $2n$ degrees of freedom. For module j, the following system of equations is valid:

$$\left.\begin{array}{l} J_1\ddot{q}_{1j} + c_1(q_{1j} - q_{1,j-1}) - c_1(q_{1,j+1} - q_{1j}) - c\Pi'(q_{2j} - \Pi'q_{1j}) = 0; \\ J_2\ddot{q}_{2j} + c_2(q_{2j} - q_{2,j-1}) - c_2(q_{2,j+1} - q_{2j}) + c(q_{2j} - \Pi'q_{1j}) = 0, \end{array}\right\} \quad (10.1)$$

In order to simplify spreading and transformation, in case of recording of system of Eq. (10.1), the moments of inertia J_j are reduced to the main shaft and are included as additives $\Delta J_{1j} = J_j\Pi'^2$ the moment of inertia J_j (here and below argument φ, when writing the functions, is omitted). The particular solution of system (10.1), on the basis of the conditional oscillator method, is found in the form:

$$q_{1j} = X_j \sin \int_0^t \Omega(t)dt; \quad q_{2j} = Y_j \sin \int_0^t \Omega(t)dt, \quad (10.2)$$

where $X_j = \tilde{X}\exp(ij\gamma), Y_j = \tilde{Y}\exp(ij\gamma)$ $(i = \sqrt{-1})$; $\Omega(t)$ is the "natural" frequency.

Substituting (10.2) into (10.1) and after some simplifications, we get:

$$\left.\begin{array}{r} [2c_1(1 - \cos\gamma) + \Pi'c - J_1\Omega^2]\tilde{X} - c\Pi'\tilde{Y} = 0; \\ -c\Pi'\tilde{X} + [2c_2(1 - \cos\gamma) + c - J_2\Omega^2]\tilde{Y} = 0. \end{array}\right\} \tag{10.3}$$

Let us introduce the following conditional notes: $\zeta_1 = c_1/c$; $\zeta_2 = c_2/c$; $k_1 = \sqrt{c_1/J_1}$; $k_2 = \sqrt{c_2/J_2}$; $\chi = k_2/k_1$; $v = \Omega/k_1$. In this case, the nontrivial solution of (10.3) corresponds to the quadratic equation

$$\rho_2 L^2 + \rho_1 L + \rho_0 = 0, \tag{10.4}$$

where

$$\begin{aligned} \rho_0 &= (\Pi'^2 - \zeta_1 v^2)(1 - \zeta_2\chi^{-2}v^2) - \Pi'^2; \\ \rho_1 &= 2[\zeta_2(\Pi'^2 - \zeta_1 v^2) + \zeta_1(1 - \zeta_2\chi^{-2}v^2)]; \\ \rho_2 &= 4\zeta_1\zeta_2; \\ L &= 1 - \cos\gamma. \end{aligned}$$

It can be shown that, $\rho_1^2 - 4\rho_0\rho_2 \geq 0$, so the roots of the Eq. (10.4), L_1, L_2, are real numbers. Thus, $\gamma_{1,2} = 2\Pi r \pm \arccos(1 - L_{1,2})$ at $0 < L_{1,2} < 2$; $\gamma_{1,2} = \operatorname{arccosh}(1 - L_{1,2})$; at $L_{1,2} < 0$; $\gamma_{1,2} = \gamma_{1,2}^0 = \operatorname{arccosh}|1 - L_{1,2}|$ at $L_{1,2} > 2$.

Further, we represent the amplitude functions X and Y in the following form:

$$\left.\begin{array}{l} X(j) = \sum\limits_{r=1}^{2} \beta_{1r}(h_{1r}f_{jr} + h_{2r}u_{jr}), \\ Y(j) = \sum\limits_{r=1}^{2} \beta_{2r}(h_{1r}f_{jr} + h_{2r}u_{jr}), \end{array}\right\} \tag{10.5}$$

where

$$\begin{aligned} \beta_{11} &= 1; \quad \beta_{12} = \Pi'(2\zeta_1 L_1 + 1 - \zeta_1\chi^{-2}v^2)^{-1}; \\ \beta_{21} &= \Pi'(2\zeta_1 L_2 + 1 - \zeta_1\chi^{-2}v^2)^{-1}; \quad \beta_{22} = 1; \end{aligned}$$

$$f_{jr} = \begin{cases} \cos j\gamma_r & (0 < L_r < 2); \\ \cosh j\gamma_r & (L_r \leq 0); \\ (-1)^j\cosh j\gamma_r^0 & (L_r \geq 2); \end{cases} \qquad u_{jr} = \begin{cases} \sin\gamma_r & (0 < L_r \leq 2); \\ \sinh\gamma_r & (L_r \leq 0); \\ (-1)^j\sinh\gamma_r^0 & (L_r \geq 2). \end{cases}$$

Herewith, the load in section j of subsystems 1 and 2 are determined as

$$Q_{1j} = c_1(X(j+1) - X(j)); \quad Q_{2j} = c_2(Y(j+1) - Y(j)).$$

To determine the spectrum of slowly varying "natural" frequencies, we use the boundary conditions $Q_{10} = X(0)R_0$, $Q_{1n} = 0$, $Q_{20} = 0$, $Q_{2n} = 0$, where $R_0 = \xi(v)c$ is the dynamic stiffness at the "input" (see Fig. 10.1). Then, taking into account (10.5) and the introduced above dimensionless parameters, we obtain the following system of uniform algebraic equations with respect to h_{1r}, h_{2r}:

$$\left.\begin{array}{l}
\displaystyle\sum_{r=1}^{2} \beta_{1r}(v)\left\{h_{1r}\left[f_{1r}(v) - \xi^{-1}(v)\varsigma_1\right] + h_{2r}u_{1r}(v)\right\} = 0; \\[4mm]
\displaystyle\sum_{r=1}^{2} \beta_{2r}(v)\left\{h_{1r}[f_{1r}(v) - 1] + h_{2r}u_{1r}(v)\right\} = 0; \\[4mm]
\displaystyle\sum_{r=1}^{2} \beta_{1r}(v)\left\{h_{1r}\left[f_{n+1,r}(v) - f_{nr}(v)\right] + h_{2r}\left[u_{n+1,r}(v) - u_{nr}(v)\right]\right\} = 0; \\[4mm]
\displaystyle\sum_{r=1}^{2} \beta_{2r}(v)\left\{h_{1r}\left[f_{n+1,r}(v) - f_{nr}(v)\right] + h_{2r}\left[u_{n+1,r}(v) - u_{nr}(v)\right]\right\} = 0.
\end{array}\right\} \quad (10.6)$$

Converting the determinant of this system into zero, we obtain the formal frequency equation, whose solutions are the slowly-changing, dimensionless "natural" frequencies $v(\varphi)$.

Further, we will turn to the more general case of a drive with the circular structure, when the dynamic model of the cyclic mechanism is the oscillatory contour of the arbitrary form, formed with the serial connection of inertial, elastic and kinematic elements (J, c, Π).

In this case, the matrix method of description, for the regular systems, is preferred. Let A, B, C, D be the elements of the first and second rows of the cyclic mechanism's transition matrix (see Sect. 8.1). Then, the matrix form of the recursive expressions, for module j, has the form

$$\begin{bmatrix} K_{1j} \\ Q_{1j} \\ K_{2j} \\ Q_{2j} \end{bmatrix} = \begin{bmatrix} 1 & c_1^{-1} & 0 & 0 \\ AB^{-1} & A(Bc_1)^{-1} + 1 & -B^{-1} & -(Bc_2)^{-1} \\ 0 & 0 & 1 & c_2^{-1} \\ -B^{-1} & -(Bc_1)^{-1} & DB^{-1} & D(Bc_2)^{-1} + 1 \end{bmatrix} \begin{bmatrix} K_{1,j-1} \\ Q_{1,j-1} \\ K_{2,j-1} \\ Q_{2,j-1} \end{bmatrix}. \quad (10.7)$$

Here $K_{1j}, K_{2j}, Q_{1j}, Q_{2j}$ are the amplitudes of oscillations and forces of the main shaft 1 and executive member 2.

For the model, of the mechanism, presented in the Fig. 10.1:

$$\begin{aligned}
A &= \Pi' - J_1\Omega^2(c\Pi')^{-1}; \\
B &= (c\Pi')^{-1}; \\
C &= -(\Pi')^{-1}\Omega^2\left[J_2 - J_1(1 - J_2\Omega^2/c)\right]; \\
D &= (\Pi')^{-1}(1 - J_2\Omega^2/c)
\end{aligned}$$

(see Table 8.1).

The recursive relations (10.7) can be considered as the uniform system of differential equations, the non-trivial solution, of which we are looking for, in the form $K_{rj} = \lambda K_{r,j-1}$, $Q_{rj} = \lambda Q_{r,j-1}$, where the characteristic exponents λ are determined as the roots of the following reciprocal equation:

$$\lambda^4 + a\lambda^3 + b\lambda^2 + a\lambda + 1 = 0. \tag{10.8}$$

Using well-known substitution, $\lambda + \lambda^{-1} = z$, we transform Eq. (10.8) into two quadratic equations, whose roots are:

$$\lambda_{1,2,3,4} = 0.5(z_{1,2} \mp \sqrt{z_{1,2}^2 - 4}),$$

where $z_{1,2} = 0.5\left[-a \pm \sqrt{a^2 - 4(b-2)}\right]$.

For determining coefficients a and b in general, we use the D.K Faddeev method [22], the use of which leads to the dependencies

$$a = -\text{Sp}\boldsymbol{\Gamma} = -\sum_{k=1}^{4} g_{kk}; \quad b = 0.5\left(\sum_{k,s=1}^{4} g_{kk}g_{ss} - \sum_{k,s=1}^{4} {}^* g_{ks}g_{sk}\right), \tag{10.9}$$

where g_{ks} are the elements included in (10.7), transition matrix $\boldsymbol{\Gamma}$, (an asterisk, in case of the sign of sum, means the omission of a member $s = k$).

On the basis of (10.7), (10.9), we get $a = -\left[4 + A(Bc_1)^{-1} + D(Bc_2)^{-1}\right]$; $b = 2B^{-1}(Ac_1^{-1} + Dc_2^{-1}) + (B^2c_1c_2)^{-1}(C-1) + 6$.

It can be shown that $a^2 - 4(b-2) = B^{-2}\left[(A/c_1 - D/c_2)^2 + 4/(c_1c_2)\right] \geq 0$. Hence, it follows that the numbers $z_{1,2}$ are real. Herewith, $\gamma_k = \arccos(0.5z_k)$ if $|z_k| < 2$, $\gamma_k = \text{arccosh}(0.5z_k)$ if $z_k > 2$ and $\gamma_k = \text{arccosh}(0.5|z_k|) + i\pi$ if $z_k < -2$.

The spectrum of "natural" frequencies can be determined on the basis of (10.6), however, the calculations show that these results are very sensitive to the accuracy of calculations, notably for higher frequencies. The use of the matrix equation appears to be more preferably:

$$[K_{1n}, 0, K_{2n}, 0]^{\text{T}} = \boldsymbol{\Gamma}^n[1, R_0, K_{20}, 0]^{\text{T}}. \tag{10.10}$$

On the basis of (10.10), the formal frequency equation can be represented as

$$w_{43}(\nu)[w_{21}(\nu) + w_{22}(\nu)\xi(\nu)] - w_{23}(\nu)[w_{41}(\nu) + w_{42}(\nu)\xi(\nu)] = 0, \tag{10.11}$$

where w_{ik} are the entries of the matrix $\mathbf{W} = \boldsymbol{\Gamma}^n$; $\xi(\nu) = c\zeta_1/R_0(\nu)$. (If the main shaft, having constant angular velocity, is connected with elastic elements c_0, with the input section of the drive, we have $R_0 = c_0$.) For the model, under consideration, $w_{21}(\nu) = \Pi'^2 - \zeta_1\nu^2$; $w_{22}(\nu) = 1 - \nu^2 + \zeta_1^{-1}\Pi'^2$; $w_{23} = -\Pi'$; $w_{41} = -\Pi'$; $w_{42} = -\zeta_1^{-1}\Pi'^2$; $w_{43}(\nu) = 1 - \nu^2\chi^{-2}\zeta_2$.

Fig. 10.2 Areas of existence
of solutions
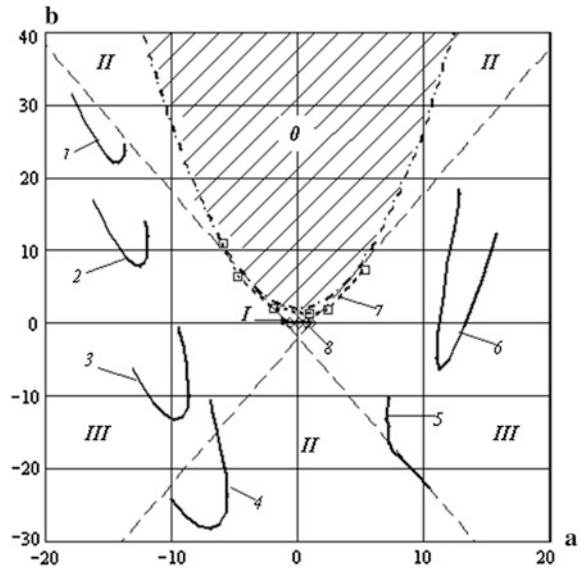
For the visual exposure of the areas of existence of solutions and their mathe-
matical form, it is proposed to use the coordinate plane $a - b$ [63, 64]. In Fig. 10.2,
for the above initial data, the solutions areas are shown, which correspond to the
trigonometric or hyperbolic form of oscillations [see (10.5)].

In the area I the hatched area 0, the solutions are absent. In the area I,
expressions $X(j)$ and $Y(j)$ are described with the trigonometric functions; in area II,
with the hyperbolic functions; in area III, with the mixed expressions.

Curves 1–6 correspond to the first set of input data, the narrow areas shown, with
the squares of curve 7, correspond to the second set. Curve 8 corresponds to the
results obtained with one variant of the system decomposition (see Sect.10.2).

When $\Pi'(\varphi) \to 0$, which corresponds to the dwell of the machine's executive
body, the original dynamic model is divided into two unrelated regular oscillatory
systems, which we will name as partial. Each of these subsystems corresponds to
dependence (10.5) to (10.6), in which, we should now accept $\beta_{12} = 0$ and $\beta_{21} = 0$.

The "natural" frequencies of the executive member's partial system, consisting
of n identical blocks, are determined with the following dependence:

$$p_{r2} = k_2\sqrt{\zeta_2^{-1} + 2[1 - \cos((r - 1)\pi/n)]} \qquad (r = \overline{1, n}). \tag{10.12}$$

It follows that the whole spectrum of "natural" frequencies is in the interval

$$k_2 \zeta_2^{-0.5} \leq p_{r2} < k_2 \sqrt{\zeta_2^{-1} + 4}.$$

Segment 8 on the X-axis corresponds to this result. The oscillation mode, in accordance with (10.5), is described with dependence

$$Y_r(j) = \cos[\pi(j-1)(r-1)/n] + (-1)^{r-1}\tan[0.5\pi(r-1)/n]$$
$$\times \sin[\pi(j-1)(r-1)/n].$$

Similarly, on the basis of (10.6), for the partial system of the main shaft, we obtain the following frequency equation, whose roots are the frequencies p_{r1}:

$$(1 + \xi(v))\cos(n + 0.5)\theta(v) - \cos(n - 0.5)\theta(v) = 0, \qquad (10.13)$$

where, $\theta(v) = \arccos \kappa(v)$; $\kappa(v) = 1 - 0.5v^2$; $v = p_{r1}/k_1$; $k_1 = \sqrt{c_1/J_1}$.

Although the Eq. (10.13) is transcendental, its solution, as per the numerical methods, is not difficult. However, for quick evaluation of the influence of the dynamic stiffness, on the "input" $R_0(v)$, mapped with function $\xi(v) = c_1/R_0(v)$, the two limiting cases $|R_0(v)| \to \infty$ and $R_0(v) \to 0$ are of interest. In the first case, $\cos(n + 0.5)\theta \to 0$, then $\theta_r = \theta_r^{(1)} = \pi(r - 0.5)/(n + 0.5)$. In the second case, on the basis of (10.13), we obtain $\theta_r = \theta_r^{(2)} = \pi r/n$. In both limiting cases the "natural" frequencies are

$$p_{r1}^{(1,2)} = 2k_1 \sin 0.5\theta_r^{(1,2)}. \qquad (10.14)$$

More detailed analysis of the effect $R_0(v)$ on the frequency spectrum, we will consider using the example, where the oscillatory system, at the "input", consists of serial connections of the massive disk (this is equivalent to "clamping" of the corresponding section), the elastic element c_0 and inertial element J_0. Then, $R_0(v) = c_0(1 - v^2\chi_0^{-2})$, where $R_0(v) = c_0(1 - v^2\chi_0^{-2})$ $\chi_0 = k_0/k_1$, $k_0 = \sqrt{c_0/J_0}$. On the other hand, as per (10.13), we have $\tilde{R}_0(v) = R_0(v)/c = F(v)$, where $F(v) = \cos[(n - 0.5)\theta(v)]/\cos[(n + 0.5)\theta(v)] - 1$.

For number of values of χ_0, in Fig. 10.3, solid lines represent the typical graphs $\tilde{R}_0(v)$, whereas the hatch-dotted lines represent $F(v)$. The points of intersection of the two curves correspond to the given parameters. The points of intersection of $F(v)$, with the abscissa axis, correspond to $\tilde{R}_0(v) = 0$. The second limiting case ($\tilde{R}_0(v) \to \infty$) is shown by the hatched line. The corresponding frequencies are determined as per (10.14).

The sensitivity of the frequency spectrum, to the boundary conditions, is proportional to the cotangent of the inclination angle of the tangent line to the curve $F(v)$, at the point of intersection with the curve $\tilde{R}_0(v)$. The analysis of the graphs

Fig. 10.3 To the analysis of
edge effect on the frequency
spectrum
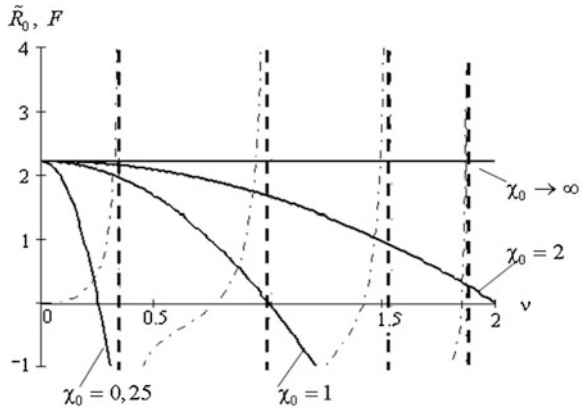
shows that the substantial influence, of dynamic stiffness of the drive, can be expected in case of closeness of these points to the abscissa axis.

It should be noted that the estimation of the influence of dynamic stiffness, at the "input" $R_0(\nu)$, allows us to answer the question, about how much is the taking into account of the dynamic stiffness of the drive, in the unit dynamic model, justified. The feasibility of decomposition, in this case, is associated with significant differences of the frequency spectra ranges of the partial systems, because of which the instability of calculations can occur.

In the particular cases under consideration, the variability of "natural" frequencies, due to non-stationary communication, implemented in the cyclic mechanism, was not taken into account. Therefore, we consider another case, corresponding to the relatively low stiffness of the executive body, where we can take $c_2 = 0$. Thus, the initial dynamic model is transformed into a system of branching structures. Then, the formal frequency equation (10.13) and dependence (10.14) retain the same form, however, now $\theta = \theta_{*r} = \arccos(\kappa_{*r}(\nu))$, where

$$\kappa_{*r} = 1 - 0.5 p_{*r}^2 c_1^{-1} \left[J_1 + J_2 (\Pi'(\varphi))^2 (1 - p_{*r}^2 J_2/c)^{-1} \right]. \qquad (10.15)$$

When $R_0 = c_0$, we have $\xi = \text{const}$, therefore, the roots of Eq. (10.13) θ_{*r}, do not depend on ν. Then, Eq. (10.15), with respect to p_{*r}, is reduced to a biquadratic equation. In a more general case, when $R_0 = R_0(\nu)$, dependencies (10.13) and (10.15) form the system of equations. The analysis showed that, from the point of decomposition, the case of "rigid" cyclic mechanism ($c \to \infty$), is of interest. Then, Eq. (10.15) implies

$$p_{*r} = \sqrt{2(1 - \cos\theta_{*r}) c_1 / \left[J_1 + J_2 \Pi'^2(\varphi) \right]}. \qquad (10.16)$$

Under the above introduced dimensionless parameters, dependence (10.15) takes the form

$$v_{*r} = p_{*r}/k_1 = 2|\sin 0.5\,\theta_{*r}|/\sqrt{\zeta_2 \zeta_1^{-1} \chi^{-2} \Pi'^2(\varphi) + 1}. \qquad (10.17)$$

A comparison of the frequency spectra, of the original model and the partial systems, shows their proximity, and in many cases, clearly points to the "origin" of the components of these spectra.

These differences, in the frequency spectra, are mainly due to the fact that in the considered partial systems, in case of increase in function $\Pi'(\varphi)$, only the decreasing character, of frequency response, appears, which is associated with the increase in the reduced moment of inertia, while the tightening role of the executive body is not reflected.

Analysis, of the partial systems, is also of interest as a way of reducing the machine's vibration activity. At the first glance, it seems that for the cyclic machines, with operating speeds usually quite far from the resonant modes, the spectrum of the "natural" frequencies is not important. It should, however, be kept in mind that due to the clearances and pulsed nature of excitation, along with the low-frequency vibrations of machine's elements, are generated free accompanying vibrations, whose intensity is often much greater than from the vibrations of the basic low harmonics (see Sects. 4.1 and 5.3). As the analysis shows, the vibration activity of the system increases significantly, with increase in the connectedness of the subsystems; which is evident from the frequency spectra of the partial systems, overlapping in the low "natural" frequencies area. Furthermore, in such cases, because of the variability of the system's parameters, the effect of the loss of stability occurs in limited segments of the kinematic cycle, reminiscent of the beat mode, when ascending intervals are alternated with intervals of amplitude attenuation (described in Chap. 12).

10.2 Model of a Ring Structure, with Absolutely Rigid Main Shaft

Schematization of the working body as a subsystem with lumped parameters We will concretize the problem, using the example of the dynamic model shown in Fig. 10.4.

Using the methodology, described in Sect. 9.2 and taking the boundary conditions $Q_0 = 0$, $Q_n = 0$, we obtain with (10.13):

$$\cos(n - 0.5)\gamma - \cos(n + 0.5)\gamma = 0,$$

Fig. 10.4 Dynamic model
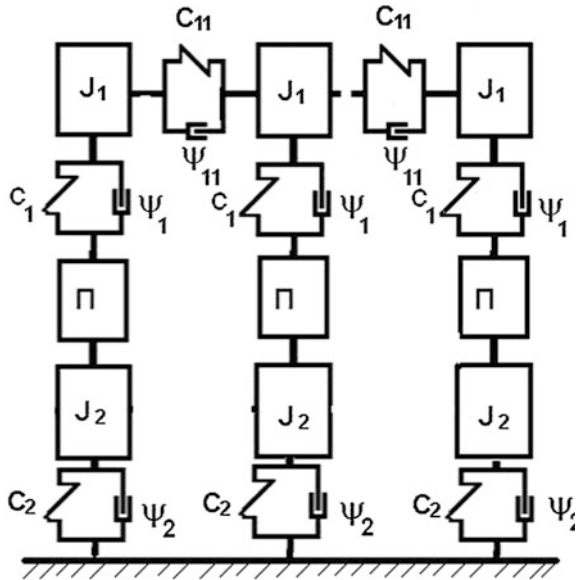
whose solution is $\gamma = (r-1)\pi/n$, where $r = \overline{1, n}$. Therefore, the formal frequency equation can be represented as follows:

$$1 + 0.5R(p)/c_{11} = \cos\frac{(r-1)\pi}{n}. \tag{10.18}$$

It can be shown that for this model $R(p) = -A/B$, where A, B are the appropriate elements of the mechanism's transition matrix (see Sect. 8.1). Thus, in this case the frequency Eq. (10.18) reduces to

$$
\begin{aligned}
J_1 J_2 p^4 &- [J_1(c_2 + c_1 \Pi'^2(\varphi)) + J_2(c_1 + 4c_{11}\sin^2\frac{j\pi}{2n})p^2 \\
&+ c_1 c_2 + 4c_{11}(c_2 + c_1 \Pi'^2(\varphi))\sin^2\frac{j\pi}{2n}] = 0.
\end{aligned}
\tag{10.19}
$$

Thus, to determine $2n$ "natural" frequencies p_{jr} $(r = \overline{1, n}; \; j = 1, 2)$, we should solve Eq. (10.19) n times. The n values of frequencies p_{jr} correspond to each value of j, moreover, when $j = 1$ the elements J_1 and J_2 oscillate in phase, while, when $j = 2$, in anti-phase. Assuming $J_2 = 0$, the oscillatory system has n degrees of freedom. Then,

$$p_r = p_0\sqrt{\zeta_2/(\Pi'^2 + \zeta_2) + 4\zeta_{11}\sin^2\frac{(r-1)\pi}{2n}}, \tag{10.20}$$

where $p_0 = \sqrt{c_1/J_1}$; $\zeta_{11} = c_{11}/c$; $\zeta_2 = c_2/c_1$.

As Π' depends on the angle φ, the "natural" frequency, according to (10.20), varies in the range

$$p_0 \le p_r(\varphi) \le 2p_0 \sqrt{\zeta_{11}}. \tag{10.21}$$

Regardless of the number of mechanisms, the lowest "natural" frequency of the entire system $J_2 = 0$ is equal to the frequency of the transfer mechanism.

The oscillation mode in accordance with (10.5), (10.6) is determined as

$$a_s^{(r)} = \cos(s\gamma_2 - \gamma_0)/\cos\gamma_0, \tag{10.22}$$

where, $\gamma_0 = -(n + 0.5)\pi(r - 1)/n$; s is the number of cross sections.

In Fig. 10.5, the mode shapes of oscillation, when $n = 8$ and $r = \overline{1, 4}$, are represented.

It is interesting that, when $J_2 = 0$, the "natural" frequency's variability combines with the oscillatory mode's stationary nature, for the regular symmetrical oscillatory system under consideration, which is usually characteristic for the systems with constant parameters. This property can be treated as quasi-stationary nature.

For small values of ζ_{11}, the frequency range, according to (10.21), is very narrow. Then, for sufficiently large number of mechanisms, there is an increased density of the frequency spectrum, to which the possibility of spatial localization of the oscillations (see Chap. 12) is related. When $c_2 \to \infty$ or $J_2 \to \infty$, the frequency doesn't depend on φ. Note that in this case the problem reduces to the study of the classical chain of identical isotropic harmonic oscillators, with the assumption that the interaction takes place only between adjacent oscillators. Then,

Fig. 10.5 Oscillatory mode shapes
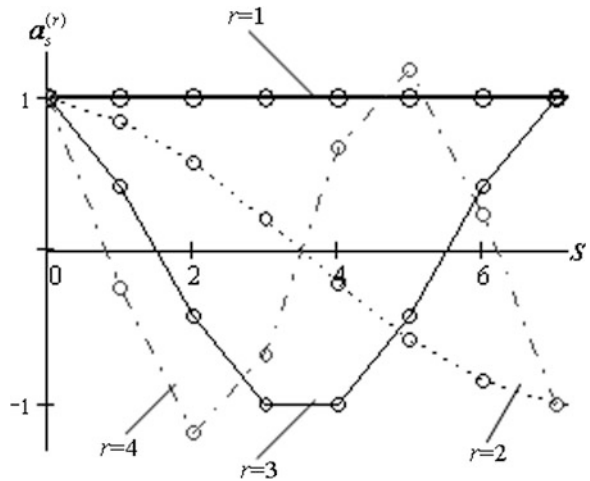
$$p_r = p_0 \sqrt{1 + 4\zeta_{11} \sin^2 \frac{(r-1)\pi}{2n}}. \tag{10.23}$$

Schematization of the working body as the subsystem with distributed parameters In order to keep the system strictly regular for this model, the ends of the working member should be "grown" with extensions of length $\Delta l/2$, where Δl is the distance between the calculated cross sections of the mechanism's driven links. Entries of the transition matrix of the repeating unit are defined as: $g_{11} = g_{22} = \cos\theta$, $g_{12} = \sigma p^{-1} \sin\theta$, where $\theta = p\Delta l/g_0$; $g_0 = \sqrt{GI/\rho}$; $\sigma = 1/\sqrt{GI\rho}$; I, ρ is the polar moment of inertia and the "mass" moment of inertia of the unit length, respectively; G is the shear modulus.

We obtain the dependence describing the mechanism's dynamic stiffness with the method described above

$$R(p) = 2[\cos \Pi \frac{r-1}{n} - \cos\theta(p)]c_{11}\theta(p)/\sin\theta(p). \tag{10.24}$$

On the other hand, analyzing the mechanism's transition matrix, we get

$$R(p) = \frac{J_1 J_2 p^4 - [J_2 c_1 + J_1(c_2 + c_1 \Pi'^2)]p^2 + c_1 c_2}{c_2 + c_1 \Pi'^2 - J_2 p^2}. \tag{10.25}$$

Equating (10.24) and (10.25), we obtain the transcendental equation, whose roots are the "natural" frequencies p_{jr}. When $J_2 = 0$ $R(p) = c_* - J_1 p^2$, where $c_* = c_1 c_2/(c_1 \Pi'^2 + c_2)$. In this case, the formal frequency equation reduces to

$$[\cos(\pi \frac{r-1}{n}) - \cos\theta(\nu)]\theta(\nu)\sin^{-1}\theta(\nu) - 0.5\zeta_2^{-1}(\zeta_0 - \nu^2) = 0, \tag{10.26}$$

where, $\nu = p/p_0$; $\zeta_2 = c_2/c_1$; $\zeta_0 = (1 + \Pi'^2 \zeta_2^{-1})^{-1}$.

When $\sin\theta \approx \theta$, the roots of Eqs. (10.19) and (10.26) coincide. In engineering calculations the differences between the considered schematization options are usually small, when $p < 0.5 g_0/\Delta l$. In Fig. 10.6 the typical graphs $\nu(n)$ built on the basis of (10.26), with the following initial data $J_1 = J_2 = 0.03 \, \text{kg m}^2$; $\tilde{n}_1 = 7 \times 10^4 \, \text{N m}$; $\tilde{n}_2 = 10^5 \, \text{N m}$; $\tilde{n}_{11} = GI/\Delta l = 5 \times 10^4 \, \text{N m}$; $\Pi' = \alpha \sin\varphi$; $\alpha = 0.8$ are presented.

The variable height of location of "points", in the graphs, corresponds to the change of the frequency, when $0 \le |\Pi'| \le |\Pi'|_{max}$. The graphs clearly show the rapprochement of the frequency spectra for a large number of modules, which may lead to amplitude modulation of oscillations (see Chap. 12).

Fig. 10.6 Dependence of the "natural" frequencies from a number of modules
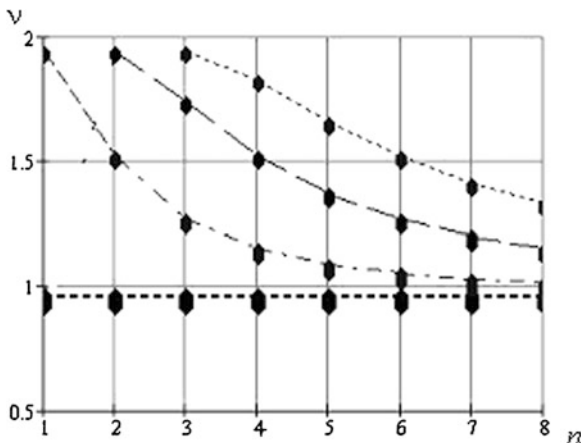
Analysis of the partial systems is of interest, for the development of the methods to reduce the machine's vibration activity. Initially it seems that, for the cyclic machines, whose operating speeds are usually quite far from the resonant modes, the "natural" frequencies' spectra are not important.

It should, however, be borne in mind that in case of the presence of clearances and pulsed nature of force and kinematic perturbations, along with the low-frequency vibrations of machine's elements, at steady speeds, the free accompanying vibrations arise, the intensity of which is usually much greater than the oscillations on the basic low harmonic. The analysis shows that the system's vibration activity increases in a large measure with increase in the connectivity of subsystems, which is evident from the overlapping of the frequency spectra of the partial systems in the area of low "natural" frequencies. Moreover, in such cases, because of the variability of the parameters, the effect of loss of stability, in the limited sections of the kinematic cycle, takes place, resembling the beat mode, when the amplitude growth areas are interspersed with areas of attenuation (see Sect. 5.3.1).

In conclusion, we will note the usual assumptions about the small influence of dissipation on the "natural" frequencies, was used above.

However, the influence on the upper boundary of the frequency of condensation can be significant, leading to the "smearing" of the boundary [33].

10.3 Model of Branched-Ring Structure, with Lumped Parameters

Dynamic model   Let us consider the dynamic model with lumped elements, fragment of which is shown in Fig. 10.7. We use the following notation: J_v are the moments of inertia; c, c_v, Δ_c are the stiffness coefficients; ψ_v, ψ are the dissipation
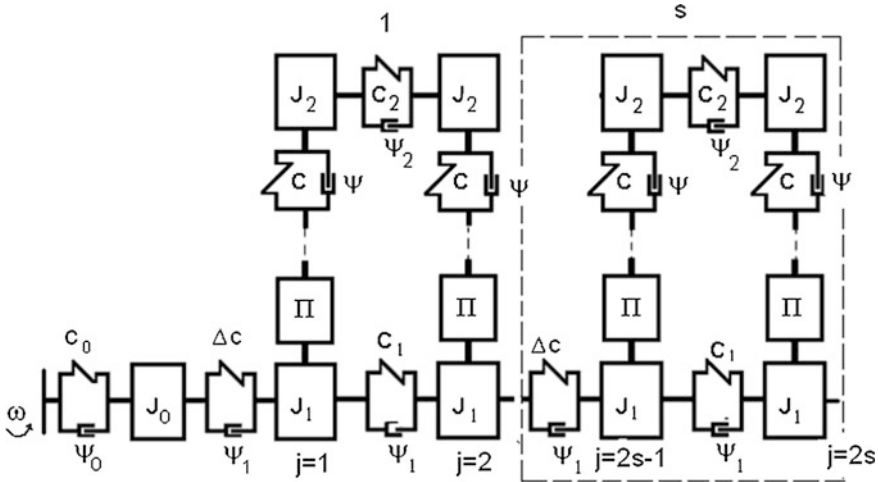
Fig. 10.7 Dynamic model of the branched-ring structure

coefficients; Π is the kinematic analogue of the cyclic mechanism ($\Pi(\varphi)$ is the position function); ω is the nominal angular velocity of the main shaft.

It is assumed that the dynamic characteristics, of the main shaft and the executive member, are reduced to the input and output links of the cyclic mechanisms, and the angular velocity at the "input", ω, is constant; which, in first approximation, is provided by the rational choice of parameters of the drive and transmission gears. The transfer mechanism, at the "input" of the main shaft, is mapped in the model, with the serial connection of the elastic-dissipative element c_0, ψ_0 (Kelvin-Voigt element) and the inertial element J_0.

Let φ_{1j}, φ_{2j} be the absolute angular position of the inertial elements of the main shaft and the executive body, where $j = \overline{0, n}$ is the number of sections. Then, $\varphi_{1j} = \varphi_1^0 + x_j$, $\varphi_{2j} = \varphi_2^0 + y_j$, where, $\varphi_1^0 = \omega t$, $\varphi_2^0 = \Pi(\varphi_1^0)$ are the ideal angle coordinates in the program motion; x_j, y_j are the deviations from the program motion (dynamic errors) with respect to the main shaft and the executive member.

In case of motion without clearances, we represent the position function $\Pi(\varphi_{1j})$ as the truncated Taylor series

$$\Pi(\varphi_j) = \Pi(\varphi_1^0 + x_j) \approx \Pi(\varphi_1^0) + \Pi'(\varphi_1^0)x_j \quad (j = \overline{1, n+1}), \tag{10.27}$$

where $(\ )' = d\Pi/d\varphi_1^0$.

Recursive dependencies and the transition matrices We will select, in the dynamic model, the repeating unit, bounded by the hatched line, to which, taking into account (10.27), corresponds the system of differential equations with slowly varying coefficients. The variability of this system's coefficients is due to the

change of geometric transfer function $\Pi'(\varphi)$, carrying out the functional relation-ship between the main shaft and the executive members. In particular, at the dwells $(\Pi' = 0)$, this bond is broken and the system of equations is split into two. As this dynamic model is a special case of the model of circular structure, considered in Sect. 10.1, the system of differential equation is omitted here. Repeated module that defines the regular properties of the system, in our case, is more complex and differs significantly from the previously considered ones.

Let us take $\varphi_1^0 = \omega t$ as the "dimensionless time", and $p(\varphi_0)$ as the slowly varying frequency of free oscillations. We will find free vibrations in the form $x_j = X_j(\varphi_1^0) \sin(\int p(\varphi_1^0) d\varphi_1^0)$ and $y_j = Y_j(\varphi_1^0) \sin(\int p(\varphi_1^0) d\varphi_1^0)$. When determining the frequency and modal characteristics, we can ignore the weak influence of dissipative forces.

Using the modified transition matrices, we can write for module s, the following recursive relationships:

$$X_j = X_{j-1} + M_{j-1}^+/\Delta c; \quad X_{j+1} = X_j + M_j^+/c_1;$$
$$M_j^+ = M_{j-1}^+ + B^{-1}(AX_j - Y_j); \tag{10.28}$$
$$M_{j+1}^+ = M_j^+ + B^{-1}(AX_{j+1} - Y_{j+1}); \quad Q_j^+ = B^{-1}(DY_j - X_j),$$

where M_j, Q_j are the peak values of the moments on the main shaft and executive member (here and below signs "+" and "−" correspond to the infinitely small deviations to the right and to the left of the section; A, B and C, D are the elements of the first and second rows of the modified transition matrix of the cyclic mechanism (see Chap. 8). In particular, if the cyclic mechanism is composed of serial connection of elements $J_1 - \Pi - c - J_2$, then $A = \Pi' - J_1 p^2/(c\Pi')$; $B = (c\Pi')^{-1}$; $C = (AD - 1)/B$; $D = (1 - J_2 p^2/c)/\Pi'$.

We introduce the following functions into consideration:

$$A/B = R_1; \quad B^{-1} = R_2;$$
$$D/B = R_3; \quad D^{-1} = R_4;$$
$$b_{11} = (1 + R_3/c_2)(2 + R_3/c_2)^{-1};$$
$$b_{12} = R_4(2 + R_3/c_2)^{-1};$$
$$b_{21} = b_{11}(1 + R_3/c_2) - R_2/c_2;$$
$$b_{22} = b_{12}(1 + R_3/c_2).$$

In addition to dependencies (10.28), we have the additional conditions $Q_{2j-1}^- = 0$ and $Q_{2j}^+ = 0$, whose inclusion leads to the following recursive relationships:

$$\begin{bmatrix} X_{j+1} \\ M_{j+1} \end{bmatrix} = \begin{pmatrix} \gamma_{11} & \gamma_{12} \\ \gamma_{21} & \gamma_{22} \end{pmatrix} \begin{bmatrix} X_{j-1} \\ M_{j-1} \end{bmatrix}, \tag{10.29}$$

where

$$\gamma_{11} = \frac{1 + (R_1 - b_{11}R_2)/c_1}{1 + b_{12}R_2/c_1};$$

$$\gamma_{12} = \frac{\Delta c^{-1}[c_1^{-1}(R_1 - b_{11}R_2) + 1] + c_1^{-1}}{1 + b_{12}R_2/c_1};$$

$$\gamma_{21} = (R_1 - R_2R_4)(1 + \gamma_{11});$$

$$\gamma_{22} = 1 + (R_1 - R_2R_4)(\Delta c^{-1} + \gamma_{12}).$$

Generally we can represent (10.29) as follows:

$$Z_s = \mathbf{\Gamma}_s Z_{s-1} \qquad (s = \overline{1,N}), \tag{10.30}$$

where s is the module number (in our case $j = 2s - 1$); $\mathbf{\Gamma}_s$ is the transition matrix; Z_{s-1}, Z_s are the state vectors in sections $j = 2(s - 1)$ и $j = 2s$.

Frequency and modal analysis Dependencies (10.29), (10.30) describe the uniform linear system of differential equations, as before, we look for the solution in the form $X_s = \eta X_{s-1}$, $M_s = \eta M_{s-1}$, where η is the characteristic factor. Taking into account the calculations in Sect. 9.1, we get $\eta = \kappa \pm i\sqrt{1 - \kappa^2}$, where $\kappa = 0.5(\gamma_{11} + \gamma_{22}) = 0.5\,\mathrm{Sp}\tilde{\mathbf{A}}_s$; $\mathrm{Sp}\mathbf{\Gamma}_s$ is the spur of the matrix $\mathbf{\Gamma}_s$; $i = \sqrt{-1}$. At $\kappa < 1$

$$\left.\begin{array}{l} X_s = h_1 \cos s\theta + h_2 \sin s\theta; \\ M_s/\Delta c = h_1[\cos(s + 1)\theta - \cos s\theta] + h_2[\sin(s + 1)\theta - \sin s\theta]. \end{array}\right\} \tag{10.31}$$

When $\kappa > 1$ ($\mathrm{Im}\,\eta = 0$), taking $\kappa = \mathrm{ch}\,\theta$, we get the dependencies, which are different from (10.31), only in terms of replacing trigonometric functions with the same name hyperbolic functions. When $\kappa < -1$, we should take $\theta = \theta^0 + i\Pi$; then $\kappa = -\cosh\theta^0 < -1$. Hence, on the basis of the Moivre theorem $\cosh(s\theta) = (-1)^s\cosh(s\theta^0)$ and $\sinh(s\theta) = (-1)^s\sinh(s\theta^0)$. With these corrections, the dependencies for the case $\kappa > 1$ are valid.

Further, we will take into account the boundary conditions. If $c_0 \to \infty$, then $X_0 = 0$, $M_N = 0$. Then, with (10.31), we obtain

$$\theta_r = \pi\frac{2r - 1}{2(N + 0.5)} \qquad r = \overline{1,N}. \tag{10.32}$$

Here r is the shape mode number (for section $s = 2j$); $N = 0.5(n + 1)$ is the number of the modules.

If the drive mechanism with the reduced stiffness coefficient c_0 and reduced moment of inertia J_0 (see Fig. 10.7) is used at the "input", then the value of θ_r, on the basis of (10.31), is determined from the transcendental equation

$$(1 + \zeta) \cos[(N + 0.5)\theta] - \zeta \, \cos[(N - 0.5)\theta] = 0, \tag{10.33}$$

where, $\zeta = \Delta c/(c_0 - J_0 p^2)$.

Thus, now parameter ζ, depends on the dynamic stiffness of the transfer mechanism $R_0(p) = c_0 - J_0 p^2$, which is the function of the desired frequency p. In general, dynamic stiffness describes the whole subsystem at the "input", including dynamic characteristics of the motor.

If $|\kappa| > 1$, then Eq. (10.33) takes the following form

$$\begin{aligned}
(1 + \zeta)\cosh[(N + 0.5)\theta] - \zeta \cosh[(N - 0.5)\theta] = 0 \quad (\kappa > 1); \\
(1 + \zeta)\sinh[(N + 0.5)\theta^0] - \zeta \sinh[(N - 0.5)\theta^0] = 0 \quad (\kappa < -1),
\end{aligned} \tag{10.34}$$

where, $\theta = \text{arccosh} \, \kappa; \quad \theta^0 = \text{arccosh}|\kappa|$.

When $c_0 \gg J_0 p^2$, we have $R_0 \approx c_0 > 0$, and $R_0 \approx -J_0 p^2 < 0$ at $c_0 \ll J_0 p^2$.

To determine "natural" frequencies in case of $\kappa < 1$, we should use the following equation:

$$\cos \theta_r = 0.5[\gamma_{11}(p_r) + \gamma_{22}(p_r)]. \tag{10.35}$$

Taking into account (10.28), the four values of "natural" frequencies $p_{rv}(\varphi)$ $(v = \overline{1,4})$ correspond to the fixed value of r. In Fig. 10.8, the graphs $p_r(\varphi_1^0)$ are represented using the following original data: $J_1 = 0.5$; $c_1 = 2.25 \times 10^4$, $c_2 = 2.25 \times 10^4$, $\Delta c = 5 \times 10^3 \, \text{N m}$; $\Pi' = r_0 \, \sin \varphi$; $r_0 = 1$; $\zeta = 2$; $n = 2 \, \text{N}$.

Let us note here that, contrary to the traditional notions, the ascending order of the "natural" frequencies does not necessarily correspond to the increase in the mode number r (see the top curve family in the graph). As it was already mentioned, the number r characterizes for module $s = 2j$, the "mode shape", only for the main shaft output cross-section. Meanwhile, inside each module, at the fixed

Fig. 10.8 Graphs of the "natural" frequencies
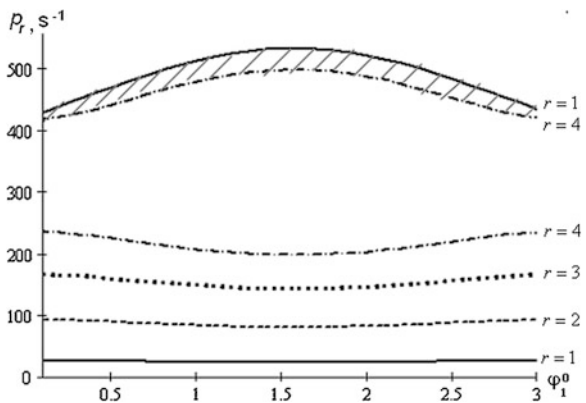
value of r, can be another four modes, which correspond to the frequencies p_{rv}. The hatched area corresponds to the vicinity of the "condensation point" $p_* = \sqrt{c/J_2}$, where the high density of the frequency spectrum takes place.

The oscillation mode shape of the main shaft, at frequency p_{rv}, is determined for section $s = 2j$ using (10.31), when $\theta = \theta_r$ and the following values of h_1 and h_2 ($\zeta \neq 0$):

$$h_1 = 1; \quad h_{2r} = (1 - \cos \theta_r + \zeta^{-1})/\sin \theta_r.$$

For sections with odd number of j, on the basis of (10.28), we have

$$X_r(2j - 1) = X_r[2(j - 1)] + M_r[2(j - 1)]/\Delta c.$$

As the analysis shows, the hyperbolic mode of oscillations, when $\kappa > 1$, is evident of the attenuation of the amplitude of free oscillations, as per the distance from the "input section" ("spatial attenuation").

A similar effect is observable, when $\kappa < -1$, but in this case the adjacent modules oscillate in anti-phase. Both of these modes are possible in the vicinity of the condensation points p_*, so they are not clearly expressed, and usually appear in the form of beats.

We will note here that, for large-scale systems, the important advantage of the method based on the properties of the regular systems, is the ability to restrict the analysis of the most realistic mode of oscillations, inherent to the working frequency range. Therewith, it is possible to get a concise and convenient form of the mathematical model of complex machine drives, with a large number of degrees of freedom.

Forced oscillations For the analysis of forced oscillations, we take into account the dissipative forces, which could be neglected in the frequency and modal analysis. We will restrict ourselves to the consideration of quasi-harmonic oscillations. In this case, to account for structural damping, we use the stiffness coefficient representation in complex form [59]. Herewith, $\tilde{c} = c(1 + 2\delta i)$, $\tilde{c}_v = c_v(1 + 2\delta_v i)$ ($v = 0, 1, 2$); $\Delta\tilde{c} = \Delta c(1 + 2\delta_1 i)$, where, c, c_v, Δc are the corresponding stiffness coefficients; $\delta = \psi/(4\pi)$, $\delta_v = \psi_v/(4\pi)$; ψ, ψ_v are the dissipation coefficients; $i = \sqrt{-1}$; ω is the nominal angular velocity of the main shaft.

As the generalized coordinates, we take the dynamic errors of the main shaft $x_j = \varphi_{1j} - \varphi_1^0$ and executive member $y_j = \varphi_{2j} - \varphi_2^0$, where φ_{1j}, φ_{2j} are the absolute angular coordinates of the inertial elements of the main shaft and executive member, j is the number of the section $\varphi_1^0 = \omega t$, $\varphi_2^0 = \Pi(\varphi_1^0)$.

Specifying the smallness of dynamic errors, it should be borne in mind that the accelerations and the loads caused by these errors can be comparable and in many cases, can be much larger, than the corresponding characteristics that arise due to the program motion. Therefore, the comparatively small values of x_j, y_j are only

evident of the acceptable kinematic precision, but in any case do not justify ignoring the excited oscillations in dynamic calculations (see Chaps. 4 and 5).

Transition matrices One of the specific features of cyclic mechanical systems is the fact that the most important disturbing factor is the program motion of the actuator. Most often the frequencies of kinematic excitation ω and 2ω are associated with the translational motion of the actuator. If the moment of inertial forces is $M = -J_2\omega^2\Pi''$, then after transformation to the main shaft, the reduced moment is $M \cdot \Pi'$. Typically lower "natural" frequencies are substantially higher than the indicated frequencies, so at first, we analyze the oscillations under the influence of perturbation, arising from the technological and other forces, whose frequency can be comparable with the spectrum of "natural" frequencies. It should be borne in mind that the spectrum of "natural" frequencies slowly changes, due to the variability of the first geometric transfer function, which we take as $\Pi'(\varphi_1^0) = \Pi'_* \sin \omega t$.

Each module $s = \overline{1, N}$ has three distinct cross-sections: $j = 2(s - 1)$ ("input" is the first mechanism), $j = 2s - 1$ (second mechanism), $j = 2s$ ("exit"). Let the periodic driving moment $M(t)$ be applied to the executive member, in the sections $j = 2(s - 1)$ and $j = 2s - 1$; we represent it as Fourier series

$$M(t) = \sum_{m=-\infty}^{\infty} M_m \exp\left(im\omega t\right) = M_0 + \sum_{m=1}^{\infty} |M_m| \cos\left(m\omega t + \alpha_m\right), \qquad (10.36)$$

where, $M_m = \tau^{-1} \int_{-\tau/2}^{\tau/2} M(t)\exp\left(-im\omega t\right)dt$; $\tau = 2\pi/\omega$, $\alpha_m = \arg M_m$.

As already noted, strictly speaking, the parameters of the oscillatory system are variable, however, in case of marked features of the spectrum of "natural" frequencies, function Π' can be averaged over a period τ. Some details will be discussed below.

Furthermore, we will write, for harmonic m, the matrix dependence, forming the connection between the complex state vectors in the cross sections $j = 2(s - 1)$ and $j = 2s - 1$:

$$[a_1, Q_1, a_2, Q_2]_{j=2s-1}^{\mathrm{T}} = \Lambda[a_1, Q_1, a_2, Q_2]_{j=2(s-1)}^{\mathrm{T}}, \qquad (10.37)$$

where a_ν, Q_ν are the complex amplitudes of oscillations and moments in the corresponding sections of the main shaft ($\nu = 1$) and executive member ($\nu = 2$); $\Lambda = \Lambda_1\Lambda_2\Lambda_1$ is the transition matrix (the index m is omitted here and hereafter);

$$\Lambda_1 = \begin{bmatrix} 1 & 0 & 0 & 0 \\ R_1 & 1 & -R_2 & 0 \\ 0 & 0 & 1 & 0 \\ R_2 & 0 & R_3 & 1 \end{bmatrix}; \quad \Lambda_2 = \begin{bmatrix} 1 & c_1^{-1} & 0 & 0 \\ 0 & 1 & 0 & 0 \\ 0 & 0 & 1 & c_2^{-1} \\ 0 & 0 & 0 & 1 \end{bmatrix}. \qquad (10.38)$$

Here Λ_1 corresponds to the transfer mechanism, and Λ_2 to the elastodissipative characteristics of the given part of the main shaft and the executive member (the inertial characteristics are included in matrix Λ_1 as reduced additional components of moments of inertia J_1 and J_2).

The moments $M = |M| \exp(i\omega t)$ are applied to the two inertial elements of the under consideration module s of the executive member. Then, taking into account the rule of signs, we have, $Q_2(2s - 2) = -M$, $Q_2(2s - 1) = M$ (in order to simplify the process of indexation, the section number is shown as the function's argument.) Hence, with (10.37), (10.38), we have

$$\left.\begin{array}{l} \lambda_{43}[a_2(2s - 2)] = -\lambda_{41}[a_1(2s - 2)] - \lambda_{42}[Q_1(2s - 2)] + (1 + \lambda_{44})M; \\ -\lambda_{33}[a_2(2s - 2)] + a_2(2s - 1) = \lambda_{31}[a_1(2s - 2)] - \lambda_{34}M, \end{array}\right\} \quad (10.39)$$

where λ_{ik} are the corresponding entries of the transition matrix $\Lambda = \|\lambda_{ik}\|$.

On the basis of (10.37)–(10.39), we exclude the amplitude functions of oscillations and loads, of the executive body and then, we get the following matrix recursive relationships:

$$\begin{bmatrix} a_1(2s - 1) \\ Q_1(2s - 1) \end{bmatrix} = \begin{bmatrix} g_{11} & g_{12} \\ g_{21} & g_{22} \end{bmatrix} \begin{bmatrix} a_1(2s - 2) \\ Q_1(2s - 2) \end{bmatrix} + M \begin{bmatrix} \xi_1 \\ \xi_2 \end{bmatrix}, \quad (10.40)$$

where

$$g_{11} = \lambda_{11} - \lambda_{13}\lambda_{41}\lambda_{43}^{-1};$$
$$g_{12} = \lambda_{12} - \lambda_{13}\lambda_{42}\lambda_{43}^{-1};$$
$$g_{21} = \lambda_{21} - \lambda_{23}\lambda_{41}\lambda_{43}^{-1};$$
$$g_{22} = \lambda_{22} - \lambda_{23}\lambda_{42}\lambda_{43}^{-1};$$
$$\xi_1 = \lambda_{13}\lambda_{43}^{-1}(1 + \lambda_{44}) - \lambda_{14};$$
$$\xi_2 = \lambda_{23}\lambda_{43}^{-1}(1 + \lambda_{44}) - \lambda_{24}.$$

The transition matrix from section $j = 2s - 1$ till $j = 2s$ has the form

$$\begin{bmatrix} a_1(2s) \\ Q_1(2s) \end{bmatrix} = \begin{bmatrix} 1 & \Delta\tilde{c}^{-1} \\ 0 & 1 \end{bmatrix} \begin{bmatrix} a_1(2s - 1) \\ Q_1(2s - 1) \end{bmatrix} \quad (10.41)$$

(10.40) and (10.41) define the transition matrix for the main shaft, within one module:

$$[a_1(2s), Q_1(2s)]^{\mathrm{T}} = \mathbf{U}[a_1(2s - 2), Q_1(2s - 2)]^{\mathrm{T}} + M[\xi_1, \xi_2]^{\mathrm{T}}, \quad (10.42)$$

where

$$\mathbf{U} = \|u_{ik}\|;$$
$$u_{11} = g_{11} + g_{21}\Delta\tilde{c}^{-1};$$
$$u_{11} = g_{11} + g_{21}\Delta\tilde{c}^{-1};$$
$$u_{12} = g_{12} + g_{22}\Delta\tilde{c}^{-1};$$
$$u_{21} = g_{21};$$
$$u_{22} = g_{22}.$$

The considered system has branched structure (cross-sections $j = 2s$) and closed contour only appears in the internal structure of every module.

Determination of amplitude-frequency and phase-frequency characteristics
The recursive relation (10.42) is the matrix form of the non-uniform system of differential equations, which can be represented as

$$\begin{bmatrix} a_1(2s) \\ Q_1(2s) \end{bmatrix} = \begin{bmatrix} u_{11} & u_{12} \\ u_{21} & u_{22} \end{bmatrix}^s \begin{bmatrix} a_1(0) \\ a_1(0)R_0 \end{bmatrix} + M \begin{bmatrix} z_{1s} \\ z_{2s} \end{bmatrix}. \qquad (10.43)$$

Here $Z_s = [z_{1s}, \quad z_{2s}]^{\mathrm{T}} = \sum_{k=0}^{s-1} \mathbf{U}^{s-k-1}\xi$; $\xi = [\xi_1, \quad \xi_2]^{\mathrm{T}}$; $a_1(0)$ is the complex amplitude in section $j = 0$; $R_0 = (\tilde{c}_{02} - J_0\omega^2)\tilde{c}_{01}/(\tilde{c}_{01} + \tilde{c}_{02})$ is the dynamic stiffness at the "input" of the regular sub-system (generally function R_0 can have more complex form and include the characteristics of the motor and drive transfer mechanisms).

To determine $a_1(0)$, we use the boundary condition $Q_1(2N) = 0$, (the absence of moment on the end of the main shaft). Using (10.43), we write

$$a_1(0)(u_{21}^{(N)} + u_{22}^{(N)}R_0) + Mz_{2,N} = 0.$$

Hence,

$$a_1(0) = -\frac{M z_{2,N}}{u_{21}^{(N)} + u_{22}^{(N)}R_0}. \qquad (10.44)$$

Here and below $u_{vk}^{(s)}(s = \overline{1,N})$ corresponds to the relevant entry of matrix U^s.

On the basis of (10.43) and (10.44), at the given frequency $m\omega$, the complex values of the amplitude of oscillations and loads of the main shaft in sections $j = 2s$ ("output" of the module s) are determined. The corresponding amplitudes, in intermediate sections $j = 2s - 1$, are now easy to find, with the help of dependence (10.41):

$$a_1(2s - 1) = a_1(2s) - Q_1(2s)\Delta\tilde{c}^{-1}; \quad Q_1(2s - 1) = Q_1(2s).$$

A more efficient way to describe the modes of oscillation and to take into account the boundary conditions, is based on using the properties of regular

oscillatory systems. We will consider the following functions: $\chi = 0.5(u_{11} + u_{22}) = 0.5\,\mathrm{SpU}$, (SpU is the spur of matrix U); when $|\chi| \le 1$ $\theta = \arccos \chi$, $f_s = \cos s\theta$, $v_s = \sin s\theta$; when $\chi > 1$ $\theta = \mathrm{arccosh}\chi$, $f_s = \cosh s\theta$, $v_s = \sinh s\theta$; when $\chi < -1$ $\theta = \mathrm{arcosh}|\chi| + i\Pi$ $(i = \sqrt{-1})$. Then, the solution of the non-uniform differential equation can be represented as

$$a_1(2s) = h_1 f_s + h_2 v_s + z_{1s}M,$$

where, h_1, h_2 are the slowly varying functions, which are determined from the boundary conditions.

The accounting of the boundary conditions leads to the following system of algebraic equations, with respect to h_1 and h_2:

$$\left.\begin{array}{l} h_1(u_{11} + u_{12}R_0 - f_1) + h_2 v_1 = 0; \\ h_1(u_{22}f_N - f_{N-1}) + h_2(u_{22}v_N - v_{N-1}) = \mu. \end{array}\right\}$$

Hence,

$$h_1 = \mu\Psi_{12}/\Delta; \quad h_2 = \mu\Psi_{11}/\Delta,$$

where

$$\begin{aligned} \Delta &= \Psi_{11}\Psi_{22} - \Psi_{12}\Psi_{21}; \\ \Psi_{11} &= -u_{11} - u_{12}R_0 + f_1; \\ \Psi_{22} &= u_{22}v_N - v_{N-1}; \\ \Psi_{12} &= v_1; \\ \Psi_{21} &= u_{22}f_N - f_{N-1}; \\ \mu &= (u_{22}\xi_1 - u_{12}\xi_2)M. \end{aligned}$$

So, the dependencies, which determine the amplitude values for all characteristic sections of the main shaft, are obtained. Thus, the problem is reduced to analyzing the amplitudes of the executive body's forced vibrations, for each selected module. Using (10.37), taking into account (10.43), we obtain

$$\left.\begin{array}{l} a_2(2s) = \lambda_{43}^{-1}[\lambda_{41}a_1(2s) + \lambda_{42}Q_1(2s) + (1 + \lambda_{44})M]; \\ a_2(2s - 1) = \lambda_{31}[a_1(2s - 2)] + \lambda_{32}[Q_1(2s - 2)] + \lambda_{33}[a_2(2s - 2)] - \lambda_{34}M. \end{array}\right\}$$

$$(10.45)$$

The resulting amplitude values are the complex values, the module of which $|a_k|$, defines the frequency response and the argument defines the phase-frequency response.

Fig. 10.9 Areas of existence of the trigonometric and hyperbolic oscillatory modes
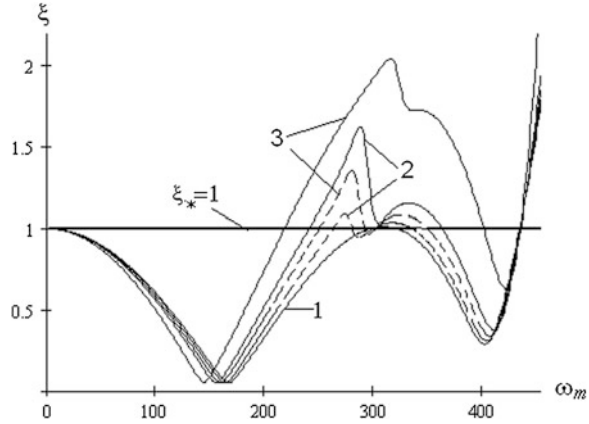
To illustrate the developed methods of calculation, we take $\tilde{n} = 1.5 \times 10^4$, $\Delta\tilde{n} = 2.5 \times 10^4 \,\text{N m}; \delta = \delta_v = 0.03$ (due to small values of the damping coefficients δ_v, the absolute value of the complex stiffness is almost identical to the stiffness of the corresponding element).

The oscillatory mode, depending on ω_m, can be described both as trigonometric, as well as hyperbolic functions (see above). In Fig. 10.9 the graphs of the function $\chi(\omega_m)$, establishing the boundaries of the relevant areas, are represented.

As noted above, when $|\chi| \leq \chi_* = 1$, the shape mode is trigonometric, and when $\chi > 1$, it is hyperbolic. In this case, we accept the following original: $c_{01} = c_{02} = 2 \times 10^5 \,\text{N m}, \tilde{n} = 1.5 \times 10^4$, $\Delta\tilde{n} = 2.5 \times 10^4 \,\text{N m}, J_0 = 0.02, \ J_1 = 0.5, \ J_2 = 0.2 \,\text{kg m}^2; \ N = s_{\max} = 4$ is the number of modules.

The solid lines correspond to $\Pi'_* = 1$ and the hatched ones to $\Pi'_* = 0.2$. Curves 1, 2, 3 correspond to $\varphi_1^0 = 0; \ 0.7; \ \Pi/2$.

As can be seen in the graph, in case of slow variation of parameters, due to the variability of the geometric characteristics of the mechanisms, in a certain frequency range, not only the quantitative, but also the qualitative changes in oscillatory modes are possible. When decreasing Π'_* the curves do not cross the line χ_*, and the oscillatory mode is close to the traditional trigonometric form.

Here above, to determine the amplitude of forced oscillations, the averaged values of the first geometric transfer function $\Pi'(\varphi_1^0)$, were used. As shown in [64], when Π' as compared to an external perturbation, is a slowly varying function (i.e. $\omega_m \gg \omega$), no significant frequency transformation of the given harmonic occurs. The accounting of the variability of Π', in these cases, only leads to the amplitude modulation of oscillations resembling the beat mode and to some "blurring" of the resonance's peaks.

If function Π' and driving moment have comparable frequencies, then when $m = 1$ the conditions of harmonic balance are performed in the transition matrix $\Lambda_\Pi = \text{diag}\{\Pi'_*/2, \ 2/\Pi'_*\}$. This situation typically arises, when disturbance was caused by the inertial forces of the translational motion, with the full revolution of

the input link. The transition through element Π is accompanied by not only the amplitude, but also the frequency transformation, as well as substitution of sinusoidal members with cosine and vice versa, which corresponds to the phase shift of $\pi/2$ [64].

When using the transition matrix, of the considered form, it should be borne in mind that the frequency of the driving part's excitation is twice the frequency of the driven part. In case of sufficient difference of frequencies ω and 2ω, from the resonance zones, the forced oscillations, with corresponding frequencies, are close to the static deformations under the kinetostatic load. In such cases, the frequency transformation is not so essential. For example, in case of ratio ω, to the lowest "natural" frequency, is less than 1/8, the difference in the coefficient of dynamicity for frequencies ω and 2ω, doesn't exceed 5 %.

10.4 Model of Multisection Drive with Branched-Ring Structure and Distributed Parameters

Dynamic model   In the systems under consideration, an array of the generalized coordinates and varied parameters is usually difficult to observe, which justifies the use of continuum idealization, with which the elastic, inertial and dissipative properties of the system are reflected as integral characteristics, forming some sort of a pseudo medium [44, 63, 64]. A similar method (aggregation) is widely used in studies, not only of complex mechanical objects, but also of automation, economy and others [47]. Figure 10.10 shows the dynamic model, which consists of the drive mechanism, schematized as torsional subsystem $(s = 0)$ and repetitive modules $(s = \overline{1, N})$, one of which is selected by the hatched line. Each module of the corresponding section of the drive is formed by an area of the main shaft, associated
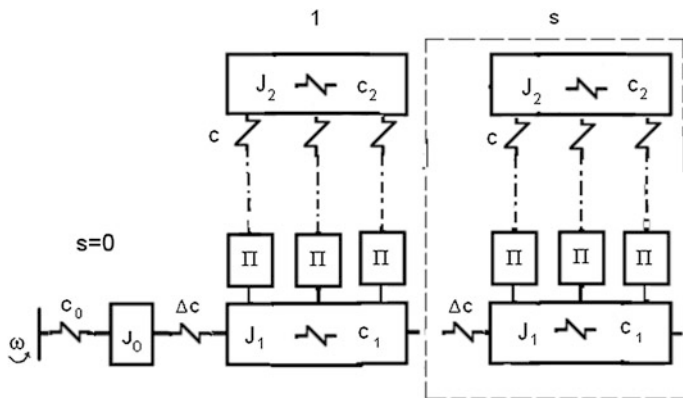
Fig. 10.10   Continual dynamic model

with the executive member with n identical cyclic mechanisms, and with neighboring sub-systems, with elastic elements, with stiffness coefficient Δc.

According to the modification of the continuum idealization method, we represent n identical mechanisms in the form of a pseudo medium. This environment, formed by "smearing" of the elastic and inertial characteristics, along the axis of the corresponding shafts, has the property to transfer moments and motion, only along the layer of the medium, and the interaction between the layers has place only through the sub-systems of the main shaft and the executive body. The characteristic of pseudo-medium is the distributed modified transition matrix

$$\tilde{\Gamma} = \prod_u^1 \tilde{\Gamma}_i = \begin{bmatrix} A(p) & B(p) \\ C(p) & D(p) \end{bmatrix} \quad (i = \overline{1, u}), \tag{10.46}$$

where u is the number of elements in the mechanism, $\tilde{\Gamma}_i$ is the transition matrix of the element.

So, particularly, if the mechanism is formed by combining the inertial, elastic and kinematic elements $J - c - \Pi$ (Π is the position function), then

$$\tilde{\Gamma}_J = \begin{bmatrix} 1 & 0 \\ -p^2 Jn/l & 1 \end{bmatrix}; \quad \tilde{\Gamma}_c = \begin{bmatrix} 1 & l/(cn) \\ 0 & 1 \end{bmatrix}; \quad \tilde{\Gamma}_\Pi = \begin{bmatrix} \Pi'(\varphi_1^*) & 0 \\ 0 & \Pi'(\varphi_1^*)^{-1} \end{bmatrix}. \tag{10.47}$$

Here, l is the length of the shaft's portion; $\Pi'(\varphi_1^*) = d\varphi_2^*/d\varphi_1^*$ is the first geometric transfer function.

Frequency and modal analysis   We will select, in the random module s, the subsystem with circular structure, consisting of two shafts, with distributed parameters. These subsystems are connected with pseudo-medium, which as per (10.46) and (10.47), takes into account the elastic, inertial and kinematic characteristics of the cyclic mechanisms. At the stage of determination of frequency and modal properties of the drive, the dissipative forces, without loss of accuracy, can be omitted. That fragment of the module s is described with the following system of differential equations:

$$\frac{\partial}{\partial t}\left(\rho_\nu \frac{\partial \varphi_\nu}{\partial t}\right) - G\left[\frac{\partial}{\partial x}\left(I_\nu(x) \frac{\partial \varphi_\nu}{\partial x}\right)\right] - M_\nu(\varphi_1, \varphi_2) = 0 \qquad (\nu = 1, 2), \tag{10.48}$$

where $\varphi_\nu(x, t) = \varphi_\nu^*(t) + q_\nu(x, t)$; φ_ν^* is the ideal rotation angle of the shaft ν, implemented in the program motion ($\varphi_1^* = \omega t$, $\varphi_2^* = \Pi(\varphi_1^*)$); q_ν is the dynamic error; I_ν, ρ_ν are the polar moments of inertia for area and mass of the shaft's unit length ν; G is the shear modulus; M_ν is the torque, exerted by the mechanisms, on area of length l of the shaft (see below).

We will represent the approximate particular solution of the uniform system of equations obtained on the grounds of (10.48) as

$$q_1 = X(x, \tau)\Psi(t); \quad q_2 = Y(x, \tau)\Psi(t). \tag{10.49}$$

Here, τ is the "slow time" (usually $\tau = \varphi_1^*$).

Further, we will separate the "slow" components of function M_v from the fast ones, having taken $M_v = \mu_v(x, \tau)\Psi(t)$. In accordance with the method of conditional oscillator, for each form, the solution can be covered by one additional condition, under which $\partial^2 q_v/\partial t^2 \approx -p^2(\tau)q_v$, where the function $p(\tau)$ can be considered as the variable "natural" frequency (see Sect. 5.2). It can be shown that the slowly varying amplitude functions of the reactive moments are described as follows:

$$\mu_1 = \mu_{11}X + \mu_{12}Y; \quad \mu_2 = \mu_{21}X + \mu_{22}Y, \tag{10.50}$$

where, $\mu_{11} = -A/B; \quad \mu_{22} = -D/B; \quad \mu_{12} = \mu_{21} = B^{-1}$.

Taking $I_v(x) = \text{const}$, while taking into account (10.48)–(10.50), for the mode under consideration, we have

$$\left.\begin{array}{l} X'' + R_{11}X + R_{12}Y = 0; \quad Y'' + R_{21}X + R_{22}Y = 0; \\ \ddot{\Psi} + p^2(\tau)\Psi = 0, \end{array}\right\} \tag{10.51}$$

where

$$R_{11} = (\rho_1 p^2 + \mu_{11})/(GI_1);$$
$$R_{22} = (\rho_2 p^2 + \mu_{22})/(GI_2);$$
$$R_{12} = \mu_{12}/(GI_1);$$
$$R_{21} = \mu_{21}/(GI_2);$$
$$(\ )' = \partial/\partial x; \dot{(\ )} = \partial/\partial t.$$

The characteristic equation, in accordance with (10.51), can be written as

$$\lambda^4 + \lambda^2(R_{11} + R_{22}) + R_{11}R_{22} - R_{12}R_{21} = 0. \tag{10.52}$$

Hence,

$$\lambda_{1,2}^2 = 0.5\left[-(R_{11} + R_{22}) \mp \sqrt{(R_{11} - R_{22})^2 + 4R_{12}R_{21}}\right]. \tag{10.53}$$

Since $R_{12}R_{21} = (B^2G^2I_1I_2)^{-1}$, the radicand in (10.53) is always positive; therefore, the roots of Eq. (10.52) can be either real or imaginary. When $\lambda_1^2 < 0$, $\lambda_2^2 < 0$, functions X and Y have trigonometric form; when $\lambda_1^2 > 0$, $\lambda_2^2 > 0$, they are described with hyperbolic functions; when $\lambda_1^2 < 0$, $\lambda_2^2 > 0$, they have a mixed form.

Let us take the following functions into consideration:

$$f_k(x) = \begin{cases} \cos(\theta_k x/l) & (\lambda_k^2 < 0); \\ \text{ch}(\theta_k x/l) & (\lambda_k^2 > 0); \end{cases} \qquad v_k(x) = \begin{cases} \sin(\theta_k x/l) & (\lambda_k^2 < 0); \\ \text{sh}(\theta_k x/l) & (\lambda_k^2 > 0), \end{cases} \quad (10.54)$$

where, $\theta_k = |\lambda_k(\tau)|l$.

Let's turn to the continuum subsystem of the arbitrary module s, for which the solution of system (10.51), with reference to (10.54), has the form

$$\left. \begin{aligned} X_s(x) &= h_{1s}f_1(x) + h_{2s}v_1(x) + h_{3s}f_2(x) + h_{4s}v_2(x); \\ Y_s(x) &= \beta_1[h_{1s}f_1(x) + h_{2s}v_1(x)] + \beta_2[h_{3s}f_2(x) + h_{4s}v_2(x)], \end{aligned} \right\} \quad (10.55)$$

where, $\beta_k = -(R_{11} + \lambda_k^2)/R_{12} = -R_{21}/(R_{22} + \lambda_k^2); \ k = 1, 2; \ x \in [0, l]$ function β_k can be interpreted as a slowly varying factor of the spatial form).

Further, we will take into account the boundary conditions. Torque, at the ends of the section of the executive body, is zero. While determining the appropriate boundary conditions, it must be borne in mind that function Y describes the dynamic error, which differs from deformation $\Delta Y = Y - \Pi(X)$. For small values of X we have $\Delta Y \approx Y - \Pi'X = (\beta_{1,2} - \Pi')X$. Then,

$$\Delta Y_s'(0) = h_{2s}(\beta_1 - \Pi')v_1'(0) + h_{4s}(\beta_2 - \Pi')v_2'(0) = 0. \quad (10.56)$$

On the basis of (10.55), (10.56), taking into account $f_k(0) = 1, \ v_k(0) = 0,$ $\Delta Y_s'(l) = 0$, we get

$$\left. \begin{aligned} h_{2s} &= \tilde{h}_{2s}X_s'(0); \quad h_{4s} = \tilde{h}_{4s}X_s'(0); \quad h_{3s} = X_s(0) - h_{1s}; \\ h_{1s} &= \frac{f_2'(l)(\beta_2 - P)X_s(0) + [\tilde{h}_{2s}v_1'(l)(\beta_1 - \Pi') + \tilde{h}_{4s}v_2'(l)(\beta_2 - \Pi')]X_s'(0)}{f_2'(l)(\beta_2 - \Pi') - f_1'(l)(\beta_1 - \Pi')}, \end{aligned} \right\} \quad (10.57)$$

where, $\tilde{h}_{2s} = -(\beta_2 - \Pi')/[v_1'(0)(\beta_2 - \beta_1)]; \quad \tilde{h}_{4s} = (\beta_1 - \Pi')/[v_2'(0)(\beta_1 - \beta_2)].$

In case of the given boundary conditions, $X_s(0)$ and $X_s'(0)$, all the parameters of the solution, with reference to (10.57), are the known functions of the unknown θ_1 and θ_2, which will be found below. So $X_s(l)$ and $X_s'(l)$ are determined as

$$\begin{aligned} X_s(l) &= h_{1s}f_1(l) + h_{2s}v_1(l) + h_{3s}f_2(l) + h_{4s}v_2(l); \\ X_s'(l) &= h_{1s}f'(l) + h_{2s}v_1'(l) + h_{3s}f_2'(l) + h_{4s}v_2'(l). \end{aligned} \quad (10.58)$$

The dependencies (10.57), (10.58) define the transition matrix $\mathbf{Z} = \|z_{kj}\|$

$$\begin{bmatrix} X_s(l) \\ X_s'(l) \end{bmatrix} = \begin{bmatrix} z_{11} & z_{12} \\ z_{21} & z_{22} \end{bmatrix} \begin{bmatrix} X_s(0) \\ X_s'(0) \end{bmatrix}. \quad (10.59)$$

While determining the elements of the transition matrix $\mathbf{Z}$ we can avoid the cumbersome analytical calculations. For the purpose, it is enough to make two simple calculations, when $X_s^{(1)}(0) = 1$, $X_s'^{(1)}(0) = 0$ and $X(0)_s^{(2)} = 0$, $X_s'^{(2)}(0) = 1$. It is easy to see that, according to (10.59), $X_s^{(1)}(l) = z_{11}$, $X_s'^{(1)}(l) = z_{21}$, $X_s^{(2)}(l) = z_{21}$, $X_s'^{(2)}(l) = z_{22}$. (Here the superscript in parentheses corresponds to the calculation number.)

The transition matrix for the module s is defined as $\mathbf{U} = \mathbf{ZW}$, where $\mathbf{W}$ is the transition matrix of the connecting element (clutch) between adjacent sections of the main shaft. In Fig. 10.10, the clutch is schematized as an elastic element Δc, and its inertial properties are taken into account, during reduction to the elements of the continual subsystem. Of course, if necessary, without restricting the generality of approach, the dynamic structure of this element may be more complex. In the considered case $u_{11} = z_{11}$; $u_{12} = z_{11}\zeta_1 + z_{12}$; $u_{21} = z_{21}$; $u_{22} = z_{21}\zeta_1 + z_{22}$, where $\zeta_1 = c_1/\Delta c$; $c_1 = GI_1/l$.

So the problem is reduced to the analysis of the regular oscillatory system, defined by the following recursive dependencies:

$$X_s(l) = u_{11}X_{s-1}(l) + u_{21}X_{s-1}'(l); \quad X_s'(l) = u_{21}X_{s-1}(l) + u_{22}X_{s-1}'(l). \quad (10.60)$$

On the basis of analysis of the system of differential equations (10.60), we have $\theta_k = \arccos\chi_k$ at $|\chi_k| < 1$, $\theta_k = \text{Arch}\chi_k$ at $\chi_k > 1$ и $\theta_k^0 = \text{Arcch}|\chi_k|$; $\chi_k < -1$, Where

$$\chi_k = 0.5(u_{11} + u_{22})_k. \quad (10.61)$$

Taking into account the boundary conditions on the main shaft, when $|\chi_k| < 1$, we arrive at the following equation :

$$(\zeta + 1)\cos[(n + 0.5)\gamma] - \zeta\,\cos[(n - 0.5)\gamma] = 0, \quad (10.62)$$

where, $\zeta = \Delta c/(c_0 - J_0 p^2)$, n is the number of modules.

Function $c_0 - J_0 p^2$ describes the dynamic stiffness at the "input", which in this case has a fairly simple form. For engineering estimates the limiting cases are very informative. In particular, if the drive based mechanism has the relatively large flywheel mass or large stiffness, $\zeta \to 0$. Then, on the basis of (10.62), we have

$$\gamma_j = (2j - 1)\pi/(2n + 1) \quad (j = \overline{1, n}). \quad (10.63)$$

In case of relatively small dynamic stiffness $|\zeta| \to \infty$, at the same time

$$\gamma_j = \pi j/n \qquad (j = \overline{1, n - 1}). \quad (10.64)$$

Here j is the number of the shape mode, accurately reflecting the constant amplitude values of free oscillations in the cross-sections of the main shaft $X_s(0)$, corresponding to the boundaries between the modules.

In case of arbitrary ζ, we have $(2j-1)/(2n+1) < \gamma_j/\pi < j/n$. For example, when $n = 4$ and $j = 1$, we have $0.222 < \gamma_2/\pi < 0.25$, which in this case indicates the relatively small effect of the boundary conditions at the "input". If we could restrict ourselves to taking into account the elastic element $(c_0 \gg J_0 p^2)$, while schematizing the driven mechanism, parameter γ_j doesn't depend on the desired frequency p, but only on the number of modules n.

After determination of γ_j, with reference to (10.62) or (10.63), (10.64) formula (10.61) obtains the meaning of a frequency equation. Thus, in particular, when $|\chi_k| < 1$

$$[u_{11}(p,\varphi) + u_{22}(p,\varphi)]_k = 2\cos\gamma_j(n,\zeta). \tag{10.65}$$

Since $k = 1, 2$, then (10.65) corresponds to the two equations, covering all the spectrum of "natural" frequencies. For illustration and qualitative estimation of the results of the analysis we take the following initial data: $\rho_1 = (J_{10} + J_1 n)l^{-1} = 0.5$; $\rho_2 = (J_{20} + J_2 n)l^{-1} = 0.3$ kg m^2; $G_1 I_1/l^2 = 10^4$ N; $GI_2/l^2 = 2.5 \times 10^3$ N; $\Delta c = 2 \times 10^3$ N m.

The mechanisms, schematized as serial connections of the kinematic analogy of the mechanism, which corresponds to the position function $\Pi(\varphi_1^*)$ and elastic element c, when $\Pi' = \alpha \sin\varphi_1^*$, $cnl^{-1} = 4 \times 10^3$. The inertial characteristics of the input and output links of the mechanism are taken into account while determining ρ_1 and ρ_2. With reference to (10.47) $A = \Pi'$; $B = l(cnp)^{-1}$; $C = 0$; $D = (\Pi')^{-1}$. On the basis of (10.55), it can be shown that when $p < p_*$, the functions X_s and Y_s have the trigonometric form and when $p > p_*$, the mixed form, where

$$p_*(\varphi_1^*) = \sqrt{c[J_2^{-1} + J_1^{-1}\Pi'^2(\varphi_1^*)]}. \tag{10.66}$$

The graph $p_*(\varphi_1^*)$, which separates, according to (10.66), the two areas of the solutions, is shown in Fig. 10.11. Other graphs correspond to the slowly changing "natural" frequencies, defined as per (10.60)–(10.66), when $N = 4$, $\zeta = 2$, $\alpha = 1$ (curve number corresponds to the number r). The area with the high density of frequency spectrum distribution (curves 4–8), is directly adjacent to curve p_*, which is located in the vicinity of the so-called condensation point $p^0 = \sqrt{c/J_2} = 119\,\text{s}^{-1}$. For certain values of $\Pi'(\varphi_1^*)$ the effect of frequency "splitting" is observed (curves 3 and 8, 4 and 7, 5 and 6) and the disappearance of some components of the frequency spectrum (curves 4–7).

During modal analysis, we first consider the oscillatory modes of the main shaft K_{sj} and the form of dimensionless loading moments $\tilde{M}_{sj}$, which correspond to the input section of module s (see Fig. 10.10) and the number of form j, when $K_{0s} = 1$.

Fig. 10.11 Graphs of the
"natural" frequencies
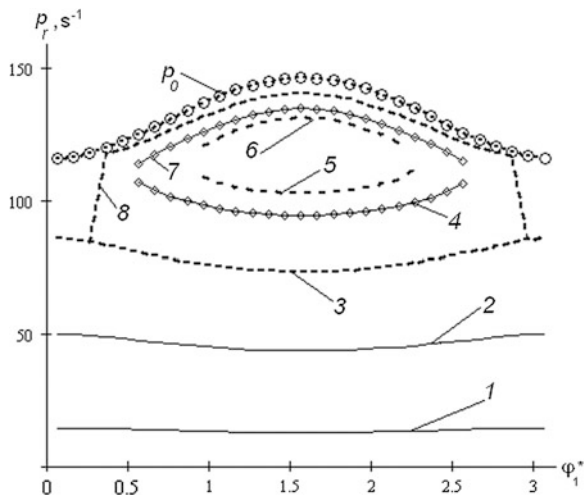
$$K_{sj} = b_1 \cos s\gamma + b_2 \sin s\gamma;$$
$$\tilde{M}_{sj} = b_1[\cos (s + 1)\gamma_j - \cos s\gamma_j] + b_2[\sin (s + 1)\gamma_j - \sin s\, \gamma_j]. \tag{10.67}$$

Let's call these forms stroboscopic. Graphs K_{sj} and $\tilde{M}_{sj}$ are shown in Fig. 10.12. Let us note that the number of "natural" frequencies r generally does not correspond to the mode number j. This is because the stroboscopic mode (10.67) characterizes the ratio of amplitudes of selected sections s. Meanwhile, the additional modes can arise within each module, in case of fixed s. In particular, in the
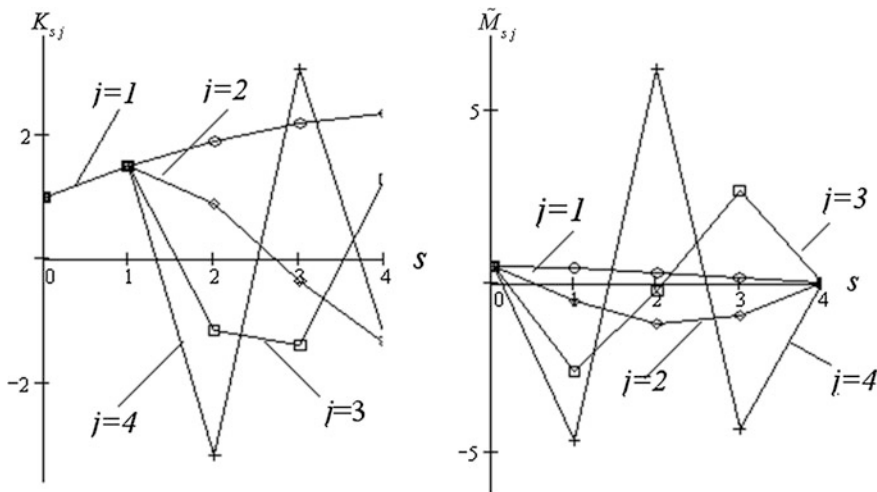
Fig. 10.12 Oscillatory mode shapes in sections s

graphs $p_r(\varphi_1^*)$ (see Fig. 10.11), curves 3 and 8 correspond to the stroboscopic form $j = 3$, and curves 4–7 to the form $j = 4$. In the vicinity of the condensation point the oscillatory modes do not have clearly expressed character and in the "pure form" are practically unlikely to be identified.

In the Fig. 10.13, the graphs of functions $X_{sj}(x/l)$ (solid curves) and $Y_{sj}(x/l)$ (highlighted lines) are represented, which characterize the distribution of amplitudes of free vibrations, directly in the subsystem of each module. At the same time
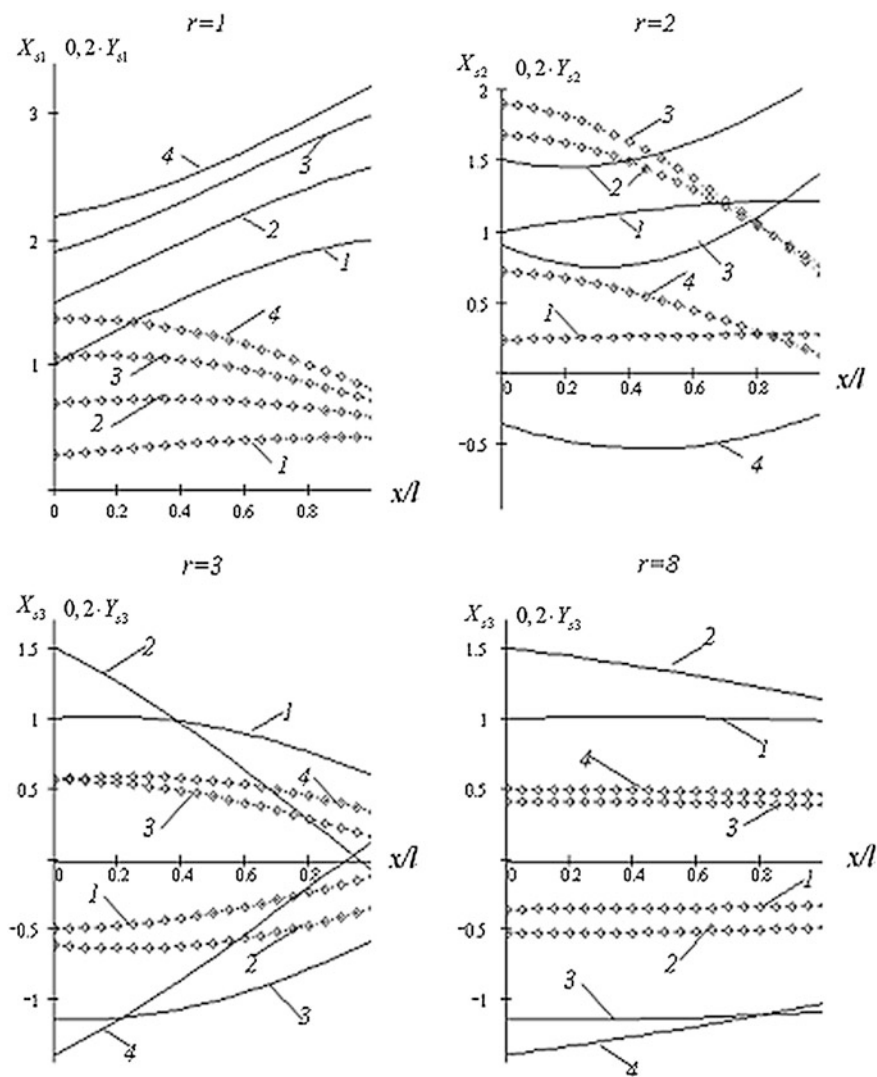
Fig. 10.13 Mode shapes of the subsystems

the number of the curve corresponds to the number of the module s, and each graph corresponds to the number of frequency r.

It follows from the analysis of graphs that for the chosen parameters at the lowest frequency ($r = 1$, $j = 1$) the oscillations of the main shaft and the executive body occur in a single phase, when $r = 2$, $j = 2$ the in-phase oscillations are violated only in the last module. When $r = 3$, 8, è $j = 3$, the oscillations appear to be of anti-phase nature for both subsystems of all the modules, and the shape mode of the executive body is weakly dependent on the oscillatory mode of the main shaft.

Forced oscillations To calculate forced oscillations we can use several approaches. One of them is the transition to the quasi-normal coordinates, based on the identified time-dependent modes of free oscillations, which corresponds to the approximate expansion in the series of "natural" modes. Here we will restrict ourselves to the consideration of the simplified method for estimating the level of forced vibrations under harmonic kinematic excitation $\varepsilon = d^2\varphi_2^*/dt^2 = \omega^2 d^2\varphi_2^*/d\varphi_1^{*2}$. Let us represent ε as a Fourier series $\varepsilon = \omega^2 \sum_{m=1}^{\infty} m^2 w_m \cos(m\varphi_1^* + \vartheta_m)$ and average the functions $\Pi'(\varphi_1^*) = d\varphi_2^*/d\varphi_1^*$ in the interval 2π. After substitution in (10.48), we obtain the particular solution of the system equation (10.51) for harmonic m:

$$\left.\begin{array}{l} X_m^* = - R_{12}^{(m)} m^2 \omega^2 w_k / (R_{11}^{(m)} R_{22}^{(m)} - R_{12}^{(m)} R_{21}^{(m)}); \\ Y_m^* = R_{11}^{(m)} m^2 \omega^2 w_k / (R_{11}^{(m)} R_{22}^{(m)} - R_{12}^{(m)} R_{21}^{(m)}). \end{array}\right\} \tag{10.68}$$

Here the upper index (m) corresponds to the substitution of $m\omega$ instead of p. To determine the amplitude-frequency characteristics (AFC), we should use (10.57), (10.67), (10.68). Omitting the calculations, we obtain the following system of non-uniform differential equations

$$\begin{bmatrix} a_{1,s} \\ \tilde{M}_{1,s} \end{bmatrix} = \begin{bmatrix} u_{11}(m\omega) & u_{12}(m\omega) \\ u_{21}(m\omega) & u_{22}(m\omega) \end{bmatrix} \begin{bmatrix} a_{1,s-1} \\ \tilde{M}_{1,s-1} \end{bmatrix} + \begin{bmatrix} u_{11}(m\omega)X^* \\ 0 \end{bmatrix}. \tag{10.69}$$

In case of the given boundary conditions, the amplitude-frequency characteristic (AFC), in sections s of the main shaft and the executive member $a_{1s}(m\omega, s)$, $a_{2s}(m\omega, s)$, are defined as

$$\begin{array}{l} a_{1s} = \left|(b_1 \cos s\gamma + b_2 \sin s\gamma)/\Delta + X_1^*\right|, \\ a_{2s} = \left|\beta_1(b_1 \cos s\gamma + b_2 \sin s\gamma)/\Delta + Y_1^*\right|, \end{array} \tag{10.70}$$

where

$$\begin{array}{l} b_1 = -X^* \zeta^{-1} \cos[(N + 0.5)\gamma]/\Delta, \\ b_2 = -X^* \zeta^{-1} \sin[(N + 0.5)\gamma]/\Delta, \\ \Delta = \cos[(N + 0.5)\gamma](1 + \zeta^{-1}) - \cos[(N + 0.5)\gamma]. \end{array}$$

Using (10.69) to determine γ, we obtain a dependence, which differs from (10.65), only that frequency p is replaced by $m\omega$:

$$0.5[u_{11}(m\omega) + u_{22}(m\omega)] = \cos\gamma(m\omega). \tag{10.71}$$

Thus, when calculating AFC for harmonic $m\omega$, we can use (10.65) with coefficients b_1, b_2 and γ, obtained from (10.70), (10.71). It is easy to confirm that $\Delta = 0$, when $m\omega = p_r$, i.e. it corresponds to the resonant mode (without dissipation).

Here above, while determining AFC, we used the averaging of function $d\varphi_2^*/d\varphi_1^* = \Pi'(\varphi_1^*)$ that, strictly speaking, is valid only for small deviations of the function from the mean, or when $m \gg 1$. For small values of m the force and kinematic connection between the main shaft and the executive body requires clarification. For example, when moment $M_2 = M_2^* \cos\omega t$ is applied to the output link, then the moment transferred to the input link is $M_1 = \Pi'(\varphi_1^*)M_2^* \cos\omega t$. Then, when $\Pi'(\varphi_1^*) = \alpha \sin\omega t$, we have $M_1 = 0.5M_2^*\alpha \sin 2\omega t$. It is shown in [62], using the method of harmonic balance that the passage through element Π (see Fig. 10.10), is accompanied not only by amplitude transformation (0.5α instead of α), but by frequency transformation (2ω instead of ω); except for that, there is mutual replacement of sin and cos functions. This case occurs in practice with the "strong" harmonics $m = 1$. In the system under consideration, in this case, it is sufficient to replace, in the transition matrices, ω with 2ω and twice reduce the estimated amplitude of the first geometric transfer function of the mechanism Π'.

In Fig. 10.14, the frequency response (AFC), adjusted in this manner, is presented for given initial data and $s = 4$. Herewith, $a_1(\omega)$ (curve 1) corresponds to the main shaft, and $0.2a_2(\omega)$ to the executive body. It follows from the graphs that significant increase in the amplitude of the executive body, takes place in the vicinity of the
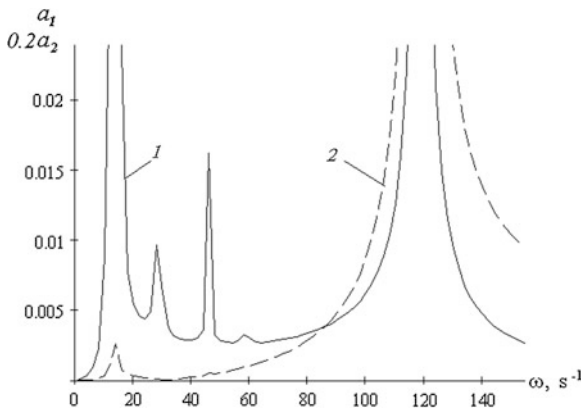
Fig. 10.14 Amplitude–frequency characteristic

lowest partial frequency of the main shaft subsystem in case of the first oscillatory mode $(j = 1)$ and in the zone of the condensation point $p^0 = \sqrt{c/J_2}$.

When calculating the modes, which are sufficiently far from the resonance zones, the influence of ω is usually small and the system is under quasi-static loading. Then, the constant term of the characteristic Eq. (10.52) is close to zero and, consequently, $\lambda_1 \approx 0$. This case is discussed in detail in [63, 64].

Chapter 11
Regular Cyclic Systems with Translational Motion of the Actuator

In the modern technological machines and automatic lines the identical cyclic mechanisms, operating in a parallel circuit, are often used for the implementation of the translational program motion of the actuators. These schematic and design solutions are fairly common in the textile, printing, packaging machines and other industries, for moving not only the massive tables or carriages, but also for the relatively compliant working bodies, forming the beam and frame structures.

Hereunder, we will discuss some regular dynamic models of this class. First of all we analyze a fairly general model, in which the main shaft and the executive body are schematized as the torsional and bending subsystems, with distributed parameters, and the cyclic mechanisms, as the subsystems with lumped parameters. Furthermore we discuss some important particular cases for the greater "transparency" of the arising effects, as well as for the elimination poor conditionality of calculation procedures in case of the limit transitions.

11.1 Dynamic Model of the General Form

11.1.1 Frequency and Modal Analysis

Let us assume that the main shaft 1 and the executive body 2 are schematized as torsional and bending subsystems with the distributed parameters. The cyclic mechanisms 3, connecting these subsystems, are schematized in the form of chain with discrete elements $J - \Pi - c - m$ (Fig. 11.1). Here J, m are the moments of inertia of the input link and mass of the output link of the mechanism; Π is the nonlinear operator that performs the transformation of the main shaft's rotation angle φ to coordinate $\Pi(\varphi)$ according to the predetermined position function (see Chap. 1). The dynamic model has the lattice structure, in which to each repeating unit, at the constraints break, three reactions should be applied: torque M_φ (to the main shaft), the bending moment M_y and shear force Q (to the executive body). Let us note here that in case of rational designing, the unaccounted bending oscillations of the main shaft, in such systems usually play a secondary role, as an acceptable range of partial frequencies of the bending subsystem always can be achieved by installing additional
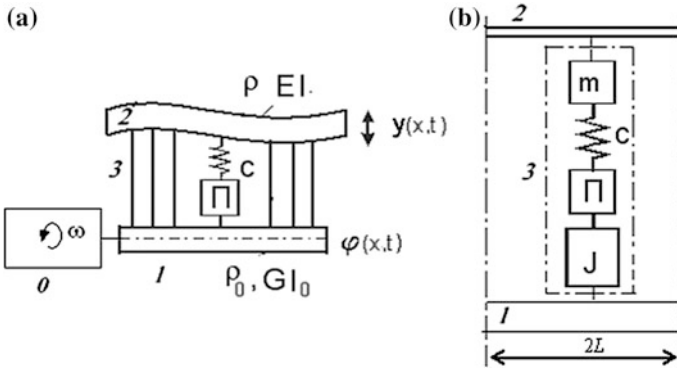
Fig. 11.1 Dynamic model of the torsion-bending system: **a** is the general form of the model; **b** is the repeating unit of the regular system

supporting bearings. The dynamic characteristics of the kinematic chain, connecting the main shaft with the motor 0, in general, can be taken into account with the choice of the appropriate dynamic stiffness at the "input" (see Sect. 5.7.4).

Let us accept the following notations: E, G are the elastic and shear modulus; I_0 is the polar moment of inertia of the main shaft; ρ_0, ρ are the moments of inertia of the main shaft and the mass of the executive body, per unit length; I_i, m_i are the discrete masses and moments of inertia; c_i are the stiffness coefficients; $2L$ is the length of the repeating unit (module).

In case of using accepted drive schematization, the concentrated moments of inertia J and masses m are attached to the mechanism's subsystem. We divide the module into three sections: in front of the mechanism (section **I**), the mechanism (section **II**), behind the mechanism (section **III**). For the mathematical description of the model, we will use the modified transition matrices (see 8.1). Let us recall that the modified transition matrices, unlike the traditional ones, take into account the slow variation of the parameters, corresponding to the linearization of the nonlinear position function, in the vicinity of the program motion. At the same time when $\Pi(\varphi) \approx \Pi(\varphi_*) + \Pi'(\varphi_*)\Delta\varphi$ where $\varphi_* = \omega t$; $\Delta\varphi$ is the dynamic error in the considered section of the main shaft; $(\ )' = \partial\Pi/\partial\varphi$.

In accordance with the conditional oscillator method, we search the free oscillations as follows:

$$\Delta\varphi_* = X(\varphi_*) \sin \int p(\varphi_*)d\varphi_*; \quad \Delta y = Y(\varphi_*) \sin \int p(\varphi_*)d\varphi_*,$$

where X, Y are the amplitudes of torsion and bending oscillations.

Transition through the arbitrary module s for some oscillatory mode corresponds to the transformation of the six-dimensional state vectors $\mathbf{T}_{s-1} \rightarrow \mathbf{T}_s$,

$$\mathbf{T}_s = \Gamma\mathbf{T}_{s-1}, \tag{11.1}$$

Here Γ is the transition matrix; $\mathbf{T} = \mathbf{T}(X, M_\varphi, Y, \alpha, M_y, Q)$, where, M_φ, M_y, α, Q are the amplitudes of the moments in case of the torsion and bending oscillations, the rotation angles of the sections and shear forces.

We represent the transition matrix as follows:

$$\Gamma = \Gamma_3 \Gamma_2 \Gamma_1, \tag{11.2}$$

where $\Gamma_1 = \Gamma_3$ are the transition matrices for sections **I** and **III**, Γ_2 is the mechanism's transition matrix

$$\Gamma_1 = \Gamma_3 = \begin{pmatrix} \Gamma_\varphi & 0 \\ 0 & \Gamma_Y \end{pmatrix}.$$

Here

$$\Gamma_\varphi = \begin{pmatrix} \cos\theta_\varphi(p) & \sigma p^{-1}\sin\theta_\varphi(p) \\ -\sigma^{-1}p\sin\theta_\varphi(p) & \cos\theta_\varphi(p) \end{pmatrix},$$

$$\Gamma_Y = \begin{pmatrix} \kappa_1(p) & \kappa_2(p)L & \kappa_3(p)L^2(EI)^{-1} & \kappa_4(p)L^3(EI)^{-1} \\ \kappa_4(p)\xi^4(p)L^3 & \kappa_1(p) & \kappa_2(p)L(EI)^{-1} & \kappa_3(p)L^2(EI)^{-1} \\ \kappa_3(p)\xi^4(p)L^2EI & \kappa_4(p)\xi^4(p)L^3EI & \kappa_1(p) & \kappa_2(p)L \\ \kappa_2(p)\xi^4(p)LEI & \kappa_3(p)\xi^4(p)L^2EI & \kappa_4(p)L^3 & \kappa_1(p) \end{pmatrix},$$

where $\theta_\varphi(p) = pL\sqrt{\rho_0/(GI_0)}$; $\sigma = (GI_0\rho_0)^{-0.5}$; $\xi(p) = \sqrt[4]{\rho p^2/(EI)}$; $\kappa_j = K_j(\theta)/\theta^{j-1}(j = \overline{1,3})$; K_j are the Krylov's functions, in case of the argument $\theta = \theta(p) = L\xi(p)$.

For real values of the parameters the functions can usually be represented as the truncated Maclaurin series.

Then the functions κ_j take the form $\kappa_1 \approx 1 + \theta^4/4!$; $\kappa_2 \approx 1 + \theta^4/5!$; $\kappa_3 \approx 1/2 + \theta^4/6!$; $\kappa_4 \approx 1/6 + \theta^4/7!$. Unlike the functions of Krylov, at $\theta \to 0$, none of the functions κ_j tend to zero, which increases the accuracy of calculations and eliminates the difficulty of limiting transitions. Let us note that the case $\theta = 0$ corresponds to the situation, when the "natural" frequencies of the system very weakly depend on the inertial characteristics of the beam. The matrix Γ_2 (mechanism) is as follows:

$$\Gamma_2 = \begin{pmatrix} 1 & 0 & 0 & 0 & 0 & 0 \\ c\Pi'_* - Jp^2 & 1 & -c\Pi'_* & 0 & 0 & 0 \\ 0 & 0 & 1 & 0 & 0 & 0 \\ 0 & 0 & 0 & 1 & 0 & 0 \\ 0 & 0 & 0 & c_\alpha & 1 & 0 \\ c\Pi'_* & 0 & mp^2 - c & 0 & 0 & 1 \end{pmatrix}$$

Here $\Pi'_* = \Pi'(\varphi_*)$, where the argument φ_* plays the role of the "slow time" (c_α see below).

The characteristic equation (11.3) corresponds to the matrix Γ:

$$\lambda^6 + h_1\lambda^5 + h_2\lambda^4 + h_3\lambda^3 + h_2\lambda^2 + h_1\lambda + 1 = 0. \tag{11.3}$$

Here it is taken into account that due to the module's dynamic symmetry, when we change the order of the section numbering, its dynamic properties remain unchanged. Equation (11.3) is reciprocal.

The roots of the characteristic equation can be defined as the eigenvalues of matrix Γ.

However, in this case the structure of the solution, described usually with the combination of trigonometric and hyperbolic functions remains in the latent form.

The coefficients of the Eq. (11.3) h_i according to (9.3) are defined as follows:

$$\left.\begin{array}{lll} h_1 = -\operatorname{Sp}\mathbf{G}_1; & \mathbf{B}_1 = \mathbf{G}_1 - h_1\mathbf{E}^0; & \mathbf{G}_2 = \mathbf{G}_1\mathbf{B}_1; \\ h_2 = -\frac{1}{2}\operatorname{Sp}\mathbf{G}_2; & \mathbf{B}_2 = \mathbf{G}_2 - h_2\mathbf{E}^0; & \mathbf{G}_3 = \mathbf{G}_1\mathbf{B}_2; \\ h_3 = -\frac{1}{3}\operatorname{Sp}\mathbf{G}_3; & \mathbf{B}_3 = \mathbf{G}_3 - h_3\mathbf{E}^0, \end{array}\right\} \tag{11.4}$$

where $\mathbf{G}_1 = \Gamma$; $\operatorname{Sp}\mathbf{G}_i$ is the spur of the matrix $\mathbf{G}_i$; $\mathbf{E}^0$ is the unit matrix.

Using substitution $z = \lambda + \lambda^{-1}$, which is applied usually for reciprocal equations, reduce (11.3) to the form of the cubic equation [76, 78]

$$z^3 + h_1 z^2 - (3 - h_2)z - 2h_1 + 3h_3 = 0. \tag{11.5}$$

Equation (11.5) has three different real roots, if

$$\Lambda = \Lambda_1^2 + \Lambda_2^3 < 0, \tag{11.6}$$

where $\Lambda_1 = -\frac{h_1^3}{27} + \frac{(3+h_2)h_1}{6} + \frac{2h_1 - 3h_3}{2}$; $\qquad \Lambda_2 = -[3(3 + h_2) + h_1]/9$.

In this case $z_1 = -2w\cos\frac{\phi}{3}$, $z_{2,3} = 2w\cos\frac{\pi\pm\phi}{3}$, where, $w = \operatorname{sgn}\Lambda_1\sqrt{|\Lambda_2|}$, $\phi = \arccos(\Lambda_1/w^3)$.

The characteristic numbers λ are the roots of the equation $\lambda^2 - z\lambda + 1 = 0$:

$$\lambda_{kj} = 0.5z_k \pm \sqrt{0.25z_k^2 - 1}, \tag{11.7}$$

where $k = 1,\ 2,\ 3,\ j = 1,\ 2$, (signs "plus" and "minus").

It follows from (11.7) that (11.6) is the necessary, but nonsufficient, condition for the characteristic number λ_k to be real; $|z_k| > 2$ is the additional condition. When $|z_k| < 2$, the functions $\lambda_{kj}(p, \varphi_*)$ are the mutually conjugate complex numbers. Accepting into (11.7) $\operatorname{Re}\lambda_{kj} = 0.5z_k = \cos\gamma_k$, we have $\lambda_{kj} = \cos\gamma_k \pm i\sin\gamma_k = e^{\pm i\gamma_k}$. For this case the particular solution has the trigonometric form. When $\Lambda > 0$, Eq. (11.5) has one real and two complex solutions: $z_1 = -2w\cosh\frac{\phi_1}{3}$; $z_{2,3} = w(\cosh\frac{\phi_1}{3} \pm i\sqrt{3}\sinh\frac{\phi_1}{3})$, where, $\phi_1 = \operatorname{Arccosh}\frac{\Lambda_1}{3}$. When $\Lambda = 0$ $(\Lambda_1^2 = -\Lambda_2^3)$, among the three real roots, two coincide.

For frequency and modal analysis, several ways can be used, which are equivalent from the theoretical point of view. However, the implementation of some of them causes certain computational difficulties, associated with the high dimensionality of the system, as well as with the rapid growth of the hyperbolic functions and their differences. Because of this, obtaining satisfactory accuracy of calculations is often a challenging task. In our case the problem is additionally complicated, because of the system's parameters and sometimes of the variability of boundary conditions. As the analysis showed, in this task a slightly modified method of initial parameters [64] proved to be most effective, the application of which, we will illustrate by the example of the model of the drive for loop-forming members in the knitting machine. For simplified estimation of the mutual influence of the module's torsion and bending subsystems, we will consider the criterion,

$$\chi = \sqrt{\frac{GI_p(\rho L + m)L^2}{12EI(\rho_0 L + J)}},$$

which in the first approximation is equal to the ratio of the partial frequencies of these subsystems.

First of all let us consider the unilateral drive, when the main shaft in section $s = 0$, connected with the transfer mechanisms, connected to the engine (see Fig. 9.2, the drive M1). Without narrowing the scope of this approach, we assume that the cross section $s = 0$ of the main shaft rotates with constant angular velocity ω. This assumption, which corresponds to the absence of oscillations at the "input", is easily eliminated by the introduction of dynamic stiffness of the transfer mechanisms. However, in this case further complication, of an already complex model, is inappropriate, since in this case the dynamic effects, which arise directly in the studied regular system, can be masked. The design specifics of the joint of the output link, of the cyclic mechanism, with the executive organ, play a major role in the formation of natural frequency spectrum. This factor is reflected in the dynamic model with the stiffness coefficient c_α. Let us discuss some extreme cases: pivotal connection (case 1: $c_\alpha = 0$) and clamping (case 2 $c_\alpha \to \infty$).

Case 1 In case of pivotal connection of the output link with the executive member the state vector, in section s is defined as $\mathbf{T}_s = \Gamma^s \mathbf{T}_0$, where $\mathbf{T}_0 = \left(0, M_{\varphi 0}, Y_0, \alpha_0, 0. 0\right)^{\mathrm{T}}$; $M_{\varphi 0}, Y_0, \alpha_0$ are the unknown boundary conditions. When $s = n$, we have $\mathbf{T}_n = (X_n, 0, Y_n, \alpha_n, 0, 0)^{\mathrm{T}}$. Hence,

$$\left.\begin{array}{l} g_{22}(p, \varphi_*)M_{\varphi 0} + g_{23}(p, \varphi_*)Y_0 + g_{24}(p, \varphi_*)\alpha_0 = 0; \\ g_{52}(p, \varphi_*)M_{\varphi 0} + g_{53}(p, \varphi_*)Y_0 + g_{54}(p, \varphi_*)\alpha_0 = 0; \\ g_{62}(p, \varphi_*)M_{\varphi 0} + g_{63}(p, \varphi_*)Y_0 + g_{64}(p, \varphi_*)\alpha_0 = 0. \end{array}\right\} \tag{11.8}$$

Here $g_{jv}(p, \varphi_*)$ are the corresponding matrix entries $\Gamma^n = \left\|g_{jv}\right\|$, when $j = 2, 5, 6$; $v = 2, 3, 4$.

Inverting the determinant of system (11.8) to zero, we obtain the following frequency equation.

$$\begin{vmatrix} g_{22}(p, \varphi_*) + g_{23}(p, \varphi_*) + g_{24}(p, \varphi_*) \\ g_{52}(p, \varphi_*) + g_{53}(p, \varphi_*) + g_{54}(p, \varphi_*) \\ g_{62}(p, \varphi_*) + g_{63}(p, \varphi_*) + g_{64}(p, \varphi_*) \end{vmatrix} = 0. \tag{11.9}$$

Let's note here that in view of the variability of $g_{j\nu}(\varphi_*)$, for each of the oscillatory modes, we have the slowly varying frequency of free oscillations. With the bilateral drive (see Fig. 9.2, drives M1, M2), we should take $T_n = (0, \ M_{\varphi n}, \ Y_n, \ \alpha_n, \ 0, \ 0)^T$, which corresponds to the assumption $X_n = 0$.

In this case the frequency equation has the form (11.9) $j = 2, 5, 6; \nu = 2, 3, 4$.

$$\begin{vmatrix} g_{12}(p, \varphi_*) + g_{13}(p, \varphi_*) + g_{14}(p, \varphi_*) \\ g_{52}(p, \varphi_*) + g_{53}(p, \varphi_*) + g_{54}(p, \varphi_*) \\ g_{62}(p, \varphi_*) + g_{63}(p, \varphi_*) + g_{64}(p, \varphi_*) \end{vmatrix} = 0. \tag{11.10}$$

The ranges of "natural" frequencies $p(\varphi_*)$, with unilateral or bilateral drives, for the typical case, are shown in the Fig. 11.2.

The graphs of $p(\varphi_*)$, changing during half of the period of kinematic cycle for the models with unilateral (M1) or bilateral (M2) drives (see Fig. 9.2), are shown in the Fig. 11.3. (For plotting the graphs we used the data of loop-forming mechanisms of the knitting machine).

The cases of frequency spectra split, arising in case of "jump" from one mode to the other and with the degeneration of some oscillatory mode shapes, are represented in the graphs. It can lead to the spatial localization of oscillations and to an increase in the system's vibration activity (see Chap. 12). As it should be expected, in case of a bilateral drive, the frequency spectrum shifts to higher values.

The frequency spectrum can be divided into two parts: the low-frequency range (acoustic or Debye spectrum) and the high-frequency range (optical or Born spectrum). In the range of acoustic frequencies, with the increase in the first transfer function $\Pi'(\varphi_*)$, the "natural" frequency decreases, and in the optical frequency range, it grows.
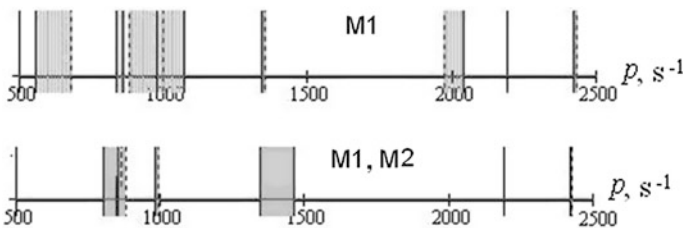
Fig. 11.2 Spectra of "natural" frequencies, in case of unilateral or bilateral drives
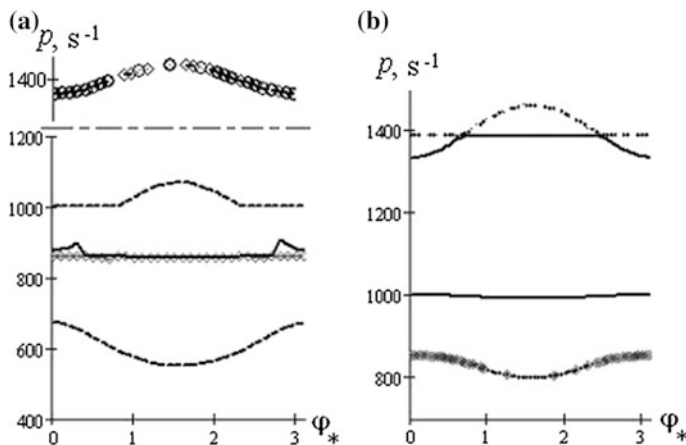
Fig. 11.3 Graphs of variation of "natural" frequencies (case 1)

Case 2 Further will we assume that the executive body is firmly attached to the ends of the mechanism's output links. Then, at the end of the section **I** and at the beginning of section **III** (see above), we should accept $\alpha_j = 0$. Using this additional condition, instead of the transition matrix Γ_1, we obtain $\Gamma_1^* = \left\| \gamma_{ij}^* \right\|_{5 \times 5}$, where $\gamma_{ij}^* = \gamma_{ij} - \gamma_{i4} \gamma_{4j} / \gamma_{44}$, γ_{ij} are the entries of the transition matrix Γ_1. Finally the transition matrix of one module takes the form

$$\Gamma^* = (\Gamma_1^*)^{-1} \Gamma_2^* \Gamma_1^*. \tag{11.11}$$

Here matrix Γ_2^* is obtained from the transition matrix of the mechanism Γ_2, by excluding the fourth row and fourth column.

When taking into account the boundary conditions, we obtain the following frequency equation for the unilateral drive: $f_{22}f_{53} - f_{52}f_{23} = 0$, and for the bilateral one $f_{12}f_{53} - f_{52}f_{13} = 0$. Here f_{jv} are the corresponding elements of the transition matrix of the system $\Gamma_n^* = (\Gamma^*)^n$.

Some graphs $p(\varphi_*)$, for the frequencies, whose values are located in the vicinity of the dominant partial frequency $p_* = \sqrt{c/m}$, are represented in Fig. 11.4. In this case, the solid curves correspond to the unilateral drive and hatched ones correspond to the bilateral one.

The contrary influence of the executive body on the frequency spectrum formation, in both considered cases is of interest. The dynamic stiffness of the executive body, in case of the unilateral drive, decreases, in case of increase in the connectivity of the two subsystems and in case of the bilateral drive—increases. In the latter case, vibrations of the subsystems are in anti-phase and the executive body acts as a "stiffener" for the torsional subsystem.

Fig. 11.4 Graphs of the change of "natural" frequencies (case 2)
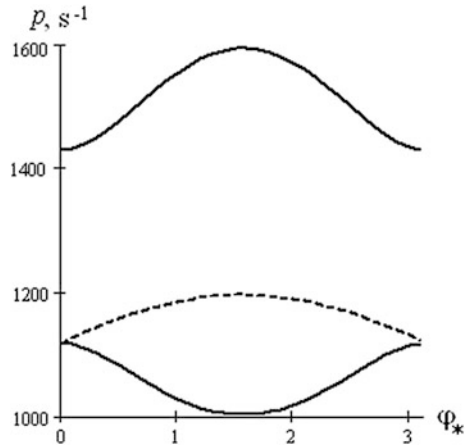
The variability of "natural" frequencies can lead to the violation of dynamic stability conditions on the finite intervals of the kinematic cycle (see Sect. 5.3.1). The amplitudes of the free oscillations, excited by the collisions in the clearances and abrupt changes in external disturbances, in some time intervals, are increasing.

Non-stationary oscillatory mode shapes To determine the state vector $\mathbf{T}_s$, with reference to (11.10), it is necessary to accurately find the unknown boundary conditions $M_{\varphi 0}$, α_0, to the constant. In this problem it is convenient to set $Y_0 = Y_0^*$ (for example, $Y_0^* = 1$). Then

$$
\begin{bmatrix} M_{\varphi 0} \\ \alpha_0 \end{bmatrix} = \begin{pmatrix} g_{52}(p, \varphi_*) & g_{54}(p, \varphi_*) \\ g_{63}(p, \varphi_*) & g_{63}(p, \varphi_*) \end{pmatrix}^{-1} \begin{bmatrix} g_{53}(p, \varphi_*) \\ g_{63}(p, \varphi_*) \end{bmatrix}. \tag{11.12}
$$

Thus, all the elements of vector $\mathbf{T}_0$ are now known.

We can see, in Fig. 11.5, the typical graphs of the non-stationary oscillatory mode shapes for unilateral drives. In the graphs the odd numbers correspond to the torsional oscillatory mode shapes on the main shaft. The even numbers correspond to the bending oscillations of the actuator; the asterisk corresponds to the lower end of the range ($\varphi_* = 0$).

In the range of low-frequencies $550 \div 655\,\mathrm{s}^{-1}$ (Fig. 11.5a) the oscillatory modes are similar to the static deformations in case of decreasing dynamic stiffness with the growth of $\Pi'(\varphi_*)$. In the next frequency range $855 \div 865\,\mathrm{s}^{-1}$ (Fig. 11.5b) in case of change in $\varphi_* = \overline{0, \pi/2}$, a substantial transformation of modes occurs (curves 2, 2*). We can see, in Fig. 11.5c, the oscillatory modes (curves 1, 1*, 2, 2*) in case of frequencies adjacent to the previous range, which also show the abrupt change of the oscillatory modes within the kinematic cycle. It is interesting that the mode shape of torsional oscillations, of the main shaft, in this case, is close to the first mode, but with the significant difference of the actuator's mode shapes.
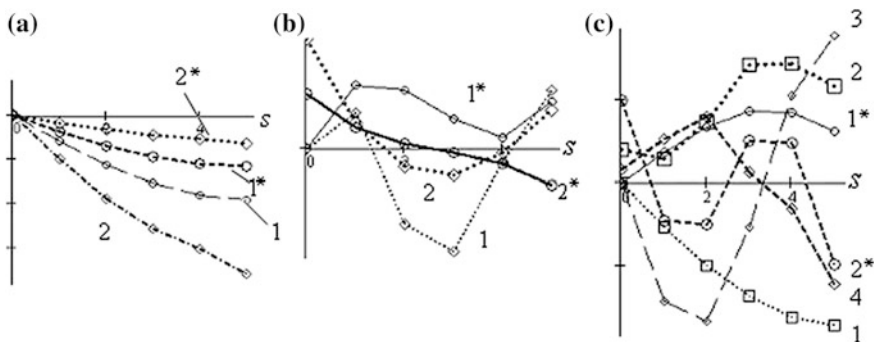
Fig. 11.5 Oscillatory mode shapes; **a** low frequency range (quasi-static regimes), **b** mid-frequency range, c) high-frequency range

Furthermore, the graph shows the single-node modes, occurring when the frequency is $\sim 2{,}000$ c^{-1} (curves 3, 4).

The presented above technique is of interest for the dynamic synthesis of this class of oscillatory systems. In particular it is not difficult to estimate the degree of connectedness of torsional and flexural sub-systems and the possibility of decomposition of the original dynamic model. If mode 2* is getting close to the inclined line, then it means that the executive body, at the given frequency, manifests itself as a non-deformable solid body. We should note the importance of the preliminary estimation of degeneration of modes and arising of new modes, within the kinematic cycle, as it is connected with the effect of spatial localization and growth in the system's vibration activity (see Chap. 12). There is another way to determine the oscillatory mode, based on the expansion of the state vector in terms of eigenvectors:

$$\mathbf{T_s} = \mathbf{V}\Psi^s\mathbf{V}^{-1}\mathbf{T}_0 \tag{11.13}$$

Here $\mathbf{V}$ is the eigenvector of matrix, $\Gamma, \Psi^s = \mathrm{diag}\{\lambda_1^s, \ldots \lambda_6^s\}$. However, as calculations show, in case of implementation of this approach hypersensitivity, to the accuracy of calculation, occurs, for the case, when the oscillating system forms a lattice, in which the torsional and flexural subsystems are interconnected with the subsystem with variable parameters, imitating a number of identical cyclic mechanisms.

11.1.2 Forced Oscillations

While developing the methodology for the research of forced oscillations, we will consider the more general case of the regular system, when the influence of dissipation is also taken into account. This is due to the fact that in the zone of high-frequency spectrum density, dissipation not only limits the level of oscillations, in

the resonant modes, but often plays the decisive role in the formation of the higher frequency range for vibration activity. The variability of parameters is caused by the slow change of the position function $\Pi(\varphi)$, which serves as the operator of the non-stationary connection, between the main shaft and the executive body. In dwells of the executive body, as well as in the vicinity of the small values of $d\Pi/d\varphi$, the dynamic connection between the torsional and flexural oscillatory systems is broken. In such cases some effects, inherent to the systems with variable structure, are revealed. To account for the position dissipative forces, we use the complex representation of the elastic modulus and stiffness coefficients (see Chap. 6):

$$\bar{E} = E(1 + 2i\delta_j); \quad \bar{G} = G(1 + 2i\delta_j); \quad \bar{c}_j = c(1 + 2i\delta_j)$$

where $i = \sqrt{-1}$; $\delta_j = \vartheta_j/(2\pi)$, ϑ_j is the logarithmic decrement of the corresponding element.

While studying the forced oscillations, we will consider the typical, for the cyclic mechanisms, situation, when the frequency of the investigated harmonic $\Omega = j\omega$ ($j = 1, 2, 3, \ldots$) is much greater than the rotation speed of the main shaft ω. It can be shown that in this case the cyclic mechanism is not the source of the excitation only, but also leads to the slow displacement of resonant frequencies and to the arising of the wideband frequency spectrum, with higher vibration activity. For methodological reasons, we will consider the most complicated case, typical for the high-speed machines, where the most important role is played by the kinematic excitation. Let the amplitude of acceleration of the program motion, on the considered harmonic, be w (here and below, for simplicity the harmonic number is omitted).

Kinematic excitation, which defines the distributed and concentrated inertial forces of the translational motion, at the considered frequency, is proportional to $w = \Pi''_*\Omega^2$. Then on the basis of (11.1) and (11.2) the component of the transition matrix, corresponding to the excitation in the given module is equal to:

$$\mathbf{U}(\Omega, \varphi) = \Gamma_1(\Omega)\Gamma_2(\Omega, \varphi)\mathbf{U}_1(\Omega) + \Gamma_1(\Omega, \varphi)\mathbf{U}_2(\Omega) + \mathbf{E}\mathbf{U}_1(\Omega), \qquad (11.14)$$

where $\mathbf{U}_1 = -w\rho(0, 0, g_{33} - 1, g_{43}, g_{53}, g_{63})^{\mathrm{T}}$; $\mathbf{U}_2 = -w(0, 0, 0, 0, 0, m)^{\mathrm{T}}$, where g_{ij} are the entries of the transition matrix Γ_k, which differ from (11.1) and (11.2) by substituting Ω instead of p (the subscripts 1, 2, 3 meet the number of the portion of the module), $\mathbf{E}$ is the unit matrix. The state vector on the boundary of the arbitrary module s can be represented as follows:

$$\mathbf{T}_s = \Gamma^s\mathbf{T}_0 + \sum_{r=0}^{s-1} \Gamma^{n-r-1}\mathbf{U}. \qquad (11.15)$$

Vector $\mathbf{T}_0$, which corresponds to the boundary conditions, when $s = 0$, contains three unknown boundary conditions T_{02}, T_{03}, T_{04} (the second index corresponds to the row number). When $s = n$, for the unilateral drive, we obtain

$$
\left.\begin{array}{l}
T_{n2}(T_{02}, T_{03}, T_{04}) = 0; \\
T_{n5}(T_{02}, T_{03}, T_{04}) = 0; \\
T_{n6}(T_{02}, T_{03}, T_{04}) = 0.
\end{array}\right\} \tag{11.16}
$$

We represent (11.16) in matrix form as

$$
\mathbf{S}_0 \cdot \theta_0 = -\theta_w. \tag{11.17}
$$

Here $\theta_0 = (T_{02}, T_{03}, T_{04})^{\mathrm{T}}$ is the vector of the unknown boundary conditions, formed with non-zero elements of vector $\mathbf{T}_0$; θ_w is the vector defined by the kinematic excitation ($w \neq 0$); $\mathbf{S}_0$ is the matrix (3×3) of coefficients of the system of linear equation (11.17).

To determine matrix $\mathbf{S}_0$, three calculations, when $w = 0$, $s = n$, should be carried-out as per expression (11.16), taking $\mathbf{T}_0^{(1)} = (0, 1, 0, 0, 0, 0)^{\mathrm{T}}$; $\mathbf{T}_0^{(2)} = (0, 0, 1, 0, 0, 0)^{\mathrm{T}}$; $\mathbf{T}_0^{(3)} = (0, 0, 0, 1, 0, 0)^{\mathrm{T}}$. Then $\mathbf{S}_0 = \left[\mathbf{T}_{n*}^{(1)} \ \mathbf{T}_{n*}^{(2)} \ \mathbf{T}_{n*}^{(3)} \right]$, where $\mathbf{T}_{n*}^{(v)}$ is the vector, formed with the second, fifth and sixth row of the vector $\mathbf{T}_n$ at given above "fictitious" boundary conditions and the calculation number v.

Further, we accept in (11.15) $\mathbf{T}_0 = \mathbf{0}$, ($w \neq 0$); wherein the second, fifth and sixth rows of the obtained vector $\mathbf{T}_{n*}$ define the vector θ_w. As per (11.17) we have

$$
\theta_0 = -\mathbf{S}_0^{-1} \cdot \theta_w. \tag{11.18}
$$

Since (11.18) defines the previously unknown boundary conditions, (11.15) allows us to find the complex amplitudes of the six characteristics, describing the flexural-torsional oscillations of the system. For systems with bilateral drive the problem is solved in a similar manner with an appropriate choice of boundary conditions. Some qualitative indicators of the forced oscillations, in the considered class of dynamic models, are illustrated by the example of results of analysis of calculations, carried out using data for the warp knitting machine.

Influence of module numbers n We can see, in Fig. 11.6, the normalized amplitude-frequency characteristics (AFC) of the executive body $Y(\Omega)$ and the main shaft $X(\Omega)$, plotted for unilateral drive, when $n = 2; 4; 5$ (curves 1, 2, 3 correspondingly) and the fixed value of $\varphi_* = \pi/2$. (Here and below, when illustrating AFC, the normalized amplitude of excitation w/Ω^2 is used). Functions $X(\Omega)$, $Y(\Omega)$ are defined as the modules of the corresponding complex values.

The analysis of the graphs shows that with growth of n the lower resonant frequency decreases significantly. In addition to that oscillations of the executive body, in the frequency range near the point of condensation, abruptly increase.

Influence of the variability of parameters of cyclic mechanisms These results correspond to the value $\Pi'_{\max}$, when the connectedness, between the torsional subsystem of the main shaft and bending subsystem of the executive body, is maintained artificially at the maximum level. The question arises that how much
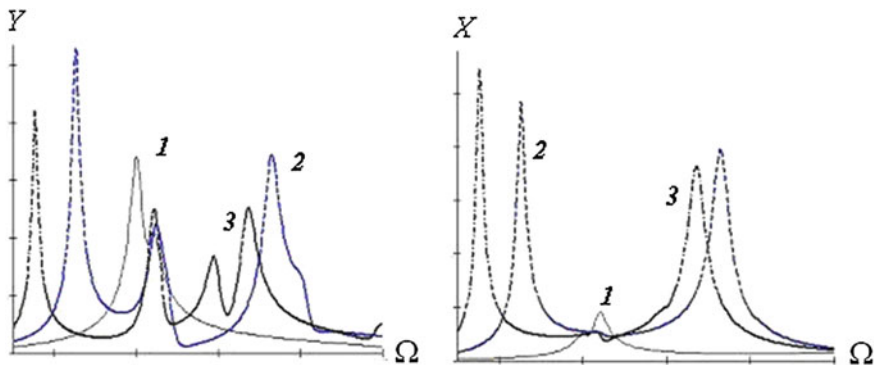
Fig. 11.6 To the analysis of the influence, of number of modules, on AFC

does the slow change of parameters, caused by the variability of Π', is manifested in the frequency and phase response?

It is clearly seen, in the Fig. 11.7, that the discontinuity of the dynamic connections, in case of working body's dwell, qualitatively changes the character of oscillations: several resonant modes arise, instead of one. In such cases the beat mode is observed, which is accompanied by the change of the oscillatory modes and high vibration activity of the system.

In Fig. 11.8, the selected curve corresponds to Π'_{max}, which in case of $\Omega < p_*$ is the lower boundary of the region and while $\Omega > p_*$ it is the upper boundary. The selected point is of interest, where amplitudes don't depend on Π'; therefore the system loses its rheonomous properties.

Influence of dissipation Here-above we considered the amplitude-frequency-characteristic (AFC), in case of small values of dissipation. A comparison of these characteristics with similar frequency responses, obtained without dissipation,

Fig. 11.7 Transformation of AFC when $\Pi' = \Pi'_{max}$ (*curve 1*) and $\Pi' = 0$ (*curve 2*)
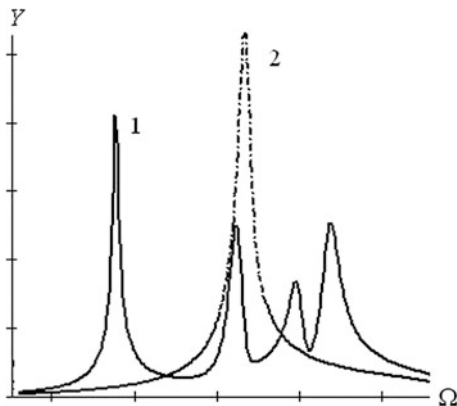
Fig. 11.8 Areas of increased vibration activity
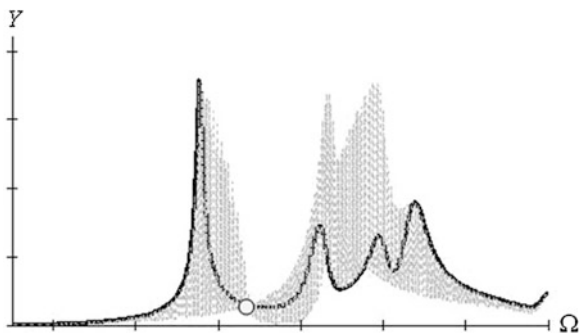
shows that apart from the natural unlimited increase in amplitudes in the resonant mode, in the absence of dissipation, the resonant zones abruptly shrink and in case of high-frequencies, such resonances appear, which completely appear to be suppressed in the presence of dissipation. Similar conclusions, while analyzing the effect of dissipation in the chains, are given in [33].

Analysis of the phase-frequency characteristic (PFC) In Fig. 11.9 we can see the phase-frequency characteristics $\gamma(\Omega)$ when n = 2, 4, 5 (curves 1, 2, 3) and $\Pi' = \Pi'_{max}$. The function $\gamma(\Omega)$ is defined as the argument of complex amplitudes $\bar{X}(\Omega)$, $\bar{Y}(\Omega)$.

The work performed under harmonic excitation is proportional to $\sin\gamma$, so the level of oscillation depends on the proximity of the phase shift γ to the value of $\pi/2$. The graphs show that at higher frequencies, taking into account the dissipation, the value of γ is much lower than this value, so the resonance is substantially suppressed. In the absence of dissipation, at these frequencies, PFC intersects the line $\pi/2$, which reflects AFC of the executive body.

To illustrate the influence of variability of parameters on the value and location of frequency ranges with increased amplitude levels, in Fig. 11.10, we plotted graphs of PFC, when n = 5 and changes, in small increments, of the first transfer function $0 \leq \Pi' \leq \Pi'_{max}$.

Fig. 11.9 Phase-frequency characteristics
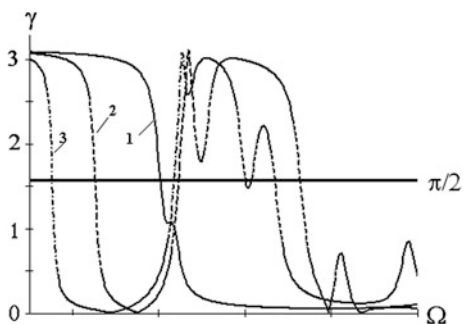
Fig. 11.10 To the analysis of the phase-frequency characteristic in case of variable parameters
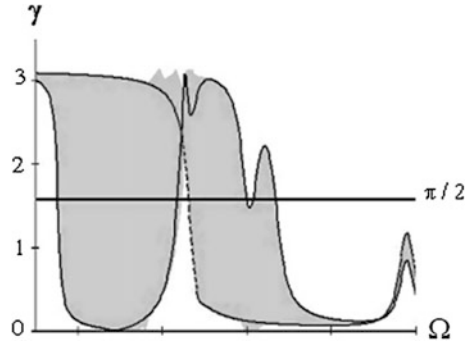
The graphs identify the areas, in which PFC intersects line $\pi/2$ all the time. Of course this is only an indirect indication of the potential for large amplitudes, because the excitation of resonant oscillations is not instantaneous and implementation of this possibility depends on the speed of the transition across the identified frequency ranges. However, in case of sufficiently large extent of these areas, we can expect an increase in the system's vibration activity. The modes of resonant oscillations, in the first approximation, correspond to the modes of free oscillations (see above). We should also bear in mind the unstable character of the modes and the possibility of jump from one form to another.

11.2 Bending Vibrations of the Actuator, Mounted on the Output Links of Identical Cyclic Mechanisms

Dynamic model Figure 11.11 represents the dynamic model, in which the working body (WB) is accepted as the flexural oscillatory system, with distributed

Fig. 11.11 Dynamic model
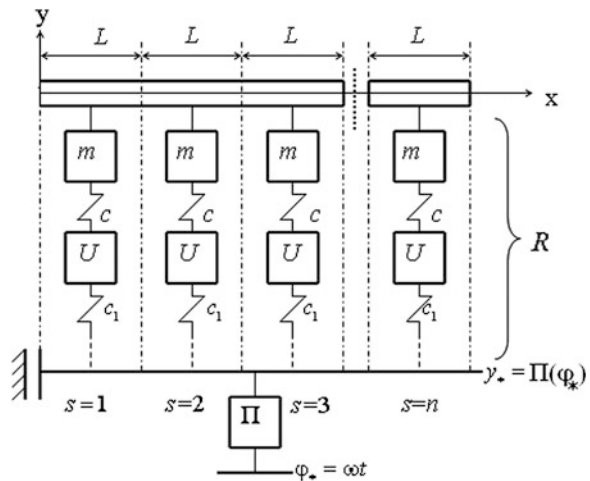
parameters and the driving cyclic mechanisms are accepted as the serial connection of discrete elements (see below). Let us accept that area s corresponds to $x \in [x_s, x_{s+1}]$. The free oscillations of the working body $y(x, t)$ are described with differential equation as follows:

$$EI \frac{\partial^4 y}{\partial x^4} + \rho \frac{\partial^2 y}{\partial t^2} = 0, \tag{11.19}$$

where ρ is the mass of unit length; EI is the bending stiffness (E is the normal modulus; I is the equatorial moment of inertia).

Taking into account the non-stationary boundary conditions, we are looking for the approximate particular solution of Eq. (11.19) as follows:

$$y(x, t) = Y(x, \tau) \cos \Phi(t), \tag{11.20}$$

where $Y(x, \tau)$ is the oscillatory mode; τ is the "slow time".

In accordance to the conditional oscillator method (see Sect. 5.2) for each of the oscillatory modes the solution can be added with the condition of the form:

$$2 \frac{\partial Y}{\partial \tau}(x_*, \tau)p(\tau) + Y(x_*, \tau)\frac{dp}{d\tau}(\tau) = 0. \tag{11.21}$$

Here $p(\tau) = d\Phi/dt$ is the variable "natural" frequency, x_* is the coordinate of the arbitrary section. Under the condition of slow variation of parameters on the basis of (11.19)–(11.21), we obtain the following ordinary differential equation:

$$\frac{\partial^4 Y}{\partial x^4}(x, \tau) - \alpha^4 Y(x_*, \tau) = 0, \tag{11.22}$$

where $\alpha^4 = \rho p^2(\tau)/(EI)$.

Analysis of the transition matrix of the regular element Let us select one block in the dynamic model, consisting of the beam portion s and the mechanism s and introduce the following functions: $\eta_1(s) = Y(x_s)$; $\eta_2(s) = L\varphi(x_s)$; $\eta_3(s) = M(x_s)L^2/(EI)$; $\eta_4(s) = Q(x_s)L^3/(EI)$, where Y, φ, M, Q are the slowly varying amplitudes of strains, rotation angles, bending moments and shear forces in the appropriate section. (For brevity the τ is omitted in the argument of "slow time".) Then on the basis of (11.20) and (11.21), with respect to this model, we can write the following matrix equation:

$$[\eta_1(s+1), \eta_2(s+1), \eta_3(s+1), \eta_4(s+1)]^{\mathrm{T}} = \Gamma [\eta_1(s), \eta_2(s), \eta_3(s), \eta_4(s)]^{\mathrm{T}} \tag{11.23}$$

Here

$$\Gamma = \begin{bmatrix} \kappa_1 & \kappa_2 & \kappa_3 & \kappa_4 \\ \theta^4 \kappa_4 & \kappa_1 & \kappa_2 & \kappa_3 \\ \theta^4 \kappa_3 & \theta^4 \kappa_4 & \kappa_1 & \kappa_2 \\ \theta^4 \kappa_2 - \zeta \kappa_1 & \theta^4 \kappa_3 - \zeta \kappa_2 & \theta^4 \kappa_4 - \zeta \kappa_3 & \kappa_1 - \zeta \kappa_4 \end{bmatrix} \qquad (11.24)$$

$\theta(\tau) = L\sqrt[4]{\rho p^2 / EI}$; $p(\tau)$ is the slow varying "natural" frequency; $\kappa_1 = K_1(\theta)$; $\kappa_2 = K_2(\theta)/\theta$; $\kappa_3 = K_3(\theta)/\theta^2$; $\kappa_4 = K_4(\theta)/\theta^3$; $K_j(\theta)$ are the Krylov's functions; $\zeta(\tau) = \xi R(\tau)$; $\xi = L^3/(EI)$; $R(\tau)$ is the cyclic mechanism's dynamic stiffness.

The dynamic stiffness is defined as $R = D/B$, where B, D are the elements of the second column of the transition mechanism. Below while illustrating, we will restrict ourselves to taking into account the elements of the model, shown in Fig. 11.11, namely the variable mechanism stiffness reduced to the output link. Then

$$R(\varphi_*) = c/[1 + \zeta_0 U t^2(\varphi_*)] - mp^2, \qquad (11.25)$$

where $\zeta_0 = c/c_1$, $U'(\varphi_*) = r_0 \sin \varphi_*$ (the "slow time" in this case is the main shaft's rotation angle φ_*).

In case of small values of θ, the Krylov functions can be represented as the truncated Maclaurin series

$$\kappa_1 \approx 1 + \frac{\theta^4}{4!}; \quad \kappa_2 \approx 1 + \frac{\theta^4}{5!}; \quad \kappa_3 \approx \frac{1}{2} + \frac{\theta^4}{6!}; \quad \kappa_4 \approx \frac{1}{6} + \frac{\theta^4}{7!}$$

Thus, in contrast to the Krylov functions, when $\theta \to 0$, none of the functions κ_j tend to zero, eliminating the difficulty of extreme transitions.

The matrix equation (11.23) is equivalent to the system of differential equations, whose solution is sought in the form $\eta_j(s) = C_j^0 \lambda^s$, where C_j^0 are in general the slowly varying functions of time. After substituting in (11.24), we find that the characteristic numbers λ are equal to the eigenvalues of the transition matrix. We use the generalized form of the characteristic equation, whose coefficients are governed by (9.3). Let us recall here that the areas of the system, under consideration, do not change their properties, in case of change of numbering of sections $s + 1 \rightleftarrows s$, so the characteristic equation appears to be reciprocal:

$$\lambda^4 + a\lambda^3 + b\lambda^2 + a\lambda + 1 = 0. \qquad (11.26)$$

Here

$$a = -\mathrm{Sp}\Gamma = -\sum_{i=1}^{4} \gamma_{ii}; \quad b = 0.5(\sum_{i,j=1}^{4} {}^*\gamma_{ii}\gamma_{jj} - \sum_{i,j=1}^{4} {}^*\gamma_{ij}\gamma_{ji}), \qquad (11.27)$$

where γ_{ij} are the elements of the transition matrix Γ; an asterisk at the sign of the sum means the omission of the member $i = j$.

On the basis of (11.24) and (11.27) we get

$$a = \zeta\kappa_4 - 4\kappa_1; := 2 + 4(\kappa_1^2 - \theta^4\kappa_3^2) - 2\zeta(\kappa_1\kappa_4 - \kappa_2\kappa_3). \tag{11.28}$$

We present the solution of Eq. (11.26) as follows

$$\lambda_{1,2,3,4} = 0.5(z_{\text{I, II}} \pm \sqrt{z_{\text{I, II}}^4 - 4}); \; z_{\text{I, II}} = 0.5(-a \pm \sqrt{a^2 - 4b + 8}). \tag{11.29}$$

For the evident representation of the structure of characteristic exponents and form of solutions, as before, we use the plane of parameters $b - a$, which is shown in the Fig. 11.12.

In region 0, solutions are not available, in area I they are described with the trigonometric functions (λ are the complex-conjugate numbers), in area II they are described with the hyperbolic functions (λ are the real numbers), and in area III they have the mixed form (one pair of the roots λ are the complex conjugate numbers and the other are the real numbers). The graph shows the locus of points $b(p)$, $a(p)$ for the following initial data $EI = 1.757 \times 10^5 \, \text{N} \cdot \text{m}$; $\rho = 2 \, \text{kg/m}$; $L = 0.5 \, \text{m}$; $m = 4 \, \text{kg}$; $c = 5 \times 10^5 \, \text{N/m}$; $n = 6$; $r_0 = 0.5 \, \text{m}$; $p = (0 \div 4{,}000) \, \text{s}^{-1}$; $\zeta_0 = 0.1 \div 10$; $\varphi_* \in [0, \pi]$.

Definition of "natural" frequencies and non-stationary oscillatory shape mode Using the boundary conditions, we write

$$[\eta_1(n), \eta_2(n), 0, 0]^\text{T} = \Gamma^n[\eta_1(0), \eta_2(0), 0]^\text{T}. \tag{11.30}$$

Fig. 11.12 Areas of existence of solutions
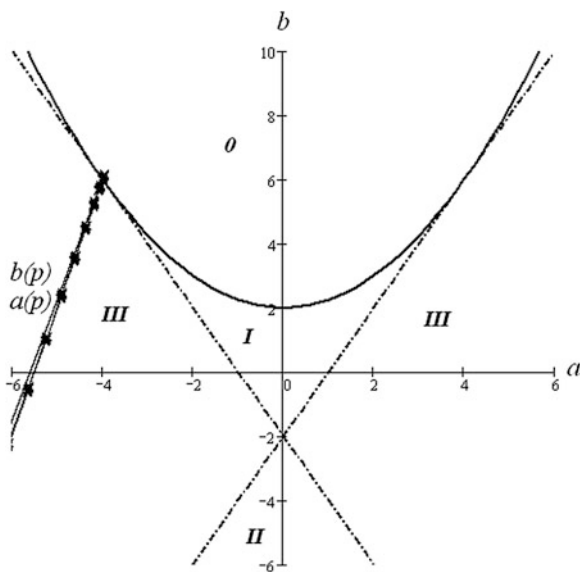
Since in case of free oscillations, the oscillatory mode is determined accurately within the range of an arbitrary constant, we take $\eta_1(0) = 1$. The matrix equation (11.30) corresponds to the uniform system of four algebraic equations, whose determinant, for the non-trivial solution, is equal to zero. However, the practical use of the formal frequency equation, obtained similarly, becomes complicated, since it has the high order and it should be solved for each fixed point in time. Let us consider, for now, just two ways of simplified determination of "natural" frequencies, using the regularity properties of the system. Let us write the matrix equation (11.30) for two consecutive segments s, $s+1$ and we will exclude variables η_2 and η_4 from the obtained equations. At that we get the next uniform system of differential equations:

$$\left.\begin{array}{l} \eta_1(s+1) + \eta_1(s-1) - \eta_1(s)(2\kappa_1 - \zeta\kappa_4) - 2\kappa_3\eta_3(s) = 0; \\ \eta_3(s+1) + \eta_3(s-1) - 2\eta_3(s)\kappa_1 - \eta_1(s)(2\theta^4\kappa_3 - \zeta\kappa_2) = 0. \end{array}\right\} \quad (11.31)$$

Since the characteristic exponents λ_k are determined already, we can represent the solution of system (11.31) as follows:

$$\eta_1(s) = \sum_{k=1}^{2} \beta_k(h_{k1}f_{ks} + h_{k2}v_{ks}); \quad \eta_3(s) = \sum_{k=1}^{2} (h_{k1}f_{ks} + h_{k2}v_{ks}), \quad (11.32)$$

where h_{k1}, h_{k2} are the arbitrary slowly varying functions, determined by the extreme conditions; $f_{ks} = \cos s\sigma_k$, $v_{ks} = \sin s\sigma_k$, $\sigma_k = \arccos 0.5z_k$ when $|z_k| < 2$; $f_{ks} = \cosh s\sigma_k$, $v_{ks} = \sinh s\sigma_k$, $\sigma_k = \mathrm{Arccosh}(0.5z_k)$ when $z > 2$ and $\sigma_k = \mathrm{Arccosh}(0.5z_k) + i\pi$ when $z_k < -2$ $(i = \sqrt{-1})$; function β_k corresponds to the eigenvector and in our case is determined as

$$\beta_k = (f_{k1} - 1)/(\theta^4\kappa_3 - 0.5\zeta\kappa_2) \quad (k = 1, 2; \quad \beta_1 \neq \beta_2) \quad (11.33)$$

The formal frequency equation can be represented as

$$H_1(p) - H_2(p) = 0, \quad (11.34)$$

where $H_k = \beta_k(\Lambda_1 + f_{k1}\Lambda_2) - f_{k1} + (\pm 1 - f_{kn})(\beta_k\Lambda_2 - 1)v_{k1}/v_{kn}$; $k = 1, 2$ (in case of double signs the plus corresponds to the symmetric mode, the minus corresponds to the anti-symmetric mode); $\Lambda_1 = \theta^4(\kappa_3 - \kappa_1\kappa_4/\kappa_2) + \zeta(\theta^4\kappa_4^2/\kappa_2 - \kappa_2)$; $\Lambda_2 = \theta^4\kappa_4^2/\kappa_2$ (in case of $\theta \to 0$, we have $\Lambda_1 \to -\zeta$ and $\Lambda_2 \to 0$).

The oscillatory modes in the cross sections s for the displacements and bending moments are determined by dependencies (11.31) and (11.32) for the obtained from (11.34) "natural" frequencies and $h_{11} = 1$; $h_{12} = (\pm 1 - f_{1n})/v_{1n}$; $h_{21} = -1$; $h_{22} = -h_{12}$.

The second method of determining the "natural" frequencies is based directly on the matrix equation (11.23), using the symmetry conditions of the dynamic model. Thus, obtained in such a way frequency equation is

$$[1 \mp g_{11}(p, \varphi_*)][1 \pm g_{22}(p, \varphi_*)] \mp g_{12}(p, \varphi_*)g_{21}(p, \varphi_*) = 0, \qquad (11.35)$$

where $g_{ij}(p, \varphi_*)$ are the corresponding entries of the matrix Γ^n; different signs correspond to the symmetric and anti-symmetric oscillatory modes.

In Fig. 11.13a, we can see the graphs $p(\varphi_*)$, for a number of lower frequencies, when $\zeta_0 = 5$ and accepted above input data. The analysis has shown that in some cases of change in φ_* the jump from one mode shape to the other are observed (the similar case in the graph is shown with a hatched line).

Of particular interest is the frequency, which corresponds to such oscillatory mode, in case of which all the supports of the working organ oscillate with uniform amplitude. It is obvious that this case corresponds to $\lambda_k = 1$. Then, on the basis of the characteristic equation (11.26) taking into account (11.35), we obtain

$$\zeta(p)[(\kappa_1 - 1)\kappa_4 - \kappa_2\kappa_3] - 2[(1 - \kappa_1)^2 + \theta^4(p)\kappa_3^2] = 0. \qquad (11.36)$$

Under given initial data, Fig. 11.13b shows the graphs of $p(\varphi_*)$, obtained on the basis of (11.36) for $\zeta_0 = 0.2$ (curve 1), $\zeta_0 = 1$ (curve 2), $\zeta_0 = 5$ (curve 3). In case of $\theta \to 0$ we have $\zeta \to 0$; in this case the non-inertial elastic beam moves along with the bearings, without deformation, i.e. like a rigid body.

On the graph, this case corresponds to the hatch-dot curves. Often with the specific values of the parameters, this frequency appears to be the lowest. Let us note that for uniformly distributed harmonic load, the strongest excitation, in case of resonance, takes place sometimes at this frequency.
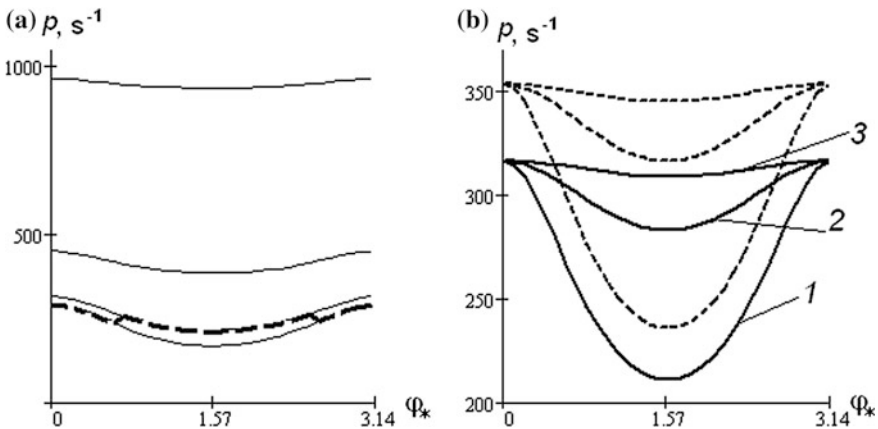
Fig. 11.13 Graphs of "natural" frequencies; a case $\lambda \neq 1$, b case $\lambda = 1$

If in the model (see Fig. 11.11), we take the extreme mechanisms to be absolutely rigid, then Eq. (11.36) has a very simple solution $\sigma_r = \sigma_{0r} = \pi r/n$ ($r = \overline{1, n-1}$) when $h_{12} = 1$; $h_{11} = h_{21} = h_{22} = 0$. At the same time the "natural" frequencies p_r are determined using the equation

$$\zeta(p_{0r}) - 2(\kappa_1 - \cos \sigma_{0r})^2/[\kappa_4(\kappa_1 - \cos \sigma_{0r}) - \kappa_2\kappa_3] = 0. \qquad (11.37)$$

When $\theta = 0$, we get

$$\zeta(p_{0r}) = -12(1 - \cos \sigma_{0r})^2/(2 + \cos \sigma_{0r}) \qquad (11.38)$$

We can use the obtained results for effective estimation of the roots of more complicated Eqs. (11.34) and (11.35): $p_{0,r-1} < p_r < p_{0r}$. As it can be seen from the graphs, with increase in value of ζ_0 the influence of variability of parameters, on the frequency characteristic of the system, increases. The variability of parameters can lead to local distortions of dynamic stability in some parts of the kinematic cycle, when the attenuated free oscillations, caused by dissipative forces, alternate with increasing oscillations (see Sect. 5.3.1).

11.3 Vibrations of Multisection Drives for Moving the Massive Actuators

Dynamic and mathematic models In Fig. 11.14 we can see the dynamic model, consisting of the subsystem of the driving mechanism, schematized as the torsional subsystem $s = 0$ and repeated modules ($s = \overline{1, n}$). Each module of the corresponding section of the drive is formed by the portion of the main shaft, connected
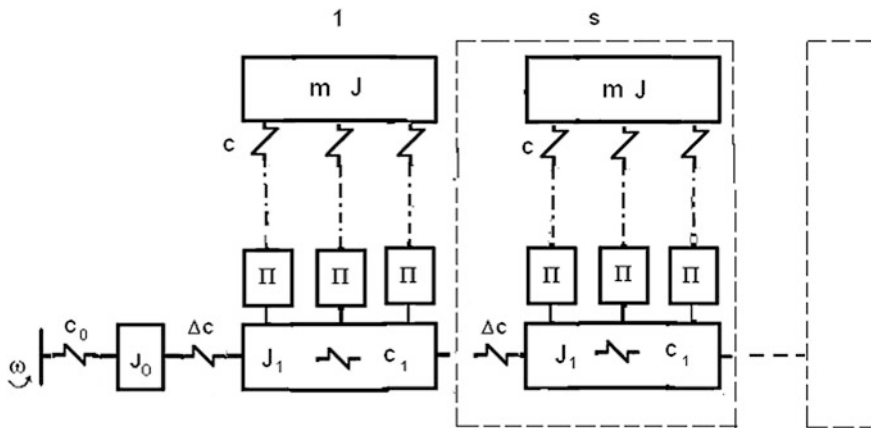
Fig. 11.14 Dynamic model

with the absolutely rigid executive body by the v identical cyclic mechanisms, performing its progressive program motion. Thus we consider the other extreme case, when the executive body has heightened rigidity and the relatively high torsional compliance of the long main shaft is substantially the determining factor in the formation of the spectrum of "natural" frequencies. This situation, in particular, takes place in the tapping carriage mechanism of a number of combers, in the needle table moving mechanism of the needle punchers, etc.

Sections are linked to each other by the elastic elements (for example, couplings, or portions of the main shaft) with torsional stiffness Δc. Let us emphasize here that in the program motion (i.e. excluding the elastic properties of the system), the executive body should move strictly progressively, however, taking into account the oscillations, this movement appears to be plane-parallel, which in many cases leads to the mismatch of the movements, at the ends and to the violations of the technological process.

Let us use the modified method of continual idealization (see Sects. 9.3 and 10.4) and present v identical mechanisms, in the form of pseudo-medium formed by "smearing" of the elastic and inertial characteristics, along the main shaft's axis. This medium, as well as its mechanical prototype has the property to transfer the load and motion, only along the layer of the medium, and the interaction between the layers is realized only through the subsystems of the main shaft and the executive body.

Frequency analysis of the single-section drive (n = 1) First of all let us consider the case, where the system, under consideration, consists of a single module. Let us write the uniform system of differential equations, based on which we can conduct the frequency and modal analysis (dissipative forces at this stage can be omitted):

$$-\frac{\partial}{\partial t}\left(\rho\frac{\partial \varphi}{\partial t}\right) + G\left[\frac{\partial}{\partial x}\left(I(x)\frac{\partial \varphi}{\partial x}\right)\right] - Q_1 = 0; \tag{11.39}$$

$$-m\ddot{y}_c = \int_0^l Q_2\,dx; \quad -J\ddot{\gamma} = \int_0^l Q_2(x - x_c)\,dx. \tag{11.40}$$

Here $\varphi(x, t)$, I, ρ is the rotation angle, polar moment of inertia and reduced mass moment of inertia of the main shaft; m, J are the mass and moment of inertia of the executive body, relative to the center of mass x_c; y_c, γ are the displacements of the center of mass and rotation angle of the executive body, G is the shear modulus, Q_1, Q_2 are the linear reactive moment and force applied from the mechanism to the corresponding subsystem.

Let us represent the approximate solution of Eq. (11.39) as follows

$$\varphi = X(x, \tau)\Psi(t), \quad y = Y(x, \tau)\Psi(t),$$

where τ is the "slow" time.

After the separation of slow components of functions Q_1 and Q_2, we can show that the Eqs. (11.39) and (11.40) in the amplitude functions X and Y are connected by the following equations

$$\left.\begin{array}{l} X'' + P_1(\tau)X = -P_2(\tau)Y; \\ Y = a + \gamma x, \end{array}\right\} \tag{11.41}$$

where $\quad a = X(0); \gamma = \partial Y/\partial x = \mathrm{const}; P_1 = (\rho p^2 + \mu_1)/(GI_1); P_2 = \mu_2/(GI_1);$
$\mu_1 = \sum\limits_{u=1}^{v} A_u/B_u;$ is the slowly varying "natural" frequency; $A,\ B$ are the elements of the pseudo medium transition matrix $\Gamma_{\mathrm{m}} = \begin{pmatrix} A & B \\ C & D \end{pmatrix}$, which connect both subsystems in the unified oscillation system (see Sect. 8.1).

If we schematize the mechanism, in the form of the chain $\Pi - c$, where Π reflects the coordinate transformation in the mechanism, and c the reduced stiffness, then

$$\Gamma_{\mathrm{m}} = \Gamma_{\mathrm{c}}\,\Gamma_{\Pi} = \begin{pmatrix} 1 & l/(cn) \\ 0 & 1 \end{pmatrix} \begin{pmatrix} \Pi'_* & 0 \\ 0 & (\Pi'_*)^{-1} \end{pmatrix} \tag{11.42}$$

Here l is the calculated length of the section; $\Pi'_* = d\Pi/d\varphi_*$ is the first geometric transfer function (the speed analogue); $\varphi_* = \omega t$. On the basis of (11.42), $A = \Pi'_*;\ B = l/(vc\Pi'_*);\ C = 0;\ D = (\Pi'_*)^{-1}.$

According to (11.40) and (11.42) the conditions of dynamic equilibrium of the executive body in the amplitude functions can be written as

$$-mp^2 Y(x_{\mathrm{c}}) = B^{-1} \int\limits_0^l (X - DY)\,dx; \quad -Jp^2\gamma = B^{-1} \int\limits_0^l (X - DY)x\,dx. \tag{11.43}$$

The solution can be represented as

$$X = h_1 f + h_2 v + \beta(a + \gamma x). \tag{11.44}$$

Here $\quad \beta = -P_2/P_1; f = \cos\theta, v = \sin\theta \quad$ at $\quad P_1 > 0; f = \cosh\theta, v = \sinh\theta \quad$ at $P_1 < 0$, where $\theta = \lambda x,\ \lambda = \sqrt{|P|},\ h_1, h_2$ are the slowly varying functions (see below).

Let's introduce the following notation: $J/m = r_*^2; x_{\mathrm{c}}/l = \chi_1; r_*/l = \chi_2;$

$S = l(C - \rho p^2 D)/[mp^2(B\rho p^2 - A)]$. Substituting (11.44) in (11.43) and solving with (11.41), the obtained system of the two algebraic equations, with respect to a and γ, we get

$$a = l(g_{11}h_1 + g_{12}h_2); \qquad \gamma = g_{21}h_1 + g_{22}h_2, \qquad (11.45)$$

where $g_{11} = [\xi_{11}(\chi_2^2 + S/3) - \xi_{21}(\chi_1 + S/2]/\Delta; \quad g_{12} = [\xi_{12}(\chi_2^2 + S/3) - \xi_{22}(1 + S/2)]/\Delta;$

$$g_{21} = [\xi_{21}(1 + S) - 0.5S\xi_{11}]/\Delta; \; g_{22} = [\xi_{22}(1 + S) - 0.5\xi_{12}S]\Delta^{-1};$$
$$\Delta = (1 + S)(\chi_2^2 + S/3) - 0.5S(\chi_1 + 0.5S).$$

Functions ξ_{ij}, included in g_{ij}, depending on the sign of P_1 are expressed through trigonometric or hyperbolic functions in case of the argument $\theta_* = \lambda l$ (Table 11.1). After substituting (11.45) in (11.44) we get

$$\begin{aligned} X &= h_1[f + \beta(g_{11}l + g_{21}x)] + h_2[v + \beta(g_{12}l + g_{22}x)]; \\ \frac{\partial X}{\partial x} &= h_1(\frac{\partial f}{\partial x} + \beta g_{21}) + h_2(\frac{\partial v}{\partial x} + \beta g_{22}). \end{aligned} \qquad (11.46)$$

Let's take $X(0) = K_{01}; \frac{\partial X}{\partial x}(0) = N_{01}; X_1(l) = K_1; \frac{\partial X}{\partial x}(l) = N_1$. Then on the basis of (11.46)

$$\begin{bmatrix} K_{01} \\ N_{01} \end{bmatrix} = \Gamma_0 \begin{bmatrix} h_1 \\ h_2 \end{bmatrix}; \qquad \begin{bmatrix} K_1 \\ N_1 \end{bmatrix} = \Gamma_1 \begin{bmatrix} h_1 \\ h_2 \end{bmatrix} \qquad (11.47)$$

Elements of matrices Γ_0 and Γ_1 are determined with the following dependencies:
$\gamma_{11}^{(0)} = 1 + \beta g_{11}l; \; \gamma_{12}^0 = \beta g_{12}l; \; \gamma_{21}^{(0)} = \beta g_{21}l; \; \gamma_{22}^{(0)} = \lambda + \beta g_{22}; \; \gamma_{11}^{(1)} = f_* + \beta l(g_{11} + g_{21}); \; \gamma_{12}^{(1)} = \beta l(g_{12} + g_{22}) + v_*; \; \gamma_{21}^{(1)} = (\partial f/\partial x)_* + \beta g_{21}; \; \gamma_{22}^{(1)} = (\partial v/\partial x)_* + \beta g_{22}$, where the asterisk meets the argument $\theta_* = |\lambda|l$.

It follows from (11.47) that

$$\begin{bmatrix} h_1 \\ h_2 \end{bmatrix} = \Gamma_0^{-1} \begin{bmatrix} K_{01} \\ N_{01} \end{bmatrix}.$$

Located between the sections of element J_0 and $x = 0$ is the elastic element with the torsional stiffness Δc. In this case, the transition matrix of the single module has the form

Table 11.1 Dependencies for functions ξ_{ij}

Condition	ξ_{11}	ξ_{12}	ξ_{21}	ξ_{22}
$P_{00} > 0$	$-\dfrac{\sin\theta_*}{mp^2 B\theta_*}$	$-\dfrac{1 - \cos\theta_*}{mp^2 B\theta_*}$	$\dfrac{\theta_* \sin\theta_* - (1 - \cos\theta_*)}{mp^2 B\theta_*^2}$	$\dfrac{\sin\theta_* - \theta_* \cos\theta_*}{mp^2 B\theta_*^2}$
$P_{00} < 0$	$-\dfrac{\sinh\theta_*}{mp^2 B\theta_*}$	$-\dfrac{\cosh\theta_* - 1}{mp^2 B\theta_*}$	$\dfrac{-\theta_* \sinh\theta_* - (1 - \cosh\theta_*)}{mp^2 B\theta_*^2}$	$\dfrac{\sin h\theta_* - \theta_* \cosh\theta_*}{mp^2 B\theta_*^2}$

$$\Gamma = \Gamma_1 \Gamma_0^{-1} \Gamma_{\Delta c}, \tag{11.48}$$

where $\Gamma_{\Delta c} = \begin{pmatrix} 1 & \Delta c^{-1} \\ 0 & 1 \end{pmatrix}$.

Thus, the following matrix relationship occurs between the state vectors in section J_0 and at the end of the module $s = 1$:

$$\begin{bmatrix} K_1 \\ 0 \end{bmatrix} = \begin{pmatrix} \gamma_{11} & \gamma_{12} \\ \gamma_{21} & \gamma_{22} \end{pmatrix} \begin{bmatrix} K_0 \\ N_0 \end{bmatrix} \tag{11.49}$$

Here γ_{ij} are the entries of the matrix Γ; K_0 is the amplitude in the section of the element J_0.

With reference to (11.49) and boundary conditions, we get the frequency equation

$$\gamma_{21}(p, \varphi_*) + \zeta(p)\gamma_{22}(p, \varphi_*) = 0. \tag{11.50}$$

Here, $\zeta(p) = \Delta c / R_0(p)$, $R_0(p)$ is the dynamic stiffness of the drive ("input").

Let us emphasize here that because of the dependence of the transition matrix on φ_* the "natural" frequencies are variable. We now consider some ultimate special cases. It can be shown that $\det\|g_{ij}\| = \Delta^{-1} \det\|\xi_{ij}\|$ so when $\Delta \to 0$ we have $\det\|g_{ij}\| \to \infty$, therefore with reference to (11.44) and (11.45) when $a \neq 0$, $\gamma \neq 0$ we get $h_1 = h_2 = 0$.

This condition implies

$$S_*^2 + 2S_*(6\chi_2^2 - 3\chi_1 + 12) + 12\chi_2^2 = 0,$$

Hence, the equation $S(p) = S_*$ defines two "natural" frequencies assuming an absolutely rigid shaft, disconnected from the drive. Other ultimate case occurs when $\det\|\xi_{ij}\| = 0$. Then $\det\|g_{ij}\| = 0$, that when $h_1 \neq 0$, $h_2 \neq 0$ is possible only when $a = 0$, $\gamma = 0$, when the executive body doesn't take part in the oscillatory process. This situation arises, for example, in some frequency ranges, when the working body substantially plays the role of framing ($\theta_* = 2\pi k$, $k = \overline{1, \infty}$) or in case of relatively small values of mechanism's stiffness ($B \to \infty$).

Frequency and modal analysis When $\kappa \leq 1$, and $\kappa = \cos\theta_*$, we have

$$\left.\begin{array}{l} K_s = h_1 \cos s\theta_* + h_2 \sin s\theta_*; \\ N_s = h_1[\cos(s + 1)\theta_* - \cos s\theta_*] + h_2[\sin(s + 1)\theta_* - \sin\theta_*], \ (s = \overline{0, n}). \end{array}\right\} \tag{11.51}$$

Here, K_s, N_s corresponds to the cross section of the main shaft at the end of the module s.

On the basis of (11.51), taking into account the boundary conditions, we obtain the transcendental equation relative to θ_*:

$$[1 + \zeta(p)] \cos[(n + 0.5)\theta_*] - \zeta(p) \cos[(n - 0.5)\theta_*] = 0. \tag{11.52}$$

where $\zeta(p) = \Delta c / R_0(p)$, R_0 is the dynamic stiffness of the driving mechanism ("input").

If the dynamic stiffness at the "input" is independent of p (see above), we have $\zeta = const$, therefore, the solution of Eq. (11.52) can be obtained regardless of the dynamic characteristics of module s. Since the oscillatory shape modes reflect the amplitude values only "selectively", i.e. only in certain sections of the main shaft, they to some extent have conditional nature (such modes were called above as stroboscopic). Figure 11.15 shows the shape modes when n = 5 (j is the mode number). When $\zeta \to \infty$ $\theta_j = j\pi/n$, where $j = \overline{1,n}$ is the number of the main shaft's oscillatory mode (on sections s). In another ultimate case, when $\zeta \to 0$, $\theta_j = \pi(2j - 1)/(n + 1)$. As it was shown in Sect. 9.1,

$$0.5 \, \mathrm{Sp}\, \Gamma(p) = \kappa(p) = \cos \theta_*(p), \tag{11.53}$$

where $\mathrm{Sp}\, \Gamma(p)$ is the spur of the matrix $\Gamma(p)$ [see (11.48)].

Let us remind here that the number of mode j, corresponding to the sections s of the main shaft, cannot coincide with the number of frequency r. The point is that each mode j corresponds to several values of r, the number of which is equal to the number of "partial" frequencies of the single module subsystem.

Here above we considered the most common case, when $\kappa \le 1$. Such a situation usually occurs over almost the entire frequency range, and is violated only under certain values of ζ in the narrow bands near the "partial" frequencies of the module. When $\kappa > 1$ ($\mathrm{Im}\,\lambda = 0$), taking $\kappa = \cosh\theta$ and having performed the similar calculations, we get expressions differing from the ones above, only in a way that the trigonometric functions are replaced with the cognominal hyperbolic ones.

When $\kappa < -1$ the condition $\kappa = \cosh\theta$ is satisfied only when $\theta = \theta^0 + i\pi$. Then $\cos(\theta^0 + i\pi) = \cosh\theta^0\cosh i\pi + \sinh\theta^0\sinh i\pi = -\mathrm{ch}\,\theta^0 \le -1$. Thus, in this

Fig. 11.15 Oscillatory mode shapes
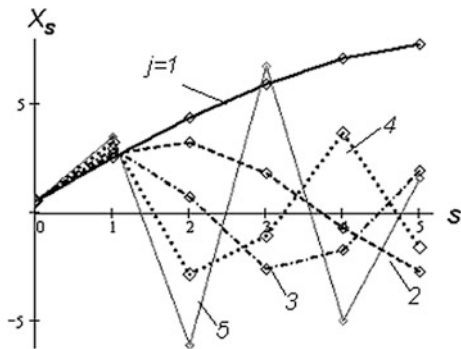
case, we should accept $\cosh\theta^0 = -\kappa$. Then $\cosh j\theta = (-1)^j \cosh j\theta^0$ and $\sinh j\theta = (-1)^j \sinh j\theta^0$. Taking into account the given corrections, the dependencies are valid for the case $\kappa > 1$.

As the analysis shows, these modes are usually very unstable. The mode instability, at different stages of the kinematic cycle, often manifests itself as a jump from one shape mode to another or to complete mode degeneration.

Here above, during drive's frequency analysis, the two methods were combined, to facilitate the study of complex oscillatory systems of large dimensions. The first one of these comprises of the use, for each module, of the method of continuum idealization, in which the elastic and inertial properties of the system are reflected by some integral characteristic. This allows us to operate with the generalized representation of variables and to reduce their number. A similar approach (aggregation) is becoming more common in the study of complex objects in mechanics, automatic control systems, economy [47]. The second method, based on the theory of regular systems, allows us in the given case to reduce the task, of studying the multi-section drive vibrations, to the analysis of a single repeating module.

Such a combined approach is of particular interest in solving the problems of dynamic analysis and synthesis of the automatic machines and automatic lines of light, textile, printing and a number of other industries, in which the cyclic mechanisms are widely used in zones of large extension of the technological process.

11.4 Torsion-Bending Vibrations of Branched-Ring Structured Systems

Dynamic model In Fig. 11.16, the dynamic model of the branched-circular structure is represented, in which the input link (main shaft) is presented as the torsional subsystem and the output link (executive body) as the bending subsystem.

The following conditional notations are accepted here: J_i are the moments of inertia; m_i are the masses; c_i are the coefficients of torsional $((i = 0, 1, 2)$ and longitudinal $(i = 3)$ stiffness; Ψ are the reduced to the corresponding elements coefficients of dissipation. $\Pi(\varphi)$ is the position function. Without narrowing the scope of generality in the formulation of the problem, we accept $\varphi_0(t) = \varphi_*(t) = \omega t$.

The reduced dynamic model consists of three integrated subsystems, corresponding to the main shaft, cyclic mechanisms and executive body. On the main shaft, gear can be noticed, which in this case is represented as the connection $c_{01} - J_0 - c_{02}$, but generally it can be reflected with the corresponding dynamic stiffness R_0. The other part of the model is a set of n repeating modules corresponding to the sections of the drive. The arbitrary module s, selected with hatch-dotted line consists of the block of the circular structure and the connecting
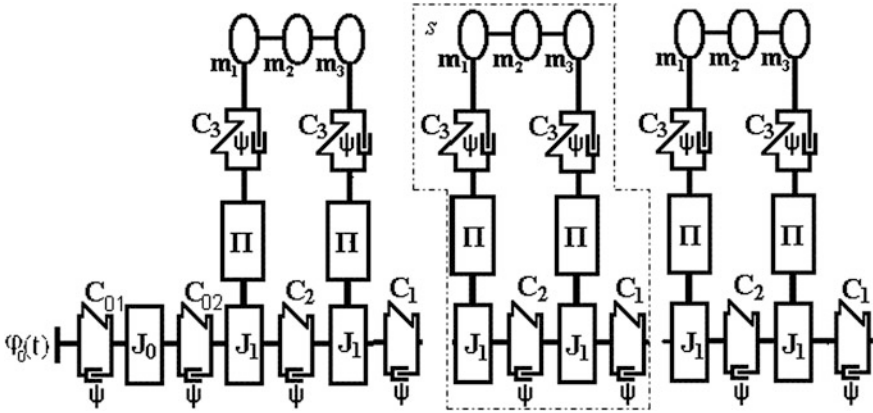
Fig. 11.16 Dynamic model

elastic member corresponding to the stiffness c_1 of the main shaft portion or to the clutch (to account for the inertial properties of the element, we can use its dynamic stiffness). The block of the circular structure is formed with the main shaft portion $J_1 - c_2 - J_1$, executive body represented as the elastic beam with masses $(m_1 = m_3 = m, \quad m_2)$ and with two cyclic mechanisms $(\Pi - c, \Psi)$.

The elastic characteristics of the beam depend, among other factors, on the design of bearings (supports) at the points of its connection to the output links of the cyclic mechanisms. When planning the support two extreme cases are possible: clamping (case 1) and pivotal connection (case 2). If we take the moment of inertia of the beam I_2 and mass per unit of the length $\tilde{m}_2$ as constants, then we can take, in the first case, $e_{22} = \ell^3/(192EI_2), e_{31} = e_{13} = \ell^3/(12EI_2), m_2 = 32\tilde{m}_2\ell/75$, and in the second case $e_{22} = \ell^3/(48EI_2), e_{31} = e_{13} = 0, m_2 = 48\,\tilde{m}_2\,\ell/\pi^2$, where ℓ is the length of the beam, E is the normal modulus, e_{ik} are the influence coefficients. When the actuator is absolutely rigid the dynamic errors in the first case, for all masses, are equal and in the second case they linearly vary along the beam (see 11.3). In particular, the dynamic error of the mass m_2 is then equal to half of the sum of the values defined in the bearing's sections.

Mathematic model of the arbitrarily given module For frequency and modal analysis, Let us use the method of studying the regular systems. Let us take $\varphi_* = \omega t$ as the "dimensionless time", where ω is the ideal angular speed of the main shaft. Let φ_j, y_j be the coordinates of the absolute angular displacements of the main shaft and linear displacements of shape. Then $\varphi_j = \varphi_* + \Delta\varphi_j$, $y_j = \Pi(\varphi_*) + \Delta y_j$, where $\Delta\varphi_j$, Δy_j are the dynamic errors; $\Pi(\varphi_*)$ is the position function, which describes the displacement of the executive body in the program motion. With zero-clearance motion and small dynamic errors, we have $\Pi(\varphi_j) = \Pi(\varphi_* + \Delta\varphi_j) \approx \Pi(\varphi_*) + \Pi'(\varphi_*)\Delta\varphi_j$, where $\Pi' = d\Pi/d\varphi_*$. When determining the frequency and modal characteristics we can ignore the weak influence of dissipative forces. Repeating unit s (see Fig. 11.16) has five degrees of

freedom and is described by the following system of differential equations (repetitive index s is omitted completely):

$$
\left.
\begin{aligned}
&J_1 \Delta \underset{1}{\ddot{\varphi}} + c_1(\Delta\varphi_1 - \Delta\varphi_0) - c_2(\Delta\varphi_3 - \Delta\varphi_1) - c_3\Pi'_*\left(\Delta y_1 - \Pi'_*\Delta\varphi_1\right) = 0; \\
&J_1 \Delta \underset{3}{\ddot{\varphi}} + c_2(\Delta\varphi_3 - \Delta\varphi_1) - c_1(\Delta\varphi_4 - \Delta\varphi_3) - c_3\Pi'_*\left(\Delta y_3 - \Pi'_*\Delta\varphi_3\right) = 0; \\
&m_1 \Delta \underset{1}{\ddot{y}} + c_3\left(\Delta y_1 - \Pi'_*\Delta\varphi_1\right) + e_{13}^{-1}(\Delta y_1 - \Delta y_3) + 0.25 e_{22}^{-1}(\Delta y_1 - 2\Delta y_2 + \Delta y_3) = F_1(t); \\
&m_2 \Delta \underset{2}{\ddot{y}} + e_{22}^{-1}(\Delta y_2 - 0.5\Delta y_1 - 0.5\Delta y_3) = F_2(t); \\
&m_3 \Delta \underset{3}{\ddot{y}} + c_3\left(\Delta y_3 - \Pi'_*\Delta\varphi_3\right) + 0.25 e_{22}^{-1}(\Delta y_1 - 2\Delta y_2 + \Delta y_3) + e_{13}^{-1}(\Delta y_3 - \Delta y_1) = F_3(t).
\end{aligned}
\right\}
$$

$$(11.54)$$

Here in addition to the previously introduced notations, we accept $e_{13}^{-1} = e_{31}^{-1}$ is the influence factor different from zero in case of clamping of the beam's ends (see above); $F_i(t) = F_T(t) - \Pi''(\omega t)\omega^2 m_i$, where F_T is the technological resistance; $\Pi'' = d^2\Pi/d\varphi_*^2$.

The accepted indexing of coordinates corresponds to the following relationship, linking the number of coordinate v in this block $\left(v = \overline{1,3}\right)$; the number of repeating module $s = \overline{1,n}$; number of section, counted from the origin of the regular part of the system $j = 3s - 3 + v$. The total number of degrees of freedom is equal to $H = H_0 + H_p$, where H_0 corresponds to the mechanism's gear (for the model in Fig. 11.16, we have $H_0 = 1$), H_p corresponds to the regular system $\left(H_p = 5n\right.$, where n is the number of sections). Taking into account the slow change of the "natural" frequencies $p(\varphi_*)$ according to the conditional oscillator method, the free oscillations are looked for in the form

$$
\Delta\varphi_v = K_v \sin \int p(\varphi_*)d\varphi_*; \quad \Delta y_v = Y_v \sin \int p(\varphi_*)d\varphi_*. \tag{11.55}
$$

After substitution of (11.55) in the uniform system of differential equations, corresponding to the system (11.54), we get

$$
\left.
\begin{aligned}
&M_1/(J_1\omega^2) + (p_2^2 + p_3^2\rho^{-2}\Pi_*'^2 - p^2)K_1 - p_2^2K_3 - \Pi'_*p_3^2\rho^{-2}Y_1 = 0; \\
&-p_2^2K_1 + \left(p_2^2 + p_3^2\rho^{-2}\Pi_*'^2 - p^2\right)K_3 - \Pi'_*p_3^2\rho^{-2}Y_3 - M_4/(J_1\omega^2) = 0; \\
&-p_3^2\Pi'_*K_1 + (p_3^2 + p_{13}^2 + 0.25p_{22}^2\mu - p^2)Y_1 - 0.5p_{22}^2\mu Y_2 + \left(0.25p_{22}^2\mu - p_{13}^2\right)Y_3 = 0; \\
&-0.5p_{22}^2Y_1 + \left(p_{22}^2 - p^2\right)Y_2 - 0.5p_{22}^2Y_3 = 0; \\
&-p_3^2\Pi'_*K_3 + \left(0.25p_{22}^2\mu - p_{13}^2\right)Y_1 - 0.5p_{22}^2\mu Y_2 + \left(p_3^2 + p_{13}^2 + 0.25p_{22}^2\mu - p^2\right)Y_3 = 0,
\end{aligned}
\right\}
$$

$$(11.56)$$

where $p_1^2 = c_1/(J_1\omega^2)$; $p_2^2 = c_2/(J_1\omega^2)$; $p_3^2 = c_3/(m\omega^2)$; $p_{22}^2 = (e_{22}m_2\omega^2)^{-1}$; $p_{13}^2 = (e_{13}m\omega^2)^{-1}$ (in case of ball-bearings we should accept $p_{13} = 0$); $\mu = m_2/m$; $\rho^2 = J_1/m$; $(m_1 = m_3 = m)$; $\Pi'_* = \Pi'(\varphi_*)$ M_v are the reactive moments.

Taking $K_1 = 0$, $K_4 = 0$ into (11.56) and converting the determinant to zero, we obtain the equation determining the slowly varying "partial" frequencies. The variability of the amplitude functions is related to the slow change of the geometrical transfer function of the cyclic mechanisms.

Employment of the theory of regular systems to construct the mathematic model with a multi-modular structure The system of equations (11.56) consists of two amplitude functions, corresponding to the boundaries of the selected module s, namely K_1 (the section at the input $s-1$) and K_4 (section at the "output" s). Using the procedure outlined in Sects. 10.4 and 11.3, [19] for torsional branched-circular regular systems, we can write the transition matrix, which connects the amplitude functions in the cross sections $s-1$ and s.

$$\begin{bmatrix} K_s \\ N_s \end{bmatrix} = \begin{pmatrix} g_{11}(\varphi_*) & g_{12}(\varphi_*) \\ g_{21}(\varphi_*) & g_{22}(\varphi_*) \end{pmatrix} \begin{bmatrix} K_{s-1} \\ N_{s-1} \end{bmatrix}, \tag{11.57}$$

where $N_s = M_s/(J_1\omega^2)$; M_s is the amplitude value of inertia in section s. Let us recall that in Eq. (11.56) for simplification of recording index s, we omitted $(K_i = K_{s,i})$. Returning to the original indexes for the given module s we have $K_1 = K_{s-1}$, $K_4 = K_s$, $N_1 = N_{s-1}$, $N_4 = N_s$.

Further, let us dwell on the methodology of determining the functions $g_{kv}(\varphi_*)$, which are the elements of the transition matrix, in the recursive dependencies (11.57). On the basis of the fourth equation of (11.56) we have

$$Y_2 = 0.5p_{22}^2(Y_1 + Y_3)/(p_{22}^2 - p^2). \tag{11.58}$$

After substitution of (11.58) in the third and fifth equation of this system, we will write

$$\begin{aligned} u_{11}(p)Y_1 + u_{12}(p)Y_3 &= p_3^2\Pi_*'K_1; \\ u_{21}(p)Y_1 + u_{22}(p)Y_3 &= p_3^2\Pi_*'K_3, \end{aligned} \tag{11.59}$$

where

$$lu_{11}(p) = u_{22}(p) = p_3^2 + p_{13}^2 + 0.25p_{22}^2\mu\left[1 - p_{22}^2/(p_{22}^2 - p^2)\right] - p^2,$$
$$u_{12}(p) = u_{21}(p) = 0.25p_{22}^2\mu\left[1 - p_{22}^2/(p_{22}^2 - p^2)\right] - p_{13}^2.$$

Hence

$$Y_1 = \Pi_*'(\sigma_1K_1 - \sigma_2K_3); \quad Y_3 = \Pi_*'(\sigma_1K_3 - \sigma_2K_1), \tag{11.60}$$

where $\sigma_1 = p_3^2u_1/(u_1^2 - u_2^2)$, $\sigma_2 = p_3^2u_2/(u_1^2 - u_2^2)$.

After substitution of (11.60) in the first two equations of the system of equations (11.56), we have

$$N_1 = -a_{11}K_1 + a_{12}K_3; \quad N_4 = -a_{21}K_1 + a_{22}K_3. \tag{11.61}$$

Here $a_{11} = a_{22} = p_2^2 + p_3^2\Pi_*'^2\rho^{-2}(1 - \sigma_1) - p^2$; $a_{12} = a_{21} = p_2^2 - \Pi_*'^2\rho^{-2}\sigma_2$.

It follows from (11.61) that:

$$K_3 = (a_{11}K_1 + N_1)/a_{12}; \quad N_4 = -a_{21}K_1 + a_{22}(a_{11}K_1 + N_1)/a_{12};$$
$$K_4 = K_3 + N_4/p_1^2. \tag{11.62}$$

So $K_3 = K_3(K_1, N_1)$; $K_4 = K_4(K_1, N_1)$; $N_4 = N_4(K_1, N_1)$. At the same time it follows on the basis of (11.61) and (11.62):

$$g_{11} = K_4(1,0) = a_{11}/a_{12} + (a_{11}^2 - a_{12}^2)/(a_{12}p_1^2); \quad g_{12} = K_4(0,1) = (1 + a_{11}p_1^{-2})/a_{12};$$
$$g_{21} = N_4(1,0) = (a_{11}^2 - a_{12}^2)/a_{12}; \quad g_{22} = N_4(0,1) = a_{11}/a_{12}. \tag{11.63}$$

The transition matrix entries are subjected to famous functional relation $g_{11}g_{22} - g_{12}g_{21} = 1$.

Composing the frequency equation on the basis of the theory of regular systems The relation (11.57), written in matrix form, fits the following homogeneous system of linear differential equations.

$$\left.\begin{array}{l} K_s = g_{11}K_{s-1} + g_{12}N_{s-1}; \\ N_s = g_{21}K_{s-1} + g_{22}N_{s-1}, \end{array}\right\}$$

The solution of which, we find in the form $K_s = \lambda K_{s-1}$; $N_s = \lambda N_{s-1}$. Then,

$$\left.\begin{array}{l} (g_{11} - \lambda)K_{s-1} + g_{12}N_{s-1} = 0; \\ g_{21}K_{s-1} + (g_{22} - \lambda)N_{s-1} = 0. \end{array}\right\}$$

Excluding the trivial zero solution, we convert the system determinant into zero. The roots, of the so obtained characteristic equation are $\lambda = \kappa \pm i\sqrt{1 - \kappa^2}$, where $i = \sqrt{-1}$; $\kappa = 0.5(g_{11} + g_{22}) = 0.5\text{Sp}\,\Gamma = \left[1 - p_{22}^2/(p_{22}^2 - p^2)\right] - p^2$.

Here $\text{Sp}\,\Gamma$ is the spur of the transition matrix. When $\kappa \leq 1$, taking $\kappa = \cos\theta$, we have:

$$\left.\begin{array}{l} K_s = h_1 \cos s\theta + h_2 \sin s\theta; \\ N_s = h_1[\cos(s+1)\theta - \cos s\theta] + h_2[\sin(s+1)\theta - \sin\theta]. \end{array}\left(s = \overline{0,n}\right)\right\} \tag{11.64}$$

Let's write the boundary conditions corresponding to the considered model: $N_0 = \zeta(p) = c_1/R_0(p)$, $N_{n+1} = 0$, where $R_0(p)$ is the dynamic stiffness of the driving mechanism. For the model represented in the Fig. 11.16, $R_0(p) = c_{02}(c_{01} - J_0p^2)/(c_{01} + c_{02} - J_0p^2)$. In a particular case $R_0 = c_{02}$ when $c_{01} \to \infty$ and $R_0 \approx c_{01}c_{02}/(c_{01} + c_{02})$ when $c_{01} \gg J_0p^2$. Then the dynamic

stiffness doesn't depend on the frequency p; at the same time $\zeta \simeq c_1/c_0$, where c_0 is the reduced stiffness coefficient of the driving gear at the "input". On the basis of (11.64), taking into account the boundary conditions we get the following transcendental equation, determining the function $\theta(p)$:

$$(1 + \zeta(p)) \cos[(n + 0.5)\theta] - \zeta(p) \cos[(n - 0.5)\theta] = 0. \qquad (11.65)$$

In case, when the boundary conditions do not depend on the frequency p, we have $\zeta = \text{const}$ (see above) and therefore the solution of (11.65) can be obtained regardless of the dynamic characteristics of the module. In particular when $R_0 \to 0$ $\theta_r = \pi r/n$, where $r = \overline{1,n}$ is the number of the oscillatory mode of the main shaft, and in the other ultimate case, when $R_0 \to \infty$ we have $\theta_r = \pi(2r - 1)/(2n + 1)$. Let us note here that the study of frequency characteristics of the systems, is advisable to begin with review of these cases, since in case of "long" chains the ultimate effect is often detected; this effect has the negligibly weak influence of the boundary conditions of the main shaft on the analyzed frequency.

The formal frequency equation has the form:

$$0.5[g_{11}(p) + g_{22}(p)] - \cos \theta(p) = 0. \qquad (11.66)$$

Thus, for the original system with $H = 5n + 1$ degrees of freedom in the concise form the frequency equation (11.66) is obtained, solving which in today's computing environments is easy.

The possible forecasting during dynamic synthesis, using this approach, is of particular interest.

Study of the spectrum of "natural" frequencies   First of all let us consider a few special cases, being of some interest not only to simplify the calculations, but also to identify the opportunities for system decomposition. The fact is that in the vicinity of the ultimate cases often there is a loss of the roots of equations and other computational difficulties. This is usually caused by physical prerequisites, appearing in the weak dynamic connectedness, between the individual subsystems.

Suppose, for example, the partial frequencies of bending subsystem are practically determined with reduced stiffness coefficients of the cyclic mechanisms. In this case $p_{22}^2 \ll p_3^2$, $p_{13}^2 \ll p_3^2$. Then, we should take $\sigma_1 = p_3^2/(p_3^2 - p^2)$, $\sigma_2 = 0$ in the dependencies (11.58)–(11.63). For this case, in the Fig. 11.17a, the graphs of the slowly changing "natural" frequencies, for the four sections of the drive ($n = 4$) and the sufficiently dense distribution of the dimensionless frequency parameters $p_r (p_1 = 44.7; p_2 = 20; p_3 = 15)$ are represented. (The numbering of the curves corresponds to the oscillatory mode of the main shaft.)

As follows from the graphs, there is significant variability of the frequency characteristics, within the kinematic cycle, which can lead to loss of local dynamic stability (see below). It is of interest that the lower frequency of the system meets the third (two-node) mode of the main shaft, which is associated with the specific interaction with the bending subsystem.
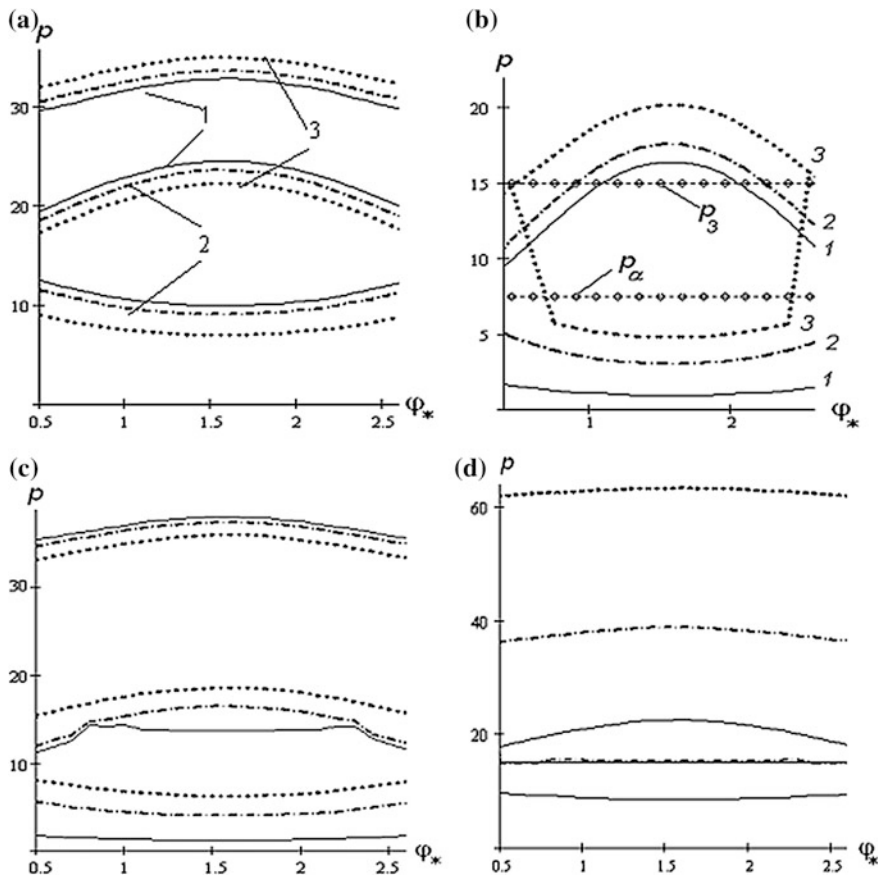
Fig. 11.17 Frequency characteristics; **a** low stiffness of the mechanism, **b** a large stiffness of the actuator, **c** a large stiffness of the mechanism, **d** a large stiffness of the shaft

As another extreme case we will consider the situation, when the executive body can be schematized in the form of the solid, which has the mass $m_{\Sigma} = \sum_{i=1}^{3} m_i$ and moment of inertia about the center of mass J_{α}. In our case $m_{\Sigma} = m(2 + \mu)$, $J_{\alpha} = 0.5\, l^2 m(2 + \mu)$, where l is the length of the executive body module. In this case the dimensionless partial frequency, of the turning oscillations, is equal to $p_{\alpha} = p_3/\sqrt{2 + \mu}$.

After some simple calculations, we find that the functions $\sigma_1(p)$ and $\sigma_2(p)$, included in the relation (11.60), are now defined as

$$\sigma_1(p) = p_3^2 / \left[2p_3^2 - (2 + \mu)p^2 \right] + 0.5 p_{\alpha}^2 / \left(p_{\alpha}^2 - p^2 \right),$$
$$\sigma_2(p) = p_3^2 / \left[2p_3^2 - (2 + \mu)p^2 \right] - 0.5 p_{\alpha}^2 / \left(p_{\alpha}^2 - p^2 \right).$$

In Fig. 11.17b the graphs of $p(\varphi_*)$, with the same initial data, but taking into account the features of the considered case, are represented. The chart shows the most significant "strong" frequencies. The adopted above frequencies indexing corresponds to the first three oscillatory modes of the main shaft. In addition we can see the curves for p_α and p_3, which are represented for comparative purposes. In qualitative terms, as compared to the previous special case, the influence of the low-frequency turning oscillations of the executive body in the formation of the "strong" lower frequencies of the main shaft, is seen. When $\Pi'_* \approx 0$, the effect of degeneration of certain oscillatory modes, accompanied by "hops" from one curve to the other, is observed. As in the previous case, the regularity of the system leads to the appearance of frequency bands with high density of frequencies.

In case, when the absolutely rigid actuator moves in the guide, excluding the possibility of turning oscillations, the tightening role of the executive body, in the formation of the frequency spectrum, appears. As a result of frequency analysis, this case is joined by the structural solution, which implements termination in the bearings of the executive body.

In addition to the above special cases, in Fig. 11.17c, d, graphs of $p(\varphi_*)$, for the relatively high values of p_*, are shown. In the first case ($p_1 = 14.1$; $p_2 = 20$; $p_3 = 15$; $p_4 = 16.3$) Here, we again see the effect of concentration of frequency spectrum and jumps in case of degeneration of certain oscillatory modes. (The numbering of the curves in Fig. 11.17d corresponds to the notes to Fig. 11.17a). With relatively rigid main shaft ($p_1 = 141, 4$; $p_2 = 63.2$; $p_3 = 11.5$; $p_4 = 5.16$) the frequency spectrum has the traditional view (Fig. 11.17d). In this case the lower frequencies correspond to the lower mode shapes of the main shaft, practically zones with high density of frequency spectrum and also degeneration of the mode shapes may be lacking.

In Fig. 11.18 the typical graphics of the oscillatory modes, for sections s, of the main shaft (Fig. 11.18a) and Y_1, Y_2, Y_3 which correspond to module s on the executive body Y_j, are shown. At the same time the cases of the in-phase (see Fig. 11.18b) and anti-phase (see Fig. 11.18c) oscillatory mode of the main shaft ends are identified.

Dynamic stability in the finite time interval The dynamic effect, associated with the violation of the dynamic stability, in case of slow variation of these parameters, is described in Sect. 5.3.1. Let us recall that this effect means the appearance of intervals, in which instead of the traditional attenuation of free accompanying oscillations, there occurs an increase in amplitudes. Since in case of certain intensity, of this increase, the vibration activity abruptly grows, the conditions excluding this phenomenon should be fixed during the dynamic synthesis. Basically, the method of suppression of this effect is that the energy withdrawn due to dissipation, during the oscillatory period, must exceed the input energy, related to the specific influence of the time-dependent connections.

With reference to the considered model, the sufficient condition for dynamic stability, in an arbitrary time interval, is given by
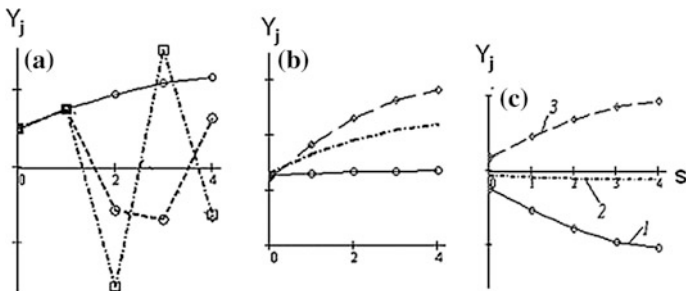
Fig. 11.18 Typical graphs of the mode shapes: r = 1, 2, 3 is the frequency number; **a** mode shapes of the shaft, **b** in-phase mode shapes of the executive body, **c** anti-phase mode shapes of the executive body
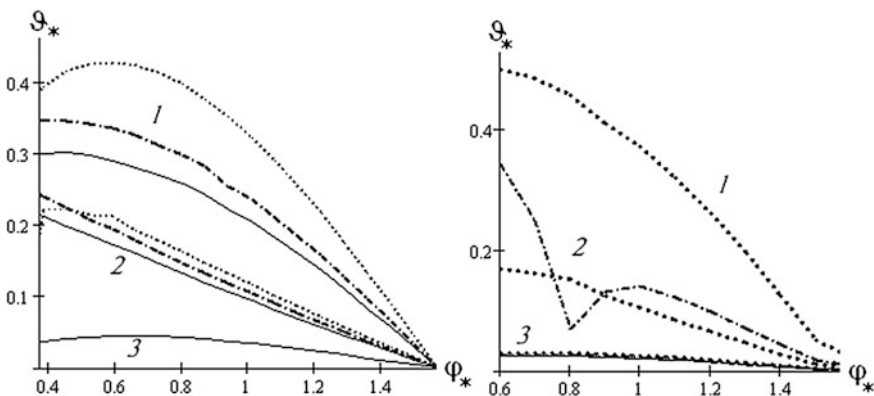
Fig. 11.19 Graphs of the logarithmic decrement's critical values

$$\vartheta_r > \vartheta_{r*} = \xi \pi p_r^{-2} dp_r / d\varphi_*,$$

where ϑ_r, ϑ_{r_*} is the reduced to the mode r logarithmic decrement and its critical value; ξ is the factor, which takes the value respective to 1, 2, 3, for oscillations, vibratory speed and vibratory accelerations.

We can see in Fig. 11.19, the graphs of critical values of ϑ_{r*} (for accelerations) in two cases, corresponding to the frequency characteristics, given in Fig. 11.17a, c.

Thus, as above, the curves shown with solid lines correspond to the first mode of the main shaft's oscillations, hatch-dotted lines to the second mode and the dotted ones to the third form. The numbering corresponds to the first, second and third frequency (in ascending order) for every mode. The graphs' analysis suggests the possible violations of dynamic stability conditions at the real level of the system's dissipation. The results of computer simulation, of oscillations of the system under consideration, taking into account dissipation and clearances, are represented in Sect. 12.2.

Chapter 12
Energy Exchange in the Regular Cyclic Oscillatory Systems. Spatial Localization of Vibrations

12.1 Brief Information About the Energy Transfer in Oscillatory Systems

Introductory remarks In the problems of the machine dynamics, we often face a variety of effects, associated with energy transfer from one subsystem to another or energy exchange between different oscillatory shape modes. Sometimes these effects are positive, helping protect machines and mechanisms against vibrations. In other cases, these effects lead to undesirable redistribution of oscillations and their localization in some units, links, sections etc.

When designing machines with increased length of technological processing zone, it is necessary that the oscillations of the long working bodies would be close to the in-phase ones. Failure to do so leads to the occurrence of undesirable dynamic effects and in addition to the various defects of the products, such as yarn divergency and edge defects in the manufacture of fabrics, yarn breakages, damage to the printed products in printing machines, violations of the specified accuracy and surface finish in machine tools and other. However, in the real conditions, it is not always possible to keep the in-phase oscillations, in case of a relatively large number of cyclic driving mechanisms. In such cases, it is necessary to suppress the spatial energy localization of the oscillations, when in certain sections, the strict dynamic regularity of the system is violated [12, 25, 37], to which the occurrence of clear extremes in oscillatory shape modes is often related.

It should be noted that the problem under consideration is of a general nature and is found in various areas of physics. In particular, in quantum mechanics, it is known as the so-called Landau-Zener tunneling, in which the energy exchange occurs between the two levels under the action of the external force [32]. The mechanical analog of tunneling was proposed. It is a system of two weakly coupled oscillators, in which the partial frequency of one of them changes slowly over time and covers the area of the internal resonance. Besides, if the transfer of energy from one oscillator to the other one is irreversible, there occurs a kind of a trap for the

Fig. 12.1 Energy transfer in coupled oscillators with varying parameters
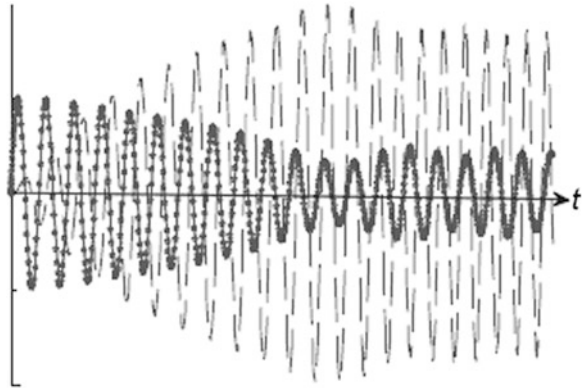
"capture" of the vibratory energy. Figure 12.1 shows graphs, illustrating the transfer of vibrations from one subsystem (solid line) to another (the hatched line) [32].

Dynamic damping in case of forced excitation Dynamic damping is a well-known and vivid manifestation of energy transfer. Dynamic absorber (DA), is the extra mass m_2, connected to the main mass m_1, with the elastic element, to reduce the amplitude of the forced oscillations of the main mass (Fig. 12.2a). In the torsion oscillation system (Fig. 12.2b) the role of the dynamical absorber performs subsystem consisting of the disk with the moment of inertia J_2 and elastic element with stiffness coefficient c_2.

In the future, without restricting the scope of generality, we will illustrate the main points for the model, shown in Fig. 12.2a. Let the mass m_1 be applied with the driving force $F_1 \cos \omega t$. Then the amplitude of the forced oscillations of mass m_1 is equal to

$$A_1 = F_1(c_2 - m_2\omega^2)/[(c_1 + c_2 - m_1\omega^2)(c_2 - m_2\omega^2) - c_2^2]. \tag{12.1}$$

When $c_2 - m_2\omega^2 = 0$, we get $A_1 = 0$. The following expression corresponds to this condition: $\omega = \omega_* = \sqrt{c_2/m_2} = p_2$, where p_2 is the corresponding partial frequency.

Fig. 12.2 Dynamic absorbers
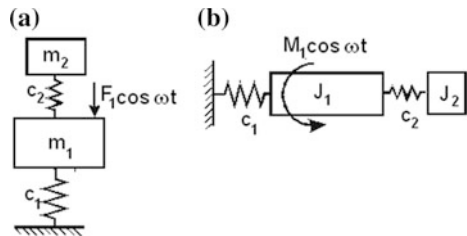
Let us emphasize here that the numerator and denominator of formula (12.1) do not vanish simultaneously, since the root of the numerator is the partial frequency, and the root of the denominator $\Delta(\omega^2) = 0$ is the natural frequency. These frequencies in the absence of multiple frequencies do not coincide. Out of structural considerations usually we assign the value of m_2, after which the stiffness coefficient of the elastic element is defined as $c_2 = m_2\omega_*^2$.

The physical essence of dynamic damping lies in the fact that in case of relevant configuration, the reaction of the dynamic damper applied to the basic mass, during steady mode, is equal to the driving force, but is opposite in direction. Dynamic damping is a special case of anti-resonance (see Sect. 4.2).

Figure 12.3 shows the amplitude-frequency characteristics (AFC) in the absence of a dynamic absorber (curve 1) and after its installation (curve 2). The estimated regime, in which $A_1 = 0$, corresponds to the frequency ω_*. If the value of ω is not strictly constant, but varies in a certain frequency range, the amplitude A_1, in the vicinity of the resonant frequency $\omega = k_1$ and $\omega = k_2$, wherein k_i are the natural frequencies, can significantly increase. In such cases an additional damper is installed, between the dynamic absorber and the main mass, which causes certain resistance, providing an outflow of vibration energy. In such cases AFC has the shape of curve 3.

It is easy to see that in the frequency range $\Delta\omega$, shown in Fig. 12.3, with hatched line, the installation of the damper has led to the increase in the amplitude of forced oscillations, since now the phase of oscillation damper is not strictly opposite to the phase of the driving force. This effect shows that the inclusion of the resistance does not always lead to the decrease in the amplitude of oscillations.

Dynamic damping in case of kinematic excitation   Let us consider the dynamic models, which differ from those shown in Fig. 12.2, only due to the fact that instead of the driving force or torque, we have kinematic excitation. In this case, the "input" of the elastic member c_1 is forcibly moved, according to the predetermined position function of the cyclic mechanism $\Pi(\varphi)$. Suppose, for example, the program motion of the mass m_1 is described as $x = r_0(1 - \cos \omega t)$. Let us adopt the dynamic errors as the generalized coordinates, i.e. the deviations from the program motion. In the system of coordinates under consideration, which undergoes a translation motion according to the specified program motion, in addition to the external forces, we

Fig. 12.3 To the analysis of the dynamic damping
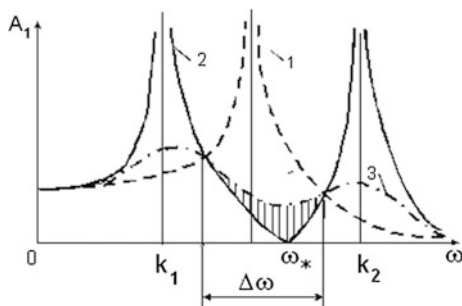
must take into account the inertial forces $F_i(t) = -m_i\omega^2\Pi''(\omega t); \; i = 1, 2$. Let us introduce the dynamic factor $\kappa = A_1/r_0$. Defining, as per the abovementioned method, A_1, we get

$$\kappa = \left| \frac{\omega^2[p_2^2(1+\mu) - \omega^2]}{\omega^4 - [(1+\mu)p_2^2 + p_1^2]\omega^2 + p_1^2 p_2^2} \right|, \tag{12.2}$$

where, $\mu = m_2/m_1$, $p_i = \sqrt{c_i/m_i}$, $i = 1, 2$.

When, $\omega = \sqrt{c_2(m_1 + m_2)/(m_1 m_2)}$, according to (12.2), we have $\kappa = 0$; it is the evidence of the complete unloading of the mechanism's drive in this mode. Let us represent dependence (12.2) in the following form:

$$\kappa = \left| \frac{z_1^2[z_2^2(1+\mu) - z_1^2]}{z_1^4 - [(1+\mu)z_2^2 + 1]z_1^2 + z_2^2} \right|,$$

where, $z_i = \omega/p_i$.

When $z_2 = z_2^* = \sqrt{1+\mu}$, we have $\kappa = 0$, and when $\mu = 0 - \kappa = 1/\left|1 - z_1^2\right|$, which, as expected, corresponds to the system with one degree of freedom. The violation of frequency tuning, when $m_2 \ll m_1$, caused by the proximity to the resonance zone, can lead to high dynamic loads. Furthermore, the amplitude of vibrations in the dynamic absorber significantly increases. It should be noted that, with regard to the problem of reducing the vibration activity in cyclic mechanisms, dynamic damping of vibration is usually not the most effective way and is preceded as per effectiveness by dynamic unloading.

Spatial localization in the classical chain Spatial localization in oscillatory chains [25, 37] is directly related to the class of problems discussed in this chapter. Hereunder we will limit our observation to brief information from the classical theory of chains, which will used for further discussion. Let us consider the model, which we have already referred to in Sect. 9.1 (see Fig. 9.1). Let the stiffness coefficient c in the section $s = 0$ differ by the amount of Δc. Then the equations of motion, similar to (9.1), take the following form

$$\ddot{q}_s + c_1(2q_s - q_{s-1} - q_{s+1}) + (c + \Delta c)q_s = 0. \tag{12.3}$$

Here q_s is the coordinate of the corresponding mass. Parameter Δc, following the terminology used in the classical theory of chains, in regards to the problems of crystallography, will be called as "inclusion" (Below we use the dimensionless form of the parameters, when $m = 1$, $c_1 = 1$, $\tilde{c} = c/c_1 = c$). As shown in [37], looking for the solution in the form $q_s = A\exp(\Omega s + ipt)$, we get

$$\Omega = 0.5\Delta c/c_1; \ p^2 = c - 0.25\Delta c^2/c_1.$$

This solution corresponds to the localized standing wave, whereas the "inclusion" has reduced the lower frequency p. The localization region can be estimated as $\Delta n \approx 2c_1/|\Delta c|$. In case of having two inclusions, we accordingly have two areas of localization, in phase and anti-phase forms of oscillations (Fig. 12.4). With the increase in the "distance" s_*, between the inclusions, the effective stiffness decreases exponentially.

For the classical model this problem is concretized in [25] using the example of vibrations of a string, as well as the Euler-Bernoulli and Timoshenko beam with lumped inclusions. However, as the analysis showed, in regard to the class of problems under consideration, the effects, observed during experiments and computer simulations, do not fit into the framework of the classical theory.

This is primarily due to the fact, that instead of pointed masses, we have repetitive modules, which form complex structures with variable parameters and non-linear elements. Furthermore, the "inclusions", which in the class of problems under consideration, are associated with the deviations from regularity, because of the design and other factors, which violate the strict dynamic similarity of the modules, are significantly modified. In particular, not only the lumped elements of the dynamic model can act as "inclusions", but also the phase shifts of the argument of the position function φ_i, arising due to the drive's oscillations $\Delta\varphi_i$ and even the small effect of dissipation. Nevertheless, the analysis of the classical models gives very valuable insights of qualitative nature about the given problem and in some cases, even, useful preliminary estimates.

Energy transfer in the cyclic system with variable parameters Let us illustrate the transfer of oscillatory energy using the example of the dynamic model of a cyclic mechanism with an elastic actuator, to which the structural formula $1 - \Pi - 1$ (see Sect. 2.5) corresponds, when we have serial connection of the elements $J_0 - c_1 - J_1 - \Pi - c_2 - J_2$. Let us adopt the following notation: $\varphi_* = \omega_* t$ is the ideal coordinate of J_0 when $\omega_* = $ const; J_i are the moments of inertia; c_i are the

Fig. 12.4 Spatial localization in the classical chain
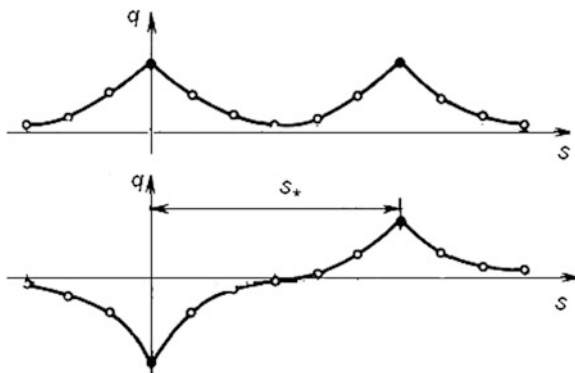
stiffness coefficients; $\varphi_1 = \varphi_* + q_1$; $\varphi_2 = \Pi(\varphi_*) + q_2$ where φ_i are the absolute angular coordinates of the corresponding inertial elements; q_i are the generalized coordinates, equal to the absolute dynamic errors, i.e. deviations from the given program motion.

This model, after linearization in the vicinity of the program motion (see Sect. 5.1), is described by the following system of differential equations (in relation to the considered problem the driving forces are excluded).

$$\left.\begin{array}{c}\ddot{q}_1 + k_1(2\delta_1\dot{q}_1 + k_1 q_1) + J_2 J_1^{-1} k_2 \Pi'_*[2\delta_2(\Pi'\dot{q}_1 - \dot{q}_2) + k_2(\Pi'_* q_1 - q_2)] = 0; \\ \ddot{q}_2 + k_2[2\delta_2(\dot{q}_2 - \Pi'_*\dot{q}_1) + k_2(q_2 - \Pi'_* q_1)] = 0, \end{array}\right\}$$

$$(12.4)$$

where $k_i = \sqrt{c_i/J_i}$; $\delta_i = \psi_i/(4\pi)$; ψ_i are the reduced dissipation coefficients $(i = 1, 2)$; $\Pi'_* = d\Pi/d\varphi$ when $\varphi = \varphi_*$.

The graph of the second transfer function of the given program motion is shown in Fig. 12.5. The results are reported for the two combinations of partial frequencies: $k_1 = 20\,\text{s}^{-1}$, $k_2 = 30\,\text{s}^{-1}$ (option 1) and $k_1 = k_2 = 30\,\text{s}^{-1}$ (option 2). The variable "natural" frequencies p_1, p_2 are displayed in the graphs of $p_i(\varphi_*)$ (Fig. 12.6).

Let at $\varphi = 0$, the subsystem of the output link, receive an impulse perturbation $(\dot{q}_2(0) \neq 0)$. The graphs of $q_1(\varphi_*)$ (solid line) and $q_2(\varphi_*)$ (dotted line) are represented in Fig. 12.7. For greater clarity in the graphs, the dissipative members in system of Eq. (12.4) have been omitted. Since, in case of $\Pi'(0) = 0$, the subsystems are unrelated, the reserve kinetic energy in case of $\Pi' \neq 0$ is redistributed between both the subsystems. A comparison of the two graphs shows that in case of equality of partial frequencies, the original level of the amplitudes in both subsystems is fully restored, at the end of the kinematic cycle. Unlike the case considered in paper [32] (see Fig. 12.1), the "trap" function is performed, by the cyclic system, only partially: within the kinematic cycle, but generally exchange of energy between the subsystems is observed during the cycle, whereas a fraction of the transferred energy is largely dependent on the ratio of the partial frequencies.

Fig. 12.5 Graph of $\Pi''(\varphi_*)$
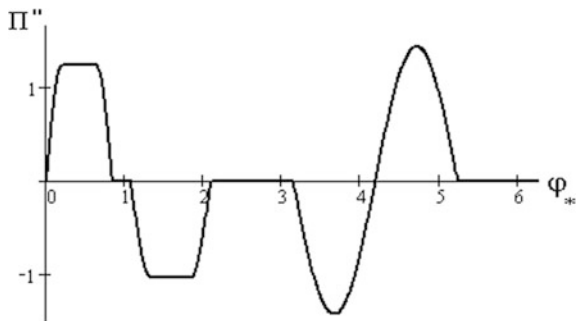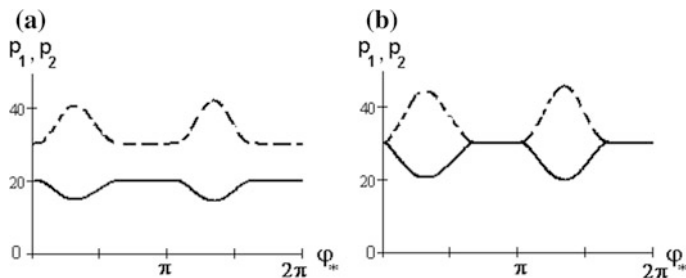
Fig. 12.6 Graphs of the change in "natural" frequencies: **a** option 1; **b** option 2
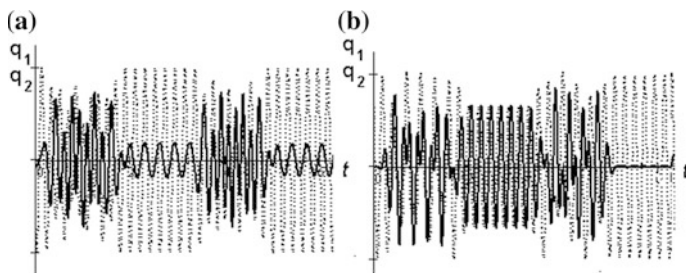
Fig. 12.7 Energy exchange between subsystems: **a** option 1; **b** option 2

As shown by the analysis, when taking dissipation into account, one of the subsystems, in case of relatively higher coefficients of dissipation, can act as the effective means of reducing the level of oscillations in the second subsystem.

12.2 Computer Simulation of Vibrations in Regular Cyclic Systems, Taking into Account the Clearances and Dissipative Forces

The clearances, in the kinematic pairs of cyclic mechanisms, significantly influence the dynamic loads in the elements of the drive and dynamic accuracy, when reproducing the given laws of program motion, while determining the level of excited oscillations. The need to improve the "zero-clearance" model, instigated by repeatedly closed oscillating contours, is primarily related to its static indetermination [28]. At the same time, as shown by the experience of operation of the given class of machines and experimental data, dynamic loads are not distributed among the actuators evenly and strongly depend on the size of the clearances. Some of the mechanisms, operating in the parallel circuit, are often rather lightly loaded and even play a negative role as a source of excitation of oscillations due to collisions in the clearances [28–31]. In regards to the study of spatial localization in the regular

cyclic systems, described in previous chapters, the consideration of clearances is of special interest. The point of the matter is that spatial localization occurs in the natural frequencies, particularly in the clearances, we have periodic impact pulses, which cause and support the accompanying oscillations at these frequencies (see Chap. 7). Dynamic effects associated with the clearances are illustrated below with reference to the two models, the frequency analysis of which are given in Sects. 10.1 and 11.4.

12.2.1 Torsion System of Ring Structure

Let us consider the dynamic model of the drive (Fig. 12.8), consisting of the subsystems of the main shaft ($k = 1$) and the executive body ($k = 2$), connected to the main shaft with n cyclic mechanisms [17, 29, 73]. Each of the mechanisms is presented as a serial connection of the elements, taking into account the inertial, elastodissipative and kinematic characteristics, as well as the reduced clearance Δs_j in the kinematic pairs. The following notations were adopted here: $J_{j,k}$ are the moments of inertia; $c_{j,k}$, c_j are the stiffness coefficients; $\psi_{j,k}$, ψ_j are the dissipation coefficients; $\Pi(\varphi_{j,1})$ is the position function. It is assumed that the dynamic characteristics of the main shaft and the executive body are reduced to the sections of the input and output links of the cyclic mechanisms. Apart from that, the "input" angular velocity ω is assumed to be constant, which, in the first approximation, usually corresponds to the real machines, in case of rational choice of characteristics of the electric motor and the gears. The oscillatory system under consideration has $2n + 1$ degrees of freedom.

In comparison with the model discussed in Sect. 10.1, this model is supplemented with elements Δs_j, that correspond to the clearances. As generalized coordinates, we will accept dynamic errors, equal to the deviations of the absolute coordinates, in the relevant sections of the inertial elements, from the program motion coordinates. Thus, for the main shaft $q_1 = \varphi_{1,1} - \varphi_0$, $q_{2(j-1)} = \varphi_{j,1} - \varphi_0$,

Fig. 12.8 Dynamic model of the ring structure
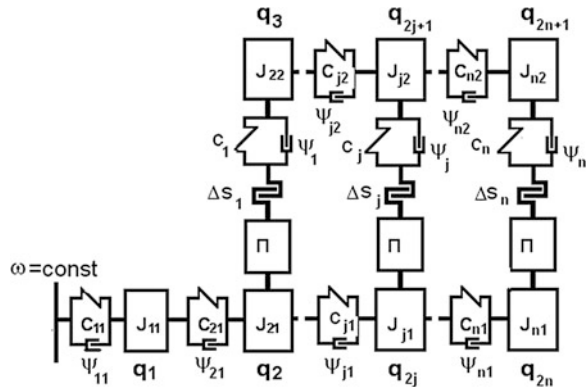
where $\varphi_0 = \omega t$, $j = \overline{1, n+1}$ and for the executive body $q_{2j-1} = \varphi_{j,2} - \Pi(\varphi_0)$ $(j \geq 2)$. On the other hand $\varphi_{j,2} = \Pi(\varphi_{j,1}) \pm 0.5\Delta s_j$.

The following system of non-linear differential equations, with slowly varying coefficients, corresponds to the adopted dynamic model:

$$
\left.
\begin{aligned}
& q_1'' + 2p_{1,1}\delta_{1,1}q_1' + p_{1,1}^2 q_1 - [2p_{2,1}\delta_{2,1}(q_2' - q_1') + p_{2,1}^2(q_2 - q_1)]\rho_{2,1} = w_1(\varphi_0); \\[2mm]
& q_{2(j-1)}'' + 2\delta_{j,1}p_{j,1}(q_{2(j-1)}' - q_{2(j-2)}') + p_{j,1}^2(q_{2(j-1)} - q_{2(j-2)}) \\
& \quad - [2\delta_{j+1,1}p_{j+1,1}(q_{2j}' - q_{2(j-1)}') + p_{j+1,1}^2(q_{2j} - q_{2(j-1)})]\rho_{j+1,1} \\
& \quad - \rho_j\Lambda_j[2\delta_jp_jZ_j' + p_j^2 Z_j - 0.5\Delta s_j \mathrm{sign}Z_j] = w_{2(j-1)}(\varphi_0); \\[2mm]
& q_{2j-1}'' + 2\delta_{j,2}p_{j,2}(q_{2j-1}' - q_{2j-3}') + p_{j,2}^2(q_{2j-1} - q_{2j-3}) \\
& \quad - [2\delta_{j+1,2}p_{j+1,2}(q_{2j+1}' - q_{2j-1}') + p_{j+1,2}^2(q_{2j+1} - q_{2j-1})]\rho_{j+1,2} \\
& \quad + \Lambda_j[2\delta_jp_jZ_j' + p_j^2 Z_j - 0.5\Delta s_j \mathrm{sign}Z_j] = w_{2j-1}(\varphi_0).
\end{aligned}
\right\}
$$

$$
\tag{12.5}
$$

Here $p_{j,k}^2 = c_{j,k}/(J_{j,k}\omega^2)$; $p_j^2 = c_j/(J_{j,2}\omega^2)$; $\rho_{j+1,k} = J_{j+1,k}/J_{j,k}$; $\rho_j = J_{j,2}/J_{j,1}$. (when $j = 2$ it should be accepted that $q_0 = q_1$, $q_0' = q_1'$, $p_{2,2} = 0$, and when $j = n + 1 - p_{n+2,1} = 0$, $p_{n+2,2} = 0$); $Z_j = q_{2j-1} - \Pi'(\varphi_0)q_{2(j-1)}$; $Z_j' = q_{2j-1}' - \Pi'(\varphi_0)q_{2(j-1)}'$; $\delta_i = \psi_i/(4\pi)$; $\Lambda_j = \Lambda_j(|Z_j| - 0.5\Delta s_j)$; is the unit function ($\Lambda_j = 1$ when $|Z_j| > 0.5\Delta s_j$; $\Lambda_j = 0$ when $|Z_j| \leq 0.5\Delta s_j$). In order to exclude the sliding modes, when calculating, it is advisable to use the smooth approximation of the unit function: $\Lambda_j \approx 0.5\{1 + 2\pi^{-1}\arctan[(|Z_j| - 0.5\Lambda s_j)L]\}$, where $L \gg |Z_j|/\Delta s_j$; $\Pi(\varphi_0) = r_0(1 - \cos\varphi_0)$.

The system of the Eq. (12.5) is composed for the general case of the models of the type under consideration. When the models have a regular structure and $j \geq 2$, we have

$$
\begin{aligned}
& c_{j1} = c_1, \ J_{j1} = J_1, \ c_{j2} = c_2, \ J_{j2} = J_2, \ c_j = c; \ p_{j,1} = p_1, \\
& p_{j,2} = p_2, \ p_j = p_0, \ \delta_{j,1} = \delta_1, \ \delta_{j,2} = \delta_2, \\
& \delta_j = \delta, \ \rho_{j+1,k} = 1, \rho_j = J_2/J_1; \Delta s_j = \Delta s.
\end{aligned}
$$

Hereunder, when selecting the input data for computer simulation, we use average values of parameters of loop-forming parts of the warp knitting machines. We have identified two typical cases of excitation of oscillations, when resurfacing in the clearances, which are illustrated in Fig. 12.9, in the graphs og $q_i(\varphi_0)$, $q_i''(\varphi_0)$, obtained for steady-state modes, when $n = 4$, $\Delta s = 0.004$ rad (the boundaries of the clearance are shown with hatched lines at the adopted scale).

When $r_0 = 0.2$ (Fig. 12.9a) the oscillatory mode is practically implemented, in case of which the executive body oscillates almost synchronously (*mode type 1*), and the influence of the parameters of the main shaft's subsystem and the stiffness
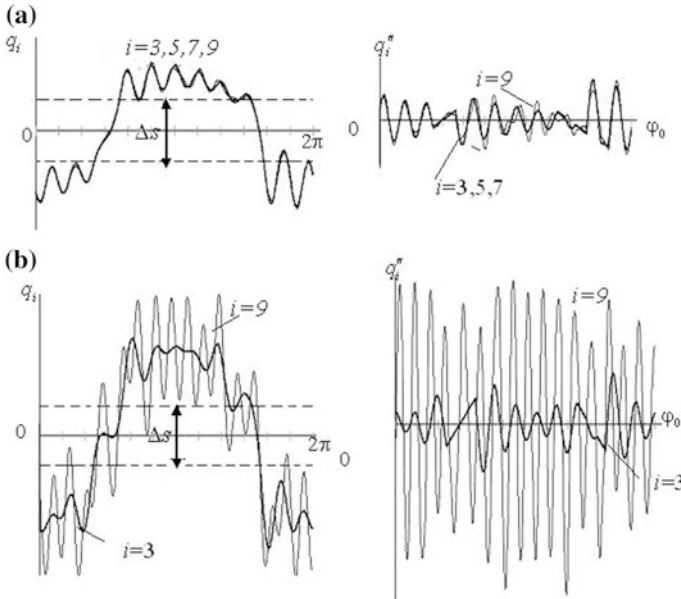
Fig. 12.9 Typical variants of excitation of oscillations, during passage through the clearance

coefficients c_2 is weak. When $r_0 = 0.5$ (Fig. 12.9b) graphs of q_i, q_i'', for the first three mechanisms $(i = 3, 5, 7)$, differ a little, however, there are clearly expressed continuous oscillations at coordinate q_9, which are inherent to vibration-impact regimes (*regime type 2*). Here we can see the effect of spatial localization of oscillations, which will be analyzed hereunder. Similar dynamic effects were also detected experimentally.

Figure 12.10 shows an experimental recording of dynamic loads, which arise in loop-forming mechanism of the knitting machine, when $n = 3$. The increased level of oscillations in the last mechanism is clearly shown in the recording.

Fig. 12.10 Oscillogram of dynamic loads: *1, 2, 3* are the numbers of the mechanisms; *4* is the angular velocity of the shaft
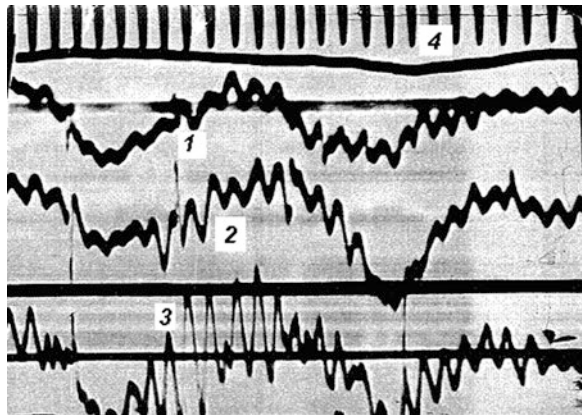
12.2.2 Torsion-Bending System of Branched-Ring Structure

Figure 12.11 represents the dynamic model of the branched-circular structure, wherein the input link (main shaft) is represented as torsional subsystem, and the output link (the executive body) as the bending subsystem. Thus, this model differs from the model described in Sect. 11.4, taking into account the clearances and dissipative forces.

Let us recall the previously accepted conventions: J_i are the moments of inertia; m_i are the masses; c_i are the coefficients of torsion $(i = 0, 1, 2)$ and longitudinal $(i = 3)$ stiffness; ψ is the dissipation coefficients, reduced to the corresponding elements; Δs is the clearance of the mechanism, reduced to the output link; Π is the analogue of the mechanism corresponding to the angular coordinate transformation, from the input link of the mechanism to the linear coordinate of the output link, according to the position function $\Pi(\varphi)$.

Let us select the dynamic errors, equal to the deviations of the absolute coordinates, in the relevant sections of the inertial elements, from the coordinates of the program motion, as the generalized coordinates. Thus, for the main shaft $q_1 = \varphi_1 - \varphi_0$; $q_{5s-3} = q_{s,1} - \varphi_0$; $q_{5s-2} = \varphi_{s,3} - \varphi_0$, where s is the number of the module, $\varphi_{s,j}$ is the angle of rotation in the cross section j of module s $(s = \overline{1, n})$, and for the executive body $q_{5s} = y_{s,2} - \Pi(\varphi)$; $q_{5s+1} = y_{s,3} - \Pi(\varphi)$, where $y_{s,j}$ is the absolute coordinate in the appropriate section $(j = 1, 2, 3)$. In the model the inertial elements, which correspond to the adopted generalized coordinates, are shown.

When composing the mathematical model, we will use the transition to the dimensionless time $\varphi_0 = \omega t$ and introduce the following functions: $\Psi_{s1} = q_{5s-3} - q_{5s-7}$; $\Psi_{s2} = q_{5s-2} - q_{5s-3}$; $\Psi_{s3} = q_{5s-1} - \Pi'_* q_{5s-3}$; $\Psi_{s4} = q_{5s+1} - \Pi'_* q_{5s-2}$; $\Psi_{s5} = q_{5s-1} - q_{5s+1}$; where $\Pi'_*(\varphi_3) = d\Pi/d\varphi_0$ corresponds to the first geometrical function of cyclic mechanism in the program motion (hereunder the prime marks the derivatives with respect to dimensionless time φ_0). For the selected
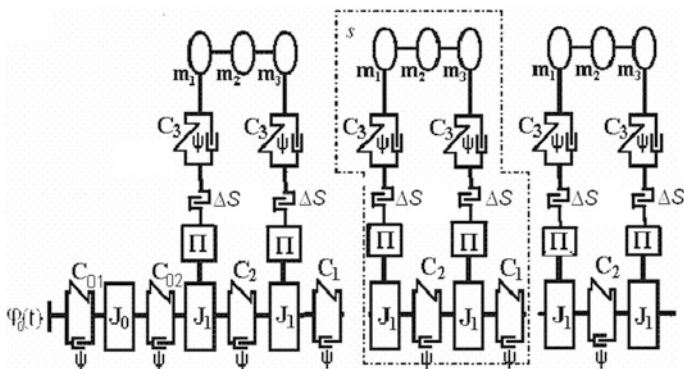
Fig. 12.11 Dynamic model of the branched-ring structure

module s, the system of differential equations, after linearization in the vicinity of the program motion, is reduced to the following form:

$$\left.\begin{array}{l}
q''_{5s-3} + p_1(2\delta_1\Psi'_{s1} + p_1\Psi_{s1}) - p_2(2\delta_2\Psi'_{s2} + p_2\Psi_{s2}) \\
- mJ_1^{-1}p_3\Pi'_*(2\delta_3\Psi'_{s3} + p_3\Psi_{s3} - 0.5\Delta s\,\mathrm{sign}\Psi_{s3})\Lambda_1 = 0\,; \\
q''_{5s-2} + p_2(2\delta_2\Psi'_{s2} + p_2\Psi_{s2}) - p_1(2\delta_1\Psi'_{s6} + p_1\Psi_{s6}) \\
- mJ_1^{-1}p_4\Pi'_*(2\delta_4\Psi'_{s4} + p_4\Psi_{s4} - 0.5\Delta s\,\mathrm{sign}\Psi_{s4})\Lambda_2 = 0\,; \\
q''_{5s-1} + p_3(2\delta_3\Psi'_{s3} + p_3\Psi_{s3} - 0.5\Delta s\,\mathrm{sign}\Psi_{s3})\Lambda_1 \\
+ p_4\mu\delta_4(q'_{5s-1} - 2q'_{5s} + q'_{5s+1}) + 0.25p_4^2\mu^2(q_{5s-1} - 2q_{5s} + q_{5s+1}) = F_1/(m\omega^2)\,; \\
p_2(2\delta_2\Psi'_{s2} + p_2\Psi_{s2}) - p_1(2\delta_1\Psi'_{s6} + p_1\Psi_{s6}) - \\
q''_{5s} + p_4(2\delta_4q'_{5s} + p_4q_{5s}) - 0.5p_4(\sqrt{2}\delta_4\Psi'_{s5} + p_4\Psi_{s5}) = F_2/(m_2\omega^2)\,; \\
q''_{5s+1} + p_3(2\delta_3\Psi'_{s4} + p_3\Psi_{s4} - 0.5\Delta s\,\mathrm{sign}\Psi_{s4})\Lambda_2 \\
+ p_4\mu\delta_4(q'_{5s-1} - 2q'_{5s} + q'_{5s+1}) + 0.25p_4^2\mu^2(q_{5s-1} - 2q_{5s} + q_{5s+1}) = F_1/(m\omega^2)\,.
\end{array}\right\}$$
(12.6)

When $s = 1$ we should accept $q_{5s-7} = q_1$; when $s = n + 1$ $q_{5j+1} \equiv 0$. In system (12.6), in addition to the above notations, we also accept $p_2^2 = c_2/(J_1\omega^2)$; $p_3^2 = c_3/(m\omega^2)$; $p_4^2 = (e_{22}\mu^2\omega^2)^{-1}$; $\mu^2 = m_2/m$; $\delta_i = \psi_i/(4\pi)$; $\Lambda_1 = 0.5 + \pi^{-1}\mathrm{arctg}[(|\Psi_{s3}| - 0.5\Delta s)/\varepsilon]$; $\Lambda_2 = 0.5 + \pi^{-1}\mathrm{arctg}[(|\Psi_{s4}| - 0.5\Delta s)/\varepsilon]$; $F = F_T - \Pi''_i\omega^2$, where F_T is the force of the technological resistance. Functions Λ_1 and Λ_2, when $\varepsilon \ll \Psi_{sj}/\Delta s$ implement the so-called smooth approximation of clearance, which excludes the occurrence of sliding modes during calculations.

One of the most important issues, facing the designer during designing, is related to the feasibility of installation of the intermediate mechanism. In the given case, in Fig. 12.12, the fragment of the model (module s) is represented. Each inertial element in the model corresponds to the appropriate number of generalized coordinate.

Fig. 12.12 Repeated module in case of installation of the additional mechanism
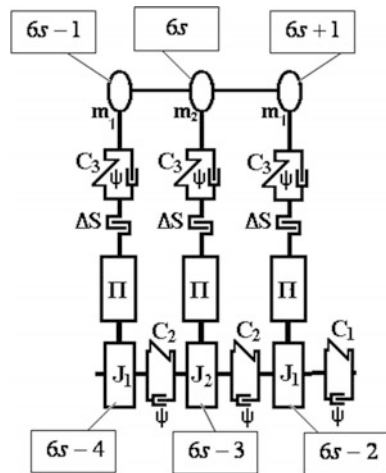
On the one hand, it should be expected that the installation of the additional mechanism must tighten the system and reduce the level of oscillations, but on the other hand, it leads to the increase in the mass of the executive body and the reduced moment of inertia of the drive. These conflicting tendencies do not allow us, a priori, to give a definite answer to the question.

Without the intermediate mechanism (model 1), the repeating unit has five degrees of freedom and after its installation (model 2), it has six degrees of freedom. The total number of degrees of freedom for the first model is equal to $H = 5n + H_0$ and for the second—$H = 6n + H_0$, where n is the number of modules, H_0 is the number of degrees of freedom of the driving mechanism.

For model 2 the system of the differential equations has the following form:

$$\left.\begin{array}{l} q''_{6s-4} + p_1(2\delta_1\Psi'_{s1} + p_1\Psi_{s1}) - p_2(2\delta_2\Psi'_{s2} + p_2\Psi_{s2}) \\ - m J_1^{-1}p_3\Pi'_*(2\delta_3\Psi'_{s3} + p_3\Psi_{s3} - 0.5\Delta s \, \mathrm{sign}\Psi_{s3})\Lambda_1 = 0\,; \\ q''_{6s-3} + p_{2*}(2\delta_2\Psi'_{s2} + p_{2*}\Psi_{s2}) - p_{2*}(2\delta_1\Psi'_{s3} + p_{2*}\Psi_{s3}) \\ - m_2 J_2^{-1}p_4\Pi'_*(2\delta_4\Psi'_{s4} + p_4\Psi_{s4} - 0.5\Delta s \, \mathrm{sign}\Psi_{s4})\Lambda_2 = 0; \\ q''_{6s-2} + p_2(2\delta_2\Psi'_{s2} + p_2\Psi_{s2}) - p_1(2\delta_1\Psi'_{s7} + p_1\Psi_{s7}) \\ - m J_1^{-1}p_3\Pi'_*(2\delta_4\Psi'_{s4} + p_3\Psi_{s4} - 0.5\Delta s \, \mathrm{sign}\Psi_{s4})\Lambda_3 = 0\,; \\ q''_{6s-1} + p_3(2\delta_3\Psi'_{s4} + p_3\Psi_{s4} - 0.5\Delta s \, \mathrm{sign}\Psi_{s4})\Lambda_1 \\ + p_4\mu\delta_4(q'_{6s-1} - 2q'_{6s} + q'_{6s+1}) + 0.25p_4^2\mu^2(q_{6s-1} - 2q_{6s} + q_{6s+1}) = F_1/(m\omega^2); \\ q''_{6s} + p_4(2\delta_4 q'_{6s} + p_4 q_{6s}) - 0.5p_4(\sqrt{2}\delta_4\Psi'_{s5} + p_4\Psi_{s5}) \\ + p_4(2\delta_4\Psi'_4 + p_4\Psi_{s4} - 0.5\Delta s \, \mathrm{sign}\Psi_{s4})\Lambda_2 = F_2/(m_2\omega^2); \\ q''_{6s+1} + p_3(2\delta_3\Psi'_{s6} + p_3\Psi_{s6} - 0.5\Delta s \, \mathrm{sign}\Psi_{s6})\Lambda_3 \\ + p_4\mu\delta_4(q'_{6s-1} - 2q'_{6s} + q'_{6s+1}) + 0.25p_4^2\mu^2(q_{5s-1} - 2q_{5s} + q_{5s+1}) = F_1/(m\omega^2); \end{array}\right\}$$

$$(12.7)$$

In the system of the Eq. (12.7), the functions Ψ_{sj}, Λ_1, Λ_2, Λ_3 are defined as follows: $\Psi_{s1} = q_{6s-4} - q_{6s-8}$ (when $s = 1$, $\Psi_{21} = q_2 - q_1$); $\Psi_{s2} = q_{6s-3} - q_{6s-4}$; $\Psi_{s3} = q_{6s-2} - q_{6s-3}$; $\Psi_{s4} = q_{6s-1} - \Pi'_* q_{6s-4}$; $\Psi_{s5} = q_{6s} - \Pi'_* q_{6s-3}$; $\Psi_{s6} = q_{6s} - \Pi'_* q_{6s-2}$; $\Lambda_1 = 0.5 + \pi^{-1}\arctan[(|\Psi_{s4}| - 0.5\Delta s)/\varepsilon]$; $\Lambda_2 = 0.5 + \pi^{-1}\arctan[(|\Psi_{s5}| - 0.5\Delta s)/\varepsilon]$; $\Lambda_3 = 0.5 + \pi^{-1}\arctan[(|\Psi_{s6}| - 0.5\Delta s)/\varepsilon]$. In addition to the previously introduced notations, we also adopt $p_{2*}^2 = c_2/(J_2\omega^2)$.

Figure 12.13 shows the graphs of oscillations Δy_j and functions $\Delta y''_j$, proportional to the vibration accelerations $(\Delta\ddot{y}_j = \omega^2\Delta y''_j)$. The sections corresponding to the location of the inertial elements are accepted as estimation points. To estimate the values of deformations in the graphs, lines 3 are plotted, which are the boundaries of the clearance Δs.

For model 1 (Fig. 12.13a), when passing through the clearance, clearly set apart are the group of curves 1, corresponding to the average cross section of the working body and the group of the curves 2, corresponding to the coordinates of the utmost sections, directly connected through the cyclic mechanism, to the main shaft. For model 2 (Fig. 12.13b), with an additional mechanism in the middle section of the
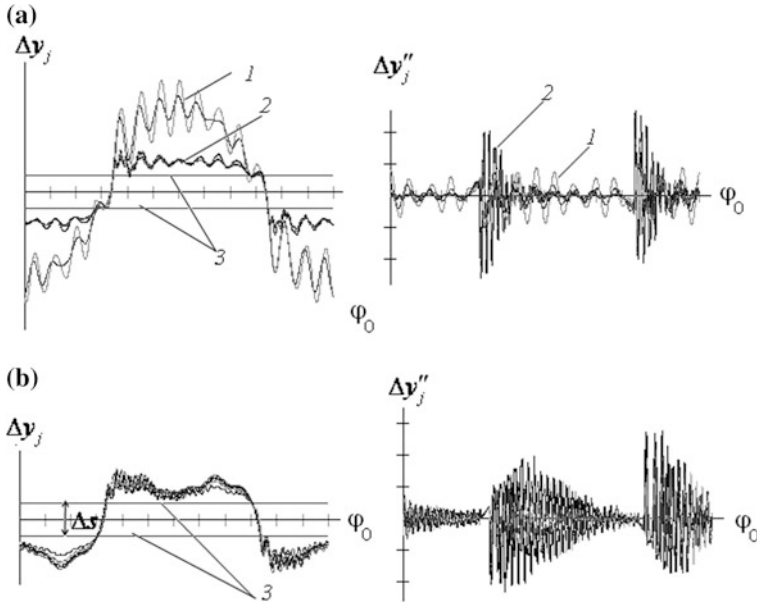
Fig. 12.13 Results of computer simulations

working body, has nearly synchronous oscillations in all sections. When comparing the graphs of acceleration, the marked advantages of this model are not so obvious, which is evident from the zones of growing amplitudes, which leads to the increase in the vibration activity. In the given example, the maximum accelerations, in case of resurfacing in the clearance, are more than twice greater than the maximum accelerations in program motion. The obtained results testify to the results of the analytical study.

12.3 Spatial Localization of Vibrations

12.3.1 Parametric Analysis of the Results of the Computer Simulation

Let us analyze the prerequisite for violations of the synchronous mode of oscillation using the example of the regular model of the circular structure, considered in Sect. 12.2.1 (see Fig. 12.8). Among the possible causes of this effect, we can highlight the following ones: the nonlinear factors, associated with clearances; interference of the oscillations in the dense frequency spectrum and the variability of the parameters; the phase shifts in the argument of the position function $\Pi(\varphi)$ in the different sections of the main shaft. We will show that in the system under consideration, when analyzing the conditions of occurrence of spatial localization of oscillations, we can limit ourselves to the linear formulation of the problem. To eliminate the

influence of the nonlinear factors, we will perform a numerical experiment, in which the clearances are equal to zero and the excitation is caused by the same initial conditions in each estimated section of the working body.

Some results of computer simulation are shown in Fig. 12.14. Fragments 1.1 and 1.2 (Fig. 12.14a) illustrate the change of oscillatory accelerations on the main shaft and the executive body, when n = 5. In the vicinity of $t = 0$ the curves 1 and 2, corresponding to the coordinates q_2 И q_6 (see Fig. 12.8), are almost in-phase, however, subsequently the phase shifts arise, which are associated with significant excitations on the executive body. Let us note that the observed effect conforms to the results obtained above, during the analysis of the mechanical analogue of tunneling of oscillations (see Fig. 12.1).

When $c_{52} = 0$, the dynamic model is transformed into a branched-circular structure. The similar graphs in Fig. 12.11b correspond to this case. Now, the phase shifts on the main shaft are close to zero, during all time intervals (fragment 2.1) and the oscillations attenuate in all sections of the executive body (fragment 2.2).

12.3.2 Analysis of the Factors Influencing Spatial Localization

Conditions of occurrence of spatial localization   It can be assumed that the strong additional excitations of mechanism *n* (see Fig. 12.14a, fragment 1.2) is associated with the specific action of the subsystem, formed by the previous mechanisms,
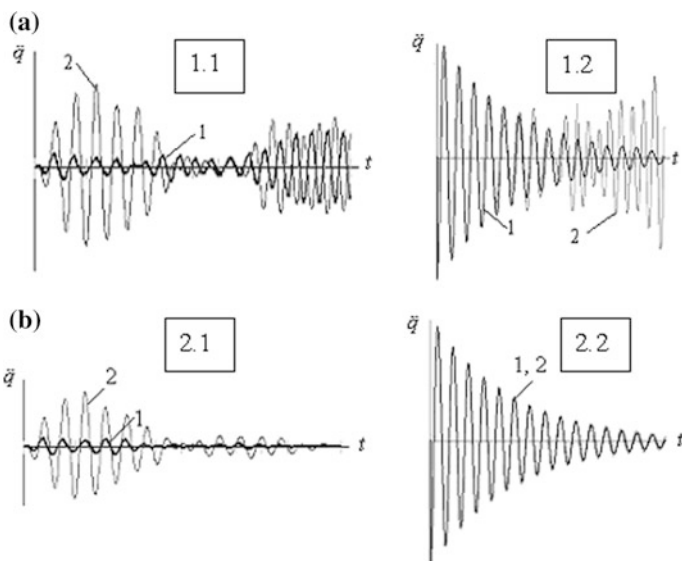
Fig. 12.14 To the analysis of the free oscillations, taking into account the variability of parameters

which in case of synchronous oscillations, manifests itself as a massive inertial member. The justification of this assumption is confirmed by the analysis of the simplified analog of the original model (Fig. 12.15). Let us conditionally divide the original model into the massive part, including $n - n_*$ modules, in which the in-phase oscillations (type 1) dominate and n_* modules with violation of the phase synchronization. Let us recall that before the violation of the phase synchronism, the oscillatory mode is implemented, in which the elastic elements c_2 practically do not participate in the oscillations (see Sect. 12.1).

To get some ideas of the influence of the system's parameters, on the conditions of occurrence of spatial localization, we will investigate the function $\Delta^{-1}(p)$, which is inversely proportional to the modulus of the frequency determinant. This function, which is proportional to the resonant amplitude and to the coefficient of accumulation of perturbations (see Chap. 4), can be considered as an analogue of the frequency response. However, in this case it should be taken into account that the system parameters change slowly, which, as it will be shown below, also plays a significant role.

In Fig. 12.16 depicts some of the results of model analysis, conducted under the following normalized parameter values: $J_1 = J_2 = 1$; $c = |c|(1 + 2\delta i)$; $i = \sqrt{-1}$ (here we used the complex form of consideration of dissipation, when $\delta = 0.03$; $r_0 = 0.8$; $n = 6$; $|c| = 1$); $\zeta_k = |c_k|/|c|$ $(k = 0, 1, 2)$; $\zeta_0 = 4$; $\zeta_1 = 2$; ζ_2, n^*. In the graphs the thick line corresponds to Π'_{max}; apart from that the area corresponding to the whole range of variation of $\Pi'(\varphi)$ is highlighted.

The frequency $p \approx 1$ corresponds to the in-phase oscillations mode. Spatial localization should be expected exactly in the vicinity of this frequency. Since the violations of the phase synchronism originate in the module, which is the remotest from the drive, we must first accept $n_* = 1$.

The first two graphs (Fig. 12.16a) differ by the parameter ζ_2, herewith for $\zeta_2 = 0$ the connection between the subsystems on the driven link is broken. The narrow splash of amplitude, observed in case of internal resonance, corresponds to the steady state, which in case of slow variation of the "natural" frequency has no time

Fig. 12.15 Simplified analogue of the initial dynamic model
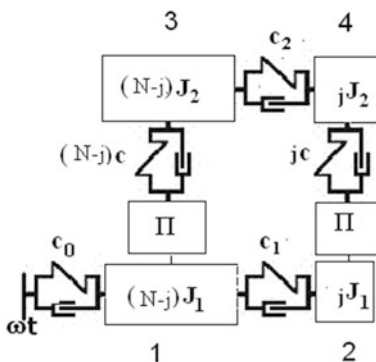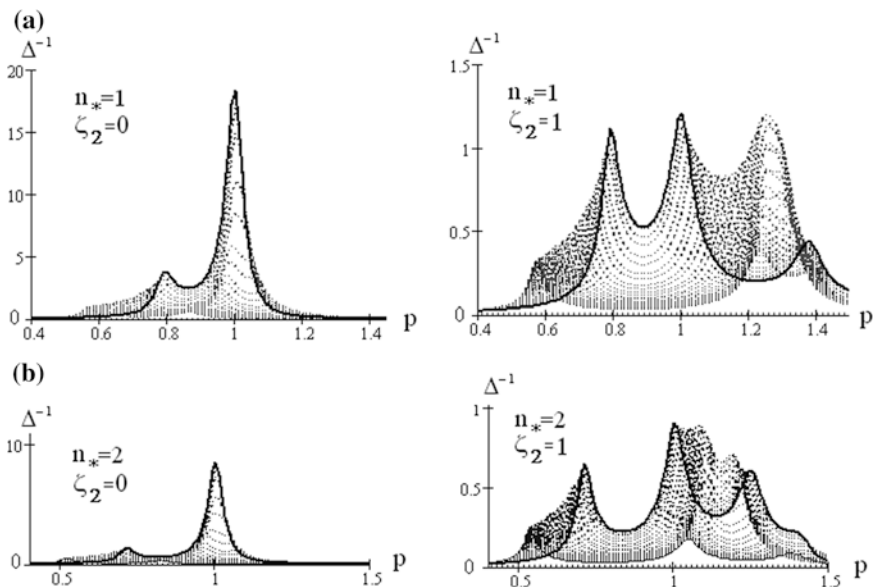
Fig. 12.16 Analogue of the amplitude-frequency characteristics

to be implemented. We can see in the second graph, when $\zeta_2 \neq 0$, the broad frequency band that overlaps the floating frequency of the internal resonance, which leads to the beat mode.

It can be shown that in the revealed frequency range the phase shifts are close to the value of $\pi/2$, whereby the energetic connection between the subsystems appears to be maximum. This fact turns out to be the deciding factor in the transfer of energy from one subsystem to the other. When $n^* = 2$, the graphs are of the similar kind (Fig. 12.16b) and differ only by the smaller excitation.

The influence of variability of the program motion (parameter r_0) Further, we will use the obtained results, to estimate the determining factors of the spatial localization in the model, shown in Fig. 12.8. To compare the intensity of the excited oscillations, as criterion, we choose the ratio of the maximum vibratory acceleration in this section of the executive body to the maximum of acceleration in the program motion $\xi_i = \max|q_i''/r_0|$ when $\Pi'' = r_0 \cos \varphi$. The parameter r_0 in this case is equal to the maximum value of the first geometric transfer function of the cyclic mechanism $\Pi' = r_0 \sin \varphi$, which is the determining factor, influencing the variability of their "natural" frequencies (see Chap. 5).

Figure 12.17 shows the graphs ξ_3 (line 1), ξ_9 (line 2), obtained by computer simulation when $p_0 = 10\,\mathrm{c}^{-1}$, $\zeta_2 = c_2/c = 1,25$ [notations correspond to the system of Eq. (12.5)]. The curves 3, 4 correspond to the results of the theoretical studies (see below). When $0.15 \leq r_0 \leq 0.3$ the repeated collisions in the clearance are absent, in this case for all mechanisms $\xi_i \approx$ const for the fixed value of r_0.

When $r_0 > 0.3$, the vibroimpact modes type 2 (see Fig. 12.9) occur on the last mechanism that leads to the abrupt increase in the value of ξ_9. With the increase in the number of mechanisms n the violations of the synchrony of oscillations of the executive body increase. For the vibration modes type 1 the frequency of the excited oscillations is close to the case $c_1 \rightarrow \infty$ and is described as follows:

$$p_r \approx p_0\sqrt{1 + 2\zeta_2[1 - \cos((r-1)\pi/n)]} \qquad (r = \overline{1,n}), \qquad (12.8)$$

where, $\zeta_2 = c_2/c$; $p_0 = \sqrt{c/J_2}$.

We can represent the reduced stiffness coefficient of the mechanism n, taking into account the compliance of the main shaft, approximately as $c_* \approx c/[1 + \zeta_{1*}^{-1}\Pi'^2(\varphi_0)]$, where $\zeta_{1*}^{-1} = \zeta_{11}^{-1} + \zeta_1^{-1}n, \zeta_{11} = c_{11}/c, c_{11}$ is the stiffness coefficient at the "input" into the regular system (see Fig. 12.8). At the same time formula (12.8) is reduced to the following form:

$$p_*(\varphi_0) = p_0\sqrt{\zeta_2 + (1 + \zeta_{1*}^{-1}\Pi'^2(\varphi_0))^{-1}}. \qquad (12.9)$$

Using (12.9) and the calculated dependencies, represented in Sect. 7.1, for a single impact pulse, when passing through the clearance, it is possible to estimate additional accelerations determined with the parameter ξ_i (see Fig. 12.17, curve 3).

From here on, we will use the energy method of approximate estimation of the possibility of occurrence of increasing oscillations, for excluding which we will require $\Delta\text{Å} = \Delta\text{Å}_+ - \Delta\text{Å}_- < 0$, where $\Delta\text{Å}_+$, $\Delta\text{Å}_-$ is the introduced and withdrawn energy, per one period of oscillation.

Taking into account that at the initial stage of violations of synchrony of vibrations, we have sufficient proximity of the values of p_0 and p_* and accept $q_{2n-1} \approx A\sin(p\varphi_0 + \alpha)$. Then $\Delta\text{Å}_+ \approx \pi\tilde{n}_2\Delta\dot{A}(\dot{A} + \Delta\dot{A})\sin\gamma$, $\Delta\text{Å}_- \approx \vartheta_*c_*(A + \Delta A)^2$,

Fig. 12.17 To the analysis of the criterion $\xi_i = \max\left|q_i''/r_0\right|$
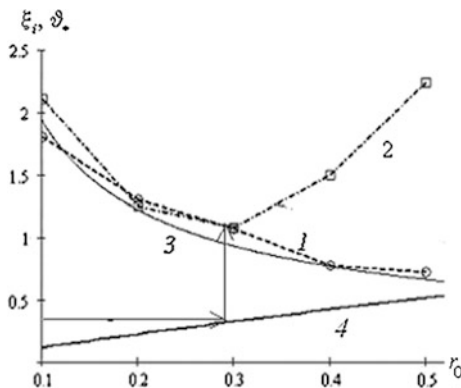
where γ is the phase shift in the oscillations of the n and n $-$ 1 mechanisms; $\vartheta_* = 2\pi\delta_*$ is the reduced value of the logarithmic decrement. It follows:

$$\Delta A/A < \vartheta_*/(\pi\varsigma_{2*} \sin\gamma - \vartheta_*), \tag{12.10}$$

where $\zeta_{2*} = c_2/c_*$.

Usually when $\Delta A/A > 0.1 \div 0.15$, the condition (12.10) is violated, and, as shown by computer simulation $\gamma \approx \pi/2$. If we take the function $\Delta A/A$ inversely proportional to the ratio of c/c_* then when $\gamma = \pi/2$, using (12.10) we obtain the following condition:

$$\vartheta < \vartheta_* = \pi\zeta_{2*}/(1 + \zeta_{1*} r_0^{-1}). \tag{12.11}$$

We can see in Fig. 12.17, the graph of $\vartheta_*(r_0)$ (curve 4), for the accepted above data. In our case $\vartheta \approx 0.2$ ($\delta \approx 0.03$); with this the condition $r_0 < 0.25 \div 0.3$ must be satisfied. Thus, in spite of the approximate nature of the above calculations, this result is in good agreement with the results of computer simulations.

In (12.10), (12.11) only one factor of possible increase in amplitudes is taken into account, namely that one which is associated with structural changes of the implemented form, caused by the "attachment" of the elastic element c_2.

Another factor is the slow change of the "natural" frequency, which may reduce the effective dissipation coefficient and even lead to the so-called negative dissipation (see Sect. 5.3.1). As a result of this, the violations of the dynamic stability can occur in a limited period of time. In this case, the effective value of the logarithmic decrement is defined by the following expression (see Sect. 5.3.1):

$$\tilde{\vartheta} = \vartheta - \vartheta_p, \tag{12.12}$$

where

$$\vartheta_p(\varphi_0) = \frac{(u - 0.5)\pi r^2 \sin 2\varphi_0}{2p\varsigma_{1*}v^3(\varphi_0)(1 + \varsigma_{1*}^{-1}r^2 \sin^2\varphi_0)^2};$$

$u = 0, 1, 2$ for oscillations, vibration velocities and vibration accelerations, respectively.

The analysis of (12.12) shows that in reality the value of $\max|\vartheta_p|$ can be comparable and sometimes even exceeds the original value of the logarithmic decrement ϑ. Then $\tilde{\vartheta}_{\min} \approx 0$ or even $\tilde{\vartheta}_{\min} < 0$. This effect is particularly evident for the vibration acceleration ($u = 2$) for relatively flexible main shaft. Extreme of the function ϑ_p, in case of harmonic position function, is usually located in the vicinity of $\varphi_0 = 3\pi/4$ and $\varphi_0 = 5\pi/4$. This explains, the observed during the experiments, phase shifts of the maximum oscillation zones, caused by a clearance, relative to the moment of transition through the clearance.

Non-stationary interference forms. Beats As already mentioned, in proximity of
the "natural" frequencies the energy is transferred from one form into another. The
behavior of the system in such cases, was figuratively described, by Mandelstam, as
"contagious" [36]. Because of the variability of the frequencies in this case the
observed energy transfer has non-stationary character. Herewith, it should be borne
in mind that the time required to reach the extreme values of partial frequencies,
which under the current transfer function $\Pi'(\varphi)$ corresponds to the angle $\varphi = \pi/2$,
plays a certain role.

We can see, in Fig. 12.18, the graphs of the dimensionless "natural" frequencies
$v_{0r}(n) = p_r(n)/p_0$, built as per formula (12.9), when $r = 1; 2$. The height of
"columns" corresponds to the range of variation of frequencies, when the position
function of the mechanism is $\Pi(\varphi)$. For a small number of modules n the areas of
the frequency variation are almost not overlapping, at the same time, for the large
values of density of frequencies condensation, increases abruptly. This situation, of
course, does not correspond to the multiple frequencies, since it corresponds to the
different moments of the "slow" time, however, it provides evidence of the prox-
imity of the frequencies in these forms. Herewith, for the same frequency range, it is
possible to have both the in-phase oscillations (r = 1), as well as the oscillations in
anti-phase (r = 2). Suppose that in each cycle there are impulse disturbances, which
cause the free oscillations of the system. Such excitations are met in practice, in
case of sampling small clearances, when the nonlinear effect, inherent to the
clearances, substantially does not occur and only causes the short impact impulse
due to the quick change of the function $\Pi'(\varphi)$ (see Chap. 7).

After simple calculations, we find that in order to achieve the maximum of the
beats, it is necessary to satisfy the condition $2\zeta/|\Delta v| < \eta$, where $|\Delta v| = |v_j(r_1) - v_j(r_2)|$ is the frequency detuning; r_1, r_2 are the numbers of the adjacent
oscillatory modes; η is the number of the periods of free oscillations in the period
$2\pi/\omega$.

Fig. 12.18 The ranges of variation of the dimensionless "natural" frequencies
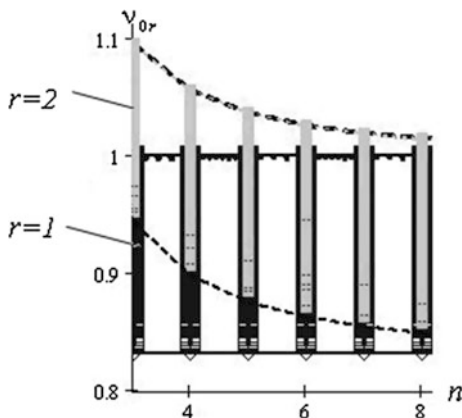
We should also take into account the system's dissipation and the possibility of accumulation of perturbations in the steady state. Consideration of these factors leads to the following sufficiently effective assessment of the effect [77]:

$$\chi = \frac{v^2(r_1)\sin[0.5\pi\eta|\Delta v/(r_1)|]}{\sqrt{\Delta v^2 + (\vartheta/\pi)^2 v(r_1)^4}}.$$

(12.13)

Here, χ is the criterion, which characterizes the increase in the level of amplitude, in case of beats, by energy transfer from one form to another; $\vartheta = 0.5\psi$ is the logarithmic decrement.

We can see in Fig. 12.19 the typical plots, when $\chi(\eta, n)$ at $n = 3, n = 5, n = 6$. For the first two cases the curves correspond to the averaged around φ value of the function Π'^2, and when $n = 6$, the curves are the boundaries of the crosshatched regions, obtained when $0 \le |\Pi'| \le |\Pi'|_{max}$.

Analysis of the graphs show that in case of increase in the number of mechanisms n, the value of χ_{max} typically increases, although with particular frequency tuning η the situations can arise, where the lower value of n corresponds to the higher value of χ (see, for example, the case $n = 5$ and $n = 6$ in the vicinity of $\eta \approx 20$).

We often come across the need to use the theory of regular systems for the study of quasi-regular systems, when there are deviations from the strict spatial periodic structure of the dynamic model. Essentially, we are talking about the already mentioned "inclusions", the consideration of which can lead to the localization of oscillations in certain sections. In this case, the system is particularly sensitive to disruption of spatial symmetry.

Estimation of the influence of vibro-impact regimes Here above, on the basis of the linear system, with variable parameters, we observed the dynamic effects from the single collision, in case of adjustment of clearance and the conditions for the excitation of vibro-impact regimes.

Fig. 12.19 Graphs of the criterion $\chi(\eta)$
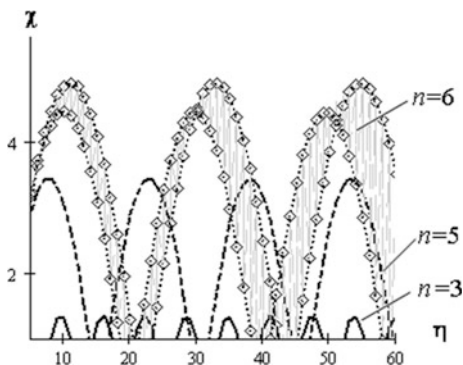
In case of their occurrence, due to nonlinear factors, the frequency spectrum of oscillations may change significantly, for the analysis of which, we will use the method of harmonic force linearization [4]. Then, if $\left|(\xi_0^*)^{-1}\cos\varphi_0\right| \geq 1$, we have $\nu(\varphi_0) = \nu_0(\varphi_0)$, where $\nu_0(\varphi_0)$ corresponds to formula (12.9). In case of breach of this condition

$$\nu(\varphi_0) = p_*/p_0 = \sqrt{\zeta_2 + \nu_0^2(\varphi_0)[1 + 2\Delta s(\pi\xi_{0*}r)^{-1}\eta^2\sqrt{1 - \xi_{0*}^{-2}\cos^2(\varphi_0)}]}. \tag{12.14}$$

With (12.14) we obtained the family of graphs $\nu(\varphi_0, \varsigma_2)$ (Fig. 12.20). In case of synchronous mode of oscillations and rigid main shaft ($\varsigma_1 \to \infty$) we have $\nu = 1$ (line 1). The rest of the graphs correspond to $\zeta_1 = 2.5$ when $\zeta_2 = 0; 0.05; 0.5; 1; 2$ (accordingly curves 2–6).

With the increase in the coefficient of stiffness c_2 the width of the "cavity" grows on the frequency characteristics, corresponding to the resurfacing in the clearance, however, their depth decreases, which is in line with the physical representations of the considered vibration modes with "soft" nonlinearity. During computer simulations, it was revealed that in case of real level of dissipation and breach of the synchronous oscillatory modes, the process of reaching the steady state, usually takes about 3–5 rotation periods of the main shaft.

For the approximate estimation of levels of amplitude, in case of steady state, we can use the analysis of the effect of the parametric pulse, described in Sect. 5.5, where it's been shown that in case of the impulsive nature of variation of the "natural" frequency, the maximum factor of the increase in amplitude for the period $T_\omega = 2\pi/\omega$ is determined as

$$\kappa_T = \exp(-\bar{\vartheta}_*\bar{p}_*)\prod_{i=1}^{N}|\Delta\nu_i|,$$

where $\Delta\nu_i$ is the relative depth of frequency pulsation, caused by the clearance (mean values are marked with a dash); N is the number of resurfacings in the

Fig. 12.20 Graphs of variation of "natural" frequencies, taking into account the clearances
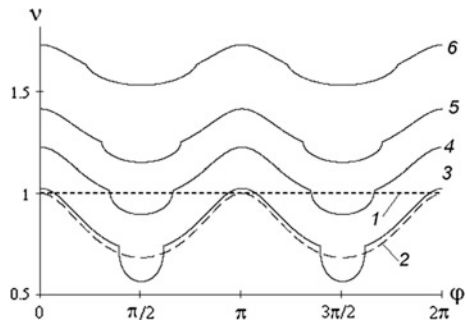
clearance for the period T_ω (in the absence of vibro-impact modes $N = 2$). For the steady-state regimes, we have $\kappa_{max} = \kappa_T \mu$, where $\mu = [1 - \exp(-\bar{\vartheta}_* \bar{p}_*)]^{-1}$ is the factor of accumulation of disturbances. Thus

$$\kappa_{max} = [\exp(\bar{\vartheta}_* \bar{p}_*) - 1]^{-1} \prod_{i=1}^{N} |\Delta v_i| \qquad (12.15)$$

As it can be seen in the graphs, $v(\varphi_0)$, in case of breach of form phase synchronism, the frequency, of the excited oscillations, increases, due to the inclusion of additional stiffness and decreases in case of the breach of the kinematic contact in the clearance. The least dynamic effect should be expected at $|\Delta v_i| \to \min$, where these two trends cancel each other.

The coefficients κ_{max}, obtained using formulae (12.15), are in good agreement with the results of computer simulations. Specifically, for the mode $r_0 = 0.5$ (see Fig. 12.17, curves 1 and 2), this coefficient corresponds to the relative difference in the value of ξ_9 / ξ_3.

A combined analysis of these dependencies shows that in case of dynamic synthesis the reasonable compromise should be considered, since we should take into account the opposite tendencies of influence of partial frequencies of the mechanism (parameter p). For large values of p the level of excitation, due to the single resurfacing in the clearance, increase and for small values, the coefficient of accumulation of disturbances and the amplitude of oscillations caused by kinematic excitation, which occurs when $\Pi''(\varphi_0) \neq 0$.

Thus, to ensure the normal operation of the drives of such class, the number of the mechanisms must be restricted in such a way, as to exclude the possibility of the break-down of in-phase oscillatory form and arising of the vibro-impact regimes. In such cases, one of the appropriate methods, of constructive solutions of this problem of dynamic synthesis, is the transition to the multi-modular structure of the drive, where the long executive body is replaced with separate sections, with the limited number of mechanisms (see Fig. 12.14). The sections are still connected to the general main shaft. In addition to the criteria ξ_i for comparing the vibration modes, particularly informative during the estimation of intensity of possible vibro-impact modes, caused by the clearances, is factor K_Δ: which is the number of discontinuities in the kinematic chain, for one period of the kinematic cycle. For modes shown in Fig. 12.9b, we have $K_\Delta = 5$ on the first mechanism (i = 3), and $K_\Delta = 9$ on the last (i = 9). The removal of the elastic member between the last two blocks (see Fig. 12.8, $c_{42} = 0$) leads to the decrease in the criterion ξ_9 from 2.52 to 0.63 and the number of breaks K_s, in this case, is reduced from nine to two.

In conclusion we shall note that with respect to the class of systems under consideration, we have to face the same difficulties, which occur in the description of complex dynamic systems, formed of bearing structures, with lots of fixing elements [7, 19].

In particular in case of the frequency spectrum of high density, expansion into series of natural forms appears to be ineffective [37]. For the given problem the

variability of the parameters leads to additional complications; thus within the same kinematic cycle occurs the structural transformation of the system, accompanied by the degeneration of certain forms of oscillations and the appearance of new ones.

Slowly varying coincident waves, which are manifested in the form of spatial localization of the oscillations in the certain areas of the objects under consideration, occur in the system. At the same time the excited free accompanying oscillations often do not decay, because there is an energy "make-up" due to parametric effects. The study of the given problem, of course, cannot be considered exhausted, both in general terms and with respect to the considered class of problems [1].

---

[1]   In the development of this issue, see : Vulfson I. I. Energy transfer in vibratory systems of drives with cyclic mechanisms. Journal of machinery manufacture and reliability . V.42, No4, 2013. Pp.– 261-268.

Appendix
Method of Harmonic Linearization

General information A brief description of this method is restricted, only to the applied side of the issue. Let the restoring force and resistance be described by the nonlinear function $-P(q, \dot{q})$. Then the differential equation, describing the oscillations of the system, with one degree of freedom, in case of the action of the harmonic driving force, takes the form

$$a\ddot{q} + P(q, \dot{q}) = F_0 + F_1 \sin \omega t \qquad (A.1)$$

or after dividing by the factor of inertia a

$$\ddot{q} + U(q, \dot{q}) = W_0 + W_1 \sin \omega t, \qquad (A.2)$$

where $U = P/a$; $W_0 = F_0/a$; $W_1 = F_1/a$.

By analogy to the linear oscillatory system an approximate solution of Eq. (A.2) will be sought in the form

$$q^0 = A_0 + A \sin(\omega t - \gamma). \qquad (A.3)$$

After substitution of (A.3) in $U(q, \dot{q})$, this function appears to be periodic, and therefore it can be represented as the Fourier series

$$U(q^0, \dot{q}^0) = U_0 + U_c \cos \varphi + U_s \sin \varphi + \text{higher harmonic}, \qquad (A.4)$$

where $\varphi = \omega t - \gamma$.

We assume that the higher harmonics (A.4) have little influence on the formation of the approximate solutions (A.3), i.e. on A_0, A_1. This assumption is realized if the oscillations are close to harmonic. In this case the judgment, about the validity of this assumption, should be based on the physical background, for example, on the experiment, operating experience, etc.

Let us note here that in the problems of nonlinear mechanics, the performance of the approximate analytical methods largely depends on how correctly the form of the approximate solutions is "guessed".

We will further introduce the formal linear differential equation

$$\ddot{q}^0 + 2n\dot{q}^0 + k^2 q^0 + S = W_0 + W_1 \sin \omega t, \tag{A.5}$$

where, n, k^2 are some unknown functions, and S is the unknown constant.

On the other hand, Eq. (A.2), taking into account (A.3), (A.4) and the above assumptions, can be written as

$$\ddot{q}^0 + U_c \cos \varphi + U_s \sin \varphi + U_0 = W_0 + W_1 \sin \omega t. \tag{A.6}$$

Comparing (A.6) and (A.5), we obtain

$$2n\dot{q}^0 + k^2 q^0 + S = U_c \cos \varphi + U_s \sin \varphi + U_0.$$

Then, taking into account (A.3), after the equalization of the coefficients at $\cos \varphi$, $\sin \varphi$ and free terms, we get $k^2 A_0 + S = U_0$; $2nA\omega = U_c$; $k^2 A = U_s$.

Using formulae for determining the Fourier coefficients, we finally obtain

$$\left.\begin{array}{l} S(A, A_0) = \dfrac{1}{2\pi} \displaystyle\int_0^{2\pi} U(q^0, \dot{q}^0) d\varphi - k^2(A, A_0)A_0; \\[3ex] 2n(A, A_0) = \dfrac{1}{\pi A \omega} \displaystyle\int_0^{2\pi} U(q^0, \dot{q}^0) \cos \varphi \, d\varphi; \\[3ex] k^2(A, A_0) = \dfrac{1}{\pi A} \displaystyle\int_0^{2\pi} U(q^0, \dot{q}^0) \sin \varphi \, d\varphi. \end{array}\right\} \tag{A.7}$$

These functions are called the *harmonic linearization coefficients*. So, using the accepted assumptions, the nonlinear differential equation (A.2), in case of using the accepted approximate solutions, is formally equivalent to the linear differential equation (A.5), the coefficients of which n, k^2, S, are the known functions of the unknown parameters of solution A, A_0.

For small values of n, function k corresponds to the frequency of free oscillations, which now, in contrast to the linear case, depends on the level of amplitude.

Coefficient $2n$, as in case of the linear oscillations, characterizes the dissipative properties of the system, which, as already noted, in the engineering problems, are usually evaluated by the dissipation coefficient ψ or by the logarithmic decrement ϑ. For the formal linear equation (A.5), the valid relationship is $n/k = \delta = \vartheta/(2\pi)$.

At the same time

$$2n(A, A_0) = \vartheta k(A, A_0)/\pi. \tag{A.8}$$

It can be shown that (A.8), when taking into account the approximate solutions (A.3), is energetically equivalent to the corresponding expressions in (A.7), however, quite often, it is more convenient, while solving engineering problems, since an analytical description of the dissipative forces, in many cases, is not possible or is very difficult. Meanwhile, the definition of parameters ϑ or ψ generally does not cause difficulties, even in those cases, where these parameters are dependent on the amplitude levels of A, A_0.

Strictly speaking, the real dissipative forces, arising in case of machine and mechanism oscillations, are always nonlinear, so their inclusion in previous chapters, devoted to the linear oscillations, essentially also meets the harmonic linearization of these forces. In this case, according to (A.8), when $k = \text{const}$ and $\lambda = \text{const}$, we have $n = \text{const}$, which allows us to use the linear differential equations to analyze system oscillations (see Chap. 6).

Let us mention the following important property of the linearization coefficients, which allows us to reduce the complex non-linear functions to the combination of more simple ones.

If the nonlinear function U can be represented as a sum $U = \sum\limits_{i=1}^{s} U_i$ then the coefficients of harmonic linearization are defined as the sum of the corresponding partial values

$$n = \sum_{i=1}^{s} n_i; \ k^2 = \sum_{i=1}^{s} k_i^2; \ U = \sum_{i=1}^{s} U_{0i}.$$

No limiting requirements are required from the form of the function $U(q, \dot{q})$. In particular, these functions can be composed of individual segments and have discontinuities of the first kind. We will emphasize that harmonic linearization, in contrast to the usual linearization, when the nonlinear function is replaced by the linear one, does not require that q and $\dot{q}$ should be quite small. The only limitation here is the proximity to the harmonic oscillations.

Forced nonlinear oscillations   For greater clarity, we will consider the widespread case $U_0 = 0$ and $A_0 = 0$ that means no constant component in the driving force $(F_0 = 0)$ and an odd function $P(q)$, described in Eq. (A.1) the nonlinear restoring force $(P(q) = -P(-q))$.

To solve Eq. (A.1), obtained by harmonic linearization method, we use the solution for the linear system with one degree of freedom (see Sect. 4.1.2)

$$A = \frac{W_1}{\sqrt{[k^2(A) - \omega^2]^2 + 4n^2(A)\omega^2}}; \qquad (A.9)$$

$$\tan\gamma = \frac{2n(A)\omega}{k^2(A) - \omega^2}. \qquad (A.10)$$

However, the performed linearization leads to the fact that the coefficients of harmonic linearization k^2 and n are the functions of unknown amplitude of forced oscillation A. Therefore if for the linear system, formula (A.9) is the final calculation expression, then now it appears to be the equation with respect to A.

To construct the frequency response $A(\omega)$ it is convenient to use the following method. Take square from both sides of the Eq. (A.9) and write it as follows:

$$A^2\{[k^2(A) - \omega^2]^2 + 4n^2(A)\omega^2\} = W_1^2. \qquad (A.11)$$

Relative to ω, the Eq. (A.11) is the biquadratic one. So it allows us to determine ω as the appropriate values of this equation's roots. The resonance mode corresponds to the condition

$$k(A_*) = \omega, \qquad (A.12)$$

where A_* is the amplitude of resonance.

Then according to (A.9) $2n(A_*)A_*\omega = W_1$, or with reference to (A.8), (A.12)

$$\vartheta A_* k^2(A_*)/\pi = W_1. \qquad (A.13)$$

Thus, the resonant amplitude A_* can be determined as the root of the Eq. (A.13); herewith the phase shift γ according to (A.10) is equal to $\pi/2$.

We will consider the characteristics of nonlinear forced oscillations, using the example of the cubic characteristic of the restoring force $-c_0 q(1 + \xi q^2)$. With $\xi > 0$ the characteristic is termed as "hard", with $\xi < 0$ the one—as "soft", and when $\xi = 0$ it is linear. For given example Eq. (A.1) has the form of Duffing equation

$$a\ddot{q} + b_0\dot{q} + c_0 q(1 + \xi q^2) = F_1 \sin \omega t,$$

and after dividing by the coefficient a

$$\ddot{q} + 2n_0\dot{q} + k_0^2 q(1 + \xi q^2) = W_1 \sin \omega t, \qquad (A.14)$$

where $2n_0 = b_0/a$; $k_0^2 = c_0/a$.

So with the account of the above mentioned, about the symmetry of nonlinearity and the oscillatory process

$$U(q^0, \dot{q}^0) = 2n_0 A\omega \cos \varphi + k_0^2 A \sin \varphi (1 + \xi A^2 \sin^2 \varphi); \left.\begin{array}{c} \\ \\ \end{array}\right\}.$$
$$q^0 = A \sin \varphi; \varphi = \omega t - \gamma.$$

According to (A.1)

$$2n(A) = (\pi A\omega)^{-1} \int_0^{2\pi} [2n_0 A\omega \cos \varphi + k_0^2 (A \sin \varphi + \xi A^3 \sin^3 \varphi)] \cos \varphi d\varphi;$$

$$k^2(A) = (\pi A)^{-1} \int_0^{2\pi} [2n_0 A\omega \cos \varphi + k_0^2 (A \sin \varphi + \xi A^3 \sin^3 \varphi)] \sin \varphi d\varphi.$$

After integration, we have $2n = 2n_0$ and

$$k^2(A) = (1 + 0.75\xi A^2)k_0^2. \tag{A.15}$$

Dependence $\omega = k_0\sqrt{1 + 0.75\xi A^2}$ obtained from (A.15), when $k = \omega$, defines the so-called skeleton curve shown in the graphs $A(\omega)$, with hatch-dotted line (Fig. A.1). To construct the graph of the amplitude-frequency characteristic, we substitute (A.15) into Eq. (A.11) and convert it into the biquadratic equation relative to ω:

$$\omega^4 - 2[k^2(A) - 2n^2(A)]\omega^2 + k^4(A) - W_I^2/A^2 = 0.$$

After solving the given equation we get

$$\omega = \sqrt{k^2(A) - 2n^2(A) \pm \sqrt{W_I^2/A^2 - 4n^2(A)[k^2(A) - n^2(A)]}}. \tag{A.16}$$
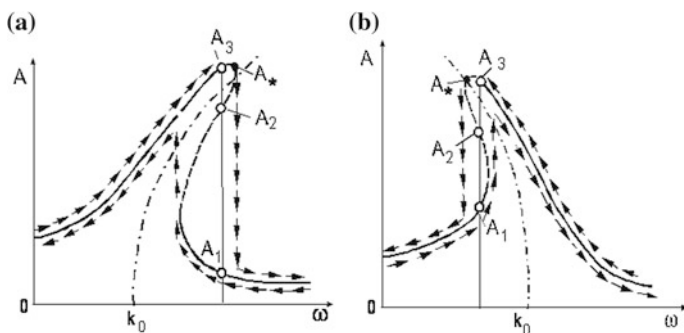
Fig. A.1 Amplitude-frequency characteristic (AFC)

When $\xi > 0$ ("hard" characteristic), the resonance peak inclines to the right (Fig. A.1a) and when $\xi < 0$ ("soft" characteristic), to the left (Fig. A.1b).

Because of the inclination of AFC *several values of the amplitudes of forced vibrations (A_1, A_2, A_3) correspond to one frequency in the certain fixed frequency range* limited by the inflection points. In addition to that, the zone of increased amplitudes now covers a much larger frequency range, as compared to the frequency response of the linear system. The resonant amplitude A_* is determined from the Eq. (A.13) in the reference to (A.15):

$$A_*(1 + 0.75\xi A_*^2)\vartheta k_0^2 - \pi W_1 = 0. \tag{A.17}$$

Here ϑ is logarithmic decrement.

The change of amplitudes, caused by the smooth increase or decrease in frequency ω, is represented on AFC, using arrows. In the vicinity of inflection points the hopping from one branch of the characteristic to another occurs, which is accompanied by an abrupt change in the amplitude of forced oscillations. Thus, the implementation of a mode may depend on the conditions of entrance into this mode.

In general, when $U_0 \neq 0$, we have $A_0 \neq 0$, and the values A and A_0 are determined by the system of equations obtained on the basis of (A.7). Then

$$k^2 = k_0^2[1 + \xi(3A_0^2 + 0.75A^2)].$$

Stability of the modes of forced oscillations We will use the energy method, for the determination of the stability of the identified periodic modes. In case of forced oscillations the introduced energy is defined as $\Delta E_+ = \pi A F_1 \sin \gamma$ and the withdrawn one as $\Delta E_- = 2\pi n \omega A^2 a$.

The indicative graph $\Delta E = \Delta E_+ - \Delta E_-$ for the fixed value of ω, to which the three modes with amplitudes A_1, A_2, A_3 correspond, is represented in Fig. A.2.

Obviously when $\Delta E > 0$ the amplitude increases, otherwise, it decreases, when $\Delta E < 0$. When $\Delta E = 0$, the regime is stationary. However for practical implementation of this mode, it is necessary for it to be stable. In other words, in case of deviations $\Delta A_i = A - A_i \,(i = 1, 2, 3)$, the condition $\Delta A_i \to 0$; $A \to A_i$ is satisfied. Using these simple considerations, we can easily verify that amplitudes A_1 and A_3 correspond to the stable regimes and amplitude A_2 to the unstable regime. The stability condition can be written as follows:

$$\partial(\Delta E)/\partial A < 0 \quad (A = A_i) \tag{A.18}$$

Fig. A.2 To the definition of the conditions of stability of the forced oscillations
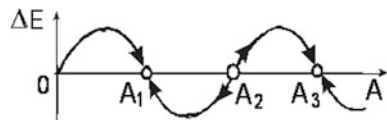
It turns out that the stable regimes in the zone, before resonance, have a positive AFC slope, and in the zone after resonance they have the negative slope of the response curve. The branches of the response (AFC), shown in the Fig. A.1, with hatched lines, correspond to the unstable regimes. Unstable branch of the frequency response is limited by the inflection points, at which the tangent to the graph $A(\omega)$ is vertical. Despite the fact that the unstable modes can not practically be implemented, the corresponding, to these regimes, branch of the response is of particular interest.

Suppose, for example, the system oscillated in the steady state regime with amplitude A_1, and then as a result of an accidental disturbance (e.g. impact) it experiences amplitude increment $\Delta A > 0$. Obviously if $A_1 + \Delta A < A_2$, then $\Delta E < 0$ and therefore, we return to the mode $A = A_1$. However, if $A_1 + \Delta A > A_2$, then $\Delta E > 0$ and further system oscillations occur with amplitude A_3.

The dependence of the regime of the implemented forced oscillations, from the initial conditions, is detected similarly.

If the initial amplitude A_0 is smaller than A_2, then $A \rightarrow A_1$ and when $A_0 > A_2$, we have $A \rightarrow A_3$. Thus, the unstable regime in the first approximation serves as a "dividing line" between the two stable states.

References

1. Antonyuk, E. Ya. (1988). *Dynamics of the mechanisms with variable structure*. Kiev: Nauk. dumka (in Russian).
2. Astashev, V. K. (1971). *The dynamics of an oscillator impacting a limiter*. Machinovedenie (Machine science) (2) (in Russian).
3. Astashev, V. K., & Babitsky,V. I. (2007). *Ultrasonic processes and machines*. Berlin: Springer.
4. Babitsky, V. I. (1998). *Theory of vibro-impact systems and applications*. Berlin: Springer.
5. Babitsky, V. I., & Krupenin, V. L. (2001). *Vibration in strongly nonlinear discontinuous system*. Berlin: Springer.
6. Banakh, L. Ya. (1981). *The study of the dynamics of regular and quasi-regular systems by means group theory*. Kolebaniya slozhnyh uprugih system, 5–11 (in Russian).
7. Banakh, L., & Kempner, M. (2010). *Vibrations of mechanical systems with regular structure*. New York: Springer.
8. Biderman, V. L. (1980). *Theory of mechanical oscillations*. Moscow: Vyshaja shkola (in Russian).
9. Blekhman, I. I. (1999). *Vibrational mechanics*. Singapore: World Scientific.
10. Blekhman, I. I., Myshkis, A. D., & Panovko Ya, G. (1983). *Mechanics and Applied Mathematics*., Logic and features of the mathematics applications Moskow: Nauka. (in Russian).
11. Bogoliubov, N. N., & Mitropolsky, Ju. A. (1958). *Asymptotic methods in the theory of nonlinear oscillations*. New York: Gordon & Breach.
12. Brilloin, L., & Parodi, M. (1959). *Propagation of waves in periodic structures*. Moscow: Izd-vo inostr. lit. (in Russian).
13. Briskin, E. S., Zhoga, V. V., Maloletov, A. V., & et al. (2009). *Dynamics and motion control of walking machines to the cycle movers*. In E. S. Briskin (Ed.), Mashinostroenie, Moscow (in Russian).
14. Dresig, H. (2005). *Schwingungen mechanischer Antriebssysteme*. Berlin: Springer (in German).
15. Dresig, H., & Holzweiβig, F. (2010). *Dynamics of Machinery*. New York: Springer.
16. Dresig, H., & Vulfson, I. I. (1989). *Dynamik der Mechanismen*. Wien, New York: Springer (in German).
17. Dubowsky, S. (1974). On predicting the dynamic effects of clearances in planar mechanisms. *ASME Journal of Engineering for Industry, 93*(1), 317–323.
18. Kreynin, G. V. (Ed.). (1988). *Handbook: Dynamics of machines and machine control*. Moscow: Mashinostroenie (in Russian).
19. Filippov, A. P. (1970). *Oscillations of the deformed systems*. Moscow: Mashinostroenie (Russian).
20. Freman, N., & Freman, P. (1967). *JWKB-approximation*. Amsterdam: North Holland Publ. Comp (in Russian).

21. Frolov, K. V., Popov, S. A., & et al. (2005). *Theory of mechanisms and mechanics of machines: a textbook for the stud. of universities*. In K. V. Frolov. Vysh. shk. (in Russian).
22. Gantmakher, F. R. (1966). *The theory of matrices*. Moscow: Nauka. (in Russian).
23. Heines, R. S. (1980). A theory of contact loss at revolute joints with clearance. *Journal Mechanical Engineering Science, 22*(3), 129–136.
24. Hitrik, V. E., & Shmakov, V. A. (1978). Study of laws sliding friction in the nonstationary modes of motion. Vibrotechnika, 2(32), 97–106. (in Russian).
25. Indeytsev, D. A., Kuznetsov, N. G., Motygin, O. V., et al. (2007). *Localization of linear waves*. Saint-Petersburg: Saint-Psb. Univ. (in Russian).
26. Kolovsky, M. Z. (1989). *Machines dynamics*. Leningrad: Mashinostroenie (in Russian).
27. Kolovsky, M. Z. (1966). *Nonlinear theory of the vibroprotected systems*. Moscow: Nauka (in Russian).
28. Kolovsky, M. Z. (1963). Effect of high-frequency disturbances on the resonant oscillations in the nonlinear system. *Dinamika i prochnost mashin, LPI., 226*, 7–17. (in Russian).
29. Kolovsky, M. Z., Evgrafov, A. N., & et al. (2006). *Advanced theory of mechanisms and machines: textbook*. Academia, Springer (in Russian).
30. Kolsch, H. (1993). *Simulation und Indefikation von Bauteilen mit statische Hysterese*. Dämpfung und Nichtlinearität Düsseldorf : VDI . Verlag, 179–194 (in German).
31. Korn, G., & Korn, T. (1961). *Mathematical handbook for scientists and engineers*. New York: Mgraw-Hill Book Company.
32. Kovaleva, A., Manevitch, L., & Kosevich, Y. (2011). Fresnel integrals and irreversible energy transfer in an oscillatory system with time-dependent parameters. Physical Review E. 2011. V. 83, 026602-1-12.
33. Landa, P. S. (1996). *Nonlinear oscillations and waves in dynamical systems*. Dordrecht: Kluwer.
34. Lurie, A. I. (2002). *Analytical mechanics*. Berlin: Springer.
35. Magnus, K. (1965). *Vibrations*. Glasgow: Blackie & Son.
36. Mandelstam, L. I. (1972). *Lectures on the theory of oscillations*. Moscow: Nauka. (in Rusian).
37. Manevich, L. I., Mihlin, Ju. V., & Pilipchuk, S. K. (1989). *The method of normal oscillations for essentially nonlinear systems*. Moscow: Nauka. (in Rusian).
38. Markovets, A. V., & Mazin, L. S. (2010). *The dynamic analysis of the mechanism of transporting sewing machines material*. Saint-Petersburg: SPGUTD. (in Rusian).
39. Vulfson, I. I., Yerikhov, M. E., Kolovsky, M. Z. & et al. (1996). Mechanics of machines. In G. A. Smirnov (Ed.), *Textbook for technical colleges.* Moscow: Vysshaya shkola (in Russian).
40. Mitropolskii, Ju. A. (1964). *Problems of the asymptotic theory of nonstationary oscillations*. Moscow: Nauka. (in Russian).
41. Nagaev, R. F. (1985). *Mechanical processes with repetitive attenuated collisions*. Moscow: Nauka. (in Russian).
42. Nashif, A., Jones, D., & Henderson, J. (1985). *Vibration damping*. New York: J. Wiley.
43. Veits, V. L. (Ed.). (1983). *Nonlinear problems of machines dynamics and strength*. Len.Gos. Univ. (in Russian).
44. Palmov, V. A. (1976). *Oscillations of elasto-plastic bodies*. Berlin: Springer.
45. Panovko, Ya. G. (1960). *Inner damping due to the vibration of elastic systems*. Moscow: Fizmatgiz. (in Russian).
46. Panovko, Y. G. (1985). *Mechanics of deformable solid body*. Moscow: Nauka (in Russian).
47. Pervozvannskii, A. A., & Gaytsgori, V. G. (1979). *Decomposition, aggregation and approximate optimization*. Moscow: Nauka.
48. Pfeiffer, F. (2008). *Mechanical system dynamics*. Berlin: Springer.
49. Pisarenko, G. S. (1962). *Energy dissipation at the mechanical oscillations*. Kiev: AN.USSR (in Russian).
50. Pozhbelko, V. I. (1989). *Inertially-pulsed machines drives with dynamic links*. Mocow: Mashinostroenie. (in Russian).

51. Poludov, A. N. (1979). *The program unloaders of the cyclic mechanisms*. Lvov: Visha shkola. (in Russian).
52. Rößler, J. (1982). Zur Modellierung von Schwingungssystemen, die periodisch übersetzende Getriebe Enhalten. Technische Mechanik, No. 3, 39-43.
53. Semenov, Y. A. (2010). *Dynamics of the machines*. Part 1: textbook. Izd. Politehn.un-ta, Saint-Petersburg (in Russian).
54. Senevirtane, L. D., & Earles, S. W. (1992). Chaotic behavior exhibited during contact loss in a clearance-joint of four bar mechanism. *Mechanism and Machine Theory, 27*(3), 307–321.
55. Sorokin, E. S. (1958). *Dynamics calculations of the bearing structures*. Moscow: Gosstroyizdat. (in Russian).
56. Ponomarev, S. D., Biederman, V. L., Liharev, K. K. & et al. (1959). *Strength calculations in mechanical engineering* (Vol. 3). Moscow: Mashgiz (in 3 v, in Russian).
57. Veitz, V. L., Kolovsky, M. Z., & Kochura, A. E. (1984). *Dynamical controlled machine aggregates*. Moscow: Nauka (in Russian).
58. Frolov, K. V. (Ed.). (1995). *Handbook: Vibration in engineering*. (2nd ed., Vol. 6). rev. and add. Moscow: Mashinostroenie (in Russian).
59. Vulfson, I. I. (1969). Oscillations of systems with parameters depending on the time. *Prikladnaya matematika i mexanika., 33*(2), 331–337. (in Russian).
60. Vulfson, I. I. (1970). Determination of the reduced dissipation parameters at biharmonic vibrations. *Vibrotehnika, 3*(5), 33–41. (in Russian).
61. Vulfson, J. I. (1973). Analytical investigation of the vibrations of mechanisms caused by parametric impulses. *Mechanism and Machine Theory, 10*(4), 305–313.
62. Vulfson, I. I. (1976). *Dynamic analysis of cyclic mechanisms*. Leningrad: Mashinostroenie (in Russian).
63. Vulfson, I. I. (1988). *Vibroactivity of branched and ring structured mechanical drives*. New York: Hemisphere Publ. Corp. (Translation from Russian, Mashinostroenie, Leningrad, 1986).
64. Vulfson, I. I. (1990). *Vibrations in machines with cyclic action mechanisms*. Leningrad: Mashinostroenie (in Russian).
65. Vulfson, I. I. (1991). Influence of vibration on the limits of spring closing in mechanisms with nonretaining links. *Journal of Machinery Manufacture and Reliability, 1*, 21–26.
66. Vulfson, I. I. (1994). Optimization of the parameters of vibratory systems of cyclic mechanisms teaching clearances into account. *Journal of Machinery Manufacture and Reliability, 3*, 7–13.
67. Vulfson, I. I. (1998). Analysis of differential-cyclic mechanism with nonlinear position feedback. *Journal of Machinery Manufacture and Reliability*, 3, 74–79.
68. Vulfson, I. I. (1999). Nonlinear vibration in cyclic mechanisms induced by nonstationary friction forces in kinematic pairs. *Journal of Machinery Manufacture and Reliability, 4*, 20–26.
69. Vulfson, I. I. (2001). Study of dynamics of mechanisms with frequency independent amplitude of the forced oscillations. *Journal of Machinery Manufacture and Reliability, 1*, 37–42.
70. Vulfson, I. I. (2001). On a nonlinear dynamic model of a mechanism with anomalous characteristics. *Journal of Machinery Manufacture and Reliability, 4*, 10–15.
71. Vulfson, I. I. (2005). Appearance of subharmonic resonances in multiple-frequency excitation. *Journal of Machinery Manufacture and Reliability*, 2, 1–7.
72. Vulfson, I. I. (2005). Nonlinear resonant oscillations of a drive at the amplitude-modulation frequency of high-frequency excitation. *Journal of Machinery Manufacture and Reliability, 6*, 13–17.
73. Vulfson, I. I. (2007). On decomposition of regular vibration systems of cycle machines incorporating idential ring-structured modules. *Journal of Machinery Manufacture and Reliability, 36*(4), 15–22.
74. Vulfson, I. I. (2008). Some nonlinear effects of machine dynamics. *Journal of Vibroingeneering*. *10*(4), 442–450.

75. Vulfson, I. I. (2008).*Vibrations in machines: Textbook for technical colleges*. St-Petersburg: SPGUTD (in Russian).
76. Vulfson, I. I. (2009). Method of frequency analysis of the multisection drives of the cyclic machines, forming torsion - bending systems of branched-ring structures.: Teoriya mehanizmov i mashin. V.7, N 1(13), 32–41, (in Russian).
77. Vulfson, I. I. (2011). Phase synchronism and space localization of vibrations of cyclic machine tips with symmetrical dynamic structure. *Journal of Machinery Manufacture and Reliability*, *40*(1), 12–18.
78. Vulfson, I. I. (2011). A modification of the generalized dynamic model of multiply regular vibratory systems of cyclic machines. *Journal of Machinery Manufacture and Reliability, 40* (5), 3–10.
79. Vulfson, I. I. (2012). Effect of low-frequency oscillations in the nonlinear dissipative forces. *Izv. Vuzov. Prikladnaya Nelineinaya Dinamika, 4*(4),51–65 (in Russian).
80. Vulfson, I. I. (2013). Energy transfer in vibratory systems of drives with cyclic mechanisms. *Journal of Machinery Manufacture and Reliability, 42*(4), 261–268.
81. Vulfson, I. I., & Georgadze, Z. N. (1990). Reduction of vibroactivity of cyclic mechanisms with dual programmable control. *Vibration Engineering*, *4*, 107–115.
82. Vulfson, I. I., & Khorungin, V. S. (1983). Oscillatory distortions of spatial linkage kinematic characteristics. *Mechanism and Machine Theory*, *16*, 137–146.
83. Vulfson, I. I., & Kolovsky, M. Z. (1968). *Nonlinear problems of machines dynamics*. Leningrad: Mashinostroenie, (in Russian).
84. Vulfson, I. I., & Levit, V. L. (1988). Distribution of dynamic loads in closed drives with clearances and phase errors of mechanisms. *Soviet Machine Science, 1*, 67–73.
85. Vulfson, I. I., & Preobrazhenskaya, M. V. (1997). A mathematical model and the frequency characteristics of a spatial mechanism with allowance for hinge clearances. *Journal of Machinery Manufacture and Reliability*, *2*, 8–15 (in Russian).
86. Vulfson, I. I., & Preobrazhenskaya, M. V. (1995). Parametric pulses during shockless reversals in linkage clearances. *Machinery Manufacture and Reliability*, *5*, 24–31.
87. Vulfson, I. I., & Preobrazhenskaya, M. V. (2008). Study of the vibrational modes excited due to the clearances of the cyclic mechanisms, connected with general executive body. *Machinery Manufacture and Reliability, 1*, 33–39 (in Russian).
88. Vulfson, I. I., & Vulfson, M. N. (2004). Refined equivalent linearization of the positional dissipative forces in oscillations with several frequencies. *Journal of Machinery Manufacture and Reliability*, *4*, 17–23.
89. Vulfson, I. I., & Vulfson, M. N. (2006). Study of forced drive oscillations based on model with distributed elastodissipative element. *Journal of Machinery Manufacture and Reliability*, *2*, 3–8.
90. Wu, C. L. S., & Earles, S. W. E. (1977). A determination of contact loss at a bearing of a linkage mechanism. *ASME Journal of Engineering for Industry, 99*(2), 375–380.
91. Wulfson, J. I. (1982). Zur Methodik der Untersuchung enzwungener Schwingungen in einem verzweigtem Mechanismensystem regulärer Struktur. *Technische Mechanik, 3*, 44–47.

Index